Universidad de Concepción
Dirección de Postgrado
Facultad de Ciencias Físicas y Matemáticas
Programa de Doctorado en Ciencias Aplicadas
con Mención en Ingeniería Matemática

# MÉTODOS DE ELEMENTOS VIRTUALES MIXTOS PARA PROBLEMAS NO LINEALES EN MECÁNICA DE FLUIDOS

## (MIXED VIRTUAL ELEMENT METHODS FOR NONLINEAR PROBLEMS IN FLUIDS MECHANICS)

Tesis para optar al grado de Doctor en Ciencias
Aplicadas con mención en Ingeniería Matemática

Edgar Mauricio Munar Benitez
CONCEPCIÓN-CHILE
2019

Profesor Guía: Gabriel N. Gatica Pérez
CI$^2$MA y Departamento de Ingeniería Matemática
Universidad de Concepción, Chile

Cotutor: Filánder A. Sequeira Chavarría
Escuela de Matemática,
Universidad Nacional, Costa Rica

**Mixed Virtual Element Methods for Nonlinear Problems in Fluid Mechanics**

Edgar Mauricio Munar Benitez

**Directores de Tesis:** Gabriel N. Gatica, Universidad de Concepción, Chile.
Filánder A. Sequeira, Universidad Nacional, Costa Rica.

**Director de Programa:** Rodolfo Rodríguez, Universidad de Concepción, Chile.

## Comisión evaluadora

Prof. Giuseppe Vacca, Universitá degli studi di milano-Bicocca.

Prof. Alexey Chernov, University of Oldenburg, Germany.

Prof. Sundararajan Natarajan, Institute of Technology-Madras, India.

## Comisión examinadora

Firma: _____
Prof. Eligio Colmenares, Universidad del Bío-Bío, Chile.

Firma: _____
Prof. Michael Karkulik, Universidad Técnica Federico Santa María, Chile.

Firma: _____
Prof. Gabriel Gatica, Universidad de Concepción, Chile.

Firma: _____
Prof. David Mora, Universidad del Bío-Bío, Chile.

Calificación: _____

Concepción, Diciembre 18 de 2019

# Abstract

In this thesis we introduce and analyze further applications of the Virtual Element Method (VEM), which can be interpreted as an evolution of the Mimetic Finite Differences method offering high order approximation spaces on computational meshes consisting of polygonal/polyhedral elements. In particular, we focus our analysis on mixed discretizations (mixed-VEM) of some nonlinear problems in fluids mechanics. Also, we are interested in developing the tools required to implement adaptive algorithms that are able to take advantage of the flexibility offered by such general meshes.

Firstly, we propose and analyze a mixed-VEM for a dual-mixed formulation of a nonlinear Brinkman model of porous media flow. We introduce the main features for the corresponding discrete scheme, which employs an explicit piecewise-polynomial subspace and a virtual element subspace to approximate the gradient of velocity and the pseudostress, respectively. The velocity and the pressure are computed via simple postprocessing formulae. In turn, the associated computable discrete nonlinear operator is defined in terms of the $\mathrm{L}^2$-orthogonal projector onto a suitable space of polynomials, which allows the explicit integration of the terms involving deviatoric tensors that appear in the original setting. The well-posedness of the discrete scheme and the associated a priori error estimates for the virtual element solution, as well as for the fully computable projection of it, are derived. Several numerical results illustrating the good performance of the method and confirming the theoretical rates of convergence are presented.

Next, a mixed-VEM for a pseudostress-velocity formulation of the Navier-Stokes equations is proposed and analyzed. We describe the main VEM ingredients that are required for our discrete analysis, which, besides projectors commonly utilized for related models, include, as the main novelty, the simultaneous use of virtual element subspaces for $\mathbf{H}^1$ and $\mathbb{H}(\mathbf{div})$ in order to approximate the velocity and the pseudostress, respectively. The pressure is computed via a postprocessing formula. Then, the discrete bilinear and trilinear forms involved, their main properties and the associated mixed virtual scheme are defined, and the corresponding solvability analysis is performed using appropriate fixed-point arguments. Moreover, Strang-type estimates are applied to derive the a priori error estimates for the two components of the virtual element solution as well as for the fully computable projections of them and the postprocessed pressure. Furthermore, some numerical examples confirming the theoretical error bounds and illustrating the performance of the proposed discrete scheme are reported.

Additionally, we extend our study and propose a mixed-VEM for the Boussinesq problem. Here, the main unknows are given by the pseudostress tensor, the velocity and the temperature, and as before, the pressure is computed via postprocessing. The discrete problem is treated employing a mixed-VEM for the scheme associated with the fluid equations in such a way that the pseudostress and the velocity are approximated on virtual element subspaces of $\mathbb{H}(\mathbf{div})$ and $\mathbf{H}^1$, respectively, whereas another VEM

is proposed to approximate the temperature on a virtual element subspace of $H^1$. The corresponding solvability analysis is performed by using fixed-point strategies. Further, Strang-type estimates are applied to derive the a priori error estimates for the components of the virtual element solution as well as for the fully computable projections of them and the postprocessed pressure.

Finally, we present an a posteriori error analysis for the mixed-VEM applied to second order elliptic equations in divergence form and with mixed boundary conditions. The resulting error estimator is of residual-type. It only depends on quantities directly available from the VEM solution and applies on very general polygonal meshes. Properties of interpolation operators, Helmholtz decompositions, inverse inequalities and localization techniques based on bubble functions are used for the analysis. Then, via the inclusion of a fully local postprocessing of the mixed-VEM solution, we show that the estimator provides a reliable and efficient control on the broken H(div)-norm error between the exact and the postprocessed flux. In the same way, we propose an a posteriori error analysis of a mixed-VEM discretization for the nonlinear Brinkman model described above. For the analysis we make use again of the aforementioned techniques. For both problems, we provide numerical experiments showing the quality of ours adaptive schemes.

# Resumen

En esta tesis introducimos y analizamos aplicaciones adicionales del Método de Elementos Virtuales (VEM), el cual puede ser interpretado como una evolución del método de Diferencias Finitas Miméticas, técnica que ofrece espacios de aproximación de alto orden sobre mallas computacionales que consisten de elementos poligonales/poliedrales. Enfocamos nuestro análisis en discretizaciones mixtas (mixed-VEM) de algunos problemas no lineales en mecánica de fluidos. Además, estamos interesados en desarrollar las herramientas necesarias para implementar algoritmos adaptativos que puedan aprovechar la flexibilidad que ofrecen estas mallas generales.

En primer lugar, proponemos y analizamos un mixed-VEM para una formulación dual-mixta de un modelo no lineal de Brinkman para flujo en medios porosos. Introducimos las características principales del esquema discreto asociado, en el cual empleamos un espacio de polinomios a trozos y un espacio virtual para aproximar el gradiente de velocidad y el pseudoesfuerzo, respectivamente. La velocidad y la presión se calculan mediante fórmulas de postprocesamiento. A su vez, el operador no lineal discreto asociado se define en términos del proyector $\mathrm{L}^2$-ortogonal sobre un espacio polinomial adecuado, lo que permite el cálculo explícito de los términos que involucran los tensores desviadores que aparecen en la formulación continua. Se establece que el esquema discreto está bien puesto y se derivan estimaciones de error a priori asociadas a la solución virtual, así como para la proyección computable de ésta. Se presentan varios resultados numéricos que ilustran el buen desempeño del método y confirman las tasas teóricas de convergencia.

Luego, un mixed-VEM para una formulación pseudoesfuerzo-velocidad de las ecuaciones de Navier-Stokes se propone y se analiza. Describimos los principales ingredientes que se requieren para nuestro análisis discreto, el cual hace uso de proyectores comúnmente usados en este contexto, incluyendo, como principal novedad, el uso simultáneo de subespacios de elementos virtuales para $\mathbf{H}^1$ y $\mathbb{H}(\mathbf{div})$, con el fin de aproximar la velocidad y el pseudoesfuerzo, respectivamente. La presión se calcula mediante una fórmula de postprocesamiento. Luego, se definen las formas bilineales y trilineales discretas involucradas, el esquema virtual asociado, y el análisis de solubilidad correspondiente es realizado usando argumentos de punto fijo. Además, estimaciones tipo Strang son aplicadas para derivar las estimaciones de error a priori tanto para las dos componentes de la solución virtual, como para las proyecciones computables de éstas y la presión postprocesada. Mas aún, se presentan algunos ejemplos numéricos que confirman las cotas de error teóricas e ilustran el rendimiento del esquema discreto.

Adicionalmente, extendemos nuestro estudio y proponemos un mixed-VEM para el problema de Boussinesq. Las principales incógnitas están dadas por el tensor de pseudoesfuerzo, la velocidad y la temperatura, y al igual que antes la presión es calculada por postproceso. El problema discreto se

plantea empleando un enfoque mixed-VEM para el esquema asociado con las ecuaciones del fluido, de tal manera que el pseudoesfuerzo y la velocidad se aproximan en subespacios de elementos virtuales de $\mathbb{H}(\mathbf{div})$ y $\mathbf{H}^1$, respectivamente, mientras que un VEM se propone para aproximar la temperatura en un subespacio virtual de $\mathrm{H}^1$. Además, se aplican estimaciones tipo Strang para derivar las estimaciones de error a priori para las componentes de la solución virtual, así como para las proyecciones computables de éstas y la presión postprocesada.

Finalmente, presentamos un análisis de error a posteriori para el mixed-VEM aplicado a ecuaciones elípticas de segundo orden en forma de divergencia y con condiciones de frontera mixtas. El estimador de error resultante es de tipo residual. Solo depende de cantidades directamente disponibles de la solución VEM y aplica para mallas poligonales muy generales. Propiedades de operadores de interpolación, descomposiciones de Helmholtz, desigualdades inversas y técnicas de localización basadas en funciones burbuja se utilizan para el análisis. Mediante la inclusión de un posprocesamiento completamente local de la solución mixed-VEM, mostramos que el estimador proporciona un control confiable y eficiente sobre el error en la norma H(div) por tramos, entre el flujo aproximado y el postprocesado. De la misma manera, proponemos un análisis de error a posteriori para una discretización mixed-VEM del modelo no lineal de Brinkman descrito anteriormente. Para el análisis hacemos uso nuevamente de técnicas antes mencionadas. Para ambos problemas, proporcionamos experimentos numéricos que muestran la calidad de nuestros esquemas adaptativos.

# Agradecimientos

En primer lugar quiero agradecer a Yura, mi compañera de vida y madre de mis hijas, quien durante cerca de 5 años ha esperado pacientemente y en la distancia que yo adelantara mis estudios. Espero que la vida me dé la oportunidad de poder recompensarle cada instante que pasamos lejos. A mi hija mayor, Lina, *la pilluela*, a quien me tocó verla crecer en la distancia, gracias por permitirme ser tu padre y no reprocharme los momentos que me he perdido contigo. A Isa, quien nació durante esta aventura, cada pirueta y sonrisa de ella eran como un viento fresco en medio de todo. Las tres son todas mis razones.

A mis padres, quienes siempre me han animado y apoyado a seguir formándome no solo académicamente, sino que a través de su ejemplo me han inspirado a ser una mejor persona y un mejor padre. No tengo como pagarles tantos sacrificios que han hecho por mí, tantas palabras de apoyo, las muchas veces que me han tendido la mano, y las innumerables ocasiones que han estado pendiente de mis hijas. Estoy seguro que el poder culminar mis estudios también es un triunfo de ellos. A mis hermanos, Migue, Boli, Mace y Jota, quienes cada uno a su manera y como han podido me han ayudado durante estos años. Gracias totales.

A mi tia Betty y todos mis primos, quenes me acogieron cada vez que los visitaba en Santiago. Me hacian sentir como en casa.

A mi suegra Mery, por estar pendiente de Linita el primer año de mis estudios. A Liliana, con quien a pesar de tener profundas diferencias, debo agradecerle tantas veces que estuvo pendiente de Yura y de mis hijas. A Deiver y Eduardo, por compartir con mi familia, y porque hicieron que mi ausencia les fuera más llevadera a ellas. Quedo profundamente agradecido con ustedes.

A Silvia Ramírez, quien este último año no solo me abrió las puertas de su casa sino que me dio la oportunidad de conocer su sencilla visión de la vida. Con seguridad cada charla y cada consejo quedará muy presente en mi vida. Mi gratitud por siempre.

A todos mis compañeros del doctorado, los que se han ido y los que se quedan, gracias por tantas charlas durante el almuerzo, por cada discusión académica y sobretodo por cada partido de futbol. De manera especial quiero agradecer a Eduardo, Ivan, Rafa y Luis, quienes me tendieron la mano muchas veces, quizás más de la cuenta. A cada uno de los amigos con quienes pude compartir en cada reunión y cada asado, hicieron que mi estadía en Chile fuera más acogedora. Muchas gracias a todos.

A mi director de tesis, el profesor Gabriel Gatica, por su tiempo, su disposición, sus retadas, sus consejos, por entender que en ocasiones tenía que viajar a mi país por estar pendiente de mi familia, por guiar mi trabajo y por estar dispuesto a formar parte de mi crecimiento como investigador. A mi co-director de tesis, el profesor Filander Sequeira, quien ha sido parte importante en el desarrollo de

mi tesis doctoral, en especial en la implementación de todos los códigos que la componen.

Al profesor Andrea Cangiani, quien muy amablemente me recibió y orientó durante mi pasantía en Univertsiy of Leicester. Por las muchas veces que hemos conversado sobre VEM y otros métodos poligonales. Grazie Mille!

A Raimund Burguer y Rodolfo Rodriguez, por su excelente gestión cuando cada uno de ellos ha sido director del programa de doctorado, lo cual se vio reflejado en los apoyos de financiamiento que gestionaron para poder sostenerme el primer año, y asistir a distintos congresos en Chile.

A los profesores del Doctorado con quienes tuve la oportunidad de tomar cursos: Gabriel Gatica, Raimund Burguer, Romel Bustinza, Leonardo Figueroa, Dhanya Rajendran. Cada uno de sus cursos ayudó a mi formación en el análisis numérico.

A los colaboradores del DIM y del CI$^2$MA, por ayudarme en los diversos trámites. A lorena, Paola, Jorge, Cecilia, Micaela. También, a quienes fueron parte, Jacqueline, Angelina y Eduardo, quienes en su momento me brindaron su ayuda en diferentes aspectos. Muchas gracias.

A Chile y cada uno de los chilenos, quienes me acogieron durante tantos años y me brindaron la oportunidad de conocerlos. Me voy convencido de que todo este aprendizaje cultural me ha ayudado a entender la diversidad de pensamiento.

A los diferentes proyectos, Beca REDOC.CTA, por brindarme financiamiento mi primer año de estudios, a CONICYT, poque a través de la Beca de doctorado Nacional pude financiarme 3 años y medio de estudios, además de la pasantía y gastos relacionados a asistencia a eventos. Al programa de financiamiento BASAL para apoyo a centros científicos y tecnológicos de excelencia a través del proyecto AFB 170001 del CMM, por apoyarme en el último tramo de redacción de este trabajo. Sin duda culminar mi estudios hubiera sido imposible sin todo este apoyo institucional. Mi gratitud por siempre.

Edgar Mauricio Munar Benitez

# Contents

# List of Tables

# List of Figures

# Introduction

Many complex physical phenomena can be modeled by partial differential equations (PDEs), but since it is generally not possible to find the solution to these problems in an exact form, it is necessary to get an approximation via computational methods. The construction of numerical methods that allow not only to solve approximately the PDE but also to handle meshes with complex geometries, is one of the most challenging problems for the numerical analysis community. Thereby, enabling the use of general meshes and with few restrictions would allow numerical methods to adapt in a better way to the anisotropic character of some PDE solutions, e.g., modeling of polycrystalline materials [1], material design [52], discrete fracture network [3], and the approximation of solutions with singularities via mesh refinement. The first attempts to enable the use of polygonal/polyhedral meshes began in the early '70s from the seminal works of Wachspress [93, 94]. Since then, various approaches have been proposed, including: polygonal/polyhedral finite elements (PFEMs), mimetic finite differences (MFDs), Galerkin polygonal/polyhedral discontinuous (DG-PFEMs), Trefftz finite elements (T-FEMs), finite elements based on boundary elements method (BEM-based FEM), and recently, virtual elements methods (VEMs).

PFEMs were introduced in [89] by using the ideas given by [93, 94]. This approach provides shape functions composed of rational, logarithmic and trigonometric functions, which makes its implementation neither simpler nor more efficient than the classical finite element method. In turn, MFD preserves the fundamental properties of mathematical and physical models such as conservation laws, positivity and symmetry of the solution, as well as discrete versions of Green's identities [17]. The DG-PFEM was introduced in [82, 96, 73] as an extension of the standard discontinuous Galerkin method [11], with the aim to handle general meshes. DG-PFEMs can be considered as hybrid methods between classical finite element methods and finite volume methods, since they approximate the solution using arbitrary degree polynomials on the elements, which are coupled using numerical flow functions [37]. On the other hand, T-FEM uses two different sets of functions to approximate the solutions, one for the boundary and other for the interior domain [50]. Furthermore, BEM-based FEM uses basis functions similar to those of T-FEM but implicitly defined, which are treated locally by means boundary integral operators [50, 85, 86, 95]. Finally, the VEM, first introduced in [13], emerges as a method that allows to generalize the MFD, in the sense that it is proposed in a variational context and further allows to define degrees of freedom into the elements, which are linked to the test functions. This enables to design high-order methods with VEM in a simpler way than MFD.

The VEM approach has received a great interest in recent years due to its ability to deal with polygonal/polyhedral meshes, the flexibility in the construction of conforming and non-conforming approximation spaces, and the easily to implement associated adaptive algorithms. Since it was in-

troduced for the first time in [13], the amount of publications using VEM are continuously increasing, and applications in many fields, including solid and fluid mechanics have been proposed (see e.g.,[10, 20, 21, 25, 30, 31, 32, 39, 76, 78, 80, 90], and the references therein). The basic idea of VEM consists of the utilization of suitable discrete spaces to approximate the PDE solution, which do not need to be known explicitly in order to implement the method, but only the degrees of freedom are required. However, these spaces must contain certain subspaces of polynomials to define suitable projectors. These projectors are defined using the bilinear forms involved in the variational formulation and their computation is guaranteed suitably choosing the degrees of freedom of the discrete spaces. All these ingredients allow to define discrete bilinear forms that mimic the original ones and that provide still consistency and stability of the resulting discrete scheme. An interesting aspect of VEM is given by the fact that it applies on general meshes, which allows to implement adaptive algorithms very easily and efficiently. The reason of the latter is because hanging nodes are easily treated as new nodes, so that the elements that contain them are taken as new polygonal/polyhedral. Hence, local refinements can be performed on polygonal/polyhedral meshes using few elements, in contrast to classical mesh refinement techniques for triangular meshes, which suffer from the fact that local refinement propagates into neighbouring regions. Recently, several works have been proposed in this regard, however, all of them focused on primal schemes (see, e.g.,[24, 38, 26, 81, 79, 44]).

According to the above discussion, the purpose of this thesis is to continue exploring the applicability of VEM to nonlinear problems in fluid mechanics and their corresponding adaptive strategies. In particular, we are interested in proposing mixed-VEM for Brinkman, Navier-Stokes and Boussinesq models, however, whose main aspects could be adapted to other types of problems. In all cases, we prove that each discrete scheme is well-posed and establish the corresponding a priori error estimates. Our concern in the first three Chapters of this thesis is to analyze mixed-VEM for the aforementioned problems, while the last two are devoted to developing adaptive strategies for some of them.

The present thesis is organized as follows. In **Chapter** 1, we extend the results obtained in [31] to a class of Brinkman models whose viscosity depends nonlinearly on the gradient of the velocity. In order to deal with the aforedescribed nonlinearity, we follow [58] and introduce the gradient of the velocity as a new unknown. Thereby, the system is formulated in terms of a pseudostress tensor and the gradient of the velocity, whereas the velocity and the pressure of the fluid are computed via postprocessing formulae. Moreover, we modify the resulting variational formulation by augmenting it with a redundant equation arising from the constitutive law relating the pseudostress and the velocity, which allows us to apply known results from nonlinear functional analysis to prove that the continuous scheme is well-posed. Next, based on the approach introduced in [32], we propose a mixed-VEM discretization where an approximation for the pseudostress is sought in a virtual subspace of $\mathbb{H}(\mathbf{div})$, whereas for the gradient of the velocity piecewise-polynomials are employed. We show the well-posedness of the discrete scheme and derive the associated a priori error estimates for the virtual element solution as well as for the fully computable projection of it. Furthermore, we also introduce a second element-by-element postprocessing formula for the pseudostress, which yields an optimally convergent approximation of this unknown with respect to the broken $\mathbb{H}(\mathbf{div})$-norm. The contents of this chapter gave rise to the following paper:

[68] G. N. Gatica, M. Munar, and F. A. Sequeira, *A mixed virtual element method for a nonlinear Brinkman model of porous media flow.* **Calcolo**, 55 (2018), pp. Art. 21, 36.

In **Chapter** 2, we propose and analyze a mixed-VEM for a pseudostress-velocity formulation of the two-dimensional Navier-Stokes equations. We follow [35] and employ a dual-mixed approach based on the introduction of a nonlinear pseudostress linking the usual linear one for the Stokes equations and the convective term. In this way, the aforementioned new tensor together with the velocity constitute the only unknowns of the problem, whereas the pressure is computed via a postprocessing formula. Banach fixed-point and Lax-Milgram theorems are applied to conclude the well-posedness of the continuous formulation. Next, using the ideas from [4, 15], we introduce virtual element spaces in order to approximate the velocity and the pseudostress. Then, the discrete bilinear and trilinear forms involved, their main properties and the associated mixed virtual scheme are defined, and the corresponding solvability analysis is performed using again fixed-point arguments. Moreover, Strang-type estimates are applied to derive the *a priori* error estimates for the two components of the virtual element solution as well as for the fully computable projections of them and the postprocessed pressure. The contents of this chapter gave rise to the following paper:

[69] G. N. Gatica, M. Munar, and F. A. Sequeira, *A mixed virtual element method for the Navier-Stokes equations.* **Math. Models Methods Appl. Sci**, 28 (2018), pp. 2719–2762.

In **Chapter** 3, we extend the ideas from **Chapter** 2 to develop a mixed-VEM for the two-dimensional Boussinesq problem. We follow [46] and introduce a pseudostress tensor depending nonlinearly on the velocity, which allows to obtain an equivalent model where the main unknowns are given by the aforementioned pseudostress tensor, the velocity and the temperature, whereas the pressure is computed via a postprocessing formula. Fixed point strategies are used to analyze the well-posedness of the resulting continuous formulation. Regarding the discrete problem, we follow the approach employed in [69], and couple it with a VEM for the convection-diffusion equation modelling the temperature. More precisely, we use a mixed-VEM for the scheme associated with the fluid equations in such a way that the pseudostress and the velocity are approximated on virtual element subspaces, whereas another VEM is proposed to approximate the temperature on a virtual element subspace. In this way, we make use of projectors onto suitable polynomial spaces, which allow the explicit computation of the terms that appear in the forms involved in the scheme for the fluid equations as well as in the forms associated to the heat equation. Next, the corresponding solvability analysis is performed using again fixed-point arguments. Further, Strang-type estimates are applied to derive the *a priori* error estimates for the components of the virtual element solution as well as for the fully computable projections of them and the postprocessed pressure. This chapter gave rise to the following preprint:

[67] G. N. Gatica, M. Munar, and F. A. Sequeira, *A mixed virtual element method for the Boussinesq problem on polygonal meshes.* Preprint 2019-32, Centro de Investigación en Ingeniería Matemática, Universidad de Concepción, Chile [available at: `https://www.ci2ma.udec.cl/publicaciones/prepublicaciones`].

In **Chapter** 4, we present an a posteriori error analysis for the mixed-VEM applied to second order elliptic equations in divergence form with mixed boundary conditions. The resulting error estimator is of residual-type. It only depends on quantities directly available from the VEM solution and applies on very general polygonal meshes. The proof of the upper bound relies on a global inf-sup condition,

a suitable Helmholtz decomposition, and the local approximation properties of a Clément-type interpolant. In turn, standard inverse inequalities and localization techniques based on bubble functions are the main tools yielding the lower bound. Then, via the inclusion of a fully local postprocessing of the mixed VEM solution, we also show that the estimator provides a reliable and efficient control on the error between the exact and the postprocessed flux. This chapter gave rise to the following preprint:

[40] A. Cangiani and M. Munar, *A posteriori error estimates for mixed virtual element methods.* Preprint 2019-10, Centro de Investigación en Ingeniería Matemática, Universidad de Concepción, Chile [available at: `https://www.ci2ma.udec.cl/publicaciones/prepublicaciones`].

Finally, in **Chapter** 5, we develop an a posteriori error analysis for the mixed-VEM employed in [68]. More precisely, we use the approach from [40] to develop a posteriori error estimates and the corresponding adaptive strategy. For this purpose, we propose a residual-type estimator, which involves fully computable approximations of the pseudostress variable. Next, for the respective analysis we follow [40], and apply suitable Helmholtz decompositions, local approximation properties of interpolation operators, inverse inequalities and localization techniques based on bubble functions. The contents of this chapter will appear in the following work currently in preparation:

M. Munar, and F. A. Sequeira, *A posteriori error analysis of a mixed virtual element method for a nonlinear Brinkman model of porous media flow.* **In preparation**.

Throughout the five chapters of this thesis, the theoretical results such as: orders of convergence, reliability and efficiency of the corresponding residual-based a posteriori error estimators, are illustrated through several numerical examples, which also highlight the good performance of the proposed discrete schemes and the associated adaptive algorithms. The computational implementations were obtained using MATLAB code and the illustrator PARAVIEW.

# Introducción

Muchos fenómenos físicos complejos pueden ser modelados por ecuaciones diferenciales parciales (PDEs), pero dado que generalmente no es posible encontrar soluciones exactas, se hace necesario obtener aproximaciones de éstas usando métodos computacionales. La construcción de métodos numéricos que permitan no solo resolver de manera aproximada las PDEs sino que también tengan la capacidad de manipular mallas con geometrias complejas es un reto para la comunidad científica, en particular la del Análisis Numérico. De este modo, habilitar el uso de mallas generales y con pocas restricciones permitiría a los métodos numéricos adaptarse de una mejor manera al carácter anisótropico de algunas soluciones PDE, por ejemplo, en problemas relacionados con materiales policristalinos [1], diseño de materiales [52], mallas de fracturas discretas [3], y la aproximación de soluciones con singularidades vía refinamiento de mallas. Los primeros intentos para habilitar el uso de mallas poligonales/poliedrales se dieron al inicio de los 70' con los artículos de Wachspress [93, 94]. A partir de estos trabajos se han venido proponiendo diversos enfoques, entre los cuales podemos mencionar: elementos finitos poligonales/poliedrales (PFEMs), diferencias finitas miméticas (MFDs), Galerkin discontinuos poligonales/poliedrales (DG-PFEMs), elementos finitos Trefftz (T-FEMs), elementos finitos basados en elementos de frontera (BEM-based FEM), y recientemente elementos virtuales (VEMs).

Los PFEMs fueron introducidas en [89] usando las ideas expuestas en [93, 94]. Este enfoque proporciona funciones de forma consistentes de funciones racionales, logarítmicas y trigonométricas, lo que hace que su implementación no sea ni más simple ni más eficiente comparada con la del FEM clásico. A su vez, el MFD preserva las propiedades fundamentales de los modelos matemáticos y físicos tales como leyes de conservación, positividad y simetría de la solución, así como también versiones discretas de las identidas de Green [17]. El DG-PFEM fue introducido en [82, 96, 73] como una extensión del método de Galerkin discontinuo clásico estándar [11], con el objetivo de manipular mallas generales. DG-PFEMs pueden ser considerados como métodos híbridos entre los FEM clásicos y los métodos de volúmenes finitos, ya que aproximan la solución empleando polinomios de grado arbitrario sobre los elementos, los cuales a su vez son acoplados usando funciones de flujo numérico [37]. Por otro lado, los T-FEMs usan dos conjuntos diferentes de funciones para aproximar las soluciones, unos para la frontera y otros para el interior del dominio [50]. Por otra parte, el BEM-based FEM usa funciones base similares a las de T-FEM pero definidas implícitamente y son tratadas localmente por medio de operadores de integrales de frontera [50, 85, 86, 95]. Finalmente, el VEM fue introducido en [13] y surge como un método que permite generalizar el MFD, en el sentido que se propone en un contexto variacional y a su vez permiten definir grados de libertad en el interior de los elementos, los cuales están ligados a las funciones test. Lo anterior facilita el diseño de métodos de alto orden con VEM de manera más simple que con los MFDs.

El enfoque VEM ha recibido mucha atención en los últimos años debido a su capacidad para tratar con mallas poligonales/poliedrales, la flexibilidad en la construcción de los espacios de aproximación, conformes y no conformes, y la facilidad con la que se pueden implementar algoritmos adaptativos. Desde su introducción in [13], la cantidad de publicaciones está creciendo continuamente, y aplicaciones en muchos campos, incluyendo mecánica de sólidos y fluidos han sido propuestos. (ver por ejemplo, [10, 20, 21, 25, 30, 31, 32, 39, 76, 78, 80, 90], y las referencias allí mencionadas). La idea básica del VEM consiste en la utilización de espacios discretos adecuados para aproximar la solución de la PDE, los cuales no necesitan ser conocidos explícitamente con el fin de implementar el método, ya que sólo se requieren los grados de libertad asociados. Sin embargo, estos espacios deben contener ciertos subespacios de polinomios para poder definir los proyectores adecuados. Estos proyectores se definen usando las fomas bilinales involucradas en la formulación variacional, y su cálculo se garantiza escogiendo adecuadamente los grados de libertad asociados a los espacios discretos. Todos estos ingredientes permiten definir formas bilineales discretas que mimetizan el comportamientos de sus pares continuos y que permiten probar la estabilidad y consistencia del esquema discreto resultante. Un aspecto interesante de VEM está dado por el hecho de que es capaz de manipular mallas generales, lo cual permite implementar algoritmos adaptativos de manera más fácil y eficiente. La razón de esto último es porque los nodos colgantes son fácilmente tratados como nuevos nodos, de tal manera que los elementos que los contienen son tomados como nuevos polígonos/poliedros de la malla. Por lo tanto, los refinamientos locales pueden ser realizados sobre mallas generales usando pocos elementos, en contraste con las técnicas de refinamiento usadas en los elementos finitos clásicos, las cuales sufren del hecho de que el refinamiento se propaga a regiones vecinas. Recientemente, varios trabajos han sido propuestos, sin embargo, todos ellos están enfocados en esquemas primales (ver por ejemplo, [24, 38, 26, 81, 79, 44]).

Acorde a lo expuesto anteriormente, el propósito de esta tesis es continuar explorando la aplicabilidad de VEM a problemas no lineales en mecánica de fluidos y sus correspondientes estrategias adaptativas. En particular, estamos interesados en proponer esquemas mixtos para los modelos de Brinkman, Navier-Stokes y Boussinesq, cuyas principales ideas pueden adaptarse a otro tipo de problemas. En todos los casos, se prueba que cada esquema discreto está bien puesto y se establecen las estimaciones de error a priori correspondientes. Los tres primeros capítulos de esta tesis conciernen al estudio de los problemas mencionados anteriormente, mientras que los últimos dos están dedicados al desarrollo de estrategias adaptativas para algunos de ellos.

La presente tesis está organizada como sigue. En el **Capítulo** 1 extendemos los resultados obtenidos en [31] a una clase de modelos de Brinkman cuya viscosidad depende no linealmente del gradiente de la velocidad. Para tratar con la no linealidad antes mencionada, seguimos [58] e introducimos el gradiente de la velocidad como una nueva incógnita. De esta manera, el sistema se formula en términos de un pseudoesfuerzo y el gradiente de la velocidad, mientras que la velocidad y la presión se calculan usando formulas de postprocesamiento. Además, modificamos la formulación variacional resultante adicionando una ecuación redundante proveniente de la ley constitutiva que relaciona el pseudoesfuerzo y la velocidad, lo que nos permite aplicar resultados conocidos del análisis funcional no lineal para probar que el esquema continuo está bien puesto. Luego, basado en el enfoque introducido en [32], proponemos una discretización mixed-VEM donde se busca una aproximación para el pseudoesfuerzo en un espacio virtual de $\mathbb{H}(\mathbf{div})$, mientras que para el gradiente de la velocidad se emplean polinomios a trozos. Mostramos que el esquema discreta está bien puesto y derivamos las correspondientes estima-

ciones de error a priori para la solución virtual, así como también para las proyecciones computables de ésta. Adicionalmente, también introducimos un segundo postprocesamiento del pseudoesfuerzo, el cual proporciona convergencia óptima respecto a la norma $\mathbb{H}(\mathbf{div})$ por tramos. El contenido de este capítulo dio lugar al siguiente artículo:

[68] G. N. Gatica, M. Munar, and F. A. Sequeira, *A mixed virtual element method for a nonlinear Brinkman model of porous media flow.* **Calcolo**, 55 (2018), pp. Art. 21, 36.

En el **Capítulo** 2 proponemos y analizamos un mixed-VEM para una formulación pseudoesfuerzo-velocidad de las ecuaciones de Navier-Stokes en 2D. Seguimos [35] y empleamos un enfoque dual-mixto basado en la introducción de un pseudoesfuerzo no lineal que relaciona las ecuaciones de Stokes con el término convectivo. De esta manera, el tensor antes mencionado junto con la velocidad constituyen las únicas incógnitas del problema, mientras que la presión se calcula vía una formula de postprocesamiento. Teoremas del punto fijo de Banach y de Lax-Milgram se aplican para concluir que la formulación continua está bien puesta. Posteriormente, usando las ideas expuestas en [4, 15], introducimos espacios de elementos virtuales con el fin de aproximar la velocidad y el pseudoesfuerzo. Luego, se definen las formas bilineales y trilineales involucradas, sus principales propiedades y el esquema virtual asociado, y el análisis de solubilidad correspondiente se realiza usando otra vez argumentos de punto fijo. Además, estimaciones tipo Strang se aplican para derivar estimaciones de error *a priori* para la solución virtual, así como para las proyecciones computables de éstas y la presión postprocesada. El contenido de este capítulo dio lugar al siguiente artículo:

[69] G. N. Gatica, M. Munar, and F. A. Sequeira, *A mixed virtual element method for the Navier-Stokes equations.* **Math. Models Methods Appl. Sci**, 28 (2018), pp. 2719–2762.

En el **Capítulo** 3 extendemos las ideas descritas en [69] para desarrollar un mixed-VEM para el problema de Boussinesq. Seguimos [46] e introducimos un tensor de pseudoesfuerzo dependiendo no linealmente de la velocidad, el cual permite obtener un modelo equivalente donde las principales incógnitas están dadas por el pseudoesfuerzo antes mencionado, la velocidad y la temperatura, mientras que la presión es calculada usando una fórmula de postprocesamiento. Estrategias de punto fijo se usan para establecer que la formulación continua resultante está bien puesta. Respecto al problema discreto, seguimos el enfoque empleado en [69], y lo acoplamos con un VEM para la ecuación convección-difusión que modela la temperatura. De manera más precisa, usamos un mixed-VEM para el esquema asociado con las ecuaciones del fluido de tal manera que, tanto el pseudoesfuerzo como la velocidad se aproximan usando espacios virtuales, mientras que se propone un VEM para aproximar la temperatura también sobre un espacio virtual adecuado. De esta manera, hacemos uso de proyectores sobre espacios polinomiales adecuados, los cuales permiten la integración explícita de los términos que aparecen tanto en las formas bilineales y trilineales asociadas a las ecuaciones del fluido, como a las asociadas a las ecuaciones del calor. Luego, el análisis de solubilidad correspondiente se realiza usando nuevamente estrategias de punto fijo. Además, se usan estimaciones tipo Strang para derivar estimaciones de error tanto para los componentes de la solución virtual como para las proyecciones computables de éstas y la presión postprocesada. El contenido de este capítulo dio lugar a la siguiente prepublicación:

[67] G. N. Gatica, M. Munar, and F. A. Sequeira, *A mixed virtual element method for the Boussinesq problem on polygonal meshes.* Preprint 2019-32, Centro de Investigación en Ingeniería Matemática, Universidad de Concepción, Chile [available at: `https://www.ci2ma.udec.cl/publicaciones/prepublicaciones`].

En el **Capítulo** 4 presentamos un análisis de error a posteriori para el mixed-VEM aplicado a ecuaciones elípticas de segundo orden en forma de divergencia y con condiciones de frontera mixtas. El estimador de error es de tipo residual. Solo depende de cantidades directamente disponibles a partir de la solución VEM y aplica sobre mallas poligonales generales. La prueba de la cota superior recae sobre una condición inf-sup global, una descomposición de Helmholtz, y propiedades de aproximación locales de un interpolante tipo Clément. A su vez, desigualdades inversas estándar y técnicas de localización basadas en funciones burbuja son las principales herramientas que proporcionan la cota inferior. Luego, por medio de la inclusión de un postproceso local de la solución VEM, también mostramos que el estimador provee un control confiable y eficiente para el error entre el flujo exacto y el postprocesado. Este capítulo dio origen a la siguiente prepublicación:

[40] A. Cangiani and M. Munar, *A posteriori error estimates for mixed virtual element methods.* Preprint 2019-10, Centro de Investigación en Ingeniería Matemática, Universidad de Concepción, Chile [available at: `https://www.ci2ma.udec.cl/publicaciones/prepublicaciones`].

Finalmente, en el **Capítulo** 5 desarrollamos un análisis de error a posteriori para la discretización mixed-VEM empleada en [68]. Más precisamente, usamos el enfoque expuesto en [40] para desarrolar estimaciones de errores a posteriori y la correspondiente estrategia adaptativa. Para este propósito, proponemos un estimador tipo residual que involucra aproximaciones completamente computables del pseudoesfuerzo. Luego, para el respectivo análisis seguimos [40], y aplicamos despomposiciones de Helmholtz, propiedades de aproximación locales de operadores de interpolación, desigualdades inversas y técnicas de localización basadas en funciones burbujas. Este capítulo aparecerá en el siguiente trabajo, actualmente en preparación:

M. Munar, and F. A. Sequeira, *A posteriori error analysis of a mixed virtual element method for a nonlinear Brinkman model of porous media flow.* **In preparation**.

A traves de los cínco capitulos de esta tesis, los resultados teóricos como: ordenes de convergencias, confiabilidad y eficiencia de los correspondientes estimadores de error a posteriori, se ilustran por medio de varios ejemplos numéricos. Las implementaciones computacionales fueron obtenidas usando código MATLAB y el ilustrador PARAVIEW.

# CHAPTER 1

# A mixed virtual element method for a nonlinear Brinkman model of porous media flow

## 1.1 Introduction

The numerical solution of diverse linear and nonlinear boundary value problems in fluid mechanics by means of the VEM technique has become a very promising research subject during recent years. In fact, we first refer to [10, 20, 39], where several virtual element methods, including stream function-based, divergence free, and non-conforming schemes, have been proposed for the classical velocity-pressure formulation of the Stokes equation. In turn, the method from [20] has been recently extended in [21] to the two-dimensional Navier-Stokes equations, thus yielding, up to our knowledge, the first VEM approach for this nonlinear model. On the other hand, and concerning the use of *dual-mixed* formulations, that is those in which the main unknown usually lives in either a vectorial $\mathbf{H}(\mathrm{div})$ or a tensorial $\mathbb{H}(\mathbf{div})$ space, we remark that several contributions have concentrated on the combination of VEM and pseudostress-based approaches, being the latter motivated by the need of circumventing the symmetry requirement of the usual stress-based methods. In particular, a mixed-VEM for the pseudostress-velocity formulation of the Stokes problem, in which the pressure is computed via a postprocessing formula, was introduced in [30]. The analysis in [30] is then extended in [31] to derive two mixed virtual element methods for the two-dimensional Brinkman problem. An interesting feature of both schemes in [31] refers to their robustness as the Stokes limit of the Brinkman model is approached. The corresponding pseudostress-based dual-mixed finite element methods for this model and its nonlinear version had been previously developed in [57, 58], respectively. More recently, another virtual element method for the Brinkman equations, though not employing the same dual-mixed approach from the aforementioned references, has been proposed in [90]. In addition, the approach from [30, 31] was extended in [32] to the case of quasi-Newtonian Stokes flows. More precisely, a virtual element method for an augmented mixed variational formulation of the class of nonlinear Stokes models studied in [64] (see also [70, 71]) is introduced and analyzed in [32]. Furthermore, in the recent work [69] we considered the same variational formulation from [35] (see also [33, 34]) and proposed, up to our knowledge, the first dual-mixed virtual element method for the Navier-Stokes equations. Indeed, the approach employed in [69] is based on the introduction of a nonlinear pseudostress linking the convective term with the usual pseudostress for the Stokes equations. We end this paragraph by highlighting that,

besides the basic principles of the VEM philosophy (cf. [13, 28]), most of the aforedescribed works on mixed VEM for pseudostress-based variational formulations have made extensive use of the key contributions provided in [4, 15, 14]. In particular, the exact computations of the $\mathrm{L}^2$-projections onto suitable spaces of polynomials have certainly enriched the potential applications of the $\mathrm{H}^1$ and H(div) conforming cases.

According to the foregoing discussion, and in order to continue developing pseudostrees-based mixed virtual element methods for nonlinear models in fluid mechanics, we now aim to extend the analysis and results from [32, 69] to the case of the problem studied in [58]. In other words, the purpose of the present chapter is to extend the analysis and results from [31] to a class of Brinkman models whose viscosity depends nonlinearly on the gradient of the velocity, which is a characteristic feature of quasi-Newtonian Stokes flows (see, e.g. [61, 64, 71, 74]). In order to deal with the aforedescribed nonlinearity, we follow [58] and introduce the gradient of the velocity as a new unknown. Moreover, we modify the resulting variational formulation by augmenting it with a redundant equation arising from the constitutive law relating the pseudostress and the velocity gradient, which allows us to apply known results from nonlinear functional analysis.

The rest of this chapter is organized as follows. In Section 1.2 we define the boundary value problem of interest, introduce its pseudostress-based mixed formulation, and provide the associated well-posedness result. Next, in Section 1.3 we follow [15, 14] to introduce the virtual element subspace that will be employed. This includes the basic assumptions on the polygonal mesh, the definition of the local virtual element space, and the projections and interpolants to be utilized together with their respective approximation properties. Further, we introduce a fully calculable local discrete nonlinear operator. Then, we set the corresponding mixed virtual element method, and apply the classical theory of nonlinear operators to conclude its well-posedness. In turn, in Section 1.4 we employ suitable bounds and identities satisfied by the nonlinear operator and the projectors and interpolators involved, to derive the a priori error estimates and corresponding rates of convergence for the virtual solution as well as for the computable projection of it. In addition, we follow the ideas from [59, 60] to construct a second approximation for the pseudostress variable $\boldsymbol{\sigma}$, which yields an optimal rate of convergence in the broken $\mathbb{H}(\mathbf{div})$-norm. We remark that this new postprocessing formula can be used in general for any H(div)-conforming VEM scheme. Finally, several numerical examples showing the good performance of the method, confirming the rates of convergence for regular and singular solutions, and illustrating the accurateness obtained with the approximate solutions, are reported in Section 1.5.

We end this section with several notations to be used throughout the **Chapter 1**. Firstly, we let $\mathbb{I}$ be the identity matrix in $\mathrm{R}^{2\times 2}$, and for any $\boldsymbol{\tau} := (\tau_{ij})$, $\boldsymbol{\zeta} := (\zeta_{ij}) \in \mathrm{R}^{2\times 2}$, we set

$$\boldsymbol{\tau}^{\mathrm{t}} := (\tau_{ji})\,, \quad \mathrm{tr}(\boldsymbol{\tau}) := \sum_{i=1}^{2} \tau_{ii}, \quad \boldsymbol{\tau}^{\mathrm{d}} := \boldsymbol{\tau} - \frac{1}{2}\,\mathrm{tr}(\boldsymbol{\tau})\,\mathbb{I}\,, \quad \text{and} \quad \boldsymbol{\tau} : \boldsymbol{\zeta} := \sum_{i,j=1}^{2} \tau_{ij}\zeta_{ij},$$

which denote, respectively, the transpose, the trace, and the deviator of the tensor $\boldsymbol{\tau}$, and the tensorial product between $\boldsymbol{\tau}$ and $\boldsymbol{\zeta}$. Next, given a bounded domain $\mathcal{O} \subseteq \mathrm{R}^2$, with polygonal boundary $\partial\mathcal{O}$, we utilize standard notations for Lebesgue spaces $\mathrm{L}^p(\mathcal{O})$, $p > 1$, and Sobolev spaces $\mathrm{H}^s(\mathcal{O})$, $s \in \mathrm{R}$, with norm $\|\cdot\|_{s,\mathcal{O}}$ and seminorm $|\cdot|_{s,\mathcal{O}}$. In particular, $\mathrm{H}^{1/2}(\partial\mathcal{O})$ is the space of traces of functions of $\mathrm{H}^1(\mathcal{O})$ and $\mathrm{H}^{-1/2}(\partial\mathcal{O})$ denotes its dual. Moreover, by $\mathbf{M}$ and $\mathbb{M}$ we will refer to the corresponding vector and tensorial counterparts of the generic scalar functional space M, and $\|\cdot\|$, with no subscripts, will stand

for the natural norm of either an element or an operator in any product functional space. Furthermore, we recall that

$$\mathbb{H}(\mathbf{div};\mathcal{O}) := \left\{ \boldsymbol{\tau} \in \mathbb{L}^2(\mathcal{O}) : \quad \mathbf{div}(\boldsymbol{\tau}) \in \mathbf{L}^2(\mathcal{O}) \right\},$$

equipped with the usual norm

$$\|\boldsymbol{\tau}\|^2_{\mathbf{div};\mathcal{O}} := \|\boldsymbol{\tau}\|^2_{0,\mathcal{O}} + \|\mathbf{div}(\boldsymbol{\tau})\|^2_{0,\mathcal{O}} \qquad \forall\, \boldsymbol{\tau} \in \mathbb{H}(\mathbf{div};\mathcal{O}),$$

is a Hilbert space. Finally, we employ $\mathbf{0}$ to denote a generic null vector, null tensor or null operator, and use $C$ and $c$, with or without subscripts to denote generic constants independent of the discretization parameters, which may take different values at different places.

## 1.2 The continuous problem

### 1.2.1 The model problem

Let $\Omega$ be a bounded domain in $\mathrm{R}^2$ with polygonal boundary $\Gamma$. Given a volume force $\mathbf{f} \in \mathbf{L}^2(\Omega)$ and a Dirichlet datum $\mathbf{g} \in \mathbf{H}^{1/2}(\Gamma)$, we seek a tensor $\boldsymbol{\sigma}$ (pseudostress), a vector field $\mathbf{u}$ (velocity), and a scalar field $p$ (pressure), such that

$$\begin{aligned} \boldsymbol{\sigma} = \mu(|\nabla \mathbf{u}|)\nabla \mathbf{u} - p\,\mathbb{I} \quad \text{in} \quad \Omega, \quad \alpha \mathbf{u} - \mathbf{div}(\boldsymbol{\sigma}) = \mathbf{f} \quad \text{in} \quad \Omega, \\ \mathrm{div}(\mathbf{u}) = 0 \quad \text{in} \quad \Omega, \quad \mathbf{u} = \mathbf{g} \quad \text{on} \quad \Gamma, \quad \text{and} \quad \int_\Omega p = 0, \end{aligned} \tag{1.1}$$

where $\mu : \mathrm{R}^+ \to \mathrm{R}$ is the nonlinear kinematic viscosity function of the fluid, and $\alpha > 0$ is a constant approximation of the viscosity divided by the permeability. In addition, note according to the incompressibility of the fluid, that $\mathbf{g}$ must satisfy the compatibility condition $\int_\Gamma \mathbf{g} \cdot \boldsymbol{\nu} = 0$, where $\boldsymbol{\nu}$ is the unit outward normal on $\Gamma$, and that the uniqueness of a pressure solution is ensured by the last equation of (1.1).

In what follows, we let $\mu_{ij} : \mathrm{R}^{2\times 2} \to \mathrm{R}$ be the mapping given by $\mu_{ij} := \mu(|\mathbf{r}|)r_{ij}$ for each $\mathbf{r} := (r_{ij}) \in \mathrm{R}^{2\times 2}$ and for each $i, j \in \{1, 2\}$. Then, throughout this chapter we assume that $\mu$ is of class $C^1$ and that there exist $\gamma_0, \alpha_0 > 0$ such that for each $\mathbf{r} := (r_{ij}), \mathbf{s} := (s_{ij}) \in \mathrm{R}^{2\times 2}$, there hold

$$|\mu_{ij}(\mathbf{r})| \leq \gamma_0 |\mathbf{r}|, \quad \text{and} \quad \left| \frac{\partial}{\partial r_{kl}} \mu_{ij}(\mathbf{r}) \right| \leq \gamma_0 \quad \forall\, i, j, k, l \in \{1, 2\}, \tag{1.2}$$

and

$$\sum_{i,j,k,l=1}^{2} \frac{\partial}{\partial r_{kl}} \mu_{ij}(\mathbf{r}) s_{ij} s_{kl} \geq \alpha_0 |\mathbf{s}|^2. \tag{1.3}$$

A classical example of nonlinear functions $\mu$ is given by the well-known Carreau law in fluid mechanics (see e.g. [77, 88])

$$\mu(s) := \rho_0 + \rho_1 (1 + s^2)^{(\beta-2)/2} \qquad \forall\, s \geq 0, \tag{1.4}$$

where $\rho_0, \rho_1 > 0$ and $\beta > 1$. In particular, note that with $\beta = 2$ we recover the usual linear Brinkman model. It is easy to check that (1.4) satisfies the assumptions (1.2) and (1.3) for all $\rho_0, \rho_1 > 0$ and for all $\beta \in [1, 2]$, with

$$\gamma_0 = \rho_0 + \rho_1 \left\{ \frac{|\beta - 2|}{2} + 1 \right\} \quad \text{and} \quad \alpha_0 = \rho_0. \tag{1.5}$$

### 1.2.2 The continuous formulation

Here we proceed as in [58] to derive a weak formulation for (1.1). In fact, we begin by observing that the first equation of (1.1) together with the incompressibility condition are equivalent to the pair of equations given by

$$\boldsymbol{\sigma}^{\mathrm{d}} \,=\, \mu(|\nabla\mathbf{u}|)\nabla\mathbf{u} \quarin \quad \Omega \quad \text{and} \quad p \,=\, -\frac{1}{2}\mathrm{tr}(\boldsymbol{\sigma}) \quad \text{in} \quad \Omega\,, \tag{1.6}$$

whence introducing the auxiliary unknown $\mathbf{t} := \nabla\mathbf{u}$ in $\Omega$, we can rewrite (1.1) as follows:

$$\begin{aligned} \mathbf{t} \,=\, \nabla\mathbf{u} \quad \text{in} \quad \Omega, \quad \boldsymbol{\sigma}^{\mathrm{d}} \,=\, \mu(|\mathbf{t}|)\mathbf{t} \quad \text{in} \quad \Omega\,, \qquad \alpha\mathbf{u} - \mathbf{div}(\boldsymbol{\sigma}) \,=\, \mathbf{f} \quad \text{in} \quad \Omega\,, \\ \mathrm{tr}(\mathbf{t}) \,=\, 0 \quad \text{in} \quad \Omega\,, \quad \mathbf{u} \,=\, \mathbf{g} \quad \text{on} \quad \Gamma\,, \quad \text{and} \quad \int_\Omega \mathrm{tr}(\boldsymbol{\sigma}) = 0\,. \end{aligned} \tag{1.7}$$

In this way, we notice from the fourth and last equation of (1.7) that the unknowns $\mathbf{t}$ and $\boldsymbol{\sigma}$ live in the spaces

$$\mathbb{L}^2_{\mathrm{tr}}(\Omega) \,:=\, \big\{\mathbf{s} \in \mathbb{L}^2(\Omega) : \quad \mathrm{tr}(\mathbf{s}) = 0\big\}\,,$$

and

$$\mathbb{H}_0(\mathbf{div};\Omega) \,:=\, \left\{\boldsymbol{\zeta} \in \mathbb{H}(\mathbf{div};\Omega) : \quad \int_\Omega \mathrm{tr}(\boldsymbol{\zeta}) = 0\right\},$$

respectively. Then, testing the first and second equation of (1.7) with $\boldsymbol{\tau} \in \mathbb{H}_0(\mathbf{div};\Omega)$ and $\mathbf{s} \in \mathbb{L}^2_{\mathrm{tr}}(\Omega)$, respectively, integrating by parts, using the Dirichlet condition for $\mathbf{u}$, and denoting by $\langle\cdot,\cdot\rangle$ the duality pairing between $\mathbf{H}^{-1/2}(\Gamma)$ and $\mathbf{H}^{1/2}(\Gamma)$, we arrive at

$$\int_\Omega \mu(|\mathbf{t}|)\mathbf{t} : \mathbf{s} \,-\, \int_\Omega \mathbf{s} : \boldsymbol{\sigma}^{\mathrm{d}} \,=\, 0 \qquad \forall\, \mathbf{s} \in \mathbb{L}^2_{\mathrm{tr}}(\Omega)\,, \tag{1.8}$$

and

$$\int_\Omega \mathbf{t} : \boldsymbol{\tau}^{\mathrm{d}} \,+\, \int_\Omega \mathbf{u} \cdot \mathbf{div}(\boldsymbol{\tau}) \,=\, \langle \boldsymbol{\tau}\boldsymbol{\nu}, \mathbf{g}\rangle \qquad \forall\, \boldsymbol{\tau} \in \mathbb{H}_0(\mathbf{div};\Omega)\,, \tag{1.9}$$

where we used the fact that $\mathbf{t} = \mathbf{t}^{\mathrm{d}}$, which implies the equality $\int_\Omega \mathbf{t} : \boldsymbol{\tau} = \int_\Omega \mathbf{t} : \boldsymbol{\tau}^{\mathrm{d}}$. In turn, the velocity is replaced from the third equation of (1.7), that is

$$\mathbf{u} \,=\, \frac{1}{\alpha}\big\{\mathbf{f} \,+\, \mathbf{div}(\boldsymbol{\sigma})\big\} \quad \text{in} \quad \Omega\,, \tag{1.10}$$

whence (1.9) becomes

$$\int_\Omega \mathbf{t} : \boldsymbol{\tau}^{\mathrm{d}} \,+\, \frac{1}{\alpha}\int_\Omega \mathbf{div}(\boldsymbol{\sigma}) \cdot \mathbf{div}(\boldsymbol{\tau}) \,=\, -\frac{1}{\alpha}\int_\Omega \mathbf{f} \cdot \mathbf{div}(\boldsymbol{\tau}) \,+\, \langle \boldsymbol{\tau}\boldsymbol{\nu}, \mathbf{g}\rangle \qquad \forall\, \boldsymbol{\tau} \in \mathbb{H}_0(\mathbf{div};\Omega)\,.$$

The foregoing equation together with (1.8) yield at first instance the following variational formulation of (1.7): Find $\mathbf{t} \in X := \mathbb{L}^2_{\mathrm{tr}}(\Omega)$ and $\boldsymbol{\sigma} \in H := \mathbb{H}_0(\mathbf{div};\Omega)$ such that

$$\begin{aligned} \int_\Omega \mu(|\mathbf{t}|)\mathbf{t} : \mathbf{s} \,-\, \int_\Omega \mathbf{s} : \boldsymbol{\sigma}^{\mathrm{d}} \,&=\, 0 && \forall\, \mathbf{s} \in X\,, \\ \int_\Omega \mathbf{t} : \boldsymbol{\tau}^{\mathrm{d}} \,+\, \frac{1}{\alpha}\int_\Omega \mathbf{div}(\boldsymbol{\sigma}) \cdot \mathbf{div}(\boldsymbol{\tau}) \,&=\, -\frac{1}{\alpha}\int_\Omega \mathbf{f} \cdot \mathbf{div}(\boldsymbol{\tau}) \,+\, \langle \boldsymbol{\tau}\boldsymbol{\nu}, \mathbf{g}\rangle && \forall\, \boldsymbol{\tau} \in H\,. \end{aligned} \tag{1.11}$$

However, in order to analyse the solvability of (1.11), we need to perform a suitable modification of it. More precisely, given a stabilization parameter $\kappa > 0$ to be suitably chosen later on, we incorporate into (1.11) the following redundant Galerkin term:

$$\kappa \int_\Omega \{\boldsymbol{\sigma}^{\mathrm{d}} - \mu(|\mathbf{t}|)\mathbf{t}\} : \boldsymbol{\tau}^{\mathrm{d}} \;=\; 0 \qquad \forall\, \boldsymbol{\tau} \in \mathbb{H}_0(\mathbf{div};\Omega)\,,$$

which leads to the augmented formulation: Find $(\mathbf{t},\boldsymbol{\sigma}) \in X \times H$ such that

$$[\mathbf{A}(\mathbf{t},\boldsymbol{\sigma}),(\mathbf{s},\boldsymbol{\tau})] \;=\; [\mathbf{F},(\mathbf{s},\boldsymbol{\tau})] \qquad \forall\,(\mathbf{s},\boldsymbol{\tau}) \in X \times H\,, \tag{1.12}$$

where $[\cdot,\cdot]$ stands for the duality pairing between $(X \times H)'$ and $X \times H$, $\mathbf{A} : X \times H \to (X \times H)'$ is the nonlinear operator

$$\begin{aligned}[\mathbf{A}(\mathbf{r},\boldsymbol{\zeta}),(\mathbf{s},\boldsymbol{\tau})] \;:=\; & \int_\Omega \mu(|\mathbf{r}|)\mathbf{r} : \mathbf{s} - \int_\Omega \mathbf{s} : \boldsymbol{\zeta}^{\mathrm{d}} + \int_\Omega \mathbf{r} : \boldsymbol{\tau}^{\mathrm{d}} \\ & + \kappa \int_\Omega \{\boldsymbol{\zeta}^{\mathrm{d}} - \mu(|\mathbf{r}|)\mathbf{r}\} : \boldsymbol{\tau}^{\mathrm{d}} + \frac{1}{\alpha}\int_\Omega \mathbf{div}(\boldsymbol{\zeta})\cdot\mathbf{div}(\boldsymbol{\tau})\,,\end{aligned} \tag{1.13}$$

and $\mathbf{F} : X \times H \to \mathrm{R}$ is the bounded linear functional

$$[\mathbf{F},(\mathbf{s},\boldsymbol{\tau})] \;:=\; -\frac{1}{\alpha}\int_\Omega \mathbf{f}\cdot\mathbf{div}(\boldsymbol{\tau}) \;+\; \langle \boldsymbol{\tau}\boldsymbol{\nu},\mathbf{g}\rangle, \tag{1.14}$$

for all $(\mathbf{r},\boldsymbol{\zeta}),(\mathbf{s},\boldsymbol{\tau}) \in X \times H$. In addition, we also observe that we can write

$$\begin{aligned}[\mathbf{A}(\mathbf{r},\boldsymbol{\zeta}),(\mathbf{s},\boldsymbol{\tau})] \;:=\; & [\mathbb{A}(\mathbf{r}),\mathbf{s} - \kappa\boldsymbol{\tau}^{\mathrm{d}}] - \textstyle\int_\Omega \mathbf{s} : \boldsymbol{\zeta}^{\mathrm{d}} + \int_\Omega \mathbf{r} : \boldsymbol{\tau}^{\mathrm{d}} \\ & + \kappa \int_\Omega \boldsymbol{\zeta}^{\mathrm{d}} : \boldsymbol{\tau}^{\mathrm{d}} + \frac{1}{\alpha}\int_\Omega \mathbf{div}(\boldsymbol{\zeta})\cdot\mathbf{div}(\boldsymbol{\tau})\,,\end{aligned} \tag{1.15}$$

for each $(\mathbf{r},\boldsymbol{\zeta}),(\mathbf{s},\boldsymbol{\tau}) \in X \times H$, where $\mathbb{A} : X \to X'$ is the auxiliary nonlinear operator defined by

$$[\mathbb{A}(\mathbf{r}),\mathbf{s}] \;:=\; \int_\Omega \mu(|\mathbf{r}|)\mathbf{r} : \mathbf{s} \qquad \forall\, \mathbf{r},\mathbf{s} \in X.$$

At this point we recall from [64, Lemma 2.1] that $\mathbb{A}$ is Lipschitz-continuous and strongly monotone, that is, with the constants $\gamma_0$ and $\alpha_0$ specified in (1.2) and (1.3), respectively, there hold

$$\|\mathbb{A}(\mathbf{r}) - \mathbb{A}(\mathbf{s})\|_{X'} \;\leq\; \gamma_0\|\mathbf{r}-\mathbf{s}\|_{0,\Omega}\,, \tag{1.16}$$

and

$$[\mathbb{A}(\mathbf{r}) - \mathbb{A}(\mathbf{s}),\mathbf{r}-\mathbf{s}] \;\geq\; \alpha_0\|\mathbf{r}-\mathbf{s}\|^2_{0,\Omega}\,, \tag{1.17}$$

for each $\mathbf{r},\mathbf{s} \in X$. In addition, employing the Cauchy-Schwarz inequality and the estimate (1.16), we deduce from (1.15) that $\mathbf{A}$ is Lipschitz-continuous with constant $L_{\mathbf{A}} := \max\{1,\kappa,\gamma_0,\frac{1}{\alpha}\}$, that is

$$\|\,\mathbf{A}(\mathbf{t},\boldsymbol{\sigma}) - \mathbf{A}(\mathbf{r},\boldsymbol{\zeta})\,\|_{(X\times H)'} \;\leq\; L_{\mathbf{A}}\,\|(\mathbf{t},\boldsymbol{\sigma}) - (\mathbf{r},\boldsymbol{\zeta})\|_{X\times H} \qquad \forall\,(\mathbf{t},\boldsymbol{\sigma}),\,(\mathbf{r},\boldsymbol{\zeta}) \,\in\, X\times H\,. \tag{1.18}$$

Moreover, in what follows we show that $\mathbf{A}$ is strongly monotone as well. For this purpose, we need the following technical result.

**Lemma 1.1.** *There exists $c(\Omega) > 0$, depending only on $\Omega$, such that*

$$c(\Omega)\,\|\boldsymbol{\tau}\|_{0,\Omega}^2 \;\leq\; \|\boldsymbol{\tau}^{\mathrm{d}}\|_{0,\Omega}^2 \;+\; \|\mathbf{div}(\boldsymbol{\tau})\|_{0,\Omega}^2 \qquad \forall\, \boldsymbol{\tau} \in H.$$

*Proof.* See [29, Chapter IV, Proposition 3.1] □

Then, the announced result on $\mathbf{A}$ is established as follows.

**Lemma 1.2.** *Let $\mathbf{A}$ be the nonlinear operator defined in (1.13). Assume that, given $\delta \in \left(0, \dfrac{2}{\gamma_0}\right)$, the parameter $\kappa$ lies in $\left(0, \dfrac{2\delta\alpha_0}{\gamma_0}\right)$. Then, there exists a positive constant $C_{SM}$, independent of $h$, such that for all $(\mathbf{r},\boldsymbol{\zeta}), (\mathbf{s},\boldsymbol{\tau}) \in X \times H$ there holds*

$$[\mathbf{A}(\mathbf{r},\boldsymbol{\zeta}) - \mathbf{A}(\mathbf{s},\boldsymbol{\tau}), (\mathbf{r},\boldsymbol{\zeta}) - (\mathbf{s},\boldsymbol{\tau})] \;\geq\; C_{SM}\|(\mathbf{r},\boldsymbol{\zeta}) - (\mathbf{s},\boldsymbol{\tau})\|_{X\times H}^2.$$

*Proof.* Given $(\mathbf{r},\boldsymbol{\zeta}), (\mathbf{s},\boldsymbol{\tau}) \in X \times H$, we obtain from (1.15) that

$$\begin{aligned}[\mathbf{A}(\mathbf{r},\boldsymbol{\zeta}) - \mathbf{A}(\mathbf{s},\boldsymbol{\tau}), (\mathbf{r},\boldsymbol{\zeta}) - (\mathbf{s},\boldsymbol{\tau})] \;&=\; [\mathbb{A}(\mathbf{r}) - \mathbb{A}(\mathbf{s}), \mathbf{r} - \mathbf{s}] \\ &- \kappa\,[\mathbb{A}(\mathbf{r}) - \mathbb{A}(\mathbf{s}), (\boldsymbol{\zeta} - \boldsymbol{\tau})^{\mathrm{d}}] \;+\; \kappa\,\|(\boldsymbol{\zeta} - \boldsymbol{\tau})^{\mathrm{d}}\|_{0,\Omega}^2 \;+\; \frac{1}{\alpha}\,\|\mathbf{div}(\boldsymbol{\zeta} - \boldsymbol{\tau})\|_{0,\Omega}^2\,,\end{aligned}$$

from which, using the Cauchy-Schwarz and Young inequalities, the Lipschitz-continuity and strong monotonicity properties of the operator $\mathbb{A}$, and Lemma 1.1, we find that

$$\begin{aligned}&[\mathbf{A}(\mathbf{r},\boldsymbol{\zeta}) - \mathbf{A}(\mathbf{s},\boldsymbol{\tau}), (\mathbf{r},\boldsymbol{\zeta}) - (\mathbf{s},\boldsymbol{\tau})] \\ &\geq\; \left(\alpha_0 - \frac{\kappa\gamma_0}{2\delta}\right)\|\mathbf{r} - \mathbf{s}\|_{0,\Omega}^2 \;+\; \kappa\left(1 - \frac{\gamma_0\delta}{2}\right)\|(\boldsymbol{\zeta} - \boldsymbol{\tau})^{\mathrm{d}}\|_{0,\Omega}^2 \;+\; \frac{1}{\alpha}\,\|\mathbf{div}(\boldsymbol{\zeta} - \boldsymbol{\tau})\|_{0,\Omega}^2 \\ &\geq\; \left(\alpha_0 - \frac{\kappa\gamma_0}{2\delta}\right)\|\mathbf{r} - \mathbf{s}\|_{0,\Omega}^2 \;+\; c(\Omega)\,\min\left\{\kappa\left(1 - \frac{\gamma_0\delta}{2}\right), \frac{1}{2\alpha}\right\}\|\boldsymbol{\zeta} - \boldsymbol{\tau}\|_{0,\Omega}^2 \;+\; \frac{1}{2\alpha}\|\mathbf{div}(\boldsymbol{\zeta} - \boldsymbol{\tau})\|_{0,\Omega}^2\,.\end{aligned}$$

Finally, it suffices to choose $C_{SM} := \min\left\{\left(\alpha_0 - \dfrac{\kappa\gamma_0}{2\delta}\right), c(\Omega)\,\min\left\{\kappa\left(1 - \dfrac{\gamma_0\delta}{2}\right), \dfrac{1}{2\alpha}\right\}, \dfrac{1}{2\alpha}\right\}$. □

Hence, the well-posedness of the variational formulation (1.12) is provided by the following theorem.

**Theorem 1.3.** *Assume that $\mathbf{f} \in \mathbf{L}^2(\Omega), \mathbf{g} \in \mathbf{H}^{1/2}(\Gamma)$, and that the parameter $\kappa$ satisfy the conditions required by* Lemma 1.2. *Then, there exists a unique $(\mathbf{t},\boldsymbol{\sigma}) \in X \times H$ solution of (1.12). Moreover, there exists a positive constant $C$, depending only on $\Omega, \alpha_0, \gamma_0, \kappa$ and $\alpha$, such that*

$$\|(\mathbf{t},\boldsymbol{\sigma})\|_{X\times H} \;\leq\; C\left\{\|\mathbf{f}\|_{0,\Omega} \;+\; \|\mathbf{g}\|_{1/2,\Gamma}\right\}.$$

*Proof.* Thanks to the Lipschitz-continuity and the strong monotonicity of the operator $\mathbf{A}$, the proof is a straightforward application of [97, Theorem 25.B]. □

## 1.3 The mixed virtual element method

In this section we introduce and analyze a mixed virtual element scheme for the continuous formulation (1.12). An explicit piecewise polynomial subspace and a suitable virtual element subspace are employed for approximating $\mathbf{t} \in X$ and $\boldsymbol{\sigma} \in H$, respectively. While all the definitions and results concerning the latter subspace, including its associated interpolation operator and main approximation properties, are available in [15, 32], most of the corresponding details are recalled in what follows for convenience of the reader. We begin with some preliminaries.

### 1.3.1 Preliminaries

Let $\{\mathcal{T}_h\}_{h>0}$ be a family of decompositions of $\Omega$ in polygonal elements. Then, for each $K \in \mathcal{T}_h$ we denote its diameter by $h_K$, and define, as usual, $h := \max\{h_K : K \in \mathcal{T}_h\}$. Furthermore, in what follows we assume that there exists a constant $C_{\mathcal{T}} > 0$ such that for each decomposition $\mathcal{T}_h$ and for each $K \in \mathcal{T}_h$ there hold:

a) the ratio between the shortest edge and the diameter $h_K$ of $K$ is bigger than $C_{\mathcal{T}}$, and

b) $K$ is star-shaped with respect to a ball $B$ of radius $C_{\mathcal{T}} h_K$ and center $\mathbf{x}_B \in K$.

We recall here that, as consequence of the above hypotheses, one can show that each $K \in \mathcal{T}_h$ is simply connected, and that there exists an integer $N_{\mathcal{T}}$ (depending only on $C_{\mathcal{T}}$), such that the number of edges of each $K \in \mathcal{T}_h$ is bounded above by $N_{\mathcal{T}}$.

Now, given an integer $\ell \geq 0$ and $\mathcal{O} \subseteq \mathrm{R}^2$, we let $\mathrm{P}_\ell(\mathcal{O})$ be the space of polynomials on $\mathcal{O}$ of degree up to $\ell$, we set $\mathbf{P}_\ell(\mathcal{O}) := [\mathrm{P}_\ell(\mathcal{O})]^2$ and $\mathbb{P}_\ell(\mathcal{O}) := [\mathrm{P}_\ell(\mathcal{O})]^{2\times 2}$. Furthermore, given an edge $e$ of $\mathcal{T}_h$ with barycentric $x_e$ and diameter $h_e$, we introduce the following set of $(\ell+1)$ normalized monomials on $e$

$$\mathcal{B}_\ell(e) := \left\{ \left( \frac{x - x_e}{h_e} \right)^j \right\}_{0 \leq j \leq \ell},$$

which certainly constitutes a basis on $\mathrm{P}_\ell(e)$. Similarly, given $K \in \mathcal{T}_h$ with barycenter $\mathbf{x}_K$, we define the following set of $\frac{1}{2}(\ell+1)(\ell+2)$ normalized monomials

$$\mathcal{B}_\ell(K) := \left\{ \left( \frac{\mathbf{x} - \mathbf{x}_K}{h_K} \right)^{\boldsymbol{\alpha}} \right\}_{0 \leq |\boldsymbol{\alpha}| \leq \ell},$$

which is a basis of $\mathrm{P}_\ell(K)$. Notice that in the definition of $\mathcal{B}_\ell(K)$ above, we have made use of the multi-index notation, that is, given $\mathbf{x} := (x_1, x_2)^{\mathrm{t}} \in \mathrm{R}^2$ and $\boldsymbol{\alpha} := (\alpha_1, \alpha_2)^{\mathrm{t}}$, with non-negative integers $\alpha_1, \alpha_2$, we set $\mathbf{x}^{\boldsymbol{\alpha}} := x_1^{\alpha_1} x_2^{\alpha_2}$ and $|\boldsymbol{\alpha}| := \alpha_1 + \alpha_2$. Furthermore, for $e$ and $K$ as indicated, we define

$$\boldsymbol{\mathcal{B}}_\ell(e) := \Big\{ (q,0)^{\mathrm{t}} : q \in \mathcal{B}_\ell(e) \Big\} \cup \Big\{ (0,q)^{\mathrm{t}} : q \in \mathcal{B}_\ell(e) \Big\},$$

and

$$\boldsymbol{\mathcal{B}}_\ell(K) := \Big\{ (q,0)^{\mathrm{t}} : q \in \mathcal{B}_\ell(K) \Big\} \cup \Big\{ (0,q)^{\mathrm{t}} : q \in \mathcal{B}_\ell(K) \Big\}.$$

On the other hand, for each integer $\ell \geq 0$, we let $\mathcal{G}_\ell(K)$ be a basis of $\big(\nabla \mathrm{P}_{\ell+1}(K)\big)^\perp \cap \mathbf{P}_\ell(K)$, which is the $\mathbf{L}^2(K)$-orthogonal of $\nabla \mathrm{P}_{\ell+1}(K)$ in $\mathbf{P}_\ell(K)$, and denote its tensorial counterpart as follows:

$$\boldsymbol{\mathcal{G}}_\ell(K) := \left\{ \begin{pmatrix} \mathbf{q} \\ \mathbf{0} \end{pmatrix} : \mathbf{q} \in \mathcal{G}_\ell(K) \right\} \cup \left\{ \begin{pmatrix} \mathbf{0} \\ \mathbf{q} \end{pmatrix} : \mathbf{q} \in \mathcal{G}_\ell(K) \right\} .$$

While in what follows we use the aforedescribed decomposition of $\mathbf{P}_\ell(K)$ (and hence of its tensorial version $\mathbb{P}_\ell(K)$), we remark that, alternatively, one could also consider more modern choices, not necessarily orthogonal, that have been proposed recently, such as $\mathbf{P}_k(K) = \nabla \mathrm{P}_{k+1} \oplus \mathbf{x}^\perp \mathrm{P}_{k-1}(K)$, where, given $\mathbf{x} := (x_1, x_2) \in \mathrm{R}^2$, $\mathbf{x}^\perp$ denotes the rotated vector $(-x_2, x_1)$. Actually, it is not difficult to see that it suffices to choose any space $\mathcal{G}(K)$ such that $\mathbf{P}_\ell(K) = \nabla \mathrm{P}_{\ell+1} \oplus \mathcal{G}(K)$.

### 1.3.2 The virtual element space and its approximation properties

Given an integer $k \geq 0$, we define the finite dimensional subspaces of $X$ and $H$, respectively, as

$$X_k^h := \left\{ \mathbf{s} \in X : \quad \mathbf{s}\big|_K \in X_k^K \quad \forall\, K \in \mathcal{T}_h \right\} \tag{1.19}$$

and

$$H_k^h := \left\{ \boldsymbol{\tau} \in H : \quad \boldsymbol{\tau}\big|_K \in H_k^K \quad \forall\, K \in \mathcal{T}_h \right\} , \tag{1.20}$$

where, given $K \in \mathcal{T}_h$, $X_k^K := \mathbb{P}_k(K)$ and $H_k^K$ is the space introduced in [15, Section 3.1], namely

$$\begin{aligned} H_k^K := \Big\{ \boldsymbol{\tau} \in \mathbb{H}(\mathbf{div}; K) \cap \mathbb{H}(\mathbf{rot}; K) : \quad & \boldsymbol{\tau}\boldsymbol{\nu}|_e \in \mathbf{P}_k(e) \quad \forall \text{ edge } e \in \partial K , \\ & \mathbf{div}(\boldsymbol{\tau}) \in \mathbf{P}_k(K) \quad \text{and} \quad \mathbf{rot}(\boldsymbol{\tau}) \in \mathbf{P}_{k-1}(K) \Big\} . \end{aligned} \tag{1.21}$$

The degrees of freedom guaranteeing unisolvency for each $\boldsymbol{\tau} \in H_k^K$ are defined by (see e.g. [14, Section 3.6], [15, 31])

$$\begin{aligned} & \int_e \boldsymbol{\tau}\boldsymbol{\nu} \cdot \mathbf{q} && \forall\, \mathbf{q} \in \boldsymbol{\mathcal{B}}_k(e) , \quad \forall \text{ edge } e \in \partial K , \\ & \int_K \boldsymbol{\tau} : \nabla \mathbf{p} && \forall\, \mathbf{p} \in \boldsymbol{\mathcal{B}}_k(K) \setminus \{(1,0)^{\mathbf{t}}, (0,1)^{\mathbf{t}}\} , \\ & \int_K \boldsymbol{\tau} : \boldsymbol{\rho} && \forall\, \boldsymbol{\rho} \in \boldsymbol{\mathcal{G}}_k(K) . \end{aligned} \tag{1.22}$$

In turn, we let $\mathcal{P}_k^K : \mathbf{L}^2(K) \to \mathbf{P}_k(K)$ and $\boldsymbol{\mathcal{P}}_k^K : \mathbb{L}^2(K) \to \mathbb{P}_k(K)$ be the orthogonal projectors. Then, for each integer $m \in \{0, 1, \ldots, k+1\}$ there hold the following approximation properties:

$$\|\mathbf{v} - \mathcal{P}_k^K(\mathbf{v})\|_{0,K} \leq C h_K^m |\mathbf{v}|_{m,K} \qquad \forall\, \mathbf{v} \in \mathbf{H}^m(K) , \tag{1.23}$$

and

$$\|\boldsymbol{\tau} - \boldsymbol{\mathcal{P}}_k^K(\boldsymbol{\tau})\|_{0,K} \leq C h_K^m |\boldsymbol{\tau}|_{m,K} \qquad \forall\, \boldsymbol{\tau} \in \mathbb{H}^m(K) . \tag{1.24}$$

We now introduce the interpolation operator $\boldsymbol{\Pi}_k^K : \mathbb{H}^1(K) \to H_k^K$, which is defined for each $\boldsymbol{\tau} \in \mathbb{H}^1(K)$ as the unique $\boldsymbol{\Pi}_k^K(\boldsymbol{\tau})$ in $H_k^K$ such that

$$\begin{aligned} 0 &= \int_e (\boldsymbol{\tau} - \boldsymbol{\Pi}_k^K(\boldsymbol{\tau}))\boldsymbol{\nu} \cdot \mathbf{q} \quad \forall\, \mathbf{q} \in \boldsymbol{\mathcal{B}}_k(e)\,, \quad \forall \text{ edge } e \in \partial K\,, \\ 0 &= \int_K (\boldsymbol{\tau} - \boldsymbol{\Pi}_k^K(\boldsymbol{\tau})) : \nabla \mathbf{p} \quad \forall\, \mathbf{p} \in \boldsymbol{\mathcal{B}}_k(K) \setminus \{(1,0)^{\mathbf{t}}, (0,1)^{\mathbf{t}}\}\,, \\ 0 &= \int_K (\boldsymbol{\tau} - \boldsymbol{\Pi}_k^K(\boldsymbol{\tau})) : \boldsymbol{\rho} \quad \forall\, \boldsymbol{\rho} \in \boldsymbol{\mathcal{G}}_k(K)\,. \end{aligned} \tag{1.25}$$

Concerning the approximation properties of $\boldsymbol{\Pi}_k^K$, we first recall from [15, eq. (3.19)] (see also [25, Lemma 6] for a closely related estimate) that for each $\boldsymbol{\tau} \in \mathbb{H}^s(K)$, with $1 \leq s \leq k+1$, there holds

$$\|\boldsymbol{\tau} - \boldsymbol{\Pi}_k^K(\boldsymbol{\tau})\|_{0,K} \;\leq\; C\, h_K^s\, |\boldsymbol{\tau}|_{s,K}\,. \tag{1.26}$$

In addition, for each $\mathbf{p} \in \boldsymbol{\mathcal{B}}_k(K)$ we readily find that

$$\int_K \mathbf{div}(\boldsymbol{\tau} - \boldsymbol{\Pi}_k^K(\boldsymbol{\tau})) \cdot \mathbf{p} \;=\; -\int_K (\boldsymbol{\tau} - \boldsymbol{\Pi}_k^K(\boldsymbol{\tau})) : \nabla \mathbf{p} + \int_{\partial K} (\boldsymbol{\tau} - \boldsymbol{\Pi}_k^K(\boldsymbol{\tau}))\boldsymbol{\nu} \cdot \mathbf{p} \;=\; 0,$$

which, thanks to the fact $\mathbf{div}(\boldsymbol{\Pi}_k^K(\boldsymbol{\tau})) \in \mathbf{P}_k(K)$, implies that

$$\mathbf{div}(\boldsymbol{\Pi}_k^K(\boldsymbol{\tau})) \;=\; \mathcal{P}_k^K(\mathbf{div}(\boldsymbol{\tau})) \qquad \forall\, \boldsymbol{\tau} \in \mathbb{H}^1(K)\,. \tag{1.27}$$

In this way, applying (1.27) and (1.23), we deduce that for each $\boldsymbol{\tau} \in \mathbb{H}^1(K)$, such that $\mathbf{div}(\boldsymbol{\tau}) \in \mathbf{H}^s(K)$, with $0 \leq s \leq k+1$, there holds

$$\|\mathbf{div}(\boldsymbol{\tau}) - \mathbf{div}(\boldsymbol{\Pi}_k^K(\boldsymbol{\tau}))\|_{0,K} \;\leq\; C\, h_K^s\, |\mathbf{div}(\boldsymbol{\tau})|_{s,K}\,, \tag{1.28}$$

which, together with (1.26), allows us to prove the following lemma.

**Lemma 1.4.** *Let $K \in \mathcal{T}_h$, and let $s$ be an integer such that $1 \leq s \leq k+1$. Then, there exists a constant $C > 0$, independent of $K$, such that for each $\boldsymbol{\tau} \in \mathbb{H}^s(K)$ such that $\mathbf{div}(\boldsymbol{\tau}) \in \mathbf{H}^s(K)$, there holds*

$$\|\boldsymbol{\tau} - \boldsymbol{\Pi}_k^K(\boldsymbol{\tau})\|_{\mathbf{div};K} \;\leq\; C\, h_K^s \left\{ |\boldsymbol{\tau}|_{s,K} \,+\, |\mathbf{div}(\boldsymbol{\tau})|_{s,K} \right\}. \tag{1.29}$$

*Proof.* It follows straightforwardly from (1.26) and (1.28). □

### 1.3.3 The discrete scheme

In what follows we define the mixed virtual element scheme itself for our nonlinear problem (1.12). In this regard, we first notice, thanks to (1.21), that the functional $\mathbf{F}$ (cf. (1.14)) is explicitly computable for all $(\mathbf{s}, \boldsymbol{\tau}) \in X_k^h \times H_k^h$, whereas for each $K \in \mathcal{T}_h$ the local version $\mathbf{A}^K : (X_k^K \times H_k^K) \to (X_k^K \times H_k^K)'$ of the nonlinear operator $\mathbf{A}$, which is defined for all $(\mathbf{r}, \boldsymbol{\zeta}), (\mathbf{s}, \boldsymbol{\tau}) \in X_k^K \times H_k^K$ by

$$\begin{aligned} [\mathbf{A}^K(\mathbf{r}, \boldsymbol{\zeta}), (\mathbf{s}, \boldsymbol{\tau})] \;:=\; & \int_K \mu(|\mathbf{r}|)\mathbf{r} : \mathbf{s} \,-\, \int_K \mathbf{s} : \boldsymbol{\zeta}^{\mathrm{d}} \,+\, \int_K \mathbf{r} : \boldsymbol{\tau}^{\mathrm{d}} \\ & + \kappa \int_K \{\boldsymbol{\zeta}^{\mathrm{d}} - \mu(|\mathbf{r}|)\mathbf{r}\} : \boldsymbol{\tau}^{\mathrm{d}} \,+\, \frac{1}{\alpha} \int_K \mathbf{div}(\boldsymbol{\zeta}) \cdot \mathbf{div}(\boldsymbol{\tau})\,, \end{aligned} \tag{1.30}$$

is not computable since $\boldsymbol{\zeta}$ and $\boldsymbol{\tau}$ are not known on the whole $K \in \mathcal{T}_h$. In order to deal with this difficulty, we now recall, as it was remarked in [15, Section 3.2], that the degrees of freedom introduced in (1.22) do allow the explicit calculation of $\boldsymbol{\mathcal{P}}_k^K(\boldsymbol{\tau})$ for each $\boldsymbol{\tau} \in H_k^K$. Indeed, given $\mathbf{p} \in \mathbb{P}_k(K)$, we utilize the decomposition $\mathbb{P}_k(K) = \boldsymbol{\mathcal{G}}_k^{\perp}(K) \oplus \boldsymbol{\mathcal{G}}_k(K)$ to write $\mathbf{p} = \nabla \mathbf{q} + \boldsymbol{\rho}$, with $\mathbf{q} \in \mathbf{P}_{k+1}(K)$ and $\boldsymbol{\rho} \in \boldsymbol{\mathcal{G}}_k(K)$, whence we find that

$$\int_K \boldsymbol{\tau} : \mathbf{p} \;=\; \int_K \boldsymbol{\tau} : \nabla \mathbf{q} + \int_K \boldsymbol{\tau} : \boldsymbol{\rho} \;=\; -\int_K \mathbf{q} \cdot \mathbf{div}(\boldsymbol{\tau}) + \int_{\partial K} \boldsymbol{\tau}\boldsymbol{\nu} \cdot \mathbf{q} + \int_K \boldsymbol{\tau} : \boldsymbol{\rho}\,.$$

In this way, it readily follows from (1.21) and (1.22) that the foregoing expression, and hence $\boldsymbol{\mathcal{P}}_k^K(\boldsymbol{\tau})$, are both computable. Then, we now let $\mathbf{A}_h^K : (X_k^K \times H_k^K) \to (X_k^K \times H_k^K)'$ be the computable local discrete nonlinear operator approximating (1.30), which is defined by

$$\begin{aligned}[\mathbf{A}_h^K(\mathbf{r},\boldsymbol{\zeta}),(\mathbf{s},\boldsymbol{\tau})] \;:=\; &\int_K \mu(|\mathbf{r}|)\,\mathbf{r} : \big(\mathbf{s} - \kappa(\boldsymbol{\mathcal{P}}_k^K(\boldsymbol{\tau}))^{\mathrm{d}}\big) \;-\; \int_K (\boldsymbol{\mathcal{P}}_k^K(\boldsymbol{\zeta}))^{\mathrm{d}} : \mathbf{s} \;+\; \int_K (\boldsymbol{\mathcal{P}}_k^K(\boldsymbol{\tau}))^{\mathrm{d}} : \mathbf{r} \\ &+\; \kappa \int_K (\boldsymbol{\mathcal{P}}_k^K(\boldsymbol{\zeta}))^{\mathrm{d}} : (\boldsymbol{\mathcal{P}}_k^K(\boldsymbol{\tau}))^{\mathrm{d}} \;+\; \frac{1}{\alpha}\int_K \mathbf{div}(\boldsymbol{\zeta}) \cdot \mathbf{div}(\boldsymbol{\tau}) \;+\; \mathcal{S}^K(\boldsymbol{\zeta} - \boldsymbol{\mathcal{P}}_k^K(\boldsymbol{\zeta}), \boldsymbol{\tau} - \boldsymbol{\mathcal{P}}_k^K(\boldsymbol{\tau}))\,,\end{aligned} \tag{1.31}$$

for all $(\mathbf{r},\boldsymbol{\zeta}),(\mathbf{s},\boldsymbol{\tau}) \in X_k^K \times H_k^K$, where $\mathcal{S}^K : H_k^K \times H_k^K \to \mathrm{R}$ is any symmetric and positive bilinear form verifying (see [13, Section 4.6] or [15, Section 3.3])

$$\widehat{c}_0 \|\boldsymbol{\zeta}\|_{0,K}^2 \;\leq\; \mathcal{S}^K(\boldsymbol{\zeta},\boldsymbol{\zeta}) \;\leq\; \widehat{c}_1 \|\boldsymbol{\zeta}\|_{0,K}^2 \qquad \forall\, \boldsymbol{\zeta} \in H_k^K, \tag{1.32}$$

with constants $\widehat{c}_0, \widehat{c}_1 > 0$ depending only on $C_{\mathcal{T}}$. In particular, for the numerical results reported below in Section 1.5 we take $\mathcal{S}^K$ as the bilinear form whose associated matrix with respect to the canonical basis of $H_k^K$ determined by the degrees of freedom (1.22), is the identity matrix. Equivalently, letting $n_k^K$ be the dimension of $H_k^K$ and denoting by $m_{j,K}$, $j \in \{1,2,\ldots,n_k^K\}$, the degrees of freedom given by (1.22), we set

$$\mathcal{S}^K(\boldsymbol{\zeta},\boldsymbol{\tau}) \;:=\; \sum_{j=1}^{n_k^K} m_{j,K}(\boldsymbol{\zeta})\, m_{j,K}(\boldsymbol{\tau}) \qquad \forall\,(\boldsymbol{\zeta},\boldsymbol{\tau}) \,\in\, H_k^K \times H_k^K\,.$$

According to (1.31), we now introduce the global discrete nonlinear operator $\mathbf{A}_h : (X_k^h \times H_k^h) \to (X_k^h \times H_k^h)'$ as

$$[\mathbf{A}_h(\mathbf{r},\boldsymbol{\zeta}),(\mathbf{s},\boldsymbol{\tau})] \;:=\; \sum_{K \in \mathcal{T}_h} [\mathbf{A}_h^K(\mathbf{r},\boldsymbol{\zeta}),(\mathbf{s},\boldsymbol{\tau})] \qquad \forall\,(\mathbf{r},\boldsymbol{\zeta}),(\mathbf{s},\boldsymbol{\tau}) \in X_k^h \times H_k^h. \tag{1.33}$$

Therefore, the mixed virtual element scheme associated with the augmented formulation (1.12) reads: Find $(\mathbf{t}_h,\boldsymbol{\sigma}_h) \in X_k^h \times H_k^h$ such that

$$[\mathbf{A}_h(\mathbf{t}_h,\boldsymbol{\sigma}_h),(\mathbf{s}_h,\boldsymbol{\tau}_h)] \;=\; [\mathbf{F},(\mathbf{s}_h,\boldsymbol{\tau}_h)] \qquad \forall\,(\mathbf{s}_h,\boldsymbol{\tau}_h) \in X_k^h \times H_k^h\,. \tag{1.34}$$

### 1.3.4 Analysis of the discrete scheme

In this section we develop the solvability analysis of our mixed virtual element scheme (1.34). First, recalling that the local orthogonal projectors $\mathcal{P}_k^K : \mathbf{L}^2(K) \to \mathbf{P}_k(K)$ and $\boldsymbol{\mathcal{P}}_k^K : \mathbb{L}^2(K) \to \mathbb{P}_k(K)$ were

introduced in Section 1.3.2, we now denote by $\mathcal{P}_k^h$ and $\boldsymbol{\mathcal{P}}_k^h$, respectively, its global counterparts, that is, given $\mathbf{v} \in \mathbf{L}^2(\Omega)$ and $\boldsymbol{\zeta} \in \mathbb{L}^2(\Omega)$, we let

$$\mathcal{P}_k^h(\mathbf{v})\big|_K := \mathcal{P}_k^K(\mathbf{v}\big|_K) \quad \text{and} \quad \boldsymbol{\mathcal{P}}_k^h(\boldsymbol{\zeta})\big|_K := \boldsymbol{\mathcal{P}}_k^K(\boldsymbol{\zeta}\big|_K) \quad \forall\, K \in \mathcal{T}_h.$$

Further, given the local bilinear form $\mathcal{S}^K : H_k^K \times H_k^K \to \mathrm{R}$, we now define the symmetric and positive definite global bilinear form $\mathcal{S}_h : H_k^h \times H_k^h \to \mathrm{R}$ as

$$\mathcal{S}_h(\boldsymbol{\zeta}, \boldsymbol{\tau}) \;:=\; \sum_{K \in \mathcal{T}_h} \mathcal{S}^K(\boldsymbol{\zeta}|_K, \boldsymbol{\tau}|_K) \qquad \forall\, (\boldsymbol{\zeta}, \boldsymbol{\tau}) \in H_k^h,$$

which according to (1.32), satisfies

$$\widehat{c}_0 \|\boldsymbol{\zeta}\|_{0,\Omega}^2 \;\leq\; \mathcal{S}_h(\boldsymbol{\zeta}, \boldsymbol{\zeta}) \;\leq\; \widehat{c}_1 \|\boldsymbol{\zeta}\|_{0,\Omega}^2 \qquad \forall\, \boldsymbol{\zeta} \in H_k^h. \tag{1.35}$$

Now, the Lipschitz-continuity of the discrete nonlinear operator $\mathbf{A}_h$ on $X_k^h \times H_k^h$ (cf. (1.33)) is established in the following lemma.

**Lemma 1.5.** *There exists a constant $\gamma > 0$, independent of $h$, such that*

$$\|\mathbf{A}_h(\mathbf{t}, \boldsymbol{\sigma}) - \mathbf{A}_h(\mathbf{r}, \boldsymbol{\zeta})\|_{(X \times H)'} \;\leq\; \gamma \|(\mathbf{t}, \boldsymbol{\sigma}) - (\mathbf{r}, \boldsymbol{\zeta})\|_{X \times H} \qquad \forall\, (\mathbf{t}, \boldsymbol{\sigma}), (\mathbf{r}, \boldsymbol{\zeta}) \in X_k^h \times H_k^h\,. \tag{1.36}$$

*Proof.* Given $(\mathbf{t}, \boldsymbol{\sigma}), (\mathbf{r}, \boldsymbol{\zeta}), (\mathbf{s}, \boldsymbol{\tau}) \in X_k^h \times H_k^h$, we first observe that

$$\begin{aligned}
[\mathbf{A}_h(\mathbf{t}, \boldsymbol{\sigma}) - \mathbf{A}_h(\mathbf{r}, \boldsymbol{\zeta}), (\mathbf{s}, \boldsymbol{\tau})] \;&=\; [\mathbb{A}(\mathbf{t}) - \mathbb{A}(\mathbf{r}), \mathbf{s} - \kappa(\boldsymbol{\mathcal{P}}_k^h(\boldsymbol{\tau}))^{\mathrm{d}}] - \int_\Omega \mathbf{s} : (\boldsymbol{\mathcal{P}}_k^h(\boldsymbol{\sigma} - \boldsymbol{\zeta}))^{\mathrm{d}} \\
&+ \quad \int_\Omega (\mathbf{t} - \mathbf{r}) : (\boldsymbol{\mathcal{P}}_k^h(\boldsymbol{\tau}))^{\mathrm{d}} \;+\; \kappa \int_\Omega (\boldsymbol{\mathcal{P}}_k^h(\boldsymbol{\sigma} - \boldsymbol{\zeta}))^{\mathrm{d}} : (\boldsymbol{\mathcal{P}}_k^h(\boldsymbol{\tau}))^{\mathrm{d}} \\
&+ \quad \mathcal{S}_h((\boldsymbol{\sigma} - \boldsymbol{\zeta}) - \boldsymbol{\mathcal{P}}_k^h(\boldsymbol{\sigma} - \boldsymbol{\zeta}), \boldsymbol{\tau} - \boldsymbol{\mathcal{P}}_k^h(\boldsymbol{\tau})) \;+\; \frac{1}{\alpha} \int_\Omega \mathbf{div}(\boldsymbol{\sigma} - \boldsymbol{\zeta}) \cdot \mathbf{div}(\boldsymbol{\tau})\,.
\end{aligned}$$

Then, applying the Cauchy-Schwarz inequality, the Lipschitz-continuity of the operator $\mathbb{A}$ (cf. (1.16)), and the upper bound in (1.35), we find that

$$[\mathbf{A}_h(\mathbf{t}, \boldsymbol{\sigma}) - \mathbf{A}_h(\mathbf{r}, \boldsymbol{\zeta}), (\mathbf{s}, \boldsymbol{\tau})] \;\leq\; \gamma \|(\mathbf{t}, \boldsymbol{\sigma}) - (\mathbf{r}, \boldsymbol{\zeta})\|_{X \times H} \|(\mathbf{s}, \boldsymbol{\tau})\|_{X \times H},$$

with $\gamma$ depending only on $\gamma_0$ (cf. (1.2), (1.16)), $\kappa$, $\frac{1}{\alpha}$, and $\widehat{c}_1$. In this way, the foregoing equation leads to (1.36), which ends the proof of the lemma. □

The following result provides the discrete analogue of Lemma 1.2.

**Lemma 1.6.** *Let $\mathbf{A}_h$ be the nonlinear operator defined in (1.33). Assume that the parameter $\kappa$ satisfy the conditions required by* lemma 1.2. *Then, there exists a positive constant $\widetilde{C}_{SM}$, independent of $h$, such that for all $(\mathbf{r}_h, \boldsymbol{\zeta}_h), (\mathbf{s}_h, \boldsymbol{\tau}_h) \in X_k^h \times H_k^h$ there holds*

$$[\mathbf{A}_h(\mathbf{r}_h, \boldsymbol{\zeta}_h) - \mathbf{A}_h(\mathbf{s}_h, \boldsymbol{\tau}_h), (\mathbf{r}_h, \boldsymbol{\zeta}_h) - (\mathbf{s}_h, \boldsymbol{\tau}_h)] \geq \widetilde{C}_{SM} \|(\mathbf{r}_h, \boldsymbol{\zeta}_h) - (\mathbf{s}_h, \boldsymbol{\tau}_h)\|_{X \times H}^2.$$

*Proof.* Given $(\mathbf{r}_h,\boldsymbol{\zeta}_h),(\mathbf{s}_h,\boldsymbol{\tau}_h)\in X_k^h\times H_k^h$, we have from (1.31) and (1.33) that

$$\begin{aligned}[\mathbf{A}_h(\mathbf{r}_h,\boldsymbol{\zeta}_h)-\mathbf{A}_h(\mathbf{s}_h,\boldsymbol{\tau}_h),(\mathbf{r}_h,\boldsymbol{\zeta}_h)-(\mathbf{s}_h,\boldsymbol{\tau}_h)] &= [\mathbb{A}(\mathbf{r}_h)-\mathbb{A}(\mathbf{s}_h),\mathbf{r}_h-\mathbf{s}_h]\\ &+\kappa\,\|(\boldsymbol{\mathcal{P}}_k^h(\boldsymbol{\zeta}_h-\boldsymbol{\tau}_h))^{\mathrm{d}}\|_{0,\Omega}^2-\kappa[\mathbb{A}(\mathbf{r}_h)-\mathbb{A}(\mathbf{s}_h),(\boldsymbol{\mathcal{P}}_k^h(\boldsymbol{\zeta}_h-\boldsymbol{\tau}_h))^{\mathrm{d}}]\\ &+\frac{1}{\alpha}\|\mathbf{div}(\boldsymbol{\zeta}_h-\boldsymbol{\tau}_h)\|_{0,\Omega}^2+\mathcal{S}_h((\boldsymbol{\zeta}_h-\boldsymbol{\tau}_h)-\boldsymbol{\mathcal{P}}_k^h(\boldsymbol{\zeta}_h-\boldsymbol{\tau}_h),(\boldsymbol{\zeta}_h-\boldsymbol{\tau}_h)-\boldsymbol{\mathcal{P}}_k^h(\boldsymbol{\zeta}_h-\boldsymbol{\tau}_h)).\end{aligned}$$

Then, using the Cauchy-Schwarz and Young inequalities, the Lipschitz-continuity and strong monotonicity properties of the operator $\mathbb{A}$ (cf. (1.16), (1.17)), and the lower bound in (1.35), we get

$$\begin{aligned}[\mathbf{A}_h(\mathbf{r}_h,\boldsymbol{\zeta}_h)-\mathbf{A}_h(\mathbf{s}_h,\boldsymbol{\tau}_h),(\mathbf{r}_h,\boldsymbol{\zeta}_h)-(\mathbf{s}_h,\boldsymbol{\tau}_h)] &\geq \left(\alpha_0-\frac{\kappa\gamma_0}{2\delta}\right)\|\mathbf{r}_h-\mathbf{s}_h\|_{0,\Omega}^2\\ &+\kappa\left(1-\frac{\gamma_0\delta}{2}\right)\|\boldsymbol{\mathcal{P}}_k^h((\boldsymbol{\zeta}_h-\boldsymbol{\tau}_h)^{\mathrm{d}})\|_{0,\Omega}^2+\frac{1}{\alpha}\|\mathbf{div}(\boldsymbol{\zeta}_h-\boldsymbol{\tau}_h)\|_{0,\Omega}^2\\ &+\widehat{c}_0\,\|(\boldsymbol{\zeta}_h-\boldsymbol{\tau}_h)^{\mathrm{d}}-(\boldsymbol{\mathcal{P}}_k^h(\boldsymbol{\zeta}_h-\boldsymbol{\tau}_h))^{\mathrm{d}}\|_{0,\Omega}^2 \qquad (1.37)\\ &\geq \left(\alpha_0-\frac{\kappa\gamma_0}{2\delta}\right)\|\mathbf{r}_h-\mathbf{s}_h\|_{0,\Omega}^2+\frac{1}{\alpha}\|\mathbf{div}(\boldsymbol{\zeta}_h-\boldsymbol{\tau}_h)\|_{0,\Omega}^2\\ &+\eta\left\{2\|(\boldsymbol{\mathcal{P}}_k^h(\boldsymbol{\zeta}_h-\boldsymbol{\tau}_h))^{\mathrm{d}}\|_{0,\Omega}^2+2\,\|(\boldsymbol{\zeta}_h-\boldsymbol{\tau}_h)^{\mathrm{d}}-(\boldsymbol{\mathcal{P}}_k^h(\boldsymbol{\zeta}_h-\boldsymbol{\tau}_h))^{\mathrm{d}}\|_{0,\Omega}^2\right\},\end{aligned}$$

where $\eta:=\frac{1}{2}\min\left\{\kappa\left(1-\frac{\gamma_0\delta}{2}\right),\widehat{c}_0\right\}$. Next, applying the parallelogram law in the last term of the foregoing inequality, we arrive at

$$2\,\|(\boldsymbol{\mathcal{P}}_k^h(\boldsymbol{\zeta}_h-\boldsymbol{\tau}_h))^{\mathrm{d}}\|_{0,\Omega}^2+2\,\|(\boldsymbol{\zeta}_h-\boldsymbol{\tau}_h)^{\mathrm{d}}-(\boldsymbol{\mathcal{P}}_k^h(\boldsymbol{\zeta}_h-\boldsymbol{\tau}_h))^{\mathrm{d}}\|_{0,\Omega}^2\geq\|(\boldsymbol{\zeta}_h-\boldsymbol{\tau}_h)^{\mathrm{d}}\|_{0,\Omega}^2,$$

which replaced back into (1.37), and using Lemma 1.1, finishes the proof with the constant

$$\widetilde{C}_{SM}:=\min\left\{\left(\alpha_0-\frac{\kappa\gamma_0}{2\delta}\right),\ c(\Omega)\min\left\{\eta,\frac{1}{2\alpha}\right\},\ \frac{1}{2\alpha}\right\}. \qquad (1.38)$$

□

Now, looking again the definition (1.31), one could infer that the bilinear form $\mathcal{S}^K$, which is stabilizing the term $\kappa\displaystyle\int_K(\boldsymbol{\mathcal{P}}_k^K(\boldsymbol{\zeta}))^{\mathrm{d}}:(\boldsymbol{\mathcal{P}}_k^K(\boldsymbol{\tau}))^{\mathrm{d}}$, needs to be multiplied by $\kappa$ as well. Nevertheless, as shown by (1.38), the constant that really matters is not the one resulting from these two terms only, but the final one providing the strong monotonicity of the nonlinear operator $\mathbf{A}_h$, namely $\widetilde{C}_{SM}$, which also depends on $\alpha$ and the unknown constant $c(\Omega)$ (cf. Lemma 1.1). Perhaps, an alternative procedure to be considered is the multiplication of $\mathcal{S}^K$ by an arbitrary parameter $\xi$ to be chosen so as to maximize either $\widetilde{C}_{SM}$ or some of the three expressions defining it.

The unique solvability and stability of the actual Galerkin scheme (1.34) is established now

**Theorem 1.7.** *Assume that given $\delta\in\left(0,\frac{2}{\gamma_0}\right)$, the parameter $\kappa$ lies in $\left(0,\frac{2\delta\alpha_0}{\gamma_0}\right)$. Then, there exists a unique $(\mathbf{t}_h,\boldsymbol{\sigma}_h)\in X_k^h\times H_k^h$ solution of (1.34), and there exists a positive constant $C$, independent of $h$, such that*

$$\|(\mathbf{t}_h,\boldsymbol{\sigma}_h)\|_{X\times H}\leq C\left\{\|\mathbf{f}\|_{0,\Omega}+\|\mathbf{g}\|_{1/2,\Gamma}\right\}.$$

*Proof.* Thanks to Lemmas 1.5 and 1.6, the proof is a direct application of [97, Theorem 25.B]. □

## 1.4 The a priori error estimates

We now aim to derive the priori error estimates for the continuous and discrete formulations (1.12) and (1.34). For this, given the local interpolation $\boldsymbol{\Pi}_k^K$ introduced in the Section 1.3.2, we denote by $\boldsymbol{\Pi}_k^h$ its global counterpart, that is, for all $\boldsymbol{\zeta} \in \mathbb{H}(\mathbf{div};\Omega)$ such that $\boldsymbol{\zeta}\big|_K \in \mathbb{H}^1(K)$ for all $K \in \mathcal{T}_h$, we let

$$\boldsymbol{\Pi}_k^h(\boldsymbol{\zeta})\big|_K \;:=\; \boldsymbol{\Pi}_k^K(\boldsymbol{\zeta}\big|_K) \qquad \forall\, K \in \mathcal{T}_h\,.$$

We begin our analysis with the following lemma.

**Lemma 1.8.** *There exists a constant $c_1 > 0$, depending only on $\kappa$ and $\widehat{c}_1$ (cf. (1.32)), such that*

$$\begin{aligned}&[\mathbf{A}_h(\mathbf{r}_h,\boldsymbol{\zeta}_h) - \mathbf{A}(\mathbf{r}_h,\boldsymbol{\zeta}_h),(\mathbf{s}_h,\boldsymbol{\tau}_h)]\\ &\leq\; c_1\left\{\|\boldsymbol{\zeta}_h - \boldsymbol{\mathcal{P}}_k^h(\boldsymbol{\zeta}_h)\|_{0,\Omega} \,+\, \|\mu(|\mathbf{r}_h|)\,\mathbf{r}_h - \boldsymbol{\mathcal{P}}_k^h\big(\mu(|\mathbf{r}_h|)\,\mathbf{r}_h\big)\|_{0,\Omega}\right\}\|(\mathbf{s}_h,\boldsymbol{\tau}_h)\|_{X\times H}\end{aligned}$$

*for all $(\mathbf{r}_h,\boldsymbol{\zeta}_h),(\mathbf{s}_h,\boldsymbol{\tau}_h) \in X_k^h \times H_k^h$.*

*Proof.* We first observe, according to the definitions of $\mathbf{A}_h$ (cf. (1.31), (1.33)) and $\mathbf{A}$ (cf. (1.13)), that

$$\begin{aligned}[\mathbf{A}_h(\mathbf{r}_h,\boldsymbol{\zeta}_h) - \mathbf{A}(\mathbf{r}_h,\boldsymbol{\zeta}_h),(\mathbf{s}_h,\boldsymbol{\tau}_h)] \;&=\; \int_\Omega \left\{\boldsymbol{\zeta}_h^{\mathrm{d}} - (\boldsymbol{\mathcal{P}}_k^h(\boldsymbol{\zeta}_h))^{\mathrm{d}}\right\} : \mathbf{s}_h + \int_\Omega \left\{(\boldsymbol{\mathcal{P}}_k^h(\boldsymbol{\tau}_h))^{\mathrm{d}} - \boldsymbol{\tau}_h^{\mathrm{d}}\right\} : \mathbf{r}_h\\ &+\, \kappa \int_\Omega \left\{\boldsymbol{\tau}_h^{\mathrm{d}} - (\boldsymbol{\mathcal{P}}_k^h(\boldsymbol{\tau}_h))^{\mathrm{d}}\right\} : \mu(|\mathbf{r}_h|)\,\mathbf{r}_h \,+\, \kappa \int_\Omega (\boldsymbol{\mathcal{P}}_k^h(\boldsymbol{\zeta}_h))^{\mathrm{d}} : (\boldsymbol{\mathcal{P}}_k^h(\boldsymbol{\tau}_h))^{\mathrm{d}} \,-\, \kappa \int_\Omega \boldsymbol{\zeta}_h^{\mathrm{d}} : \boldsymbol{\tau}_h^{\mathrm{d}}\\ &+\, \mathcal{S}_h(\boldsymbol{\zeta}_h - \boldsymbol{\mathcal{P}}_k^h(\boldsymbol{\zeta}_h), \boldsymbol{\tau}_h - \boldsymbol{\mathcal{P}}_k^h(\boldsymbol{\tau}_h))\,,\end{aligned}$$

for all $(\mathbf{r}_h,\boldsymbol{\zeta}_h),(\mathbf{s}_h,\boldsymbol{\tau}_h) \in X_k^h \times H_k^h$. Then, using that $\mathbf{s}_h\big|_K$ and $\mathbf{r}_h\big|_K$ belong to $\mathbb{P}_k(K)$ for each $K \in \mathcal{T}_h$, we deduce that the first two terms on the right hand side of the foregoing equation vanish. In turn, since it is clear that

$$\int_\Omega \left\{\boldsymbol{\tau}_h^{\mathrm{d}} - (\boldsymbol{\mathcal{P}}_k^h(\boldsymbol{\tau}_h))^{\mathrm{d}}\right\} : \boldsymbol{\mathcal{P}}_k^h\big(\mu(|\mathbf{r}_h|)\,\mathbf{r}_h\big) \;=\; 0\,,$$

the third term can be rewritten as

$$\kappa \int_\Omega \left\{\boldsymbol{\tau}_h^{\mathrm{d}} - (\boldsymbol{\mathcal{P}}_k^h(\boldsymbol{\tau}_h))^{\mathrm{d}}\right\} : \left\{\mu(|\mathbf{r}_h|)\,\mathbf{r}_h - \boldsymbol{\mathcal{P}}_k^h\big(\mu(|\mathbf{r}_h|)\,\mathbf{r}_h\big)\right\},$$

whereas the fourth one reduces to $\kappa \displaystyle\int_\Omega (\boldsymbol{\mathcal{P}}_k^h(\boldsymbol{\zeta}_h))^{\mathrm{d}} : \boldsymbol{\tau}_h^{\mathrm{d}}$, and hence $\mathbf{A}_h$ becomes

$$\begin{aligned}[\mathbf{A}_h(\mathbf{r}_h,\boldsymbol{\zeta}_h) - \mathbf{A}(\mathbf{r}_h,\boldsymbol{\zeta}_h),(\mathbf{s}_h,\boldsymbol{\tau}_h)] \;&=\; \kappa \int_\Omega (\boldsymbol{\mathcal{P}}_k^h(\boldsymbol{\zeta}_h) \,-\, \boldsymbol{\zeta}_h)^{\mathrm{d}} : \boldsymbol{\tau}_h^{\mathrm{d}} \,+\, \mathcal{S}_h(\boldsymbol{\zeta}_h - \boldsymbol{\mathcal{P}}_k^h(\boldsymbol{\zeta}_h), \boldsymbol{\tau}_h - \boldsymbol{\mathcal{P}}_k^h(\boldsymbol{\tau}_h))\\ &+\, \kappa \int_\Omega \left\{\boldsymbol{\tau}_h^{\mathrm{d}} - (\boldsymbol{\mathcal{P}}_k^h(\boldsymbol{\tau}_h))^{\mathrm{d}}\right\} : \left\{\mu(|\mathbf{r}_h|)\,\mathbf{r}_h - \boldsymbol{\mathcal{P}}_k^h\big(\mu(|\mathbf{r}_h|)\,\mathbf{r}_h\big)\right\}.\end{aligned}$$

In this way, using the Cauchy-Schwarz inequality, the symmetry of $\mathcal{S}_h$, and the upper bound in (1.35),

we find that

$$\begin{aligned}
&[\mathbf{A}_h(\mathbf{r}_h,\boldsymbol{\zeta}_h)-\mathbf{A}(\mathbf{r}_h,\boldsymbol{\zeta}_h),(\mathbf{s}_h,\boldsymbol{\tau}_h)]\\
&\quad\leq\ \kappa\left\{\|\boldsymbol{\zeta}_h-\boldsymbol{\mathcal{P}}_k^h(\boldsymbol{\zeta}_h)\|_{0,\Omega}\ +\ \|\mu(|\mathbf{r}_h|)\,\mathbf{r}_h-\boldsymbol{\mathcal{P}}_k^h\big(\mu(|\mathbf{r}_h|)\,\mathbf{r}_h\big)\|_{0,\Omega}\right\}\|\boldsymbol{\tau}_h\|_{0,\Omega}\\
&\qquad+\ \left\{\mathcal{S}_h(\boldsymbol{\zeta}_h-\boldsymbol{\mathcal{P}}_k^h(\boldsymbol{\zeta}_h),\boldsymbol{\zeta}_h-\boldsymbol{\mathcal{P}}_k^h(\boldsymbol{\zeta}_h))\right\}^{1/2}\left\{\mathcal{S}_h(\boldsymbol{\tau}_h-\boldsymbol{\mathcal{P}}_k^h(\boldsymbol{\tau}_h),\boldsymbol{\tau}_h-\boldsymbol{\mathcal{P}}_k^h(\boldsymbol{\tau}_h))\right\}^{1/2}\\
&\quad\leq\ c_1\left\{\|\boldsymbol{\zeta}_h-\boldsymbol{\mathcal{P}}_k^h(\boldsymbol{\zeta}_h)\|_{0,\Omega}\ +\ \|\mu(|\mathbf{r}_h|)\,\mathbf{r}_h-\boldsymbol{\mathcal{P}}_k^h\big(\mu(|\mathbf{r}_h|)\,\mathbf{r}_h\big)\|_{0,\Omega}\right\}\|(\mathbf{s}_h,\boldsymbol{\tau}_h)\|_{X\times H}\,,
\end{aligned}$$

with $c_1 := 2\,\max\{\kappa,\widehat{c}_1\}$, which completes the proof. □

Then, we have the following main result.

**Theorem 1.9.** *Let $(\mathbf{t},\boldsymbol{\sigma})\in X\times H$ and $(\mathbf{t}_h,\boldsymbol{\sigma}_h)\in X_k^h\times H_k^h$ be the unique solutions of the continuous and discrete schemes (1.12) and (1.34), respectively, and assume that $\boldsymbol{\sigma}\big|_K\in\mathbb{H}^1(K)$ for all $K\in\mathcal{T}_h$. Then, there exists a positive constant $C>0$, independent of $h$, such that*

$$\|\mathbf{t}-\mathbf{t}_h\|_{0,\Omega}+\|\boldsymbol{\sigma}-\boldsymbol{\sigma}_h\|_{\mathbf{div};\Omega}\leq C\left\{\|\mathbf{t}-\boldsymbol{\mathcal{P}}_k^h(\mathbf{t})\|_{0,\Omega}+\|\boldsymbol{\sigma}-\boldsymbol{\Pi}_k^h(\boldsymbol{\sigma})\|_{\mathbf{div};\Omega}+\|\boldsymbol{\sigma}-\boldsymbol{\mathcal{P}}_k^h(\boldsymbol{\sigma})\|_{0,\Omega}\right\}. \quad (1.39)$$

*Proof.* We begin by observing, due to the triangle inequality, that

$$\|\mathbf{t}-\mathbf{t}_h\|_{0,\Omega}+\|\boldsymbol{\sigma}-\boldsymbol{\sigma}_h\|_{\mathbf{div};\Omega}\ \leq\ \|\mathbf{t}-\boldsymbol{\mathcal{P}}_k^h(\mathbf{t})\|_{0,\Omega}+\|\boldsymbol{\sigma}-\boldsymbol{\Pi}_k^h(\boldsymbol{\sigma})\|_{\mathbf{div};\Omega}+\|\delta_h^{\mathbf{t}}\|_{0,\Omega}+\|\delta_h^{\boldsymbol{\sigma}}\|_{\mathbf{div};\Omega}, \quad (1.40)$$

where $(\delta_h^{\mathbf{t}},\delta_h^{\boldsymbol{\sigma}}):=(\boldsymbol{\mathcal{P}}_k^h(\mathbf{t})-\mathbf{t}_h,\boldsymbol{\Pi}_k^h(\boldsymbol{\sigma})-\boldsymbol{\sigma}_h)\in X_k^h\times H_k^h$. Then, applying the strong monotonicity of $\mathbf{A}_h$ (cf. Lemma 1.6) with $(\mathbf{r}_h,\boldsymbol{\zeta}_h):=(\boldsymbol{\mathcal{P}}_k^h(\mathbf{t}),\boldsymbol{\Pi}_k^h(\boldsymbol{\sigma}))$ and $(\mathbf{s}_h,\boldsymbol{\tau}_h):=(\mathbf{t}_h,\boldsymbol{\sigma}_h)$, and the equations (1.34) and (1.12), we obtain that

$$\begin{aligned}
\widetilde{C}_{SM}\|(\delta_h^{\mathbf{t}},\delta_h^{\boldsymbol{\sigma}})\|_{X\times H}^2\ &\leq\ [\mathbf{A}_h(\boldsymbol{\mathcal{P}}_k^h(\mathbf{t}),\boldsymbol{\Pi}_k^h(\boldsymbol{\sigma}))-\mathbf{A}_h(\mathbf{t}_h,\boldsymbol{\sigma}_h),(\delta_h^{\mathbf{t}},\delta_h^{\boldsymbol{\sigma}})]\\
&=\ [\mathbf{A}_h(\boldsymbol{\mathcal{P}}_k^h(\mathbf{t}),\boldsymbol{\Pi}_k^h(\boldsymbol{\sigma})),(\delta_h^{\mathbf{t}},\delta_h^{\boldsymbol{\sigma}})]-[\mathbf{A}_h(\mathbf{t}_h,\boldsymbol{\sigma}_h),(\delta_h^{\mathbf{t}},\delta_h^{\boldsymbol{\sigma}})]\\
&=\ [\mathbf{A}_h(\boldsymbol{\mathcal{P}}_k^h(\mathbf{t}),\boldsymbol{\Pi}_k^h(\boldsymbol{\sigma})),(\delta_h^{\mathbf{t}},\delta_h^{\boldsymbol{\sigma}})]-[\mathbf{A}(\mathbf{t},\boldsymbol{\sigma}),(\delta_h^{\mathbf{t}},\delta_h^{\boldsymbol{\sigma}})]\,,
\end{aligned}$$

from which, adding and subtracting $[\mathbf{A}(\boldsymbol{\mathcal{P}}_k^h(\mathbf{t}),\boldsymbol{\Pi}_k^h(\boldsymbol{\sigma})),(\delta_h^{\mathbf{t}},\delta_h^{\boldsymbol{\sigma}})]$, we obtain

$$\begin{aligned}
\widetilde{C}_{SM}\|(\delta_h^{\mathbf{t}},\delta_h^{\boldsymbol{\sigma}})\|_{X\times H}^2\ &\leq\ [\mathbf{A}_h(\boldsymbol{\mathcal{P}}_k^h(\mathbf{t}),\boldsymbol{\Pi}_k^h(\boldsymbol{\sigma}))-\mathbf{A}(\boldsymbol{\mathcal{P}}_k^h(\mathbf{t}),\boldsymbol{\Pi}_k^h(\boldsymbol{\sigma})),(\delta_h^{\mathbf{t}},\delta_h^{\boldsymbol{\sigma}})]\\
&\qquad+\ [\mathbf{A}(\boldsymbol{\mathcal{P}}_k^h(\mathbf{t}),\boldsymbol{\Pi}_k^h(\boldsymbol{\sigma}))-\mathbf{A}(\mathbf{t},\boldsymbol{\sigma}),(\delta_h^{\mathbf{t}},\delta_h^{\boldsymbol{\sigma}})]\,.
\end{aligned} \quad (1.41)$$

The two expressions on the right-hand side of (1.41) are bounded in what follows. Indeed, we first apply Lemma 1.8 to obtain

$$\begin{aligned}
&[\mathbf{A}_h(\boldsymbol{\mathcal{P}}_k^h(\mathbf{t}),\boldsymbol{\Pi}_k^h(\boldsymbol{\sigma}))-\mathbf{A}(\boldsymbol{\mathcal{P}}_k^h(\mathbf{t}),\boldsymbol{\Pi}_k^h(\boldsymbol{\sigma})),(\delta_h^{\mathbf{t}},\delta_h^{\boldsymbol{\sigma}})]\ \leq\ c_1\left\{\|\boldsymbol{\Pi}_k^h(\boldsymbol{\sigma})-\boldsymbol{\mathcal{P}}_k^h\big(\boldsymbol{\Pi}_k^h(\boldsymbol{\sigma})\big)\|_{0,\Omega}\right.\\
&\qquad+\ \left.\|\mu(|\boldsymbol{\mathcal{P}}_k^h(\mathbf{t})|)\,\boldsymbol{\mathcal{P}}_k^h(\mathbf{t})-\boldsymbol{\mathcal{P}}_k^h\big(\mu(|\boldsymbol{\mathcal{P}}_k^h(\mathbf{t})|)\,\boldsymbol{\mathcal{P}}_k^h(\mathbf{t})\big)\|_{0,\Omega}\right\}\|(\delta_h^{\mathbf{t}},\delta_h^{\boldsymbol{\sigma}})\|_{X\times H}\,.
\end{aligned} \quad (1.42)$$

Then, adding and subtracting $\boldsymbol{\sigma} - \boldsymbol{\mathcal{P}}_k^h(\boldsymbol{\sigma})$, we find that

$$\begin{aligned}
&\|\boldsymbol{\Pi}_k^h(\boldsymbol{\sigma}) - \boldsymbol{\mathcal{P}}_k^h\big(\boldsymbol{\Pi}_k^h(\boldsymbol{\sigma})\big)\|_{0,\Omega} \\
&\quad \leq \Big\{ \|\boldsymbol{\sigma} - \boldsymbol{\Pi}_k^h(\boldsymbol{\sigma})\|_{0,\Omega} + \|\boldsymbol{\sigma} - \boldsymbol{\mathcal{P}}_k^h(\boldsymbol{\sigma})\|_{0,\Omega} + \|\boldsymbol{\mathcal{P}}_k^h\big(\boldsymbol{\sigma} - \boldsymbol{\Pi}_k^h(\boldsymbol{\sigma})\big)\|_{0,\Omega} \Big\} \\
&\quad \leq 2 \Big\{ \|\boldsymbol{\sigma} - \boldsymbol{\Pi}_k^h(\boldsymbol{\sigma})\|_{0,\Omega} + \|\boldsymbol{\sigma} - \boldsymbol{\mathcal{P}}_k^h(\boldsymbol{\sigma})\|_{0,\Omega} \Big\} .
\end{aligned} \tag{1.43}$$

In turn, adding and subtracting $\mu(|\mathbf{t}|)\,\mathbf{t} - \boldsymbol{\mathcal{P}}_k^h\big(\mu(|\mathbf{t}|)\,\mathbf{t}\big)$, we deduce that

$$\begin{aligned}
\|\mu(|\boldsymbol{\mathcal{P}}_k^h(\mathbf{t})|)\,\boldsymbol{\mathcal{P}}_k^h(\mathbf{t}) - \boldsymbol{\mathcal{P}}_k^h\big(\mu(|\boldsymbol{\mathcal{P}}_k^h(\mathbf{t})|)\,\boldsymbol{\mathcal{P}}_k^h(\mathbf{t})\big)\|_{0,\Omega} &\leq \|\mu(|\boldsymbol{\mathcal{P}}_k^h(\mathbf{t})|)\,\boldsymbol{\mathcal{P}}_k^h(\mathbf{t}) - \mu(|\mathbf{t}|)\,\mathbf{t}\|_{0,\Omega} \\
+ \quad \|\mu(|\mathbf{t}|)\,\mathbf{t} - \boldsymbol{\mathcal{P}}_k^h\big(\mu(|\mathbf{t}|)\,\mathbf{t}\big)\|_{0,\Omega} &+ \Big\| \boldsymbol{\mathcal{P}}_k^h\Big(\mu(|\mathbf{t}|)\,\mathbf{t} - \mu(|\boldsymbol{\mathcal{P}}_k^h(\mathbf{t})|)\,\boldsymbol{\mathcal{P}}_k^h(\mathbf{t})\Big)\Big\|_{0,\Omega} ,
\end{aligned} \tag{1.44}$$

from which, applying the boundedness of $\boldsymbol{\mathcal{P}}_k^h$, the Lipschitz-continuity estimate (1.16), and the fact that $\mu(|\mathbf{t}|)\,\mathbf{t} = \boldsymbol{\sigma}^{\mathtt{d}}$ (cf. (1.7)), we conclude the existence of a constant $c > 0$, depending on $\gamma_0$ (cf. (1.16)), such that

$$\|\mu(|\boldsymbol{\mathcal{P}}_k^h(\mathbf{t})|)\,\boldsymbol{\mathcal{P}}_k^h(\mathbf{t}) - \boldsymbol{\mathcal{P}}_k^h\big(\mu(|\boldsymbol{\mathcal{P}}_k^h(\mathbf{t})|)\,\boldsymbol{\mathcal{P}}_k^h(\mathbf{t})\big)\|_{0,\Omega} \leq c \Big\{ \|\mathbf{t} - \boldsymbol{\mathcal{P}}_k^h(\mathbf{t})\|_{0,\Omega} + \|\boldsymbol{\sigma} - \boldsymbol{\mathcal{P}}_k^h(\boldsymbol{\sigma})\|_{0,\Omega} \Big\} . \tag{1.45}$$

Finally, the Lipschitz-continuity of $\mathbf{A}$ (cf. (1.18)) yields

$$\begin{aligned}
&[\mathbf{A}(\boldsymbol{\mathcal{P}}_k^h(\mathbf{t}), \boldsymbol{\Pi}_k^h(\boldsymbol{\sigma})) - \mathbf{A}(\mathbf{t}, \boldsymbol{\sigma}), (\delta_h^{\mathbf{t}}, \delta_h^{\boldsymbol{\sigma}})] \\
&\quad \leq \sqrt{2}\, L_{\mathbf{A}} \Big\{ \|\mathbf{t} - \boldsymbol{\mathcal{P}}_k^h(\mathbf{t})\|_{0,\Omega} + \|\boldsymbol{\sigma} - \boldsymbol{\Pi}_k^h(\boldsymbol{\sigma})\|_{\mathbf{div};\Omega} \Big\} \, \|(\delta_h^{\mathbf{t}}, \delta_h^{\boldsymbol{\sigma}})\|_{X \times H} .
\end{aligned} \tag{1.46}$$

In this way, (1.41), (1.42), (1.43), (1.45) and (1.46) yield the existence of $C := C(\widetilde{C}_{SM}, c_1, \gamma_0, L_{\mathbf{A}}) > 0$, such that

$$\|\delta_h^{\mathbf{t}}\|_{0,\Omega} + \|\delta_h^{\boldsymbol{\sigma}}\|_{\mathbf{div};\Omega} \leq C \Big\{ \|\mathbf{t} - \boldsymbol{\mathcal{P}}_k^h(\mathbf{t})\|_{0,\Omega} + \|\boldsymbol{\sigma} - \boldsymbol{\Pi}_k^h(\boldsymbol{\sigma})\|_{\mathbf{div};\Omega} + \|\boldsymbol{\sigma} - \boldsymbol{\mathcal{P}}_k^h(\boldsymbol{\sigma})\|_{0,\Omega} \Big\} ,$$

which, together with (1.40), gives (1.39) and ends the proof of the theorem. □

Having established the a priori error estimates for our unknowns, we now provide the corresponding rate of convergence.

**Theorem 1.10.** *Let $(\mathbf{t}, \boldsymbol{\sigma}) \in X \times H$ and $(\mathbf{t}_h, \boldsymbol{\sigma}_h) \in X_k^h \times H_k^h$ be the unique solutions of the continuous and discrete schemes (1.12) and (1.34), respectively. Assume that for some $s \in [1, k+1]$ there hold $\mathbf{t}|_K$, $\boldsymbol{\sigma}|_K \in \mathbb{H}^s(K)$, and $\mathbf{div}(\boldsymbol{\sigma})|_K \in \mathbf{H}^s(K)$ for each $K \in \mathcal{T}_h$. Then, there exists $C > 0$, independent of $h$, such that*

$$\|\mathbf{t} - \mathbf{t}_h\|_{0,\Omega} + \|\boldsymbol{\sigma} - \boldsymbol{\sigma}_h\|_{\mathbf{div};\Omega} \leq C\, h^s \sum_{K \in \mathcal{T}_h} \Big\{ |\mathbf{t}|_{s,K} + |\boldsymbol{\sigma}|_{s,K} + |\mathbf{div}(\boldsymbol{\sigma})|_{s,K} \Big\} . \tag{1.47}$$

*Proof.* It follows from (1.39) and a straightforward application of the approximation properties provided by (1.24) and (1.29). □

### 1.4.1 Computable approximations of $\boldsymbol{\sigma}, p$ and $\mathbf{u}$

We now introduce the fully computable approximation of $\boldsymbol{\sigma}_h$ given by

$$\widehat{\boldsymbol{\sigma}}_h \ := \ \boldsymbol{\mathcal{P}}_k^h(\boldsymbol{\sigma}_h), \tag{1.48}$$

and establishes next the corresponding a priori error estimate in the $\mathbb{L}^2(\Omega)$-norm, which yields exactly the same rate of convergence given by Theorem 1.10.

**Lemma 1.11.** *There exists a positive constant $C$, independent of $h$, such that*

$$\|\boldsymbol{\sigma} - \widehat{\boldsymbol{\sigma}}_h\|_{0,\Omega} \leq C \left\{ \|\mathbf{t} - \boldsymbol{\mathcal{P}}_k^h(\mathbf{t})\|_{0,\Omega} + \|\boldsymbol{\sigma} - \boldsymbol{\Pi}_k^h(\boldsymbol{\sigma})\|_{\mathbf{div};\Omega} + \|\boldsymbol{\sigma} - \boldsymbol{\mathcal{P}}_k^h(\boldsymbol{\sigma})\|_{0,\Omega} \right\}. \tag{1.49}$$

*Proof.* The proof is similar to [31, Lemma 5.2]. □

Next, as suggested by (1.6) and (1.10), and proceeding as in [31, Section 5.2], we define

$$p_h \ := \ -\frac{1}{2}\mathrm{tr}(\widehat{\boldsymbol{\sigma}}_h) \quad \text{and} \quad \mathbf{u}_h \ := \ \frac{1}{\alpha}\left\{ \mathcal{P}_k^h(\mathbf{f}) + \mathbf{div}(\boldsymbol{\sigma}_h) \right\}, \tag{1.50}$$

which constitute fully computable approximations of the pressure and velocity, respectively. Then, we notice from (1.6) and the first equation of (1.50) that there holds

$$\|p - p_h\|_{0,\Omega} \ = \ \frac{1}{2}\|\mathrm{tr}(\boldsymbol{\sigma} - \widehat{\boldsymbol{\sigma}}_h)\|_{0,\Omega} \ \leq \ \frac{1}{\sqrt{2}}\|\boldsymbol{\sigma} - \widehat{\boldsymbol{\sigma}}_h\|_{0,\Omega},$$

which, together with (1.49), gives the a priori error estimate for the pressure, that is

$$\|p - p_h\|_{0,\Omega} \leq C \left\{ \|\mathbf{t} - \boldsymbol{\mathcal{P}}_k^h(\mathbf{t})\|_{0,\Omega} + \|\boldsymbol{\sigma} - \boldsymbol{\Pi}_k^h(\boldsymbol{\sigma})\|_{\mathbf{div};\Omega} + \|\boldsymbol{\sigma} - \boldsymbol{\mathcal{P}}_k^h(\boldsymbol{\sigma})\|_{0,\Omega} \right\}. \tag{1.51}$$

In turn, starting from (1.10) and the second equation of (1.50), and then using again from (1.10) that $\mathbf{f} = \alpha\mathbf{u} - \mathbf{div}(\boldsymbol{\sigma})$, we arrive at

$$\|\mathbf{u} - \mathbf{u}_h\|_{0,\Omega} \leq C \left\{ \|\mathbf{u} - \mathcal{P}_k^h(\mathbf{u})\|_{0,\Omega} + \|\mathbf{div}(\boldsymbol{\sigma}) - \mathcal{P}_k^h(\mathbf{div}(\boldsymbol{\sigma}))\|_{0,\Omega} + \|\mathbf{div}(\boldsymbol{\sigma} - \boldsymbol{\sigma}_h)\|_{0,\Omega} \right\},$$

from which, bounding $\|\mathbf{div}(\boldsymbol{\sigma} - \boldsymbol{\sigma}_h)\|_{0,\Omega}$ by $\|(\mathbf{t}, \boldsymbol{\sigma}) - (\mathbf{t}_h, \boldsymbol{\sigma}_h)\|_{X \times H}$, and employing the a priori error estimate (1.39) (cf. Theorem 1.9), we conclude that

$$\begin{aligned} \|\mathbf{u} - \mathbf{u}_h\|_{0,\Omega} \ \leq \ C \Big\{ & \|\mathbf{u} - \mathcal{P}_k^h(\mathbf{u})\|_{0,\Omega} \ + \ \|\mathbf{div}(\boldsymbol{\sigma}) - \mathcal{P}_k^h(\mathbf{div}(\boldsymbol{\sigma}))\|_{0,\Omega} \\ & + \ \|\mathbf{t} - \boldsymbol{\mathcal{P}}_k^h(\mathbf{t})\|_{0,\Omega} \ + \ \|\boldsymbol{\sigma} - \boldsymbol{\Pi}_k^h(\boldsymbol{\sigma})\|_{\mathbf{div};\Omega} \ + \ \|\boldsymbol{\sigma} - \boldsymbol{\mathcal{P}}_k^h(\boldsymbol{\sigma})\|_{0,\Omega} \Big\}. \end{aligned} \tag{1.52}$$

In this way, we are now able to provide the theoretical rates of convergence for $\widehat{\boldsymbol{\sigma}}_h$, $p_h$, and $\mathbf{u}_h$.

**Theorem 1.12.** *Let $(\mathbf{t}, \boldsymbol{\sigma}) \in X \times H$ and $(\mathbf{t}_h, \boldsymbol{\sigma}_h) \in X_k^h \times H_k^h$ be the unique solutions of the continuous and discrete schemes (1.12) and (1.34), respectively. In addition, let $\widehat{\boldsymbol{\sigma}}_h$ and $(p_h, \mathbf{u}_h)$ be the discrete approximations introduced in (1.48) and (1.50), respectively. Assume that for some $s \in [1, k+1]$ there hold $\mathbf{t}\big|_K$, $\boldsymbol{\sigma}\big|_K \in \mathbb{H}^s(K)$, $\mathbf{div}(\boldsymbol{\sigma})\big|_K \in \mathbf{H}^s(K)$, and $\mathbf{u}\big|_K \in \mathbf{H}^s(K)$ for each $K \in \mathcal{T}_h$. Then, there exist positive constants $C_1$ and $C_2$, independent of $h$, such that*

$$\|\boldsymbol{\sigma} - \widehat{\boldsymbol{\sigma}}_h\|_{0,\Omega} + \|p - p_h\|_{0,\Omega} \ \leq \ C_1\, h^s \sum_{K \in \mathcal{T}_h} \left\{ |\mathbf{t}|_{s,K} + |\boldsymbol{\sigma}|_{s,K} + |\mathbf{div}(\boldsymbol{\sigma})|_{s,K} \right\}, \tag{1.53}$$

*and*

$$\|\mathbf{u}-\mathbf{u}_h\|_{0,\Omega} \leq C_2\, h^s \sum_{K\in\mathcal{T}_h} \Big\{ |\mathbf{u}|_{s,K} + |\mathbf{t}|_{s,K} + |\boldsymbol{\sigma}|_{s,K} + |\mathbf{div}(\boldsymbol{\sigma})|_{s,K} \Big\}. \tag{1.54}$$

*Proof.* It follows from (1.49), (1.51), (1.52), and a straightforward application of the approximation properties provided by (1.23), (1.24) and (1.29). □

### 1.4.2 A convergent approximation of $\boldsymbol{\sigma}$ in the broken $\mathbb{H}(\mathbf{div})$-norm

In this section we proceed as in [31, Section 5.3] and construct a second approximation, denoted by $\boldsymbol{\sigma}_h^\star$, for the pseudostress variable $\boldsymbol{\sigma}$, which has an optimal rate of convergence in the broken $\mathbb{H}(\mathbf{div})$-norm. To this end, for each $K \in \mathcal{T}_h$ we let $(\cdot,\cdot)_{\mathbf{div};K}$ be the usual $\mathbb{H}(\mathbf{div};K)$-inner product with induced norm $\|\cdot\|_{\mathbf{div};K}$, and let $\boldsymbol{\sigma}_h^\star\big|_K := \boldsymbol{\sigma}_{h,K}^\star \in \mathbb{P}_{k+1}(K)$ be the unique solution of the local problem

$$(\boldsymbol{\sigma}_{h,K}^\star, \boldsymbol{\tau}_h)_{\mathbf{div};K} = \int_K \widehat{\boldsymbol{\sigma}}_h : \boldsymbol{\tau}_h \;+\; \int_K \mathbf{div}(\boldsymbol{\sigma}_h)\cdot\mathbf{div}(\boldsymbol{\tau}_h) \qquad \forall\, \boldsymbol{\tau}_h \in \mathbb{P}_{k+1}(K). \tag{1.55}$$

We stress that $\boldsymbol{\sigma}_{h,K}^\star$ can be explicitly computed for each $K \in \mathcal{T}_h$, independently. Then, the rate of convergence for the broken $\mathbb{H}(\mathbf{div};\Omega)$-norm of $\boldsymbol{\sigma}-\boldsymbol{\sigma}_h^\star$ is established as follows.

**Theorem 1.13.** *Assume that the hypotheses of Theorem 1.10 are satisfied. Then, there exists a positive constant $C$, independent of $h$, such that*

$$\left\{ \sum_{K\in\mathcal{T}_h} \|\boldsymbol{\sigma}-\boldsymbol{\sigma}_{h,K}^\star\|^2_{\mathbf{div};K} \right\}^{1/2} \leq C\, h^s \sum_{K\in\mathcal{T}_h} \Big\{ |\mathbf{t}|_{s,K} + |\boldsymbol{\sigma}|_{s,K} + |\mathbf{div}(\boldsymbol{\sigma})|_{s,K} \Big\}. \tag{1.56}$$

*Proof.* From [31, Lemma 5.3] and the first part in the proof of [31, Theorem 5.5], we find that there exists $C>0$, independent of $h$, such that for each $K \in \mathcal{T}_h$ there holds

$$\|\boldsymbol{\sigma}-\boldsymbol{\sigma}_{h,K}^\star\|_{\mathbf{div};K} \leq C \Big\{ \|\boldsymbol{\sigma}-\widehat{\boldsymbol{\sigma}}_h\|_{0,K} \;+\; \|\mathbf{div}(\boldsymbol{\sigma}-\boldsymbol{\sigma}_h)\|_{0,K}$$
$$+ \|\boldsymbol{\sigma}-\boldsymbol{\mathcal{P}}_{k+1}^K(\boldsymbol{\sigma})\|_{0,K} \;+\; |\boldsymbol{\sigma}-\boldsymbol{\mathcal{P}}_{k+1}^K(\boldsymbol{\sigma})|_{1,K} \Big\},$$

which, after bounding $\|\mathbf{div}(\boldsymbol{\sigma}-\boldsymbol{\sigma}_h)\|_{0,K}$ by $\|\boldsymbol{\sigma}-\boldsymbol{\sigma}_h)\|_{\mathbf{div},K}$, becomes

$$\|\boldsymbol{\sigma}-\boldsymbol{\sigma}_{h,K}^\star\|_{\mathbf{div};K} \leq C \Big\{ \|\boldsymbol{\sigma}-\widehat{\boldsymbol{\sigma}}_h\|_{0,K} \;+\; \|\boldsymbol{\sigma}-\boldsymbol{\sigma}_h\|_{\mathbf{div},K}$$
$$+ \|\boldsymbol{\sigma}-\boldsymbol{\mathcal{P}}_{k+1}^K(\boldsymbol{\sigma})\|_{0,K} \;+\; |\boldsymbol{\sigma}-\boldsymbol{\mathcal{P}}_{k+1}^K(\boldsymbol{\sigma})|_{1,K} \Big\}.$$

Next, summing up the squares of the foregoing equation over all $K \in \mathcal{T}_h$, and employing the estimates (1.47) and (1.53), and the approximation properties of $\boldsymbol{\mathcal{P}}_{k+1}^K$ (cf. [30, Lemma 3.4]), we conclude (1.56), thus ending the proof. □

At this point we remark that, while the use of Raviart-Thomas of order $k \geq 0$ instead of $\mathbb{P}_{k+1}(K)$ in (1.55) could seem more natural, it is not clear whether the approximation properties of the corresponding orthogonal projector with respect to the $\mathbb{H}(\mathbf{div};K)$-inner product, which up to the authors' knowledge are unknown, would yield at least the same rates of convergence already guaranteed by Theorem 1.13. The advantage of employing $\mathbb{P}_{k+1}(K)$ is precisely that the respective approximation properties are well established in the literature.

## 1.5 Numerical results

In this section we present three numerical experiments illustrating the performance of the augmented mixed virtual element scheme (1.34) introduced and analized in Sections 3.3 and 3.4, respectively. More precisely, in all the computations we consider the specific virtual element subspaces $X_k^h$ and $H_k^h$ (cf. (1.19)-(1.20)) and associated discrete nonlinear operator $\mathbf{A}_h$ (cf. (1.33)) determined by the definitions of the local subspaces $X_k^K$ and $H_k^K$, and the $\mathbb{L}^2$-orthogonal projector $\boldsymbol{\mathcal{P}}_k^K$, respectively, with $k \in \{0,1,2\}$. Here we recall, as already remarked in [32, Section 4.1], that the projector introduced in [30, Section 4] is applicable only when the viscosity $\mu$ is constant. In fact, this approach was utilized in [31] for the linear Brinkman problem. Now, as in [31, Section 6], the zero mean condition for tensors in the space $H_k^h$ is imposed via a real Lagrange multiplier, which means that, instead of (1.34), we solve the following modified discrete scheme: Find $((\mathbf{t}_h,\boldsymbol{\sigma}_h),\lambda_h) \in (X_k^h \times H_k^h) \times \mathrm{R}$ such that

$$\begin{aligned} [\mathbf{A}_h(\mathbf{t}_h,\boldsymbol{\sigma}_h),(\mathbf{s}_h,\boldsymbol{\tau}_h)] + \lambda_h \int_\Omega \mathrm{tr}(\boldsymbol{\tau}_h) &= [\mathbf{F},(\mathbf{s}_h,\boldsymbol{\tau}_h)] \qquad \forall\, (\mathbf{s}_h,\boldsymbol{\tau}_h) \in X_k^h \times H_k^h, \\ \beta_h \int_\Omega \mathrm{tr}(\boldsymbol{\sigma}_h) &= 0 \qquad\qquad\qquad \forall\, \beta_h \in \mathrm{R}, \end{aligned} \tag{1.57}$$

where $\lambda_h$ is an artificial unknown introduced just to keep the symmetry of (1.34). Concerning the decompositions of $\Omega$ employed in our computations, we consider quasi-uniform triangles, distorted squares, and distorted hexagons, where the term "*distorted*" refers here to perturbations of quadrilateral and hexagonal meshes, respectively.

We begin by introducing additional notations. In what follows, $N$ stands for the total number of degrees of freedom (unknowns) of (1.57), that is

$$N := 2(k+1) \times \{\text{number of edges } e \in \mathcal{T}_h\} + \frac{(k+2)(7k+3)}{2} \times \{\text{number of elements } K \in \mathcal{T}_h\} + 1.$$

Also, the individual errors are defined by

$$\mathtt{e}(\mathbf{t}) := \|\mathbf{t}-\mathbf{t}_h\|_{0,\Omega}, \quad \mathtt{e}_0(\boldsymbol{\sigma}) := \|\boldsymbol{\sigma}-\widehat{\boldsymbol{\sigma}}_h\|_{0,\Omega}, \quad \mathtt{e}(\mathbf{u}) := \|\mathbf{u}-\mathbf{u}_h\|_{0,\Omega}, \quad \mathtt{e}(p) := \|p-\widehat{p}_h\|_{0,\Omega},$$

$$\mathtt{e}_{\mathrm{div}}(\boldsymbol{\sigma}) := \left\{ \sum_{K\in\mathcal{T}_h} \|\boldsymbol{\sigma}-\widehat{\boldsymbol{\sigma}}_h\|^2_{\mathbf{div};K} \right\}^{1/2} \quad \text{and} \quad \mathtt{e}(\boldsymbol{\sigma}^\star) := \left\{ \sum_{K\in\mathcal{T}_h} \|\boldsymbol{\sigma}-\boldsymbol{\sigma}_h^\star\|^2_{\mathbf{div};K} \right\}^{1/2},$$

where $\widehat{\boldsymbol{\sigma}}_h, \boldsymbol{\sigma}_h^\star$ and $(\widehat{p}_h,\mathbf{u}_h)$ are computed according to (1.48), (1.55), and (1.50), respectively, whereas the associated experimental rates of convergence are given by

$$\mathtt{r}(\cdot) := \frac{\log(\mathtt{e}(\cdot)/\mathtt{e}'(\cdot))}{\log(h/h')},$$

where $\mathtt{e}$ and $\mathtt{e}'$ denote the corresponding errors for two consecutive meshes with sizes $h$ and $h'$, respectively. In turn, the nonlinear algebraic systems arising from (1.57) are solved by the Newton method with a tolerance of $10^{-6}$ and taking as initial iteration the solution of the linear Brinkman problem with $\mu = 1$ (three iterations were required to achieve the given tolerance in each example). The numerical results presented below were obtained using a MATLAB code, in which all the resulting linear systems are solved by the usual instruction "\".

In Example 1 we take the unit square $\Omega := (0,1)^2$, set $\alpha = 1$, and consider the nonlinear viscosity $\mu$ given by the Carreau law (1.4) with $\rho_0 = 2$, $\rho_1 = 1$, and $\beta = 5/3$, that is

$$\mu(s) \ := \ 2 \ + \ (1+s^2)^{-1/6} \quad \forall \, s \geq 0 \, .$$

In addition, we choose the data $\mathbf{f}$ and $\mathbf{g}$ so that the exact solution is given by

$$\mathbf{u}(\mathbf{x}) \ := \ \begin{pmatrix} -\cos(\pi x_1)\sin(\pi x_2) \\ \\ \sin(\pi x_1)\cos(\pi x_2) \end{pmatrix} \quad \text{and} \quad p(\mathbf{x}) \ := \ x_1^2 - x_2^2$$

for all $\mathbf{x} := (x_1, x_2)^{\mathbf{t}} \in \Omega$.

In Example 2 we consider again $\Omega := (0,1)^2$, $\alpha = 1$, and the nonlinear viscosity given by (1.4), but now with $\rho_0 = \rho_1 = 1/2$, and $\beta = 3/2$, that is

$$\mu(s) \ := \ \frac{1}{2} + \frac{1}{2}(1+s^2)^{-1/4} \quad \forall \, s \geq 0 \, .$$

In this case, the data $\mathbf{f}$ and $\mathbf{g}$ are chosen so that the exact solution is given by

$$\mathbf{u}(\mathbf{x}) \ := \ \begin{pmatrix} x_1^2(x_2+1)\exp(-x_1)\left((x_2+1)\cos(x_2+1) + 2\sin(x_2+1)\right) \\ \\ x_1(x_1-2)(x_2+1)^2\exp(-x_1)\sin(x_2+1) \end{pmatrix},$$

and

$$p(\mathbf{x}) \ := \ \sin(2\pi x_1)\sin(2\pi x_2)$$

for all $\mathbf{x} := (x_1, x_2)^{\mathbf{t}} \in \Omega$.

In Example 3 we take the $L$-shaped domain $\Omega := (-1,1)^2 \setminus [0,1]^2$, set again $\alpha = 1$, and consider the same nonlinearity $\mu$ from Example 2. Then, we choose the data $\mathbf{f}$ and $\mathbf{g}$ so that the exact solution is given by

$$\mathbf{u}(\mathbf{x}) \ := \ \begin{pmatrix} (1 + x_1 - \exp(x_1))(1 - \cos(x_2)) \\ \\ (1 - \exp(x_1))(\sin(x_2) - x_2) \end{pmatrix} \quad \text{and} \quad p(\mathbf{x}) \ := \ (x_1^2 + x_2^2)^{1/3} - p_0$$

for all $\mathbf{x} := (x_1, x_2)^{\mathbf{t}} \in \Omega$, where $p_0 \in \mathrm{R}$ is such that $\int_\Omega p = 0$. Note in this example that the partial derivatives of $p$, and hence, in particular $\mathbf{div}(\boldsymbol{\sigma})$, are singular at the origin. More precisely, because of the power $1/3$, there holds $\boldsymbol{\sigma} \in \mathbb{H}^{5/3-\epsilon}(\Omega)$ and $\mathbf{div}(\boldsymbol{\sigma}) \in \mathbf{H}^{2/3-\epsilon}(\Omega)$ for each $\epsilon > 0$.

Finally, we remark that for all three examples the explicit constants $\gamma_0$ and $\alpha_0$ are defined according to (1.5), and that the stabilization parameter $\kappa$ is taken as suggested by the midpoints of the intervals specified in Lemma 1.2, that is $\delta = \dfrac{1}{\gamma_0}$ and $\kappa = \dfrac{\delta\,\alpha_0}{\gamma_0} = \dfrac{\alpha_0}{\gamma_0^2}$.

In Tables 1.1 up to 1.6 we summarize the convergence history of the augmented mixed virtual element scheme (1.57) as applied to Example 1 and 2. We notice there that the rate of convergence $O(h^{k+1})$ predicted by Theorems 1.12 and 1.13 (when $s = k+1$) is achieved by all the unknowns for these smooth examples, for triangular as well as for quadrilateral and hexagonal meshes. In particular, these results confirm that our postprocessed stress $\boldsymbol{\sigma}_h^\star$ improves in one power the non-satisfactory order provided by the first approximation $\widehat{\boldsymbol{\sigma}}_h$ with respect to the broken $\mathbb{H}(\mathbf{div})$-norm. Next, in Tables 1.7 up to 1.9 we

display the corresponding convergence history of Example 3. As predicted by the theory, and due to the limited regularity of $p$ and $\boldsymbol{\sigma}$ in this case, we observe that the orders $O(h^{\min\{k+1,5/3\}})$ and $O(h^{2/3})$ are attained by $(\boldsymbol{\sigma}_h, p_h)$ and $\boldsymbol{\sigma}_h^\star$, respectively. However, the rates of convergence in Tables 1.8 and 1.9 oscillate more than expected, which, besides the singularity of this example, might be caused by the strong irregular character of the meshes. In addition, we observe that $\mathbf{u}_h$ shows a convergence rate of $O(h^{\min\{k,5/3\}+1})$. This behaviour of the error $\|\mathbf{u}-\mathbf{u}_h\|_{0,\Omega}$ is explained by the fact that, as shown by (1.52), it depends on the regularity of $\mathbf{u}$, $\mathbf{t}$, $\boldsymbol{\sigma}$ and $\mathbf{div}(\boldsymbol{\sigma})$. A very common way to overcome this drawback is the use of adaptive algorithms based on suitable a posteriori error estimators. This issue will be addressed in a forthcoming work.

Finally, in order to graphically illustrate the accurateness of our discrete scheme, in Figures 1.1 and 1.2 we display some components of the approximate solutions for Example 1 and 3, respectively. They all correspond to those obtained with the first mesh of each kind (triangles, quadrilaterals and hexagons, respectively) and for the polynomial degree $k = 2$

| $k$ | $h$ | $N$ | $\mathtt{e}(\mathbf{t})$ | $\mathtt{r}(\mathbf{t})$ | $\mathtt{e}_0(\boldsymbol{\sigma})$ | $\mathtt{r}_0(\boldsymbol{\sigma})$ | $\mathtt{e}_{\mathrm{div}}(\boldsymbol{\sigma})$ | $\mathtt{r}_{\mathrm{div}}(\boldsymbol{\sigma})$ | $\mathtt{e}(\mathbf{u})$ | $\mathtt{r}(\mathbf{u})$ | $\mathtt{e}(p)$ | $\mathtt{r}(p)$ | $\mathtt{e}(\boldsymbol{\sigma}^\star)$ | $\mathtt{r}(\boldsymbol{\sigma}^\star)$ |
|---|---|---|---|---|---|---|---|---|---|---|---|---|---|---|
| | 0.0566 | 7601 | 1.43e-1 | −− | 3.91e-1 | −− | 3.79e+1 | −− | 3.10e-2 | −− | 6.49e-2 | −− | 1.62e-0 | −− |
| | 0.0404 | 14841 | 1.02e-1 | 1.00 | 2.80e-1 | 1.00 | 3.79e+1 | 0.00 | 2.17e-2 | 1.06 | 4.63e-2 | 1.01 | 1.15e-0 | 1.00 |
| 0 | 0.0218 | 50961 | 5.50e-2 | 1.00 | 1.51e-1 | 1.00 | 3.79e+1 | 0.00 | 1.15e-2 | 1.03 | 2.49e-2 | 1.00 | 6.22e-1 | 1.00 |
| | 0.0150 | 106409 | 3.80e-2 | 1.00 | 1.04e-1 | 1.00 | 3.79e+1 | 0.00 | 7.90e-3 | 1.01 | 1.72e-2 | 1.00 | 4.30e-1 | 1.00 |
| | 0.0118 | 173281 | 2.98e-2 | 1.00 | 8.16e-2 | 1.00 | 3.79e+1 | 0.00 | 6.18e-3 | 1.00 | 1.35e-2 | 1.00 | 3.37e-1 | 1.00 |
| | 0.0566 | 26451 | 3.25e-3 | −− | 8.80e-3 | −− | 1.58e-0 | −− | 7.35e-4 | −− | 7.85e-4 | −− | 4.49e-2 | −− |
| | 0.0404 | 51731 | 1.66e-3 | 2.00 | 4.49e-3 | 2.00 | 1.13e-0 | 1.00 | 3.72e-4 | 2.03 | 3.93e-4 | 2.06 | 2.30e-2 | 1.99 |
| 1 | 0.0218 | 177971 | 4.81e-4 | 2.00 | 1.30e-3 | 2.00 | 6.09e-1 | 1.00 | 1.07e-4 | 2.01 | 1.11e-4 | 2.04 | 6.68e-3 | 2.00 |
| | 0.0150 | 371865 | 2.30e-4 | 2.00 | 6.23e-4 | 2.00 | 4.21e-1 | 1.00 | 5.11e-5 | 2.00 | 5.29e-5 | 2.02 | 3.20e-3 | 2.00 |
| | 0.0118 | 605761 | 1.41e-4 | 2.00 | 3.82e-4 | 2.00 | 3.30e-1 | 1.00 | 3.13e-5 | 2.00 | 3.23e-5 | 2.02 | 1.96e-3 | 2.00 |
| | 0.0566 | 54051 | 5.95e-5 | −− | 1.93e-4 | −− | 4.83e-2 | −− | 1.31e-5 | −− | 3.24e-5 | −− | 2.97e-3 | −− |
| | 0.0404 | 105771 | 2.17e-5 | 3.00 | 7.06e-5 | 2.99 | 2.48e-2 | 1.99 | 4.72e-6 | 3.03 | 1.15e-5 | 3.08 | 1.11e-3 | 2.94 |
| 2 | 0.0218 | 364131 | 3.40e-6 | 3.00 | 1.10e-5 | 3.00 | 7.20e-3 | 2.00 | 7.31e-7 | 3.01 | 1.73e-6 | 3.06 | 1.76e-4 | 2.97 |
| | 0.0150 | 761025 | 1.12e-6 | 3.00 | 3.65e-6 | 3.00 | 3.44e-3 | 2.00 | 2.41e-7 | 3.00 | 5.64e-7 | 3.04 | 5.83e-5 | 2.99 |
| | 0.0118 | 1239841 | 5.40e-7 | 3.00 | 1.75e-6 | 3.00 | 2.11e-3 | 2.00 | 1.16e-7 | 3.00 | 2.69e-7 | 3.03 | 2.81e-5 | 2.99 |

Table 1.1: Example 1, history of convergence using triangles (table produced by the author).

| $k$ | $h$ | $N$ | $\mathtt{e}(\mathbf{t})$ | $\mathtt{r}(\mathbf{t})$ | $\mathtt{e}_0(\boldsymbol{\sigma})$ | $\mathtt{r}_0(\boldsymbol{\sigma})$ | $\mathtt{e}_{\mathrm{div}}(\boldsymbol{\sigma})$ | $\mathtt{r}_{\mathrm{div}}(\boldsymbol{\sigma})$ | $\mathtt{e}(\mathbf{u})$ | $\mathtt{r}(\mathbf{u})$ | $\mathtt{e}(p)$ | $\mathtt{r}(p)$ | $\mathtt{e}(\boldsymbol{\sigma}^\star)$ | $\mathtt{r}(\boldsymbol{\sigma}^\star)$ |
|---|---|---|---|---|---|---|---|---|---|---|---|---|---|---|
| | 0.0461 | 8716 | 1.18e-1 | −− | 3.16e-1 | −− | 3.79e+1 | −− | 2.73e-2 | −− | 2.84e-2 | −− | 1.42e-0 | −− |
| | 0.0359 | 14356 | 9.16e-2 | 1.00 | 2.46e-1 | 1.00 | 3.79e+1 | 0.00 | 2.09e-2 | 1.06 | 2.16e-2 | 1.08 | 1.10e-0 | 1.00 |
| 0 | 0.0183 | 54561 | 4.68e-2 | 1.00 | 1.26e-1 | 1.00 | 3.79e+1 | 0.00 | 1.05e-2 | 1.03 | 1.06e-2 | 1.06 | 5.64e-1 | 1.00 |
| | 0.0135 | 101281 | 3.43e-2 | 1.00 | 9.21e-2 | 1.00 | 3.79e+1 | 0.00 | 7.67e-3 | 1.01 | 7.80e-3 | 1.00 | 4.14e-1 | 1.00 |
| | 0.0101 | 179841 | 2.58e-2 | 1.00 | 6.90e-2 | 1.00 | 3.79e+1 | 0.00 | 5.74e-3 | 1.01 | 5.84e-3 | 1.01 | 3.10e-1 | 1.00 |
| | 0.0461 | 28456 | 2.72e-3 | −− | 7.56e-3 | −− | 1.40e-0 | −− | 5.81e-4 | −− | 1.41e-3 | −− | 3.56e-2 | −− |
| | 0.0359 | 46936 | 1.64e-3 | 2.02 | 4.53e-3 | 2.04 | 1.09e-0 | 1.00 | 3.50e-4 | 2.02 | 7.79e-4 | 2.35 | 2.15e-2 | 2.00 |
| 1 | 0.0183 | 178817 | 4.25e-4 | 2.01 | 1.16e-3 | 2.03 | 5.57e-1 | 1.00 | 9.12e-5 | 2.01 | 1.68e-4 | 2.29 | 5.64e-3 | 1.99 |
| | 0.0135 | 332161 | 2.28e-4 | 2.01 | 6.22e-4 | 2.02 | 4.09e-1 | 1.00 | 4.90e-5 | 2.00 | 8.38e-5 | 2.23 | 3.04e-3 | 2.00 |
| | 0.0101 | 590081 | 1.28e-4 | 2.01 | 3.48e-4 | 2.01 | 3.07e-1 | 1.00 | 2.75e-5 | 2.00 | 4.46e-5 | 2.19 | 1.71e-3 | 2.00 |
| | 0.0461 | 56771 | 4.28e-5 | −− | 1.39e-4 | −− | 3.57e-2 | −− | 8.52e-6 | −− | 3.33e-5 | −− | 1.89e-3 | −− |
| | 0.0359 | 93691 | 2.00e-5 | 3.03 | 6.46e-5 | 3.06 | 2.16e-2 | 2.00 | 4.00e-6 | 3.00 | 1.47e-5 | 3.24 | 9.09e-4 | 2.92 |
| 2 | 0.0183 | 357281 | 2.64e-6 | 3.02 | 8.56e-6 | 3.02 | 5.68e-3 | 1.99 | 5.35e-7 | 3.00 | 1.85e-6 | 3.09 | 1.24e-4 | 2.97 |
| | 0.0135 | 663841 | 1.04e-6 | 3.01 | 3.36e-6 | 3.01 | 3.06e-3 | 1.99 | 2.11e-7 | 3.00 | 7.07e-7 | 3.10 | 4.90e-5 | 3.00 |
| | 0.0101 | 1179521 | 4.36e-7 | 3.02 | 1.41e-6 | 3.02 | 1.72e-3 | 2.00 | 8.89e-8 | 3.00 | 2.92e-7 | 3.07 | 2.07e-5 | 3.00 |

Table 1.2: Example 1, history of convergence using quadrilaterals (table produced by the author).

| $k$ | $h$ | $N$ | $\mathtt{e}(\mathbf{t})$ | $\mathtt{r}(\mathbf{t})$ | $\mathtt{e}_0(\boldsymbol{\sigma})$ | $\mathtt{r}_0(\boldsymbol{\sigma})$ | $\mathtt{e}_{\mathrm{div}}(\boldsymbol{\sigma})$ | $\mathtt{r}_{\mathrm{div}}(\boldsymbol{\sigma})$ | $\mathtt{e}(\mathbf{u})$ | $\mathtt{r}(\mathbf{u})$ | $\mathtt{e}(p)$ | $\mathtt{r}(p)$ | $\mathtt{e}(\boldsymbol{\sigma}^\star)$ | $\mathtt{r}(\boldsymbol{\sigma}^\star)$ |
|---|---|---|---|---|---|---|---|---|---|---|---|---|---|---|
| | 0.0439 | 11262 | 1.24e-1 | −− | 3.53e-1 | −− | 3.79e+1 | −− | 2.63e-2 | −− | 8.67e-2 | −− | 1.42e-0 | −− |
| | 0.0342 | 18255 | 9.61e-2 | 1.04 | 2.70e-1 | 1.08 | 3.79e+1 | 0.00 | 2.05e-2 | 1.00 | 6.05e-2 | 1.44 | 1.11e-0 | 1.00 |
| 0 | 0.0251 | 33870 | 7.01e-2 | 1.02 | 1.95e-1 | 1.05 | 3.79e+1 | 0.00 | 1.50e-2 | 1.01 | 3.94e-2 | 1.39 | 8.12e-1 | 1.00 |
| | 0.0182 | 64243 | 5.04e-2 | 1.02 | 1.39e-1 | 1.04 | 3.79e+1 | 0.00 | 1.08e-2 | 1.00 | 2.55e-2 | 1.34 | 5.89e-1 | 1.00 |
| | 0.0132 | 121206 | 3.64e-2 | 1.01 | 9.99e-2 | 1.03 | 3.79e+1 | 0.00 | 7.86e-3 | 1.00 | 1.67e-2 | 1.31 | 4.27e-1 | 1.00 |
| | 0.0439 | 33782 | 2.28e-3 | −− | 6.27e-3 | −− | 1.39e-0 | −− | 5.01e-4 | −− | 9.82e-4 | −− | 3.07e-2 | −− |
| | 0.0342 | 54761 | 1.39e-3 | 1.99 | 3.80e-3 | 2.01 | 1.09e-0 | 0.99 | 3.04e-4 | 2.01 | 5.47e-4 | 2.35 | 1.85e-2 | 2.03 |
| 1 | 0.0251 | 101606 | 7.43e-4 | 2.02 | 2.04e-3 | 2.02 | 7.99e-1 | 1.00 | 1.63e-4 | 2.01 | 2.86e-4 | 2.08 | 1.01e-2 | 1.97 |
| | 0.0182 | 192871 | 3.91e-4 | 1.99 | 1.07e-3 | 1.99 | 5.80e-1 | 0.99 | 8.55e-5 | 2.00 | 1.50e-4 | 2.00 | 5.35e-3 | 1.96 |
| | 0.0132 | 363614 | 2.05e-4 | 2.00 | 5.61e-4 | 2.01 | 4.20e-1 | 1.00 | 4.49e-5 | 2.00 | 7.34e-5 | 2.22 | 2.81e-3 | 2.00 |
| | 0.0439 | 65059 | 3.60e-5 | −− | 1.23e-4 | −− | 3.20e-2 | −− | 6.53e-6 | −− | 3.65e-5 | −− | 1.59e-3 | −− |
| | 0.0342 | 105463 | 1.70e-5 | 3.01 | 5.74e-5 | 3.05 | 1.93e-2 | 2.02 | 3.11e-6 | 2.98 | 1.71e-5 | 3.05 | 7.85e-4 | 2.84 |
| 2 | 0.0251 | 195683 | 6.79e-6 | 2.96 | 2.30e-5 | 2.95 | 1.05e-2 | 1.96 | 1.22e-6 | 3.03 | 6.81e-6 | 2.97 | 3.06e-4 | 3.03 |
| | 0.0182 | 371577 | 2.59e-6 | 2.99 | 8.84e-6 | 2.96 | 5.58e-3 | 1.96 | 4.66e-7 | 2.98 | 2.60e-6 | 2.98 | 1.21e-4 | 2.87 |
| | 0.0132 | 700291 | 9.85e-7 | 3.01 | 3.36e-6 | 3.01 | 2.93e-3 | 2.00 | 1.77e-7 | 3.01 | 9.84e-7 | 3.02 | 4.58e-5 | 3.03 |

Table 1.3: Example 1, history of convergence using hexagons (table produced by the author).

| $k$ | $h$ | $N$ | $\mathtt{e}(\mathbf{t})$ | $\mathtt{r}(\mathbf{t})$ | $\mathtt{e}_0(\boldsymbol{\sigma})$ | $\mathtt{r}_0(\boldsymbol{\sigma})$ | $\mathtt{e}_{\mathrm{div}}(\boldsymbol{\sigma})$ | $\mathtt{r}_{\mathrm{div}}(\boldsymbol{\sigma})$ | $\mathtt{e}(\mathbf{u})$ | $\mathtt{r}(\mathbf{u})$ | $\mathtt{e}(p)$ | $\mathtt{r}(p)$ | $\mathtt{e}(\boldsymbol{\sigma}^\star)$ | $\mathtt{r}(\boldsymbol{\sigma}^\star)$ |
|---|---|---|---|---|---|---|---|---|---|---|---|---|---|---|
| | 0.0566 | 7601 | 1.26e-1 | −− | 1.13e-1 | −− | 7.17e-0 | −− | 2.23e-2 | −− | 4.60e-2 | −− | 4.12e-1 | −− |
| | 0.0404 | 14841 | 9.04e-2 | 0.98 | 8.00e-2 | 1.02 | 7.17e-0 | 0.00 | 1.59e-2 | 1.01 | 3.19e-2 | 1.09 | 2.94e-1 | 0.99 |
| 0 | 0.0218 | 50961 | 4.89e-2 | 0.99 | 4.28e-2 | 1.01 | 7.17e-0 | 0.00 | 8.55e-3 | 1.00 | 1.66e-2 | 1.05 | 1.59e-1 | 1.00 |
| | 0.0150 | 106409 | 3.39e-2 | 1.00 | 2.95e-2 | 1.00 | 7.17e-0 | 0.00 | 5.91e-3 | 1.00 | 1.14e-2 | 1.02 | 1.10e-1 | 1.00 |
| | 0.0118 | 173281 | 2.66e-2 | 1.00 | 2.31e-2 | 1.00 | 7.17e-0 | 0.00 | 4.63e-3 | 1.00 | 8.89e-3 | 1.02 | 8.59e-2 | 1.00 |
| | 0.0566 | 26451 | 3.16e-3 | −− | 3.74e-3 | −− | 3.98e-1 | −− | 4.47e-4 | −− | 2.06e-3 | −− | 1.86e-2 | −− |
| | 0.0404 | 51731 | 1.66e-3 | 1.92 | 1.93e-3 | 1.97 | 2.85e-1 | 1.00 | 2.28e-4 | 2.01 | 1.05e-3 | 2.00 | 9.49e-3 | 2.00 |
| 1 | 0.0218 | 177971 | 4.93e-4 | 1.96 | 5.65e-4 | 1.98 | 1.53e-1 | 1.00 | 6.59e-5 | 2.00 | 3.04e-4 | 2.00 | 2.76e-3 | 2.00 |
| | 0.0150 | 371865 | 2.37e-4 | 1.98 | 2.71e-4 | 1.99 | 1.06e-1 | 1.00 | 3.15e-5 | 2.00 | 1.45e-4 | 2.00 | 1.32e-3 | 2.00 |
| | 0.0118 | 605761 | 1.46e-4 | 1.99 | 1.66e-4 | 1.99 | 8.31e-2 | 1.00 | 1.93e-5 | 2.00 | 8.92e-5 | 2.00 | 8.09e-4 | 2.00 |
| | 0.0566 | 54051 | 6.53e-5 | −− | 1.19e-4 | −− | 2.05e-2 | −− | 5.06e-6 | −− | 7.63e-5 | −− | 6.56e-4 | −− |
| | 0.0404 | 105771 | 2.37e-5 | 3.01 | 4.34e-5 | 3.00 | 1.05e-2 | 1.99 | 1.82e-6 | 3.04 | 2.78e-5 | 3.00 | 2.39e-4 | 3.00 |
| 2 | 0.0218 | 364131 | 3.71e-6 | 3.00 | 6.77e-6 | 3.00 | 3.04e-3 | 2.00 | 2.80e-7 | 3.02 | 4.34e-6 | 3.00 | 3.74e-5 | 3.00 |
| | 0.0150 | 761025 | 1.23e-6 | 3.00 | 2.24e-6 | 3.00 | 1.45e-3 | 2.00 | 9.25e-8 | 3.01 | 1.43e-6 | 3.00 | 1.24e-5 | 3.00 |
| | 0.0118 | 1239841 | 5.90e-7 | 3.00 | 1.08e-6 | 3.00 | 8.92e-4 | 2.00 | 4.44e-8 | 3.00 | 6.88e-7 | 3.00 | 5.94e-6 | 3.00 |

Table 1.4: Example 2, history of convergence using triangles (table produced by the author).

| $k$ | $h$ | $N$ | $\mathtt{e}(\mathbf{t})$ | $\mathtt{r}(\mathbf{t})$ | $\mathtt{e}_0(\boldsymbol{\sigma})$ | $\mathtt{r}_0(\boldsymbol{\sigma})$ | $\mathtt{e}_{\mathrm{div}}(\boldsymbol{\sigma})$ | $\mathtt{r}_{\mathrm{div}}(\boldsymbol{\sigma})$ | $\mathtt{e}(\mathbf{u})$ | $\mathtt{r}(\mathbf{u})$ | $\mathtt{e}(p)$ | $\mathtt{r}(p)$ | $\mathtt{e}(\boldsymbol{\sigma}^\star)$ | $\mathtt{r}(\boldsymbol{\sigma}^\star)$ |
|---|---|---|---|---|---|---|---|---|---|---|---|---|---|---|
| | 0.0461 | 8716 | 7.05e-2 | −− | 7.54e-2 | −− | 7.17e-0 | −− | 2.04e-2 | −− | 3.89e-2 | −− | 3.54e-1 | −− |
| | 0.0359 | 14356 | 5.45e-2 | 1.02 | 5.80e-2 | 1.04 | 7.17e-0 | 0.00 | 1.58e-2 | 1.00 | 2.98e-2 | 1.05 | 2.75e-1 | 1.00 |
| 0 | 0.0183 | 54561 | 2.76e-2 | 1.01 | 2.93e-2 | 1.02 | 7.17e-0 | 0.00 | 8.09e-3 | 1.00 | 1.50e-2 | 1.03 | 1.41e-1 | 1.00 |
| | 0.0135 | 101281 | 2.02e-2 | 1.01 | 2.14e-2 | 1.01 | 7.17e-0 | 0.00 | 5.93e-3 | 1.00 | 1.09e-2 | 1.01 | 1.03e-1 | 1.00 |
| | 0.0101 | 179841 | 1.52e-2 | 1.00 | 1.60e-2 | 1.00 | 7.17e-0 | 0.00 | 4.45e-3 | 1.00 | 8.18e-3 | 1.01 | 7.74e-2 | 1.00 |
| | 0.0461 | 28456 | 1.01e-3 | −− | 2.41e-3 | −− | 3.48e-1 | −− | 2.87e-4 | −− | 1.63e-3 | −− | 1.46e-2 | −− |
| | 0.0359 | 46936 | 6.11e-4 | 1.98 | 1.46e-3 | 2.00 | 2.71e-1 | 1.00 | 1.73e-4 | 2.00 | 9.89e-4 | 2.00 | 8.87e-3 | 1.99 |
| 1 | 0.0183 | 178817 | 1.58e-4 | 2.02 | 3.82e-4 | 2.00 | 1.39e-1 | 1.00 | 4.53e-5 | 2.00 | 2.59e-4 | 2.00 | 2.32e-3 | 2.00 |
| | 0.0135 | 332161 | 8.52e-5 | 2.00 | 2.05e-4 | 2.00 | 1.02e-1 | 1.00 | 2.44e-5 | 2.00 | 1.39e-4 | 2.00 | 1.25e-3 | 2.00 |
| | 0.0101 | 590081 | 4.78e-5 | 2.01 | 1.15e-4 | 2.00 | 7.63e-2 | 1.00 | 1.37e-5 | 2.00 | 7.83e-5 | 2.00 | 7.02e-4 | 2.00 |
| | 0.0461 | 56771 | 1.19e-5 | −− | 6.99e-5 | −− | 1.48e-2 | −− | 2.78e-6 | −− | 4.90e-5 | −− | 4.31e-4 | −− |
| | 0.0359 | 93691 | 5.58e-6 | 3.01 | 3.28e-5 | 3.01 | 8.96e-3 | 2.00 | 1.30e-6 | 3.01 | 2.30e-5 | 3.01 | 2.03e-4 | 3.00 |
| 2 | 0.0183 | 357281 | 7.35e-7 | 3.02 | 4.35e-6 | 3.01 | 2.34e-3 | 2.00 | 1.74e-7 | 3.00 | 3.05e-6 | 3.01 | 2.72e-5 | 3.00 |
| | 0.0135 | 663841 | 2.90e-7 | 2.99 | 1.71e-6 | 3.00 | 1.26e-3 | 2.00 | 6.85e-8 | 3.01 | 1.20e-6 | 3.00 | 1.07e-5 | 3.00 |
| | 0.0101 | 1179521 | 1.22e-7 | 3.01 | 7.22e-7 | 3.00 | 7.08e-4 | 2.00 | 2.89e-8 | 3.00 | 5.07e-7 | 3.00 | 4.52e-6 | 3.00 |

Table 1.5: Example 2, history of convergence using quadrilaterals (table produced by the author).

| $k$ | $h$ | $N$ | $\mathtt{e}(\mathbf{t})$ | $\mathtt{r}(\mathbf{t})$ | $\mathtt{e}_0(\boldsymbol{\sigma})$ | $\mathtt{r}_0(\boldsymbol{\sigma})$ | $\mathtt{e}_{\mathrm{div}}(\boldsymbol{\sigma})$ | $\mathtt{r}_{\mathrm{div}}(\boldsymbol{\sigma})$ | $\mathtt{e}(\mathbf{u})$ | $\mathtt{r}(\mathbf{u})$ | $\mathtt{e}(p)$ | $\mathtt{r}(p)$ | $\mathtt{e}(\boldsymbol{\sigma}^\star)$ | $\mathtt{r}(\boldsymbol{\sigma}^\star)$ |
|---|---|---|---|---|---|---|---|---|---|---|---|---|---|---|
| | 0.0439 | 11262 | 6.54e-2 | −− | 7.16e-2 | −− | 7.17e-0 | −− | 1.93e-2 | −− | 3.75e-2 | −− | 3.51e-1 | −− |
| | 0.0342 | 18255 | 5.11e-2 | 0.99 | 5.58e-2 | 1.00 | 7.17e-0 | 0.00 | 1.51e-2 | 0.99 | 2.92e-2 | 1.01 | 2.74e-1 | 1.00 |
| 0 | 0.0251 | 33870 | 3.74e-2 | 1.00 | 4.08e-2 | 1.00 | 7.17e-0 | 0.00 | 1.11e-2 | 1.00 | 2.14e-2 | 1.00 | 2.01e-1 | 1.00 |
| | 0.0182 | 64243 | 2.72e-2 | 0.99 | 2.96e-2 | 0.99 | 7.17e-0 | 0.00 | 8.06e-3 | 0.99 | 1.55e-2 | 1.00 | 1.46e-1 | 0.99 |
| | 0.0132 | 121206 | 1.98e-2 | 0.99 | 2.15e-2 | 1.00 | 7.17e-0 | 0.00 | 5.85e-3 | 0.99 | 1.12e-2 | 1.00 | 1.06e-1 | 1.00 |
| | 0.0439 | 33782 | 8.53e-4 | −− | 2.06e-3 | −− | 3.46e-1 | −− | 2.61e-4 | −− | 1.40e-3 | −− | 1.25e-2 | −− |
| | 0.0342 | 54761 | 5.17e-4 | 2.01 | 1.25e-3 | 2.00 | 2.70e-1 | 1.00 | 1.60e-4 | 1.98 | 8.52e-4 | 2.00 | 7.68e-3 | 1.96 |
| 1 | 0.0251 | 101606 | 2.77e-4 | 2.01 | 6.74e-4 | 2.00 | 1.98e-1 | 1.00 | 8.57e-5 | 2.01 | 4.59e-4 | 2.00 | 4.13e-3 | 2.00 |
| | 0.0182 | 192871 | 1.46e-4 | 1.99 | 3.56e-4 | 1.98 | 1.44e-1 | 0.99 | 4.53e-5 | 1.97 | 2.42e-4 | 1.98 | 2.17e-3 | 1.99 |
| | 0.0132 | 363614 | 7.66e-5 | 2.00 | 1.87e-4 | 2.00 | 1.04e-1 | 1.00 | 2.39e-5 | 1.99 | 1.27e-4 | 2.00 | 1.14e-3 | 2.00 |
| | 0.0439 | 65059 | 2.42e-5 | −− | 6.00e-5 | −− | 1.31e-2 | −− | 2.31e-6 | −− | 4.03e-5 | −− | 3.32e-4 | −− |
| | 0.0342 | 105463 | 1.15e-5 | 2.98 | 2.89e-5 | 2.94 | 8.02e-3 | 1.96 | 1.09e-6 | 3.01 | 1.94e-5 | 2.93 | 1.57e-4 | 3.00 |
| 2 | 0.0251 | 195683 | 4.58e-6 | 2.97 | 1.14e-5 | 3.00 | 4.31e-3 | 2.00 | 4.27e-7 | 3.02 | 7.66e-6 | 3.00 | 6.19e-5 | 3.00 |
| | 0.0182 | 371577 | 1.75e-6 | 2.99 | 4.35e-6 | 2.98 | 2.27e-3 | 1.99 | 1.64e-7 | 2.97 | 2.92e-6 | 2.98 | 2.37e-5 | 2.98 |
| | 0.0132 | 700291 | 6.68e-7 | 2.99 | 1.65e-6 | 3.01 | 1.19e-3 | 2.00 | 6.26e-8 | 2.99 | 1.11e-6 | 3.01 | 9.03e-6 | 3.00 |

Table 1.6: Example 2, history of convergence using hexagons (table produced by the author).

| $k$ | $h$ | $N$ | $\mathtt{e}(\mathbf{t})$ | $\mathtt{r}(\mathbf{t})$ | $\mathtt{e}_0(\boldsymbol{\sigma})$ | $\mathtt{r}_0(\boldsymbol{\sigma})$ | $\mathtt{e}_{\mathrm{div}}(\boldsymbol{\sigma})$ | $\mathtt{r}_{\mathrm{div}}(\boldsymbol{\sigma})$ | $\mathtt{e}(\mathbf{u})$ | $\mathtt{r}(\mathbf{u})$ | $\mathtt{e}(p)$ | $\mathtt{r}(p)$ | $\mathtt{e}(\boldsymbol{\sigma}^\star)$ | $\mathtt{r}(\boldsymbol{\sigma}^\star)$ |
|---|---|---|---|---|---|---|---|---|---|---|---|---|---|---|
| | 0.0101 | 7169 | 3.97e-2 | −− | 5.43e-2 | −− | 1.56e-0 | −− | 7.75e-3 | −− | 2.71e-2 | −− | 1.15e-1 | −− |
| | 0.0673 | 16045 | 2.66e-2 | 0.98 | 3.58e-2 | 1.02 | 1.56e-0 | 0.00 | 5.08e-3 | 1.04 | 1.76e-2 | 1.06 | 8.48e-2 | 0.74 |
| 0 | 0.0372 | 52289 | 1.48e-2 | 0.99 | 1.97e-2 | 1.01 | 1.56e-0 | 0.00 | 2.78e-3 | 1.02 | 9.53e-3 | 1.03 | 5.52e-2 | 0.72 |
| | 0.0253 | 113345 | 1.00e-2 | 1.00 | 1.33e-2 | 1.01 | 1.56e-0 | 0.00 | 1.88e-3 | 1.01 | 6.43e-3 | 1.02 | 4.19e-2 | 0.71 |
| | 0.0186 | 208545 | 7.40e-3 | 1.00 | 9.80e-3 | 1.00 | 1.56e-0 | 0.00 | 1.39e-3 | 1.00 | 4.73e-3 | 1.01 | 3.39e-2 | 0.70 |
| | 0.0101 | 24921 | 9.36e-4 | −− | 1.55e-3 | −− | 1.06e-1 | −− | 2.43e-4 | −− | 9.02e-4 | −− | 3.38e-2 | −− |
| | 0.0673 | 55903 | 4.52e-4 | 1.79 | 7.83e-4 | 1.69 | 8.08e-1 | 0.68 | 1.08e-4 | 2.01 | 4.62e-4 | 1.65 | 2.57e-2 | 0.67 |
| 1 | 0.0372 | 182553 | 1.58e-4 | 1.77 | 2.89e-4 | 1.68 | 5.41e-2 | 0.68 | 3.28e-5 | 2.00 | 1.73e-4 | 1.65 | 1.73e-2 | 0.67 |
| | 0.0253 | 396033 | 8.04e-5 | 1.75 | 1.51e-4 | 1.68 | 4.17e-2 | 0.67 | 1.51e-5 | 2.00 | 9.12e-5 | 1.66 | 1.34e-2 | 0.67 |
| | 0.0186 | 728993 | 4.73e-5 | 1.74 | 9.03e-5 | 1.68 | 3.39e-2 | 0.67 | 8.18e-6 | 2.00 | 5.49e-5 | 1.66 | 1.09e-2 | 0.67 |
| | 0.0101 | 50905 | 6.23e-5 | −− | 2.78e-4 | −− | 3.96e-2 | −− | 6.02e-6 | −− | 1.92e-4 | −− | 1.93e-2 | −− |
| | 0.0673 | 114283 | 3.15e-5 | 1.68 | 1.41e-4 | 1.67 | 3.02e-2 | 0.67 | 1.92e-6 | 2.82 | 9.75e-5 | 1.67 | 1.48e-2 | 0.67 |
| 2 | 0.0372 | 373465 | 1.17e-5 | 1.67 | 5.26e-5 | 1.67 | 2.03e-2 | 0.67 | 3.67e-7 | 2.79 | 3.63e-5 | 1.67 | 9.93e-3 | 0.67 |
| | 0.0253 | 810433 | 6.13e-6 | 1.67 | 2.76e-5 | 1.67 | 1.57e-2 | 0.67 | 1.26e-7 | 2.76 | 1.90e-5 | 1.67 | 7.67e-3 | 0.67 |
| | 0.0186 | 1492033 | 3.68e-6 | 1.67 | 1.66e-5 | 1.67 | 1.28e-2 | 0.67 | 5.43e-8 | 2.75 | 1.14e-5 | 1.67 | 6.26e-3 | 0.67 |

Table 1.7: Example 3, history of convergence using triangles (table produced by the author).

| $k$ | $h$ | $N$ | $\mathtt{e}(\mathbf{t})$ | $\mathtt{r}(\mathbf{t})$ | $\mathtt{e}_0(\boldsymbol{\sigma})$ | $\mathtt{r}_0(\boldsymbol{\sigma})$ | $\mathtt{e}_{\mathrm{div}}(\boldsymbol{\sigma})$ | $\mathtt{r}_{\mathrm{div}}(\boldsymbol{\sigma})$ | $\mathtt{e}(\mathbf{u})$ | $\mathtt{r}(\mathbf{u})$ | $\mathtt{e}(p)$ | $\mathtt{r}(p)$ | $\mathtt{e}(\boldsymbol{\sigma}^\star)$ | $\mathtt{r}(\boldsymbol{\sigma}^\star)$ |
|---|---|---|---|---|---|---|---|---|---|---|---|---|---|---|
| | 0.0907 | 8561 | 2.22e-2 | −− | 3.85e-2 | −− | 1.56e-0 | −− | 6.15e-3 | −− | 2.28e-2 | −− | 1.09e-1 | −− |
| | 0.0725 | 13326 | 1.77e-2 | 1.02 | 3.03e-2 | 1.07 | 1.56e-0 | 0.00 | 4.87e-3 | 1.05 | 1.78e-2 | 1.09 | 9.42e-2 | 0.66 |
| 0 | 0.0363 | 52901 | 8.74e-3 | 1.02 | 1.47e-2 | 1.05 | 1.56e-0 | 0.00 | 2.38e-3 | 1.03 | 8.55e-3 | 1.06 | 6.13e-2 | 0.62 |
| | 0.0245 | 115589 | 5.88e-3 | 1.01 | 9.84e-3 | 1.02 | 1.56e-0 | 0.00 | 1.60e-3 | 1.02 | 5.73e-3 | 1.02 | 4.47e-2 | 0.80 |
| | 0.0191 | 190286 | 4.58e-3 | 1.00 | 7.63e-3 | 1.02 | 1.56e-0 | 0.00 | 1.24e-3 | 1.01 | 4.44e-3 | 1.02 | 3.82e-2 | 0.63 |
| | 0.0907 | 27921 | 5.40e-4 | −− | 1.33e-3 | −− | 1.06e-1 | −− | 1.72e-4 | −− | 8.71e-4 | −− | 4.23e-2 | −− |
| | 0.0725 | 43526 | 3.78e-4 | 1.59 | 9.29e-4 | 1.60 | 9.16e-2 | 0.66 | 1.12e-4 | 1.93 | 6.07e-4 | 1.62 | 3.67e-2 | 0.64 |
| 1 | 0.0363 | 173301 | 1.09e-4 | 1.79 | 3.31e-4 | 1.49 | 6.01e-2 | 0.61 | 2.79e-5 | 2.00 | 2.22e-4 | 1.45 | 2.55e-2 | 0.52 |
| | 0.0245 | 379029 | 5.08e-5 | 1.96 | 1.65e-4 | 1.78 | 4.54e-2 | 0.71 | 1.27e-5 | 2.01 | 1.12e-4 | 1.76 | 1.83e-2 | 0.84 |
| | 0.0191 | 624246 | 3.36e-5 | 1.66 | 1.05e-4 | 1.80 | 3.86e-2 | 0.66 | 7.69e-6 | 2.00 | 7.09e-5 | 1.82 | 1.58e-2 | 0.60 |
| | 0.0907 | 55681 | 9.07e-5 | −− | 3.37e-4 | −− | 4.58e-2 | −− | 4.16e-6 | −− | 2.29e-4 | −− | 2.90e-2 | −− |
| | 0.0725 | 86851 | 6.26e-5 | 1.66 | 2.32e-4 | 1.67 | 3.93e-2 | 0.69 | 2.04e-6 | 3.20 | 1.58e-4 | 1.67 | 2.52e-2 | 0.64 |
| 2 | 0.0363 | 346201 | 2.56e-5 | 1.29 | 9.17e-5 | 1.34 | 2.73e-2 | 0.53 | 3.60e-7 | 2.50 | 6.23e-5 | 1.34 | 1.81e-2 | 0.48 |
| | 0.0245 | 757465 | 1.30e-5 | 1.74 | 4.64e-5 | 1.74 | 2.00e-2 | 0.78 | 1.15e-7 | 2.90 | 3.15e-5 | 1.74 | 1.29e-2 | 0.86 |
| | 0.0191 | 1247731 | 7.87e-6 | 2.00 | 2.68e-5 | 2.19 | 1.70e-2 | 0.68 | 5.58e-8 | 2.93 | 1.81e-5 | 2.21 | 1.06e-2 | 0.77 |

Table 1.8: Example 3, history of convergence using quadrilaterals (table produced by the author).

| $k$ | $h$ | $N$ | $\mathtt{e}(\mathbf{t})$ | $\mathtt{r}(\mathbf{t})$ | $\mathtt{e}_0(\boldsymbol{\sigma})$ | $\mathtt{r}_0(\boldsymbol{\sigma})$ | $\mathtt{e}_{\mathrm{div}}(\boldsymbol{\sigma})$ | $\mathtt{r}_{\mathrm{div}}(\boldsymbol{\sigma})$ | $\mathtt{e}(\mathbf{u})$ | $\mathtt{r}(\mathbf{u})$ | $\mathtt{e}(p)$ | $\mathtt{r}(p)$ | $\mathtt{e}(\boldsymbol{\sigma}^\star)$ | $\mathtt{r}(\boldsymbol{\sigma}^\star)$ |
|---|---|---|---|---|---|---|---|---|---|---|---|---|---|---|
| | 0.0866 | 8382 | 2.26e-2 | −− | 4.02e-2 | −− | 1.56e-0 | −− | 6.62e-3 | −− | 2.41e-2 | −− | 1.18e-1 | −− |
| | 0.0462 | 28668 | 1.20e-2 | 1.01 | 2.10e-2 | 1.03 | 1.56e-0 | 0.00 | 3.49e-3 | 1.02 | 1.25e-2 | 1.04 | 7.73e-2 | 0.68 |
| 0 | 0.0315 | 61050 | 8.13e-3 | 1.02 | 1.42e-2 | 1.02 | 1.56e-0 | 0.00 | 2.38e-3 | 1.00 | 8.48e-3 | 1.02 | 5.98e-2 | 0.67 |
| | 0.0247 | 98868 | 6.38e-3 | 1.00 | 1.11e-2 | 1.02 | 1.56e-0 | 0.00 | 1.87e-3 | 1.00 | 6.63e-3 | 1.02 | 5.16e-2 | 0.61 |
| | 0.0204 | 145758 | 5.25e-3 | 1.01 | 9.16e-3 | 1.01 | 1.56e-0 | 0.00 | 1.54e-3 | 0.99 | 5.45e-3 | 1.01 | 4.60e-2 | 0.58 |
| | 0.0866 | 25142 | 5.93e-4 | −− | 1.50e-3 | −− | 1.15e-1 | −− | 1.86e-4 | −− | 9.84e-4 | −− | 4.87e-2 | −− |
| | 0.0462 | 86000 | 1.84e-4 | 1.86 | 5.45e-4 | 1.61 | 7.66e-2 | 0.65 | 5.38e-5 | 1.97 | 3.65e-4 | 1.58 | 3.24e-2 | 0.65 |
| 1 | 0.0315 | 183146 | 9.66e-5 | 1.68 | 2.96e-4 | 1.60 | 5.98e-2 | 0.65 | 2.52e-5 | 1.98 | 1.99e-4 | 1.59 | 2.63e-2 | 0.54 |
| | 0.0247 | 296600 | 6.30e-5 | 1.77 | 2.02e-4 | 1.59 | 5.16e-2 | 0.61 | 1.55e-5 | 2.01 | 1.36e-4 | 1.57 | 2.26e.2 | 0.62 |
| | 0.0204 | 437270 | 4.48e-5 | 1.76 | 1.49e-4 | 1.55 | 4.52e-2 | 0.68 | 1.06e-5 | 1.99 | 1.01e-4 | 1.53 | 2.00e-2 | 0.63 |
| | 0.0866 | 48419 | 9.62e-5 | −− | 4.32e-4 | −− | 5.08e-2 | −− | 4.09e-6 | −− | 2.98e-4 | −− | 3.35e-2 | −− |
| | 0.0462 | 165627 | 3.32e-5 | 1.69 | 1.58e-4 | 1.60 | 3.41e-2 | 0.63 | 7.64e-7 | 2.67 | 1.09e-4 | 1.59 | 2.31e-2 | 0.59 |
| 2 | 0.0315 | 352723 | 2.01e-5 | 1.31 | 9.18e-5 | 1.42 | 2.73e-2 | 0.58 | 2.65e-7 | 2.77 | 6.33e-5 | 1.43 | 1.85e-2 | 0.58 |
| | 0.0247 | 571227 | 1.24e-5 | 2.00 | 6.32e-5 | 1.55 | 2.36e-2 | 0.59 | 1.50e-7 | 2.34 | 4.38e-5 | 1.53 | 1.61e-2 | 0.56 |
| | 0.0204 | 842174 | 9.85e-6 | 1.19 | 4.76e-5 | 1.46 | 2.10e-2 | 0.61 | 8.41e-8 | 3.00 | 3.29e-5 | 1.47 | 1.44e-2 | 0.58 |

Table 1.9: Example 3, history of convergence using hexagons (table produced by the author).

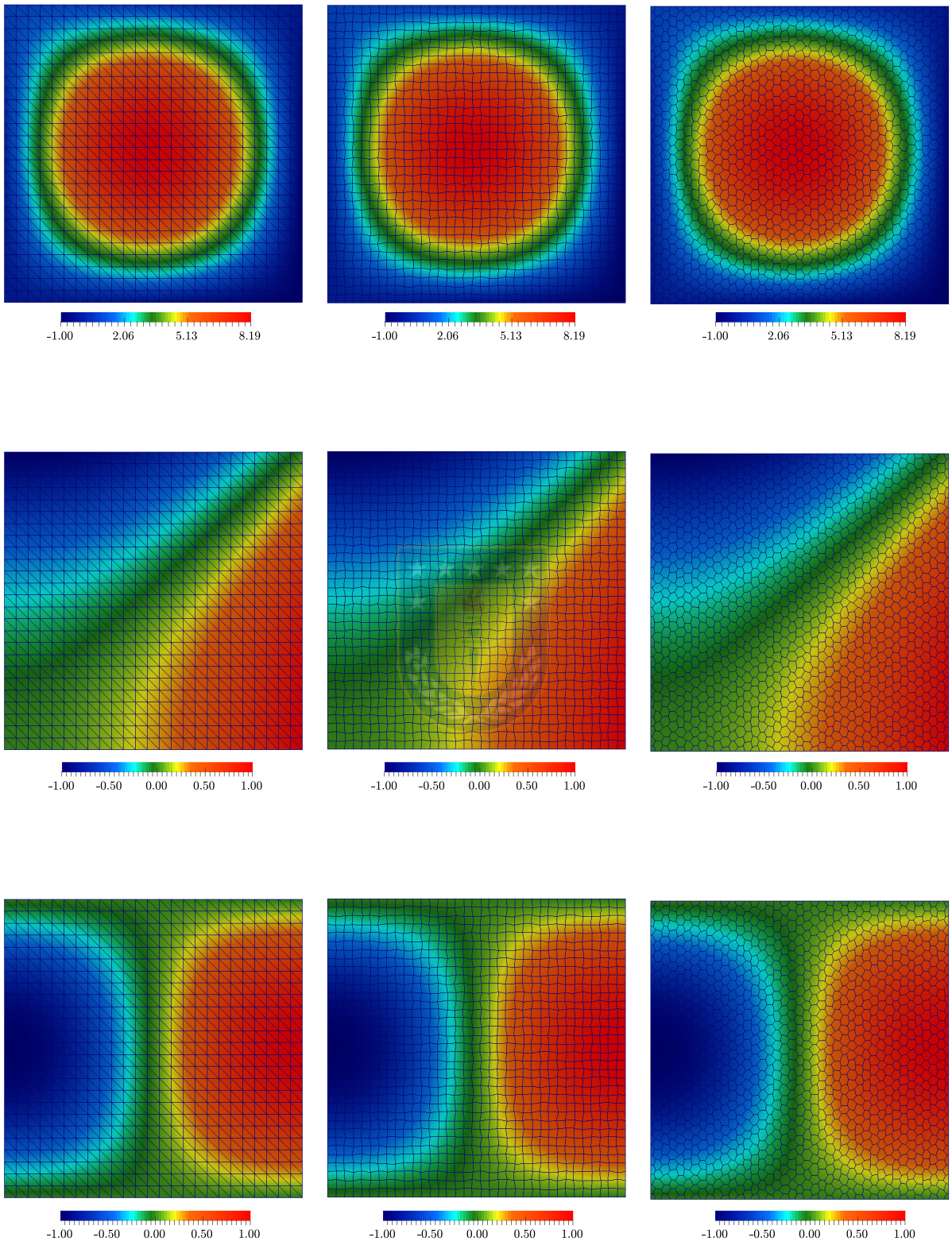


Figure 1.1: Example 1, $\sigma_{h,11}$ (top), $p_h$ (middle) and $u_{h,1}$ (bottom) (figure produced by the author).

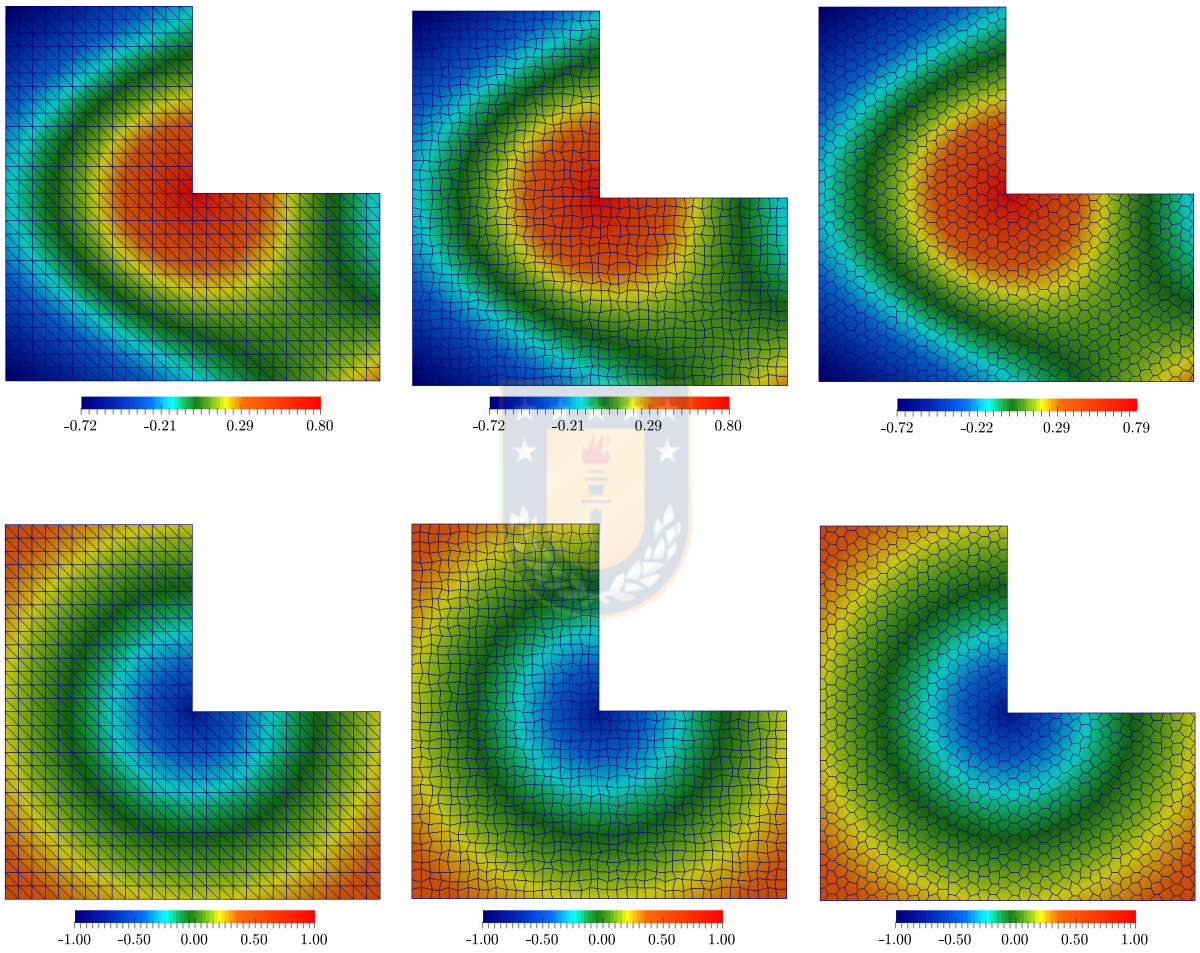


Figure 1.2: Example 3, $\sigma_{h,22}$ (top) and $p_h$ (bottom) (figure produced by the author).

# CHAPTER 2

## A mixed virtual element method for the Navier–Stokes equations

### 2.1 Introduction

The utilization of virtual element methods (VEM) in fluid mechanics has become a very active research subject in recent years. Indeed, regarding the Stokes equations, we begin by referring to [10, 20, 39], where stream function-based, divergence free, and non-conforming virtual element methods, respectively, have been developed for the classical velocity-pressure formulation of this problem. In particular, a new family of virtual elements for the Stokes problem on polygonal meshes, in which the discrete velocity is pointwise divergence-free, is provided in [20]. Moreover, the associated virtual scheme is shown to be equivalent to a problem with less degrees of freedom, thus yielding a more efficient method. In turn, the virtual element method proposed in [39] approximates the pressure using discontinuous piecewise polynomials, whereas the components of the velocity are approximated using a globally nonconforming virtual element space. In fact, the virtual element functions are locally defined as the solution of Poisson problems with polynomial Neumann boundary conditions. More recently, a family of virtual element methods for the two-dimensional Navier-Stokes equations is introduced and analyzed in [21], which constitutes, up to our knowledge, the first paper applying the VEM technique to that nonlinear model. As in [20], pointwise divergence-free discrete velocities are also obtained in [21], and hence the virtual element scheme suggested there can be seen as a natural extension of the approach provided in [20].

Furthermore, other contributions in the aforementioned direction have concentrated on the combined use of pseudostress-based dual-mixed variational formulations and virtual element methods, thus yielding the first mixed-VEM schemes known so far for the Stokes and related models in fluid mechanics (see [30, 31, 32]). Before describing the main aspects of these works in what follows, we notice that the name *dual-mixed* refers here to those formulations in which the main unknown of the resulting saddle point problem lives in either a vectorial $\mathbf{H}(\mathrm{div})$ or a tensorial $\mathbb{H}(\mathbf{div})$ space, which is precisely the case when the stress or the pseudostress is employed. Having said the above, we now recall that a mixed-VEM for the pseudostress-velocity formulation of the Stokes problem, in which the pressure is computed via a postprocessing formula, was introduced and analyzed in [30]. In particular, in order to derive the explicitly computable discrete bilinear form, a new local projector onto a suitable polynomial space, which takes into account the main features of the continuous solution and allows the explicit integration

of terms involving deviatoric tensors, is proposed there. Then, the analysis in [30] is extended in [31] to derive two mixed virtual element methods for the two-dimensional Brinkman problem. Proceeding as in [57], the equilibrium equation and the incompressibility condition are utilized in [31] to eliminate the velocity and the pressure, respectively, whence the pseudostress becomes the only unknown of the resulting dual-mixed formulation. In this way, the aforementioned two schemes arise from the use of one from two different projectors, the ad-hoc one introduced in [30] and the $\mathrm{L}^2$-orthogonal one analyzed in [15] (see also [14]). Another virtual element method for the Brinkman equations, not employing the aforementioned dual-mixed approach, is proposed in [90]. We end this paragraph by remarking that the analysis and results from [30, 31] were extended in [32] to the case of quasi-Newtonian Stokes flows, for which the nonlinear model studied in [64] (see also [70]) was considered.

In addition to the above, it is important to highlight that the incorporation of the pseudostress as one of the main unknowns of a dual-mixed variational formulation in continuum mechanics, is mainly motivated by the need of finding new ways of circumventing the symmetry requirement of the usual stress-based methods. In particular, and since in this chapter we are interested in developing a VEM scheme for a dual-mixed formulation of the Navier-Stokes equations, we begin the corresponding bibliographic discussion with [75], where a new mixed finite element method for that model was introduced and analyzed. More precisely, the main unknowns of the approach in [75] are given by the velocity, its gradient, and a modified nonlinear pseudostress tensor linking the usual stress and the convective term. A fixed-point argument and the Babuška-Brezzi theory are applied there to derive the well-posedness of the resulting continuous formulation. Then, the procedure from [75] is modified in [35] through the introduction of a new nonlinear tensor linking now the pseudostress (instead of the stress) and the convective term, which, together with the velocity, constitute the only unknowns. Suitable Galerkin type terms arising from the constitutive and equilibrium equations, and the boundary condition, are then incorporated into the formulation of [35], so that the Lax-Milgram and Banach fixed-point theorems are employed to prove the well-posedness of both the continuous and discrete schemes. In turn, the approach from [35] has been further extended to other boundary value problems, including the development of new dual-mixed formulations for the stationary Boussinesq problem (see [46, 47, 48, 49]), and for the Navier-Stokes equations with constant density and variable viscosity (see [33, 34]). Besides the methods and tools utilized in [35], the foregoing extensions also make use of the Brouwer fixed-point theorem and the Babuška-Brezzi theory.

According to the above discussion, and in order to additionally contribute in the direction drawn by [21, 32, 68], we now aim to continue extending the applicability of the VEM technique to nonlinear problems in fluid mechanics. More precisely, we consider the same variational formulation from [35] (see also [33, 34]), and develop, up to our knowledge, the first dual-mixed virtual element method for the Navier Stokes equations. Actually, following the original motivation of the virtual element philosophy, our main goal is to extend the capability of employing general polygonal meshes to design convergent Galerkin schemes for this important problem in applications, but now from the perspective of a mixed approach and its own advantages. After addressing the challenging aspects of the necessary analysis for establishing this extension, we should be able to face other relevant nonlinear models in fluid mechanics, such as Boussinesq equations, bioconvective flows, nonlinear porous media flows (for instance Darcy-Forchheimer), and diverse coupled problems arising from the interaction of some of the above (see [43, 53, 62, 72] for examples of the models we are thinking of). In particular, the virtual element methods become very suitable and advantageous for the latter since, the fact that they allow

hanging nodes and nonconvex elements, makes much easier the eventual interaction between meshes coming from different domains or from different parts of a given region. Furthermore, as already highlighted in the abstract, another motivation for considering a mixed virtual element discretization of the Navier-Stokes equations, lies on the particular variational formulation to be employed and the consequent use, simultaneously, of virtual element subspaces for $\mathbf{H}^1$ and $\mathbb{H}(\mathbf{div})$. Up to our knowledge, this seems to be the first work on virtual element methods showing this novelty.

The rest of this chapter is organized as follows. At the end of the present section we provide some useful notations. In Section 2.2 we describe our nonlinear model, recall from [35] the derivation of the augmented pseudostress-velocity formulation to be employed, and state the corresponding well-posedness result. Then, in Section 2.3 we introduce the virtual element subspaces approximating the velocity and the pseudostress in $\mathbf{H}^1$ and $\mathbb{H}(\mathbf{div})$, respectively, state their approximation properties, and define the projectors and remaining ingredients that are needed for the discrete analysis. In turn, computable discrete versions of the bilinear and trilinear forms involved, and of the corresponding functional on the right-hand side of the formulation, are locally and then globally defined in Section 2.4. In addition, the main mapping properties connecting them with their continuous versions are also proved in this section. Next, in Section 2.5 we define the associated mixed virtual element scheme, perform the solvability analysis by using suitable fixed-point arguments (as done in [35] and its further extensions), and apply Strang-type estimates to derive the *a priori* error estimates for both the virtual element solution and the fully computable projections of its components. The corresponding rates of convergence are then readily established by using the approximation properties given in Section 2.3. Furthermore, following previous works by some of the authors, an element-by-element postprocessing formula for the fully computable pseudostress is suggested at the last part of Section 2.5, which leads to an optimally convergent approximation of this unknown with respect to the broken $\mathbb{H}(\mathbf{div})$-norm. Finally, some numerical tests showing the good performance of the method, confirming the rates of convergence for solutions, and illustrating the accurateness obtained with the approximate solutions, are reported in Section 2.6.

We end the present section by providing some notations to be used along the **Chapter** 2, including those already employed above. Firstly, for any vector fields $\mathbf{v} = (v_i)_{i=1,2}$ and $\mathbf{w} = (w_i)_{i=1,2}$ we set the gradient, divergence and tensor product operators as

$$\nabla \mathbf{v} := \left( \frac{\partial v_i}{\partial x_j} \right)_{i,j=1,2}, \qquad \mathrm{div}(\mathbf{v}) := \sum_{j=1}^{2} \frac{\partial v_j}{\partial x_j}, \quad \text{and} \quad \mathbf{v} \otimes \mathbf{w} := (v_i w_j)_{i,j=1,2},$$

respectively. In addition, denoting by $\mathbb{I}$ the identity matrix of $\mathrm{R}^{2\times 2}$, and given $\boldsymbol{\tau} := (\tau_{ij})$, $\boldsymbol{\zeta} := (\zeta_{ij}) \in \mathrm{R}^{2\times 2}$, we write as usual

$$\boldsymbol{\tau}^{\mathbf{t}} := (\tau_{ji}), \quad \mathrm{tr}(\boldsymbol{\tau}) := \sum_{i=1}^{2} \tau_{ii}, \quad \boldsymbol{\tau}^{\mathrm{d}} := \boldsymbol{\tau} - \frac{1}{2}\mathrm{tr}(\boldsymbol{\tau})\,\mathbb{I}, \quad \text{and} \quad \boldsymbol{\tau} : \boldsymbol{\zeta} := \sum_{i,j=1}^{2} \tau_{ij}\zeta_{ij},$$

which corresponds, respectively, to the transpose, the trace, and the deviator tensor of $\boldsymbol{\tau}$, and to the tensorial product between $\boldsymbol{\tau}$ and $\boldsymbol{\zeta}$. Next, given a bounded domain $\mathcal{O} \subseteq \mathrm{R}^2$, with boundary $\partial\mathcal{O}$, we let $\mathbf{n}$ be the outward unit normal vector on $\partial\mathcal{O}$. Also, given $r \geq 0$ and $p > 1$, we let $\mathrm{W}^{r,p}(\mathcal{O})$ be the standard Sobolev space with norm $\|\cdot\|_{r,p,\mathcal{O}}$ and seminorm $|\cdot|_{r,p,\mathcal{O}}$. In particular, for $r = 0$ we let $\mathrm{L}^p(\mathcal{O}) := \mathrm{W}^{0,p}(\mathcal{O})$ be the usual Lebesgue space, and for $p = 2$ we let $\mathrm{H}^s(\mathcal{O}) := \mathrm{W}^{r,2}(\mathcal{O})$ be the classical Hilbertian Sobolev space with norm $\|\cdot\|_{s,\mathcal{O}}$ and seminorm $|\cdot|_{s,\mathcal{O}}$.

Furthermore, given a generic scalar functional space M, we let $\mathbf{M}$ and $\mathbb{M}$ be its vector and tensorial counterparts, respectively, whose norms and seminorms are denoted exactly as those of M. On the other hand, letting **div** (resp. **rot**) be the usual divergence operator div (resp. rotational operator rot) acting along the rows of a given tensor, we recall that the spaces

$$\mathbf{H}(\mathrm{div};\mathcal{O}) := \left\{\tau \in \mathbf{L}^2(\mathcal{O}) : \quad \mathrm{div}(\tau) \in \mathrm{L}^2(\mathcal{O})\right\},$$

$$\mathbb{H}(\mathbf{div};\mathcal{O}) := \left\{\boldsymbol{\tau} \in \mathbb{L}^2(\mathcal{O}) : \quad \mathbf{div}(\boldsymbol{\tau}) \in \mathbf{L}^2(\mathcal{O})\right\},$$

$$\mathbf{H}(\mathrm{rot};\mathcal{O}) := \left\{\tau \in \mathbf{L}^2(\mathcal{O}) : \quad \mathrm{rot}(\tau) \in \mathrm{L}^2(\mathcal{O})\right\},$$

and

$$\mathbb{H}(\mathbf{rot};\mathcal{O}) := \left\{\boldsymbol{\tau} \in \mathbb{L}^2(\mathcal{O}) : \quad \mathbf{rot}(\boldsymbol{\tau}) \in \mathbf{L}^2(\mathcal{O})\right\},$$

equipped with the usual norms

$$\begin{aligned}
\|\tau\|^2_{\mathrm{div};\mathcal{O}} &:= \|\tau\|^2_{0,\mathcal{O}} + \|\mathrm{div}(\tau)\|^2_{0,\mathcal{O}} \qquad \forall\, \tau \in \mathbf{H}(\mathrm{div};\mathcal{O}),\\
\|\boldsymbol{\tau}\|^2_{\mathbf{div};\mathcal{O}} &:= \|\boldsymbol{\tau}\|^2_{0,\mathcal{O}} + \|\mathbf{div}(\boldsymbol{\tau})\|^2_{0,\mathcal{O}} \qquad \forall\, \boldsymbol{\tau} \in \mathbb{H}(\mathbf{div};\mathcal{O}),\\
\|\tau\|^2_{\mathrm{rot};\mathcal{O}} &:= \|\tau\|^2_{0,\mathcal{O}} + \|\mathrm{rot}(\tau)\|^2_{0,\mathcal{O}} \qquad \forall\, \tau \in \mathbf{H}(\mathrm{rot};\mathcal{O}),
\end{aligned}$$

and

$$\|\boldsymbol{\tau}\|^2_{\mathbf{rot};\mathcal{O}} := \|\boldsymbol{\tau}\|^2_{0,\mathcal{O}} + \|\mathbf{rot}(\boldsymbol{\tau})\|^2_{0,\mathcal{O}} \qquad \forall\, \boldsymbol{\tau} \in \mathbb{H}(\mathbf{rot};\mathcal{O}),$$

are Hilbert spaces. Finally, in what follows we employ $\mathbf{0}$ to denote a generic null vector, null tensor or null operator, and use $C$ to denote generic constants independent of the discretization parameters, which may take different values at different places.

## 2.2 The Navier-Stokes equations

### 2.2.1 The model problem

Let $\Omega$ be a bounded polygonal domain in $\mathrm{R}^2$ with boundary $\Gamma$. In what follows we consider the stationary Navier-Stokes equations with constant viscosity $\mu > 0$. In other words, given a volume force $\mathbf{f} \in \mathbf{L}^2(\Omega)$ and a Dirichlet datum $\mathbf{g} \in \mathbf{H}^{1/2}(\Gamma)$, we seek the velocity $\mathbf{u}$ and the pressure $p$ of a fluid occupying the region $\Omega$, such that

$$\begin{aligned}
-\mu\Delta\mathbf{u} + (\nabla\mathbf{u})\,\mathbf{u} + \nabla p &= \mathbf{f} \quad \text{in} \quad \Omega, \qquad \mathrm{div}(\mathbf{u}) = 0 \quad \text{in} \quad \Omega,\\
\mathbf{u} &= \mathbf{g} \quad \text{on} \quad \Gamma, \quad \text{and} \quad \int_\Omega p = 0,
\end{aligned} \tag{2.1}$$

where the last equation in (2.1) is imposed to guarantee the uniqueness of the pressure solution. Notice here that, due to the incompressibility condition given by the second equation of (2.1), $\mathbf{g}$ must satisfy the compatibility condition

$$\int_\Gamma \mathbf{g}\cdot\mathbf{n} = 0. \tag{2.2}$$

Then, following [35] (see also [34, 46]), we introduce a pseudostress tensor defined by

$$\boldsymbol{\sigma} := \mu\nabla\mathbf{u} - \mathbf{u}\otimes\mathbf{u} - p\,\mathbb{I} \quad \text{in} \quad \Omega\,, \tag{2.3}$$

which establishes that the first equation in (2.1) can be written as the equilibrium equation

$$-\mathbf{div}(\boldsymbol{\sigma}) = \mathbf{f} \quad \text{in} \quad \Omega\,.$$

Next, it is not difficult to see that (2.3) and the incompressibility condition $\mathrm{div}(\mathbf{u}) = 0$ in $\Omega$, are equivalent to the pair of equations given by

$$\boldsymbol{\sigma}^{\mathrm{d}} = \mu\nabla\mathbf{u} - (\mathbf{u}\otimes\mathbf{u})^{\mathrm{d}} \quad \text{in} \quad \Omega \quad \text{and} \quad p = -\frac{1}{2}\,\mathrm{tr}(\boldsymbol{\sigma} + \mathbf{u}\otimes\mathbf{u}) \quad \text{in} \quad \Omega\,, \tag{2.4}$$

whence (2.1) can be rewritten as: Find the pseudostress $\boldsymbol{\sigma}$ and the velocity $\mathbf{u}$ such that

$$\begin{aligned} \boldsymbol{\sigma}^{\mathrm{d}} = \mu\nabla\mathbf{u} - (\mathbf{u}\otimes\mathbf{u})^{\mathrm{d}} \quad \text{in} \quad \Omega\,, \qquad -\mathbf{div}(\boldsymbol{\sigma}) = \mathbf{f} \quad \text{in} \quad \Omega\,, \\ \mathbf{u} = \mathbf{g} \quad \text{on} \quad \Gamma\,, \quad \text{and} \quad \int_\Omega \mathrm{tr}(\boldsymbol{\sigma} + \mathbf{u}\otimes\mathbf{u}) = 0\,. \end{aligned} \tag{2.5}$$

We stress here that we have eliminated the pressure from the original model (2.1). However, using the second equation in (2.4) we can recover $p$ by a postprocessing formula in terms of $\boldsymbol{\sigma}$ and $\mathbf{u}$.

### 2.2.2 The augmented mixed formulation

In what follows we derive a weak formulation of (2.5). To this end, and proceeding as in [34, 35], we multiply the first equation in (2.5) by $\boldsymbol{\tau} \in \mathbb{H}(\mathbf{div};\Omega)$, integrate by parts in $\Omega$, and use the Dirichlet boundary condition to deduce that

$$\int_\Omega \boldsymbol{\sigma}^{\mathrm{d}} : \boldsymbol{\tau}^{\mathrm{d}} + \mu\int_\Omega \mathbf{u}\cdot\mathbf{div}(\boldsymbol{\tau}) + \int_\Omega (\mathbf{u}\otimes\mathbf{u})^{\mathrm{d}} : \boldsymbol{\tau} = \mu\langle\boldsymbol{\tau}\mathbf{n},\mathbf{g}\rangle_\Gamma \qquad \forall\ \boldsymbol{\tau}\in\mathbb{H}(\mathbf{div};\Omega)\,.$$

In turn, the equilibrium equation, which is given by the second equation of (2.5), is rewritten as

$$\mu\int_\Omega \mathbf{v}\cdot\mathbf{div}(\boldsymbol{\sigma}) = -\mu\int_\Omega \mathbf{f}\cdot\mathbf{v} \qquad \forall\ \mathbf{v}\in\mathbf{L}^2(\Omega)\,.$$

In this way, we arrive at first instance at the following weak formulation of (2.5): Find $\boldsymbol{\sigma}\in\mathbb{H}(\mathbf{div};\Omega)$ and $\mathbf{u}$ in a suitable space, such that

$$\begin{aligned} \int_\Omega \boldsymbol{\sigma}^{\mathrm{d}} : \boldsymbol{\tau}^{\mathrm{d}} + \mu\int_\Omega \mathbf{u}\cdot\mathbf{div}(\boldsymbol{\tau}) + \int_\Omega (\mathbf{u}\otimes\mathbf{u})^{\mathrm{d}} : \boldsymbol{\tau} &= \mu\langle\boldsymbol{\tau}\mathbf{n},\mathbf{g}\rangle_\Gamma \qquad \forall\ \boldsymbol{\tau}\in\mathbb{H}(\mathbf{div};\Omega)\,, \\ \mu\int_\Omega \mathbf{v}\cdot\mathbf{div}(\boldsymbol{\sigma}) &= -\mu\int_\Omega \mathbf{f}\cdot\mathbf{v} \qquad \forall\ \mathbf{v}\in\mathbf{L}^2(\Omega)\,, \\ \int_\Omega \mathrm{tr}(\boldsymbol{\sigma}) &= -\int_\Omega \mathrm{tr}(\mathbf{u}\otimes\mathbf{u})\,. \end{aligned} \tag{2.6}$$

We now define

$$\mathbb{H}_0(\mathbf{div};\Omega) := \left\{\boldsymbol{\tau}\in\mathbb{H}(\mathbf{div};\Omega) \,:\, \int_\Omega \mathrm{tr}(\boldsymbol{\tau}) = 0\right\},$$

and recall (see [29, 56]) that there holds the decomposition

$$\mathbb{H}(\mathbf{div};\Omega) \;=\; \mathbb{H}_0(\mathbf{div};\Omega) \oplus \mathrm{R}\,\mathbb{I}\,. \tag{2.7}$$

More precisely, for each $\boldsymbol{\tau} \in \mathbb{H}(\mathbf{div};\Omega)$ there exist unique $\boldsymbol{\tau}_0 \in \mathbb{H}_0(\mathbf{div};\Omega)$ and $c := \frac{1}{2|\Omega|}\int_\Omega \mathrm{tr}(\boldsymbol{\tau}) \in \mathrm{R}$, where $|\Omega|$ denotes the measure of $\Omega$, such that $\boldsymbol{\tau} = \boldsymbol{\tau}_0 + c\,\mathbb{I}$. In particular, the third equation of (2.6) yields $\boldsymbol{\sigma} = \boldsymbol{\sigma}_0 + c\,\mathbb{I}$, with $\boldsymbol{\sigma}_0 \in \mathbb{H}_0(\mathbf{div};\Omega)$ and the constant $c$ given explicitly in terms of $\mathbf{u}$ by

$$c \;=\; -\frac{1}{2|\Omega|}\int_\Omega \mathrm{tr}(\mathbf{u}\otimes\mathbf{u}) \;=\; -\frac{1}{2|\Omega|}\,\|\mathbf{u}\|^2_{0,\Omega}\,. \tag{2.8}$$

In this way, replacing $\boldsymbol{\sigma}$ by the expression $\boldsymbol{\sigma}_0 + c\,\mathbb{I}$ in (2.6), using that $\boldsymbol{\sigma}^{\mathrm{d}} = \boldsymbol{\sigma}_0^{\mathrm{d}}$ and $\mathbf{div}(\boldsymbol{\sigma}) = \mathbf{div}(\boldsymbol{\sigma}_0)$, taking into account the condition (2.2), and denoting from now on the remaining unknown $\boldsymbol{\sigma}_0 \in \mathbb{H}_0(\mathbf{div};\Omega)$ simply by $\boldsymbol{\sigma}$, we deduce that the weak formulation of (2.5) can be written as: Find $\boldsymbol{\sigma} \in \mathbb{H}_0(\mathbf{div};\Omega)$ and $\mathbf{u}$ in a suitable space, such that

$$\begin{aligned}
\int_\Omega \boldsymbol{\sigma}^{\mathrm{d}} : \boldsymbol{\tau}^{\mathrm{d}} \,+\, \mu\int_\Omega \mathbf{u}\cdot\mathbf{div}(\boldsymbol{\tau}) \,+\, \int_\Omega (\mathbf{u}\otimes\mathbf{u})^{\mathrm{d}} : \boldsymbol{\tau} \;&=\; \mu\langle \boldsymbol{\tau}\mathbf{n}, \mathbf{g}\rangle_\Gamma \qquad \forall\, \boldsymbol{\tau} \in \mathbb{H}_0(\mathbf{div};\Omega)\,, \\
\mu\int_\Omega \mathbf{v}\cdot\mathbf{div}(\boldsymbol{\sigma}) \;&=\; -\mu\int_\Omega \mathbf{f}\cdot\mathbf{v} \qquad \forall\, \mathbf{v} \in \mathbf{L}^2(\Omega)\,.
\end{aligned}$$

On the other hand, we notice that the third term in the first equation of the foregoing system requires $\mathbf{u}$ to lie in a smaller space than $\mathbf{L}^2(\Omega)$. In fact, applying the Cauchy-Schwarz inequality, and employing the compact (and hence continuous) injection

$$\mathbf{i}_c \,:\, \mathbf{H}^1(\Omega) \to \mathbf{L}^4(\Omega) \tag{2.9}$$

(cf. the Rellich-Kondrachov theorem in Theorem 6.3 of [2] or Theorem 1.3.5 of [84]), we arrive at

$$\left|\int_\Omega (\mathbf{w}\otimes\mathbf{z})^{\mathrm{d}} : \boldsymbol{\zeta}\right| \;\le\; \|\mathbf{w}\|_{0,4,\Omega}\|\mathbf{z}\|_{0,4,\Omega}\|\boldsymbol{\zeta}\|_{0,\Omega} \;\le\; \|\mathbf{i}_c\|^2\,\|\mathbf{w}\|_{1,\Omega}\|\mathbf{z}\|_{1,\Omega}\|\boldsymbol{\zeta}\|_{0,\Omega}\,, \tag{2.10}$$

for all $\mathbf{w},\mathbf{z} \in \mathbf{H}^1(\Omega)$, and $\boldsymbol{\zeta} \in \mathbb{L}^2(\Omega)$, which suggests to look for the unknown $\mathbf{u}$ in $\mathbf{H}^1(\Omega)$ and to restrict the set of corresponding test functions $\mathbf{v}$ to the same space. Consequently, and in order to be able to analyze the present variational formulation of (2.5), we follow [35] and incorporate the following redundant Galerkin terms:

$$\begin{aligned}
\kappa_1\int_\Omega \mathbf{div}(\boldsymbol{\sigma})\cdot\mathbf{div}(\boldsymbol{\tau}) \;&=\; -\kappa_1\int_\Omega \mathbf{f}\cdot\mathbf{div}(\boldsymbol{\tau}) \qquad \forall\, \boldsymbol{\tau} \in \mathbb{H}_0(\mathbf{div};\Omega)\,, \\
\kappa_2\int_\Omega \left\{\mu\nabla\mathbf{u} - \boldsymbol{\sigma}^{\mathrm{d}} - (\mathbf{u}\otimes\mathbf{u})^{\mathrm{d}}\right\} : \nabla\mathbf{v} \;&=\; 0 \qquad\qquad\qquad \forall\, \mathbf{v} \in \mathbf{H}^1(\Omega)\,, \\
\kappa_3\int_\Gamma \mathbf{u}\cdot\mathbf{v} \;&=\; \kappa_3\int_\Gamma \mathbf{g}\cdot\mathbf{v} \qquad\qquad\qquad \forall\, \mathbf{v} \in \mathbf{H}^1(\Omega)\,,
\end{aligned}$$

where $\kappa_1$, $\kappa_2$ and $\kappa_3$ are positive parameters to be specified later. In this way, we obtain the following augmented mixed formulation: Find $\vec{\boldsymbol{\sigma}} := (\boldsymbol{\sigma},\mathbf{u}) \in \mathbf{H} := \mathbb{H}_0(\mathbf{div};\Omega)\times\mathbf{H}^1(\Omega)$ such that

$$\mathbf{A}(\vec{\boldsymbol{\sigma}},\vec{\boldsymbol{\tau}}) \;+\; \mathbf{B}(\mathbf{u};\vec{\boldsymbol{\sigma}},\vec{\boldsymbol{\tau}}) \;=\; \mathbf{F}(\vec{\boldsymbol{\tau}}) \qquad \forall\, \vec{\boldsymbol{\tau}} := (\boldsymbol{\tau},\mathbf{v}) \in \mathbf{H}\,, \tag{2.11}$$

where $\mathbf{A} : \mathbf{H} \times \mathbf{H} \to \mathrm{R}$ is the bilinear form

$$\begin{aligned}\mathbf{A}(\vec{\boldsymbol{\zeta}}, \vec{\boldsymbol{\tau}}) \;:=\; & \int_\Omega \boldsymbol{\zeta}^{\mathrm{d}} : \boldsymbol{\tau}^{\mathrm{d}} \,+\, \kappa_1 \int_\Omega \mathbf{div}(\boldsymbol{\zeta}) \cdot \mathbf{div}(\boldsymbol{\tau}) \,+\, \kappa_2 \mu \int_\Omega \nabla \mathbf{w} : \nabla \mathbf{v} \,+\, \kappa_3 \int_\Gamma \mathbf{w} \cdot \mathbf{v} \\ & - \mu \int_\Omega \mathbf{v} \cdot \mathbf{div}(\boldsymbol{\zeta}) \,+\, \mu \int_\Omega \mathbf{w} \cdot \mathbf{div}(\boldsymbol{\tau}) \,-\, \kappa_2 \int_\Omega \boldsymbol{\zeta}^{\mathrm{d}} : \nabla \mathbf{v}\end{aligned} \tag{2.12}$$

for all $\vec{\boldsymbol{\zeta}} := (\boldsymbol{\zeta}, \mathbf{w})$, $\vec{\boldsymbol{\tau}} := (\boldsymbol{\tau}, \mathbf{v}) \in \mathbf{H}$, $\mathbf{F} : \mathbf{H} \to \mathrm{R}$ is the linear functional

$$\mathbf{F}(\vec{\boldsymbol{\tau}}) \;:=\; \mu \langle \boldsymbol{\tau}\mathbf{n}, \mathbf{g} \rangle_\Gamma \,-\, \kappa_1 \int_\Omega \mathbf{f} \cdot \mathbf{div}(\boldsymbol{\tau}) \,+\, \mu \int_\Omega \mathbf{f} \cdot \mathbf{v} \,+\, \kappa_3 \int_\Gamma \mathbf{g} \cdot \mathbf{v} \tag{2.13}$$

for all $\vec{\boldsymbol{\tau}} := (\boldsymbol{\tau}, \mathbf{v}) \in \mathbf{H}$, and given $\mathbf{z} \in \mathbf{H}^1(\Omega)$, $\mathbf{B}(\mathbf{z}; \cdot, \cdot) : \mathbf{H} \times \mathbf{H} \to \mathrm{R}$ is the bilinear form

$$\mathbf{B}(\mathbf{z}; \vec{\boldsymbol{\zeta}}, \vec{\boldsymbol{\tau}}) \;:=\; \int_\Omega (\mathbf{w} \otimes \mathbf{z})^{\mathrm{d}} : \big\{ \boldsymbol{\tau} - \kappa_2 \nabla \mathbf{v} \big\} \tag{2.14}$$

for all $\vec{\boldsymbol{\zeta}} := (\boldsymbol{\zeta}, \mathbf{w})$, $\vec{\boldsymbol{\tau}} := (\boldsymbol{\tau}, \mathbf{v}) \in \mathbf{H}$. We notice here, according to (2.10) and (2.14), that there holds

$$|\, \mathbf{B}(\mathbf{z}; \vec{\boldsymbol{\zeta}}, \vec{\boldsymbol{\tau}}) \,| \;\leq\; \|\mathbf{i}_c\|^2 \, (1 + \kappa_2^2)^{1/2} \, \|\mathbf{z}\|_{1,\Omega} \, \|\vec{\boldsymbol{\zeta}}\|_{\mathbf{H}} \, \|\vec{\boldsymbol{\tau}}\|_{\mathbf{H}} \qquad \forall\, \mathbf{z} \in \mathbf{H}^1(\Omega), \; \forall\, \vec{\boldsymbol{\zeta}}, \; \vec{\boldsymbol{\tau}} \in \mathbf{H} \,. \tag{2.15}$$

Up to minor changes caused by the present non-homogeneous Dirichlet boundary condition for $\mathbf{u}$, the unique solvability of (2.11) was basically derived in [35]. In particular, it was proved there (cf. Lemma 3.1 of [35]) that for $\kappa_1$, $\kappa_3 > 0$ and $0 < \kappa_2 < 2\mu$, there exists $\alpha_{\mathbf{A}} > 0$, depending on $\kappa_1$, $\kappa_2$, $\kappa_3$, $\mu$, and the constants $c_1(\Omega)$ and $c_2(\Omega)$ (cf. Lemma 2.19 below), such that

$$\mathbf{A}(\vec{\boldsymbol{\tau}}, \vec{\boldsymbol{\tau}}) \;\geq\; \alpha_{\mathbf{A}} \, \|\vec{\boldsymbol{\tau}}\|^2_{\mathbf{H}} \qquad \forall\, \vec{\boldsymbol{\tau}} \in \mathbf{H} \,, \tag{2.16}$$

which, together with (2.15), yielded the $\mathbf{H}$-ellipticity of the bilinear form $\mathbf{A} + \mathbf{B}(\mathbf{z}; \cdot, \cdot)$ for sufficiently small $\mathbf{z}$. More precisely, for each $\mathbf{z} \in \mathbf{H}^1(\Omega)$ such that $\|\mathbf{z}\|_{1,\Omega} \leq \frac{\alpha_{\mathbf{A}}}{2 \, \|\mathbf{i}_c\|^2 \, (1+\kappa_2^2)^{1/2}}$, there holds (cf. Eq. (3.16) of [35])

$$\mathbf{A}(\vec{\boldsymbol{\tau}}, \vec{\boldsymbol{\tau}}) \,+\, \mathbf{B}(\mathbf{z}; \vec{\boldsymbol{\tau}}, \vec{\boldsymbol{\tau}}) \;\geq\; \frac{\alpha_{\mathbf{A}}}{2} \, \|\vec{\boldsymbol{\tau}}\|^2_{\mathbf{H}} \qquad \forall\, \vec{\boldsymbol{\tau}} \in \mathbf{H} \,. \tag{2.17}$$

In addition, letting $\boldsymbol{\gamma}_0 : \mathbf{H}^1(\Omega) \to \mathbf{L}^2(\Omega)$ be the usual trace operator, it was shown (cf. eqs. (3.6) and (3.9) of [35]) that there exist $C_{\mathbf{A}}$, $M_{\mathbf{F}} > 0$, depending on $\kappa_1$, $\kappa_2$, $\kappa_3$, $\mu$, and $\|\boldsymbol{\gamma}_0\|$, such that

$$|\, \mathbf{A}(\vec{\boldsymbol{\zeta}}, \vec{\boldsymbol{\tau}}) \,| \;\leq\; C_{\mathbf{A}} \, \|\vec{\boldsymbol{\zeta}}\|_{\mathbf{H}} \, \|\vec{\boldsymbol{\tau}}\|_{\mathbf{H}} \qquad \forall\, \vec{\boldsymbol{\zeta}}, \; \vec{\boldsymbol{\tau}} \in \mathbf{H} \,, \tag{2.18}$$

and

$$|\mathbf{F}(\vec{\boldsymbol{\tau}})| \;\leq\; M_{\mathbf{F}} \Big\{ \|\mathbf{f}\|_{0,\Omega} \,+\, \|\mathbf{g}\|_{0,\Gamma} \,+\, \|\mathbf{g}\|_{1/2,\Gamma} \Big\} \, \|\vec{\boldsymbol{\tau}}\|_{\mathbf{H}} \qquad \forall\, \vec{\boldsymbol{\tau}} \in \mathbf{H} \,. \tag{2.19}$$

In this way, reformulating (2.11) as a fixed-point operator equation, and assuming that $\mathbf{f}$ and $\mathbf{g}$ are suitably bounded, the well-posedness of (2.11) was established thanks to the Lax-Milgram Lemma and the Banach fixed-point Theorem. The corresponding result is stated as follows.

**Theorem 2.1.** *Let $\kappa_1$, $\kappa_3 > 0$, $0 < \kappa_2 < 2\mu$, and given $\rho \in \Big(0, \frac{\alpha_{\mathbf{A}}}{2 \, \|\mathbf{i}_c\|^2 \, (1+\kappa_2^2)^{1/2}}\Big)$ (cf. (2.9) and (2.16)), set $W_\rho := \big\{ \mathbf{z} \in \mathbf{H}^1(\Omega) : \; \|\mathbf{z}\|_{1,\Omega} \leq \rho \big\}$. In addition, assume that the data $\mathbf{f} \in \mathbf{L}^2(\Omega)$ and $\mathbf{g} \in \mathbf{H}^{1/2}(\Gamma)$ satisfy (cf. (2.19))*

$$M_{\mathbf{F}} \Big\{ \|\mathbf{f}\|_{0,\Omega} \,+\, \|\mathbf{g}\|_{0,\Gamma} \,+\, \|\mathbf{g}\|_{1/2,\Gamma} \Big\} \;\leq\; \frac{\alpha_{\mathbf{A}}}{2} \, \rho \,.$$

*Then, there exists a unique* $\vec{\boldsymbol{\sigma}} := (\boldsymbol{\sigma}, \mathbf{u}) \in \mathbf{H}$ *solution of* (2.11)*, with* $\mathbf{u} \in W_\rho$*, and there holds*

$$\|\vec{\boldsymbol{\sigma}}\|_{\mathbf{H}} \leq C_{\mathbf{T}} \left\{ \|\mathbf{f}\|_{0,\Omega} + \|\mathbf{g}\|_{0,\Gamma} + \|\mathbf{g}\|_{1/2,\Gamma} \right\}$$

*with the constant* $C_{\mathbf{T}} := \frac{2\, M_{\mathbf{F}}}{\alpha_{\mathbf{A}}}$.

*Proof.* We omit details and refer to Theorem 3.4 of [35] (see also Theorem 3.9 of [34] for a similar proof). □

## 2.3 The virtual element subspaces

### 2.3.1 Preliminaries

Let $\{\mathcal{T}_h\}_{h>0}$ be a family of decompositions of $\Omega$ in polygonal elements. For each $K \in \mathcal{T}_h$ we denote its barycenter, diameter, and number of edges by $\mathbf{x}_K$, $h_K$, and $d_K$, respectively, and define, as usual, $h := \max\{h_K : K \in \mathcal{T}_h\}$. Furthermore, in what follows we assume that there exists a constant $C_{\mathcal{T}} > 0$ such that for each decomposition $\mathcal{T}_h$ and for each $K \in \mathcal{T}_h$ there hold:

a) the ratio between the shortest edge and the diameter $h_K$ of $K$ is bigger than $C_{\mathcal{T}}$, and

b) $K$ is star-shaped with respect to a ball $B$ of radius $C_{\mathcal{T}} h_K$ and center $\mathbf{x}_B \in K$, that is , for each $x_0 \in B$, all the line segments joining $x_0$ with any $x \in K$ are contained in $K$, or equivalently, for each $x \in K$, the closed convex hull of $\{x\} \cup B$ is contained in $K$.

As consequence of the above hypotheses, one can show that each $K \in \mathcal{T}_h$ is simply connected, and that there exists an integer $N_{\mathcal{T}}$ (depending only on $C_{\mathcal{T}}$), such that $d_K \leq N_{\mathcal{T}} \quad \forall\, K \in \mathcal{T}_h$.

Now, given an integer $\ell \geq 0$ and $\mathcal{O} \subseteq \mathrm{R}^2$, we let $\mathrm{P}_\ell(\mathcal{O})$ be the space of polynomials on $\mathcal{O}$ of degree up to $\ell$, we set $\mathbf{P}_\ell(\mathcal{O}) := [\mathrm{P}_\ell(\mathcal{O})]^2$ and $\mathbb{P}_\ell(\mathcal{O}) := [\mathrm{P}_\ell(\mathcal{O})]^{2\times 2}$. Also, in what follows we use the multi-index notation, that is, given $\mathbf{x} := (x_1, x_2)^{\mathbf{t}} \in \mathrm{R}^2$ and $\boldsymbol{\alpha} := (\alpha_1, \alpha_2)^{\mathbf{t}}$, with non-negative integers $\alpha_1, \alpha_2$, we let $\mathbf{x}^{\boldsymbol{\alpha}} := x_1^{\alpha_1} x_2^{\alpha_2}$ and $|\boldsymbol{\alpha}| := \alpha_1 + \alpha_2$. Furthermore, given $K \in \mathcal{T}_h$ and an edge $e \in \partial K$ with barycentric $x_e$ and diameter $h_e$, we introduce the following sets of $(\ell+1)$ normalized monomials on $e$

$$\mathcal{B}_\ell(e) := \left\{ \left( \frac{x - x_e}{h_e} \right)^j \right\}_{0 \leq j \leq \ell},$$

and $\frac{1}{2}(\ell+1)(\ell+2)$ normalized monomials on $K$

$$\mathcal{B}_\ell(K) := \left\{ \left( \frac{\mathbf{x} - \mathbf{x}_K}{h_K} \right)^{\boldsymbol{\alpha}} \right\}_{0 \leq |\boldsymbol{\alpha}| \leq \ell},$$

which constitute basis of $\mathrm{P}_\ell(e)$ and $\mathrm{P}_\ell(K)$, respectively. In addition, denoting $\widetilde{\mathcal{B}}_1(K) := \mathcal{B}_1(K)$, we define for each integer $\ell \geq 2$,

$$\widetilde{\mathcal{B}}_\ell(K) := \mathcal{B}_\ell(K) \setminus \mathcal{B}_{\ell-2}(K),$$

which is a basis of the subspace of polynomials on $K$ of degree exactly $\ell-1$ or $\ell$. In turn, the corresponding vector and tensor versions of the foregoing sets of monomials are given by

$$\begin{aligned}\boldsymbol{\mathcal{B}}_\ell(e) &:= \Big\{(q,0)^{\mathbf{t}}: \quad q\in\mathcal{B}_\ell(e)\Big\}\cup\Big\{(0,q)^{\mathbf{t}}: \quad q\in\mathcal{B}_\ell(e)\Big\},\\ \boldsymbol{\mathcal{B}}_\ell(K) &:= \Big\{(\mathbf{q},0)^{\mathbf{t}}: \quad \mathbf{q}\in\mathcal{B}_\ell(K)\Big\}\cup\Big\{(0,\mathbf{q})^{\mathbf{t}}: \quad \mathbf{q}\in\mathcal{B}_\ell(K)\Big\},\end{aligned}$$

and

$$\widetilde{\boldsymbol{\mathcal{B}}}_\ell(K) := \Big\{(\mathbf{q},0)^{\mathbf{t}}: \quad \mathbf{q}\in\widetilde{\mathcal{B}}_\ell(K)\Big\}\cup\Big\{(0,\mathbf{q})^{\mathbf{t}}: \quad \mathbf{q}\in\widetilde{\mathcal{B}}_\ell(K)\Big\}.$$

On the other hand, for each integer $\ell\geq 0$, we let $\mathcal{G}_\ell(K)$ be a basis of $\big(\nabla\mathrm{P}_{\ell+1}(K)\big)^{\perp}\cap\mathbf{P}_\ell(K)$, which is the $\mathbf{L}^2(K)$-orthogonal of $\nabla\mathbf{P}_{\ell+1}(K)$ in $\mathbf{P}_\ell(K)$, and denote its vectorial counterparts as follow:

$$\boldsymbol{\mathcal{G}}_\ell(K) := \left\{\begin{pmatrix}\mathbf{q}\\ \mathbf{0}\end{pmatrix}: \mathbf{q}\in\mathcal{G}_\ell(K)\right\}\cup\left\{\begin{pmatrix}\mathbf{0}\\ \mathbf{q}\end{pmatrix}: \mathbf{q}\in\mathcal{G}_\ell(K)\right\}.$$

Finally, we let

$$\mathbf{H}^1(\mathcal{T}_h) := \Big\{\mathbf{v}\in\mathbf{L}^2(\Omega): \quad \mathbf{v}|_K\in\mathbf{H}^1(K) \quad \forall\, K\in\mathcal{T}_h\Big\},$$

and consider the $\mathbf{H}^1$–broken seminorm

$$|\mathbf{v}|_{1,h} := \left\{\sum_{K\in\mathcal{T}_h}\|\nabla\mathbf{v}\|^2_{0,K}\right\}^{1/2} \qquad \forall\,\mathbf{v}\in\mathbf{H}^1(\mathcal{T}_h).$$

### 2.3.2 The virtual element subspace of $\mathbf{H}^1(\Omega)$

In this section we present a suitable choice for the virtual element subspace of $\mathbf{H}^1(\Omega)$. To this end, given $K\in\mathcal{T}_h$ and an integer $k\geq 1$, we first let $\mathcal{R}_k^K:\mathbf{H}^1(K)\to\mathbf{P}_k(K)$ be the projection operator defined for each $\mathbf{v}\in\mathbf{H}^1(K)$ as the unique polynomial $\mathcal{R}_k^K(\mathbf{v})\in\mathbf{P}_k(K)$ satisfying (cf. [16])

$$\begin{aligned}\int_K\nabla\mathcal{R}_k^K(\mathbf{v}):\nabla\mathbf{q} &= \int_K\nabla\mathbf{v}:\nabla\mathbf{q} \qquad \forall\,\mathbf{q}\in\mathbf{P}_k(K),\\ \int_{\partial K}\mathcal{R}_k^K(\mathbf{v}) &= \int_{\partial K}\mathbf{v}.\end{aligned} \tag{2.20}$$

Notice, however, that a modified version of $\mathcal{R}_k^K$ can be found in [4]. Also, it is readily seen from the first equation of (2.20) that

$$|\mathcal{R}_k^K(\mathbf{v})|_{1,K}\leq|\mathbf{v}|_{1,K} \qquad \forall\,\mathbf{v}\in\mathbf{H}^1(K). \tag{2.21}$$

In addition, we recall from Lemma 5.1 of [16] that for integers $s\in[1,k+1]$ and $m\in[1,s]$, there holds

$$\|\mathbf{v}-\mathcal{R}_k^K(\mathbf{v})\|_{m,K}\leq C\,h_K^{s-m}\,|\mathbf{v}|_{s,K} \qquad \forall\,\mathbf{v}\in\mathbf{H}^s(K), \quad \forall\,K\in\mathcal{T}_h. \tag{2.22}$$

Furthermore, we now consider the finite-dimensional subspace of $\mathbf{C}(\partial K)$ given by

$$\mathbb{B}_k(\partial K) := \Big\{\mathbf{v}\in\mathbf{C}(\partial K): \quad \mathbf{v}|_e\in\mathbf{P}_k(e), \quad \forall\text{ edge } e\subseteq\partial K\Big\},$$

define the following local virtual element space of order $k$ (see, e.g. [4])

$$V_k^K := \Big\{ \mathbf{v} \in \mathbf{H}^1(K) : \quad \mathbf{v}|_{\partial K} \in \mathbb{B}_k(\partial K)\,, \quad \Delta \mathbf{v}|_K \in \mathbf{P}_k(K)\,, \\ \text{and} \quad \int_K \big\{ \mathcal{R}_k^K(\mathbf{v}) - \mathbf{v} \big\} \cdot \mathbf{p} \;=\; 0 \qquad \forall\, \mathbf{p} \in \widetilde{\boldsymbol{\mathcal{B}}}_k(K) \Big\}\,, \tag{2.23}$$

and recall from [4] the following degrees of freedom for a given $\mathbf{v} \in V_k^K$

$$\begin{aligned} m_{i,v}^V(\mathbf{v}) &:= \text{value of } \mathbf{v} \text{ at the } i\text{th vertex of } K\,, \quad \forall\, i \text{ vertex of } K \\ m_e^V(\mathbf{v}) &:= \text{values of } \mathbf{v} \text{ at } k-1 \text{ uniformly spaced points on } e\,,\ \forall\, e \in \partial K\,, \text{ for } k \geq 2\,, \\ m_{\mathbf{q},K}^V(\mathbf{v}) &:= \text{value of } \int_K \mathbf{v} \cdot \mathbf{q}\,,\ \forall\, \mathbf{q} \in \boldsymbol{\mathcal{B}}_{k-2}(K)\,, \text{ for } k \geq 2\,. \end{aligned} \tag{2.24}$$

Then, the following result summarizes the unisolvency of (2.24) with respect to $V_k^K$.

**Lemma 2.2.** *Let $k \geq 1$ be an integer. Then the amount of degrees of freedom defined by (2.24) is given by $n_{k,K}^V := \dim V_k^K = 2k\,d_K + k(k-1)$. In addition, they are unisolvent with respect to $V_k^K$.*

*Proof.* We refer to Propositions 1 and 2 in [4] for details. □

In what follows we show that for each $\mathbf{v} \in V_k^K$ its projection $\mathcal{R}_k^K(\mathbf{v})$ can be computed explicitly by using the degrees of freedom defined in (2.24). In fact, we begin by noticing that, given $\mathbf{v} \in V_k^K$ and $\mathbf{q} \in \mathbf{P}_k(K)$, the right-hand side of the first equation of (2.20) can be integrated by parts to yield

$$\int_K \nabla \mathbf{v} : \nabla \mathbf{q} \;=\; -\int_K \mathbf{v} \cdot \Delta \mathbf{q} \;+\; \int_{\partial K} (\nabla \mathbf{q}) \mathbf{n} \cdot \mathbf{v}\,.$$

Since $\Delta \mathbf{q} \in \mathbf{P}_{k-2}(K)$, the first term on the right-hand side of the foregoing equation can be computed by using the moments $m_{\mathbf{q},K}^V(\mathbf{v})$, whereas for the second one the degrees of freedom given by $m_{i,v}^V(\mathbf{v})$ and $m_e^V(\mathbf{v})$ are employed. In turn, it is straightforward to see that the right-hand side of the second equation of (2.20) can be calculated using also $m_{i,v}^V(\mathbf{v})$ and $m_e^V(\mathbf{v})$.

Furthermore, we now denote by $\{m_{j,K}^V(\mathbf{v})\}_{j=1}^{n_{k,K}^V}$ the degrees of freedom defined by (2.24), and let $\Pi_k^K : \mathbf{H}^1(K) \to V_k^K$ be the associated local interpolation operator, that is, given $\mathbf{v} \in \mathbf{H}^1(K)$, $\Pi_k^K(\mathbf{v})$ is the unique element in $V_k^K$ such that $\quad m_{j,K}^V(\mathbf{v} - \Pi_k^K(\mathbf{v})) \;=\; 0 \qquad \forall\, j \in \big\{1, 2, \ldots, n_{k,K}^V\big\}\,.$

The following lemma establishes the approximation properties of $\Pi_k^K$.

**Lemma 2.3.** *Let $k, m$ and $s$ be integers such $0 \leq m \leq 1$ and $2 \leq s \leq k+1$. Then, there exists a constant $C > 0$, independent of $K$, such that for each $K \in \mathcal{T}_h$, there holds*

$$|\mathbf{v} - \Pi_k^K(\mathbf{v})|_{m,K} \;\leq\; C\, h_K^{s-m}\, |\mathbf{v}|_{s,K} \qquad \forall\, \mathbf{v} \in \mathbf{H}^s(K)\,.$$

*Proof.* See Proposition 4 of [4]. □

We end this section by establishing the virtual element space on the whole $\Omega$. Indeed, for every polygonal decomposition $\mathcal{T}_h$ of $\Omega$, and for every integer $k \geq 1$, we consider the following virtual element subspace of $\mathbf{H}^1(\Omega)$

$$V_k^h := \left\{ \mathbf{v} \in \mathbf{H}^1(\Omega) : \quad \mathbf{v}|_K \in V_k^K \quad \forall\, K \in \mathcal{T}_h \right\}. \tag{2.25}$$

In addition, we remark here that, for a given $\mathbf{v} \in V_k^h$, the local degrees of freedom defined by $m_{i,v}^V(\mathbf{v})$ and $m_e^V(\mathbf{v})$ in (2.24), together with the fact that $\mathbf{v}|_e \in \mathbf{P}_k(e) \quad \forall\, e \in \mathcal{T}_h$ (cf. (2.23)), guarantee the continuity of the trace of $\mathbf{v}$ across the edges $e$ of $\mathcal{T}_h$. It follows that $\mathbf{v} \in \mathbf{H}^1(\Omega)$, which confirms that $V_k^h$ is in fact a $\mathbf{H}^1(\Omega)$-conforming subspace. According to this discussion and Lemma 2.3, the approximation property of $V_k^h$ is given by:

$(\mathbf{AP}_h^{\mathbf{u}})$ : there exists $C > 0$, independent of $h$, such that for each integer $s \in [2, k+1]$ there holds

$$\mathrm{dist}(\mathbf{v}, V_k^h) := \inf_{\mathbf{v}_h \in V_k^h} \|\mathbf{v} - \mathbf{v}_h\|_{1,\Omega} \;\leq\; C h^{s-1} \left\{ \sum_{K \in \mathcal{T}_h} |\mathbf{v}|_{s,K}^2 \right\}^{1/2}$$

for all $\mathbf{v} \in \mathbf{H}^1(\Omega)$ such that $\mathbf{v}|_K \in \mathbf{H}^s(K) \quad \forall\, K \in \mathcal{T}_h$.

### 2.3.3 The virtual element subspace of $\mathbb{H}_0(\mathbf{div}; \Omega)$

Throughout this section we consider an integer $k \geq 1$. Then, given $K \in \mathcal{T}_h$, we introduce the local virtual element space $H_k^K$ of order $k$ as follows (see, e.g. [15, 28, 30, 14])

$$\begin{aligned} H_k^K := \Big\{ \boldsymbol{\tau} \in \mathbb{H}(\mathbf{div}; K) \cap \mathbb{H}(\mathbf{rot}; K) \;:\; & \boldsymbol{\tau}\mathbf{n}|_e \in \mathbf{P}_k(e) \quad \forall \text{ edge } e \in \partial K\,, \\ & \mathbf{div}(\boldsymbol{\tau})|_K \in \mathbf{P}_{k-1}(K)\,, \quad \text{and} \quad \mathbf{rot}(\boldsymbol{\tau})|_K \in \mathbf{P}_{k-1}(K) \Big\}\,, \end{aligned} \tag{2.26}$$

whose local degrees of freedom are given by (see [14])

$$\begin{aligned} m_{\mathbf{q},\mathbf{n}}^H(\boldsymbol{\tau}) &:= \int_e \boldsymbol{\tau}\mathbf{n} \cdot \mathbf{q} \qquad \forall\, \mathbf{q} \in \boldsymbol{\mathcal{B}}_k(e)\,, \quad \forall \text{ edge } e \in \partial K\,, \\ m_{\mathbf{q},\mathbf{div}}^H(\boldsymbol{\tau}) &:= \int_K \boldsymbol{\tau} : \nabla \mathbf{q} \qquad \forall\, \mathbf{q} \in \boldsymbol{\mathcal{B}}_{k-1}(K) \setminus \{(1,0)^{\mathbf{t}}, (0,1)^{\mathbf{t}}\}\,, \\ m_{\boldsymbol{\rho},\mathbf{rot}}^H(\boldsymbol{\tau}) &:= \int_K \boldsymbol{\tau} : \boldsymbol{\rho} \qquad \forall\, \boldsymbol{\rho} \in \boldsymbol{\mathcal{G}}_k(K)\,. \end{aligned} \tag{2.27}$$

The unisolvency of (2.27) in $H_k^K$ is summarized as follows.

**Lemma 2.4.** *The amount of local degrees of freedom defined in (2.27) is given by*

$$n_{k,K}^H := \dim H_k^K = 2\left\{(k+1)(d_K + k) - 1\right\},$$

*where $d_K$ is the number of edges of $K \in \mathcal{T}_h$. In addition, the local degrees of freedom (2.27) are unisolvent in $H_k^K$.*

*Proof.* See Theorem 1 of [14] for details. □

At this point we remark that the introduction of the local virtual element space $H_k^K$ (cf. (2.26)) has been motivated only by its previous use in the design of a mixed virtual element method for the Stokes equations (see [30]), which, in turn, has simply followed the approach suggested in the seminal work [28], in which the basic principles of the mixed virtual element schemes were established. A cheaper space, in terms of degrees of freedom, is the following one originally proposed in [15] for $k \geq 0$

$$H_k^K := \Big\{ \boldsymbol{\tau} \in \mathbb{H}(\mathbf{div}; K) \cap \mathbb{H}(\mathbf{rot}; K) : \quad \boldsymbol{\tau}\mathbf{n}|_e \in \mathbf{P}_k(e) \quad \forall \text{ edge } e \in \partial K \,, \\ \mathbf{div}(\boldsymbol{\tau})|_K \in \mathbf{P}_k(K) \,, \quad \text{and} \quad \mathbf{rot}(\boldsymbol{\tau})|_K \in \mathbf{P}_{k-1}(K) \Big\} \,, \tag{2.28}$$

which has been recently employed by some of the present authors in [31, 68]. Since the analysis that follows should also apply to (2.28) instead of (2.26), we plan to incorporate the use of (2.28) in a forthcoming paper dealing with the computational implementation of the resulting mixed virtual element scheme to be defined later on in (2.66).

We now gather all the degrees of freedom (2.27) in the set $\{m_{j,K}^H(\boldsymbol{\tau})\}_{j=1}^{n_{k,K}^H}$, and then, we introduce the interpolation operator $\boldsymbol{\Pi}_k^K : \mathbb{H}^1(K) \to H_k^K$, which is defined for each $\boldsymbol{\tau} \in \mathbb{H}^1(K)$ as the unique $\boldsymbol{\Pi}_k^K(\boldsymbol{\tau})$ in $H_k^h$ such that

$$m_{j,K}^H(\boldsymbol{\tau} - \boldsymbol{\Pi}_k^K(\boldsymbol{\tau})) \;=\; 0 \qquad \forall\, j \in \{1, 2, \ldots, n_{k,K}^H\} \,.$$

Concerning the approximation properties of $\boldsymbol{\Pi}_k^K$, we first recall from Eq. (3.19) in [15] that for each integer $s \in [1, k+1]$ there exists $C > 0$, independent of $K$, such that

$$\|\boldsymbol{\tau} - \boldsymbol{\Pi}_k^K(\boldsymbol{\tau})\|_{0,K} \;\leq\; C\, h_K^s\, |\boldsymbol{\tau}|_{s,K} \qquad \forall\, \boldsymbol{\tau} \in \mathbb{H}^s(K) \,. \tag{2.29}$$

In addition, similarly to Eq. (3.14) in [31], it is easy to check that

$$\mathbf{div}(\boldsymbol{\Pi}_k^K(\boldsymbol{\tau})) \;=\; \mathcal{P}_{k-1}^K(\mathbf{div}(\boldsymbol{\tau})) \qquad \forall\, \boldsymbol{\tau} \in \mathbb{H}^1(K) \,,$$

where $\mathcal{P}_{k-1}^K : \mathbf{L}^2(K) \to \mathbf{P}_{k-1}(K)$ is the orthogonal projector (see Section 2.3.4 below). In this way, applying (2.34) we deduce that for each integer $s \in [0, k]$ there exists $C > 0$, independent of $K$, such that

$$\|\mathbf{div}(\boldsymbol{\tau}) - \mathbf{div}(\boldsymbol{\Pi}_k^K(\boldsymbol{\tau}))\|_{0,K} \;\leq\; C\, h_K^s\, |\mathbf{div}(\boldsymbol{\tau})|_{s,K} \qquad \forall\, \boldsymbol{\tau} \in \mathbb{H}^1(K) \text{ with } \mathbf{div}(\boldsymbol{\tau}) \in \mathbf{H}^s(K) \,. \tag{2.30}$$

The foregoing estimate together with (2.29) yields the following result.

**Lemma 2.5.** *For each integer $s \in [1, k]$ there exists $C > 0$, independent of $K$, such that*

$$\|\boldsymbol{\tau} - \boldsymbol{\Pi}_k^K(\boldsymbol{\tau})\|_{\mathbf{div};K} \;\leq\; C\, h_K^s \Big\{ |\boldsymbol{\tau}|_{s,K} \,+\, |\mathbf{div}(\boldsymbol{\tau})|_{s,K} \Big\} \qquad \forall\, \boldsymbol{\tau} \in \mathbb{H}^s(K) \text{ with } \mathbf{div}(\boldsymbol{\tau}) \in \mathbf{H}^s(K) \,.$$

*Proof.* It follows straightforwardly from (2.29) and (2.30). □

Finally, for every integer $k \geq 1$ we define the global virtual element subspaces of $\mathbb{H}_0(\mathbf{div}; \Omega)$ as

$$H_k^h := \Big\{ \boldsymbol{\tau} \in \mathbb{H}_0(\mathbf{div}; \Omega) : \quad \boldsymbol{\tau}|_K \in H_k^K \quad \forall\, K \in \mathcal{T}_h \Big\} \,. \tag{2.31}$$

Note here that given $\boldsymbol{\tau} \in H_k^h$, the local degrees of freedom defined by $m^H_{\mathbf{q},\mathbf{n}}(\boldsymbol{\tau})$ in (2.27), along with the fact that $\boldsymbol{\tau}\mathbf{n}|_e \in \mathbf{P}_k(e) \quad \forall$ edge $e \in \mathcal{T}_h$ (cf. (2.26)), guarantee the continuity of the normal components of $\boldsymbol{\tau}$ across the edges $e$ of $\mathcal{T}_h$. It follows that $\boldsymbol{\tau} \in \mathbb{H}(\mathbf{div};\Omega)$, which confirms that $H_k^h$ is in fact contained in $\mathbb{H}(\mathbf{div};\Omega)$. Also, using this and Lemma 2.5, it is easy to obtain the following approximation property:

($\mathbf{AP}^{\boldsymbol{\sigma}}_h$) For each integer $s \in [1,k]$ there exists $C>0$, independent of $h$, such that

$$\mathrm{dist}(\boldsymbol{\tau}, H_k^h) := \inf_{\boldsymbol{\tau}_h \in H_k^h} \|\boldsymbol{\tau}-\boldsymbol{\tau}_h\|_{\mathbf{div};\Omega} \leq C\, h^s \left\{ \sum_{K\in\mathcal{T}_h} \left( |\boldsymbol{\tau}|^2_{s,K} + |\mathbf{div}(\boldsymbol{\tau})|^2_{s,K} \right) \right\}^{1/2}$$

for all $\boldsymbol{\tau} \in \mathbb{H}_0(\mathbf{div};\Omega)$ such that $\boldsymbol{\tau}|_K \in \mathbb{H}^s(K)$ and $\mathbf{div}(\boldsymbol{\tau})|_K \in \mathbf{H}^s(K)$, for all $K \in \mathcal{T}_h$.

### 2.3.4 $\mathbf{L}^2$-orthogonal projections

We now let $\mathcal{P}_k^K : \mathbf{L}^2(K) \to \mathbf{P}_k(K)$ and $\boldsymbol{\mathcal{P}}_k^K : \mathbb{L}^2(K) \to \mathbb{P}_k(K)$ be the vectorial and tensorial versions of the $\mathrm{L}^2(K)$-orthogonal projector, respectively, which, given $\mathbf{v} \in \mathbf{L}^2(K)$ and $\boldsymbol{\tau} \in \mathbb{L}^2(K)$, are characterized by

$$\mathcal{P}_k^K(\mathbf{v}) \in \mathbf{P}_k(K) \quad \text{and} \quad \int_K \mathcal{P}_k^K(\mathbf{v})\cdot\mathbf{q} = \int_K \mathbf{v}\cdot\mathbf{q} \qquad \forall\, \mathbf{q} \in \mathbf{P}_k(K) \tag{2.32}$$

and

$$\boldsymbol{\mathcal{P}}_k^K(\boldsymbol{\tau}) \in \mathbb{P}_k(K) \quad \text{and} \quad \int_K \boldsymbol{\mathcal{P}}_k^K(\boldsymbol{\tau}) : \mathbf{p} = \int_K \boldsymbol{\tau} : \mathbf{p} \qquad \forall\, \mathbf{p} \in \mathbb{P}_k(K)\,, \tag{2.33}$$

respectively. In addition, it is well-known (see, e.g. [30, Lemma 3.4]) that, given integers $k$, $s$, and $m$ such that $k \geq 0$, $s \in [1, k+1]$, and $m \in [0, s]$, there hold the following approximation properties

$$\|\mathbf{v} - \mathcal{P}_k^K(\mathbf{v})\|_{m,K} \leq C\, h_K^{s-m}\, |\mathbf{v}|_{s,K} \qquad \forall\, \mathbf{v} \in \mathbf{H}^s(K)\,, \quad \forall\, K \in \mathcal{T}_h\,, \tag{2.34}$$

and

$$\|\boldsymbol{\tau} - \boldsymbol{\mathcal{P}}_k^K(\boldsymbol{\tau})\|_{m,K} \leq C\, h_K^{s-m}\, |\boldsymbol{\tau}|_{s,K} \qquad \forall\, \boldsymbol{\tau} \in \mathbb{H}^s(K)\,, \quad \forall\, K \in \mathcal{T}_h\,. \tag{2.35}$$

In addition, we remark here that the degrees of freedom given by (2.24) do allow the explicit calculation of the right-hand side of (2.32) (and hence of $\mathcal{P}_k^K(\mathbf{v})$) for each $\mathbf{v} \in V_k^K$. Indeed, it is easy to see first that the degrees of freedom given by $m^V_{\mathbf{q},K}(\mathbf{v})$ (cf. (2.24)) yields the computation of $\int_K \mathbf{v}\cdot\mathbf{q}$ when $\mathbf{q} \in \boldsymbol{\mathcal{B}}_{k-2}(K)$, whereas for $\mathbf{q} \in \widetilde{\boldsymbol{\mathcal{B}}}_k(K)$ we recall from (2.23) that

$$\int_K \mathbf{v}\cdot\mathbf{q} = \int_K \mathcal{R}_k^K(\mathbf{v})\cdot\mathbf{q}\,, \tag{2.36}$$

and then use that $\mathcal{R}_k^K(\mathbf{v})$ is explicitly computable for each $\mathbf{v} \in V_k^K$ .

On the other hand, we now aim to derive additional approximation properties for the projection $\mathcal{P}_k^K$. The goal is to extend the estimate (2.34) to the case of general Sobolev spaces. To this end, we need to recall from Section 3.3 of [30] some preliminary notations and technical results. Indeed, for each element $K \in \mathcal{T}_h$ we first define $\widetilde{K} := T_K(K)$, where $T_K : \mathrm{R}^2 \to \mathrm{R}^2$ is the bijective affine mapping defined by

$$T_K(\mathbf{x}) := \frac{\mathbf{x} - \mathbf{x}_B}{h_K} \quad \forall\, \mathbf{x} \in \mathrm{R}^2\,.$$

Then, as it was remarked in Section 3.3 of [30], it is easy to see that the diameter $h_{\widetilde{K}}$ of $\widetilde{K}$ is 1, the shortest edge of $\widetilde{K}$ is bigger than $C_{\mathcal{T}}$ (which follows from assumptions (i) and (ii) above), and $\widetilde{K}$ is star-shaped with respect to a ball $\widetilde{B}$ of radius $C_{\mathcal{T}}$ and centered at the origin. Then, by connecting each vertex of $\widetilde{K}$ to the center of $\widetilde{B}$, that is to the origin, we generate a partition of $\widetilde{K}$ into $d_{\widetilde{K}}$ triangles $\widetilde{\Delta}_i$, $i \in \{1,2,\ldots,d_{\widetilde{K}}\}$, where $d_{\widetilde{K}} \leq N_{\mathcal{T}}$, and for which the minimum angle condition is satisfied. The later means that there exists a constant $c_{\mathcal{T}} > 0$, depending only on $C_{\mathcal{T}}$ and $N_{\mathcal{T}}$, such that $\widetilde{h}_i(\widetilde{\rho}_i)^{-1} \leq c_{\mathcal{T}} \quad \forall\, i \in \{1,2,\ldots,d_{\widetilde{K}}\}$, where $\widetilde{h}_i$ is the diameter of $\widetilde{\Delta}_i$ and $\widetilde{\rho}_i$ is the diameter of the largest ball contained in $\widetilde{\Delta}_i$. We also let $\widehat{\Delta}$ be the canonical triangle of $\mathrm{R}^2$ with corresponding parameters $\widehat{h}$ and $\widehat{\rho}$, and for each $i \in \{1,2,\ldots,d_{\widetilde{K}}\}$ we let $F_i : \mathrm{R}^2 \to \mathrm{R}^2$ be the bijective linear mapping, say $F_i(\mathbf{x}) := B_i\mathbf{x} \quad \forall\, \mathbf{x} \in \mathrm{R}^2$, with $B_i \in \mathrm{R}^{2\times 2}$ invertible, such that $F_i(\widehat{\Delta}) = \widetilde{\Delta}_i$. We remark that the fact that the origin is a vertex of each triangle $\widetilde{\Delta}_i$ allows to choose $F_i$ as indicated.

In what follows, given $K \in \mathcal{T}_h$ and $\mathbf{v} \in \mathbf{L}^2(K)$, we let $\widetilde{\mathbf{v}} := \mathbf{v} \circ T_K^{-1} \in \mathbf{L}^2(\widetilde{K})$. Also, we recall from the Introduction that given $r \geq 0$, $p > 1$, $p \neq 2$, and an arbitrary domain $\mathcal{O} \subseteq \mathrm{R}^2$, $\|\cdot\|_{r,p,\mathcal{O}}$ and $|\cdot|_{r,p,\mathcal{O}}$ stand for the norm and seminorm, respectively, of the Sobolev space $\mathrm{W}^{r,p}(\mathcal{O})$ and its vectorial and tensorial versions. Then, we have the following result.

**Lemma 2.6.** *Given an integer $\ell \geq 0$, there holds $\widetilde{\mathcal{P}_\ell^K(\mathbf{v})} = \mathcal{P}_\ell^{\widetilde{K}}(\widetilde{\mathbf{v}})$ for all $\mathbf{v} \in \mathbf{L}^2(K)$. In addition, for integers $r$, $s \geq 0$ and for $p \geq 2$, there holds $\mathcal{P}_\ell^{\widetilde{K}} \in \mathcal{L}(\mathbf{W}^{r,p}(\widetilde{K}), \mathbf{W}^{s,p}(\widetilde{K}))$, with $\|\mathcal{P}_\ell^{\widetilde{K}}\|_{\mathcal{L}(\mathbf{W}^{r,p}(\widetilde{K}),\mathbf{W}^{s,p}(\widetilde{K}))}$ independent of $\widetilde{K}$.*

*Proof.* We begin by recalling from Lemma 3.2 of [30] that $\widetilde{\mathcal{P}_\ell^K(\mathbf{v})} = \mathcal{P}_\ell^{\widetilde{K}}(\widetilde{\mathbf{v}})$ for all $\mathbf{v} \in \mathbf{L}^2(K)$. Next, denoting $N_\ell := (\ell+1)(\ell+2)$, we let $\{\widetilde{\boldsymbol{\varphi}}_1, \widetilde{\boldsymbol{\varphi}}_2, \ldots, \widetilde{\boldsymbol{\varphi}}_{N_\ell}\}$ be a $\mathbf{L}^2(\widetilde{K})$-orthonormal basis of $\mathbf{P}_\ell(\widetilde{K})$, which yields $\mathcal{P}_\ell^{\widetilde{K}}(\widetilde{\mathbf{v}}) = \sum_{j=1}^{N_\ell} \langle \widetilde{\mathbf{v}}, \widetilde{\boldsymbol{\varphi}}_j \rangle_{0,\widetilde{K}}\, \widetilde{\boldsymbol{\varphi}}_j \qquad \forall\, \widetilde{\mathbf{v}} \in \mathbf{L}^2(\widetilde{K})$. Now, given $p \geq 2$, we let $q$ be the conjugate of $p$, that is $q := \frac{p}{p-1}$. Thus, using the triangle and Hölder inequalities, we find that for any pair of non-negative integers $r$ and $s$ there holds

$$\begin{aligned}
\|\mathcal{P}_\ell^{\widetilde{K}}(\widetilde{\mathbf{v}})\|_{s,p,\widetilde{K}} &\leq \left\{ \sum_{j=1}^{N_\ell} \|\widetilde{\boldsymbol{\varphi}}_j\|_{0,q,\widetilde{K}} \|\widetilde{\boldsymbol{\varphi}}_j\|_{s,p,\widetilde{K}} \right\} \|\widetilde{\mathbf{v}}\|_{0,p,\widetilde{K}} \\
&\leq \left\{ \sum_{j=1}^{N_\ell} \|\widetilde{\boldsymbol{\varphi}}_j\|_{0,q,\widetilde{K}} \|\widetilde{\boldsymbol{\varphi}}_j\|_{s,p,\widetilde{K}} \right\} \|\widetilde{\mathbf{v}}\|_{r,p,\widetilde{K}} \qquad \forall\, \widetilde{\mathbf{v}} \in \mathbf{W}^{r,p}(\widetilde{K})\,,
\end{aligned}$$

which proves that $\mathcal{P}_\ell^{\widetilde{K}} \in \mathcal{L}(\mathbf{W}^{r,p}(\widetilde{K}), \mathbf{W}^{s,p}(\widetilde{K}))$ with

$$\|\mathcal{P}_\ell^{\widetilde{K}}\|_{\mathcal{L}(\mathbf{W}^{r,p}(\widetilde{K}),\mathbf{W}^{s,p}(\widetilde{K}))} \leq \sum_{j=1}^{N_\ell} \|\widetilde{\boldsymbol{\varphi}}_j\|_{0,q,\widetilde{K}} \|\widetilde{\boldsymbol{\varphi}}_j\|_{s,p,\widetilde{K}}\,.$$

In this way, applying the same arguments from the last part of the proof of Lemma 3.2 in [30], we deduce that $\|\mathcal{P}_\ell^{\widetilde{K}}\|_{\mathcal{L}(\mathbf{W}^{r,p}(\widetilde{K}),\mathbf{W}^{s,p}(\widetilde{K}))}$ is bounded independently of $\widetilde{K}$. In fact, using the afore described decomposition of $\widetilde{K}$, we can write

$$\|\widetilde{\boldsymbol{\varphi}}_j\|_{s,p,\widetilde{K}} = \left\{ \sum_{t=0}^{s} |\widetilde{\boldsymbol{\varphi}}_j|^p_{t,p,\widetilde{K}} \right\}^{1/p} = \left\{ \sum_{t=0}^{s} \sum_{i=1}^{d_{\widetilde{K}}} |\widetilde{\boldsymbol{\varphi}}_j|^p_{t,p,\widetilde{\Delta}_i} \right\}^{1/p}.$$

In turn, applying the usual scaling properties, we deduce the existence of a constant $\widetilde{C}_t > 0$, depending only on $t$, such that

$$|\widetilde{\boldsymbol{\varphi}}_j|_{t,p,\widetilde{\Delta}_i} \leq \widetilde{C}_t\, \widetilde{h}_i^{-t+2/p} |\widehat{\boldsymbol{\varphi}}_{j,i}|_{t,p,\widehat{\Delta}}\,,$$

where $\widehat{\boldsymbol{\varphi}}_{j,i} := \widetilde{\boldsymbol{\varphi}}_j|_{\widetilde{\Delta}_i} \circ F_i \in \mathbf{P}_l(\widehat{\Delta})$. Then, according to the equivalence of norms in $\mathbf{P}_l(\widehat{\Delta})$, we find that

$$|\widetilde{\boldsymbol{\varphi}}_j|_{t,p,\widetilde{\Delta}_i} \leq \widetilde{C}_t\, \widetilde{h}_i^{-t+2/p} \|\widehat{\boldsymbol{\varphi}}_{j,i}\|_{t,p,\widehat{\Delta}} \leq \widetilde{C}_t\, \widetilde{h}_i^{-t+2/p}\, \widehat{C}\, \|\widehat{\boldsymbol{\varphi}}_{j,i}\|_{0,\widehat{\Delta}}\,,$$

with a constant $\widehat{C} > 0$ depending on $t$, $p$, $\ell$, and $\widehat{\Delta}$. Moreover, applying again the scaling properties, we have that

$$\|\widehat{\boldsymbol{\varphi}}_{j,i}\|_{0,\widehat{\Delta}} \leq C_0\, \widetilde{h}_i^{-1}\, \|\widetilde{\boldsymbol{\varphi}}_j\|_{0,\widetilde{\Delta}_i} \leq C_0\, \widetilde{h}_i^{-1}\, \|\widetilde{\boldsymbol{\varphi}}_j\|_{0,\widetilde{K}} = C_0\, \widetilde{h}_i^{-1}\,,$$

with a constant $C_0 > 0$ depending only on $\widehat{\Delta}$, and using that $1 \leq \widetilde{h}_i^{-1} \leq C_{\mathcal{T}}^{-1}$, we get

$$|\widetilde{\boldsymbol{\varphi}}_j|_{t,p,\widetilde{\Delta}_i} \leq \widetilde{C}_t\, \widehat{C}\, C_0\, \widetilde{h}_i^{-t+2/p-1} \leq \widetilde{C}_t\, \widehat{C}\, C_0\, \widehat{C}_{\mathcal{T}}\,,$$

where

$$\widehat{C}_{\mathcal{T}} := \begin{cases} 1 & \text{if} \quad -t+2/p-1 \geq 0 \\ C_{\mathcal{T}}^{t+1-2/p} & \text{if} \quad -t+2/p-1 < 0 \end{cases}\,.$$

Finally, since $d_{\widetilde{K}} \leq N_{\mathcal{T}}$, we conclude that $\|\widetilde{\boldsymbol{\varphi}}_j\|_{s,p,\widetilde{K}}$ is bounded by a constant depending only on $s$, $p$, $N_{\mathcal{T}}$, $C_{\mathcal{T}}$, $\widehat{\Delta}$, and $\ell$. The estimate for $\|\widetilde{\boldsymbol{\varphi}}_j\|_{0,q,\widetilde{K}}$ proceeds similarly, and hence further details are omitted, thus concluding the proof. □

The next result is taken from Lemma 4.3.8 of [27].

**Lemma 2.7.** *Let $\mathcal{O}$ be star-shaped with respect to a ball $B$ with radius $\rho > \frac{1}{2}\rho_{\max}$, where $\rho_{\max} := \max\{\rho : \mathcal{O}$ is star-shaped with respect to a ball of radius $\rho\}$. In addition, given an integer $s \geq 0$, $p \geq 1$, and $\mathbf{v} \in \mathbf{W}^{s,p}(\mathcal{O})$, we let $\mathbf{Q}^s(\mathbf{v})$ be the Taylor polynomial of degree $s$ of $\mathbf{v}$ averaged over $B$. Then, there holds*

$$|\mathbf{v} - \mathbf{Q}^s(\mathbf{v})|_{m,p,\mathcal{O}} \leq C\, d^{s-m}\, |\mathbf{v}|_{s,p,\mathcal{O}} \qquad \forall\, m \in \{0,1,\ldots,s\}\,,$$

*where $d = \mathrm{diam}(\mathcal{O})$ and $C > 0$ depends on $s$ and the chunkiness parameter $d/\rho_{\max}$.*

The following lemma establishes the approximation properties of the projector $\mathcal{P}_k^K : \mathbf{L}^2(K) \to \mathbf{P}_k(K)$ with respect to more general Sobolev norms.

**Lemma 2.8.** *Let $K \in \mathcal{T}_h$ and $k$, $s$, $m$, and $p$ be integers such that $k \geq 0$, $0 \leq m \leq s \leq k+1$, and $p \geq 2$. Then, there exists a constant $C > 0$, independent of $K$, such that*

$$|\mathbf{v} - \mathcal{P}_k^K(\mathbf{v})|_{m,p,K} \leq C\, h_K^{s-m}\, |\mathbf{v}|_{s,p,K} \qquad \forall\, \mathbf{v} \in \mathbf{W}^{s,p}(K)\,. \tag{2.37}$$

*Proof.* Given $K \in \mathcal{T}_h$ and $\mathbf{v} \in \mathbf{W}^{s,p}(K)$, we first observe, thanks to the scaling properties, that there hold

$$|\widetilde{\mathbf{v}}|_{m,p,\widetilde{K}} \leq C_m\, h_K^{m-2/p}\, |\mathbf{v}|_{m,p,K} \quad \text{and} \quad |\mathbf{v}|_{m,p,K} \leq \widetilde{C}_m\, h_K^{-m+2/p}\, |\widetilde{\mathbf{v}}|_{m,p,\widetilde{K}}\,, \tag{2.38}$$

where $C_m$ and $\widetilde{C}_m$ are positive constants depending only on $m$. In turn, letting $\widetilde{\mathbf{Q}}^s(\widetilde{\mathbf{v}})$ be the Taylor polynomial of order $s$ of $\widetilde{\mathbf{v}}$ averaged over a ball of radius $> \frac{1}{2}\widetilde{\rho}_{\max}$, we have that $\widetilde{\mathbf{Q}}^s(\widetilde{\mathbf{v}}) \in \mathbf{P}_{s-1}(\widetilde{K}) \subseteq \mathbf{P}_k(\widetilde{K})$, which certainly yields

$$\mathcal{P}_k^{\widetilde{K}}(\widetilde{\mathbf{Q}}^s(\widetilde{\mathbf{v}})) = \widetilde{\mathbf{Q}}^s(\widetilde{\mathbf{v}})\,. \tag{2.39}$$

Recall here that $h_{\widetilde{K}} := \mathrm{diam}(\widetilde{K}) = 1$ and that $\widetilde{K}$ is star-shaped with respect to a ball $\widetilde{B}$ of radius $C_{\mathcal{T}}$ and centered at the origin. It follows, using (2.38), that

$$|\mathbf{v} - \mathcal{P}_k^K(\mathbf{v})|_{m,p,K} \;\leq\; \widetilde{C}_m\, h_K^{-m+2/p}\, |\widetilde{\mathbf{v}} - \widetilde{\mathcal{P}_k^K(\mathbf{v})}|_{m,p,\widetilde{K}} \;=\; \widetilde{C}_m\, h_K^{-m+2/p}\, |\widetilde{\mathbf{v}} - \mathcal{P}_k^{\widetilde{K}}(\widetilde{\mathbf{v}})|_{m,p,\widetilde{K}}\,,$$

and along with (2.39), we obtain from Lemmas 2.6 (with $r = s = m$) and 2.7 (with $\mathcal{O} = \widetilde{K}$), that

$$\begin{aligned}
|\mathbf{v} - \mathcal{P}_k^K(\mathbf{v})|_{m,p,K} &\leq \widetilde{C}_m\, h_K^{-m+2/p}\, |(I - \mathcal{P}_k^{\widetilde{K}})(\widetilde{\mathbf{v}} - \widetilde{\mathbf{Q}}^s(\widetilde{\mathbf{v}}))|_{m,p,\widetilde{K}} \\
&\leq \widetilde{C}_m\, \|I - \mathcal{P}_k^{\widetilde{K}}\|_{\mathcal{L}(\mathbf{W}^{m,p}(\widetilde{K}),\mathbf{W}^{m,p}(\widetilde{K}))} h_K^{-m+2/p} \|\widetilde{\mathbf{v}} - \widetilde{\mathbf{Q}}^s(\widetilde{\mathbf{v}})\|_{m,p,\widetilde{K}} \\
&\leq C\, h_K^{-m+2/p}\, h_{\widetilde{K}}^{s-m}\, |\widetilde{\mathbf{v}}|_{s,p,\widetilde{K}} \;=\; C\, h_K^{-m+2/p}\, |\widetilde{\mathbf{v}}|_{s,p,\widetilde{K}} \\
&\leq C\, h_K^{-m+2/p}\, h_K^{s-2/p}\, |\mathbf{v}|_{s,p,K} \;=\; C\, h_K^{s-m}\, |\mathbf{v}|_{s,p,K}\,,
\end{aligned}$$

which completes the proof of the lemma. □

As a consequence of the previous lemma, we have the following result.

**Lemma 2.9.** *Let $K \in \mathcal{T}_h$ and $k$, $s$, and $p$ be integers such that $k \geq 0$, $0 \leq s \leq k+1$, and $p \geq 2$. Then, there exists a constant $M_k \geq 1$, independent of $K$, such that*

$$|\mathcal{P}_k^K(\mathbf{v})|_{s,p,K} \;\leq\; M_k\, |\mathbf{v}|_{s,p,K} \qquad \forall\, \mathbf{v} \in \mathbf{W}^{s,p}(K)\,.$$

*Proof.* It follows by adding and subtracting $\mathbf{v}$ and then employing the triangle inequality and Lemma 2.8 with $m = s$. □

We end this section by remarking that for the case $s = 0$ and $p = 4$, Lemma 2.9 yields

$$\|\mathcal{P}_k^K(\mathbf{v})\|_{0,4,K} \;\leq\; M_k\, \|\mathbf{v}\|_{0,4,K} \qquad \forall\, \mathbf{v} \in \mathbf{L}^4(K)\,, \quad \forall\, K \in \mathcal{T}_h\,. \tag{2.40}$$

## 2.4 The discrete forms

We begin by introducing the global virtual element subspaces of $\mathbf{H} := \mathbb{H}_0(\mathbf{div};\Omega) \times \mathbf{H}^1(\Omega)$. More precisely, given $k \geq 1$, we set

$$\mathbf{H}_k^h \;:=\; H_k^h \times V_k^h\,,$$

where $H_k^h$ and $V_k^h$ have been defined in (2.31) and (2.25), respectively. Hence, the main goal of this section is to propose computable discrete versions $\mathbf{A}_h : \mathbf{H}_k^h \times \mathbf{H}_k^h \to \mathrm{R}$ and $\mathbf{B}_h(\mathbf{z};\,\cdot\,,\,\cdot\,) : \mathbf{H}_k^h \times \mathbf{H}_k^h \to \mathrm{R}$, for each $\mathbf{z} \in V_k^h$, of the bilinear forms $\mathbf{A}$ (cf. (2.12)) and $\mathbf{B}(\mathbf{z};\cdot,\cdot)$ (cf. (2.14)), respectively. Additionally, a computable discrete version of the functional $\mathbf{F}$ (cf. (2.13)) is also presented here.

### 2.4.1 The discrete bilinear form $\mathbf{A}_h$

According to the definition of the spaces $V_k^h$ (cf. (2.25)) and $H_k^h$ (cf. (2.31)), we observe from (2.12) that, given $\vec{\boldsymbol{\zeta}} := (\boldsymbol{\zeta}, \mathbf{w})$, $\vec{\boldsymbol{\tau}} := (\boldsymbol{\tau}, \mathbf{v}) \in \mathbf{H}_k^h$, $\mathbf{A}(\vec{\boldsymbol{\zeta}}, \vec{\boldsymbol{\tau}})$ is not explicitly computable because of the following three terms:

$$A^{K,\mathrm{d}}(\boldsymbol{\zeta}, \boldsymbol{\tau}) := \int_K \boldsymbol{\zeta}^{\mathrm{d}} : \boldsymbol{\tau}^{\mathrm{d}}\,, \qquad A^{K,\nabla}(\mathbf{w}, \mathbf{v}) := \kappa_2 \mu \int_K \nabla \mathbf{w} : \nabla \mathbf{v}\,, \quad \text{and} \quad \kappa_2 \int_K \boldsymbol{\zeta}^{\mathrm{d}} : \nabla \mathbf{v}\,, \tag{2.41}$$

in which the tensors $\boldsymbol{\zeta}^{\mathrm{d}}$, $\boldsymbol{\tau}^{\mathrm{d}}$, $\nabla \mathbf{w}$ and $\nabla \mathbf{v}$ are not known on each $K \in \mathcal{T}_h$. This is the reason why in what follows we define discrete computable versions of the forms in (2.41), all them in terms of some suitable projection operators.

We begin by defining the discrete local bilinear form $A_h^{K,\mathrm{d}} : H_k^K \times H_k^K \to \mathrm{R}$ as follows

$$A_h^{K,\mathrm{d}}(\boldsymbol{\zeta}, \boldsymbol{\tau}) := A^{K,\mathrm{d}}(\boldsymbol{\mathcal{P}}_k^K(\boldsymbol{\zeta}), \boldsymbol{\mathcal{P}}_k^K(\boldsymbol{\tau})) + \mathcal{S}^{K,\mathrm{d}}(\boldsymbol{\zeta} - \boldsymbol{\mathcal{P}}_k^K(\boldsymbol{\zeta}), \boldsymbol{\tau} - \boldsymbol{\mathcal{P}}_k^K(\boldsymbol{\tau})) \qquad \forall\, \boldsymbol{\zeta}, \boldsymbol{\tau} \in H_k^K\,, \tag{2.42}$$

where $\mathcal{S}^{K,\mathrm{d}} : H_k^K \times H_k^K \to \mathrm{R}$ is the bilinear form associated to the identity matrix in $\mathrm{R}^{n_{k,K}^H \times n_{k,K}^H}$ with respect to a basis of $H_k^K$. Equivalently, we set

$$\mathcal{S}^{K,\mathrm{d}}(\boldsymbol{\zeta}, \boldsymbol{\tau}) := \sum_{i=1}^{n_{k,K}^H} m_{i,K}^H(\boldsymbol{\zeta}) m_{i,K}^H(\boldsymbol{\tau}) \qquad \forall\, \boldsymbol{\zeta}, \boldsymbol{\tau} \in H_k^K\,,$$

where $m_{i,K}^H$, $i \in \{1, \ldots, n_{k,K}^H\}$, are the degrees of freedom defined in (2.27).

The following estimates concerning $\mathcal{S}^{K,\mathrm{d}}$ will be very useful in what follows.

**Lemma 2.10.** *There exist constants $\widehat{c}_0, \widehat{c}_1 > 0$, depending only on $C_{\mathcal{T}}$, such that*

$$\widehat{c}_0 \|\boldsymbol{\zeta}\|_{0,K}^2 \leq \mathcal{S}^{K,\mathrm{d}}(\boldsymbol{\zeta}, \boldsymbol{\zeta}) \leq \widehat{c}_1 \|\boldsymbol{\zeta}\|_{0,K}^2 \qquad \forall\, \boldsymbol{\zeta} \in H_k^K\,, \quad \forall\, K \in \mathcal{T}_h\,. \tag{2.43}$$

*Proof.* See Eqs. (3.36) and (6.2) in [15] (see also Eq. (5.8) in [28] and Lemma 4.5 of [30]). □

As a consequence of Lemma 2.10 and the properties of $\boldsymbol{\mathcal{P}}_k^K$, we have the following result.

**Lemma 2.11.** *For each $K \in \mathcal{T}_h$, there holds*

$$A_h^{K,\mathrm{d}}(\mathbf{p}, \boldsymbol{\tau}) = A^{K,\mathrm{d}}(\mathbf{p}, \boldsymbol{\tau}) \qquad \forall\, \mathbf{p} \in \mathbb{P}_k(K)\,, \quad \forall\, \boldsymbol{\tau} \in H_k^K\,. \tag{2.44}$$

*In addition, there exist constants $\alpha_1$, $\alpha_2 > 0$, independent of $h$ and $K$, such that*

$$|A_h^{K,\mathrm{d}}(\boldsymbol{\zeta}, \boldsymbol{\tau})| \leq \alpha_2 \|\boldsymbol{\zeta}\|_{0,K} \|\boldsymbol{\tau}\|_{0,K} \qquad \forall\, \boldsymbol{\zeta}, \boldsymbol{\tau} \in H_k^K\,, \tag{2.45}$$

*and*

$$\alpha_1 \|\boldsymbol{\zeta}^{\mathrm{d}}\|_{0,K}^2 \leq A_h^{K,\mathrm{d}}(\boldsymbol{\zeta}, \boldsymbol{\zeta}) \leq \alpha_2 \|\boldsymbol{\zeta}\|_{0,K}^2 \qquad \forall\, \boldsymbol{\zeta} \in H_k^K\,. \tag{2.46}$$

*Proof.* Let $\mathbf{p} \in \mathbb{P}_k(K)$ and $\boldsymbol{\tau} \in H_k^K$. Then, bearing in mind the definitions of $A_h^{K,\mathrm{d}}$ (cf. (2.42)), $A^{K,\mathrm{d}}$ (cf. (2.41)), and $\boldsymbol{\mathcal{P}}_k^K$ (cf. (2.33)), and using that certainly $\boldsymbol{\mathcal{P}}_k^K(\mathbf{p}) = \mathbf{p}$ and $\mathbf{p}^{\mathrm{d}} \in \mathbb{P}_k(K)$, we deduce that

$$A_h^{K,\mathrm{d}}(\mathbf{p}, \boldsymbol{\tau}) = \int_K \mathbf{p}^{\mathrm{d}} : \big(\boldsymbol{\mathcal{P}}_k^K(\boldsymbol{\tau})\big)^{\mathrm{d}} = \int_K \boldsymbol{\mathcal{P}}_k^K(\boldsymbol{\tau}) : \mathbf{p}^{\mathrm{d}} = \int_K \boldsymbol{\tau} : \mathbf{p}^{\mathrm{d}} = A^{K,\mathrm{d}}(\mathbf{p}, \boldsymbol{\tau})\,,$$

which establishes (2.44). In turn, applying the Cauchy-Schwarz inequality and the upper bound in (2.43), we find that for each $\boldsymbol{\zeta}, \boldsymbol{\tau} \in H_k^K$ there holds

$$\begin{aligned} |A_h^{K,\mathrm{d}}(\boldsymbol{\zeta},\boldsymbol{\tau})| \;&\leq\; \|\boldsymbol{\mathcal{P}}_k^K(\boldsymbol{\zeta})\|_{0,K}\|\boldsymbol{\mathcal{P}}_k^K(\boldsymbol{\tau})\|_{0,K} \\ &+\quad \left\{\mathcal{S}^{K,\mathrm{d}}(\boldsymbol{\zeta}-\boldsymbol{\mathcal{P}}_k^K(\boldsymbol{\zeta}),\boldsymbol{\zeta}-\boldsymbol{\mathcal{P}}_k^K(\boldsymbol{\zeta}))\right\}^{1/2}\left\{\mathcal{S}^{K,\mathrm{d}}(\boldsymbol{\tau}-\boldsymbol{\mathcal{P}}_k^K(\boldsymbol{\tau}),\boldsymbol{\tau}-\boldsymbol{\mathcal{P}}_k^K(\boldsymbol{\tau}))\right\}^{1/2} \\ &\leq\quad \|\boldsymbol{\zeta}\|_{0,K}\|\boldsymbol{\tau}\|_{0,K} \,+\, \widehat{c}_1\,\|\boldsymbol{\zeta}-\boldsymbol{\mathcal{P}}_k^K(\boldsymbol{\zeta})\|_{0,K}\|\boldsymbol{\tau}-\boldsymbol{\mathcal{P}}_k^K(\boldsymbol{\tau})\|_{0,K} \\ &\leq\quad (1+\widehat{c}_1)\,\|\boldsymbol{\zeta}\|_{0,K}\|\boldsymbol{\tau}\|_{0,K}\,, \end{aligned}$$

which is (2.45) with $\alpha_2 := 1+\widehat{c}_1$. Next, employing triangle inequality, the definition of $A^{K,\mathrm{d}}$ (cf. (2.41)), and the lower bound in (2.43), we deduce that

$$\begin{aligned} \|\boldsymbol{\zeta}^{\mathrm{d}}\|_{0,K}^2 \;&\leq\; 2\,\|(\boldsymbol{\mathcal{P}}_k^K(\boldsymbol{\zeta}))^{\mathrm{d}}\|_{0,K}^2 \,+\, 2\,\|(\boldsymbol{\zeta}-\boldsymbol{\mathcal{P}}_k^K(\boldsymbol{\zeta}))^{\mathrm{d}}\|_{0,K}^2 \\ &\leq\quad 2\,\|(\boldsymbol{\mathcal{P}}_k^K(\boldsymbol{\zeta}))^{\mathrm{d}}\|_{0,K}^2 \,+\, \frac{2}{\widehat{c}_0}\Big\{\widehat{c}_0\,\|\boldsymbol{\zeta}-\boldsymbol{\mathcal{P}}_k^K(\boldsymbol{\zeta})\|_{0,K}^2\Big\} \\ &\leq\quad 2\,A^{K,\mathrm{d}}(\boldsymbol{\mathcal{P}}_k^K(\boldsymbol{\zeta}),\boldsymbol{\mathcal{P}}_k^K(\boldsymbol{\zeta})) \,+\, \frac{2}{\widehat{c}_0}\,\mathcal{S}^{K,\mathrm{d}}(\boldsymbol{\zeta}-\boldsymbol{\mathcal{P}}_k^K(\boldsymbol{\zeta}),\boldsymbol{\zeta}-\boldsymbol{\mathcal{P}}_k^K(\boldsymbol{\zeta}))\,, \end{aligned}$$

which yields the lower bound in (2.46) with $\alpha_1 := \Big(2\max\big\{1,(\widehat{c}_0)^{-1}\big\}\Big)^{-1}$. Finally, we remark that the upper bound in (2.46) follows straightforwardly from (2.45). □

On the other hand, we define the discrete local bilinear form $A_h^{K,\nabla} : V_k^K \times V_k^K \to \mathrm{R}$ as

$$A_h^{K,\nabla}(\mathbf{w},\mathbf{v}) \;:=\; A^{K,\nabla}(\mathcal{R}_k^K(\mathbf{w}),\mathcal{R}_k^K(\mathbf{v})) \,+\, \mathcal{S}^{K,\nabla}(\mathbf{w}-\mathcal{R}_k^K(\mathbf{w}),\mathbf{v}-\mathcal{R}_k^K(\mathbf{v})) \quad \forall\ \mathbf{w},\mathbf{v}\in V_k^K\,, \tag{2.47}$$

where $\mathcal{R}_k^K$ is defined in (2.20), and $\mathcal{S}^{K,\nabla} : V_k^K \times V_k^K \to \mathrm{R}$ is the bilinear form associated to the identity matrix in $\mathrm{R}^{n_{k,K}^V \times n_{k,K}^V}$ with respect to a basis of $V_k^K$, that is,

$$\mathcal{S}^{K,\nabla}(\mathbf{w},\mathbf{v}) \;:=\; \sum_{i=1}^{n_{k,K}^V} m_{i,K}^V(\mathbf{w})\,m_{i,K}^V(\mathbf{v}) \qquad \forall\ \mathbf{w},\mathbf{v}\in V_k^K\,,$$

where, as indicated in Section 2.3.2, $m_{i,K}^V$, $i\in\{1,\ldots,n_{k,K}^V\}$, are the degrees of freedom defined by (2.24).

Similarly to Lemma 2.10, the following result establishes the estimates for $\mathcal{S}^{K,\nabla}$.

**Lemma 2.12.** *There exist constants $\widetilde{c}_0,\widetilde{c}_1>0$, depending only on $C_{\mathcal{T}}$, such that*

$$\widetilde{c}_0\,|\mathbf{w}|_{1,K}^2 \;\leq\; \mathcal{S}^{K,\nabla}(\mathbf{w},\mathbf{w}) \;\leq\; \widetilde{c}_1\,|\mathbf{w}|_{1,K}^2 \qquad \forall\ \mathbf{w}\in V_k^K\,,\quad \forall\ K\in\mathcal{T}_h\,. \tag{2.48}$$

*Proof.* It follows from Eq. (4.20) in Section 4.6 of [13]. □

Now, as a consequence of the previous lemma and the properties of the projector $\mathcal{R}_k^K$ (cf. (2.20)), we deduce the following result.

**Lemma 2.13.** *For each $K \in \mathcal{T}_h$ there holds*

$$A_h^{K,\nabla}(\mathbf{q},\mathbf{v}) \;=\; A^{K,\nabla}(\mathbf{q},\mathbf{v}) \quad \forall\, \mathbf{q} \in \mathbf{P}_k(K)\,, \quad \forall\, \mathbf{v} \in V_k^K\,, \tag{2.49}$$

*and there exist positive constants $\beta_1, \beta_2$, independent of $h$ and $K$, such that*

$$|A_h^{K,\nabla}(\mathbf{w},\mathbf{v})| \;\leq\; \beta_2\, |\mathbf{w}|_{1,K} |\mathbf{v}|_{1,K} \tag{2.50}$$

*and*

$$\beta_1\, |\mathbf{w}|_{1,K}^2 \;\leq\; A_h^{K,\nabla}(\mathbf{w},\mathbf{w}) \;\leq\; \beta_2\, |\mathbf{w}|_{1,K}^2 \tag{2.51}$$

*for all $\mathbf{w}, \mathbf{v} \in V_k^K$.*

*Proof.* Given $\mathbf{q} \in \mathbf{P}_k(K)$, it is clear from (2.20) that $\mathcal{R}_k^K(\mathbf{q}) = \mathbf{q}$. In addition, given $\mathbf{v} \in V_k^K$, it follows from the definitions of $A_h^{K,\nabla}$ (cf. (2.47)), $A^{K,\nabla}$ (cf. (2.41)), and $\mathcal{R}_k^K$ (cf. (2.20)), that

$$A_h^{K,\nabla}(\mathbf{q},\mathbf{v}) \;=\; \kappa_2\mu \int_K \nabla\mathbf{q} : \nabla\mathcal{R}_k^K(\mathbf{v}) \;=\; \kappa_2\mu \int_K \nabla\mathcal{R}_k^K(\mathbf{v}) : \nabla\mathbf{q} \;=\; \kappa_2\mu \int_K \nabla\mathbf{v} : \nabla\mathbf{q} = A^{K,\nabla}(\mathbf{q},\mathbf{v})\,,$$

which proves (2.49). Now, for the estimate (2.50) we apply the Cauchy-Schwarz inequality, the upper bound in (2.48), and (2.21), to establish that for each $\mathbf{w}, \mathbf{v} \in V_k^K$ there holds

$$\begin{aligned}
|A_h^{K,\nabla}(\mathbf{w},\mathbf{v})| \;&\leq\; \kappa_2\mu\, |\mathcal{R}_k^K(\mathbf{w})|_{1,K} |\mathcal{R}_k^K(\mathbf{v})|_{1,K} \\
&+\; \big\{\mathcal{S}^{K,\nabla}(\mathbf{w}-\mathcal{R}_k^K(\mathbf{w}),\mathbf{w}-\mathcal{R}_k^K(\mathbf{w}))\big\}^{1/2} \big\{\mathcal{S}^{K,\nabla}(\mathbf{v}-\mathcal{R}_k^K(\mathbf{v}),\mathbf{v}-\mathcal{R}_k^K(\mathbf{v}))\big\}^{1/2} \\
&\leq\; \kappa_2\mu\, |\mathbf{w}|_{1,K} |\mathbf{v}|_{1,K} \,+\, \widetilde{c}_1\, |\mathbf{w}-\mathcal{R}_k^K(\mathbf{w})|_{1,K} |\mathbf{v}-\mathcal{R}_k^K(\mathbf{v})|_{1,K} \\
&\leq\; \beta_2\, |\mathbf{w}|_{1,K} |\mathbf{v}|_{1,K}\,,
\end{aligned}$$

with $\beta_2 := \kappa_2\mu + 4\,\widetilde{c}_1$. Next, using the lower bound in (2.48), we easily obtain

$$\begin{aligned}
|\mathbf{w}|_{1,K}^2 \;&\leq\; 2\,|\mathcal{R}_k^K(\mathbf{w})|_{1,K}^2 \,+\, 2\,|\mathbf{w}-\mathcal{R}_k^K(\mathbf{w})|_{1,K}^2 \\
&\leq\; 2\,|\mathcal{R}_k^K(\mathbf{w})|_{1,K}^2 \,+\, \frac{2}{\widetilde{c}_0}\Big\{\widetilde{c}_0\,|\mathbf{w}-\mathcal{R}_k^K(\mathbf{w})|_{1,K}^2\Big\} \\
&\leq\; 2\,A^{K,\nabla}(\mathcal{R}_k^K(\mathbf{w}),\mathcal{R}_k^K(\mathbf{w})) \,+\, \frac{2}{\widetilde{c}_0}\,\mathcal{S}^{K,\nabla}(\mathbf{w}-\mathcal{R}_k^K(\mathbf{w}),\mathbf{w}-\mathcal{R}_k^K(\mathbf{w}))\,,
\end{aligned}$$

which establishes (2.51) with $\beta_1 := \big(2\max\{1,(\widetilde{c}_0)^{-1}\}\big)^{-1}$. Finally, the upper bound of (2.51) follows straightforwardly from (2.50). □

The following two lemmas compare $A^{K,\mathrm{d}}$ and $A^{K,\nabla}$ with their computable versions $A_h^{K,\mathrm{d}}$ and $A_h^{K,\nabla}$, respectively.

**Lemma 2.14.** *Let $\alpha_2$ be the constant from (2.45) (cf. proof of Lemma 2.11). Then, for each $K \in \mathcal{T}_h$ there holds*

$$|A^{K,\mathrm{d}}(\boldsymbol{\zeta},\boldsymbol{\tau}) - A_h^{K,\mathrm{d}}(\boldsymbol{\zeta},\boldsymbol{\tau})| \;\leq\; \alpha_2\, \|\boldsymbol{\zeta} - \boldsymbol{\mathcal{P}}_k^K(\boldsymbol{\zeta})\|_{0,K} \|\boldsymbol{\tau}\|_{0,K} \qquad \forall\, \boldsymbol{\zeta},\, \boldsymbol{\tau} \in H_k^K\,. \tag{2.52}$$

*Proof.* Let $\boldsymbol{\zeta}, \boldsymbol{\tau} \in H_k^K$. Then, from the definitions of $A^{K,\mathrm{d}}$ (cf. (2.41)), $A_h^{K,\mathrm{d}}$ (cf. (2.42)), and $\boldsymbol{\mathcal{P}}_k^K$ (cf. (2.33)), along with Lemma 2.10, it follows that

$$\begin{aligned}
|A^{K,\mathrm{d}}(\boldsymbol{\zeta},\boldsymbol{\tau}) - A_h^{K,\mathrm{d}}(\boldsymbol{\zeta},\boldsymbol{\tau})| \,&\leq\, \left| \int_K \boldsymbol{\zeta}^{\mathrm{d}} : \boldsymbol{\tau} - \int_K (\boldsymbol{\mathcal{P}}_k^K(\boldsymbol{\zeta}))^{\mathrm{d}} : \boldsymbol{\mathcal{P}}_k^K(\boldsymbol{\tau}) \right| \\
&+\quad \left\{ \mathcal{S}^{K,\mathrm{d}}(\boldsymbol{\zeta} - \boldsymbol{\mathcal{P}}_k^K(\boldsymbol{\zeta}), \boldsymbol{\zeta} - \boldsymbol{\mathcal{P}}_k^K(\boldsymbol{\zeta})) \right\}^{1/2} \left\{ \mathcal{S}^{K,\mathrm{d}}(\boldsymbol{\tau} - \boldsymbol{\mathcal{P}}_k^K(\boldsymbol{\tau}), \boldsymbol{\tau} - \boldsymbol{\mathcal{P}}_k^K(\boldsymbol{\tau})) \right\}^{1/2} \\
&\leq\quad \left| \int_K \left(\boldsymbol{\zeta} - \boldsymbol{\mathcal{P}}_k^K(\boldsymbol{\zeta})\right)^{\mathrm{d}} : \boldsymbol{\tau} \right| + \widehat{c}_1 \|\boldsymbol{\zeta} - \boldsymbol{\mathcal{P}}_k^K(\boldsymbol{\zeta})\|_{0,K} \, \|\boldsymbol{\tau} - \boldsymbol{\mathcal{P}}_k^K(\boldsymbol{\tau})\|_{0,K} \\
&\leq\quad \|\boldsymbol{\zeta} - \boldsymbol{\mathcal{P}}_k^K(\boldsymbol{\zeta})\|_{0,K} \|\boldsymbol{\tau}\|_{0,K} \,+\, \widehat{c}_1 \|\boldsymbol{\zeta} - \boldsymbol{\mathcal{P}}_k^K(\boldsymbol{\zeta})\|_{0,K} \, \|\boldsymbol{\tau}\|_{0,K} \\
&=\quad \alpha_2 \, \|\boldsymbol{\zeta} - \boldsymbol{\mathcal{P}}_k^K(\boldsymbol{\zeta})\|_{0,K} \, \|\boldsymbol{\tau}\|_{0,K} \,,
\end{aligned}$$

which yields (2.52), thus completing the proof. □

**Lemma 2.15.** *Let $\beta_2 > 0$ be the constant from (2.50) (cf. proof of Lemma 2.13). Then, for each $K \in \mathcal{T}_h$ there holds*

$$|A^{K,\nabla}(\mathbf{w},\mathbf{v}) - A_h^{K,\nabla}(\mathbf{w},\mathbf{v})| \;\leq\; \beta_2 \, |\mathbf{w} - \mathcal{R}_k^K(\mathbf{w})|_{1,K} |\mathbf{v}|_{1,K} \qquad \forall\, \mathbf{w}, \mathbf{v} \in V_k^K \,. \tag{2.53}$$

*Proof.* Let $\mathbf{v}, \mathbf{w} \in V_k^h$. Then, according to the definitions of $A^{K,\nabla}$ (cf. (2.41)), $A_h^{K,\nabla}$ (cf. (2.47)), and $\mathcal{R}_k^K$ (cf. (2.20)), and using (2.48), we find that

$$\begin{aligned}
|A^{K,\nabla}(\mathbf{w},\mathbf{v}) - A_h^{K,\nabla}(\mathbf{w},\mathbf{v})| \;&\leq\; \kappa_2 \mu \left| \int_K \nabla \mathbf{w} : \nabla \mathbf{v} - \int_K \nabla \mathcal{R}_k^K(\mathbf{w}) : \nabla \mathcal{R}_k^K(\mathbf{v}) \right| \\
&+ \left\{ \mathcal{S}^{K,\nabla}(\mathbf{w} - \mathcal{R}_k^K(\mathbf{w}), \mathbf{w} - \mathcal{R}_k^K(\mathbf{w})) \right\}^{1/2} \left\{ \mathcal{S}^{K,\nabla}(\mathbf{v} - \mathcal{R}_k^K(\mathbf{v}), \mathbf{v} - \mathcal{R}_k^K(\mathbf{v})) \right\}^{1/2} \\
&\leq\; \kappa_2 \mu \left| \int_K \nabla\big(\mathbf{w} - \mathcal{R}_k^K(\mathbf{w})\big) : \nabla \mathbf{v} \right| + \widetilde{c}_1 \, |\mathbf{w} - \mathcal{R}_k^K(\mathbf{w})|_{1,K} |\mathbf{v} - \mathcal{R}_k^K(\mathbf{v})|_{1,K} \\
&\leq\; \kappa_2 \mu \, |\mathbf{w} - \mathcal{R}_k^K(\mathbf{w})|_{1,K} |\mathbf{v}|_{1,K} \,+\, 2\,\widetilde{c}_1 \, |\mathbf{w} - \mathcal{R}_k^K(\mathbf{w})|_{1,K} |\mathbf{v}|_{1,K} \\
&\leq\; \beta_2 \, |\mathbf{w} - \mathcal{R}_k^K(\mathbf{w})|_{1,K} |\mathbf{v}|_{1,K} \,,
\end{aligned}$$

which shows (2.53), thus finishing the proof. □

Having provided the above analysis, we now introduce the complete local discrete bilinear form $\mathbf{A}_h^K : \mathbf{H}_k^K \times \mathbf{H}_k^K \to \mathrm{R}$ in terms of $A_h^{K,\mathrm{d}}$, $A_h^{K,\nabla}$, and $\boldsymbol{\mathcal{P}}_k^K$, as

$$\begin{aligned}
\mathbf{A}_h^K(\vec{\boldsymbol{\zeta}}, \vec{\boldsymbol{\tau}}) \;:=\; & A_h^{K,\mathrm{d}}(\boldsymbol{\zeta},\boldsymbol{\tau}) \,+\, \kappa_1 \int_K \mathbf{div}(\boldsymbol{\zeta}) \cdot \mathbf{div}(\boldsymbol{\tau}) \,+\, A_h^{K,\nabla}(\mathbf{w},\mathbf{v}) \,+\, \kappa_3 \int_{\partial K \cap \Gamma} \mathbf{w} \cdot \mathbf{v} \\
& - \mu \int_K \mathbf{v} \cdot \mathbf{div}(\boldsymbol{\zeta}) \,+\, \mu \int_K \mathbf{w} \cdot \mathbf{div}(\boldsymbol{\tau}) \,-\, \kappa_2 \int_K (\boldsymbol{\mathcal{P}}_k^K(\boldsymbol{\zeta}))^{\mathrm{d}} : \boldsymbol{\mathcal{P}}_k^K(\nabla \mathbf{v})
\end{aligned} \tag{2.54}$$

for all $\vec{\boldsymbol{\zeta}} := (\boldsymbol{\zeta}, \mathbf{w})$, $\vec{\boldsymbol{\tau}} := (\boldsymbol{\tau}, \mathbf{v}) \in \mathbf{H}_k^K := H_k^K \times V_k^K$. It is important to remark here that the integrals $\displaystyle\int_K \mathbf{v} \cdot \mathbf{div}(\boldsymbol{\zeta})$ and $\displaystyle\int_K \mathbf{w} \cdot \mathbf{div}(\boldsymbol{\tau})$ are both computable. Indeed, using the fact that $\mathbf{div}(\boldsymbol{\zeta}) \in \mathbf{P}_{k-1}(K)$, we decompose it as $\mathbf{div}(\boldsymbol{\zeta}) = \mathbf{div}(\boldsymbol{\zeta})_{k-2} + \mathbf{div}(\boldsymbol{\zeta})_{k-1}$, where $\mathbf{div}(\boldsymbol{\zeta})_{k-2} \in \mathbf{P}_{k-2}(K)$ and $\mathbf{div}(\boldsymbol{\zeta})_{k-1}$ is a polynomial of degree exactly $= k-1$. In this way, we obtain

$$\int_K \mathbf{v} \cdot \mathbf{div}(\boldsymbol{\zeta}) \;=\; \int_K \mathbf{v} \cdot \mathbf{div}(\boldsymbol{\zeta})_{k-2} \,+\, \int_K \mathbf{v} \cdot \mathbf{div}(\boldsymbol{\zeta})_{k-1} \,, \tag{2.55}$$

and observe that the two terms on the right hand side of the foregoing identity can be computed explicitly by using the degrees of freedom given by $m^V_{\mathbf{q},K}(\mathbf{v})$ (cf. (2.24)) and (2.36) (see also (2.23)), respectively. Certainly, since $\mathbf{div}(\boldsymbol{\tau}) \in \mathbf{P}_{k-1}(K)$, the same observation as above is valid for the computation of $\displaystyle\int_K \mathbf{w}\cdot\mathbf{div}(\boldsymbol{\tau})$.

Similarly, integrating by parts we observe that

$$\begin{aligned}\int_K \nabla\mathbf{v} : \mathbf{p} \;&=\; -\int_K \mathbf{v}\cdot\mathbf{div}(\mathbf{p}) \,+\, \int_{\partial K}\mathbf{p}\mathbf{n}\cdot\mathbf{v}\\ &=\; -\int_K \mathcal{P}^K_{k-1}(\mathbf{v})\cdot\mathbf{div}(\mathbf{p}) \,+\, \int_{\partial K}\mathbf{p}\mathbf{n}\cdot\mathbf{v} \qquad \forall\, \mathbf{p}\in\mathbb{P}_k(K)\,,\end{aligned}$$

which yields the explicit computation of $\boldsymbol{\mathcal{P}}^K_k(\nabla\mathbf{v}) \quad \forall\, \mathbf{v}\in V^K_k$.

Hence, we define the global discrete bilinear form $\mathbf{A}_h : \mathbf{H}^h_k \times \mathbf{H}^h_k \to \mathrm{R}$ as

$$\mathbf{A}_h(\vec{\boldsymbol{\zeta}},\vec{\boldsymbol{\tau}}) \;:=\; \sum_{K\in\mathcal{T}_h}\mathbf{A}^K_h(\vec{\boldsymbol{\zeta}},\vec{\boldsymbol{\tau}}) \qquad \forall\, \vec{\boldsymbol{\zeta}},\vec{\boldsymbol{\tau}}\in\mathbf{H}^h_k\,. \tag{2.56}$$

In turn, in what follows we denote by $\mathcal{R}^h_k$, $\mathcal{P}^h_k$, and $\boldsymbol{\mathcal{P}}^h_k$, the global counterparts of the projections $\mathcal{R}^K_k$ (cf. (2.20)), $\mathcal{P}^K_k$ (cf. (2.32)), and $\boldsymbol{\mathcal{P}}^K_k$ (cf. (2.33)), respectively. In other words, for each $K\in\mathcal{T}_h$ we let

$$\mathcal{R}^h_k(\mathbf{z})|_K \;:=\; \mathcal{R}^K_k(\mathbf{z}|_K)\,, \quad \mathcal{P}^h_k(\mathbf{v})|_K \;:=\; \mathcal{P}^K_k(\mathbf{v}|_K)\,, \quad \text{and} \quad \boldsymbol{\mathcal{P}}^h_k(\boldsymbol{\tau})|_K \;:=\; \boldsymbol{\mathcal{P}}^K_k(\boldsymbol{\tau}|_K)\,,$$

for all $\mathbf{z}\in\mathbf{H}^1(\Omega)$, $\mathbf{v}\in\mathbf{L}^2(\Omega)$, and $\boldsymbol{\tau}\in\mathbb{L}^2(\Omega)$.

The following two lemmas, which refer to the relationship between $\mathbf{A}_h$ and $\mathbf{A}$, can be seen as the global analogues of (2.44) - (2.49) (cf. Lemmas 2.11 and 2.13) and Lemmas 2.14 - 2.15.

**Lemma 2.16.** *There holds*

$$\mathbf{A}_h(\vec{\mathbf{p}},\vec{\boldsymbol{\tau}}) \;=\; \mathbf{A}(\vec{\mathbf{p}},\vec{\boldsymbol{\tau}}) \quad \forall\,\vec{\mathbf{p}}\in\mathbb{P}_k(\Omega)\times\mathbf{P}_k(\Omega)\,, \quad \forall\,\vec{\boldsymbol{\tau}}\in\mathbf{H}^K_k\,.$$

*Proof.* Let $\vec{\mathbf{p}} := (\mathbf{p},\mathbf{q})\in\mathbb{P}_k(\Omega)\times\mathbf{P}_k(\Omega)$ and $\vec{\boldsymbol{\tau}} := (\boldsymbol{\tau},\mathbf{v})\in\mathbf{H}^K_k$. Then, noting that $\boldsymbol{\mathcal{P}}^K_k(\mathbf{p}) = \mathbf{p}$ and $\mathbf{p}^{\mathrm{d}}\in\mathbb{P}_k(\Omega)$, and employing the characterization of $\boldsymbol{\mathcal{P}}^K_k$ (cf. (2.33)), we observe that

$$\int_K (\boldsymbol{\mathcal{P}}^K_k(\mathbf{p}))^{\mathrm{d}} : \boldsymbol{\mathcal{P}}^K_k(\nabla\mathbf{v}) \;=\; \int_K \mathbf{p}^{\mathrm{d}} : \boldsymbol{\mathcal{P}}^K_k(\nabla\mathbf{v}) \;=\; \int_K \mathbf{p}^{\mathrm{d}} : \nabla\mathbf{v}\,.$$

which, together with (2.44), (2.49), and the definitions of $\mathbf{A}_h$ (cf. (2.56)) and $\mathbf{A}^K_h$ (cf. (2.54)), yield the required identity. □

**Lemma 2.17.** *There exists a constant $L_{\mathbf{A}} > 0$, depending only on $\alpha_2$, $\beta_2$ and $\kappa_2$, such that*

$$|\mathbf{A}(\vec{\boldsymbol{\zeta}},\vec{\boldsymbol{\tau}}) - \mathbf{A}_h(\vec{\boldsymbol{\zeta}},\vec{\boldsymbol{\tau}})| \;\leq\; L_{\mathbf{A}}\Big\{\|\boldsymbol{\zeta}-\boldsymbol{\mathcal{P}}^h_k(\boldsymbol{\zeta})\|_{0,\Omega} \,+\, |\mathbf{w}-\mathcal{R}^h_k(\mathbf{w})|_{1,h}\Big\}\|\vec{\boldsymbol{\tau}}\|_{\mathbf{H}} \tag{2.57}$$

*for all $\vec{\boldsymbol{\zeta}} := (\boldsymbol{\zeta},\mathbf{w}), \vec{\boldsymbol{\tau}} := (\boldsymbol{\tau},\mathbf{v})\in\mathbf{H}^K_k$.*

*Proof.* It follows from the definitions of $\mathbf{A}$ (cf. (2.12)) and $\mathbf{A}_h$ (cf. (2.56)) that

$$\mathbf{A}(\vec{\boldsymbol{\zeta}},\vec{\boldsymbol{\tau}}) - \mathbf{A}_h(\vec{\boldsymbol{\zeta}},\vec{\boldsymbol{\tau}}) = \sum_{K\in\mathcal{T}_h}\Big\{A^{K,\mathrm{d}}(\boldsymbol{\zeta},\boldsymbol{\tau}) - A_h^{K,\mathrm{d}}(\boldsymbol{\zeta},\boldsymbol{\tau}) + A^{K,\nabla}(\mathbf{w},\mathbf{v}) - A_h^{K,\nabla}(\mathbf{w},\mathbf{v}) - \kappa_2\int_K \boldsymbol{\zeta}^{\mathrm{d}} : \nabla\mathbf{v} + \kappa_2\int_K (\boldsymbol{\mathcal{P}}_k^K(\boldsymbol{\zeta}))^{\mathrm{d}} : \boldsymbol{\mathcal{P}}_k^K(\nabla\mathbf{v})\Big\}.$$

Next, thanks to the fact that $(\boldsymbol{\mathcal{P}}_k^K(\boldsymbol{\zeta}))^{\mathrm{d}} \in \mathbb{P}_k(K)$, along with (2.33), we have

$$\int_K (\boldsymbol{\mathcal{P}}_k^K(\boldsymbol{\zeta}))^{\mathrm{d}} : \boldsymbol{\mathcal{P}}_k^K(\nabla\mathbf{v}) = \int_K (\boldsymbol{\mathcal{P}}_k^K(\boldsymbol{\zeta}))^{\mathrm{d}} : \nabla\mathbf{v}\,,$$

which implies that

$$|\mathbf{A}(\vec{\boldsymbol{\zeta}},\vec{\boldsymbol{\tau}}) - \mathbf{A}_h(\vec{\boldsymbol{\zeta}},\vec{\boldsymbol{\tau}})| \leq \sum_{K\in\mathcal{T}_h}\Big\{|A^{K,\mathrm{d}}(\boldsymbol{\zeta},\boldsymbol{\tau}) - A_h^{K,\mathrm{d}}(\boldsymbol{\zeta},\boldsymbol{\tau})| + \big|A^{K,\nabla}(\mathbf{w},\mathbf{v}) - A_h^{K,\nabla}(\mathbf{w},\mathbf{v})\big| + \kappa_2\Big|\int_K \big(\boldsymbol{\zeta} - \boldsymbol{\mathcal{P}}_k^K(\boldsymbol{\zeta})\big)^{\mathrm{d}} : \nabla\mathbf{v}\Big|\Big\}.$$

Now, employing the Cauchy-Schwarz inequality, (2.52), and (2.53), we find that

$$\begin{aligned}|\mathbf{A}(\vec{\boldsymbol{\zeta}},\vec{\boldsymbol{\tau}}) - \mathbf{A}_h(\vec{\boldsymbol{\zeta}},\vec{\boldsymbol{\tau}})| &\leq \sum_{K\in\mathcal{T}_h}\Big\{\alpha_2\,\|\boldsymbol{\zeta} - \boldsymbol{\mathcal{P}}_k^K(\boldsymbol{\zeta})\|_{0,K}\|\boldsymbol{\tau}\|_{0,K} \\ &\quad + \beta_2\,|\mathbf{w} - \mathcal{R}_k^K(\mathbf{w})|_{1,K}|\mathbf{v}|_{1,K} + \kappa_2\,\|\boldsymbol{\zeta} - \boldsymbol{\mathcal{P}}_k^K(\boldsymbol{\zeta})\|_{0,K}|\mathbf{v}|_{1,K}\Big\} \\ &\leq \max\{\alpha_2+\kappa_2,\beta_2\}\left(\sum_{K\in\mathcal{T}_h}\Big\{\|\boldsymbol{\zeta} - \boldsymbol{\mathcal{P}}_k^K(\boldsymbol{\zeta})\|_{0,K}^2 + |\mathbf{w} - \mathcal{R}_k^K(\mathbf{w})|_{1,K}^2\Big\}\right)^{1/2}\|\vec{\boldsymbol{\tau}}\|_{\mathbf{H}}\,,\end{aligned}$$

which is (2.57) with $L_{\mathbf{A}} := \max\{\alpha_2+\kappa_2,\beta_2\}$. □

Next, we prove the boundedness and ellipticity properties of $\mathbf{A}_h$. We begin with the first of them.

**Lemma 2.18.** *There exists a constant $\widetilde{C}_{\mathbf{A}} > 0$, independent of $h$, such that*

$$|\mathbf{A}_h(\vec{\boldsymbol{\zeta}},\vec{\boldsymbol{\tau}})| \leq \widetilde{C}_{\mathbf{A}}\,\|\vec{\boldsymbol{\zeta}}\|_{\mathbf{H}}\,\|\vec{\boldsymbol{\tau}}\|_{\mathbf{H}} \qquad \forall\ \vec{\boldsymbol{\zeta}},\vec{\boldsymbol{\tau}} \in \mathbf{H}_k^h\,.$$

*Proof.* The result follows straightforwardly from the definition of $\mathbf{A}_h$ (cf. (2.56)), the estimates (2.45) and (2.50) (cf. Lemmas 2.11 and 2.13), the Cauchy-Schwarz and trace inequalities, and the boundedness of $\boldsymbol{\mathcal{P}}_k^h$. We omit further details and just mention that $\widetilde{C}_{\mathbf{A}}$ depends on $\mu$, $\alpha_2$, $\beta_2$, $\kappa_1$, $\kappa_3$, and $\|\boldsymbol{\gamma}_0\|$. □

In turn, for the second property we require the estimates provided by the following lemma.

**Lemma 2.19.** *There exist constants $c_1(\Omega)$, $c_2(\Omega) > 0$, independent of $h$, such that*

$$c_1(\Omega)\,\|\boldsymbol{\tau}\|_{0,\Omega}^2 \leq \|\boldsymbol{\tau}^{\mathrm{d}}\|_{0,\Omega}^2 + \|\mathbf{div}(\boldsymbol{\tau})\|_{0,\Omega}^2 \qquad \forall\ \boldsymbol{\tau} \in \mathbb{H}_0(\mathbf{div};\Omega)$$

*and*

$$c_2(\Omega)\,\|\mathbf{v}\|_{1,\Omega}^2 \leq |\mathbf{v}|_{1,\Omega}^2 + \|\mathbf{v}\|_{0,\Gamma}^2 \qquad \forall\ \mathbf{v} \in \mathbf{H}^1(\Omega)\,.$$

*Proof.* See Proposition 3.1 in Chapter IV of [29] and Lemma 3.3 of [54], respectively. □

In this way, the $\mathbf{H}_k^h$-ellipticity of $\mathbf{A}_h$ is proved as follows.

**Lemma 2.20.** *Assume that $\kappa_1, \kappa_3 > 0$ and $0 < \kappa_2 < 2\min\{\alpha_1, \beta_1\}$, where $\alpha_1$ and $\beta_1$ are the positive constants from (2.46) and (2.51), respectively. Then, there exists a constant $\alpha(\Omega) > 0$, independent of $h$, such that*

$$\mathbf{A}_h(\vec{\boldsymbol{\tau}}, \vec{\boldsymbol{\tau}}) \;\geq\; \alpha(\Omega)\, \|\vec{\boldsymbol{\tau}}\|^2_{\mathbf{H}} \qquad \forall\, \vec{\boldsymbol{\tau}} \in \mathbf{H}_k^h\,. \tag{2.58}$$

*Proof.* Let $\vec{\boldsymbol{\tau}}_h := (\boldsymbol{\tau}, \mathbf{v}) \in \mathbf{H}_k^h$. Then, bearing in mind the definition of the bilinear form $\mathbf{A}_h$ (cf. (2.54) and (2.56)), and employing the estimates (2.46) and (2.51), the Cauchy-Schwarz inequality, the fact that $(\boldsymbol{\mathcal{P}}_k^h(\boldsymbol{\tau}))^{\mathrm{d}} = \boldsymbol{\mathcal{P}}_k^h(\boldsymbol{\tau}^{\mathrm{d}}) \quad \forall\, \boldsymbol{\tau} \in \mathbb{L}^2(\Omega)$, and the boundedness of $\boldsymbol{\mathcal{P}}_k^h$, we find that

$$\begin{aligned}
\mathbf{A}_h(\vec{\boldsymbol{\tau}}, \vec{\boldsymbol{\tau}}) \;&\geq\; \alpha_1 \|\boldsymbol{\tau}^{\mathrm{d}}\|^2_{0,\Omega} + \kappa_1\, \|\mathbf{div}(\boldsymbol{\tau})\|^2_{0,\Omega} \,+\, \beta_1\, |\mathbf{v}|^2_{1,\Omega} + \kappa_3\, \|\mathbf{v}\|^2_{0,\Gamma} - \kappa_2 \|(\boldsymbol{\mathcal{P}}_k^h(\boldsymbol{\tau}))^{\mathrm{d}}\|_{0,\Omega}\, \|\boldsymbol{\mathcal{P}}_k^h(\nabla \mathbf{v})\|_{0,\Omega} \\
&=\; \alpha_1 \|\boldsymbol{\tau}^{\mathrm{d}}\|^2_{0,\Omega} + \kappa_1\, \|\mathbf{div}(\boldsymbol{\tau})\|^2_{0,\Omega} \,+\, \beta_1\, |\mathbf{v}|^2_{1,\Omega} + \kappa_3\, \|\mathbf{v}\|^2_{0,\Gamma} - \kappa_2 \|\boldsymbol{\mathcal{P}}_k^h(\boldsymbol{\tau}^{\mathrm{d}})\|_{0,\Omega} \|\boldsymbol{\mathcal{P}}_k^h(\nabla \mathbf{v})\|_{0,\Omega} \\
&\geq\; \alpha_1 \|\boldsymbol{\tau}^{\mathrm{d}}\|^2_{0,\Omega} + \kappa_1\, \|\mathbf{div}(\boldsymbol{\tau})\|^2_{0,\Omega} \,+\, \beta_1\, |\mathbf{v}|^2_{1,\Omega} + \kappa_3\, \|\mathbf{v}\|^2_{0,\Gamma} - \kappa_2 \|\boldsymbol{\tau}^{\mathrm{d}}\|_{0,\Omega} |\mathbf{v}|_{1,\Omega}\,,
\end{aligned}$$

which, using the Young inequality, yields

$$\mathbf{A}_h(\vec{\boldsymbol{\tau}}, \vec{\boldsymbol{\tau}}) \;\geq\; \left(\alpha_1 - \frac{\kappa_2}{2}\right) \|\boldsymbol{\tau}^{\mathrm{d}}\|^2_{0,\Omega} + \kappa_1\, \|\mathbf{div}(\boldsymbol{\tau})\|^2_{0,\Omega} + \left(\beta_1 - \frac{\kappa_2}{2}\right) |\mathbf{v}|^2_{1,\Omega} + \kappa_3\, \|\mathbf{v}\|^2_{0,\Gamma}\,.$$

Then, assuming the stipulated hypotheses on $\kappa_1, \kappa_2$ and $\kappa_3$, applying the estimates provided by Lemma 2.19, and defining the constant $\widetilde{\alpha}(\Omega) := \min\left\{\alpha_1 - \frac{\kappa_2}{2}, \frac{\kappa_1}{2}, \beta_1 - \frac{\kappa_2}{2}, \kappa_3\right\}$, it follows that

$$\begin{aligned}
\mathbf{A}_h(\vec{\boldsymbol{\tau}}, \vec{\boldsymbol{\tau}}) \;&\geq\; \widetilde{\alpha}(\Omega) \left\{ \|\boldsymbol{\tau}^{\mathrm{d}}\|^2_{0,\Omega} + \|\mathbf{div}(\boldsymbol{\tau})\|^2_{0,\Omega} + \|\mathbf{div}(\boldsymbol{\tau})\|^2_{0,\Omega} + |\mathbf{v}|^2_{1,\Omega} + \|\mathbf{v}\|^2_{0,\Gamma} \right\} \\
&\geq\; \widetilde{\alpha}(\Omega) \left\{ c_1(\Omega)\, \|\boldsymbol{\tau}\|^2_{0,\Omega} + \|\mathbf{div}(\boldsymbol{\tau})\|^2_{0,\Omega} + c_2(\Omega) \|\mathbf{v}\|^2_{1,\Omega} \right\}
\end{aligned}$$

which yields (2.58) with $\alpha(\Omega) := \widetilde{\alpha}(\Omega)\, \min\{1, c_1(\Omega), c_2(\Omega)\}$, thus completing the proof. □

Regarding an optimal choice of the parameters $\kappa_1$, $\kappa_2$, and $\kappa_3$, we follow the approach from [35] (see also [33, 34]) and adopt the criterion of maximizing the constant $\widetilde{\alpha}(\Omega)$ multiplying the ellipticity constant $\alpha(\Omega)$. In this way, $\kappa_2$ is taken as the midpoint of its range, that is $\kappa_2 = \min\{\alpha_1, \beta_1\}$, and then both $\kappa_3$ and $\frac{\kappa_1}{2}$ are chosen equal to $\min\{\alpha_1 - \frac{\kappa_2}{2}, \beta_1 - \frac{\kappa_2}{2}\} = \frac{1}{2}\min\{\alpha_1, \beta_1\}$. In case the constants $\alpha_1$ and $\beta_1$ are not known explicitly, then we proceed as in the continuous case (see [35]) and replace above $\min\{\alpha_1, \beta_1\}$ by $\mu$, thus yielding heuristic choices for these stabilization parameters.

We end this section by noticing that after taking another look to the definition of $\mathbf{A}_h^K$ (cf. (2.54)), particularly to the expression defining $A_h^{K,\nabla}$ (cf. (2.47)), one could conjecture that the bilinear form $\mathcal{S}^{K,\nabla}$, which is acting as a stabilizer of the term

$$A^{K,\nabla}(\mathcal{R}_k^K(\mathbf{w}), \mathcal{R}_k^K(\mathbf{v})) := \kappa_2\, \mu \int_K \nabla \mathcal{R}_k^K(\mathbf{w}) : \nabla \mathcal{R}_k^K(\mathbf{v})\,,$$

requires to be multiplied by $\kappa_2\,\mu$ as well. A similar comment applies to $A_h^{K,\mathrm{d}}$ (cf. (2.42)) and the chance of multiplying its components $A^{K,\mathrm{d}}$ and $\mathcal{S}^{K,\mathrm{d}}$ by the same constant. However, as proved by (2.58), the constant that really matters is not the one resulting from a couple of terms only of the whole expression defining $\mathbf{A}_h$, but the definite one yielding the ellipticity of this bilinear form, namely $\alpha(\Omega)$, which depends on several other constants and parameters. Alternatively, one could consider for instance the multiplication of the pairs $\big(A^{K,\nabla},\mathcal{S}^{K,\nabla}\big)$ and $\big(A^{K,\mathrm{d}},\mathcal{S}^{K,\mathrm{d}}\big)$ by arbitrary parameters to be chosen so as to maximize either $\alpha(\Omega)$ or some of the expressions defining them. Nevertheless, this could very well turn into just a theoretical exercise since some of the constants involved might not be known explicitly. Anyhow, the most relevant issue here is the derivation of an ellipticity constant independent of $h$, which has been indeed guaranteed by Lemma 2.20.

### 2.4.2 The discrete trilinear form $\mathbf{B}_h$

Similarly as in the previous section, we now introduce a computable discrete version of the form $\mathbf{B}$ defined in (2.14). More precisely, for each $\mathbf{z}\in V_k^h$ we let $\mathbf{B}_h(\mathbf{z};\,\cdot\,,\,\cdot\,):\mathbf{H}_k^h\times\mathbf{H}_k^h\to\mathrm{R}$ be the bilinear form defined by

$$\mathbf{B}_h(\mathbf{z};\vec{\boldsymbol{\zeta}},\vec{\boldsymbol{\tau}}) \;:=\; \int_\Omega \big(\mathcal{P}_k^h(\mathbf{w})\otimes\mathcal{P}_k^h(\mathbf{z})\big)^{\mathrm{d}} : \big\{\boldsymbol{\mathcal{P}}_k^h(\boldsymbol{\tau})-\kappa_2\boldsymbol{\mathcal{P}}_k^h(\nabla\mathbf{v})\big\} \tag{2.59}$$

for all $\vec{\boldsymbol{\zeta}}:=(\boldsymbol{\zeta},\mathbf{w}),\vec{\boldsymbol{\tau}}:=(\boldsymbol{\tau},\mathbf{v})\in\mathbf{H}_k^h$.

The following result establishes the comparison between $\mathbf{B}$ and $\mathbf{B}_h$.

**Lemma 2.21.** *Let $\mathbf{i}_c$ and $M_k\geq 1$ be specified in (2.9) and (2.40), respectively. Then, there holds*

$$\begin{aligned}|\mathbf{B}(\mathbf{z};\vec{\boldsymbol{\zeta}},\vec{\boldsymbol{\tau}})-\mathbf{B}_h(\mathbf{z};\vec{\boldsymbol{\zeta}},\vec{\boldsymbol{\tau}})| \;\leq\; (1+\kappa_2^2)^{1/2}\Big\{&\|\mathbf{w}\otimes\mathbf{z}-\boldsymbol{\mathcal{P}}_k^h(\mathbf{w}\otimes\mathbf{z})\|_{0,\Omega}\\ &+\|\mathbf{i}_c\|\,M_k\Big(\|\mathbf{w}\|_{1,\Omega}\|\mathbf{z}-\mathcal{P}_k^h(\mathbf{z})\|_{0,4,\Omega}\;+\;\|\mathbf{z}\|_{1,\Omega}\,\|\mathbf{w}-\mathcal{P}_k^h(\mathbf{w})\|_{0,4,\Omega}\Big)\Big\}\|\vec{\boldsymbol{\tau}}\|_{\mathbf{H}}\end{aligned} \tag{2.60}$$

*for all $\vec{\boldsymbol{\zeta}}:=(\boldsymbol{\zeta},\mathbf{w}),\vec{\boldsymbol{\tau}}:=(\boldsymbol{\tau},\mathbf{v})\in\mathbf{H}_k^h$ and $\mathbf{z}\in V_k^h$.*

*Proof.* Let $\vec{\boldsymbol{\zeta}}:=(\boldsymbol{\zeta},\mathbf{w}),\vec{\boldsymbol{\tau}}:=(\boldsymbol{\tau},\mathbf{v})\in\mathbf{H}_k^h$ and $\mathbf{z}\in V_k^h$. Then, from the definitions of $\mathbf{B}$ (cf. (2.14)) and $\mathbf{B}_h$ (cf. (2.59)), and after adding and subtracting suitable terms, we obtain

$$\begin{aligned}\mathbf{B}(\mathbf{z};\vec{\boldsymbol{\zeta}},\vec{\boldsymbol{\tau}})-\mathbf{B}_h(\mathbf{z};\vec{\boldsymbol{\zeta}},\vec{\boldsymbol{\tau}}) \;&=\; \int_\Omega(\mathbf{w}\otimes\mathbf{z})^{\mathrm{d}}:\{\boldsymbol{\tau}-\kappa_2\nabla\mathbf{v}\}\;-\;\int_\Omega\big(\mathcal{P}_k^h(\mathbf{w})\otimes\mathcal{P}_k^h(\mathbf{z})\big)^{\mathrm{d}}:\boldsymbol{\mathcal{P}}_k^h(\boldsymbol{\tau}-\kappa_2\nabla\mathbf{v})\\
&=\;\int_\Omega(\mathbf{w}\otimes\mathbf{z})^{\mathrm{d}}:\{\boldsymbol{\tau}-\kappa_2\nabla\mathbf{v}\}\;-\;\int_\Omega(\mathbf{w}\otimes\mathbf{z})^{\mathrm{d}}:\boldsymbol{\mathcal{P}}_k^h(\boldsymbol{\tau}-\kappa_2\nabla\mathbf{v})\\
&+\;\int_\Omega\big(\mathbf{w}\otimes\mathbf{z}-\mathcal{P}_k^h(\mathbf{w})\otimes\mathcal{P}_k^h(\mathbf{z})\big)^{\mathrm{d}}:\boldsymbol{\mathcal{P}}_k^h(\boldsymbol{\tau}-\kappa_2\nabla\mathbf{v})\\
&=\;\int_\Omega\Big\{(\mathbf{w}\otimes\mathbf{z})^{\mathrm{d}}-\boldsymbol{\mathcal{P}}_k^h\big((\mathbf{w}\otimes\mathbf{z})^{\mathrm{d}}\big)\Big\}:\{\boldsymbol{\tau}-\kappa_2\nabla\mathbf{v}\}\\
&+\;\int_\Omega\big(\mathbf{w}\otimes\mathbf{z}-\mathcal{P}_k^h(\mathbf{w})\otimes\mathcal{P}_k^h(\mathbf{z})\big)^{\mathrm{d}}:\boldsymbol{\mathcal{P}}_k^h(\boldsymbol{\tau}-\kappa_2\nabla\mathbf{v})\,,\end{aligned}$$

which, along with the Cauchy-Schwarz inequality and the fact that $\boldsymbol{\mathcal{P}}_k^h(\boldsymbol{\tau}^{\mathrm{d}}) = \big(\boldsymbol{\mathcal{P}}_k^h(\boldsymbol{\tau})\big)^{\mathrm{d}} \quad \forall\, \boldsymbol{\tau} \in \mathbb{L}^2(\Omega)$, leads to

$$\begin{aligned}
|\mathbf{B}(\mathbf{z};\vec{\boldsymbol{\zeta}},\vec{\boldsymbol{\tau}}) - \mathbf{B}_h(\mathbf{z};\vec{\boldsymbol{\zeta}},\vec{\boldsymbol{\tau}})| \;&\leq\; \|\mathbf{w}\otimes\mathbf{z} - \boldsymbol{\mathcal{P}}_k^h(\mathbf{w}\otimes\mathbf{z})\|_{0,\Omega}\,\|\boldsymbol{\tau} - \kappa_2\nabla\mathbf{v}\|_{0,\Omega} \\
&+\; \|\mathbf{w}\otimes\mathbf{z} - \mathcal{P}_k^h(\mathbf{w})\otimes\mathcal{P}_k^h(\mathbf{z})\|_{0,\Omega}\,\|\boldsymbol{\mathcal{P}}_k^h(\boldsymbol{\tau} - \kappa_2\nabla\mathbf{v})\|_{0,\Omega} \qquad (2.61)\\
&\leq\; (1+\kappa_2^2)^{1/2}\Big\{\|\mathbf{w}\otimes\mathbf{z} - \boldsymbol{\mathcal{P}}_k^h(\mathbf{w}\otimes\mathbf{z})\|_{0,\Omega} \;+\; \|\mathbf{w}\otimes\mathbf{z} - \mathcal{P}_k^h(\mathbf{w})\otimes\mathcal{P}_k^h(\mathbf{z})\|_{0,\Omega}\Big\}\,\|\vec{\boldsymbol{\tau}}\|_{\mathbf{H}}\,.
\end{aligned}$$

In turn, adding and subtracting $\mathcal{P}_k^h(\mathbf{z})$, employing the Cauchy-Schwarz inequality, and applying (2.9) and the estimate (2.40), we find that

$$\begin{aligned}
\|\mathbf{w}\otimes\mathbf{z} - \mathcal{P}_k^h(\mathbf{w})\otimes\mathcal{P}_k^h(\mathbf{z})\|_{0,\Omega} \;&=\; \|\mathbf{w}\otimes(\mathbf{z} - \mathcal{P}_k^h(\mathbf{z})) \;+\; (\mathbf{w} - \mathcal{P}_k^h(\mathbf{w}))\otimes\mathcal{P}_k^h(\mathbf{z})\|_{0,\Omega} \\
&\leq\; \|\mathbf{w}\|_{0,4,\Omega}\,\|\mathbf{z} - \mathcal{P}_k^h(\mathbf{z})\|_{0,4,\Omega} \;+\; \|\mathbf{w} - \mathcal{P}_k^h(\mathbf{w})\|_{0,4,\Omega}\,\|\mathcal{P}_k^h(\mathbf{z})\|_{0,4,\Omega} \\
&\leq\; \|\mathbf{w}\|_{0,4,\Omega}\,\|\mathbf{z} - \mathcal{P}_k^h(\mathbf{z})\|_{0,4,\Omega} \;+\; M_k\,\|\mathbf{z}\|_{0,4,\Omega}\,\|\mathbf{w} - \mathcal{P}_k^h(\mathbf{w})\|_{0,4,\Omega} \\
&\leq\; \|\mathbf{i}_c\|\,M_k\Big\{\|\mathbf{w}\|_{1,\Omega}\,\|\mathbf{z} - \mathcal{P}_k^h(\mathbf{z})\|_{0,4,\Omega} \;+\; \|\mathbf{z}\|_{1,\Omega}\,\|\mathbf{w} - \mathcal{P}_k^h(\mathbf{w})\|_{0,4,\Omega}\Big\}\,.
\end{aligned}$$

Finally, replacing the foregoing estimate into (2.61) we arrive to (2.60) and complete the proof. □

On the other hand, the boundedness of the bilinear form $\mathbf{B}_h$ is established in the following result.

**Lemma 2.22.** *There holds*

$$|\mathbf{B}_h(\mathbf{z};\vec{\boldsymbol{\zeta}},\vec{\boldsymbol{\tau}})| \;\leq\; \|\mathbf{i}_c\|^2\,M_k^2\,(1+\kappa_2^2)^{1/2}\,\|\mathbf{z}\|_{1,\Omega}\,\|\vec{\boldsymbol{\zeta}}\|_{\mathbf{H}}\,\|\vec{\boldsymbol{\tau}}\|_{\mathbf{H}} \qquad (2.62)$$

*for all* $\mathbf{z}\in V_k^h$ *and* $\vec{\boldsymbol{\zeta}},\vec{\boldsymbol{\tau}}\in\mathbf{H}_k^h$.

*Proof.* Let $\mathbf{z}\in V_k^h$, $\vec{\boldsymbol{\zeta}} := (\boldsymbol{\zeta},\mathbf{w})$, $\vec{\boldsymbol{\tau}} := (\boldsymbol{\tau},\mathbf{v}) \in \mathbf{H}_k^h$. Then, applying the Cauchy-Schwarz inequality in (2.59), and then employing the boundedness of $\boldsymbol{\mathcal{P}}_k^h$, the Cauchy-Schwarz inequality, the boundedness of $\mathbf{i}_c$ (cf. (2.9)), and the estimate (2.40), we readily obtain

$$\begin{aligned}
|\mathbf{B}_h(\mathbf{z};\vec{\boldsymbol{\zeta}},\vec{\boldsymbol{\tau}})| \;&\leq\; \|\mathcal{P}_k^h(\mathbf{w})\otimes\mathcal{P}_k^h(\mathbf{z})\|_{0,\Omega}\,\|\boldsymbol{\mathcal{P}}_k^h(\boldsymbol{\tau} - \kappa_2\nabla\mathbf{v})\|_{0,\Omega} \\
&\leq\; (1+\kappa_2^2)^{1/2}\,\|\mathcal{P}_k^h(\mathbf{w})\otimes\mathcal{P}_k^h(\mathbf{z})\|_{0,\Omega}\,\|\vec{\boldsymbol{\tau}}\|_{\mathbf{H}} \\
&\leq\; (1+\kappa_2^2)^{1/2}\,\|\mathcal{P}_k^h(\mathbf{w})\|_{0,4,\Omega}\,\|\mathcal{P}_k^h(\mathbf{z})\|_{0,4,\Omega}\,\|\vec{\boldsymbol{\tau}}\|_{\mathbf{H}} \qquad (2.63)\\
&\leq\; M_k^2\,(1+\kappa_2^2)^{1/2}\,\|\mathbf{z}\|_{0,4,\Omega}\,\|\mathbf{w}\|_{0,4,\Omega}\,\|\vec{\boldsymbol{\tau}}\|_{\mathbf{H}} \\
&\leq\; \|\mathbf{i}_c\|^2\,M_k^2\,(1+\kappa_2^2)^{1/2}\,\|\mathbf{z}\|_{1,\Omega}\,\|\mathbf{w}\|_{1,\Omega}\|\vec{\boldsymbol{\tau}}\|_{\mathbf{H}}\,,
\end{aligned}$$

which, noticing that $\|\mathbf{w}\|_{1,\Omega} \leq \|\vec{\boldsymbol{\zeta}}\|_{\mathbf{H}}$, yields (2.62) and completes the proof. □

### 2.4.3 The discrete linear form $\mathbf{F}_h$

In this section we introduce a computable discrete version $\mathbf{F}_h : \mathbf{H}_k^h \to \mathrm{R}$ of the functional $\mathbf{F}$ (cf. (2.13)). More precisely, we define

$$\mathbf{F}_h(\vec{\boldsymbol{\tau}}) \;:=\; \mu\langle\boldsymbol{\tau}\mathbf{n},\mathbf{g}\rangle_\Gamma \;-\; \kappa_1\int_\Omega \mathbf{f}\cdot\mathbf{div}(\boldsymbol{\tau}) \;+\; \mu\int_\Omega \mathcal{P}_{k-1}^h(\mathbf{f})\cdot\mathbf{v} \;+\; \kappa_3\int_\Gamma \mathbf{g}\cdot\mathbf{v}\,, \qquad (2.64)$$

which can be calculated using the fact that $\mathbf{div}(\boldsymbol{\tau})|_K \in \mathbf{P}_{k-1}(K)$ and $\boldsymbol{\tau}\mathbf{n}|_e \in \mathbf{P}_k(e)$, for each $e \in \partial K$ and for all $K \in \mathcal{T}_h$. Similarly, the degrees of freedom of $\mathbf{v}$ allow us to compute the boundary integrals $\int_\Gamma \mathbf{g} \cdot \mathbf{v}$ and the term $\int_\Omega \mathcal{P}^h_{k-1}(\mathbf{f}) \cdot \mathbf{v}$. In particular, the latter is computed locally exactly as explained for the expression in (2.55).

In addition, we have the following lemma comparing $\mathbf{F}$ and $\mathbf{F}_h$.

**Lemma 2.23.** *There exists a constant $C_{\mathrm{F}} > 0$, independent of $h$, such that*

$$|\mathbf{F}(\vec{\boldsymbol{\tau}}) - \mathbf{F}_h(\vec{\boldsymbol{\tau}})| \;\leq\; C_{\mathrm{F}}\, h\, \|\mathbf{f} - \mathcal{P}^h_{k-1}(\mathbf{f})\|_{0,\Omega}\, |\mathbf{v}|_{1,\Omega} \tag{2.65}$$

*for all $\vec{\boldsymbol{\tau}} := (\boldsymbol{\tau}, \mathbf{v}) \in \mathbf{H}^h_k$.*

*Proof.* It suffices to observe from the definitions of $\mathbf{F}$ (cf. (2.13)), $\mathbf{F}_h$ (cf. (2.64)), and $\mathcal{P}^h_{k-1}$ (cf. (2.32)), that

$$\begin{aligned} |\mathbf{F}(\vec{\boldsymbol{\tau}}) - \mathbf{F}_h(\vec{\boldsymbol{\tau}})| \;&=\; \mu \left| \int_\Omega \{\mathbf{f} - \mathcal{P}^h_{k-1}(\mathbf{f})\} \cdot \mathbf{v} \right| \;=\; \mu \left| \int_\Omega \{\mathbf{f} - \mathcal{P}^h_{k-1}(\mathbf{f})\} \cdot \{\mathbf{v} - \mathcal{P}^h_{k-1}(\mathbf{v})\} \right| \\ &\leq\; \mu\, \|\mathbf{f} - \mathcal{P}^h_{k-1}(\mathbf{f})\|_{0,\Omega}\, \|\mathbf{v} - \mathcal{P}^h_{k-1}(\mathbf{v})\|_{0,\Omega}\,, \end{aligned}$$

from which we arrive to (2.65) after applying (2.34) with $m = 0$ and $s = 1$. □

## 2.5 The virtual element scheme

We now use the discrete forms analyzed in the previous section to introduce our mixed virtual element scheme associated with (2.11), which reads: Find $\vec{\boldsymbol{\sigma}}_h := (\boldsymbol{\sigma}_h, \mathbf{u}_h) \in \mathbf{H}^h_k$ such that

$$\mathbf{A}_h(\vec{\boldsymbol{\sigma}}_h, \vec{\boldsymbol{\tau}}_h) + \mathbf{B}_h(\mathbf{u}_h; \vec{\boldsymbol{\sigma}}_h, \vec{\boldsymbol{\tau}}_h) \;=\; \mathbf{F}_h(\vec{\boldsymbol{\tau}}_h) \qquad \forall\, \vec{\boldsymbol{\tau}}_h \in \mathbf{H}^h_k\,, \tag{2.66}$$

where $\mathbf{A}_h$, $\mathbf{B}_h$ and $\mathbf{F}_h$ are the forms defined by (2.56), (2.59), and (2.64), respectively. We stress here that, and in order to insure that $\boldsymbol{\sigma}_h$ satisfies the condition $\int_\Omega \mathrm{tr}(\boldsymbol{\sigma}_h) = 0$, we follow the approach in Section 6 of [31] (see also Section 5 of [68]) and employ a Lagrange multiplier technique. More precisely, we redefine $H^h_k$ in (2.31) simply as

$$H^h_k \;:=\; \left\{ \boldsymbol{\tau} \in \mathbb{H}(\mathbf{div}; \Omega) \;:\quad \boldsymbol{\tau}|_K \in H^K_k \quad \forall\, K \in \mathcal{T}_h \right\}, \tag{2.67}$$

and reformulate (2.66), equivalently, as the discrete scheme: Find $(\vec{\boldsymbol{\sigma}}_h, \lambda_h) \in \mathbf{H}^h_k \times \mathrm{R}$ such that

$$\begin{aligned} \mathbf{A}_h(\vec{\boldsymbol{\sigma}}_h, \vec{\boldsymbol{\tau}}_h) + \mathbf{B}_h(\mathbf{u}_h; \vec{\boldsymbol{\sigma}}_h, \vec{\boldsymbol{\tau}}_h) + \lambda_h \int_\Omega \mathrm{tr}(\boldsymbol{\tau}_h) \;&=\; \mathbf{F}_h(\vec{\boldsymbol{\tau}}_h) \qquad \forall\, \vec{\boldsymbol{\tau}}_h := (\boldsymbol{\tau}_h, \mathbf{v}_h) \in \mathbf{H}^h_k\,, \\ \xi_h \int_\Omega \mathrm{tr}(\boldsymbol{\sigma}_h) \;&=\; 0 \qquad\qquad\qquad \forall\, \xi_h \in \mathrm{R}\,. \end{aligned} \tag{2.68}$$

Note here that the aforementioned condition for $\boldsymbol{\sigma}_h$ is imposed through the second equation of (2.68). In turn, it is easy to see (by taking $\boldsymbol{\tau}_h$ as the identity matrix along the first row of (2.68)) that the Lagrange multiplier $\lambda_h$ becomes a null auxiliary unknown, which confirms that (2.66) is also satisfied.

### 2.5.1 The solvability analysis

In this section we follow the approach from Section 3.2 in [34] and employ a fixed-point strategy to analyze the solvability and stability of the Galerkin scheme (2.66). To this end, we first define the discrete operator $\mathbf{T}_h : V_k^h \to V_k^h$ as

$$\mathbf{T}_h(\mathbf{z}_h) \;:=\; \mathbf{w}_h \qquad \forall\, \mathbf{z}_h \in V_k^h\,,$$

where $\mathbf{w}_h$ is the second component of the unique solution (to be confirmed below) of the discrete problem: Find $\vec{\boldsymbol{\zeta}}_h := (\boldsymbol{\zeta}_h, \mathbf{w}_h) \in \mathbf{H}_k^h$ such that

$$\mathbf{A}_h(\vec{\boldsymbol{\zeta}}_h, \vec{\boldsymbol{\tau}}_h) + \mathbf{B}_h(\mathbf{z}_h; \vec{\boldsymbol{\zeta}}_h, \vec{\boldsymbol{\tau}}_h) \;=\; \mathbf{F}_h(\vec{\boldsymbol{\tau}}_h) \qquad \forall\, \vec{\boldsymbol{\tau}}_h \in \mathbf{H}_k^h\,. \tag{2.69}$$

In this way, we realize that the augmented mixed-VEM formulation (2.66) can be rewritten as the fixed-point problem: Find $\mathbf{u}_h \in V_k^h$ such that

$$\mathbf{T}_h(\mathbf{u}_h) \;=\; \mathbf{u}_h\,. \tag{2.70}$$

Now, before studying the solvability of (2.70), we need to prove that $\mathbf{T}_h$ is well-defined, which is equivalent to the well-posedness of (2.69). Indeed, the following lemma shows that $\mathbf{T}_h$ makes sense only in a closed ball of $V_k^h$.

**Lemma 2.24.** *Suppose that the parameters $\kappa_1, \kappa_2$ and $\kappa_3$, satisfy the conditions required by Lemma 2.20. Then, there exists $\rho_0 > 0$, independent of $h$, such that for each $\rho \in (0, \rho_0)$, problem (2.69) has a unique solution $\vec{\boldsymbol{\zeta}}_h := (\boldsymbol{\zeta}_h, \mathbf{w}_h) \in \mathbf{H}_k^h$ for each $\mathbf{z}_h \in V_k^h$ such that $\|\mathbf{z}_h\|_{1,\Omega} \leq \rho$. In addition, there exists a constant $c_{\mathbf{T}} > 0$, independent of $\mathbf{z}_h$, $\mathbf{f}$, $\mathbf{g}$, and $h$, such that*

$$\|\mathbf{T}_h(\mathbf{z}_h)\|_{1,\Omega} \;=\; \|\mathbf{w}_h\|_{1,\Omega} \;\leq\; \|\vec{\boldsymbol{\zeta}}_h\|_{\mathbf{H}} \;\leq\; c_{\mathbf{T}} \left\{ \|\mathbf{f}\|_{0,\Omega} + \|\mathbf{g}\|_{0,\Gamma} + \|\mathbf{g}\|_{1/2,\Gamma} \right\}. \tag{2.71}$$

*Proof.* Let $\mathbf{z}_h \in V_k^h$. Then, thanks to the boundedness properties of $\mathbf{A}_h$ and $\mathbf{B}_h$ (cf. Lemmas 2.18 and 2.22), and defining $C_{\mathbf{AB}}(\mathbf{z}_h) := \widetilde{C}_{\mathbf{A}} + \|\mathbf{i}_c\|^2\, M_k^2\, (1+\kappa_2^2)^{1/2}\, \|\mathbf{z}_h\|_{1,\Omega}$, we find that

$$|\mathbf{A}_h(\vec{\boldsymbol{\zeta}}_h, \vec{\boldsymbol{\tau}}_h) + \mathbf{B}_h(\mathbf{z}_h; \vec{\boldsymbol{\zeta}}_h, \vec{\boldsymbol{\tau}}_h)| \;\leq\; C_{\mathbf{AB}}(\mathbf{z}_h)\, \|\vec{\boldsymbol{\zeta}}_h\|_{\mathbf{H}}\, \|\vec{\boldsymbol{\tau}}_h\|_{\mathbf{H}} \qquad \forall\, \vec{\boldsymbol{\zeta}}_h, \vec{\boldsymbol{\tau}}_h \in \mathbf{H}_k^h\,,$$

which shows that $\mathbf{A}_h + \mathbf{B}_h(\mathbf{z}_h; \cdot, \cdot)$ is bounded. Next, according to the hypotheses on $\kappa_1$, $\kappa_2$, and $\kappa_3$, we know from Lemma 2.20 that $\mathbf{A}_h$ becomes elliptic with constant $\alpha(\Omega)$, and hence, employing (2.62), we deduce that

$$\mathbf{A}_h(\vec{\boldsymbol{\tau}}_h, \vec{\boldsymbol{\tau}}_h) + \mathbf{B}_h(\mathbf{z}_h; \vec{\boldsymbol{\tau}}_h, \vec{\boldsymbol{\tau}}_h) \geq \left\{ \alpha(\Omega) - \|\mathbf{i}_c\|^2\, M_k^2\, (1+\kappa_2^2)^{1/2}\, \|\mathbf{z}_h\|_{1,\Omega} \right\} \|\vec{\boldsymbol{\tau}}_h\|_{\mathbf{H}}^2 \geq \frac{\alpha(\Omega)}{2} \|\vec{\boldsymbol{\tau}}_h\|_{\mathbf{H}}^2 \tag{2.72}$$

for all $\vec{\boldsymbol{\tau}}_h \in \mathbf{H}_k^h$, provided

$$\|\mathbf{i}_c\|^2\, M_k^2\, (1+\kappa_2^2)^{1/2}\, \|\mathbf{z}_h\|_{1,\Omega} \;\leq\; \frac{\alpha(\Omega)}{2}\,.$$

Therefore, given $\mathbf{z}_h \in V_k^h$, the ellipticity of the bilinear form $\mathbf{A}_h + \mathbf{B}_h(\mathbf{z}_h; \cdot, \cdot)$ is ensured with the constant $\frac{\alpha(\Omega)}{2}$, independent of $\mathbf{z}_h$, by requiring

$$\|\mathbf{z}_h\|_{1,\Omega} \;\leq\; \rho_0 \;:=\; \frac{\alpha(\Omega)}{2\, \|\mathbf{i}_c\|^2\, M_k^2\, (1+\kappa_2^2)^{1/2}}\,. \tag{2.73}$$

In turn, it is easy to see that, with the same constant $M_{\mathbf{F}} > 0$ from (2.19), which is independent of $\mathbf{z}_h$, $h$, and the data $\mathbf{f}$ and $\mathbf{g}$, there holds

$$|\mathbf{F}_h(\vec{\boldsymbol{\tau}}_h)| \leq M_{\mathbf{F}} \left\{ \|\mathbf{f}\|_{0,\Omega} + \|\mathbf{g}\|_{0,\Gamma} + \|\mathbf{g}\|_{1/2,\Gamma} \right\} \|\vec{\boldsymbol{\tau}}_h\|_{\mathbf{H}} \qquad \forall\, \vec{\boldsymbol{\tau}}_h \in \mathbf{H}_k^h \,,$$

which shows that $\mathbf{F}_h$ is bounded with

$$\|\mathbf{F}_h\| \leq M_{\mathbf{F}} \left\{ \|\mathbf{f}\|_{0,\Omega} + \|\mathbf{g}\|_{0,\Gamma} + \|\mathbf{g}\|_{1/2,\Gamma} \right\}. \tag{2.74}$$

Hence, a straightforward application of the Lax-Milgram lemma implies the existence of a unique solution $\vec{\boldsymbol{\zeta}}_h := (\boldsymbol{\zeta}_h, \mathbf{w}_h) \in \mathbf{H}_k^h$ of (2.69). Moreover, the corresponding continuous dependence result establishes that

$$\|\vec{\boldsymbol{\zeta}}_h\|_{\mathbf{H}} \leq \frac{2}{\alpha(\Omega)} \|\mathbf{F}_h\| \,,$$

from which, utilizing (2.74), we conclude (2.71) with $c_{\mathbf{T}} := \frac{2M_{\mathbf{F}}}{\alpha(\Omega)}$, which is clearly independent of $\mathbf{z}_h$. □

Having proved that $\mathbf{T}_h : \mathbf{H}_k^h \to \mathbf{H}_k^h$ is well defined, we now employ the Banach theorem to establish the existence of a unique fixed-point of this operator. We begin with the following result, from which a Lipschitz-continuity property of $\mathbf{T}_h$ will be derived later on (see the proof of Theorem 2.26 below).

**Lemma 2.25.** *Given $\rho \in (0, \rho_0)$, with $\rho_0$ defined by (2.73), we let*

$$W_\rho^h := \left\{ \mathbf{z}_h \in V_k^h : \quad \|\mathbf{z}_h\|_{1,\Omega} \leq \rho \right\}. \tag{2.75}$$

*Then, there holds*

$$\|\mathbf{T}_h(\mathbf{z}_{1,h}) - \mathbf{T}_h(\mathbf{z}_{2,h})\|_{1,\Omega} \leq \frac{1}{\rho_0} \|\mathbf{T}_h(\mathbf{z}_{1,h})\|_{1,\Omega} \|\mathbf{z}_{1,h} - \mathbf{z}_{2,h}\|_{1,\Omega} \qquad \forall\, \mathbf{z}_{1,h}, \mathbf{z}_{2,h} \in W_\rho^h \,. \tag{2.76}$$

*Proof.* Given $\rho \in (0, \rho_0)$ and $\mathbf{z}_{1,h}$, $\mathbf{z}_{2,h} \in W_\rho^h$, we let

$$\mathbf{u}_{1,h} = \mathbf{T}_h(\mathbf{z}_{1,h}) \qquad \text{and} \qquad \mathbf{u}_{2,h} = \mathbf{T}_h(\mathbf{z}_{2,h})$$

be the second components of the corresponding solutions $\vec{\boldsymbol{\sigma}}_{1,h}$ and $\vec{\boldsymbol{\sigma}}_{2,h}$ of the problems

$$\mathbf{A}_h(\vec{\boldsymbol{\sigma}}_{1,h}, \vec{\boldsymbol{\tau}}_h) + \mathbf{B}_h(\mathbf{z}_{1,h}; \vec{\boldsymbol{\sigma}}_{1,h}, \vec{\boldsymbol{\tau}}_h) = \mathbf{F}_h(\vec{\boldsymbol{\tau}}_h) \tag{2.77}$$

and

$$\mathbf{A}_h(\vec{\boldsymbol{\sigma}}_{2,h}, \vec{\boldsymbol{\tau}}_h) + \mathbf{B}_h(\mathbf{z}_{2,h}; \vec{\boldsymbol{\sigma}}_{2,h}, \vec{\boldsymbol{\tau}}_h) = \mathbf{F}_h(\vec{\boldsymbol{\tau}}_h) \,, \tag{2.78}$$

for all $\vec{\boldsymbol{\tau}}_h \in \mathbf{H}_k^h$, respectively. Then, applying the ellipticity of $\mathbf{A}_h + \mathbf{B}_h(\mathbf{z}_{2,h}, \cdot, \cdot)$ (cf. (2.72)) with $\vec{\boldsymbol{\tau}}_h := \vec{\boldsymbol{\sigma}}_{1,h} - \vec{\boldsymbol{\sigma}}_{2,h}$, and employing (2.77) and (2.78), we find that

$$\begin{aligned} \frac{\alpha(\Omega)}{2} \|\vec{\boldsymbol{\sigma}}_{1,h} - \vec{\boldsymbol{\sigma}}_{2,h}\|_{\mathbf{H}}^2 &\leq \mathbf{A}_h(\vec{\boldsymbol{\sigma}}_{1,h} - \vec{\boldsymbol{\sigma}}_{2,h}, \vec{\boldsymbol{\sigma}}_{1,h} - \vec{\boldsymbol{\sigma}}_{2,h}) + \mathbf{B}_h(\mathbf{z}_{2,h}; \vec{\boldsymbol{\sigma}}_{1,h} - \vec{\boldsymbol{\sigma}}_{2,h}, \vec{\boldsymbol{\sigma}}_{1,h} - \vec{\boldsymbol{\sigma}}_{2,h}) \\ &= - \mathbf{B}_h(\mathbf{z}_{1,h} - \mathbf{z}_{2,h}; \vec{\boldsymbol{\sigma}}_{1,h}, \vec{\boldsymbol{\sigma}}_{1,h} - \vec{\boldsymbol{\sigma}}_{2,h}) \,, \end{aligned}$$

which, together with the estimate obtained at the end of (2.63), yield

$$\frac{\alpha(\Omega)}{2} \|\vec{\boldsymbol{\sigma}}_{1,h} - \vec{\boldsymbol{\sigma}}_{2,h}\|_{\mathbf{H}}^2 \leq \|\mathbf{i}_c\|^2 M_k^2 (1 + \kappa_2^2)^{1/2} \|\mathbf{z}_{1,h} - \mathbf{z}_{2,h}\|_{1,\Omega} \|\mathbf{u}_{1,h}\|_{1,\Omega} \|\vec{\boldsymbol{\sigma}}_{1,h} - \vec{\boldsymbol{\sigma}}_{2,h}\|_{\mathbf{H}} \,. \tag{2.79}$$

Finally, recalling the definition of $\rho_0$ (cf. (2.73)), we see that (2.79) can be rewritten as

$$\|\vec{\boldsymbol{\sigma}}_{1,h} - \vec{\boldsymbol{\sigma}}_{2,h}\|_{\mathbf{H}} \;\leq\; \frac{1}{\rho_0}\,\|\mathbf{u}_{1,h}\|_{1,\Omega}\,\|\mathbf{z}_{1,h} - \mathbf{z}_{2,h}\|_{1,\Omega}\,,$$

which gives (2.76) and finishes the proof. □

The main result of this section is stated as follows.

**Theorem 2.26.** *Suppose that the parameters $\kappa_1, \kappa_2$ and $\kappa_3$, satisfy the conditions required by Lemma 2.20. In addition, given $\rho \in (0, \rho_0)$, with $\rho_0$ defined by (2.73), we let $W_\rho^h$ as in (2.75), and assume that the data satisfy*

$$c_{\mathbf{T}}\left\{\|\mathbf{f}\|_{0,\Omega} + \|\mathbf{g}\|_{0,\Gamma} + \|\mathbf{g}\|_{1/2,\Gamma}\right\} \;\leq\; \rho\,, \tag{2.80}$$

*with $c_{\mathbf{T}}$ given by Lemma 2.24. Then, the mixed virtual element scheme (2.66) has a unique solution $\vec{\boldsymbol{\sigma}}_h := (\boldsymbol{\sigma}_h, \mathbf{u}_h) \in \mathbf{H}_k^h$ with $\mathbf{u}_h \in W_\rho^h$, and there holds*

$$\|\vec{\boldsymbol{\sigma}}_h\|_{\mathbf{H}} \;\leq\; c_{\mathbf{T}}\left\{\|\mathbf{f}\|_{0,\Omega} + \|\mathbf{g}\|_{0,\Gamma} + \|\mathbf{g}\|_{1/2,\Gamma}\right\}. \tag{2.81}$$

*Proof.* We first notice, thanks to (2.71), that the assumption (2.80) guarantees that $\mathbf{T}_h(W_\rho^h) \subseteq W_\rho^h$. Next, using (2.76) along with (2.71) and (2.80), we obtain

$$\|\mathbf{T}_h(\mathbf{z}_{1,h}) - \mathbf{T}_h(\mathbf{z}_{2,h})\|_{1,\Omega} \;\leq\; \frac{\rho}{\rho_0}\,\|\mathbf{z}_{1,h} - \mathbf{z}_{2,h}\|_{1,\Omega} \qquad \forall\; \mathbf{z}_{1,h}, \mathbf{z}_{2,h} \in W_\rho^h\,,$$

which proves that $\mathbf{T}_h : W_\rho^h \to W_\rho^h$ is a contraction, that is a Lipschitz-continuous mapping with corresponding constant in $(0,1)$. Hence, a simple application of the Banach theorem implies the existence of a unique fixed-point $\mathbf{u}_h \in W_\rho^h$ of (2.70). In this way, the equivalence between (2.70) and the Galerkin scheme (2.66) shows that (2.66) has a unique solution $\vec{\boldsymbol{\sigma}}_h \in \mathbf{H}_k^h$, whose stability (2.81) follows directly from (2.71). □

### 2.5.2 The a priori error analysis

We now aim to derive the *a priori* estimates for the error $\|\vec{\boldsymbol{\sigma}} - \vec{\boldsymbol{\sigma}}_h\|_{\mathbf{H}}$, where $\vec{\boldsymbol{\sigma}} := (\boldsymbol{\sigma}, \mathbf{u}) \in \mathbf{H} := \mathbb{H}_0(\mathbf{div};\Omega) \times \mathbf{H}^1(\Omega)$ and $\vec{\boldsymbol{\sigma}}_h := (\boldsymbol{\sigma}_h, \mathbf{u}_h) \in \mathbf{H}_k^h := H_k^h \times V_k^h$ are the unique solutions of the continuous and discrete schemes (2.11) and (2.66), respectively. In this regard, and as suggested by Theorems 2.1 and 2.26, we first define

$$\widetilde{\rho}_0 \;:=\; \min\left\{\frac{\alpha_{\mathbf{A}}}{2\,\|\mathbf{i}_c\|^2\,(1+\kappa_2^2)^{1/2}},\; \rho_0\right\},$$

with $\mathbf{i}_c$, $\alpha_{\mathbf{A}}$, and $\rho_0$, given by (2.9), (2.16), and (2.73), respectively, and observe that the existence of $\vec{\boldsymbol{\sigma}}$ and $\vec{\boldsymbol{\sigma}}_h$ is guaranteed within the respective balls centered at the origin and with radius $\rho \in (0, \widetilde{\rho}_0)$, and under the assumptions that $\kappa_1,\ \kappa_3 > 0$, and $0 < \kappa_2 < 2\min\{\mu, \alpha_1, \beta_1\}$. In particular, we know from Theorem 2.1 that there holds

$$\|\vec{\boldsymbol{\sigma}}\|_{\mathbf{H}} \;\leq\; C_{\mathbf{T}}\left\{\|\mathbf{f}\|_{0,\Omega} + \|\mathbf{g}\|_{0,\Gamma} + \|\mathbf{g}\|_{1/2,\Gamma}\right\} \;\leq\; \rho\,. \tag{2.82}$$

We begin the analysis with a preliminary estimate for $\|\vec{\boldsymbol{\sigma}} - \vec{\boldsymbol{\sigma}}_h\|_{\mathbf{H}}$.

**Lemma 2.27.** *There exists a positive constant $C_{\mathrm{p}}$, independent of $h$, such that*

$$\|\vec{\boldsymbol{\sigma}}-\vec{\boldsymbol{\sigma}}_h\|_{\mathbf{H}} \leq C_{\mathrm{p}}\left\{\|\boldsymbol{\sigma}-\boldsymbol{\mathcal{P}}_k^h(\boldsymbol{\sigma})\|_{0,\Omega}+|\mathbf{u}-\mathcal{R}_k^h(\mathbf{u})|_{1,h}+h\,\|\mathbf{f}-\mathcal{P}_{k-1}^h(\mathbf{f})\|_{0,\Omega}\right.$$
$$\left.+\inf_{\vec{\boldsymbol{\zeta}}_h\in\mathbf{H}_k^h}\left(\|\vec{\boldsymbol{\sigma}}-\vec{\boldsymbol{\zeta}}_h\|_{\mathbf{H}}+\sup_{\substack{\vec{\boldsymbol{\tau}}_h\in\mathbf{H}_k^h\\ \vec{\boldsymbol{\tau}}_h\neq\mathbf{0}}}\frac{|\mathbf{B}(\mathbf{u};\vec{\boldsymbol{\zeta}}_h,\vec{\boldsymbol{\tau}}_h)-\mathbf{B}_h(\mathbf{u}_h;\vec{\boldsymbol{\zeta}}_h,\vec{\boldsymbol{\tau}}_h)|}{\|\vec{\boldsymbol{\tau}}_h\|_{\mathbf{H}}}\right)\right\} \tag{2.83}$$

*Proof.* It reduces to apply the first Strang lemma for linear problems (see, e.g. Theorem 4.1.1 of [45] or Theorem 11.1 of [87]) to the context given by (2.11) and (2.66). In fact, we first set

$$A(\vec{\boldsymbol{\zeta}},\vec{\boldsymbol{\tau}}) := \mathbf{A}(\vec{\boldsymbol{\zeta}},\vec{\boldsymbol{\tau}})+\mathbf{B}(\mathbf{u};\vec{\boldsymbol{\zeta}},\vec{\boldsymbol{\tau}}), \qquad F(\vec{\boldsymbol{\tau}}) := \mathbf{F}(\vec{\boldsymbol{\tau}}),$$
$$A_h(\vec{\boldsymbol{\zeta}}_h,\vec{\boldsymbol{\tau}}_h) := \mathbf{A}_h(\vec{\boldsymbol{\zeta}}_h,\vec{\boldsymbol{\tau}}_h)+\mathbf{B}_h(\mathbf{u}_h;\vec{\boldsymbol{\zeta}}_h,\vec{\boldsymbol{\tau}}_h), \quad \text{and} \quad F_h(\vec{\boldsymbol{\tau}}_h) := \mathbf{F}_h(\vec{\boldsymbol{\tau}}_h),$$

for all $\vec{\boldsymbol{\zeta}},\vec{\boldsymbol{\tau}}\in H:=\mathbf{H}$ and $\vec{\boldsymbol{\zeta}}_h,\vec{\boldsymbol{\tau}}_h\in H_h:=\mathbf{H}_k^h$. Then, employing the bounds provided by (2.15), (2.18), Lemmas 2.18 and 2.22, and (2.82), and recalling that $M_k\geq 1$ (cf. (2.40)), we deduce that the family $\{A\}\cup\{A_h\}_{h>0}$ is uniformly bounded with a constant, independent of $h$, given by

$$L_{\mathrm{B}} := \max\left\{C_{\mathbf{A}},\widetilde{C}_{\mathbf{A}}\right\}+\|\mathbf{i}_c\|^2\,M_k^2\,(1+\kappa_2^2)^{1/2}\,\widetilde{\rho}_0\,.$$

In turn, using now (2.17) and (2.72), we obtain that $\{A\}\cup\{A_h\}_{h>0}$ is uniformly elliptic with the constant

$$L_{\mathrm{E}} := \frac{1}{2}\min\{\alpha_{\mathbf{A}},\alpha(\Omega)\}\,.$$

Hence, a straightforward application of the aforementioned classic result yields

$$\|\vec{\boldsymbol{\sigma}}-\vec{\boldsymbol{\sigma}}_h\|_{\mathbf{H}} \leq C_{\mathrm{ST}}\left\{\sup_{\substack{\vec{\boldsymbol{\tau}}_h\in\mathbf{H}_k^h\\ \vec{\boldsymbol{\tau}}_h\neq\mathbf{0}}}\frac{|\mathbf{F}(\vec{\boldsymbol{\tau}}_h)-\mathbf{F}_h(\vec{\boldsymbol{\tau}}_h)|}{\|\vec{\boldsymbol{\tau}}_h\|_{\mathbf{H}}}+\inf_{\vec{\boldsymbol{\zeta}}_h\in\mathbf{H}_k^h}\left(\|\vec{\boldsymbol{\sigma}}-\vec{\boldsymbol{\zeta}}_h\|_{\mathbf{H}}\right.\right.$$
$$\left.\left.+\sup_{\substack{\vec{\boldsymbol{\tau}}_h\in\mathbf{H}_k^h\\ \vec{\boldsymbol{\tau}}_h\neq\mathbf{0}}}\frac{|\mathbf{A}(\vec{\boldsymbol{\zeta}}_h,\vec{\boldsymbol{\tau}}_h)-\mathbf{A}_h(\vec{\boldsymbol{\zeta}}_h,\vec{\boldsymbol{\tau}}_h)+\mathbf{B}(\mathbf{u};\vec{\boldsymbol{\zeta}}_h,\vec{\boldsymbol{\tau}}_h)-\mathbf{B}_h(\mathbf{u}_h;\vec{\boldsymbol{\zeta}}_h,\vec{\boldsymbol{\tau}}_h)|}{\|\vec{\boldsymbol{\tau}}_h\|_{\mathbf{H}}}\right)\right\}, \tag{2.84}$$

where $C_{\mathrm{ST}} := L_{\mathrm{E}}^{-1}\max\left\{1,L_{\mathrm{E}}+L_{\mathrm{B}}\right\}$.

Next, thanks to (2.65) (cf. Lemma 2.23), we find that

$$\sup_{\substack{\vec{\boldsymbol{\tau}}_h\in\mathbf{H}_k^h\\ \vec{\boldsymbol{\tau}}_h\neq\mathbf{0}}}\frac{|\mathbf{F}(\vec{\boldsymbol{\tau}}_h)-\mathbf{F}_h(\vec{\boldsymbol{\tau}}_h)|}{\|\vec{\boldsymbol{\tau}}_h\|_{\mathbf{H}}} \leq C_{\mathrm{F}}\,h\|\mathbf{f}-\mathcal{P}_{k-1}^h(\mathbf{f})\|_{0,\Omega}\,, \tag{2.85}$$

whereas, setting $\vec{\boldsymbol{\zeta}}_h:=(\boldsymbol{\zeta}_h,\mathbf{w}_h)$, (2.57) (cf. Lemma 2.17) gives

$$|\mathbf{A}(\vec{\boldsymbol{\zeta}}_h,\vec{\boldsymbol{\tau}}_h)-\mathbf{A}_h(\vec{\boldsymbol{\zeta}}_h,\vec{\boldsymbol{\tau}}_h)| \leq L_{\mathbf{A}}\left\{\|\boldsymbol{\zeta}_h-\boldsymbol{\mathcal{P}}_k^h(\boldsymbol{\zeta}_h)\|_{0,\Omega}+|\mathbf{w}_h-\mathcal{R}_k^h(\mathbf{w}_h)|_{1,h}\right\}\|\vec{\boldsymbol{\tau}}_h\|_{\mathbf{H}}\,.$$

Thus, adding and subtracting $\boldsymbol{\sigma}-\boldsymbol{\mathcal{P}}_k^h(\boldsymbol{\sigma})$ and $\mathbf{u}-\mathcal{R}_k^h(\mathbf{u})$, respectively, in the first and second expressions on the right-hand side of the foregoing equation, and using the boundedness of $\boldsymbol{\mathcal{P}}_k^h$ and $\mathcal{R}_k^h$ (cf. (2.21)),

we deduce that

$$
\begin{aligned}
&|\mathbf{A}(\vec{\boldsymbol{\zeta}}_h,\vec{\boldsymbol{\tau}}_h)-\mathbf{A}_h(\vec{\boldsymbol{\zeta}}_h,\vec{\boldsymbol{\tau}}_h)| \\
&\quad\leq L_{\mathbf{A}}\left\{2\|\boldsymbol{\sigma}-\boldsymbol{\zeta}_h\|_{0,\Omega}+\|\boldsymbol{\sigma}-\boldsymbol{\mathcal{P}}_k^h(\boldsymbol{\sigma})\|_{0,\Omega}+2|\mathbf{u}-\mathbf{w}_h|_{1,\Omega}+|\mathbf{u}-\mathcal{R}_k^h(\mathbf{u})|_{1,h}\right\}\|\vec{\boldsymbol{\tau}}_h\|_{\mathbf{H}} \qquad (2.86)\\
&\quad\leq L_{\mathbf{A}}\left\{3\|\vec{\boldsymbol{\sigma}}-\vec{\boldsymbol{\zeta}}_h\|_{\mathbf{H}}+\|\boldsymbol{\sigma}-\boldsymbol{\mathcal{P}}_k^h(\boldsymbol{\sigma})\|_{0,\Omega}+|\mathbf{u}-\mathcal{R}_k^h(\mathbf{u})|_{1,h}\right\}\|\vec{\boldsymbol{\tau}}_h\|_{\mathbf{H}}\,.
\end{aligned}
$$

Finally, replacing (2.85) and (2.86) back into (2.84), we arrive at (2.83) with $C_{\mathrm{p}}$ depending on $C_{\mathrm{ST}}$, $C_{\mathrm{F}}$, and $L_{\mathbf{A}}$, thus completing the proof. □

We now aim to bound the supremum in (2.83). For this purpose, we first observe that, while the estimates (2.60) (cf. Lemma 2.21) and (2.62) (cf. Lemma 2.22) were proved for $\mathbf{z}\in V_k^h$, it is easily seen that they are also valid for $\mathbf{z}\in\mathbf{H}^1(\Omega)$. Then, we have the following result.

**Lemma 2.28.** *There exists $\widetilde{C}_{\mathrm{p}}>0$, independent of $h$, but depending on $\kappa_2$, $\|\mathbf{i}_c\|$, and $M_k$, such that*

$$
\begin{aligned}
|\mathbf{B}(\mathbf{u};\vec{\boldsymbol{\zeta}}_h,\vec{\boldsymbol{\tau}}_h)-\mathbf{B}_h(\mathbf{u}_h;\vec{\boldsymbol{\zeta}}_h,\vec{\boldsymbol{\tau}}_h)| &\leq \widetilde{C}_{\mathrm{p}}\left\{\Big(\|\vec{\boldsymbol{\sigma}}\|_{\mathbf{H}}+\|\vec{\boldsymbol{\sigma}}_h\|_{\mathbf{H}}\Big)\|\vec{\boldsymbol{\sigma}}-\vec{\boldsymbol{\zeta}}_h\|_{\mathbf{H}}\right.\\
&+\|\vec{\boldsymbol{\sigma}}\|_{\mathbf{H}}\Big(\|\vec{\boldsymbol{\sigma}}-\vec{\boldsymbol{\sigma}}_h\|_{\mathbf{H}}+\|\mathbf{u}-\mathcal{P}_k^h(\mathbf{u})\|_{0,4,\Omega}\Big) \qquad (2.87)\\
&+\left.\|\mathbf{u}\otimes\mathbf{u}-\boldsymbol{\mathcal{P}}_k^h(\mathbf{u}\otimes\mathbf{u})\|_{0,\Omega}\right\}\|\vec{\boldsymbol{\tau}}_h\|_{\mathbf{H}}\,,
\end{aligned}
$$

*for all $\vec{\boldsymbol{\zeta}}_h:=(\boldsymbol{\zeta}_h,\mathbf{w}_h)$, $\vec{\boldsymbol{\tau}}_h:=(\boldsymbol{\tau}_h,\mathbf{v}_h)\in\mathbf{H}_k^h$.*

*Proof.* Let $\vec{\boldsymbol{\zeta}}_h:=(\boldsymbol{\zeta}_h,\mathbf{w}_h)$, $\vec{\boldsymbol{\tau}}_h:=(\boldsymbol{\tau}_h,\mathbf{v}_h)\in\mathbf{H}_k^h$. Then, adding and subtracting $\mathbf{B}_h(\mathbf{u};\vec{\boldsymbol{\zeta}}_h,\vec{\boldsymbol{\tau}}_h)$, we find that

$$
|\mathbf{B}(\mathbf{u};\vec{\boldsymbol{\zeta}}_h,\vec{\boldsymbol{\tau}}_h)-\mathbf{B}_h(\mathbf{u}_h;\vec{\boldsymbol{\zeta}}_h,\vec{\boldsymbol{\tau}}_h)|\leq\big|\mathbf{B}(\mathbf{u};\vec{\boldsymbol{\zeta}}_h,\vec{\boldsymbol{\tau}}_h)-\mathbf{B}_h(\mathbf{u};\vec{\boldsymbol{\zeta}}_h,\vec{\boldsymbol{\tau}}_h)\big|+\big|\mathbf{B}_h(\mathbf{u}-\mathbf{u}_h;\vec{\boldsymbol{\zeta}}_h,\vec{\boldsymbol{\tau}}_h)\big|\,. \qquad (2.88)
$$

For the second term on the right-hand side of (2.88) we apply (2.62) (cf. Lemma 2.22) and obtain

$$
\big|\mathbf{B}_h(\mathbf{u}-\mathbf{u}_h;\vec{\boldsymbol{\zeta}}_h,\vec{\boldsymbol{\tau}}_h)\big|\leq\|\mathbf{i}_c\|^2\,M_k^2\,(1+\kappa_2^2)^{1/2}\,\|\mathbf{u}-\mathbf{u}_h\|_{1,\Omega}\,\|\vec{\boldsymbol{\zeta}}_h\|_{\mathbf{H}}\,\|\vec{\boldsymbol{\tau}}_h\|_{\mathbf{H}}\,,
$$

which, adding and subtracting $\vec{\boldsymbol{\sigma}}$, yield

$$
\begin{aligned}
|\mathbf{B}_h(\mathbf{u}-\mathbf{u}_h;\vec{\boldsymbol{\zeta}}_h,\vec{\boldsymbol{\tau}}_h)| &\leq \|\mathbf{i}_c\|^2\,M_k^2\,(1+\kappa_2^2)^{1/2}\left\{\|\vec{\boldsymbol{\sigma}}-\vec{\boldsymbol{\zeta}}_h\|_{\mathbf{H}}+\|\vec{\boldsymbol{\sigma}}\|_{\mathbf{H}}\right\}\|\mathbf{u}-\mathbf{u}_h\|_{1,\Omega}\,\|\vec{\boldsymbol{\tau}}_h\|_{\mathbf{H}}\\
&\leq \|\mathbf{i}_c\|^2\,M_k^2\,(1+\kappa_2^2)^{1/2}\left\{\Big(\|\mathbf{u}\|_{1,\Omega}+\|\mathbf{u}_h\|_{1,\Omega}\Big)\|\vec{\boldsymbol{\sigma}}-\vec{\boldsymbol{\zeta}}_h\|_{\mathbf{H}}+\|\vec{\boldsymbol{\sigma}}\|_{\mathbf{H}}\,\|\mathbf{u}-\mathbf{u}_h\|_{1,\Omega}\right\}\|\vec{\boldsymbol{\tau}}_h\|_{\mathbf{H}}\,.
\end{aligned} \qquad (2.89)
$$

In addition, thanks to (2.60) (cf. Lemma 2.21), the corresponding first term is bounded as follows

$$
\begin{aligned}
\big|\mathbf{B}(\mathbf{u};\vec{\boldsymbol{\zeta}}_h,\vec{\boldsymbol{\tau}}_h)-\mathbf{B}_h(\mathbf{u};\vec{\boldsymbol{\zeta}}_h,\vec{\boldsymbol{\tau}}_h)\big| &\leq (1+\kappa_2^2)^{1/2}\left\{\|\mathbf{w}_h\otimes\mathbf{u}-\boldsymbol{\mathcal{P}}_k^h(\mathbf{w}_h\otimes\mathbf{u})\|_{0,\Omega}\right.\\
&+\left.\|\mathbf{i}_c\|\,M_k\Big(\|\mathbf{w}_h\|_{1,\Omega}\,\|\mathbf{u}-\mathcal{P}_k^h(\mathbf{u})\|_{0,4,\Omega}+\|\mathbf{u}\|_{1,\Omega}\,\|\mathbf{w}_h-\mathcal{P}_k^h(\mathbf{w}_h)\|_{0,4,\Omega}\Big)\right\}\|\vec{\boldsymbol{\tau}}_h\|_{\mathbf{H}}\,.
\end{aligned} \qquad (2.90)
$$

Now, adding and subtracting $\mathbf{u}$, it follows that

$$\mathbf{w}_h \otimes \mathbf{u} - \boldsymbol{\mathcal{P}}_k^h(\mathbf{w}_h \otimes \mathbf{u}) \,=\, (\mathbf{w}_h - \mathbf{u}) \otimes \mathbf{u} \,+\, \mathbf{u} \otimes \mathbf{u} \,-\, \boldsymbol{\mathcal{P}}_k^h\big((\mathbf{w}_h - \mathbf{u}) \otimes \mathbf{u} \,+\, \mathbf{u} \otimes \mathbf{u}\big)\,,$$

from which, using the $\mathbf{L}^2(\Omega)$-boundedness of $\boldsymbol{\mathcal{P}}_k^h$, the Cauchy-Schwarz inequality, and (2.9), we deduce that

$$\begin{aligned}\|\mathbf{w}_h \otimes \mathbf{u} - \boldsymbol{\mathcal{P}}_k^h(\mathbf{w}_h \otimes \mathbf{u})\|_{0,\Omega} \,&\leq\, 2\,\|\mathbf{u} - \mathbf{w}_h\|_{0,4,\Omega}\,\|\mathbf{u}\|_{0,4,\Omega} \,+\, \|\mathbf{u} \otimes \mathbf{u} - \boldsymbol{\mathcal{P}}_k^h(\mathbf{u} \otimes \mathbf{u})\|_{0,\Omega} \\ &\leq\, 2\,\|\mathbf{i}_c\|^2\,\|\mathbf{u} - \mathbf{w}_h\|_{1,\Omega}\,\|\mathbf{u}\|_{1,\Omega} \,+\, \|\mathbf{u} \otimes \mathbf{u} - \boldsymbol{\mathcal{P}}_k^h(\mathbf{u} \otimes \mathbf{u})\|_{0,\Omega}\,.\end{aligned} \tag{2.91}$$

In turn, similar reasonings, but employing now the $\mathbf{L}^4(\Omega)$-boundedness of $\boldsymbol{\mathcal{P}}_k^h$ (cf. (2.40)), yield

$$\|\mathbf{w}_h\|_{1,\Omega}\,\|\mathbf{u} - \mathcal{P}_k^h(\mathbf{u})\|_{0,4,\Omega} \,\leq\, \|\mathbf{i}_c\|\,(1 + M_k)\,\|\mathbf{u}\|_{1,\Omega}\,\|\mathbf{u} - \mathbf{w}_h\|_{1,\Omega} \,+\, \|\mathbf{u}\|_{1,\Omega}\,\|\mathbf{u} - \mathcal{P}_k^h(\mathbf{u})\|_{0,4,\Omega} \tag{2.92}$$

and

$$\|\mathbf{w}_h - \mathcal{P}_k^h(\mathbf{w}_h)\|_{0,4,\Omega} \,\leq\, \|\mathbf{i}_c\|\,(1 + M_k)\,\|\mathbf{u} - \mathbf{w}_h\|_{1,\Omega} \,+\, \|\mathbf{u} - \mathcal{P}_k^h(\mathbf{u})\|_{0,4,\Omega}\,. \tag{2.93}$$

In this way, replacing (2.91), (2.92), and (2.93) back into (2.90), and then using the resulting estimate together with (2.89) in (2.88), we are lead to (2.87) after bounding $\|\mathbf{u} - \mathbf{w}_h\|_{1,\Omega}$, $\|\mathbf{u} - \mathbf{u}_h\|_{1,\Omega}$, $\|\mathbf{u}\|_{1,\Omega}$, and $\|\mathbf{u}_h\|_{1,\Omega}$ by $\|\vec{\boldsymbol{\sigma}} - \vec{\boldsymbol{\zeta}}_h\|_{\mathbf{H}}$, $\|\vec{\boldsymbol{\sigma}} - \vec{\boldsymbol{\sigma}}_h\|_{\mathbf{H}}$, $\|\vec{\boldsymbol{\sigma}}\|_{\mathbf{H}}$, and $\|\vec{\boldsymbol{\sigma}}_h\|_{\mathbf{H}}$, respectively. □

As a consequence of Lemmas 2.27 and 2.28, we are able to establish the following definite *a priori* estimate for $\|\vec{\boldsymbol{\sigma}} - \vec{\boldsymbol{\sigma}}_h\|_{\mathbf{H}}$, in which we employ the expression $\mathrm{dist}(\vec{\boldsymbol{\sigma}}, \mathbf{H}_k^h)$ to denote the distance of $\vec{\boldsymbol{\sigma}}$ to $\mathbf{H}_k^h$ with respect to the product norm of $\mathbb{H}(\mathbf{div};\Omega) \times \mathbf{H}^1(\Omega)$.

**Theorem 2.29.** *Let $C_{\mathbf{T}}$, $C_{\mathrm{p}}$, and $\widetilde{C}_{\mathrm{p}}$ be the constants from Theorem 2.1, Lemma 2.27, and Lemma 2.28, respectively, and assume that the data $\mathbf{f}$ and $\mathbf{g}$ satisfy*

$$C_{\mathbf{T}}\,C_{\mathrm{p}}\,\widetilde{C}_{\mathrm{p}}\,\Big\{\|\mathbf{f}\|_{0,\Omega} \,+\, \|\mathbf{g}\|_{0,\Gamma} \,+\, \|\mathbf{g}\|_{1/2,\Gamma}\Big\} \,\leq\, \frac{1}{2}\,. \tag{2.94}$$

*Then there exists a positive constant $\widehat{C}_{\mathrm{p}}$, independent of $h$, such that*

$$\begin{aligned}\|\vec{\boldsymbol{\sigma}} - \vec{\boldsymbol{\sigma}}_h\|_{\mathbf{H}} \,\leq\, \widehat{C}_{\mathrm{p}}\,\Big\{ &\|\boldsymbol{\sigma} - \boldsymbol{\mathcal{P}}_k^h(\boldsymbol{\sigma})\|_{0,\Omega} \,+\, |\mathbf{u} - \mathcal{R}_k^h(\mathbf{u})|_{1,h} \,+\, h\,\|\mathbf{f} - \mathcal{P}_{k-1}^h(\mathbf{f})\|_{0,\Omega} \\ &+\, \|\mathbf{u} - \mathcal{P}_k^h(\mathbf{u})\|_{0,4,\Omega} \,+\, \|\mathbf{u} \otimes \mathbf{u} - \boldsymbol{\mathcal{P}}_k^h(\mathbf{u} \otimes \mathbf{u})\|_{0,\Omega} \,+\, \mathrm{dist}(\vec{\boldsymbol{\sigma}}, \mathbf{H}_k^h)\Big\}\,.\end{aligned} \tag{2.95}$$

*Proof.* It suffices to replace (2.87) back into (2.83), and then proceed to estimate the resulting terms in a suitable manner. In particular, the expressions $\|\vec{\boldsymbol{\sigma}}\|_{\mathbf{H}}$ and $\|\vec{\boldsymbol{\sigma}}_h\|_{\mathbf{H}}$ multiplying $\|\vec{\boldsymbol{\sigma}} - \vec{\boldsymbol{\zeta}}_h\|_{\mathbf{H}}$ or $\|\mathbf{u} - \mathcal{P}_k^h(\mathbf{u})\|_{0,4,\Omega}$ are bounded by $\widetilde{\rho}_0$, whereas (2.82) is used to bound $\|\vec{\boldsymbol{\sigma}}\|_{\mathbf{H}}$ in terms of the data when it multiplies the exact error $\|\vec{\boldsymbol{\sigma}} - \vec{\boldsymbol{\sigma}}_h\|_{\mathbf{H}}$. In this way, and after taking the infimum on $\vec{\boldsymbol{\zeta}}_h \in \mathbf{H}_k^h$, which yields $\mathrm{dist}(\vec{\boldsymbol{\sigma}}, \mathbf{H}_k^h)$, we are lead on the right hand side to the remaining expression

$$C_{\mathbf{T}}\,C_{\mathrm{p}}\,\widetilde{C}_{\mathrm{p}}\,\Big\{\|\mathbf{f}\|_{0,\Omega} \,+\, \|\mathbf{g}\|_{0,\Gamma} \,+\, \|\mathbf{g}\|_{1/2,\Gamma}\Big\}\,\|\vec{\boldsymbol{\sigma}} - \vec{\boldsymbol{\sigma}}_h\|_{\mathbf{H}}\,,$$

which is handled according to the assumption (2.94). Other details are omitted. □

Having established Theorem 2.29, we now provide the corresponding rates of convergence.

**Theorem 2.30.** *Let $\vec{\boldsymbol{\sigma}} := (\boldsymbol{\sigma}, \mathbf{u}) \in \mathbf{H}$ and $\vec{\boldsymbol{\sigma}}_h := (\boldsymbol{\sigma}_h, \mathbf{u}_h) \in \mathbf{H}_k^h$ be the unique solutions of the continuous and discrete schemes (2.11) and (2.66), respectively. Assume that for integers $r \in [1, k]$, $s \in [2, k+1]$, and $\ell \in [1, k+1]$, there hold $\boldsymbol{\sigma}|_K \in \mathbb{H}^r(K)$, $\mathbf{f}|_K = -\mathbf{div}(\boldsymbol{\sigma})|_K \in \mathbf{H}^r(K)$, $\mathbf{u}|_K \in \mathbf{H}^s(K)$, and $(\mathbf{u} \otimes \mathbf{u})|_K \in \mathbb{H}^\ell(K)$, for each $K \in \mathcal{T}_h$. Then, there exists a positive constant $C$, independent of $h$, such that*

$$\begin{aligned} \|\vec{\boldsymbol{\sigma}} - \vec{\boldsymbol{\sigma}}_h\|_{\mathbf{H}} &:= \|\boldsymbol{\sigma} - \boldsymbol{\sigma}_h\|_{\mathbf{div};\Omega} + \|\mathbf{u} - \mathbf{u}_h\|_{1,\Omega} \\ &\leq C\, h^{\min\{r,s-1,\ell\}} \left\{ \sum_{K \in \mathcal{T}_h} \Big( |\boldsymbol{\sigma}|_{r,K}^2 + |\mathbf{div}(\boldsymbol{\sigma})|_{r,K}^2 + |\mathbf{u}|_{s,K}^2 + |\mathbf{u} \otimes \mathbf{u}|_{\ell,K}^2 \Big) \right\}^{1/2} \\ &+ C\, h^{s-1} \left\{ \sum_{K \in \mathcal{T}_h} |\mathbf{u}|_{s-1,4,K}^4 \right\}^{1/4} . \end{aligned} \tag{2.96}$$

*Proof.* It follows from (2.95) and the approximation properties provided along the chapter. In fact, employing $(\mathbf{AP}_h^{\mathbf{u}})$ (cf. Section2.3.2) and $(\mathbf{AP}_h^{\boldsymbol{\sigma}})$ (cf. Section 2.3.3), we obtain

$$\mathrm{dist}(\mathbf{u}, V_k^h) \leq C\, h^{s-1} \left\{ \sum_{K \in \mathcal{T}_h} |\mathbf{u}|_{s,K}^2 \right\}^{1/2}$$

and

$$\mathrm{dist}(\boldsymbol{\sigma}, H_k^h) \leq C\, h^r \left\{ \sum_{K \in \mathcal{T}_h} \Big( |\boldsymbol{\sigma}|_{r,K}^2 + |\mathbf{div}(\boldsymbol{\sigma})|_{r,K}^2 \Big) \right\}^{1/2},$$

respectively, whereas straighforward applications of (2.34) and (2.35) imply

$$h\, \|\mathbf{f} - \mathcal{P}_{k-1}^h(\mathbf{f})\|_{0,\Omega} \leq C\, h^{r+1} \left\{ \sum_{K \in \mathcal{T}_h} |\mathbf{f}|_{r,K}^2 \right\}^{1/2} = C\, h^{r+1} \left\{ \sum_{K \in \mathcal{T}_h} |\mathbf{div}(\boldsymbol{\sigma})|_{r,K}^2 \right\}^{1/2},$$

$$\|\boldsymbol{\sigma} - \boldsymbol{\mathcal{P}}_k^h(\boldsymbol{\sigma})\|_{0,\Omega} \leq C\, h^r \left\{ \sum_{K \in \mathcal{T}_h} |\boldsymbol{\sigma}|_{r,K}^2 \right\}^{1/2},$$

and

$$\|\mathbf{u} \otimes \mathbf{u} - \boldsymbol{\mathcal{P}}_k^h(\mathbf{u} \otimes \mathbf{u})\|_{0,\Omega} \leq C\, h^\ell \left\{ \sum_{K \in \mathcal{T}_h} |\mathbf{u} \otimes \mathbf{u}|_{\ell,K}^2 \right\}^{1/2}.$$

In turn, (2.22) gives

$$|\mathbf{u} - \mathcal{R}_k^h(\mathbf{u})|_{1,h} \leq C\, h^{s-1} \left\{ \sum_{K \in \mathcal{T}_h} |\mathbf{u}|_{s,K}^2 \right\}^{1/2},$$

and the fact that $\mathbf{H}^s(K) \subseteq \mathbf{W}^{s-1,4}(K)$ together with (2.37) (cf. Lemma 2.8) yield

$$\|\mathbf{u} - \mathcal{P}_k^h(\mathbf{u})\|_{0,4,\Omega} \leq C\, h^{s-1} \left\{ \sum_{K \in \mathcal{T}_h} |\mathbf{u}|_{s-1,4,K}^4 \right\}^{1/4}.$$

The foregoing estimates and a simple algebraic inequality lead to (2.96), thus concluding the proof. □

We find it important to notice here, as shown in Theorem 11 of [38], that the estimate provided in Lemma 2.3 is also valid for the case $s = 1$, and hence standard Sobolev interpolation results prove that the approximation property of $V_k^h$ given by $(\mathbf{AP}_h^{\mathbf{u}})$ (see at the end of Section 2.3.2) can be extended to the range $s \in [1, k+1]$. Consequently, this result together with the ranges for $s$ in (2.22) and (2.37) imply that the regularity assumption on $\mathbf{u}$ in the foregoing theorem can also be relaxed to $s \in [1, k+1]$ and $\mathbf{u}|_K \in \mathbf{H}^s(K)$ for each $K \in \mathcal{T}_h$, thus confirming that our convergence analysis also applies to less regular solutions.

### 2.5.3 Computable approximations of $\boldsymbol{\sigma}$, $\mathbf{u}$, and $p$

We first introduce the fully computable approximations of $\boldsymbol{\sigma}_h$ and $\mathbf{u}_h$ given by

$$\widehat{\boldsymbol{\sigma}}_h := \boldsymbol{\mathcal{P}}_k^h(\boldsymbol{\sigma}_h) \qquad \text{and} \qquad \widehat{\mathbf{u}}_h := \mathcal{P}_k^h(\mathbf{u}_h)\,, \tag{2.97}$$

and establish the corresponding *a priori* error estimates in the $\mathbb{L}^2(\Omega)$-norm for $\boldsymbol{\sigma} - \widehat{\boldsymbol{\sigma}}_h$, and in the $\mathbf{L}^2(\Omega)$-norm and broken $\mathbf{H}^1$-seminorm for $\mathbf{u} - \widehat{\mathbf{u}}_h$. As shown below in Theorem 2.33, they yield exactly the same rate of convergence given by Theorem 2.30.

We begin the analysis with the following result.

**Theorem 2.31.** *Let $\vec{\boldsymbol{\sigma}} := (\boldsymbol{\sigma}, \mathbf{u}) \in \mathbf{H}$ and $\vec{\boldsymbol{\sigma}}_h := (\boldsymbol{\sigma}_h, \mathbf{u}_h) \in \mathbf{H}_k^h$ be the unique solutions of the continuous and discrete schemes (2.11) and (2.66), respectively. Then there exists a positive constant $C > 0$, independent of $h$, such that*

$$\begin{aligned} &\|\boldsymbol{\sigma} - \widehat{\boldsymbol{\sigma}}_h\|_{0,\Omega} + \|\mathbf{u} - \widehat{\mathbf{u}}_h\|_{0,\Omega} + \left\{ \sum_{K \in \mathcal{T}_h} |\mathbf{u} - \widehat{\mathbf{u}}_h|_{1,K}^2 \right\}^{1/2} \\ &\qquad \leq C \left\{ \|\vec{\boldsymbol{\sigma}} - \vec{\boldsymbol{\sigma}}_h\|_{\mathbf{H}} + \|\boldsymbol{\sigma} - \boldsymbol{\mathcal{P}}_k^h(\boldsymbol{\sigma})\|_{0,\Omega} + \left\{ \sum_{K \in \mathcal{T}_h} \|\mathbf{u} - \mathcal{P}_k^K(\mathbf{u})\|_{1,K}^2 \right\}^{1/2} \right\}. \end{aligned} \tag{2.98}$$

*Proof.* In order to bound $\|\boldsymbol{\sigma} - \widehat{\boldsymbol{\sigma}}_h\|_{0,\Omega}$, we add and subtract $\boldsymbol{\mathcal{P}}_k^h(\boldsymbol{\sigma})$, and then employ the boundedness of $\boldsymbol{\mathcal{P}}_k^h$, which gives

$$\begin{aligned} \|\boldsymbol{\sigma} - \widehat{\boldsymbol{\sigma}}_h\|_{0,\Omega} &\leq \|\boldsymbol{\sigma} - \boldsymbol{\mathcal{P}}_k^h(\boldsymbol{\sigma})\|_{0,\Omega} + \|\boldsymbol{\mathcal{P}}_k^h(\boldsymbol{\sigma}) - \boldsymbol{\mathcal{P}}_k^h(\boldsymbol{\sigma}_h)\|_{0,\Omega} \\ &\leq \|\boldsymbol{\sigma} - \boldsymbol{\mathcal{P}}_k^h(\boldsymbol{\sigma})\|_{0,\Omega} + \|\boldsymbol{\sigma} - \boldsymbol{\sigma}_h\|_{0,\Omega}\,. \end{aligned} \tag{2.99}$$

Similarly, adding and subtracting $\mathcal{P}_k^K(\mathbf{u})$, and using now the boundedness of $\mathcal{P}_k^K$ (cf. Lemma 2.9), we are lead to

$$\|\mathbf{u} - \widehat{\mathbf{u}}_h\|_{1,K} \leq \|\mathbf{u} - \mathcal{P}_k^K(\mathbf{u})\|_{1,K} + M_k \|\mathbf{u} - \mathbf{u}_h\|_{1,K} \qquad \forall\, K \in \mathcal{T}_h\,,$$

from which, taking square and summing over $K \in \mathcal{T}_h$, it follows that

$$\|\mathbf{u} - \widehat{\mathbf{u}}_h\|_{0,\Omega} + \left\{ \sum_{K \in \mathcal{T}_h} |\mathbf{u} - \widehat{\mathbf{u}}_h|_{1,K}^2 \right\}^{1/2} \leq C \left\{ \left\{ \sum_{K \in \mathcal{T}_h} \|\mathbf{u} - \mathcal{P}_k^K(\mathbf{u})\|_{1,K}^2 \right\}^{1/2} + \|\mathbf{u} - \mathbf{u}_h\|_{1,\Omega} \right\}. \tag{2.100}$$

In this way, (2.99) and (2.100) yield (2.98), which ends the proof. □

Next, according to the second equation in (2.4) and the decomposition of $\boldsymbol{\sigma}$ provided by (2.7) and (2.8), we suggest the following computable approximation of the pressure:

$$\widehat{p}_h \;:=\; -\frac{1}{2}\,\mathrm{tr}\Big(\widehat{\boldsymbol{\sigma}}_h \,+\, \widehat{c}_h\mathbb{I} \,+\, \widehat{\mathbf{u}}_h\otimes\widehat{\mathbf{u}}_h\Big) \quad \text{in} \quad \Omega\,, \qquad \text{with} \qquad \widehat{c}_h \;:=\; -\frac{1}{2|\Omega|}\,\|\widehat{\mathbf{u}}_h\|^2_{0,\Omega}\,. \tag{2.101}$$

The following lemma establishes the corresponding *a priori* error estimate.

**Theorem 2.32.** *There exists a positive constant $C>0$, independent of $h$, such that*

$$\|p-\widehat{p}_h\|_{0,\Omega} \;\leq\; C\,\Big\{\|\vec{\boldsymbol{\sigma}}-\vec{\boldsymbol{\sigma}}_h\|_{\mathbf{H}} \,+\, \|\boldsymbol{\sigma}-\boldsymbol{\mathcal{P}}^h_k(\boldsymbol{\sigma})\|_{0,\Omega} \,+\, \|\mathbf{u}-\mathcal{P}^h_k(\mathbf{u})\|_{0,4,\Omega}\Big\}\,. \tag{2.102}$$

*Proof.* According to (2.4), (2.7), (2.8), and (2.101), we have that

$$p-\widehat{p}_h \;=\; -\frac{1}{2}\mathrm{tr}\Big((\boldsymbol{\sigma}-\widehat{\boldsymbol{\sigma}}_h) \,+\, (\mathbf{u}\otimes\mathbf{u}-\widehat{\mathbf{u}}_h\otimes\widehat{\mathbf{u}}_h)\Big) \,+\, \frac{1}{2|\Omega|}\int_\Omega \mathrm{tr}(\mathbf{u}\otimes\mathbf{u}-\widehat{\mathbf{u}}_h\otimes\widehat{\mathbf{u}}_h)\,,$$

which, applying the Cauchy-Schwarz inequality, yields

$$\|p-\widehat{p}_h\|_{0,\Omega} \;\leq\; C\,\Big\{\|\boldsymbol{\sigma}-\widehat{\boldsymbol{\sigma}}_h\|_{0,\Omega} \,+\, \|\mathbf{u}\otimes\mathbf{u}-\widehat{\mathbf{u}}_h\otimes\widehat{\mathbf{u}}_h\|_{0,\Omega}\Big\}\,. \tag{2.103}$$

Then, adding and subtracting $\widehat{\mathbf{u}}_h$, and using the triangle and Cauchy-Schwarz inequalities, the boundedness of $\mathcal{P}^h_k$ (cf. (2.40)), (2.9), and the fact that $\|\mathbf{u}\|_{1,\Omega}$ and $\|\mathbf{u}_h\|_{1,\Omega}$ are bounded by $\widetilde{\rho}_0$, we find that

$$\begin{aligned}
\|\mathbf{u}\otimes\mathbf{u}-\widehat{\mathbf{u}}_h\otimes\widehat{\mathbf{u}}_h\|_{0,\Omega} \;&=\; \|\mathbf{u}\otimes(\mathbf{u}-\widehat{\mathbf{u}}_h)\|_{0,\Omega} \,+\, \|(\mathbf{u}-\widehat{\mathbf{u}}_h)\otimes\widehat{\mathbf{u}}_h\|_{0,\Omega} \\
&\leq\; \Big(\|\mathbf{u}\|_{0,4,\Omega}+\|\widehat{\mathbf{u}}_h\|_{0,4,\Omega}\Big)\,\|\mathbf{u}-\widehat{\mathbf{u}}_h\|_{0,4,\Omega} \;=\; \Big(\|\mathbf{u}\|_{0,4,\Omega}+\|\mathcal{P}^h_k(\mathbf{u}_h)\|_{0,4,\Omega}\Big)\,\|\mathbf{u}-\widehat{\mathbf{u}}_h\|_{0,4,\Omega} \\
&\leq\; \Big(\|\mathbf{u}\|_{0,4,\Omega}+M_k\,\|\mathbf{u}_h\|_{0,4,\Omega}\Big)\,\|\mathbf{u}-\widehat{\mathbf{u}}_h\|_{0,4,\Omega} \;\leq\; (1+M_k)\,\|\mathbf{i}_c\|\,\widetilde{\rho}_0\,\|\mathbf{u}-\widehat{\mathbf{u}}_h\|_{0,4,\Omega}\,.
\end{aligned} \tag{2.104}$$

In turn, adding and subtracting $\mathcal{P}^h_k(\mathbf{u})$, and employing again the boundedness of $\mathcal{P}^h_k$ and (2.9), we readily obtain

$$\begin{aligned}
\|\mathbf{u}-\widehat{\mathbf{u}}_h\|_{0,4,\Omega} \;&\leq\; \|\mathbf{u}-\mathcal{P}^h_k(\mathbf{u})\|_{0,4,\Omega} \,+\, \|\mathcal{P}^h_k(\mathbf{u}-\mathbf{u}_h)\|_{0,4,\Omega} \\
&\leq\; \|\mathbf{u}-\mathcal{P}^h_k(\mathbf{u})\|_{0,4,\Omega} \,+\, \|\mathbf{i}_c\|\,M_k\,\|\mathbf{u}-\mathbf{u}_h\|_{1,\Omega}\,.
\end{aligned} \tag{2.105}$$

Finally, (2.103), (2.104), and (2.105), together with (2.99) imply (2.102) and finish the proof. □

We end this section by providing the theoretical rates of convergence for $\widehat{\boldsymbol{\sigma}}_h$, $\widehat{\mathbf{u}}_h$, and $\widehat{p}_h$.

**Theorem 2.33.** *Let $\vec{\boldsymbol{\sigma}} := (\boldsymbol{\sigma},\mathbf{u}) \in \mathbf{H}$ and $\vec{\boldsymbol{\sigma}}_h := (\boldsymbol{\sigma}_h,\mathbf{u}_h) \in \mathbf{H}^h_k$ be the unique solutions of the continuous and discrete schemes (2.11) and (2.66), respectively. In addition, let $(\widehat{\boldsymbol{\sigma}}_h,\widehat{\mathbf{u}}_h)$ and $\widehat{p}_h$ be the discrete approximations introduced in (2.97) and (2.101), respectively. Assume that for integers $r\in[1,k]$, $s\in[1,k+1]$, and $\ell\in[1,k+1]$, there hold $\boldsymbol{\sigma}|_K\in\mathbb{H}^r(K)$, $\mathbf{f}|_K=-\mathbf{div}(\boldsymbol{\sigma})|_K\in\mathbf{H}^r(K)$, $\mathbf{u}|_K\in\mathbf{H}^s(K)$, and $(\mathbf{u}\otimes\mathbf{u})|_K\in\mathbb{H}^\ell(K)$, for each $K\in\mathcal{T}_h$. Then, there exists a positive constant $C$, independent of $h$, such that*

$$\begin{aligned}
&\|\boldsymbol{\sigma}-\widehat{\boldsymbol{\sigma}}_h\|_{0,\Omega} \,+\, \|\mathbf{u}-\widehat{\mathbf{u}}_h\|_{0,\Omega} \,+\, \Big\{\sum_{K\in\mathcal{T}_h}|\mathbf{u}-\widehat{\mathbf{u}}_h|^2_{1,K}\Big\}^{1/2} \,+\, \|p-\widehat{p}_h\|_{0,\Omega} \\
&\quad\leq\; C\,h^{\min\{r,s-1,\ell\}}\Big\{\sum_{K\in\mathcal{T}_h}\Big(|\boldsymbol{\sigma}|^2_{r,K}+|\mathbf{div}(\boldsymbol{\sigma})|^2_{r,K}+|\mathbf{u}|^2_{s,K}+|\mathbf{u}\otimes\mathbf{u}|^2_{\ell,K}\Big)\Big\}^{1/2} \\
&\quad+\;\; C\,h^{s-1}\Big\{\sum_{K\in\mathcal{T}_h}|\mathbf{u}|^4_{s-1,4,K}\Big\}^{1/4}\,.
\end{aligned} \tag{2.106}$$

*Proof.* It follows from (2.98), (2.102), Theorem 2.30, the remark right after it, and the approximation properties provided along the chapter. In particular, applying (2.37) (cf. Lemma 2.8), we readily find that

$$\left\{ \sum_{K\in\mathcal{T}_h} \|\mathbf{u}-\mathcal{P}_k^K(\mathbf{u})\|_{1,K}^2 \right\}^{1/2} \leq C\, h^{s-1} \left\{ \sum_{K\in\mathcal{T}_h} |\mathbf{u}|_{s,K}^2 \right\}^{1/2} .$$

Further details, being similar to those shown in the proof of Theorem 2.30, are omitted. □

### 2.5.4 A convergent approximation of $\boldsymbol{\sigma}$ in the broken $\mathbb{H}(\mathbf{div};\Omega)$-norm

In what follows we proceed as in Section 5.3 of [31] and propose a second approximation $\widetilde{\boldsymbol{\sigma}}_h$ of the pseudostress $\boldsymbol{\sigma}$, which yields the same rate of convergence from Theorems 2.30 and 2.33 in the broken $\mathbb{H}(\mathbf{div};\Omega)$-norm. For this purpose, we now consider for each $K\in\mathcal{T}_h$ an arbitrary but explicitly known finite dimensional subspace $\mathbb{U}(K)$ of $\mathbb{H}(\mathbf{div};K)$, to be specified later on, and let $(\cdot,\cdot)_{\mathbf{div};K}$ be the usual $\mathbb{H}(\mathbf{div};K)$-inner product with induced norm $\|\cdot\|_{\mathbf{div};K}$. Then, we let $\widetilde{\boldsymbol{\sigma}}_h\in\mathbb{L}^2(\Omega)$ be the tensor defined locally as $\widetilde{\boldsymbol{\sigma}}_h|_K := \widetilde{\boldsymbol{\sigma}}_{h,K}$, where $\widetilde{\boldsymbol{\sigma}}_{h,K}\in\mathbb{U}(K)$ is the unique solution of the problem

$$(\widetilde{\boldsymbol{\sigma}}_{h,K},\boldsymbol{\tau}_h)_{\mathbf{div};K} = \int_K \widehat{\boldsymbol{\sigma}}_h : \boldsymbol{\tau}_h + \int_K \mathbf{div}(\boldsymbol{\sigma}_h)\cdot\mathbf{div}(\boldsymbol{\tau}_h) \qquad \forall\, \boldsymbol{\tau}_h\in\mathbb{U}(K)\,. \tag{2.107}$$

Note here that the right-hand side of (2.107), and hence $\widetilde{\boldsymbol{\sigma}}_{h,K}$, is fully computable since both $\widehat{\boldsymbol{\sigma}}_h$ and $\mathbf{div}(\boldsymbol{\tau}_h)$ are. In addition, it is important to remark that $\widetilde{\boldsymbol{\sigma}}_{h,K}$ can be calculated for each $K\in\mathcal{T}_h$, independently, which certainly suggests a parallel implementation of these computations. Next, denoting by $\Pi_U^K:\mathbb{H}(\mathbf{div};K)\to\mathbb{U}(K)$ the orthogonal projector with respect to $(\cdot,\cdot)_{\mathbf{div};K}$, we have the following result establishing the *a priori* estimate for the local error $\|\boldsymbol{\sigma}-\widetilde{\boldsymbol{\sigma}}_{h,K}\|_{\mathbf{div};K}$.

**Lemma 2.34.** *For each $K\in\mathcal{T}_h$ there holds*

$$\|\boldsymbol{\sigma}-\widetilde{\boldsymbol{\sigma}}_{h,K}\|_{\mathbf{div};K} \leq \|\mathbf{div}(\boldsymbol{\sigma}-\boldsymbol{\sigma}_h)\|_{0,K} + \|\boldsymbol{\sigma}-\widehat{\boldsymbol{\sigma}}_h\|_{0,K} + \|\boldsymbol{\sigma}-\Pi_U^K(\boldsymbol{\sigma})\|_{\mathbf{div};K}\,. \tag{2.108}$$

*Proof.* It proceeds exactly as the proof of Lemma 5.3 in [31], and hence we refer to that work and omit details here. □

In this way, since we know from (2.96) (cf. Theorem 2.30) and (2.106) (cf. Theorem 2.33) that the errors $\|\mathbf{div}(\boldsymbol{\sigma}-\boldsymbol{\sigma}_h)\|_{0,\Omega}$ and $\|\boldsymbol{\sigma}-\widehat{\boldsymbol{\sigma}}_h\|_{0,\Omega}$ converge at most with order $O(h^k)$, which holds when $r=k$, $s=k+1$, and $\ell=k$, it follows from (2.108) that we need to guarantee at least the same rate for $\left\{ \sum_{K\in\mathcal{T}_h} \|\boldsymbol{\sigma}-\Pi_U^K(\boldsymbol{\sigma})\|_{\mathbf{div};K}^2 \right\}^{1/2}$. Thus, in order to achieve this goal, we take for simplicity $\mathbb{U}(K) := \mathbb{P}_k(K)$, which means that $\Pi_U^K$ becomes $\boldsymbol{\mathcal{P}}_k^K$, whence (2.35) yields

$$\|\boldsymbol{\tau}-\Pi_U^K(\boldsymbol{\tau})\|_{\mathbf{div};K} \leq \|\boldsymbol{\tau}-\Pi_U^K(\boldsymbol{\tau})\|_{1,K} \leq C\, h_K^r\, |\boldsymbol{\tau}|_{r+1,K} \qquad \forall\,\boldsymbol{\tau}\in\mathbb{H}^{r+1}(K)\,,\quad \forall\, K\in\mathcal{T}_h\,.$$

Therefore, according to the foregoing analysis, we are able to state the following theorem.

**Theorem 2.35.** *Let* $\vec{\boldsymbol{\sigma}} := (\boldsymbol{\sigma}, \mathbf{u}) \in \mathbf{H}$ *and* $\vec{\boldsymbol{\sigma}}_h := (\boldsymbol{\sigma}_h, \mathbf{u}_h) \in \mathbf{H}_k^h$ *be the unique solutions of the continuous and discrete schemes* (2.11) *and* (2.66)*, respectively. In addition, let* $\widehat{\boldsymbol{\sigma}}_h$ *and* $\widetilde{\boldsymbol{\sigma}}_h$ *be the discrete approximations of* $\boldsymbol{\sigma}$ *introduced in* (2.97) *and* (2.107)*, respectively. Assume that for integers* $r \in [1, k]$*,* $s \in [1, k+1]$*, and* $\ell \in [1, k+1]$*, there hold* $\boldsymbol{\sigma}|_K \in \mathbb{H}^{r+1}(K)$*,* $\mathbf{f}|_K = -\mathbf{div}(\boldsymbol{\sigma})|_K \in \mathbf{H}^r(K)$*,* $\mathbf{u}|_K \in \mathbf{H}^s(K)$*, and* $(\mathbf{u} \otimes \mathbf{u})|_K \in \mathbb{H}^\ell(K)$*, for each* $K \in \mathcal{T}_h$*. Then, there holds*

$$\left\{ \sum_{K \in \mathcal{T}_h} \|\boldsymbol{\sigma} - \widetilde{\boldsymbol{\sigma}}_{h,K}\|^2_{\mathbf{div};K} \right\}^{1/2} = O(h^{\min\{r, s-1, \ell\}}) .$$

We end this chapter with a remark. Regarding the eventual extension of the present analysis to the case of arbitrary small edges or other less restrictive hypotheses on the meshes, as discussed for instance in [19], we conjecture that a suitable adaptation of the main theoretical results provided in there should be applicable to our approach. In particular, the fact that the general error analysis developed in Section 3 of [19] is valid for any other linear symmetric elliptic problem, suggests that a minor modification of it would be able to deal with the bilinear forms $\mathbf{A}(\cdot,\cdot)+\mathbf{B}(\mathbf{z};\cdot,\cdot)$ and $\mathbf{A}_h(\cdot,\cdot)+\mathbf{B}_h(\mathbf{z}_h;\cdot,\cdot)$ defining the continuous and discrete schemes (2.11) and (2.66), respectively, with $\mathbf{z} \in \mathbf{H}^1(\Omega)$ and $\mathbf{z}_h \in V_k^h$. In fact, while neither of them is symmetric, they are both elliptic for suitable closed balls containing $\mathbf{z}$ and $\mathbf{z}_h$, as shown by (2.17) and (2.72), respectively. Further discussions on this matter should form part of a separate work.

## 2.6 Numerical Tests

In this section we present some numerical tests illustrating the performance of the augmented mixed virtual element scheme (2.66), which was introduced and analized in Section 2.5. By simplicity and efficiency in the implementation, in all the computations we consider, for $k \geq 0$, the following global virtual element subspace of $\mathbb{H}_0(\mathbf{div};\Omega)$:

$$H_k^h := \left\{ \boldsymbol{\tau} \in \mathbb{H}_0(\mathbf{div};\Omega) : \quad \boldsymbol{\tau}|_K \in H_k^K \quad \forall\, K \in \mathcal{T}_h \right\}, \tag{2.109}$$

where $H_k^K$ is given by (2.28). Moreover, we make use of $V_{k+1}^h$, for $k \geq 0$, as global virtual element subspace of $\mathbf{H}^1(\Omega)$. We stress that the analysis established in Section 2.5 applies for the virtual subspaces described above, also (see Chapter 3 for more details). In addition, and similarly as in [68], the zero integral mean condition for tensors in the space (2.109) is imposed via a real Lagrange multiplier. Concerning the decompositions of $\Omega$ employed in our computations, we consider uniform triangles, distorted squares and hexagonal meshes (see Figure (2.1)).

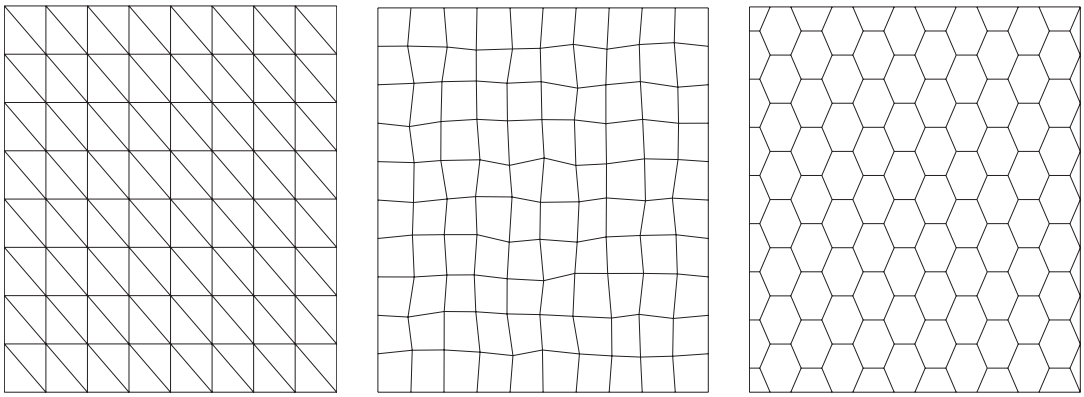

Figure 2.1: Sample meshes: triangular (left), distorted squares (center) and hexagonal (right) (figure produced by the author).

We begin by introducing some notations. In what follows, $N$ stands for the total number of degrees of freedom (unknowns) of (2.66). Further, the individual errors are defined by

$$\mathtt{e}_0(\boldsymbol{\sigma}) := \|\boldsymbol{\sigma}-\widehat{\boldsymbol{\sigma}}_h\|_{0,\Omega}, \quad \mathtt{e}_0(\mathbf{u}) := \|\mathbf{u}-\widehat{\mathbf{u}}_h\|_{0,\Omega}, \quad \mathtt{e}_1(\mathbf{u}) := |\mathbf{u}-\widehat{\mathbf{u}}_h|_{1,\Omega}\,,$$

$$\mathtt{e}(p) := \|p-\widehat{p}_h\|_{0,\Omega}, \quad \text{and} \quad \mathtt{e}(\widetilde{\boldsymbol{\sigma}}) := \left\{\sum_{K\in\mathcal{T}_h}\|\boldsymbol{\sigma}-\widetilde{\boldsymbol{\sigma}}_h\|^2_{\mathbf{div};K}\right\}^{1/2},$$

where $\widehat{\boldsymbol{\sigma}}_h, \widetilde{\boldsymbol{\sigma}}_h, \widehat{p}_h, \widehat{\mathbf{u}}_h$ are computed as in Sections 2.5.3-2.5.4, whereas the associated experimental rates of convergence are given by

$$\mathtt{r}(\cdot) := \frac{\log(\mathtt{e}(\cdot)/\mathtt{e}'(\cdot))}{\log(h/h')},$$

where $\mathtt{e}$ and $\mathtt{e}'$ denote the corresponding errors for two consecutive meshes with sizes $h$ and $h'$, respectively. In turn, the nonlinear algebraic systems are solved by the Newton method with a tolerance of $10^{-6}$ and taking as initial iteration the solution of the Stokes problem. The numerical results presented below were obtained using a MATLAB code.

### 2.6.1 Test 1

We consider the unit square $\Omega := (0,1)^2$, set $\mu = 1$ and choose the data $\mathbf{f}$ and $\mathbf{g}$ so that the exact solution is given by

$$\mathbf{u}(\mathbf{x}) := \frac{1}{2}\begin{pmatrix} \sin^2(2\pi x_1)\sin(2\pi x_2)\cos(2\pi x_2) \\ -\sin^2(2\pi x_2)\sin(2\pi x_1)\cos(2\pi x_1) \end{pmatrix} \quad \text{and} \quad p(\mathbf{x}) := \sin(2\pi x_1)\cos(2\pi x_2)$$

for all $\mathbf{x} := (x_1, x_2)^{\mathbf{t}} \in \Omega$. Here we use $\kappa_i = \mu$, for $i = 1, 2, 3$.

In Tables 2.1 up to 2.3 we summarize the convergence history of our augmented mixed virtual element scheme for the meshes in Figures 2.1. We can see the robustness of our method with respect to the mesh shape. Also, we notice that the rate of convergence $O(h^{k+1})$ is achieved by all the errors,

with exception of $\|\mathbf{u}-\widehat{\mathbf{u}}\|_{0,\Omega}$, which converge with order $k+2$. In particular, these results confirm that our postprocessed stress $\widetilde{\boldsymbol{\sigma}}_h$ improves in one power the non-satisfactory order provided by the first approximation $\widehat{\boldsymbol{\sigma}}_h$ with respect to the broken $\mathbb{H}(\mathbf{div})$-norm.

| $k$ | $h$ | $N$ | $\mathtt{e}_0(\boldsymbol{\sigma})$ | $\mathtt{r}_0(\boldsymbol{\sigma})$ | $\mathtt{e}_0(\mathbf{u})$ | $\mathtt{r}_0(\mathbf{u})$ | $\mathtt{e}_1(\mathbf{u})$ | $\mathtt{r}_1(\mathbf{u})$ | $\mathtt{e}(p)$ | $\mathtt{r}(p)$ | $\mathtt{e}(\widetilde{\boldsymbol{\sigma}})$ | $\mathtt{r}(\widetilde{\boldsymbol{\sigma}})$ |
|---|---|---|---|---|---|---|---|---|---|---|---|---|
| | 0.2000 | 443 | 3.0516e+00 | −− | 8.4195e-02 | −− | 1.5377e+00 | −− | 1.6535e+00 | −− | 2.1774e+01 | −− |
| | 0.1000 | 1683 | 1.5383e+00 | 0.9882 | 2.4385e-02 | 1.7877 | 7.5079e-01 | 1.0343 | 8.0667e-01 | 1.0355 | 1.1260e+01 | 0.9514 |
| 0 | 0.0500 | 6563 | 7.6789e-01 | 1.0023 | 6.3173e-03 | 1.9486 | 3.6779e-01 | 1.0295 | 3.9709e-01 | 1.0225 | 5.6777e+00 | 0.9879 |
| | 0.0250 | 25923 | 3.8337e-01 | 1.0022 | 1.5947e-03 | 1.9860 | 1.8247e-01 | 1.0112 | 1.9725e-01 | 1.0095 | 2.8447e+00 | 0.9970 |
| | 0.0125 | 103043 | 1.9155e-01 | 1.0010 | 3.9978e-04 | 1.9961 | 9.1007e-02 | 1.0036 | 9.8382e-02 | 1.0035 | 1.4231e+00 | 0.9993 |
| | 0.2000 | 1883 | 5.0847e-01 | −− | 6.8347e-03 | −− | 3.4928e-01 | −− | 2.4817e-01 | −− | 5.5114e+00 | −− |
| | 0.1000 | 7363 | 1.3071e-01 | 1.9598 | 9.3352e-04 | 2.8721 | 9.4423e-02 | 1.8872 | 6.1853e-02 | 2.0044 | 1.4398e+00 | 1.9366 |
| 1 | 0.0500 | 29123 | 3.3006e-02 | 1.9855 | 1.2898e-04 | 2.8555 | 2.4671e-02 | 1.9363 | 1.5441e-02 | 2.0020 | 3.6394e-01 | 1.9841 |
| | 0.0250 | 115843 | 8.2780e-03 | 1.9954 | 1.6801e-05 | 2.9406 | 6.2768e-03 | 1.9747 | 3.8527e-03 | 2.0029 | 9.1236e-02 | 1.9960 |
| | 0.0125 | 462083 | 2.0717e-03 | 1.9985 | 2.1297e-06 | 2.9798 | 1.5784e-03 | 1.9915 | 9.6187e-04 | 2.0019 | 2.2825e-02 | 1.9990 |

Table 2.1: Test 1, history of convergence using triangular meshes (table produced by the author).

| $k$ | $h$ | $N$ | $\mathtt{e}_0(\boldsymbol{\sigma})$ | $\mathtt{r}_0(\boldsymbol{\sigma})$ | $\mathtt{e}_0(\mathbf{u})$ | $\mathtt{r}_0(\mathbf{u})$ | $\mathtt{e}_1(\mathbf{u})$ | $\mathtt{r}_1(\mathbf{u})$ | $\mathtt{e}(p)$ | $\mathtt{r}(p)$ | $\mathtt{e}(\widetilde{\boldsymbol{\sigma}})$ | $\mathtt{r}(\widetilde{\boldsymbol{\sigma}})$ |
|---|---|---|---|---|---|---|---|---|---|---|---|---|
| | 0.2001 | 451 | 3.4227e+00 | −− | 1.1892e-01 | −− | 1.6403e+00 | −− | 2.0782e+00 | −− | 2.3823e+01 | −− |
| | 0.1008 | 1667 | 1.6044e+00 | 1.1038 | 4.5955e-02 | 1.3851 | 7.8520e-01 | 1.0733 | 9.6708e-01 | 1.1145 | 1.2241e+01 | 0.9701 |
| 0 | 0.0504 | 6403 | 7.2252e-01 | 1.1529 | 1.3618e-02 | 1.7577 | 3.4936e-01 | 1.1703 | 4.3965e-01 | 1.1392 | 6.1954e+00 | 0.9841 |
| | 0.0252 | 25091 | 3.4017e-01 | 1.0868 | 3.6083e-03 | 1.9162 | 1.6371e-01 | 1.0936 | 2.0796e-01 | 1.0801 | 3.1025e+00 | 0.9978 |
| | 0.0126 | 99331 | 1.6606e-01 | 1.0348 | 9.1662e-04 | 1.9775 | 7.9839e-02 | 1.0362 | 1.0164e-01 | 1.0331 | 1.5522e+00 | 0.9994 |
| | 0.2001 | 1539 | 6.5675e-01 | −− | 1.1618e-02 | −− | 4.1530e-01 | −− | 3.4226e-01 | −− | 7.0682e+00 | −− |
| | 0.1008 | 5891 | 1.6252e-01 | 2.0345 | 1.1453e-03 | 3.3754 | 1.0544e-01 | 1.9972 | 8.1907e-02 | 2.0833 | 1.8865e+00 | 1.9244 |
| 1 | 0.0504 | 23043 | 3.9542e-02 | 2.0427 | 1.1785e-04 | 3.2863 | 2.6560e-02 | 1.9926 | 1.9871e-02 | 2.0468 | 4.7887e-01 | 1.9814 |
| | 0.0252 | 91139 | 9.7434e-03 | 2.0210 | 1.3539e-05 | 3.1218 | 6.6211e-03 | 2.0042 | 4.9085e-03 | 2.0174 | 1.2062e-01 | 1.9892 |
| | 0.0126 | 362499 | 2.4296e-03 | 2.0042 | 1.6587e-06 | 3.0298 | 1.6577e-03 | 1.9984 | 1.2244e-03 | 2.0038 | 3.0172e-02 | 1.9997 |

Table 2.2: Test 1, history of convergence using distorted squares meshes (table produced by the author).

| $k$ | $h$ | $N$ | $\mathtt{e}_0(\boldsymbol{\sigma})$ | $\mathtt{r}_0(\boldsymbol{\sigma})$ | $\mathtt{e}_0(\mathbf{u})$ | $\mathtt{r}_0(\mathbf{u})$ | $\mathtt{e}_1(\mathbf{u})$ | $\mathtt{r}_1(\mathbf{u})$ | $\mathtt{e}(p)$ | $\mathtt{r}(p)$ | $\mathtt{e}(\widetilde{\boldsymbol{\sigma}})$ | $\mathtt{r}(\widetilde{\boldsymbol{\sigma}})$ |
|---|---|---|---|---|---|---|---|---|---|---|---|---|
| | 0.2033 | 487 | 3.8158e+00 | −− | 1.2242e-01 | −− | 1.7864e+00 | −− | 2.3698e+00 | −− | 2.7089e+01 | −− |
| | 0.1016 | 1799 | 1.7968e+00 | 1.0865 | 4.3996e-02 | 1.4764 | 8.7200e-01 | 1.0346 | 1.1071e+00 | 1.0979 | 1.4660e+01 | 0.8858 |
| 0 | 0.0508 | 6757 | 8.3421e-01 | 1.1070 | 1.2472e-02 | 1.8186 | 4.0486e-01 | 1.1069 | 5.1433e-01 | 1.1061 | 7.5112e+00 | 0.9648 |
| | 0.0254 | 26527 | 4.0422e-01 | 1.0453 | 3.2287e-03 | 1.9497 | 1.9528e-01 | 1.0519 | 2.4971e-01 | 1.0424 | 3.7891e+00 | 0.9872 |
| | 0.0127 | 104437 | 1.9951e-01 | 1.0187 | 8.1730e-04 | 1.9820 | 9.6348e-02 | 1.0192 | 1.2339e-01 | 1.0171 | 1.9007e+00 | 0.9953 |
| | 0.2033 | 1451 | 7.7971e-01 | −− | 1.9170e-02 | −− | 5.3975e-01 | −− | 3.9630e-01 | −− | 8.6851e+00 | −− |
| | 0.1016 | 5435 | 1.9706e-01 | 1.9843 | 1.8048e-03 | 3.4090 | 1.3721e-01 | 1.9759 | 9.9888e-02 | 1.9882 | 2.4011e+00 | 1.8549 |
| 1 | 0.0508 | 20261 | 4.9129e-02 | 2.0040 | 1.9355e-04 | 3.2211 | 3.4708e-02 | 1.9831 | 2.4594e-02 | 2.0220 | 6.2039e-01 | 1.9524 |
| | 0.0254 | 79751 | 1.2335e-02 | 1.9938 | 2.3173e-05 | 3.0622 | 8.7412e-03 | 1.9894 | 6.1517e-03 | 1.9992 | 1.5686e-01 | 1.9837 |
| | 0.0127 | 313301 | 3.0875e-03 | 1.9982 | 2.8622e-06 | 3.0172 | 2.1910e-03 | 1.9963 | 1.5379e-03 | 2.0001 | 3.9393e-02 | 1.9934 |

Table 2.3: Test 1, history of convergence using hexagonal meshes (table produced by the author).

### 2.6.2 Test 2

We consider again the unit square $\Omega := (0,1)^2$ with $\mathbf{u}(\mathbf{x}) := (x_2, -x_1)^{\mathbf{t}}$ and $p := \frac{1}{2}(x_1^2 + x_2^2) - \frac{1}{3}$ for all $\mathbf{x} := (x_1, x_2)^{\mathbf{t}} \in \Omega$. Here the data are given by $\mathbf{f} = \mathbf{0}$ and $\mathbf{g}$ is non-homogeneus. The aim of this test is to see the behavior of our method under different values of the viscosity $\mu$. Further, we use two families of uniformly generated meshes: triangular and distorted squares meshes.

| $\mu$ | $h$ | $\mathtt{e}_0(\boldsymbol{\sigma})$ | $\mathtt{r}_0(\boldsymbol{\sigma})$ | $\mathtt{e}_0(\mathbf{u})$ | $\mathtt{r}_0(\mathbf{u})$ | $\mathtt{e}_1(\mathbf{u})$ | $\mathtt{r}_1(\mathbf{u})$ | $\mathtt{e}(p)$ | $\mathtt{r}(p)$ | $\mathtt{e}(\widetilde{\boldsymbol{\sigma}})$ | $\mathtt{r}(\widetilde{\boldsymbol{\sigma}})$ | iter |
|---|---|---|---|---|---|---|---|---|---|---|---|---|
| | 0.2000 | 1.1497e-01 | −− | 2.8921e-03 | −− | 1.9715e-02 | −− | 5.8970e-02 | −− | 1.1499e-01 | −− | 3 |
| | 0.1000 | 5.6931e-02 | 1.0140 | 7.4896e-04 | 1.9492 | 7.1275e-03 | 1.4678 | 2.8734e-02 | 1.0372 | 5.6934e-02 | 1.0142 | 2 |
| 1.0 | 0.0500 | 2.8284e-02 | 1.0093 | 1.9032e-04 | 1.9764 | 2.8079e-03 | 1.3439 | 1.4144e-02 | 1.0226 | 2.8284e-02 | 1.0093 | 2 |
| | 0.0250 | 1.4099e-02 | 1.0044 | 4.7899e-05 | 1.9904 | 1.2315e-03 | 1.1891 | 7.0208e-03 | 1.0105 | 1.4099e-02 | 1.0044 | 2 |
| | 0.0125 | 7.0409e-03 | 1.0017 | 1.2004e-05 | 1.9964 | 5.8296e-04 | 1.0790 | 3.5004e-03 | 1.0041 | 7.0409e-03 | 1.0017 | 2 |
| | 0.2000 | 1.1954e-01 | −− | 2.0059e-02 | −− | 1.5762e-01 | −− | 6.0631e-02 | −− | 1.1993e-01 | −− | 3 |
| | 0.1000 | 5.7736e-02 | 1.0500 | 5.4198e-03 | 1.8879 | 6.2624e-02 | 1.3316 | 2.9033e-02 | 1.0624 | 5.7794e-02 | 1.0532 | 3 |
| 0.1 | 0.0500 | 2.8406e-02 | 1.0233 | 1.4029e-03 | 1.9498 | 2.6452e-02 | 1.2433 | 1.4190e-02 | 1.0328 | 2.8413e-02 | 1.0243 | 2 |
| | 0.0250 | 1.4116e-02 | 1.0089 | 3.5553e-04 | 1.9804 | 1.2054e-02 | 1.1338 | 7.0271e-03 | 1.0139 | 1.4117e-02 | 1.0092 | 2 |
| | 0.0125 | 7.0431e-03 | 1.0030 | 8.9317e-05 | 1.9930 | 5.7923e-03 | 1.0573 | 3.5012e-03 | 1.0051 | 7.0432e-03 | 1.0031 | 2 |
| | 0.2000 | −− | −− | −− | −− | −− | −− | −− | −− | −− | −− | – |
| | 0.1000 | 1.3667e-01 | −− | 6.9473e-02 | −− | 1.1184e+00 | −− | 5.4665e-02 | −− | 1.3923e-01 | −− | 5 |
| 0.01 | 0.0500 | 3.8918e-02 | 1.8122 | 1.5309e-02 | 2.1821 | 3.0122e-01 | 1.8926 | 1.8417e-02 | 1.5696 | 3.9322e-02 | 1.8241 | 3 |
| | 0.0250 | 1.5695e-02 | 1.3101 | 3.9109e-03 | 1.9688 | 1.2598e-01 | 1.2576 | 7.6721e-03 | 1.2634 | 1.5760e-02 | 1.3190 | 3 |
| | 0.0125 | 7.2560e-03 | 1.1131 | 9.8686e-04 | 1.9866 | 5.8637e-02 | 1.1033 | 3.5884e-03 | 1.0963 | 7.2650e-03 | 1.1173 | 3 |

Table 2.4: Test 2, history of convergence using triangular meshes ($k = 0$) (table produced by the author).

In Tables 2.4 up to 2.7 we summarize the convergence history of our augmented mixed virtual element scheme. We observe the robustness of our method with respect to different values of the viscosity. In particular, it is interesting to observe that for the first triangular mesh using $\mu = 0.01$ and $k = 0$ the method was not convergent (at least 50 iterations were used as limit), in contrast with the results when we use distorted squares meshes.

| $\mu$ | $h$ | $\mathtt{e}_0(\boldsymbol{\sigma})$ | $\mathtt{r}_0(\boldsymbol{\sigma})$ | $\mathtt{e}_0(\mathbf{u})$ | $\mathtt{r}_0(\mathbf{u})$ | $\mathtt{e}_1(\mathbf{u})$ | $\mathtt{r}_1(\mathbf{u})$ | $\mathtt{e}(p)$ | $\mathtt{r}(p)$ | $\mathtt{e}(\widetilde{\boldsymbol{\sigma}})$ | $\mathtt{r}(\widetilde{\boldsymbol{\sigma}})$ | iter |
|---|---|---|---|---|---|---|---|---|---|---|---|---|
| | 0.2000 | 3.9073e-03 | −− | 2.4332e-05 | −− | 9.7644e-04 | −− | 2.0122e-03 | −− | 3.9074e-03 | −− | 2 |
| | 0.1000 | 9.9383e-04 | 1.9751 | 2.5035e-06 | 3.2809 | 2.1036e-04 | 2.2147 | 4.9694e-04 | 2.0176 | 9.9384e-04 | 1.9751 | 2 |
| 1.0 | 0.0500 | 2.5049e-04 | 1.9883 | 2.5948e-07 | 3.2702 | 4.5885e-05 | 2.1968 | 1.2327e-04 | 2.0113 | 2.5049e-04 | 1.9883 | 2 |
| | 0.0250 | 6.2870e-05 | 1.9943 | 2.8003e-08 | 3.2120 | 1.0395e-05 | 2.1421 | 3.0682e-05 | 2.0063 | 6.2870e-05 | 1.9943 | 2 |
| | 0.0125 | 1.5748e-05 | 1.9972 | 3.1698e-09 | 3.1431 | 2.4439e-06 | 2.0887 | 7.6529e-06 | 2.0033 | 1.5748e-05 | 1.9972 | 2 |
| | 0.2000 | 3.9111e-03 | −− | 2.2105e-04 | −− | 8.5484e-03 | −− | 2.0282e-03 | −− | 3.9266e-03 | −− | 2 |
| | 0.1000 | 9.9388e-04 | 1.9764 | 2.3837e-05 | 3.2131 | 1.8494e-03 | 2.2086 | 4.9780e-04 | 2.0266 | 9.9514e-04 | 1.9803 | 2 |
| 0.1 | 0.0500 | 2.5048e-04 | 1.9884 | 2.5328e-06 | 3.2344 | 3.9376e-04 | 2.2317 | 1.2331e-04 | 2.0133 | 2.5057e-04 | 1.9897 | 2 |
| | 0.0250 | 6.2869e-05 | 1.9943 | 2.7691e-07 | 3.1933 | 8.6184e-05 | 2.1918 | 3.0685e-05 | 2.0067 | 6.2875e-05 | 1.9947 | 2 |
| | 0.0125 | 1.5748e-05 | 1.9972 | 3.1553e-08 | 3.1336 | 1.9650e-05 | 2.1329 | 7.6531e-06 | 2.0034 | 1.5748e-05 | 1.9973 | 2 |
| | 0.2000 | 5.7564e-03 | −− | 3.2083e-03 | −− | 1.1935e-01 | −− | 3.0907e-03 | −− | 6.8453e-03 | −− | 3 |
| | 0.1000 | 1.0400e-03 | 2.4686 | 2.5179e-04 | 3.6715 | 1.8994e-02 | 2.6516 | 5.6533e-04 | 2.4508 | 1.1578e-03 | 2.5638 | 2 |
| 0.01 | 0.0500 | 2.5174e-04 | 2.0465 | 2.4960e-05 | 3.3346 | 3.8198e-03 | 2.3140 | 1.2722e-04 | 2.1518 | 2.6060e-04 | 2.1514 | 2 |
| | 0.0250 | 6.2909e-05 | 2.0006 | 2.7355e-06 | 3.1897 | 8.4372e-04 | 2.1787 | 3.0907e-05 | 2.0413 | 6.3503e-05 | 2.0370 | 2 |
| | 0.0125 | 1.5749e-05 | 1.9980 | 3.1465e-07 | 3.1200 | 1.9476e-04 | 2.1151 | 7.6659e-06 | 2.0114 | 1.5788e-05 | 2.0080 | 2 |

Table 2.5: Test 2, history of convergence using triangular meshes ($k = 1$) (table produced by the author).

| $\mu$ | $h$ | $\mathtt{e}_0(\boldsymbol{\sigma})$ | $\mathtt{r}_0(\boldsymbol{\sigma})$ | $\mathtt{e}_0(\mathbf{u})$ | $\mathtt{r}_0(\mathbf{u})$ | $\mathtt{e}_1(\mathbf{u})$ | $\mathtt{r}_1(\mathbf{u})$ | $\mathtt{e}(p)$ | $\mathtt{r}(p)$ | $\mathtt{e}(\widetilde{\boldsymbol{\sigma}})$ | $\mathtt{r}(\widetilde{\boldsymbol{\sigma}})$ | iter |
|---|---|---|---|---|---|---|---|---|---|---|---|---|
| | 0.2001 | 1.2794e-01 | −− | 5.7453e-03 | −− | 3.4909e-02 | −− | 7.4355e-02 | −− | 1.2796e-01 | −− | 3 |
| | 0.1008 | 5.9107e-02 | 1.1250 | 1.6072e-03 | 1.8559 | 1.2125e-02 | 1.5406 | 3.4483e-02 | 1.1194 | 5.9110e-02 | 1.1252 | 2 |
| 1.0 | 0.0504 | 2.7790e-02 | 1.0906 | 4.2224e-04 | 1.9318 | 4.0276e-03 | 1.5928 | 1.6083e-02 | 1.1022 | 2.7791e-02 | 1.0907 | 2 |
| | 0.0252 | 1.3437e-02 | 1.0485 | 1.0707e-04 | 1.9795 | 1.3701e-03 | 1.5557 | 7.7191e-03 | 1.0591 | 1.3437e-02 | 1.0485 | 2 |
| | 0.0126 | 6.6221e-03 | 1.0211 | 2.6900e-05 | 1.9934 | 5.2109e-04 | 1.3950 | 3.7886e-03 | 1.0270 | 6.6221e-03 | 1.0211 | 2 |
| | 0.2001 | 1.4750e-01 | −− | 4.4891e-02 | −− | 2.3608e-01 | −− | 8.0185e-02 | −− | 1.4926e-01 | −− | 3 |
| | 0.1008 | 6.3914e-02 | 1.2184 | 1.3867e-02 | 1.7115 | 8.5250e-02 | 1.4840 | 3.6109e-02 | 1.1623 | 6.4240e-02 | 1.2283 | 3 |
| 0.1 | 0.0504 | 2.8747e-02 | 1.1547 | 3.9471e-03 | 1.8159 | 2.9564e-02 | 1.5305 | 1.6440e-02 | 1.1371 | 2.8794e-02 | 1.1597 | 3 |
| | 0.0252 | 1.3589e-02 | 1.0810 | 1.0438e-03 | 1.9190 | 9.5431e-03 | 1.6314 | 7.7782e-03 | 1.0797 | 1.3595e-02 | 1.0827 | 2 |
| | 0.0126 | 6.6436e-03 | 1.0327 | 2.6684e-04 | 1.9683 | 2.9243e-03 | 1.7068 | 3.7971e-03 | 1.0348 | 6.6443e-03 | 1.0332 | 2 |
| | 0.2001 | 4.5591e-01 | −− | 3.0279e-01 | −− | 2.2173e+00 | −− | 1.6058e-01 | −− | 4.8962e-01 | −− | 4 |
| | 0.1008 | 1.8046e-01 | 1.3502 | 1.1179e-01 | 1.4516 | 8.7762e-01 | 1.3503 | 6.6903e-02 | 1.2755 | 1.9495e-01 | 1.3416 | 4 |
| 0.01 | 0.0504 | 5.8930e-02 | 1.6174 | 3.2792e-02 | 1.7724 | 2.8473e-01 | 1.6268 | 2.5450e-02 | 1.3968 | 6.2885e-02 | 1.6352 | 3 |
| | 0.0252 | 2.0365e-02 | 1.5330 | 9.2352e-03 | 1.8282 | 8.8340e-02 | 1.6885 | 1.0010e-02 | 1.3462 | 2.1090e-02 | 1.5762 | 3 |
| | 0.0126 | 8.0024e-03 | 1.3479 | 2.6141e-03 | 1.8213 | 2.7949e-02 | 1.6607 | 4.2780e-03 | 1.2268 | 8.0963e-03 | 1.3816 | 3 |

Table 2.6: Test 2, history of convergence using distorted squares ($k = 0$) (table produced by the author).

| $\mu$ | $h$ | $\mathtt{e}_0(\boldsymbol{\sigma})$ | $\mathtt{r}_0(\boldsymbol{\sigma})$ | $\mathtt{e}_0(\mathbf{u})$ | $\mathtt{r}_0(\mathbf{u})$ | $\mathtt{e}_1(\mathbf{u})$ | $\mathtt{r}_1(\mathbf{u})$ | $\mathtt{e}(p)$ | $\mathtt{r}(p)$ | $\mathtt{e}(\widetilde{\boldsymbol{\sigma}})$ | $\mathtt{r}(\widetilde{\boldsymbol{\sigma}})$ | iter |
|---|---|---|---|---|---|---|---|---|---|---|---|---|
| | 0.2001 | 3.3507e-03 | −− | 1.0145e-05 | −− | 2.6306e-04 | −− | 1.7197e-03 | −− | 3.3516e-03 | −− | 2 |
| | 0.1008 | 8.4006e-04 | 2.0155 | 1.2943e-06 | 2.9997 | 7.3685e-05 | 1.8540 | 4.3312e-04 | 2.0089 | 8.3985e-04 | 2.0163 | 2 |
| 1.0 | 0.0504 | 2.1013e-04 | 2.0027 | 1.6324e-07 | 2.9923 | 1.8495e-05 | 1.9977 | 1.0869e-04 | 1.9980 | 2.1004e-04 | 2.0029 | 2 |
| | 0.0252 | 5.2499e-05 | 2.0010 | 2.0273e-08 | 3.0094 | 4.5986e-06 | 2.0079 | 2.7197e-05 | 1.9988 | 5.2476e-05 | 2.0010 | 2 |
| | 0.0126 | 1.3132e-05 | 1.9997 | 2.5687e-09 | 2.9812 | 1.1661e-06 | 1.9800 | 6.8062e-06 | 1.9991 | 1.3126e-05 | 1.9998 | 2 |
| | 0.2001 | 3.3504e-03 | −− | 6.3182e-05 | −− | 1.5263e-03 | −− | 1.7209e-03 | −− | 3.5152e-03 | −− | 2 |
| | 0.1008 | 8.3996e-04 | 2.0156 | 7.5492e-06 | 3.0952 | 4.0436e-04 | 1.9351 | 4.3319e-04 | 2.0096 | 8.5303e-04 | 2.0630 | 2 |
| 0.1 | 0.0504 | 2.1012e-04 | 2.0025 | 9.0238e-07 | 3.0698 | 9.9161e-05 | 2.0313 | 1.0870e-04 | 1.9981 | 2.1098e-04 | 2.0190 | 2 |
| | 0.0252 | 5.2499e-05 | 2.0009 | 1.0881e-07 | 3.0520 | 2.4127e-05 | 2.0392 | 2.7197e-05 | 1.9988 | 5.2538e-05 | 2.0058 | 2 |
| | 0.0126 | 1.3132e-05 | 1.9997 | 1.3640e-08 | 2.9967 | 6.0677e-06 | 1.9919 | 6.8062e-06 | 1.9991 | 1.3130e-05 | 2.0010 | 2 |
| | 0.2001 | 3.4839e-03 | −− | 7.0535e-04 | −− | 1.5854e-02 | −− | 1.8380e-03 | −− | 9.5553e-03 | −− | 2 |
| | 0.1008 | 8.4322e-04 | 2.0668 | 7.4121e-05 | 3.2823 | 3.8088e-03 | 2.0776 | 4.3855e-04 | 2.0877 | 1.6625e-03 | 2.5478 | 2 |
| 0.01 | 0.0504 | 2.1013e-04 | 2.0081 | 6.9983e-06 | 3.4107 | 7.7972e-04 | 2.2923 | 1.0893e-04 | 2.0128 | 2.8852e-04 | 2.5309 | 2 |
| | 0.0252 | 5.2494e-05 | 2.0011 | 6.7899e-07 | 3.3656 | 1.5236e-04 | 2.3556 | 2.7209e-05 | 2.0013 | 5.8404e-05 | 2.3046 | 2 |
| | 0.0126 | 1.3132e-05 | 1.9996 | 7.4758e-08 | 3.1839 | 3.2235e-05 | 2.2414 | 6.8068e-06 | 1.9996 | 1.3522e-05 | 2.1113 | 2 |

Table 2.7: Test 2, history of convergence using distorted squares ($k = 1$) (table produced by the author).

### 2.6.3 Test 3

We consider the square $\Omega := (-1/2, 3/2) \times (0, 2)$, set $\mu = 1$ and choose the data $\mathbf{f}$ and $\mathbf{g}$ so that the exact solution is given by

$$\mathbf{u}(\mathbf{x}) := \begin{pmatrix} 1 - e^{\lambda x_1}\cos(2\pi x_2) \\ \\ \dfrac{\lambda}{2\pi} e^{\lambda x_1}\sin(2\pi x_2) \end{pmatrix} \quad \text{and} \quad p(\mathbf{x}) := -\frac{1}{2}e^{2\lambda x_1} + p_0\,,$$

for all $\mathbf{x} := (x_1, x_2)^{\mathbf{t}} \in \Omega$ where $\lambda := \dfrac{-8\pi^2}{1+\sqrt{1+16\pi^2}}$ and $p_0$ is such that $\int_\Omega p = 0$. In order to emphasize the robustness of our method with respect to the parameters $\kappa_1, \kappa_2$ and $\kappa_3$, we take

$(\kappa_1,\kappa_2,\kappa_3) = (\mu,\mu,\mu)$, $(\kappa_1,\kappa_2,\kappa_3) = (\frac{3}{4}\mu,\frac{3}{2}\mu,\frac{3}{8}\mu)$ and $(\kappa_1,\kappa_2,\kappa_3) = (2\mu,3\mu,\frac{3}{2}\mu)$, which, certainly, satisfy the assumptions of Theorems 2.1 and 2.26. In Tables 2.8-2.10 we summarize the history convergence for a sequence of uniform triangular meshes. In addition, the results displayed below show slight differences, which, illustrate the robustness of our method with respect to the choice of the parameters aforementioned.

| $k$ | $h$ | $N$ | $\mathtt{e}_0(\boldsymbol{\sigma})$ | $\mathtt{r}_0(\boldsymbol{\sigma})$ | $\mathtt{e}_0(\mathbf{u})$ | $\mathtt{r}_0(\mathbf{u})$ | $\mathtt{e}_1(\mathbf{u})$ | $\mathtt{r}_1(\mathbf{u})$ | $\mathtt{e}(p)$ | $\mathtt{r}(p)$ | $\mathtt{e}(\widetilde{\boldsymbol{\sigma}})$ | $\mathtt{r}(\widetilde{\boldsymbol{\sigma}})$ |
|---|---|---|---|---|---|---|---|---|---|---|---|---|
| | 0.4000 | 443 | 8.4581e+01 | −− | 4.1314e+00 | −− | 4.8869e+01 | −− | 4.4523e+01 | −− | 8.4637e+01 | −− |
| | 0.2000 | 1683 | 5.8588e+01 | 0.5297 | 1.3427e+00 | 1.6215 | 3.1059e+01 | 0.6539 | 2.7122e+01 | 0.7151 | 5.8597e+01 | 0.5305 |
| 0 | 0.1000 | 6563 | 3.2497e+01 | 0.8503 | 3.4178e-01 | 1.9740 | 1.6384e+01 | 0.9227 | 1.4887e+01 | 0.8654 | 3.2498e+01 | 0.8505 |
| | 0.0500 | 25923 | 1.6531e+01 | 0.9751 | 9.0219e-02 | 1.9216 | 8.3932e+00 | 0.9650 | 7.4549e+00 | 0.9978 | 1.6531e+01 | 0.9751 |
| | 0.4000 | 1883 | 4.8720e+01 | −− | 7.9713e-01 | −− | 1.9297e+01 | −− | 2.1066e+01 | −− | 4.8722e+01 | −− |
| 1 | 0.2000 | 7363 | 1.4754e+01 | 1.7234 | 1.2622e-01 | 2.6589 | 5.2714e+00 | 1.8721 | 6.2340e+00 | 1.7567 | 1.4754e+01 | 1.7235 |
| | 0.1000 | 29123 | 3.7484e+00 | 1.9767 | 1.7375e-02 | 2.8608 | 1.4101e+00 | 1.9024 | 1.5015e+00 | 2.0537 | 3.7484e+00 | 1.9767 |
| | 0.0500 | 115843 | 9.3358e-01 | 2.0054 | 1.9468e-03 | 3.1578 | 3.4177e-01 | 2.0447 | 3.7195e-01 | 2.0132 | 9.3358e-01 | 2.0054 |

Table 2.8: Test 3, history of convergence using triangular meshes and $(\kappa_1,\kappa_2,\kappa_3) = (1,1,1)$ (table produced by the author).

| $k$ | $h$ | $N$ | $\mathtt{e}_0(\boldsymbol{\sigma})$ | $\mathtt{r}_0(\boldsymbol{\sigma})$ | $\mathtt{e}_0(\mathbf{u})$ | $\mathtt{r}_0(\mathbf{u})$ | $\mathtt{e}_1(\mathbf{u})$ | $\mathtt{r}_1(\mathbf{u})$ | $\mathtt{e}(p)$ | $\mathtt{r}(p)$ | $\mathtt{e}(\widetilde{\boldsymbol{\sigma}})$ | $\mathtt{r}(\widetilde{\boldsymbol{\sigma}})$ |
|---|---|---|---|---|---|---|---|---|---|---|---|---|
| | 0.4000 | 443 | 8.4717e+01 | −− | 4.1405e+00 | −− | 4.8842e+01 | −− | 4.4439e+01 | −− | 8.5059e+01 | −− |
| | 0.2000 | 1683 | 5.8599e+01 | 0.5318 | 1.3777e+00 | 1.5875 | 3.1203e+01 | 0.6464 | 2.7373e+01 | 0.6991 | 5.8661e+01 | 0.5361 |
| 0 | 0.1000 | 6563 | 3.2498e+01 | 0.8505 | 3.5414e-01 | 1.9599 | 1.6412e+01 | 0.9270 | 1.4935e+01 | 0.8741 | 3.2507e+01 | 0.8516 |
| | 0.0500 | 25923 | 1.6532e+01 | 0.9751 | 9.3447e-02 | 1.9221 | 8.3978e+00 | 0.9666 | 7.4617e+00 | 1.0011 | 1.6533e+01 | 0.9754 |
| | 0.4000 | 1883 | 4.8717e+01 | −− | 8.1890e-01 | −− | 1.9643e+01 | −− | 2.1218e+01 | −− | 4.8726e+01 | −− |
| 1 | 0.2000 | 7363 | 1.4746e+01 | 1.7241 | 1.2769e-01 | 2.6811 | 5.3204e+00 | 1.8844 | 6.2248e+00 | 1.7692 | 1.4747e+01 | 1.7243 |
| | 0.1000 | 29123 | 3.7478e+00 | 1.9763 | 1.7476e-02 | 2.8692 | 1.4188e+00 | 1.9069 | 1.5012e+00 | 2.0519 | 3.7478e+00 | 1.9763 |
| | 0.0500 | 115843 | 9.3354e-01 | 2.0052 | 1.9583e-03 | 3.1577 | 3.4461e-01 | 2.0417 | 3.7192e-01 | 2.0131 | 9.3355e-01 | 2.0053 |

Table 2.9: Test 3, history of convergence using triangular meshes and $(\kappa_1,\kappa_2,\kappa_3) = (3/4,3/2,3/8)$ (table produced by the author).

| $k$ | $h$ | $N$ | $\mathtt{e}_0(\boldsymbol{\sigma})$ | $\mathtt{r}_0(\boldsymbol{\sigma})$ | $\mathtt{e}_0(\mathbf{u})$ | $\mathtt{r}_0(\mathbf{u})$ | $\mathtt{e}_1(\mathbf{u})$ | $\mathtt{r}_1(\mathbf{u})$ | $\mathtt{e}(p)$ | $\mathtt{r}(p)$ | $\mathtt{e}(\widetilde{\boldsymbol{\sigma}})$ | $\mathtt{r}(\widetilde{\boldsymbol{\sigma}})$ |
|---|---|---|---|---|---|---|---|---|---|---|---|---|
| | 0.4000 | 443 | 8.4625e+01 | −− | 4.1581e+00 | −− | 4.8861e+01 | −− | 4.4494e+01 | −− | 8.4652e+01 | −− |
| | 0.2000 | 1683 | 5.8553e+01 | 0.5313 | 1.3744e+00 | 1.5971 | 3.1126e+01 | 0.6506 | 2.7245e+01 | 0.7077 | 5.8558e+01 | 0.5317 |
| 0 | 0.1000 | 6563 | 3.2487e+01 | 0.8499 | 3.5275e-01 | 1.9621 | 1.6399e+01 | 0.9245 | 1.4907e+01 | 0.8670 | 3.2488e+01 | 0.8500 |
| | 0.0500 | 25923 | 1.6530e+01 | 0.9748 | 9.3014e-02 | 1.9231 | 8.3958e+00 | 0.9659 | 7.4576e+00 | 0.9992 | 1.6530e+01 | 0.9748 |
| | 0.4000 | 1883 | 4.8741e+01 | −− | 8.3909e-01 | −− | 1.9918e+01 | −− | 2.1105e+01 | −− | 4.8742e+01 | −− |
| 1 | 0.2000 | 7363 | 1.4735e+01 | 1.7260 | 1.3142e-01 | 2.6746 | 5.4764e+00 | 1.8628 | 6.2172e+00 | 1.7632 | 1.4735e+01 | 1.7259 |
| | 0.1000 | 29123 | 3.7471e+00 | 1.9754 | 1.7732e-02 | 2.8898 | 1.4455e+00 | 1.9217 | 1.5013e+00 | 2.0500 | 3.7471e+00 | 1.9754 |
| | 0.0500 | 115843 | 9.3350e-01 | 2.0051 | 1.9938e-03 | 3.1528 | 3.5238e-01 | 2.0364 | 3.7187e-01 | 2.0134 | 9.3350e-01 | 2.0051 |

Table 2.10: Test 3, history of convergence using triangular meshes and $(\kappa_1,\kappa_2,\kappa_3) = (2,3,3/2)$ (table produced by the author).

# CHAPTER 3

# A mixed virtual element method for the Boussinesq problem on polygonal meshes

## 3.1 Introduction

In [69] we developed a mixed-VEM for a pseudostress-velocity formulation of the two-dimensional Navier-Stokes equations. There, we employed a dual-mixed approach based on the introduction of a nonlinear pseudostress linking the usual linear one for the Stokes equations and the convective term. In this way, the resulting continuous scheme is augmented with Galerkin type terms arising from the constitutive and equilibrium equations, and the Dirichlet boundary condition, all them multiplied by suitable stabilization parameters, so that the Banach fixed-point and Lax-Milgram theorems are applied to establish the well-posedness of the continuous scheme (cf. [35]). Regarding the discrete problem we proposed there the simultaneous use of virtual element subspaces for $\mathbf{H}^1$ and $\mathbb{H}(\mathbf{div})$ in order to approximate the velocity and the pseudostress, respectively. Then, the discrete bilinear and trilinear forms involved, their main properties, and the associated mixed virtual scheme were defined, and the corresponding solvability was performed by applying similar techniques to those for the continuous formulation. Other contributions dealing with VEM for nonlinear models include [18, 32, 68, 36, 21, 76]. More specifically, in [32] the authors proposed a mixed-VEM for quasi-Newtonian Stokes flows, whereas in [68] the approach from [32] was extend to a nonlinear Brinkman model of porous media flow. In [36] a virtual element method dealing with quasilinear elliptic problems was developed. Finally, an $\mathrm{H}^1$-conforming VEM for the Navier-Stokes equations was introduced in [21], whereas a nonconforming one was proposed in [76].

On the other hand, the development of new mixed finite element methods for the Boussinesq model has constituted a very active research topic in recent years [7, 8, 6, 46, 48, 49]. In particular, an augmented mixed-primal formulation is introduced and analyzed in [46], where the sought quantities are the pseudostress, the velocity, the temperature, and the normal heat flux through the boundary. Under sufficiently small data, it is proved there that when Raviart-Thomas, Lagrange, and discontinuous piecewise finite elements are used to approximate the above unknowns, then the resulting Galerkin method is well-posed and optimally-convergent. Similarly, two formulations for this model, based on a dual-mixed formulation for the momentum equation, and either a primal or a mixed-primal one for the energy equation, are proposed in [49]. In this case, the velocity, the trace-free gradient,

and the normal heat flux are approximated by discontinuous piecewise polynomials, whereas Raviart-Thomas and Lagrange elements are employed for the stress and the temperature, which guarantees the stability and the optimal convergence of the finite element methods. In turn, the Boussinesq problem with temperature-dependent parameters was studied in [7] for the two-dimensional case. There, the authors propose an augmented mixed-primal finite element method that approximates the pseudostress tensor with Raviart-Thomas elements of order $k+1$, the velocity and the temperature with Lagrange elements of order $k$, and the vorticity tensor and normal heat flux on the boundary with discontinuous piecewise polynomials of degree $\leq k$, thus obtaining optimal a priori error estimates as well. Later on, the approach from [7] is suitably modified in [8] to derive an augmented mixed-primal finite element method for the $n$-dimensional case, $n \in \{2,3\}$, in which the incorporation of the strain rate tensor as an auxiliary unknown plays a key role in the analysis. Discontinuous piecewise polynomial functions of degree $\leq k$, together with Raviart-Thomas and Lagrange elements of order $k$ and $k+1$, respectively, are utilized in [8] to approximate the strain rate, the vorticity, the normal heat flux, the pseudostress, the velocity, and the temperature of the fluid.

According to the above discussion and in order to continue extending the applicability of VEM to nonlinear models in fluids mechanics, we now generalize the approach from [69] to the case of the Boussinesq problem. More precisely, we consider the equations and the variational formulation from [46], and then adapt the approach from [69] to propose, up to our knowledge by the first time, a mixed-VEM for Boussinesq. In fact, the pseudostress and the velocity of the fluid are approximated by virtual element subspaces of $\mathbb{H}(\mathrm{div})$ and $\mathbf{H}^1$, respectively, whereas a virtual element subspace of $\mathrm{H}^1$ is employed to approximate the temperature. Thus, similarly as in the aforementioned references, fixed-point arguments are utilized to develop the corresponding solvability analysis, whereas Strang-type estimates are applied to derive the corresponding a priori error estimates for the components of the virtual element solution as well as for their fully calculable projections and the postprocessed pressure.

The rest of this chapter is organized as follows. At the end of the present section we provide some useful notations. In Section 3.2 we describe our nonlinear model, recall from [46] the derivation of the augmented formulation to be employed, as well as the corresponding well-posedness result. Then, in Section 3.3 we introduce the virtual element subspaces approximating the temperature, the velocity and the pseudostress in $\mathrm{H}^1$, $\mathbf{H}^1$ and $\mathbb{H}(\mathbf{div})$, respectively, state their approximation properties, and define the $\mathrm{L}^2$-projectors and remaining ingredients that are needed for the discrete analysis. In turn, computable discrete versions of the bilinear and trilinear forms involved, and of the corresponding functional on the right-hand side of the formulation, are locally and then globally defined in Section 3.4. Next, in Section 3.5 we define the associated mixed virtual element scheme, and perform its solvability analysis by using suitable fixed-point arguments. Moreover, we apply Strang-type estimates to derive the *a priori* error estimates for both the virtual element solution and the fully computable projections of its components. The corresponding rates of convergence are then readily established by using the approximation properties of the subspaces introduced in Sections 3.3 and 3.4. Finally, some numerical examples showing the good performance of the method, confirming the rates of convergence for solutions, and illustrating the accurateness obtained with the approximate solutions, are reported in Section 3.6.

For any vector fields $\mathbf{v} = (v_i)_{i=1,2}$ and $\mathbf{w} = (w_i)_{i=1,2}$, we set the gradient, divergence and tensor

product operators as

$$\nabla \mathbf{v} := \left(\frac{\partial v_i}{\partial x_j}\right)_{i,j=1,2}, \qquad \mathrm{div}\,(\mathbf{v}) := \sum_{j=1}^{2} \frac{\partial v_j}{\partial x_j}, \quad \text{and} \quad \mathbf{v} \otimes \mathbf{w} := (v_i w_j)_{i,j=1,2}\,,$$

respectively. In addition, denoting by $\mathbb{I}$ the identity matrix of $\mathrm{R}^{2\times 2}$, and given $\boldsymbol{\tau} := (\tau_{ij})$, $\boldsymbol{\zeta} := (\zeta_{ij}) \in \mathrm{R}^{2\times 2}$, we write as usual

$$\boldsymbol{\tau}^{\mathbf{t}} := (\tau_{ji})\,, \quad \mathrm{tr}(\boldsymbol{\tau}) := \sum_{i=1}^{2} \tau_{ii}, \quad \boldsymbol{\tau}^{\mathrm{d}} := \boldsymbol{\tau} - \frac{1}{2}\,\mathrm{tr}(\boldsymbol{\tau})\,\mathbb{I}\,, \quad \text{and} \quad \boldsymbol{\tau} : \boldsymbol{\zeta} := \sum_{i,j=1}^{2} \tau_{ij}\zeta_{ij},$$

which corresponds, respectively, to the transpose, the trace, and the deviator tensor of $\boldsymbol{\tau}$, and to the tensorial product between $\boldsymbol{\tau}$ and $\boldsymbol{\zeta}$. Next, given a bounded domain $\mathcal{O} \subseteq \mathrm{R}^2$ with boundary $\partial\mathcal{O}$, we let $\mathbf{n}$ be the outward unit normal vector on $\partial\mathcal{O}$. Also, given $r \geq 0$ and $1 < p \leq \infty$, we let $\mathrm{W}^{r,p}(\mathcal{O})$ be the standard Sobolev space with norm $\|\cdot\|_{r,p,\mathcal{O}}$ and seminorm $|\cdot|_{r,p,\mathcal{O}}$. In particular, for $r = 0$ we let $\mathrm{L}^p(\mathcal{O}) := \mathrm{W}^{0,p}(\mathcal{O})$ be the usual Lebesgue space, and for $p = 2$ we let $\mathrm{H}^s(\mathcal{O}) := \mathrm{W}^{r,2}(\mathcal{O})$ be the classical Hilbertian Sobolev space with norm $\|\cdot\|_{s,\mathcal{O}}$ and seminorm $|\cdot|_{s,\mathcal{O}}$. Furthermore, given a generic scalar functional space M, we let $\mathbf{M}$ and $\mathbb{M}$ be its vector and tensorial counterparts, respectively, whose norms and seminorms are denoted exactly as those of M. On the other hand, letting **div** (resp. **rot**) be the usual divergence operator div (resp. rotational operator rot) acting along the rows of a given tensor, we recall that the space

$$\mathbb{H}(\mathbf{div};\mathcal{O}) := \left\{\boldsymbol{\tau} \in \mathbb{L}^2(\mathcal{O}) : \quad \mathbf{div}\,(\boldsymbol{\tau}) \in \mathbf{L}^2(\mathcal{O})\right\},$$

and

$$\mathbb{H}(\mathbf{rot};\mathcal{O}) := \left\{\boldsymbol{\tau} \in \mathbb{L}^2(\mathcal{O}) : \quad \mathbf{rot}\,(\boldsymbol{\tau}) \in \mathbf{L}^2(\mathcal{O})\right\},$$

equipped with the usual norms

$$\|\boldsymbol{\tau}\|^2_{\mathbf{div};\mathcal{O}} := \|\boldsymbol{\tau}\|^2_{0,\mathcal{O}} + \|\mathbf{div}\,(\boldsymbol{\tau})\|^2_{0,\mathcal{O}} \qquad \forall\, \boldsymbol{\tau} \in \mathbb{H}(\mathbf{div};\mathcal{O})\,,$$

and

$$\|\boldsymbol{\tau}\|^2_{\mathbf{rot};\mathcal{O}} := \|\boldsymbol{\tau}\|^2_{0,\mathcal{O}} + \|\mathbf{rot}\,(\boldsymbol{\tau})\|^2_{0,\mathcal{O}} \qquad \forall\, \boldsymbol{\tau} \in \mathbb{H}(\mathbf{rot};\mathcal{O})\,,$$

are Hilbert spaces. Also, we define

$$\mathbb{H}_0(\mathbf{div};\mathcal{O}) := \left\{\boldsymbol{\tau} \in \mathbb{H}(\mathbf{div};\mathcal{O}) : \int_\Omega \mathrm{tr}(\boldsymbol{\tau}) = 0\right\},$$

and recall (see [29, 56]) that there holds the decomposition

$$\mathbb{H}(\mathbf{div};\mathcal{O}) = \mathbb{H}_0(\mathbf{div};\mathcal{O}) \oplus \mathrm{R}\,\mathbb{I}\,. \tag{3.1}$$

More precisely, for each $\boldsymbol{\tau} \in \mathbb{H}(\mathbf{div};\mathcal{O})$ there exist unique $\boldsymbol{\tau}_0 \in \mathbb{H}_0(\mathbf{div};\mathcal{O})$ and $c := \frac{1}{2|\mathcal{O}|}\int_{\mathcal{O}} \mathrm{tr}(\boldsymbol{\tau}) \in \mathrm{R}$, where $|\mathcal{O}|$ denotes the measure of $\mathcal{O}$, such that $\boldsymbol{\tau} = \boldsymbol{\tau}_0 + c\,\mathbb{I}$. Finally, in what follows we employ $\mathbf{0}$ to denote a generic null vector, null tensor or null operator, and use $C$ to denote generic constants independent of the discretization parameters, which may take different values at different places.

## 3.2 The model problem and its continuous formulation

Let $\Omega$ be a bounded polygonal domain in $\mathrm{R}^2$ with boundary $\Gamma$. We consider the stationary Boussinesq problem, that is, given an external force per unit mass $\mathbf{g} \in \mathbf{L}^\infty(\Omega)$ and the boundary data $\mathbf{u}_D \in \mathbf{H}^{1/2}(\Gamma)$, we are interested in finding the velocity $\mathbf{u}$, the pressure $p$ and the temperature $\varphi$ of a fluid occupying the region $\Omega$, such that

$$\begin{aligned} -\mu\,\Delta\,\mathbf{u} + (\nabla\,\mathbf{u})\,\mathbf{u} + \nabla\,p - \mathbf{g}\,\varphi = 0 \quad \text{in} \quad \Omega\,, \quad \mathrm{div}\,(\mathbf{u}) = 0 \quad \text{in} \quad \Omega\,, \quad \mathbf{u} = \mathbf{u}_D \quad \text{on} \quad \Gamma\,, \\ -\,\mathrm{div}\,(\mathbb{K}\,\nabla\,\varphi) + \mathbf{u}\cdot\nabla\,\varphi = 0 \quad \text{in} \quad \Omega \quad \text{and} \quad \varphi = 0 \quad \text{on} \quad \Gamma\,, \end{aligned} \tag{3.2}$$

where $\mu > 0$ is the fluid viscosity and $\mathbb{K} \in \mathbb{L}^\infty(\Omega)$ is a uniformly positive definite tensor describing the thermal conductivity. Note that from the incompressibility condition (cf. second equation in (3.2)) the data $\mathbf{u}_D$ must satisfy the compatibility condition $\int_\Gamma \mathbf{u}_D \cdot \mathbf{n} = 0$. In addition, the uniqueness of a pressure solution of (3.2), is ensured in the space $\mathrm{L}^2_0(\Omega) := \Big\{ q \in \mathrm{L}^2(\Omega) : \quad \int_\Omega q = 0 \Big\}$.

Now, proceeding as in [46, Section II], we introduce the pseudostress tensor

$$\boldsymbol{\sigma} := \mu\,\nabla\,\mathbf{u} - (\mathbf{u}\otimes\mathbf{u}) - p\,\mathbb{I} \quad \text{in} \quad \Omega\,, \tag{3.3}$$

and use the incompressibility condition to eliminate the pressure, so that then our model problem (3.2) can be rewritten equivalently as

$$\begin{aligned} \boldsymbol{\sigma}^{\mathrm{d}} + (\mathbf{u}\otimes\mathbf{u})^{\mathrm{d}} = \mu\,\nabla\,\mathbf{u} \quad \text{in} \quad \Omega, \quad -\,\mathbf{div}\,(\boldsymbol{\sigma}) - \mathbf{g}\,\varphi = 0 \quad \text{in} \quad \Omega\,, \quad \mathbf{u} = \mathbf{u}_D \quad \text{on} \quad \Gamma\,, \\ -\,\mathrm{div}\,(\mathbb{K}\nabla\varphi) + \mathbf{u}\cdot\nabla\varphi = 0 \quad \text{in} \quad \Omega, \quad \varphi = 0 \quad \text{on} \quad \Gamma \quad \text{and} \quad \int_\Omega \mathrm{tr}(\boldsymbol{\sigma} + \mathbf{u}\otimes\mathbf{u}) = 0\,, \end{aligned} \tag{3.4}$$

where the pressure $p$ can be approximated by the postprocessing formula

$$p = -\frac{1}{2}\,\mathrm{tr}\,(\boldsymbol{\sigma} + \mathbf{u}\otimes\mathbf{u}) \quad \text{in} \quad \Omega\,. \tag{3.5}$$

Next, following [46, Section III], and motivated by the decomposition (3.1), we test the first, second and fourth equation of (3.4), with $\boldsymbol{\tau} \in \mathbb{H}_0(\mathbf{div};\Omega)$, $\mathbf{v} \in \mathbf{H}^1(\Omega)$, and $\psi \in \mathrm{H}^1_0(\Omega)$, respectively. Then, we integrate by parts, use the boundary conditions, and enrich the resulting variational formulation with the incorporation of the following redundant terms

$$\begin{aligned} \kappa_1 \int_\Omega \Big\{ \mu\,\nabla\,\mathbf{u} - (\mathbf{u}\otimes\mathbf{u})^{\mathrm{d}} - \boldsymbol{\sigma}^{\mathrm{d}} \Big\} : \nabla\mathbf{v} &= 0 \qquad \forall\,\mathbf{v} \in \mathbf{H}^1(\Omega)\,, \\ \kappa_2 \int_\Omega \mathbf{div}\,(\boldsymbol{\sigma})\cdot\mathbf{div}\,(\boldsymbol{\tau}) + \kappa_2 \int_\Omega \mathbf{g}\,\varphi\cdot\mathbf{div}\,(\boldsymbol{\tau}) &= 0 \qquad \forall\,\boldsymbol{\tau} \in \mathbb{H}_0(\mathbf{div};\Omega)\,, \\ \kappa_3 \int_\Gamma \mathbf{u}\cdot\mathbf{v} &= \kappa_3 \int_\Gamma \mathbf{u}_D\cdot\mathbf{v} \quad \forall\,\mathbf{v} \in \mathbf{H}^1(\Omega)\,, \end{aligned}$$

with $\kappa_1, \kappa_2$ and $\kappa_3$ positives parameters to be specified later. In this way, we arrive at the following augmented formulation: Find $(\vec{\boldsymbol{\sigma}}, \varphi) := ((\boldsymbol{\sigma}, \mathbf{u}), \varphi) \in \mathbf{H} \times \mathrm{H}$ such that

$$\begin{aligned} \mathbf{A}(\vec{\boldsymbol{\sigma}}, \vec{\boldsymbol{\tau}}) + \mathbf{B}(\mathbf{u}; \vec{\boldsymbol{\sigma}}, \vec{\boldsymbol{\tau}}) &= \mathbf{F}(\varphi; \vec{\boldsymbol{\tau}}) + \mathbf{F}_D(\vec{\boldsymbol{\tau}}) \quad \forall\,\vec{\boldsymbol{\tau}} := (\boldsymbol{\tau}, \mathbf{v}) \in \mathbf{H} := \mathbb{H}_0(\mathbf{div};\Omega) \times \mathbf{H}^1(\Omega), \\ \mathbf{a}(\varphi, \psi) &= \mathrm{F}(\mathbf{u}, \varphi; \psi) \qquad \forall\,\psi \in \mathrm{H} := \mathrm{H}^1_0(\Omega)\,, \end{aligned} \tag{3.6}$$

where the forms $\mathbf{A}, \mathbf{B}$ and $\mathbf{a}$ are defined, respectively as

$$\begin{aligned}\mathbf{A}(\vec{\boldsymbol{\sigma}}, \vec{\boldsymbol{\tau}}) \;:=\; & \int_\Omega \boldsymbol{\sigma}^{\mathrm{d}} : \boldsymbol{\tau}^{\mathrm{d}} \,+\, \kappa_2 \int_\Omega \mathbf{div}\,(\boldsymbol{\sigma}) \cdot \mathbf{div}\,(\boldsymbol{\tau}) \,+\, \kappa_1\, \mu \int_\Omega \nabla \mathbf{v} : \nabla \mathbf{u} \\ & -\mu \int_\Omega \mathbf{v} \cdot \mathbf{div}\,(\boldsymbol{\sigma}) \,+\, \mu \int_\Omega \mathbf{u} \cdot \mathbf{div}\,(\boldsymbol{\tau}) \,-\, \kappa_1 \int_\Omega \boldsymbol{\sigma}^{\mathrm{d}} : \nabla \mathbf{v} + \kappa_3 \int_\Gamma \mathbf{v} \cdot \mathbf{u}\,,\end{aligned} \tag{3.7}$$

$$\mathbf{B}(\mathbf{z}; \vec{\boldsymbol{\sigma}}, \vec{\boldsymbol{\tau}}) \;:=\; \int_\Omega (\mathbf{u} \otimes \mathbf{z})^{\mathrm{d}} : \Big\{ \boldsymbol{\tau} - \kappa_1\, \nabla\, \mathbf{v} \Big\}\,, \tag{3.8}$$

and

$$\mathbf{a}(\varphi, \psi) := \int_\Omega \mathbb{K} \nabla \varphi \cdot \nabla \psi \tag{3.9}$$

for all $\vec{\boldsymbol{\sigma}} := (\boldsymbol{\sigma}, \mathbf{u}) \in \mathbf{H}$, for all $\mathbf{z} \in \mathbf{H}^1(\Omega)$, and for all $\varphi, \psi \in \mathrm{H}$. In turn, $\mathbf{F}(\varphi)$ (with a given $\varphi \in \mathrm{H}^1_0(\Omega)$), and $\mathrm{F}(\mathbf{u}, \varphi)$ (with a given $(\mathbf{u}, \varphi) \in \mathbf{H}^1(\Omega) \times \mathrm{H}^1_0(\Omega)$), are the linear functionals defined by

$$\mathbf{F}(\varphi; \vec{\boldsymbol{\tau}}) := \int_\Omega \mathbf{g}\, \varphi \cdot \Big\{ \mu\, \mathbf{v} - \kappa_2\, \mathbf{div}\,(\boldsymbol{\tau}) \Big\}\,, \tag{3.10}$$

and

$$\mathrm{F}(\mathbf{u}, \varphi; \psi) := -\int_\Omega (\mathbf{u} \cdot \nabla \varphi)\, \psi\,, \tag{3.11}$$

respectively, whereas $\mathbf{F}_D$ and $\mathrm{F}_N$ are given by

$$\mathbf{F}_D(\vec{\boldsymbol{\tau}}) := \kappa_3 \int_\Gamma \mathbf{u}_D \cdot \mathbf{v} + \mu\, \langle \boldsymbol{\tau} \mathbf{n}, \mathbf{u}_D \rangle\,. \tag{3.12}$$

We recall here that the choice of $\mathbf{H}^1(\Omega)$ and $\mathrm{H}^1_0(\Omega)$ as tests functions spaces for the velocity $\mathbf{u}$ and the temperature $\varphi$, is motivated by the convective terms at the first and fourth equation in (3.4), which require $\mathbf{u}$ and $\varphi$ to be in spaces smaller than $\mathbf{L}^2(\Omega)$ and $\mathrm{L}^2(\Omega)$, respectively. In fact, this is possible thanks to the Cauchy-Schwarz and Hölder inequalities, and the compact (and hence continuous) injections (see [35, 46] for more details)

$$\mathbf{i}_c \,:\, \mathbf{H}^1(\Omega) \to \mathbf{L}^4(\Omega) \quad \text{and} \quad \mathrm{i}_c \,:\, \mathrm{H}^1(\Omega) \to \mathrm{L}^4(\Omega)\,. \tag{3.13}$$

In this way, according to (3.8) and (3.13), we have that

$$|\mathbf{B}(\mathbf{z}; \vec{\boldsymbol{\zeta}}, \vec{\boldsymbol{\tau}})| \leq C_{\mathbf{B}} \|\mathbf{z}\|_{1,\Omega} \|\vec{\boldsymbol{\zeta}}\|_{\mathbf{H}} \|\vec{\boldsymbol{\tau}}\|_{\mathbf{H}} \quad \forall\, \mathbf{z} \in \mathbf{H}^1(\Omega), \quad \forall\, \vec{\boldsymbol{\zeta}}, \vec{\boldsymbol{\tau}} \in \mathbf{H}\,. \tag{3.14}$$

with $C_{\mathbf{B}} := \|\boldsymbol{i}_c\|^2 (1 + \kappa_1^2)^{1/2}$.

In addition, the analysis of the continuous formulation (3.6) is analogous to [46, Section III], and therefore up to minor changes caused by the homogenous Dirichlet condition for $\varphi$, its well-posedness is developed through a fixed-point strategy based on decoupling the fluid and heat equations, and then combining the classical Banach Theorem and the Lax-Milgram Theorem. In particular, it was proved there (cf. [46, Lemma 3.3]) that for $\kappa_1 \in (0, 2\mu)$ and $\kappa_2, \kappa_3 \in (0, \infty)$, there exists $\alpha_{\mathbf{A}} > 0$ (cf. [46, eq. 3.30]), depending on $\kappa_1, \kappa_2, \kappa_3, \mu$ and the constants $c_1(\Omega)$ and $c_2(\Omega)$ (cf. Lemma 3.9 below), such that

$$\mathbf{A}(\vec{\boldsymbol{\tau}}, \vec{\boldsymbol{\tau}}) \geq \alpha_{\mathbf{A}} \|\vec{\boldsymbol{\tau}}\|^2_{\mathbf{H}} \quad \forall\, \vec{\boldsymbol{\tau}} \in \mathbf{H}\,, \tag{3.15}$$

which together with (3.14), yielded the $\mathbf{H}$-ellipticity of the bilinear form $\mathbf{A}+\mathbf{B}(\mathbf{z};\cdot,\cdot)$ for sufficiently small $\mathbf{z}$, that is, for each $\mathbf{z}\in\mathbf{H}^1(\Omega)$ such that $\|\mathbf{z}\|_{1,\Omega}\leq\dfrac{\alpha_{\mathbf{A}}}{2C_{\mathbf{B}}}$, there holds (cf. [46, eq. 3.32])

$$\mathbf{A}(\vec{\boldsymbol{\tau}},\vec{\boldsymbol{\tau}})+\mathbf{B}(\mathbf{z};\vec{\boldsymbol{\tau}},\vec{\boldsymbol{\tau}})\geq\frac{\alpha_{\mathbf{A}}}{2}\|\vec{\boldsymbol{\tau}}\|^2_{\mathbf{H}}\quad\forall\,\vec{\boldsymbol{\tau}}\in\mathbf{H}\,.$$

In turn, the boundedness of the bilinear form $\mathbf{A}$ (cf. (3.7)) is obtained with a constant $C_{\mathbf{A}}>0$, depending on $\kappa_1,\kappa_2,\kappa_3,\mu$ and $\|\gamma_0\|$, where $\gamma_0:\mathbf{H}^1(\Omega)\to\mathbf{H}^{1/2}(\Gamma)$ is the usual trace operator, that is, there holds

$$|\mathbf{A}(\vec{\boldsymbol{\zeta}},\vec{\boldsymbol{\tau}})|\leq C_{\mathbf{A}}\|\vec{\boldsymbol{\zeta}}\|_{\mathbf{H}}\|\vec{\boldsymbol{\tau}}\|_{\mathbf{H}}\quad\forall\,\vec{\boldsymbol{\zeta}},\vec{\boldsymbol{\tau}}\in\mathbf{H}\,.\tag{3.16}$$

Furthermore, given $\phi\in\mathrm{H}^1_0(\Omega)$, it follows from the Cauchy-Schwarz inequality and the trace theorems in $\mathbb{H}(\mathbf{div};\Omega)$ and $\mathbf{H}^1(\Omega)$, that

$$\begin{aligned}\|\mathbf{F}(\phi;\cdot)\| &\leq C_{\mathbf{F}}\|\mathbf{g}\|_{\infty,\Omega}\|\phi\|_{0,\Omega}\,,\\ \|\mathbf{F}_D\| &\leq \kappa_3\|\gamma_0\|\|\mathbf{u}_D\|_{0,\Gamma}+\mu\|\mathbf{u}_D\|_{1/2,\Gamma}\,,\end{aligned}\tag{3.17}$$

with $C_{\mathbf{F}}:=(\mu^2+\kappa_2^2)^{1/2}$. In this way, denoting $M_{\mathbf{F}}:=\max\Big\{C_{\mathbf{F}},\kappa_3\|\gamma_0\|\Big\}$, we get

$$\|\mathbf{F}(\phi;\cdot)+\mathbf{F}_D\|\leq M_{\mathbf{F}}\Big\{\|\mathbf{g}\|_{\infty,\Omega}\|\phi\|_{0,\Omega}+\|\mathbf{u}_D\|_{0,\Gamma}+\|\mathbf{u}_D\|_{1/2,\Gamma}\Big\}\,.\tag{3.18}$$

On the other hand, it is clear from (3.9), the properties of the tensor $\mathbb{K}$, and the Poincaré inequality, that $\mathbf{a}$ is a bounded and H-elliptic bilinear form with constants $\|\mathbb{K}\|_{\infty,\Omega}$ and $\alpha_{\mathbf{a}}$, respectively. In addition, it follows from it follows from (3.11) and (3.13), that for a given $(\mathbf{z},\phi)\in\mathbf{H}^1(\Omega)\times\mathrm{H}^1_0(\Omega)$, there holds

$$\|\mathrm{F}(\mathbf{z},\phi)\|\leq M_{\mathrm{F}}\|\mathbf{z}\|_{1,\Omega}|\phi|_{1,\Omega}\,,$$

with $M_{\mathrm{F}}:=\|\boldsymbol{i}_c\|\|i_c\|$. Finally, by using the aforementioned arguments we can conclude the following result.

**Theorem 3.1.** *Let $\kappa_1\in(0,2\,\mu)$ and $\kappa_2\,,\,\kappa_3\in(0,\infty)$. Given $\rho\in\left(0,\dfrac{\alpha_{\mathbf{A}}}{2C_{\mathbf{B}}}\right)$, let $W_\rho$ be the closed ball in $\mathbf{H}^1(\Omega)\times\mathrm{H}^1_0(\Omega)$ defined by $W_\rho:=\Big\{(\mathbf{z},\phi)\in\mathbf{H}^1(\Omega)\times\mathrm{H}^1_0(\Omega):\quad\|(\mathbf{z},\phi)\|\leq\rho\Big\}$. In addition, assume that the data satisfy the assumptions*

$$c_{\mathbf{T}}\Big\{\|\mathbf{g}\|_{\infty,\Omega}+\|\mathbf{u}_D\|_{0,\Omega}+\|\mathbf{u}_D\|_{1/2,\Gamma}\Big\}\leq\rho\,,$$

*and*

$$C_{\mathbf{T}}\Big\{\|\mathbf{g}\|_{\infty,\Omega}+\|\mathbf{u}_D\|_{0,\Omega}+\|\mathbf{u}_D\|_{1/2,\Gamma}\Big\}<1\,,$$

*where $c_{\mathbf{T}}:=c_{\mathbf{T}}(\rho,M_{\mathbf{F}},\alpha_{\mathbf{A}},M_{\mathrm{F}},\alpha_{\mathbf{a}})$ and $C_{\mathbf{T}}:=C_{\mathbf{T}}(\rho,C_{\mathrm{F}},C_{\mathbf{F}},C_{\mathbf{B}},\alpha_{\mathbf{a}},\alpha_{\mathbf{A}},M_{\mathbf{F}})$ are positive constants. Then, problem (3.6) has a unique solution $((\boldsymbol{\sigma},\mathbf{u}),\varphi)\in\mathbf{H}\times\mathrm{H}$ with $(\mathbf{u},\varphi)\in W_\rho$. Moreover, there hold*

$$\|(\boldsymbol{\sigma},\mathbf{u})\|_{\mathbf{H}}\leq\frac{2M_{\mathbf{F}}}{\alpha_{\mathbf{A}}}\Big\{\rho\,\|\mathbf{g}\|_{\infty,\Omega}+\|\mathbf{u}_D\|_{0,\Gamma}+\|\mathbf{u}_D\|_{1/2,\Gamma}\Big\}\,,\tag{3.19}$$

*and*

$$\|\varphi\|_{1,\Omega}\leq\frac{2M_{\mathrm{F}}}{\alpha_{\mathbf{a}}}\rho\,\|\mathbf{u}\|_{1,\Omega}\,.\tag{3.20}$$

*Proof.* We omit details and refer to [46, Theorem 3.9]. □

## 3.3 The virtual element subspaces

In this section we introduce suitable virtual element subspaces for $\mathrm{H}^1_0(\Omega)$, $\mathbf{H}^1(\Omega)$, and $\mathbb{H}_0(\mathbf{div};\Omega)$, together to their respective approximation properties. To this end, we will assume the basic assumptions on meshes that are standard in this context (cf. [13, 28]), that is, given $\{\mathcal{T}_h\}_{h>0}$ a family of decompositions of $\Omega$ in polygonal elements $K$, and given a particular $K \in \mathcal{T}_h$, we denote its barycenter, diameter, and number of edges by $\mathbf{x}_K$, $h_K$, and $d_K$, respectively, and define, as usual, $h := \max\{h_K : K \in \mathcal{T}_h\}$. In addition, we assume that there exists a constant $C_{\mathcal{T}} > 0$ such that for each decomposition $\mathcal{T}_h$ and for each $K \in \mathcal{T}_h$ there hold:

a) the ratio between the shortest edge and the diameter $h_K$ of $K$ is bigger than $C_{\mathcal{T}}$, and

b) $K$ is star-shaped with respect to a ball $B$ of radius $C_{\mathcal{T}} h_K$ and center $\mathbf{x}_B \in K$.

Now, given an integer $\ell \geq 0$ and $\mathcal{O} \subseteq \mathrm{R}^2$, we let $\mathrm{P}_\ell(\mathcal{O})$ be the space of polynomials on $\mathcal{O}$ of degree up to $\ell$, we set $\mathbf{P}_\ell(\mathcal{O}) := [\mathrm{P}_\ell(\mathcal{O})]^2$ and $\mathbb{P}_\ell(\mathcal{O}) := [\mathrm{P}_\ell(\mathcal{O})]^{2\times 2}$. Also, in what follows we use the multi-index notation, that is, given $\mathbf{x} := (x_1, x_2)^{\mathbf{t}} \in \mathrm{R}^2$ and $\boldsymbol{\alpha} := (\alpha_1, \alpha_2)^{\mathbf{t}}$, with non-negative integers $\alpha_1, \alpha_2$, we let $\mathbf{x}^{\boldsymbol{\alpha}} := x_1^{\alpha_1} x_2^{\alpha_2}$ and $|\boldsymbol{\alpha}| := \alpha_1 + \alpha_2$. Furthermore, given $K \in \mathcal{T}_h$ and an edge $e \in \partial K$ with barycentric $x_e$ and diameter $h_e$, we introduce the following sets of $(\ell+1)$ normalized monomials on $e$

$$\mathcal{B}_\ell(e) := \left\{ \left( \frac{x - x_e}{h_e} \right)^j \right\}_{0 \leq j \leq \ell},$$

and $\frac{1}{2}(\ell+1)(\ell+2)$ normalized monomials on $K$

$$\mathcal{B}_\ell(K) := \left\{ \left( \frac{\mathbf{x} - \mathbf{x}_K}{h_K} \right)^{\boldsymbol{\alpha}} \right\}_{0 \leq |\boldsymbol{\alpha}| \leq \ell},$$

which constitute basis of $\mathrm{P}_\ell(e)$ and $\mathrm{P}_\ell(K)$, respectively. In addition, denoting $\widetilde{\mathcal{B}}_0(K) := \mathcal{B}_1(K)$, we define for each integer $\ell \geq 1$,

$$\widetilde{\mathcal{B}}_\ell(K) := \mathcal{B}_{\ell+1}(K) \setminus \mathcal{B}_{\ell-1}(K),$$

which is a basis of the subspace of polynomials on $K$ of degree exactly $\ell+1$ or $\ell$. In turn, the corresponding vector and tensor versions of the foregoing sets of monomials are given by

$$\begin{aligned} \boldsymbol{\mathcal{B}}_\ell(e) &:= \Big\{ (q,0)^{\mathbf{t}} : \quad q \in \mathcal{B}_\ell(e) \Big\} \cup \Big\{ (0,q)^{\mathbf{t}} : \quad q \in \mathcal{B}_\ell(e) \Big\}, \\ \boldsymbol{\mathcal{B}}_\ell(K) &:= \Big\{ (\mathbf{q},0)^{\mathbf{t}} : \quad \mathbf{q} \in \mathcal{B}_\ell(K) \Big\} \cup \Big\{ (0,\mathbf{q})^{\mathbf{t}} : \quad \mathbf{q} \in \mathcal{B}_\ell(K) \Big\}, \end{aligned}$$

and

$$\widetilde{\boldsymbol{\mathcal{B}}}_\ell(K) := \Big\{ (\mathbf{q},0)^{\mathbf{t}} : \quad \mathbf{q} \in \widetilde{\mathcal{B}}_\ell(K) \Big\} \cup \Big\{ (0,\mathbf{q})^{\mathbf{t}} : \quad \mathbf{q} \in \widetilde{\mathcal{B}}_\ell(K) \Big\}.$$

On the other hand, for each integer $\ell \geq 0$, we let $\mathcal{G}_\ell(K)$ be a basis of $\big(\nabla \mathrm{P}_{\ell+1}(K)\big)^\perp \cap \mathbf{P}_\ell(K)$, which is the $\mathbf{L}^2(K)$-orthogonal of $\nabla \mathrm{P}_{\ell+1}(K)$ in $\mathbf{P}_\ell(K)$, and denote its vectorial counterparts as follow:

$$\boldsymbol{\mathcal{G}}_\ell(K) := \left\{ \begin{pmatrix} \mathbf{q} \\ \mathbf{0} \end{pmatrix} : \mathbf{q} \in \mathcal{G}_\ell(K) \right\} \cup \left\{ \begin{pmatrix} \mathbf{0} \\ \mathbf{q} \end{pmatrix} : \mathbf{q} \in \mathcal{G}_\ell(K) \right\}.$$

We remark that, alternatively, one could also consider another choices, not necessarily orthogonal, that have been proposed recently, such as $\mathbf{P}_k(K) = \nabla \mathrm{P}_{k+1} \oplus \mathbf{x}^{\perp}\mathrm{P}_{k-1}(K)$, where, given $\mathbf{x} := (x_1, x_2) \in \mathrm{R}^2$, $\mathbf{x}^{\perp}$ denotes the rotated vector $(-x_2, x_1)$. Actually, it is not difficult to see that it suffices to choose any space $\mathcal{G}(K)$ such that $\mathbf{P}_\ell(K) = \nabla \mathrm{P}_{\ell+1} \oplus \mathcal{G}(K)$.

Finally, we let

$$\mathrm{H}^1(\mathcal{T}_h) := \left\{ \psi \in \mathrm{L}^2(\Omega) : \quad \psi|_K \in \mathrm{H}^1(K) \quad \forall\, K \in \mathcal{T}_h \right\},$$

and consider the $\mathrm{H}^1$-broken seminorm

$$|\psi|_{1,h} := \left\{ \sum_{K \in \mathcal{T}_h} \|\nabla \psi\|^2_{0,K} \right\}^{1/2} \qquad \forall\, \psi \in \mathrm{H}^1(\mathcal{T}_h)\,.$$

### 3.3.1 The virtual subspace of $\mathrm{H}^1(\Omega)$

Given $K \in \mathcal{T}_h$ and an integer $k \geq 0$, we first let $\mathcal{R}_k^K : \mathrm{H}^1(K) \to \mathrm{P}_{k+1}(K)$ be the projection operator defined for each $\psi \in \mathrm{H}^1(K)$ as the unique polynomial $\mathcal{R}_k^K(\psi) \in \mathrm{P}_{k+1}(K)$ satisfying (cf. [13, 16])

$$\begin{aligned} \int_K \nabla \mathcal{R}_k^K(\psi) \cdot \nabla q &= \int_K \nabla \psi \cdot \nabla q \qquad \forall\, q \in \mathrm{P}_{k+1}(K)\,, \\ \int_{\partial K} \mathcal{R}_k^K(\psi) &= \int_{\partial K} \psi\,. \end{aligned} \tag{3.21}$$

Also, it is readily seen from the first equation of (3.21) that

$$|\mathcal{R}_k^K(\psi)|_{1,K} \leq |\psi|_{1,K} \qquad \forall\, \psi \in \mathrm{H}^1(K)\,.$$

In addition, we recall from [16, Lemma 5.1] that for integers $m \in [2, k+2]$ and $\ell \in [1, m]$, there holds the approximation property

$$\|\psi - \mathcal{R}_k^K(\psi)\|_{\ell,K} \leq C\, h_K^{m-\ell}\, |\psi|_{m,K} \qquad \forall\, \psi \in \mathrm{H}^m(K)\,, \quad \forall\, K \in \mathcal{T}_h\,. \tag{3.22}$$

Furthermore, we now consider the finite-dimensional subspace of $\mathrm{C}(\partial K)$ given by

$$\mathrm{B}_k(\partial K) := \left\{ \psi \in \mathrm{C}(\partial K) : \quad \psi|_e \in \mathrm{P}_{k+1}(e)\,, \quad \forall \text{ edge } e \subseteq \partial K \right\}, \tag{3.23}$$

define the following local virtual element space (see, e.g. [4])

$$\begin{aligned} \mathcal{Q}_k^K := \Big\{ \psi \in \mathrm{H}^1(K) : \quad & \psi|_{\partial K} \in \mathrm{B}_k(\partial K)\,, \quad \Delta\, \psi \in \mathrm{P}_{k+1}(K)\,, \\ & \text{and} \quad \int_K \left\{ \mathcal{R}_k^K(\psi) - \psi \right\} q \,=\, 0 \qquad \forall\, q \in \widetilde{\mathcal{B}}_k(K) \Big\}, \end{aligned} \tag{3.24}$$

and recall from [4] the following degrees of freedom for a given $\psi \in \mathcal{Q}_k^K$

$$\begin{aligned} &i) \quad \text{the value of } \psi \text{ at the } i\text{th vertex of } K\,, \quad \forall\, i \text{ vertex of } K\,, \\ &ii) \quad \text{the values of } \psi \text{ at } k \text{ uniformly spaced points on } e\,, \ \forall\, e \in \partial K\,, \ \text{for } k \geq 1\,, \\ &iii) \quad \text{the moments } \int_K \psi\, q\,, \ \forall\, q \in \mathcal{B}_{k-1}(K)\,, \ \text{for } k \geq 1\,. \end{aligned} \tag{3.25}$$

It is well-known that for each $\psi \in \mathcal{Q}_k^K$ the projection $\mathcal{R}_k^K(\psi) \in \mathrm{P}_{k+1}(K)$ is fully computable using only the degrees of freedom (3.25) (cf. [4, 13]). In addition, for each $K \in \mathcal{T}_h$ and $\psi \in \mathrm{H}^1(K)$, we denote its $\mathcal{Q}_k^K$-interpolant by $\psi_I$, and recall next from [4] its associated approximation properties.

**Lemma 3.2.** *Let $k, \ell$ and $m$ be integers such $\ell \in [0,1]$ and $m \in [2, k+2]$. Then, there exists a constant $C > 0$, independent of $K$, such that for each $K \in \mathcal{T}_h$, there holds*

$$\|\psi - \psi_I\|_{\ell,K} \ \leq \ C\, h_K^{m-\ell}\, |\psi|_{m,K} \qquad \forall\ \psi \in \mathrm{H}^m(K)\,.$$

*Proof.* See [4, Proposition 4]. □

### 3.3.2 The virtual subspace of $\mathbf{H}^1(\Omega)$

In this section we consider the vectorial version of the virtual element space $\mathcal{Q}_k^K$ (cf. (3.24)). Indeed, given $K \in \mathcal{T}_h$ and an integer $k \geq 0$, we let $\boldsymbol{\mathcal{R}}_k^K : \mathbf{H}^1(K) \to \mathbf{P}_{k+1}(K)$ be the vectorial version of the projection operator $\mathcal{R}_k^K : \mathrm{H}^1(K) \to \mathrm{P}_{k+1}(K)$ (cf. (3.21)), whose approximation properties are consequence of (3.22), that is, for each $s \in [2, k+2]$ and $\ell \in [1, s]$, there holds

$$\|\mathbf{v} - \boldsymbol{\mathcal{R}}_k^K(\mathbf{v})\|_{\ell,K} \ \leq \ C\, h_K^{s-\ell}\, |\mathbf{v}|_{s,K} \qquad \forall\, \mathbf{v} \in \mathbf{H}^s(K)\,, \quad \forall\, K \in \mathcal{T}_h\,. \tag{3.26}$$

Further, letting $\mathbf{B}_k(\partial K)$ be the vectorial version of the set $\mathrm{B}_k(\partial K)$ (cf. (3.23)), we can define the space $V_k^K$ as

$$\begin{aligned} V_k^K \ := \ \Big\{ \mathbf{v} \in \mathbf{H}^1(K) : \quad & \mathbf{v}\big|_{\partial K} \in \mathbf{B}_k(\partial K), \qquad \Delta \mathbf{v}| \in \mathbf{P}_{k+1}(K) \\ & \text{and} \quad \int_K \{\boldsymbol{\mathcal{R}}_k^K(\mathbf{v}) - \mathbf{v}\} \cdot \mathbf{p} \ = \ 0 \qquad \forall\ \mathbf{p} \in \widetilde{\boldsymbol{\mathcal{B}}}_k(K) \Big\}\,, \end{aligned} \tag{3.27}$$

whose degrees of freedom, for a given $\mathbf{v} \in V_k^K$, are given by

$$\begin{aligned} &i) && \text{the value of } \mathbf{v} \text{ at the } i\text{th vertex of } K\,, \quad \forall\ i \text{ vertex of } K \\ &ii) && \text{the values of } \mathbf{v} \text{ at } k \text{ uniformly spaced points on } e\,,\ \forall\ e \in \partial K\,, \text{ for } k \geq 1\,, \\ &iii) && \text{the moments } \int_K \mathbf{v} \cdot \mathbf{p}\,,\ \forall\ \mathbf{p} \in \boldsymbol{\mathcal{B}}_{k-1}(K)\,, \text{ for } k \geq 1\,. \end{aligned} \tag{3.28}$$

Then, denoting by $\mathbf{v}_I$ the $V_k^K$-interpolant of $\mathbf{v} \in \mathbf{H}^1(K)$, we have the following vector version of Lemma 3.2.

**Lemma 3.3.** *Let $k, \ell$ and $m$ be integers such $\ell \in [0,1]$ and $m \in [2, k+2]$. Then, there exists a constant $C > 0$, independent of $K$, such that for each $K \in \mathcal{T}_h$, there holds*

$$\|\mathbf{v} - \mathbf{v}_I\|_{\ell,K} \ \leq \ C\, h_K^{m-\ell}\, |\mathbf{v}|_{m,K} \qquad \forall\ \mathbf{v} \in \mathbf{H}^m(K)\,.$$

### 3.3.3 The virtual subspaces of $\mathbb{H}_0(\mathbf{div}; \Omega)$

For each $K \in \mathcal{T}_h$ and $k \geq 0$, we introduce the local virtual space $H_k^K$ as follows (see, e.g. [15])

$$\begin{aligned} H_k^K \ := \ \Big\{ \boldsymbol{\tau} \in \mathbb{H}(\mathbf{div}; K) \cap \mathbb{H}(\mathbf{rot}; K) : \quad & \boldsymbol{\tau}\mathbf{n}|_e \in \mathbf{P}_k(e) \quad \forall \text{ edge } e \in \partial K, \\ & \mathbf{div}\,(\boldsymbol{\tau}) \in \mathbf{P}_k(K)\,, \quad \text{and} \quad \mathbf{rot}\,(\boldsymbol{\tau}) \in \mathbf{P}_{k-1}(K) \Big\}\,, \end{aligned} \tag{3.29}$$

whose local degrees of freedom, for a given $\boldsymbol{\tau} \in H_k^K$, are given by

$$\begin{aligned} &\int_e \boldsymbol{\tau}\mathbf{n} \cdot \mathbf{q} \qquad \forall\, \mathbf{q} \in \boldsymbol{\mathcal{B}}_k(e)\,, \quad \forall \text{ edge } e \in \partial K\,, \\ &\int_K \boldsymbol{\tau} : \nabla \mathbf{q} \qquad \forall\, \mathbf{q} \in \boldsymbol{\mathcal{B}}_k(K) \setminus \{(1,0)^{\mathbf{t}}, (0,1)^{\mathbf{t}}\}\,, \\ &\int_K \boldsymbol{\tau} : \boldsymbol{\rho} \qquad \forall\, \boldsymbol{\rho} \in \boldsymbol{\mathcal{G}}_k(K)\,. \end{aligned} \tag{3.30}$$

Now, for each $K \in \mathcal{T}_h$ and $\boldsymbol{\tau} \in \mathbb{H}^1(K)$, we denote its $H_k^K$-interpolant by $\boldsymbol{\tau}_I$, which has the following approximation properties: for each integer $r \in [1, k+1]$ there exists $C > 0$, independent of $K$, such that

$$\|\boldsymbol{\tau} - \boldsymbol{\tau}_I\|_{0,K} \;\leq\; C\, h_K^r\, |\boldsymbol{\tau}|_{r,K} \qquad \forall\, \boldsymbol{\tau} \in \mathbb{H}^r(K)\,. \tag{3.31}$$

In addition, for each integer $r \in [0, k+1]$ there exists $C > 0$, independent of $K$, such that

$$\|\mathbf{div}\,(\boldsymbol{\tau}) - \mathbf{div}\,(\boldsymbol{\tau}_I)\|_{0,K} \;\leq\; C\, h_K^r\, |\mathbf{div}\,(\boldsymbol{\tau})|_{r,K} \qquad \forall\, \boldsymbol{\tau} \in \mathbb{H}^1(K) \text{ with } \mathbf{div}(\boldsymbol{\tau}) \in \mathbf{H}^r(K)\,. \tag{3.32}$$

Then, the foregoing estimate together with (3.31) yields the following result.

**Lemma 3.4.** *For each integer $r \in [1, k+1]$ there exists $C > 0$, independent of $K$, such that*

$$\|\boldsymbol{\tau} - \boldsymbol{\tau}_I\|_{\mathbf{div};K} \;\leq\; C\, h_K^r \left\{ |\boldsymbol{\tau}|_{r,K} \,+\, |\mathbf{div}\,(\boldsymbol{\tau})|_{r,K} \right\} \qquad \forall\, \boldsymbol{\tau} \in \mathbb{H}^r(K) \text{ with } \mathbf{div}(\boldsymbol{\tau}) \in \mathbf{H}^r(K)\,.$$

*Proof.* It follows straightforwardly from (3.31) and (3.32). □

### 3.3.4 The global virtual subspaces

We now set the global virtual element subspaces of $\mathbb{H}_0(\mathbf{div};\Omega)$, $\mathrm{H}^1(\Omega)$ and $\mathbf{H}^1(\Omega)$, respectively, that is

$$H_k^h \;:=\; \left\{ \boldsymbol{\tau} \in \mathbb{H}_0(\mathbf{div};\Omega) : \quad \boldsymbol{\tau}\big|_K \in H_k^K \quad \forall\, K \in \mathcal{T}_h \right\}, \tag{3.33}$$

$$\mathcal{Q}_k^h \;:=\; \left\{ \psi \in \mathrm{H}_0^1(\Omega) : \quad \psi\big|_K \in \mathcal{Q}_k^K \quad \forall\, K \in \mathcal{T}_h \right\}, \tag{3.34}$$

and

$$V_k^h \;:=\; \left\{ \mathbf{v} \in \mathbf{H}^1(\Omega) : \quad \mathbf{v}\big|_K \in V_k^K \quad \forall\, K \in \mathcal{T}_h \right\}, \tag{3.35}$$

Then, from Lemmas 3.2, 3.3, and 3.4, the approximation properties of (3.33), (3.34) and (3.35) are given, respectively by

($\mathbf{AP}_h^{\boldsymbol{\sigma}}$) there exists $C > 0$, independent of $h$, such that for each integer $r \in [1, k+1]$ there holds

$$\mathrm{dist}(\boldsymbol{\sigma}, H_k^h) := \inf_{\boldsymbol{\zeta}_h \in H_k^h} \|\boldsymbol{\sigma} - \boldsymbol{\zeta}_h\|_{\mathrm{div};\Omega} \leq\; C\, h^r \left\{ \sum_{K \in \mathcal{T}_h} \left( |\boldsymbol{\sigma}|_{r,K}^2 \,+\, |\mathbf{div}\,(\boldsymbol{\sigma})|_{r,K}^2 \right) \right\}^{1/2}$$

for all $\boldsymbol{\sigma} \in \mathbb{H}_0(\mathbf{div};\Omega)$ such that $\boldsymbol{\sigma}|_K \in \mathbb{H}^r(K)$ and $\mathbf{div}\,(\boldsymbol{\sigma})|_K \in \mathbf{H}^r(K)$, for all $K \in \mathcal{T}_h$.

($\mathbf{AP}_h^{\varphi}$) there exists $C > 0$, independent of $h$, such that for each integer $m \in [2, k+2]$ there holds

$$\operatorname{dist}(\varphi, \mathcal{Q}_k^h) := \inf_{\phi_h \in \mathcal{Q}_k^h} \|\varphi - \phi_h\|_{1,\Omega} \leq Ch^{m-1} \left\{ \sum_{K \in \mathcal{T}_h} |\varphi|_{m,K}^2 \right\}^{1/2}$$

for all $\varphi \in \mathrm{H}_0^1(\Omega)$ such that $\varphi\big|_K \in \mathrm{H}^m(K) \quad \forall\, K \in \mathcal{T}_h$.

($\mathbf{AP}_h^{\mathbf{u}}$) there exists $C > 0$, independent of $h$, such that for each integer $s \in [2, k+2]$ there holds

$$\operatorname{dist}(\mathbf{u}, V_k^h) := \inf_{\mathbf{w}_h \in V_k^h} \|\mathbf{u} - \mathbf{w}_h\|_{1,\Omega} \leq Ch^{s-1} \left\{ \sum_{K \in \mathcal{T}_h} |\mathbf{u}|_{s,K}^2 \right\}^{1/2}$$

for all $\mathbf{u} \in \mathbf{H}^1(\Omega)$ such that $\mathbf{u}\big|_K \in \mathbf{H}^s(K) \quad \forall\, K \in \mathcal{T}_h$.

### 3.3.5 $\mathrm{L}^2$-orthogonal projections

For each $k \geq 0$, we let $\mathcal{P}_k^K : \mathrm{L}^2(K) \to \mathrm{P}_k(K)$ be the $\mathrm{L}^2(K)$-orthogonal projector, which, given $\psi \in \mathrm{L}^2(K)$, is characterized by

$$\mathcal{P}_k^K(\psi) \in \mathrm{P}_k(K) \quad \text{and} \quad \int_K \mathcal{P}_k^K(\psi)\, q = \int_K \psi\, q \quad \forall\, q \in \mathrm{P}_k(K)\,.$$

In addition, it is well-known that, given integers $k$, $s$, and $\ell$ such that $k \geq 0$, $s \in [1, k+1]$, and $\ell \in [0, s]$, there holds the following approximation property

$$\|\psi - \mathcal{P}_k^K(\psi)\|_{\ell,K} \leq C\, h_K^{s-\ell} |\psi|_{s,K} \qquad \forall\, \psi \in \mathrm{H}^s(K)\,, \quad \forall\, K \in \mathcal{T}_h\,. \tag{3.36}$$

Further, letting $\boldsymbol{\mathcal{P}}_k^K : \mathbf{L}^2(K) \to \mathbf{P}_k(K)$ and $\boldsymbol{\mathcal{P}}_k^K : \mathbb{L}^2(K) \to \mathbb{P}_k(K)$ be the vectorial and tensorial versions of the orthogonal projector $\mathcal{P}_k^K$, respectively, as consequence of (3.36) we have that, given integers $k$, $s$, and $\ell$ such that $k \geq 0$, $s \in [1, k+1]$, and $\ell \in [0, s]$, there hold

$$\|\mathbf{v} - \boldsymbol{\mathcal{P}}_k^K(\mathbf{v})\|_{\ell,K} \leq C\, h_K^{s-\ell} |\mathbf{v}|_{s,K} \qquad \forall\, \mathbf{v} \in \mathbf{H}^s(K)\,, \quad \forall\, K \in \mathcal{T}_h\,, \tag{3.37}$$

and

$$\|\boldsymbol{\tau} - \boldsymbol{\mathcal{P}}_k^K(\boldsymbol{\tau})\|_{\ell,K} \leq C\, h_K^{s-\ell} |\boldsymbol{\tau}|_{s,K} \qquad \forall\, \boldsymbol{\tau} \in \mathbb{H}^s(K)\,, \quad \forall\, K \in \mathcal{T}_h\,. \tag{3.38}$$

The following lemma establishes the approximation properties of the projector $\boldsymbol{\mathcal{P}}_k^K : \mathbf{L}^2(K) \to \mathbf{P}_k(K)$ with respect to more general Sobolev norms

**Lemma 3.5.** *Let $K \in \mathcal{T}_h$ and $k$, $s$, $m$, and $p$ be integers such that $k \geq 0$, $s \in [0, k+1]$, $\ell \in [s, k+1]$, and $p \in [2, +\infty)$. Then, there exists a constant $C > 0$, independent of $K$, such that*

$$|\mathbf{v} - \boldsymbol{\mathcal{P}}_k^K(\mathbf{v})|_{\ell,p,K} \leq C\, h_K^{s-\ell} |\mathbf{v}|_{s,p,K} \qquad \forall\ \mathbf{v} \in \mathbf{W}^{s,p}(K)\,. \tag{3.39}$$

*Proof.* See [69, Lemma 3.7]. □

As a consequence of the previous lemma, we have the following result.

**Lemma 3.6.** *Let $K \in \mathcal{T}_h$ and $k$, $s$, and $p$ be integers such that $k \geq 0$, $s \in [0, k+1]$, and $p \in [2, +\infty)$. Then, there exists a constant $C_{\mathtt{k}} \geq 1$, independent of $K$, such that*

$$|\boldsymbol{\mathcal{P}}_k^K(\mathbf{v})|_{s,p,K} \leq C_{\mathtt{k}} |\mathbf{v}|_{s,p,K} \qquad \forall\, \mathbf{v} \in \mathbf{W}^{s,p}(K)\,. \tag{3.40}$$

*Proof.* See [69, Lemma 3.8]. □

In addition, we now recall, as it was remarked in [4] (respectively [15]) that the degrees of freedom introduced in (3.25) (respectively (3.30)) do allow the explicit calculation of $\mathcal{P}_{k+1}^K(\psi)$ (respectively $\boldsymbol{\mathcal{P}}_k^K(\boldsymbol{\tau})$) for each $\psi \in \mathcal{Q}_k^K$ (respectively for each $\boldsymbol{\tau} \in H_k^K$). Further, as consequence of the above it is clear that the degrees of freedom (3.28) ensures the computability of the $\boldsymbol{\mathcal{P}}_{k+1}^K(\mathbf{v})$ for each $\mathbf{v} \in V_k^K$. Furthermore, also it is possible to compute $\boldsymbol{\mathcal{P}}_k^K(\nabla\psi)$ and $\boldsymbol{\mathcal{P}}_k^K(\nabla\mathbf{v})$ for each $\psi \in \mathcal{Q}_k^K$ and $\mathbf{v} \in V_k^K$, respectively. More details can be found in [4, 15, 68, 69]).

## 3.4 The discrete forms

We proceed as in [69, Section 4]. Indeed, we introduce a global virtual element subspace of $\mathbf{H} := \mathbb{H}_0(\mathbf{div};\Omega) \times \mathbf{H}^1(\Omega)$. More precisely, given $k \geq 0$, we set $\mathbf{H}_k^h := H_k^h \times V_k^h$, where $H_k^h$ and $V_k^h$ have been defined in (3.33) and (3.35), respectively. Further, defining $\mathbf{H}_k^K := H_k^K \times V_k^K$, it is clear that

$$\mathbf{H}_k^h := \left\{ \vec{\boldsymbol{\tau}} := (\boldsymbol{\tau}, \mathbf{v}) \in \mathbf{H} : \quad \vec{\boldsymbol{\tau}}\big|_K \in \mathbf{H}_k^K \quad \forall\, K \in \mathcal{T}_h \right\}.$$

Now, we observe that for each $K \in \mathcal{T}_h$ the local version $\mathbf{A}^K : \mathbf{H}_k^K \times \mathbf{H}_k^K \to \mathrm{R}$ of the bilinear form $\mathbf{A}$ (cf. (3.7)), which is defined for all $\vec{\boldsymbol{\zeta}} := (\boldsymbol{\zeta}, \mathbf{w})$, $\vec{\boldsymbol{\tau}} := (\boldsymbol{\tau}, \mathbf{v}) \in \mathbf{H}_k^K$ by

$$\begin{aligned}\mathbf{A}^K(\vec{\boldsymbol{\zeta}}, \vec{\boldsymbol{\tau}}) := \int_K \boldsymbol{\zeta}^{\mathrm{d}} : \boldsymbol{\tau}^{\mathrm{d}} + \kappa_2 \int_K \mathbf{div}\,(\boldsymbol{\zeta}) \cdot \mathbf{div}\,(\boldsymbol{\tau}) + \kappa_1 \mu \int_K \nabla\mathbf{w} : \nabla\mathbf{v} - \mu \int_K \mathbf{v} \cdot \mathbf{div}\,(\boldsymbol{\zeta}) \\ + \mu \int_K \mathbf{w} \cdot \mathbf{div}\,(\boldsymbol{\tau}) - \kappa_1 \int_K \boldsymbol{\zeta}^{\mathrm{d}} : \nabla\mathbf{v} + \kappa_3 \int_{\partial K \cap \Gamma} \mathbf{w} \cdot \mathbf{v}\end{aligned}$$

is not computable since the tensors $\boldsymbol{\zeta}^{\mathrm{d}}$, $\boldsymbol{\tau}^{\mathrm{d}}$, $\nabla\mathbf{w}$ and $\nabla\mathbf{v}$ are not known on each $K \in \mathcal{T}_h$. This is the reason why in what follows we define a discrete computable versions of $\mathbf{A}^K$ in terms of some suitable projection operators. Then, proceeding as in [69], by using the analysis from Section 3.3.5, we can introduce a local discrete bilinear form $\mathbf{A}_h^K : \mathbf{H}_k^K \times \mathbf{H}_k^K \to \mathrm{R}$, as

$$\begin{aligned}\mathbf{A}_h^K(\vec{\boldsymbol{\zeta}}, \vec{\boldsymbol{\tau}}) := \mathbf{A}_h^{K,\mathrm{d}}(\boldsymbol{\zeta}, \boldsymbol{\tau}) + \kappa_2 \int_K \mathbf{div}\,(\boldsymbol{\zeta}) \cdot \mathbf{div}\,(\boldsymbol{\tau}) + \mathbf{A}_h^{K,\nabla}(\mathbf{w}, \mathbf{v}) - \mu \int_K \mathbf{v} \cdot \mathbf{div}\,(\boldsymbol{\zeta}) \\ + \mu \int_K \mathbf{w} \cdot \mathbf{div}\,(\boldsymbol{\tau}) - \kappa_1 \int_K (\boldsymbol{\mathcal{P}}_k^K(\boldsymbol{\zeta}))^{\mathrm{d}} : \boldsymbol{\mathcal{P}}_k^K(\nabla\mathbf{v}) + \kappa_3 \int_{\partial K \cap \Gamma} \mathbf{w} \cdot \mathbf{v}\end{aligned}$$

for all $\vec{\boldsymbol{\zeta}} := (\boldsymbol{\zeta}, \mathbf{w})$, $\vec{\boldsymbol{\tau}} := (\boldsymbol{\tau}, \mathbf{v}) \in \mathbf{H}_k^K$, where $A_h^{K,\mathrm{d}} : H_k^K \times H_k^K \to \mathrm{R}$ and $A_h^{K,\nabla} : V_k^K \times V_k^K \to \mathrm{R}$ are the bilinear forms given by

$$A_h^{K,\mathrm{d}}(\boldsymbol{\zeta}, \boldsymbol{\tau}) := \int_K (\boldsymbol{\mathcal{P}}_k^K(\boldsymbol{\zeta}))^{\mathrm{d}} : (\boldsymbol{\mathcal{P}}_k^K(\boldsymbol{\tau}))^{\mathrm{d}} + \mathcal{S}^{K,\mathrm{d}}(\boldsymbol{\zeta} - \boldsymbol{\mathcal{P}}_k^K(\boldsymbol{\zeta}), \boldsymbol{\tau} - \boldsymbol{\mathcal{P}}_k^K(\boldsymbol{\tau})) \qquad \forall\, \boldsymbol{\zeta}, \boldsymbol{\tau} \in H_k^K\,, \tag{3.41}$$

and

$$A_h^{K,\nabla}(\mathbf{w},\mathbf{v}) := \kappa_1\mu\int_K \nabla\boldsymbol{\mathcal{R}}_k^K(\mathbf{w}):\nabla\boldsymbol{\mathcal{R}}_k^K(\mathbf{v})+\mathcal{S}^{K,\nabla}(\mathbf{w}-\boldsymbol{\mathcal{R}}_k^K(\mathbf{w}),\mathbf{v}-\boldsymbol{\mathcal{R}}_k^K(\mathbf{v}))\quad\forall\,\mathbf{w},\mathbf{v}\in V_k^K\,,\tag{3.42}$$

respectively, with $\mathcal{S}^{K,\mathrm{d}}:H_k^K\times H_k^K\to\mathrm{R}$ and $\mathcal{S}^{K,\nabla}:V_k^K\times V_k^K\to\mathrm{R}$ being symmetric and positive bilinear forms verifying (see [13, Section 4.6] or [15, Section 3.3])

$$\widehat{c}_0\|\boldsymbol{\zeta}\|_{0,K}^2\ \le\ \mathcal{S}^{K,\mathrm{d}}(\boldsymbol{\zeta},\boldsymbol{\zeta})\ \le\ \widehat{c}_1\|\boldsymbol{\zeta}\|_{0,K}^2\qquad\forall\,\boldsymbol{\zeta}\in H_k^K,$$

and

$$\widetilde{c}_0\,|\mathbf{w}|_{1,K}^2\ \le\ \mathcal{S}^{K,\nabla}(\mathbf{w},\mathbf{w})\ \le\ \widetilde{c}_1\,|\mathbf{w}|_{1,K}^2\qquad\forall\,\mathbf{w}\in V_k^K\,,$$

where $\widehat{c}_0,\widehat{c}_1,\widetilde{c}_0,\widetilde{c}_1>0$ are constants depending only on $C_{\mathcal{T}}$. In particular, we can take $\mathcal{S}^{K,\mathrm{d}}$ (respectively $\mathcal{S}^{K,\nabla}$) as the bilinear form whose associated matrix with respect to the canonical basis of $H_k^K$ (respectively $V_k^K$) determined by the degrees of freedom (3.30) (respectively (3.28)), is the identity matrix.

In addition, the bilinear form $\mathcal{S}^{K,\nabla}$, which stabilizes the term $\kappa_1\mu\displaystyle\int_K\nabla\boldsymbol{\mathcal{R}}_k^K(\mathbf{w}):\nabla\boldsymbol{\mathcal{R}}_k^K(\mathbf{v})$, does not need to be multiplied by $\kappa_1\mu$, since the constant that provides the ellipticity of $\mathbf{A}_h$ (cf. Lemma 3.10 below), involve the parameters $\kappa_2$ and $\kappa_3$, and the unknowns constants $c_1(\Omega)$ and $c_2(\Omega)$ (cf. Lemma 3.9). More information about this fact can be found in [69, Section 4.1] or [68, Section 3.4].

Now, the following two lemmas establish the properties of the bilinear forms $A^{K,\mathrm{d}}$ (cf. (3.41)) and $A^{K,\nabla}$ (cf. (3.42)), respectively.

**Lemma 3.7.** *For each $K\in\mathcal{T}_h$, there holds*

$$A_h^{K,\mathrm{d}}(\mathbf{p},\boldsymbol{\tau})\ =\ A^{K,\mathrm{d}}(\mathbf{p},\boldsymbol{\tau})\qquad\forall\,\mathbf{p}\in\mathbb{P}_k(K)\,,\quad\forall\,\boldsymbol{\tau}\in H_k^K\,.$$

*In addition, there exist constants $\alpha_1,\ \alpha_2>0$, independent of $h$ and $K$, such that*

$$|A_h^{K,\mathrm{d}}(\boldsymbol{\zeta},\boldsymbol{\tau})|\ \le\ \alpha_2\,\|\boldsymbol{\zeta}\|_{0,K}\|\boldsymbol{\tau}\|_{0,K}\qquad\forall\,\boldsymbol{\zeta},\,\boldsymbol{\tau}\in H_k^K\,,$$

*and*

$$\alpha_1\,\|\boldsymbol{\zeta}^{\mathrm{d}}\|_{0,K}^2\ \le\ A_h^{K,\mathrm{d}}(\boldsymbol{\zeta},\boldsymbol{\zeta})\ \le\ \alpha_2\,\|\boldsymbol{\zeta}\|_{0,K}^2\qquad\forall\,\boldsymbol{\zeta}\in H_k^K\,.$$

*Proof.* See [69, Lemma 4.2]. □

**Lemma 3.8.** *For each $K\in\mathcal{T}_h$ there holds*

$$A_h^{K,\nabla}(\mathbf{q},\mathbf{v})\ =\ A^{K,\nabla}(\mathbf{q},\mathbf{v})\quad\forall\,\mathbf{q}\in\mathbf{P}_k(K)\,,\quad\forall\,\mathbf{v}\in V_k^K\,,$$

*and there exist positive constants $\beta_1,\beta_2$, independent of $h$ and $K$, such that*

$$|A_h^{K,\nabla}(\mathbf{w},\mathbf{v})|\ \le\ \beta_2\,|\mathbf{w}|_{1,K}|\mathbf{v}|_{1,K}$$

*and*

$$\beta_1\,|\mathbf{w}|_{1,K}^2\ \le\ A_h^{K,\nabla}(\mathbf{w},\mathbf{w})\ \le\ \beta_2\,|\mathbf{w}|_{1,K}^2$$

*for all $\mathbf{w},\mathbf{v}\in V_k^K$.*

*Proof.* See [69, Lemma 4.4]. □

Hence, we define the global discrete bilinear form $\mathbf{A}_h : \mathbf{H}_k^h \times \mathbf{H}_k^h \to \mathrm{R}$ as

$$\mathbf{A}_h(\vec{\boldsymbol{\zeta}}, \vec{\boldsymbol{\tau}}) \;:=\; \sum_{K \in \mathcal{T}_h} \mathbf{A}_h^K(\vec{\boldsymbol{\zeta}}, \vec{\boldsymbol{\tau}}) \qquad \forall\, \vec{\boldsymbol{\zeta}}, \vec{\boldsymbol{\tau}} \in \mathbf{H}_k^h \,.$$

In turn, in what follows, for each $k \geq 0$ we denote by $\mathcal{P}_k^h$, $\boldsymbol{\mathcal{P}}_k^h$, and $\boldsymbol{\mathcal{P}}\!\!\!\boldsymbol{\mathcal{P}}_k^h$, the global counterparts of the projections $\mathcal{P}_k^K$, $\boldsymbol{\mathcal{P}}_k^K$, and $\boldsymbol{\mathcal{P}}\!\!\!\boldsymbol{\mathcal{P}}_k^K$, respectively, which were introduced in Section 3.3.5. In other words, for each $K \in \mathcal{T}_h$ we let

$$\mathcal{P}_k^h(\psi)|_K \;:=\; \mathcal{P}_k^K(\psi|_K), \quad \boldsymbol{\mathcal{P}}_k^h(\mathbf{v})|_K \;:=\; \boldsymbol{\mathcal{P}}_k^K(\mathbf{v}|_K)\,, \quad \text{and} \quad \boldsymbol{\mathcal{P}}\!\!\!\boldsymbol{\mathcal{P}}_k^h(\boldsymbol{\tau})|_K \;:=\; \boldsymbol{\mathcal{P}}\!\!\!\boldsymbol{\mathcal{P}}_k^K(\boldsymbol{\tau}|_K)\,,$$

for all $\psi \in \mathrm{L}^2(\Omega)$, $\mathbf{v} \in \mathbf{L}^2(\Omega)$, and $\boldsymbol{\tau} \in \mathbb{L}^2(\Omega)$. Next, we observe that using the properties of the projector $\boldsymbol{\mathcal{P}}\!\!\!\boldsymbol{\mathcal{P}}_k^h$ and the Lemmas 3.7 and 3.8, we can deduce the boundedness of the bilinear form $\mathbf{A}_h$, that is, there exists a positive constant $\widetilde{C}_{\mathbf{A}}$, depending only on $\kappa_1, \kappa_2, \kappa_3, \mu, \alpha_2, \beta_2$ and $\|\gamma_0\|$, such that

$$|\mathbf{A}_h(\vec{\boldsymbol{\zeta}}, \vec{\boldsymbol{\tau}})| \;\leq\; \widetilde{C}_{\mathbf{A}}\, \|\vec{\boldsymbol{\zeta}}\|_{\mathbf{H}}\, \|\vec{\boldsymbol{\tau}}\|_{\mathbf{H}} \qquad \forall\, \vec{\boldsymbol{\zeta}}, \vec{\boldsymbol{\tau}} \in \mathbf{H}_k^h \,. \tag{3.43}$$

Now, in order to prove the $\mathbf{H}_k^h$-ellipticity of the bilinear form $\mathbf{A}_h$, we require the following results.

**Lemma 3.9.** *There exist constants $c_1(\Omega)$, $c_2(\Omega) > 0$, independent of $h$, such that*

$$c_1(\Omega)\, \|\boldsymbol{\tau}\|_{0,\Omega}^2 \;\leq\; \|\boldsymbol{\tau}^{\mathrm{d}}\|_{0,\Omega}^2 + \|\mathbf{div}(\boldsymbol{\tau})\|_{0,\Omega}^2 \qquad \forall\, \boldsymbol{\tau} \in \mathbb{H}_0(\mathbf{div}; \Omega)$$

*and*

$$c_2(\Omega)\, \|\mathbf{v}\|_{1,\Omega}^2 \;\leq\; |\mathbf{v}|_{1,\Omega}^2 + \|\mathbf{v}\|_{0,\Gamma}^2 \qquad \forall\, \mathbf{v} \in \mathbf{H}^1(\Omega)\,.$$

*Proof.* See [29, Proposition 3.1, Chapter IV] and [54, Lemma 3.3], respectively. □

**Lemma 3.10.** *Assume that $\kappa_2, \kappa_3 > 0$ and $0 < \kappa_1 < 2\min\{\alpha_1, \beta_1\}$, where $\alpha_1$ and $\beta_1$ are the positive constants from Lemmas 3.7 and 3.8, respectively. Then, there holds*

$$\mathbf{A}_h(\vec{\boldsymbol{\tau}}, \vec{\boldsymbol{\tau}}) \;\geq\; \widetilde{\alpha}_{\mathbf{A}}\, \|\vec{\boldsymbol{\tau}}\|_{\mathbf{H}}^2 \qquad \forall\, \vec{\boldsymbol{\tau}} \in \mathbf{H}_k^h \,, \tag{3.44}$$

*with* $\widetilde{\alpha}_{\mathbf{A}} := \min\Big\{\alpha_1 - \frac{\kappa_1}{2}, \frac{\kappa_2}{2}, \beta_1 - \frac{\kappa_1}{2}, \kappa_3\Big\} \min\Big\{1, c_1(\Omega), c_2(\Omega)\Big\}$.

*Proof.* See [69, Lemma 4.11]. □

Regarding an optimal choice of the parameters $\kappa_1$, $\kappa_2$, and $\kappa_3$, we follow the approach from [46] (see also [33, 34]) and adopt the criterion of maximizing some of the constants defining $\widetilde{\alpha}_{\mathbf{A}}$. In this way, $\kappa_1$ is taken as the midpoint of its range, that is $\kappa_1 = \min\{\alpha_1, \beta_1\}$, and then both $\kappa_3$ and $\frac{\kappa_2}{2}$ are chosen equal to $\frac{1}{2}\min\{\alpha_1, \beta_1\}$. If the constants $\alpha_1$ and $\beta_1$ are not known explicitly, then we proceed as in the continuous case (see [46]) and replace $\min\{\alpha_1, \beta_1\}$ above by $\mu$, thus yielding heuristic choices for these stabilization parameters.

We now introduce a computable discrete version of the form $\mathbf{B}$ defined in (3.8). Indeed, for each $\mathbf{z} \in V_k^h$ we let $\mathbf{B}_h(\mathbf{z}; \cdot, \cdot) : \mathbf{H}_k^h \times \mathbf{H}_k^h \to \mathrm{R}$ be the bilinear form defined by

$$\mathbf{B}_h(\mathbf{z}; \vec{\boldsymbol{\zeta}}, \vec{\boldsymbol{\tau}}) \;:=\; \int_\Omega \big(\boldsymbol{\mathcal{P}}_{k+1}^h(\mathbf{w}) \otimes \boldsymbol{\mathcal{P}}_{k+1}^h(\mathbf{z})\big)^{\mathrm{d}} : \big\{\boldsymbol{\mathcal{P}}_k^h(\boldsymbol{\tau}) - \kappa_1 \boldsymbol{\mathcal{P}}\!\!\!\boldsymbol{\mathcal{P}}_k^h(\nabla \mathbf{v})\big\}$$

for all $\vec{\boldsymbol{\zeta}} := (\boldsymbol{\zeta}, \mathbf{w}), \vec{\boldsymbol{\tau}} := (\boldsymbol{\tau}, \mathbf{v}) \in \mathbf{H}_k^h$. In addition, the boundedness of the form $\mathbf{B}_h$ is established by (cf. [69, Lemma 4.13])

$$|\mathbf{B}_h(\mathbf{z}; \vec{\boldsymbol{\zeta}}, \vec{\boldsymbol{\tau}})| \ \leq \ \widetilde{C}_{\mathbf{B}} \, \|\mathbf{z}\|_{1,\Omega} \, \|\vec{\boldsymbol{\zeta}}\|_{\mathbf{H}} \, \|\vec{\boldsymbol{\tau}}\|_{\mathbf{H}} \tag{3.45}$$

for all $\mathbf{z} \in V_k^h$ and $\vec{\boldsymbol{\zeta}}, \vec{\boldsymbol{\tau}} \in \mathbf{H}_k^h$, with $\widetilde{C}_{\mathbf{B}} := \|\boldsymbol{i}_c\|^2 C_{\mathbf{k}}^2 (1+\kappa_1^2)^{1/2}$. Finally, for a given $\phi \in \mathcal{Q}_k^h$, we introduce the computable discrete version $\mathbf{F}_h(\phi;\cdot) : \mathbf{H}_k^h \to \mathrm{R}$ of the functional $\mathbf{F}(\phi;\cdot)$ (cf. (3.10)) given by

$$\mathbf{F}_h(\phi; \vec{\boldsymbol{\tau}}) := \int_\Omega \mathbf{g} \, \mathcal{P}_{k+1}^h(\phi) \cdot \Big\{ \mu \boldsymbol{\mathcal{P}}_{k+1}^h(\mathbf{v}) - \kappa_2 \, \mathbf{div}\,(\boldsymbol{\tau}) \Big\} \qquad \forall \, \vec{\boldsymbol{\tau}} := (\boldsymbol{\tau}, \mathbf{v}) \in \mathbf{H}_k^h \, . \tag{3.46}$$

We remark here that the functional $\mathbf{F}_D : \mathbf{H}_k^h \to \mathrm{R}$ (cf. (3.12)) is fully computable using the degrees of freedom (3.28) and (3.30). On the other hand, since the local version $\mathbf{a}^K : \mathcal{Q}_k^K \times \mathcal{Q}_k^H \to \mathrm{R}$ of the bilinear form $\mathbf{a}$ (cf. (3.9)), which is defined for all $\varphi, \psi \in \mathcal{Q}_k^K$ by

$$\mathbf{a}^K(\varphi, \psi) := \int_K \mathbb{K} \nabla \varphi \cdot \nabla \psi \, , \tag{3.47}$$

is not computable, in what follows we aim to define a computable version $\mathbf{a}_h : \mathcal{Q}_k^h \times \mathcal{Q}_k^h \to \mathrm{R}$ of the bilinear form $\mathbf{a}$ (cf. (3.9)). To this end, motivated by the fact that the tensor $\mathbb{K}$ (cf. Section 3.2) is not constant, we follow the approach from [23, Section 3.4]. Indeed, for each $q \in \mathrm{P}_{k+1}(K)$ and $\psi \in \mathcal{Q}_k^K$, and bearing in mind the orthogonal projector $\boldsymbol{\mathcal{P}}_k^K : \mathbf{L}^2(K) \to \mathbf{P}_k(K)$, a simple integration by parts yields

$$\int_K \boldsymbol{\mathcal{P}}_k^K(\mathbb{K}\nabla q) \cdot \nabla \psi = - \int_K \mathrm{div}(\boldsymbol{\mathcal{P}}_k^K(\mathbb{K}\nabla q)) \psi + \int_{\partial K} (\boldsymbol{\mathcal{P}}_k^K(\mathbb{K}\nabla q)) \cdot \mathbf{n} \, \psi \, . \tag{3.48}$$

Then, using the fact that $\mathrm{div}(\boldsymbol{\mathcal{P}}_k^K(\mathbb{K}\nabla q)) \in \mathrm{P}_{k-1}(K)$ and $(\boldsymbol{\mathcal{P}}_k^K(\mathbb{K}\nabla q)) \cdot \mathbf{n} \in \mathrm{P}_k(e)$ for each edge $e \in \partial K$, together with the knowledge of the degrees of freedom (3.25), we deduce that the expression (3.48) is fully computable. Therefore, we can introduce the projection operator $\Pi_k^K : \mathcal{Q}_k^K \to \mathrm{P}_{k+1}(K)$ defined for each $\psi \in \mathcal{Q}_k^K$ as the unique polynomial $\Pi_k^K(\psi) \in \mathrm{P}_{k+1}(K)$ satisfying (cf. [23, eq. 3.22])

$$\begin{aligned} \int_K \mathbb{K} \nabla \Pi_k^K(\psi) \cdot \nabla q \ &= \ \int_K \boldsymbol{\mathcal{P}}_k^K(\mathbb{K}\nabla q) \cdot \nabla \psi \qquad \forall \, q \in \mathrm{P}_{k+1}(K) \, , \\ \overline{\Pi_k^K(\psi)} \ &= \ \overline{\psi} \, . \end{aligned} \tag{3.49}$$

with $\overline{\psi} := \dfrac{1}{d_K} \displaystyle\sum_{\mathbf{x} \in \mathcal{V}(K)} \psi(\mathbf{x})$, where $d_K$ and $\mathcal{V}(K)$ denote the number of edges and the set of vertices of $K$, respectively. Notice that it is clear from (3.48) and (3.49) that $\Pi_k^K(\psi)$ is well-defined for each $\psi \in \mathcal{Q}_k^K$, and that $\Pi_k^K$ is indeed a projection operator. Also, it easy to see from the first equation of (3.49) and the properties of the tensor $\mathbb{K}$ that there exists $C_{\mathbb{K}} > 0$, depending only on $\mathbb{K}$, such that

$$|\Pi_k^K(\psi)|_{1,K} \ \leq \ C_{\mathbb{K}} |\psi|_{1,K} \qquad \forall \, \psi \in \mathrm{H}^1(K) \, . \tag{3.50}$$

In addition, the approximation properties of $\Pi_k^K$ are established in [23, Section 4], that is, given integers $k$, $m$ and $\ell$ such that $k \geq 0$, $m \in [2, k+2]$ and $\ell \in [1, m]$, there holds

$$\|\psi - \Pi_k^K(\psi)\|_{\ell,K} \ \leq \ C \, h_K^{m-\ell} \, |\psi|_{m,K} \qquad \forall \, \psi \in \mathrm{H}^m(K) \, , \quad \forall \, K \in \mathcal{T}_h \, . \tag{3.51}$$

Now, we can introduce a local discrete bilinear form $\mathbf{a}_h^K : \mathcal{Q}_k^K \times \mathcal{Q}_k^K \to \mathrm{R}$, which is defined by

$$\mathbf{a}_h^K(\varphi, \psi) := \mathbf{a}^K(\Pi_k^K(\varphi), \Pi_k^K(\psi)) + \mathcal{S}^{K,\Pi}(\varphi - \Pi_k^K(\varphi), \psi - \Pi_k^K(\psi)) \tag{3.52}$$

for all $\varphi, \psi \in \mathcal{Q}_k^K$, where $\mathcal{S}^{K,\Pi} : \mathcal{Q}_k^K \times \mathcal{Q}_k^K \to \mathrm{R}$ is a positive and symmetric bilinear form verifying

$$\overline{c}_0 \, |\psi|_{1,K}^2 \;\leq\; \mathcal{S}^{K,\Pi}(\psi,\psi) \;\leq\; \overline{c}_1 \, |\psi|_{1,K}^2 \qquad \forall\, \psi \in \mathcal{Q}_k^K \,, \tag{3.53}$$

with $\overline{c}_0$ $\overline{c}_1$ positives constant depending only on $C_{\mathcal{T}}$.

The following lemma establishes the properties of the bilinear form (3.52). (cf. [23])

**Lemma 3.11.** *There holds*

$$\mathbf{a}_h^K(p,\psi) = \int_K \boldsymbol{\mathcal{P}}_k^K(\mathbb{K}\nabla p)\cdot\nabla\psi \qquad \forall\, p \in \mathrm{P}_{k+1}(K)\,, \quad \forall\, \psi \in \mathcal{Q}_k^K\,, \quad \forall\, K \in \mathcal{T}_h\,,$$

*and there exist constants $\alpha_*, \alpha^* > 0$, such that*

$$\alpha_* \mathbf{a}^K(\psi,\psi) \leq \mathbf{a}_h^K(\psi,\psi) \leq \alpha^* \mathbf{a}^K(\psi,\psi) \qquad \forall\, \psi \in \mathcal{Q}_k^K\,, \quad \forall K \in \mathcal{T}_h\,.$$

*Proof.* See [23, Section 3.4]. □

In this way, we define the global discrete bilinear form $\mathbf{a}_h : \mathcal{Q}_k^h \times \mathcal{Q}_k^h \to \mathrm{R}$ as

$$\mathbf{a}_h(\varphi,\psi) \;:=\; \sum_{K\in\mathcal{T}_h} \mathbf{a}_h^K(\varphi,\psi) \qquad \forall\, \varphi,\psi \in \mathcal{Q}_k^h\,.$$

In turn, it is clear from (3.11) that, given $(\mathbf{z},\phi) \in V_k^h \times \mathcal{Q}_k^h$, the functional $\mathrm{F}(\mathbf{z},\phi;\cdot) : \mathcal{Q}_k^h \to \mathrm{R}$ (cf. (3.11)) is not computable. Therefore, we introduce a computable discrete version $\mathrm{F}_h(\mathbf{z},\phi;\cdot)$, which is given by

$$\mathrm{F}_h(\mathbf{z},\phi;\psi) := -\int_\Omega (\boldsymbol{\mathcal{P}}_{k+1}^h(\mathbf{z})\cdot\boldsymbol{\mathcal{P}}_k^h(\nabla\phi))\mathcal{P}_{k+1}^h(\psi) \tag{3.54}$$

for all $\psi \in \mathcal{Q}_k^h$.

## 3.5 The virtual element scheme and its stability analysis

We now use the discrete forms analyzed in the previous section to introduce our mixed virtual element scheme associated with (3.6), which reads: Find $(\vec{\boldsymbol{\sigma}}_h, \varphi_h) := ((\boldsymbol{\sigma}_h, \mathbf{u}_h), \varphi_h) \in \mathbf{H}_k^h \times \mathcal{Q}_k^h$ such that

$$\begin{aligned} \mathbf{A}_h(\vec{\boldsymbol{\sigma}}_h, \vec{\boldsymbol{\tau}}_h) + \mathbf{B}_h(\mathbf{u}_h; \vec{\boldsymbol{\sigma}}_h, \vec{\boldsymbol{\tau}}_h) &= \mathbf{F}_h(\varphi_h; \vec{\boldsymbol{\tau}}_h) + \mathbf{F}_D(\vec{\boldsymbol{\tau}}_h) \qquad \forall\, \vec{\boldsymbol{\tau}}_h := (\boldsymbol{\tau}_h, \mathbf{v}_h) \in \mathbf{H}_k^h\,, \\ \mathbf{a}_h(\varphi_h, \psi_h) &= \mathrm{F}_h(\mathbf{u}_h, \varphi_h; \psi_h) \qquad \forall\, \psi_h \in \mathcal{Q}_k^h\,. \end{aligned} \tag{3.55}$$

For the stability analysis of the Galerkin scheme (3.55), we follow the approach from [46, Section III.B] and employ a fixed-point strategy. Indeed, we define the discrete operators $\mathbf{S}_h : V_k^h \times \mathcal{Q}_k^h \to \mathbf{H}_k^h$ and $\widetilde{\mathbf{S}}_h : V_k^h \times \mathcal{Q}_k^h \to \mathcal{Q}_k^h$, respectively, as

$$\mathbf{S}_h(\mathbf{z}_h, \phi_h) \;:= (\mathbf{S}_{1,h}(\mathbf{z}_h, \phi_h), \mathbf{S}_{2,h}(\mathbf{z}_h, \phi_h)) = \vec{\boldsymbol{\sigma}}_h,$$

and

$$\widetilde{\mathbf{S}}_h(\mathbf{z}_h, \phi_h) := \varphi_h$$

for all $(\mathbf{z}_h,\phi_h)\in V_k^h\times\mathcal{Q}_k^h$, where $\vec{\boldsymbol{\sigma}}_h:=(\boldsymbol{\sigma}_h,\mathbf{u}_h)\in\mathbf{H}_k^h$ and $\varphi_h\in\mathcal{Q}_k^h$ are the unique solutions of the discrete problems:

$$\mathbf{A}_h(\vec{\boldsymbol{\sigma}}_h,\vec{\boldsymbol{\tau}}_h)\,+\,\mathbf{B}_h(\mathbf{z}_h;\vec{\boldsymbol{\sigma}}_h,\vec{\boldsymbol{\tau}}_h)\;=\;\mathbf{F}_h(\phi_h;\vec{\boldsymbol{\tau}}_h)+\mathbf{F}_D(\vec{\boldsymbol{\tau}}_h)\qquad\forall\,\vec{\boldsymbol{\tau}}_h\in\mathbf{H}_k^h\,,\tag{3.56}$$

and

$$\mathbf{a}_h(\varphi_h,\psi_h)=\mathrm{F}_h(\mathbf{z}_h,\phi_h;\psi_h)\quad\forall\,\psi_h\in\mathcal{Q}_k^h,\tag{3.57}$$

respectively. Next, we introduce the operator $\mathbf{T}_h:V_k^h\times\mathcal{Q}_k^h\to V_k^h\times\mathcal{Q}_k^h$ as

$$\mathbf{T}_h(\mathbf{z}_h,\phi_h):=(\mathbf{S}_{2,h}(\mathbf{z}_h,\phi_h),\widetilde{\mathbf{S}}_h(\mathbf{S}_{2,h}(\mathbf{z}_h,\phi_h),\phi_h))\quad\forall\,(\mathbf{z}_h,\phi_h)\in V_k^h\times\mathcal{Q}_k^h\,,\tag{3.58}$$

and realize that (3.55) can be rewritten as the fixed-point problem: Find $(\mathbf{u}_h,\varphi_h)\in V_k^h\times\mathcal{Q}_k^h$ such that

$$\mathbf{T}_h(\mathbf{u}_h,\varphi_h)=(\mathbf{u}_h,\varphi_h)\,.\tag{3.59}$$

The following two lemmas establish the well-posedness of (3.56) and (3.57), and hence the well-definedness of the operator $\mathbf{T}_h$.

**Lemma 3.12.** *Suppose that the parameters $\kappa_1,\kappa_2$ and $\kappa_3$, satisfy the conditions required by Lemma 3.10 and let $\rho\in\left(0,\dfrac{\widetilde{\alpha}_{\mathbf{A}}}{2\widetilde{C}_{\mathbf{B}}}\right)$. Then, the problem (3.56) has a unique solution $\vec{\boldsymbol{\sigma}}_h:=(\boldsymbol{\sigma}_h,\mathbf{u}_h)\in\mathbf{H}_k^h$ for each $(\mathbf{z}_h,\phi_h)\in V_k^h\times\mathcal{Q}_k^h$ such that $\|\mathbf{z}_h\|_{1,\Omega}\leq\rho$. Further, there exists a constant $c_{\mathbf{S}}>0$, independent of $\mathbf{z}_h,\phi_h$, and $h$, such that*

$$\|\mathbf{S}_h(\mathbf{z}_h,\phi_h)\|_{\mathbf{H}}=\|\vec{\boldsymbol{\sigma}}_h\|_{\mathbf{H}}\leq\;c_{\mathbf{S}}\left\{\|\mathbf{g}\|_{\infty,\Omega}\|\phi_h\|_{0,\Omega}+\|\mathbf{u}_D\|_{0,\Gamma}+\|\mathbf{u}_D\|_{1/2,\Gamma}\right\}.\tag{3.60}$$

*Proof.* We proceed as in [46, Lemma 3.3] (see also [69, Lemma 5.1]). In fact, given $\rho\in\left(0,\dfrac{\widetilde{\alpha}_{\mathbf{A}}}{2\widetilde{C}_{\mathbf{B}}}\right)$ and $(\mathbf{z}_h,\phi_h)\in V_k^h\times\mathcal{Q}_k^h$ such that $\|\mathbf{z}_h\|_{1,\Omega}\leq\rho$, we can deduce, using (3.44) and (3.45), that the ellipticity of the bilinear form $\mathbf{A}_h+\mathbf{B}_h(\mathbf{z}_h;\cdot,\cdot)$ is ensured with the constant $\frac{\widetilde{\alpha}_{\mathbf{A}}}{2}$. In addition, we have that

$$\|\mathbf{F}_h(\phi_h;\cdot)\|\leq C_{\mathbf{F}}\|\mathbf{g}\|_{\infty,\Omega}\|\phi_h\|_{0,\Omega}\quad\forall\varphi_h\in\mathcal{Q}_k^h\,,\tag{3.61}$$

with $C_{\mathbf{F}}$ the bound in (3.17). Then, there holds

$$\|\mathbf{F}_h(\phi_h;\cdot)+\mathbf{F}_D\|\leq M_{\mathbf{F}}\left\{\|\mathbf{g}\|_{\infty,\Omega}\|\phi_h\|_{0,\Omega}+\|\mathbf{u}_D\|_{0,\Gamma}+\|\mathbf{u}_D\|_{1/2,\Gamma}\right\},$$

where $M_{\mathbf{F}}$ is the constant in (3.18). Then, a direct application of the Lax-Milgram theorem implies the existence of a unique solution $\vec{\boldsymbol{\sigma}}_h:=(\boldsymbol{\sigma}_h,\mathbf{u}_h)\in\mathbf{H}_k^h$ of (3.56), which satisfies (3.60) with $c_{\mathbf{S}}:=\dfrac{2M_{\mathbf{F}}}{\widetilde{\alpha}_{\mathbf{A}}}$. □

**Lemma 3.13.** *For each $(\mathbf{z}_h,\phi_h)\in V_k^h\times\mathcal{Q}_k^h$, there exists a unique solutuion $\varphi_h\in\mathcal{Q}_k^h$ solution of (3.57), and there holds*

$$\|\widetilde{\mathbf{S}}_h(\mathbf{z}_h,\phi_h)\|_{1,\Omega}=\|\varphi_h\|_{1,\Omega}\leq\;c_{\widetilde{\mathbf{S}}}\,\|\mathbf{z}_h\|_{1,\Omega}|\phi_h|_{1,\Omega}\,,\tag{3.62}$$

*with $c_{\widetilde{\mathbf{S}}}$ independent of $\mathbf{z}_h,\phi_h$ and $h$.*

*Proof.* From Lemma 3.11 we deduce the boundedness and ellipticity of the bilinear form $\mathbf{a}_h$ with constants $\alpha^*\|\mathbf{a}\| = \alpha^*\|\mathbb{K}\|_{\infty,\Omega}$ and $\alpha_*\alpha_{\mathbf{a}}$, respectively. Further, for each $(\mathbf{z}_h,\phi_h)\in V_k^h\times\mathcal{Q}_k^h$, we find from (3.54), (3.13) and Lemma 3.6, that

$$\|\mathrm{F}_h(\mathbf{z}_h,\phi_h;\cdot)\| \leq \widetilde{M}_{\mathrm{F}}\|\mathbf{z}_h\|_{1,\Omega}|\phi_h|_{1,\Omega}\,, \tag{3.63}$$

with $\widetilde{M}_{\mathrm{F}} := \|\boldsymbol{i}_c\|\|i_c\|C_{\mathbf{k}}^2$ (cf. (3.13) and (3.40)). In this way, the Lax-Milgram theorem guarantees the existence of a unique solution $\varphi_h\in\mathcal{Q}_k^h$ of (3.57), and a positive constant $c_{\widetilde{\mathbf{S}}} := \dfrac{\widetilde{M}_{\mathrm{F}}}{\alpha_*\alpha_{\mathbf{a}}}$ such that (3.62) holds. □

Having proved the well-definedness of $\mathbf{T}_h$, we now aim to establish the existence of a unique fixed point for this operator. We begin with the following result.

**Lemma 3.14.** *Suppose that the parameters $\kappa_1,\kappa_2$ and $\kappa_3$, satisfy the conditions required by Lemma 3.10 and let $\rho\in\left(0,\dfrac{\widetilde{\alpha}_{\mathbf{A}}}{2\widetilde{C}_{\mathbf{B}}}\right)$. Also, let $W_\rho^h$ be the closed ball in $V_k^h\times\mathcal{Q}_k^h$ defined by*

$$W_\rho^h := \Big\{(\mathbf{z}_h,\phi_h)\in V_k^h\times\mathcal{Q}_k^h : \quad \|(\mathbf{z}_h,\phi_h)\|\leq\rho\Big\}\,, \tag{3.64}$$

*and assume that the data satisfy*

$$\widetilde{c}_{\mathbf{T}}\Big\{\|\mathbf{g}\|_{\infty,\Omega}+\|\mathbf{u}_D\|_{0,\Omega}+\|\mathbf{u}_D\|_{1/2,\Gamma}\Big\}\leq\rho\,, \tag{3.65}$$

*where $\widetilde{c}_{\mathbf{T}} := \max\Big\{(1+c_{\widetilde{\mathbf{S}}}\rho)\max\Big\{1,\rho\Big\}c_{\mathbf{S}},c_{\widetilde{\mathbf{S}}}\Big\}$. Then, there holds $\mathbf{T}_h(W_\rho^h)\subseteq W_\rho^h$.*

*Proof.* It follows by similar arguments to those used in the proof of [46, Lemma 3.5]. □

**Lemma 3.15.** *Suppose that the parameters $\kappa_1,\kappa_2$ and $\kappa_3$, satisfy the conditions required by Lemma 3.10. In addition, let $\rho\in\left(0,\dfrac{\widetilde{\alpha}_{\mathbf{A}}}{2\widetilde{C}_{\mathbf{B}}}\right)$ and $W_\rho^h$ as in Lemma 3.14 (cf. (3.64)). Then, there exists a positive constant $\widetilde{C}_{\mathbf{T}}$, such that*

$$\|\mathbf{T}_h(\mathbf{z}_h,\phi_h)-\mathbf{T}_h(\widetilde{\mathbf{z}}_h,\widetilde{\phi}_h)\| \leq \widetilde{C}_{\mathbf{T}}\Big\{\|\mathbf{g}\|_{\infty,\Omega}+\|\mathbf{u}_D\|_{0,\Omega}+\|\mathbf{u}_D\|_{1/2,\Gamma}\Big\}\|(\mathbf{z}_h,\phi_h)-(\widetilde{\mathbf{z}}_h,\widetilde{\phi}_h)\| \tag{3.66}$$

*for all $(\mathbf{z}_h,\phi_h),(\widetilde{\mathbf{z}}_h,\widetilde{\phi}_h)\in W_\rho^h$.*

*Proof.* We proceed as in [46, Lemma 3.8]. In fact, from the definition of $\mathbf{T}_h$ (cf. (3.58)) we first observe that

$$\begin{aligned}\|\mathbf{T}_h(\mathbf{z}_h,\phi_h)-\mathbf{T}_h(\widetilde{\mathbf{z}}_h,\widetilde{\phi}_h)\| &\leq \|\mathbf{S}_{2,h}(\mathbf{z}_h,\phi_h)-\mathbf{S}_{2,h}(\widetilde{\mathbf{z}}_h,\widetilde{\phi}_h)\|_{1,\Omega}\\ &\quad+\|\widetilde{\mathbf{S}}_h(\mathbf{S}_{2,h}(\mathbf{z}_h,\phi_h),\phi_h)-\widetilde{\mathbf{S}}_h(\mathbf{S}_{2,h}(\widetilde{\mathbf{z}}_h,\widetilde{\phi}_h),\widetilde{\phi}_h)\|_{1,\Omega}\,.\end{aligned} \tag{3.67}$$

The two expressions on the right-hand side of (3.67) are bounded in what follows. Indeed, letting $(\boldsymbol{\sigma}_h,\mathbf{u}_h) := \mathbf{S}_h(\mathbf{z}_h,\phi_h)$ and $(\widetilde{\boldsymbol{\sigma}}_h,\widetilde{\mathbf{u}}_h) := \mathbf{S}_h(\widetilde{\mathbf{z}}_h,\widetilde{\phi}_h)$ be the corresponding solutions of problem (3.56), and reasoning similarly as in [69, Lemma 5.2], we deduce that

$$\|\mathbf{S}_h(\mathbf{z}_h,\phi_h)-\mathbf{S}_h(\widetilde{\mathbf{z}}_h,\widetilde{\phi}_h)\|_{\mathbf{H}}\leq\frac{2}{\widetilde{\alpha}_{\mathbf{A}}}\Big\{\widetilde{C}_{\mathbf{B}}\|\mathbf{S}_{2,h}(\mathbf{z}_h,\phi_h)\|_{1,\Omega}\|\mathbf{z}_h-\widetilde{\mathbf{z}}_h\|_{1,\Omega}+C_{\mathbf{F}}\|\mathbf{g}\|_{\infty,\Omega}\|\phi_h-\widetilde{\phi}_h\|_{0,\Omega}\Big\}.$$

Then, from the foregoing inequality and Lemma 3.12, we get

$$\begin{aligned}
&\|\mathbf{S}_{2,h}(\mathbf{z}_h,\phi_h)-\mathbf{S}_{2,h}(\widetilde{\mathbf{z}}_h,\widetilde{\phi}_h)\|_{1,\Omega}\\
&\leq \frac{2}{\widetilde{\alpha}_{\mathbf{A}}}\Big\{c_{\mathbf{S}}\widetilde{C}_{\mathbf{B}}\left(\rho\|\mathbf{g}\|_{\infty,\Omega}+\|\mathbf{u}_D\|_{0,\Gamma}+\|\mathbf{u}_D\|_{1/2,\Gamma}\right)\|\mathbf{z}_h-\widetilde{\mathbf{z}}_h\|_{1,\Omega}+C_{\mathbf{F}}\|\mathbf{g}\|_{\infty,\Omega}\|\phi_h-\widetilde{\phi}_h\|_{0,\Omega}\Big\} \qquad (3.68)\\
&\leq C_{\mathbf{S}}\Big\{\|\mathbf{g}\|_{\infty,\Omega}+\|\mathbf{u}_D\|_{0,\Gamma}+\|\mathbf{u}_D\|_{1/2,\Gamma}\Big\}\|(\mathbf{z}_h,\phi_h)-(\widetilde{\mathbf{z}}_h,\widetilde{\phi}_h)\|\,,
\end{aligned}$$

with $C_{\mathbf{S}}:=\dfrac{2(1+\rho)}{\widetilde{\alpha}_{\mathbf{A}}}\max\Big\{c_{\mathbf{S}}\widetilde{C}_{\mathbf{B}},C_{\mathbf{F}}\Big\}$.

On the other hand, since $\mathbf{S}_{2,h}(\mathbf{z}_h,\phi_h),\mathbf{S}_{2,h}(\widetilde{\mathbf{z}}_h,\widetilde{\phi}_h)\in V_k^h$ we let $\varphi_h:=\widetilde{\mathbf{S}}_h(\mathbf{S}_{2,h}(\mathbf{z}_h,\phi_h),\phi_h)$ and $\widetilde{\varphi}_h:=\widetilde{\mathbf{S}}_h(\mathbf{S}_{2,h}(\widetilde{\mathbf{z}}_h,\widetilde{\phi}_h),\widetilde{\phi}_h)$ be the corresponding solutions of problem (3.57). Then, using the ellipticity of the bilinear form $\mathbf{a}$, Lemma 3.11, and adding and subtracting suitable terms, we get

$$\begin{aligned}
&\|\widetilde{\mathbf{S}}_h(\mathbf{S}_{2,h}(\mathbf{z}_h,\phi_h),\phi_h)-\widetilde{\mathbf{S}}_h(\mathbf{S}_{2,h}(\widetilde{\mathbf{z}}_h,\widetilde{\phi}_h),\widetilde{\phi}_h)\|_{1,\Omega}^2=\|\varphi_h-\widetilde{\varphi}_h\|_{1,\Omega}^2\leq(\alpha_*\alpha_{\mathbf{a}})^{-1}\mathbf{a}_h(\varphi_h-\widetilde{\varphi}_h,\varphi_h-\widetilde{\varphi}_h)\\
&\leq(\alpha_*\alpha_{\mathbf{a}})^{-1}|\mathrm{F}_h(\mathbf{S}_{2,h}(\mathbf{z}_h,\phi_h),\phi_h-\widetilde{\phi}_h;\varphi_h-\widetilde{\varphi}_h)+\mathrm{F}_h(\mathbf{S}_{2,h}(\mathbf{z}_h,\phi_h)-\mathbf{S}_{2,h}(\widetilde{\mathbf{z}}_h,\widetilde{\phi}_h),\widetilde{\phi}_h;\varphi_h-\widetilde{\varphi}_h)|\,.
\end{aligned}$$

Then, from the foregoing inequality, the boundedness of $\mathrm{F}_h$ (cf. (3.63)), the estimates (3.60) and (3.68), and the fact that $\phi_h,\widetilde{\phi}_h\in W_\rho^h$, we obtain

$$\begin{aligned}
&\|\widetilde{\mathbf{S}}_h(\mathbf{S}_{2,h}(\mathbf{z}_h,\phi_h),\phi_h)-\widetilde{\mathbf{S}}_h(\mathbf{S}_{2,h}(\widetilde{\mathbf{z}}_h,\widetilde{\phi}_h),\widetilde{\phi}_h)\|_{1,\Omega}\\
&\qquad\leq(\alpha_*\alpha_{\mathbf{a}})^{-1}\widetilde{C}_{\mathrm{F}}\Big\{\|\mathbf{S}_{2,h}(\mathbf{z}_h,\phi_h)\|_{1,\Omega}|\phi_h-\widetilde{\phi}_h|_{1,\Omega}+\rho\|\mathbf{S}_{2,h}(\mathbf{z}_h,\phi_h)-\mathbf{S}_{2,h}(\widetilde{\mathbf{z}}_h,\widetilde{\phi}_h)\|_{1,\Omega}\Big\} \qquad (3.69)\\
&\qquad\leq C_{\widetilde{\mathbf{S}}}\Big\{\|\mathbf{g}\|_{\infty,\Omega}+\|\mathbf{u}_D\|_{0,\Omega}+\|\mathbf{u}_D\|_{1/2,\Gamma}\Big\}\|(\mathbf{z}_h,\phi_h)-(\widetilde{\mathbf{z}}_h,\widetilde{\phi}_h)\|\,,
\end{aligned}$$

where $C_{\widetilde{\mathbf{S}}}:=(\alpha_*\alpha_{\mathbf{a}})^{-1}\widetilde{C}_{\mathrm{F}}(1+\rho)\max\Big\{c_{\mathbf{S}},\rho C_{\mathbf{S}}\Big\}$. Therefore, from (3.67)-(3.69) we conclude (3.66) with $\widetilde{C}_{\mathbf{T}}:=\max\{C_{\mathbf{S}},C_{\widetilde{\mathbf{S}}}\}$. □

We are ready to prove that our discrete scheme (3.55) ( equivalently, the fixed-point operator equation (3.59)) is well-posed. More precisely, we have the following result.

**Theorem 3.16.** *Suppose that the parameters $\kappa_1,\kappa_2$ and $\kappa_3$, satisfy the conditions required by Lemma 3.10, and let $\rho\in\left(0,\dfrac{\widetilde{\alpha}_{\mathbf{A}}}{2\widetilde{C}_{\mathbf{B}}}\right)$. Also, let $W_\rho^h$ as in Lemma 3.14 (cf. (3.64)), and assume that the data satisfy the assumptions (3.65) and*

$$\widetilde{C}_{\mathbf{T}}\Big\{\|\mathbf{g}\|_{\infty,\Omega}+\|\mathbf{u}_D\|_{0,\Omega}+\|\mathbf{u}_D\|_{1/2,\Gamma}\Big\}<1\,,$$

*with $\widetilde{C}_{\mathbf{T}}$ given by Lemma 3.15. Then, the mixed virtual element scheme (3.55) has a unique solution $((\boldsymbol{\sigma}_h,\mathbf{u}_h),\varphi_h)\in\mathbf{H}_k^h\times\mathcal{Q}_k^h$, with $(\mathbf{u}_h,\varphi_h)\in W_\rho^h$, and there hold*

$$\|(\boldsymbol{\sigma}_h,\mathbf{u}_h)\|_{\mathbf{H}}\leq\ \frac{2M_{\mathbf{F}}}{\widetilde{\alpha}_{\mathbf{A}}}\Big\{\rho\|\mathbf{g}\|_{\infty,\Omega}+\|\mathbf{u}_D\|_{0,\Gamma}+\|\mathbf{u}_D\|_{1/2,\Gamma}\Big\}\,, \qquad (3.70)$$

*and*

$$\|\varphi_h\|_{1,\Omega}\ \leq\ \frac{\widetilde{M}_{\mathrm{F}}}{\alpha_*\alpha_{\mathbf{a}}}\,\rho\|\mathbf{u}_h\|_{1,\Omega}\,. \qquad (3.71)$$

*Proof.* It follows from Lemmas 3.14 and 3.15, the Banach fixed-point theorem, and the estimates (3.60) and (3.62). □

### 3.5.1 A priori error estimates

We now aim to derive the *a priori* estimates for the error

$$\|(\vec{\boldsymbol{\sigma}},\varphi) - (\vec{\boldsymbol{\sigma}}_h,\varphi_h)\| := \|\vec{\boldsymbol{\sigma}} - \vec{\boldsymbol{\sigma}}_h\|_{\mathbf{H}} + \|\varphi - \varphi_h\|_{1,\Omega}\,, \tag{3.72}$$

where $(\vec{\boldsymbol{\sigma}},\varphi) := ((\boldsymbol{\sigma},\mathbf{u}),\varphi) \in \mathbf{H}\times\mathrm{H}$ and $(\vec{\boldsymbol{\sigma}}_h,\varphi_h) := ((\boldsymbol{\sigma}_h,\mathbf{u}_h),\varphi_h) \in \mathbf{H}_k^h\times\mathcal{Q}_k^h$ are the unique solutions of the continuous and discrete schemes (3.6) and (3.55), respectively. In this regard, and as suggested by Theorems 3.1 and 3.16, we first define

$$\rho_0 := \min\left\{\frac{\alpha_{\mathbf{A}}}{2C_{\mathbf{B}}}, \frac{\widetilde{\alpha}_{\mathbf{A}}}{2\widetilde{C}_{\mathbf{B}}}\right\}, \tag{3.73}$$

and observe that, under the assumptions that $\kappa_2,\kappa_3>0$, and $0<\kappa_1<2\min\{\mu,\alpha_1,\beta_1\}$, the existence of $(\vec{\boldsymbol{\sigma}},\varphi)$ and $(\vec{\boldsymbol{\sigma}}_h,\varphi_h)$ is guaranteed within the respective balls centered at the origin and with radius $\rho\in(0,\rho_0)$.

Next, recalling that the local projectors $\boldsymbol{\mathcal{R}}_k^K : V_k^K \to \mathbf{P}_{k+1}(K)$ and $\Pi_k^K : \mathcal{Q}_k^K \to \mathrm{P}_{k+1}(K)$ are introduced in Sections 3.3.2 and 3.4, respectively, we now denote by $\boldsymbol{\mathcal{R}}_k^h$ and $\Pi_k^h$ its global counterparts, respectively, that is, given $\mathbf{v}\in V_k^h$ and $\psi\in\mathcal{Q}_k^h$, we let

$$\boldsymbol{\mathcal{R}}_k^h(\mathbf{v})|_K := \boldsymbol{\mathcal{R}}_k^K(\mathbf{v}|_K) \quarad \text{and} \quad \Pi_k^h(\psi)|_K := \Pi_k^K(\psi|_K) \quad \forall\, K\in\mathcal{T}_h\,.$$

We begin our analysis with some preliminary lemmas.

**Lemma 3.17.** *There exist positive constants $L_{\mathbf{A}}$, $C_{\mathtt{p}}$, and $C_{\mathtt{q}}$, independent of $h$, such that*

$$\sup_{\substack{\vec{\boldsymbol{\tau}}_h\in\mathbf{H}_k^h\\ \vec{\boldsymbol{\tau}}_h\neq\mathbf{0}}} \frac{|(\mathbf{A}-\mathbf{A}_h)(\vec{\boldsymbol{\zeta}}_h,\vec{\boldsymbol{\tau}}_h)|}{\|\vec{\boldsymbol{\tau}}_h\|_{\mathbf{H}}} \leq L_{\mathbf{A}}\Big\{\|\vec{\boldsymbol{\sigma}}-\vec{\boldsymbol{\zeta}}_h\|_{\mathbf{H}} + \|\boldsymbol{\sigma}-\boldsymbol{\mathcal{P}}_k^h(\boldsymbol{\sigma})\|_{0,\Omega} + |\mathbf{u}-\boldsymbol{\mathcal{R}}_k^h(\mathbf{u})|_{1,h}\Big\}, \tag{3.74}$$

*and*

$$\begin{aligned}\sup_{\substack{\vec{\boldsymbol{\tau}}_h\in\mathbf{H}_k^h\\ \vec{\boldsymbol{\tau}}_h\neq\mathbf{0}}} &\frac{|(\mathbf{B}-\mathbf{B}_h)(\mathbf{u};\vec{\boldsymbol{\zeta}}_h,\vec{\boldsymbol{\tau}}_h)|}{\|\vec{\boldsymbol{\tau}}_h\|_{\mathbf{H}}}\\ &\leq C_{\mathtt{p}}\left\{\|\vec{\boldsymbol{\sigma}}-\vec{\boldsymbol{\zeta}}_h\|_{\mathbf{H}} + \|\boldsymbol{\sigma}-\boldsymbol{\mathcal{P}}_k^h(\boldsymbol{\sigma})\|_{0,\Omega} + |\mathbf{u}-\boldsymbol{\mathcal{R}}_k^h(\mathbf{u})|_{1,h} + \|\mathbf{u}-\boldsymbol{\mathcal{P}}_{k+1}^h(\mathbf{u})\|_{0,4,\Omega}\right\}\end{aligned} \tag{3.75}$$

*for all $\vec{\boldsymbol{\zeta}}_h := (\boldsymbol{\zeta}_h,\mathbf{w}_h)\in\mathbf{H}_k^h$, and*

$$\sup_{\substack{\vec{\boldsymbol{\tau}}_h\in\mathbf{H}_k^h\\ \vec{\boldsymbol{\tau}}_h\neq\mathbf{0}}} \frac{|(\mathbf{F}-\mathbf{F}_h)(\varphi;\vec{\boldsymbol{\tau}}_h)|}{\|\vec{\boldsymbol{\tau}}_h\|_{\mathbf{H}}} \leq C_{\mathtt{q}}\Big\{\|\mathbf{div}\,(\boldsymbol{\sigma}) - \boldsymbol{\mathcal{P}}_{k+1}^h(\mathbf{div}\,(\boldsymbol{\sigma}))\|_{0,\Omega} + \|\varphi-\mathcal{P}_{k+1}^h(\varphi)\|_{0,\Omega}\Big\}. \tag{3.76}$$

*Proof.* Firstly, using [69, Lemma 4.8], and by adding and subtracting suitable terms (see also [69, eq. (5.21)]), we get (3.74) with $L_{\mathbf{A}} := 3\max\Big\{\alpha_2+\kappa_1,\beta_2\Big\}$, where $\alpha_2$ and $\beta_2$ are the constants from Lemmas 3.7 and 3.8, respectively. In turn, in order to prove (3.75), we proceed as in [69, Lemma 4.12] by adding and subtracting suitable terms, which yields

$$\begin{aligned}(\mathbf{B}-\mathbf{B}_h)(\mathbf{u};\vec{\boldsymbol{\zeta}}_h,\vec{\boldsymbol{\tau}}_h) &= \int_\Omega \Big\{(\mathbf{w}_h\otimes\mathbf{u})^{\mathrm{d}} - \boldsymbol{\mathcal{P}}_k^h((\mathbf{w}_h\otimes\mathbf{u})^{\mathrm{d}})\Big\} : \Big\{\boldsymbol{\tau}_h - \kappa_1\nabla\mathbf{v}_h\Big\}\\ &\quad + \int_\Omega \Big(\mathbf{w}_h\otimes\mathbf{u} - \boldsymbol{\mathcal{P}}_{k+1}^h(\mathbf{w}_h)\otimes\boldsymbol{\mathcal{P}}_{k+1}^h(\mathbf{u}))\Big)^{\mathrm{d}} : \boldsymbol{\mathcal{P}}_k^h(\boldsymbol{\tau}_h-\kappa_1\nabla\mathbf{v}_h)\,.\end{aligned} \tag{3.77}$$

The two expressions on the right-hand side of (3.77) are bounded in what follows. In fact, adding and subtracting $\mathbf{u}$, it follows that

$$(\mathbf{w}_h \otimes \mathbf{u}) - \boldsymbol{\mathcal{P}}_k^h(\mathbf{w}_h \otimes \mathbf{u}) = (\mathbf{w}_h - \mathbf{u}) \otimes \mathbf{u} - \boldsymbol{\mathcal{P}}_k^h((\mathbf{w}_h - \mathbf{u}) \otimes \mathbf{u}) + (\mathbf{u} \otimes \mathbf{u}) - \boldsymbol{\mathcal{P}}_k^h(\mathbf{u} \otimes \mathbf{u})\,.$$

Then, using the foregoing expression, and the first equation of (3.4), we arrive at

$$\begin{aligned}
&\int_\Omega \Big\{(\mathbf{w}_h \otimes \mathbf{u})^{\mathrm{d}} - \boldsymbol{\mathcal{P}}_k^h((\mathbf{w}_h \otimes \mathbf{u})^{\mathrm{d}})\Big\} : \Big\{\boldsymbol{\tau}_h - \kappa_1 \nabla \mathbf{v}_h\Big\} \\
&\qquad = \int_\Omega \Big\{(\mathbf{w}_h - \mathbf{u}) \otimes \mathbf{u} - \boldsymbol{\mathcal{P}}_k^h((\mathbf{w}_h - \mathbf{u}) \otimes \mathbf{u})\Big\}^{\mathrm{d}} : \Big\{\boldsymbol{\tau}_h - \kappa_1 \nabla \mathbf{v}_h\Big\} \\
&\qquad + \mu \int_\Omega \Big\{\nabla \mathbf{u} - \boldsymbol{\mathcal{P}}_k^h(\nabla \mathbf{u})\Big\} : \Big\{\boldsymbol{\tau}_h - \kappa_1 \nabla \mathbf{v}_h\Big\} - \int_\Omega \Big\{\boldsymbol{\sigma} - \boldsymbol{\mathcal{P}}_k^h(\boldsymbol{\sigma})\Big\}^{\mathrm{d}} : \Big\{\boldsymbol{\tau}_h - \kappa_1 \nabla \mathbf{v}_h\Big\}\,.
\end{aligned} \tag{3.78}$$

In this way, replacing (3.78) into (3.77), using the Cauchy-Schwarz and Hölder inequalities, employing the compact injection (3.13) and the fact that $\nabla\, \boldsymbol{\mathcal{R}}_k^h(\mathbf{u})\big|_K \in \mathbb{P}_k(K)$ for all $K \in \mathcal{T}_h$, and then bounding $\|\mathbf{u} - \mathbf{w}_h\|_{1,\Omega}$ and $\|\mathbf{u}\|_{1,\Omega}$ by $\|\vec{\boldsymbol{\sigma}} - \vec{\boldsymbol{\zeta}}_h\|_{\mathbf{H}}$ and $\rho_0$, respectively, we deduce

$$\begin{aligned}
|(\mathbf{B} - \mathbf{B}_h)(\mathbf{u}; \vec{\boldsymbol{\zeta}}_h, \vec{\boldsymbol{\tau}}_h)| \leq \widehat{C}_{\mathrm{p}} \Big\{ &\|\vec{\boldsymbol{\sigma}} - \vec{\boldsymbol{\zeta}}_h\|_{\mathbf{H}} + |\mathbf{u} - \boldsymbol{\mathcal{R}}_k^h(\mathbf{u})|_{1,h} + \|\boldsymbol{\sigma} - \boldsymbol{\mathcal{P}}_k^h(\boldsymbol{\sigma})\|_{0,\Omega} \\
&+ \|(\mathbf{w}_h \otimes \mathbf{u}) - \boldsymbol{\mathcal{P}}_{k+1}^h(\mathbf{w}_h) \otimes \boldsymbol{\mathcal{P}}_{k+1}^h(\mathbf{u})\|_{0,\Omega} \Big\} \|\vec{\boldsymbol{\tau}}_h\|_{\mathbf{H}}\,,
\end{aligned} \tag{3.79}$$

with $\widehat{C}_p := (1 + \kappa_1^2)^{1/2} \max\Big\{1, 2\rho_0 \|\boldsymbol{i}_c\|^2, \mu\Big\}$. On the other hand, adding and subtracting $\boldsymbol{\mathcal{P}}_{k+1}^h(\mathbf{u})$, employing the Cauchy-Schwarz and Hölder inequalities, Lemma 3.6, and the compact injection (3.13), we find that

$$\begin{aligned}
&\|(\mathbf{w}_h \otimes \mathbf{u}) - \boldsymbol{\mathcal{P}}_{k+1}^h(\mathbf{w}_h) \otimes \boldsymbol{\mathcal{P}}_{k+1}^h(\mathbf{u})\|_{0,\Omega} \\
&\qquad \leq \|\boldsymbol{i}_c\| C_{\mathtt{k}} \Big\{ \|\mathbf{w}_h\|_{1,\Omega} \|\mathbf{u} - \boldsymbol{\mathcal{P}}_{k+1}^h(\mathbf{u})\|_{0,4,\Omega} + \|\mathbf{u}\|_{1,\Omega} \|\mathbf{w}_h - \boldsymbol{\mathcal{P}}_{k+1}^h(\mathbf{w}_h)\|_{0,4,\Omega} \Big\}\,.
\end{aligned} \tag{3.80}$$

Furthermore, using similar arguments, and bounding $\|\mathbf{u} - \mathbf{w}_h\|_{1,\Omega}$ and $\|\mathbf{u}\|_{1,\Omega}$ by $\|\vec{\boldsymbol{\sigma}} - \vec{\boldsymbol{\zeta}}_h\|_{\mathbf{H}}$ and $\rho_0$, respectively, we get

$$\begin{aligned}
&\|\mathbf{w}_h\|_{1,\Omega} \|\mathbf{u} - \boldsymbol{\mathcal{P}}_{k+1}^h(\mathbf{u})\|_{0,4,\Omega} \\
&\qquad \leq \|\boldsymbol{i}_c\|(1 + C_{\mathtt{k}}) \|\mathbf{u}\|_{1,\Omega} \|\mathbf{u} - \mathbf{w}_h\|_{1,\Omega} + \|\mathbf{u}\|_{1,\Omega} \|\mathbf{u} - \boldsymbol{\mathcal{P}}_{k+1}^h(\mathbf{u})\|_{0,4,\Omega} \\
&\qquad \leq \rho_0 \max\Big\{1, \|\boldsymbol{i}_c\|(1 + C_{\mathtt{k}})\Big\} \Big\{ \|\vec{\boldsymbol{\sigma}} - \vec{\boldsymbol{\zeta}}_h\|_{\mathbf{H}} + \|\mathbf{u} - \boldsymbol{\mathcal{P}}_{k+1}^h(\mathbf{u})\|_{0,4,\Omega} \Big\}\,,
\end{aligned} \tag{3.81}$$

and

$$\begin{aligned}
&\|\mathbf{u}\|_{1,\Omega} \|\mathbf{w}_h - \boldsymbol{\mathcal{P}}_{k+1}^h(\mathbf{w}_h)\|_{0,4,\Omega} \\
&\qquad \leq \rho_0 \Big\{ \|\boldsymbol{i}_c\|(1 + C_{\mathtt{k}}) \|\mathbf{u} - \mathbf{w}_h\|_{1,\Omega} + \|\mathbf{u} - \boldsymbol{\mathcal{P}}_{k+1}^h(\mathbf{u})\|_{0,4,\Omega} \Big\} \\
&\qquad \leq \rho_0 \max\Big\{1, \|\boldsymbol{i}_c\|(1 + C_{\mathtt{k}})\Big\} \Big\{ \|\vec{\boldsymbol{\sigma}} - \vec{\boldsymbol{\zeta}}_h\|_{\mathbf{H}} + \|\mathbf{u} - \boldsymbol{\mathcal{P}}_{k+1}^h(\mathbf{u})\|_{0,4,\Omega} \Big\}\,.
\end{aligned} \tag{3.82}$$

Therefore, replacing (3.81) and (3.82) back into (3.80), we get

$$\|(\mathbf{w}_h \otimes \mathbf{u}) - \boldsymbol{\mathcal{P}}_{k+1}^h(\mathbf{w}_h) \otimes \boldsymbol{\mathcal{P}}_{k+1}^h(\mathbf{u})\|_{0,\Omega} \leq \overline{C}_{\mathrm{p}} \Big\{ \|\vec{\boldsymbol{\sigma}} - \vec{\boldsymbol{\zeta}}_h\|_{\mathbf{H}} + \|\mathbf{u} - \boldsymbol{\mathcal{P}}_{k+1}^h(\mathbf{u})\|_{0,4,\Omega} \Big\}\,, \tag{3.83}$$

with $\overline{C}_{\mathtt{p}} := \|\boldsymbol{i}_c\| C_{\mathtt{k}} \rho_0 \max\Big\{1, \|\boldsymbol{i}_c\|(1+C_{\mathtt{k}})\Big\}$. Finally, replacing (3.83) into (3.79), and taking the supremum on $\vec{\boldsymbol{\tau}}_h \in \mathbf{H}_k^h$, we deduce (3.75) with $C_{\mathtt{p}} := \widehat{C}_{\mathtt{p}}(1+\overline{C}_{\mathtt{p}})$. Next, in order to deal with (3.76), we observe from (3.10) and (3.46) that

$$(\mathbf{F}-\mathbf{F}_h)(\varphi;\vec{\boldsymbol{\tau}}_h) = \int_\Omega \mathbf{g}\,\varphi\cdot\mu\mathbf{v}_h - \int_\Omega \mathbf{g}\,\mathcal{P}_{k+1}^h(\varphi)\cdot\mu\boldsymbol{\mathcal{P}}_{k+1}^h(\mathbf{v}_h) - \kappa_2\int_\Omega \mathbf{g}\Big\{\varphi-\mathcal{P}_{k+1}^h(\varphi)\Big\}\cdot\mathbf{div}\,(\boldsymbol{\tau}_h)\,. \tag{3.84}$$

Next, adding and subtracting $\mu\displaystyle\int_\Omega \boldsymbol{\mathcal{P}}_{k+1}^h(\mathbf{g}\varphi)\cdot\mathbf{v}_h$, and using the second equation in (3.4), we deduce that

$$\begin{aligned}
&\int_\Omega \mathbf{g}\,\varphi\cdot\mu\mathbf{v}_h - \int_\Omega \mathbf{g}\,\mathcal{P}_{k+1}^h(\varphi)\cdot\mu\boldsymbol{\mathcal{P}}_{k+1}^h(\mathbf{v}_h)\\
&\qquad = \mu\int_\Omega\Big\{\mathbf{g}\,\varphi - \boldsymbol{\mathcal{P}}_{k+1}^h(\mathbf{g}\,\varphi)\Big\}\cdot\mathbf{v}_h + \mu\int_\Omega \mathbf{g}\Big\{\varphi-\mathcal{P}_{k+1}^h(\varphi)\Big\}\cdot\boldsymbol{\mathcal{P}}_{k+1}^h(\mathbf{v}_h)\\
&\qquad = -\mu\int_\Omega\Big\{\mathbf{div}\,(\boldsymbol{\sigma}) - \boldsymbol{\mathcal{P}}_{k+1}^h(\mathbf{div}\,(\boldsymbol{\sigma}))\Big\}\cdot\mathbf{v}_h + \mu\int_\Omega \mathbf{g}\Big\{\varphi-\mathcal{P}_{k+1}^h(\varphi)\Big\}\cdot\boldsymbol{\mathcal{P}}_{k+1}^h(\mathbf{v}_h)\,.
\end{aligned} \tag{3.85}$$

Finally, replacing (3.85) into (3.84), and applying the Cauchy-Schwarz inequality, we get (3.76) with $C_{\mathtt{q}} := (4\mu^2+\kappa_2^2)^{1/2}\max\Big\{1,\|\mathbf{g}\|_{\infty,\Omega}\Big\}$. □

**Lemma 3.18.** *There exist positive constants $L_{\mathbf{a}}$ and $\widetilde{C}_{\mathtt{q}}$, independent of $h$, such that*

$$\sup_{\substack{\psi_h\in\mathcal{Q}_k^h\\ \psi_h\neq 0}}\frac{|(\mathbf{a}-\mathbf{a}_h)(\phi_h,\psi_h)|}{\|\psi_h\|_{1,\Omega}} \leq L_{\mathbf{a}}\Big\{\|\varphi-\phi_h\|_{1,\Omega} + \|\mathbb{K}\nabla\varphi - \boldsymbol{\mathcal{P}}_k^h(\mathbb{K}\nabla\varphi)\|_{0,\Omega} + |\varphi-\Pi_k^h(\varphi)|_{1,h}\Big\} \tag{3.86}$$

*for all $\phi_h\in\mathcal{Q}_k^h$, and*

$$\begin{aligned}
&\sup_{\substack{\psi_h\in\mathcal{Q}_k^h\\ \psi_h\neq 0}}\frac{|(\mathrm{F}-\mathrm{F}_h)(\mathbf{u},\varphi;\psi_h)|}{\|\psi_h\|_{1,\Omega}}\\
&\leq \widetilde{C}_{\mathtt{q}}\Big\{h\|\mathrm{div}(\mathbb{K}\nabla\varphi) - \mathcal{P}_{k+1}^h(\mathrm{div}(\mathbb{K}\nabla\varphi))\|_{0,\Omega} + |\varphi-\Pi_k^h(\varphi)|_{1,h} + \|\mathbf{u}-\boldsymbol{\mathcal{P}}_{k+1}^h(\mathbf{u})\|_{0,4,\Omega}\Big\}\,.
\end{aligned} \tag{3.87}$$

*Proof.* Given $K\in\mathcal{T}_h$, using the symmetry of the bilinear form $\mathbf{a}^K$ (cf.(3.47)), and the first equation in (3.49) with $q := \Pi_k^K(\phi_h)\in\mathrm{P}_{k+1}(K)$, the local bilinear form $\mathbf{a}_h^K$ (cf. (3.52)) can be rewritten as

$$\mathbf{a}_h^K(\phi_h,\psi_h) = \int_K \boldsymbol{\mathcal{P}}_k^K(\mathbb{K}\nabla\Pi_k^K(\phi_h))\cdot\nabla\psi_h + \mathcal{S}^{K,\Pi}(\phi_h-\Pi_k^K(\phi_h),\psi_h-\Pi_k^K(\psi_h)) \tag{3.88}$$

for all $\phi_h,\psi_h\in\mathcal{Q}_k^K$. Then, from (3.9) and (3.88), and adding and subtracting $\displaystyle\int_K \mathbb{K}\nabla\Pi_k^K(\phi_h)\cdot\nabla\psi_h$, we get

$$\begin{aligned}
(\mathbf{a}^K-\mathbf{a}_h^K)(\phi_h,\psi_h) &= \int_K \mathbb{K}\nabla(\phi_h-\Pi_k^K(\phi_h))\cdot\nabla\psi_h - \mathcal{S}^{K,\Pi}(\phi_h-\Pi_k^K(\phi_h),\psi_h-\Pi_k^K(\psi_h))\\
&\quad + \int_K\Big\{\mathbb{K}\nabla\Pi_k^K(\phi_h) - \boldsymbol{\mathcal{P}}_k^K(\mathbb{K}\nabla\Pi_k^K(\phi_h))\Big\}\cdot\nabla\psi_h
\end{aligned}$$

whence, applying the Cauchy-Schwarz inequality, using the symmetry of the bilinear form $\mathcal{S}^{K,\Pi}$, the upper bound in (3.53), and the estimate (3.50), we obtain

$$|(\mathbf{a}-\mathbf{a}_h)(\phi_h,\psi_h)| \leq \Big\{ \|\mathbb{K}\nabla\phi_h - \mathbb{K}\nabla\Pi_k^K(\phi_h)\|_{0,K} + \|\mathbb{K}\nabla\Pi_k^K(\phi_h) - \boldsymbol{\mathcal{P}}_k^K(\mathbb{K}\nabla\Pi_k^K(\phi_h))\|_{0,K} + (1+C_{\mathbb{K}})\,\overline{c}_1\,|\phi_h - \Pi_k^K(\phi_h)|_{1,K} \Big\} |\psi_h|_{1,K}\,.$$

Further, adding and subtracting suitable terms, summing over all $K \in \mathcal{T}_h$, and then taking supremum over $\psi_h \in \mathcal{Q}_k^h$, we deduce the estimate (3.86) with $L_{\mathbf{a}}$ depending only on $\mathbb{K}$ and $\overline{c}_1$. On the other hand, from (3.11) and (3.54), adding and subtracting $\displaystyle\int_\Omega \mathcal{P}_{k+1}^h(\mathbf{u}\cdot\nabla\varphi)\psi_h$, and using the fourth equation in (3.4), we find that

$$\begin{aligned}
(\mathrm{F}-\mathrm{F}_h)(\mathbf{u},\varphi;\psi_h) &= -\int_\Omega (\mathbf{u}\cdot\nabla\varphi)\psi_h + \int_\Omega (\boldsymbol{\mathcal{P}}_{k+1}^h(\mathbf{u})\cdot\boldsymbol{\mathcal{P}}_k^h(\nabla\varphi))\mathcal{P}_{k+1}^h(\psi_h)\\
&= -\int_\Omega \Big\{(\mathbf{u}\cdot\nabla\varphi) - \mathcal{P}_{k+1}^h(\mathbf{u}\cdot\nabla\varphi)\Big\}\psi_h - \int_\Omega \Big\{(\mathbf{u}\cdot\nabla\varphi) - (\boldsymbol{\mathcal{P}}_{k+1}^h(\mathbf{u})\cdot\boldsymbol{\mathcal{P}}_k^h(\nabla\varphi))\Big\}\mathcal{P}_{k+1}^h(\psi_h)\\
&= -\int_\Omega \Big\{\mathrm{div}(\mathbb{K}\nabla\varphi) - \mathcal{P}_{k+1}^h(\mathrm{div}(\mathbb{K}\nabla\varphi))\Big\}(\psi_h - \mathcal{P}_{k+1}^h(\psi_h)) - \int_\Omega \Big\{\Big(\mathbf{u}-\boldsymbol{\mathcal{P}}_{k+1}^h(\mathbf{u})\Big)\cdot\nabla\varphi\Big\}\mathcal{P}_{k+1}^h(\psi_h)\\
&\quad - \int_\Omega \Big\{\boldsymbol{\mathcal{P}}_{k+1}^h(\mathbf{u})\cdot\Big(\nabla\varphi - \boldsymbol{\mathcal{P}}_k^h(\nabla\varphi)\Big)\Big\}\mathcal{P}_{k+1}^h(\psi_h)\,,
\end{aligned}$$

whence, applying the Cauchy-Schwarz and Hölder inequalities, the approximation properties (3.36), Lemma 3.6, the fact that $\nabla\,\Pi_k^h(\varphi)\big|_K \in \mathbf{P}_k(K)$ for all $K \in \mathcal{T}_h$, and finally bounding $|\varphi|_{1,\Omega}$ and $\|\mathbf{u}\|_{1,\Omega}$ by $\rho_0$, we get (3.87) with $\widetilde{C}_{\mathtt{q}} := \max\Big\{\widehat{C}, C_{\mathtt{k}}\|i_c\|\rho_0, C_{\mathtt{k}}^2\|\boldsymbol{i}_c\|\|i_c\|\rho_0\Big\}$, where $\widehat{C}$ is the constant obtained when (3.36) is applied with $\psi_h \in \mathrm{H}^1(\Omega)$. □

Next, since we are interested in obtain an upper bound for the error $\|(\vec{\boldsymbol{\sigma}},\varphi) - (\vec{\boldsymbol{\sigma}}_h,\varphi_h)\|$ (cf. (3.72)), we first rearrange (3.6) and (3.55) as the following pairs of continuous and discrete formulations

$$\begin{aligned}
\mathbf{A}(\vec{\boldsymbol{\zeta}},\vec{\boldsymbol{\tau}}) + \mathbf{B}(\mathbf{u};\vec{\boldsymbol{\zeta}},\vec{\boldsymbol{\tau}}) &= \mathbf{F}(\varphi;\vec{\boldsymbol{\tau}}) + \mathbf{F}_D(\vec{\boldsymbol{\tau}}) \qquad \forall\,\vec{\boldsymbol{\tau}} \in \mathbf{H}\,,\\
\mathbf{A}_h(\vec{\boldsymbol{\zeta}}_h,\vec{\boldsymbol{\tau}}_h) + \mathbf{B}_h(\mathbf{u}_h;\vec{\boldsymbol{\zeta}}_h,\vec{\boldsymbol{\tau}}_h) &= \mathbf{F}_h(\varphi_h;\vec{\boldsymbol{\tau}}_h) + \mathbf{F}_D(\vec{\boldsymbol{\tau}}_h) \quad \forall\,\vec{\boldsymbol{\tau}}_h \in \mathbf{H}_k^h\,,
\end{aligned} \tag{3.89}$$

and

$$\begin{aligned}
\mathbf{a}(\varphi,\psi) &= \mathrm{F}(\mathbf{u},\varphi;\psi) \qquad \forall\,\psi \in \mathrm{H}\,,\\
\mathbf{a}_h(\varphi_h,\psi_h) &= \mathrm{F}_h(\mathbf{u}_h,\varphi_h;\psi_h) \quad \forall\,\psi_h \in \mathcal{Q}_k^h\,.
\end{aligned} \tag{3.90}$$

Then, we have the following lemma establishing a preliminary estimate for $\|\vec{\boldsymbol{\sigma}} - \vec{\boldsymbol{\sigma}}_h\|_{\mathbf{H}}$.

**Lemma 3.19.** *There exist positive constants $C_{\mathtt{d}}$ and $C_{\mathtt{r}}$, independent of $h$, such that*

$$\begin{aligned}
\|\vec{\boldsymbol{\sigma}} - \vec{\boldsymbol{\sigma}}_h\|_{\mathbf{H}} \leq\ & C_{\mathtt{d}}\Big\{\|\mathbf{div}\,(\boldsymbol{\sigma}) - \boldsymbol{\mathcal{P}}_{k+1}^h(\mathbf{div}\,(\boldsymbol{\sigma}))\|_{0,\Omega} + \|\varphi - \mathcal{P}_{k+1}^h(\varphi)\|_{0,\Omega} + \|\boldsymbol{\sigma} - \boldsymbol{\mathcal{P}}_k^h(\boldsymbol{\sigma})\|_{0,\Omega}\\
&+ |\mathbf{u} - \boldsymbol{\mathcal{R}}_k^h(\mathbf{u})|_{1,h} + \|\mathbf{u} - \boldsymbol{\mathcal{P}}_{k+1}^h(\mathbf{u})\|_{0,4,\Omega} + \mathrm{dist}(\vec{\boldsymbol{\sigma}},\mathbf{H}_k^h)\Big\}\\
&+ C_{\mathtt{r}}\Big\{\|\vec{\boldsymbol{\sigma}}\|_{\mathbf{H}} + \|\mathbf{g}\|_{\infty,\Omega}\Big\}\|(\vec{\boldsymbol{\sigma}},\varphi) - (\vec{\boldsymbol{\sigma}}_h,\varphi_h)\|\,.
\end{aligned} \tag{3.91}$$

*Proof.* Employing the bounds provided by (3.14)-(3.16) and (3.43)-(3.45), the fact that $\|\mathbf{u}\|_{1,\Omega}$ and $\|\mathbf{u}_h\|_{1,\Omega}$ are bounded by $\rho_0$ (cf.(3.73)), and recalling that $C_{\mathbf{k}} \geq 1$ (cf. Lemma 3.6), we deduce that $\mathbf{A} + \mathbf{B}(\mathbf{u};\cdot,\cdot)$ and $\mathbf{A}_h + \mathbf{B}_h(\mathbf{u}_h;\cdot,\cdot)$ are bounded and elliptic with the common constants $L_{\mathrm{B}}$ and $L_{\mathrm{E}}$, respectively, both independent of $h$, which are given by

$$L_{\mathrm{B}} := \max\left\{C_{\mathbf{A}}, \widetilde{C}_{\mathbf{A}}\right\} + \widetilde{C}_{\mathbf{B}}\rho_0 \quad \text{and} \quad L_{\mathrm{E}} := \frac{1}{2}\min\{\alpha_{\mathbf{A}}, \widetilde{\alpha}_{\mathbf{A}}\}\,.$$

In turn, $\mathbf{F}(\varphi;\cdot) + \mathbf{F}_D$ and $\mathbf{F}_h(\varphi_h;\cdot) + \mathbf{F}_D$ are bounded linear functionals in $\mathbf{H}$ and $\mathbf{H}_k^h$, respectively. Then, a straightforward application of the first Strang lemma for linear problems (see [45, Theorem 4.1.1] or [87, Theorem 11.1]) to the context (3.89) gives

$$\begin{aligned}\|\vec{\boldsymbol{\sigma}} - \vec{\boldsymbol{\sigma}}_h\|_{\mathbf{H}} \leq C_{\mathtt{st}} \Bigg\{ \sup_{\substack{\vec{\boldsymbol{\tau}}_h \in \mathbf{H}_k^h \\ \vec{\boldsymbol{\tau}}_h \neq \mathbf{0}}} \frac{|\mathbf{F}(\varphi;\vec{\boldsymbol{\tau}}_h) - \mathbf{F}_h(\varphi_h;\vec{\boldsymbol{\tau}}_h)|}{\|\vec{\boldsymbol{\tau}}_h\|_{\mathbf{H}}} + \inf_{\vec{\boldsymbol{\zeta}}_h \in \mathbf{H}_k^h} \Bigg( \|\vec{\boldsymbol{\sigma}} - \vec{\boldsymbol{\zeta}}_h\|_{\mathbf{H}} \\ + \sup_{\substack{\vec{\boldsymbol{\tau}}_h \in \mathbf{H}_k^h \\ \vec{\boldsymbol{\tau}}_h \neq \mathbf{0}}} \frac{|(\mathbf{A} - \mathbf{A}_h)(\vec{\boldsymbol{\zeta}}_h, \vec{\boldsymbol{\tau}}_h) + \mathbf{B}(\mathbf{u};\vec{\boldsymbol{\zeta}}_h, \vec{\boldsymbol{\tau}}_h) - \mathbf{B}_h(\mathbf{u}_h;\vec{\boldsymbol{\zeta}}_h, \vec{\boldsymbol{\tau}}_h)|}{\|\vec{\boldsymbol{\tau}}_h\|_{\mathbf{H}}} \Bigg) \Bigg\}\,, \end{aligned} \tag{3.92}$$

where $C_{\mathtt{st}} := L_{\mathrm{E}}^{-1}\max\{1, L_{\mathrm{E}} + L_{\mathrm{B}}\}$. Next, adding and subtracting $\mathbf{F}_h(\varphi;\vec{\boldsymbol{\tau}}_h)$, we find that

$$\mathbf{F}(\varphi;\vec{\boldsymbol{\tau}}_h) - \mathbf{F}_h(\varphi_h;\vec{\boldsymbol{\tau}}_h) = (\mathbf{F} - \mathbf{F}_h)(\varphi;\vec{\boldsymbol{\tau}}_h) + \mathbf{F}_h(\varphi - \varphi_h;\vec{\boldsymbol{\tau}}_h)\,. \tag{3.93}$$

Then, from (3.93), the estimate (3.76) in Lemma 3.17, and the boundedness of $\mathbf{F}_h$ (cf. (3.61)), we deduce that

$$\begin{aligned}&\sup_{\substack{\vec{\boldsymbol{\tau}}_h \in \mathbf{H}_k^h \\ \vec{\boldsymbol{\tau}}_h \neq \mathbf{0}}} \frac{|\mathbf{F}(\varphi;\vec{\boldsymbol{\tau}}_h) - \mathbf{F}_h(\varphi_h;\vec{\boldsymbol{\tau}}_h)|}{\|\vec{\boldsymbol{\tau}}_h\|_{\mathbf{H}}} \\ &\quad \leq C_{\mathtt{q}}\Big\{\|\mathbf{div}\,(\boldsymbol{\sigma}) - \boldsymbol{\mathcal{P}}_{k+1}^h(\mathbf{div}\,(\boldsymbol{\sigma}))\|_{0,\Omega} + \|\varphi - \mathcal{P}_{k+1}^h(\varphi)\|_{0,\Omega}\Big\} + C_{\mathbf{F}}\|\mathbf{g}\|_{\infty,\Omega}\|\varphi - \varphi_h\|_{1,\Omega}\,. \end{aligned} \tag{3.94}$$

Also, adding and subtracting suitable terms, we find that

$$\begin{aligned}&|\mathbf{B}(\mathbf{u};\vec{\boldsymbol{\zeta}}_h, \vec{\boldsymbol{\tau}}_h) - \mathbf{B}_h(\mathbf{u}_h;\vec{\boldsymbol{\zeta}}_h, \vec{\boldsymbol{\tau}}_h)| \\ &\quad \leq |(\mathbf{B} - \mathbf{B}_h)(\mathbf{u};\vec{\boldsymbol{\zeta}}_h, \vec{\boldsymbol{\tau}}_h)| + |\mathbf{B}_h(\mathbf{u} - \mathbf{u}_h;\vec{\boldsymbol{\sigma}}, \vec{\boldsymbol{\tau}}_h) - \mathbf{B}_h(\mathbf{u} - \mathbf{u}_h;\vec{\boldsymbol{\sigma}} - \vec{\boldsymbol{\zeta}}_h, \vec{\boldsymbol{\tau}}_h)|\,. \end{aligned} \tag{3.95}$$

Furthermore, by using the boundedness of $\mathbf{B}_h$ (cf. (3.45)), and bounding $\|\mathbf{u}\|_{1,\Omega}$ and $\|\mathbf{u}_h\|_{1,\Omega}$ by $\rho_0$, we get

$$\begin{aligned}&|\mathbf{B}_h(\mathbf{u} - \mathbf{u}_h;\vec{\boldsymbol{\sigma}}, \vec{\boldsymbol{\tau}}_h) - \mathbf{B}_h(\mathbf{u} - \mathbf{u}_h;\vec{\boldsymbol{\sigma}} - \vec{\boldsymbol{\zeta}}_h, \vec{\boldsymbol{\tau}}_h)| \\ &\quad \leq \widetilde{C}_{\mathbf{B}}\left(\|\vec{\boldsymbol{\sigma}}\|_{\mathbf{H}} + \|\vec{\boldsymbol{\sigma}} - \vec{\boldsymbol{\zeta}}_h\|_{\mathbf{H}}\right)\|\mathbf{u} - \mathbf{u}_h\|_{1,\Omega}\|\vec{\boldsymbol{\tau}}_h\|_{\mathbf{H}} \\ &\quad \leq \widetilde{C}_{\mathbf{B}}\left(\|\vec{\boldsymbol{\sigma}}\|_{\mathbf{H}}\|\vec{\boldsymbol{\sigma}} - \vec{\boldsymbol{\sigma}}_h\|_{\mathbf{H}} + 2\rho_0\,\|\vec{\boldsymbol{\sigma}} - \vec{\boldsymbol{\zeta}}_h\|_{\mathbf{H}}\right)\|\vec{\boldsymbol{\tau}}_h\|_{\mathbf{H}}\,. \end{aligned}$$

Then, from (3.95), the foregoing expression, and the estimate (3.75) from Lemma 3.17, we get

$$\begin{aligned}\sup_{\substack{\vec{\boldsymbol{\tau}}_h \in \mathbf{H}_k^h \\ \vec{\boldsymbol{\tau}}_h \neq \mathbf{0}}} \frac{|\mathbf{B}(\mathbf{u};\vec{\boldsymbol{\zeta}}_h, \vec{\boldsymbol{\tau}}_h) - \mathbf{B}_h(\mathbf{u}_h;\vec{\boldsymbol{\zeta}}_h, \vec{\boldsymbol{\tau}}_h)|}{\|\vec{\boldsymbol{\tau}}_h\|_{\mathbf{H}}} \leq \widetilde{C}_{\mathtt{p}}\Big\{\|\vec{\boldsymbol{\sigma}} - \vec{\boldsymbol{\zeta}}_h\|_{\mathbf{H}} + \|\boldsymbol{\sigma} - \boldsymbol{\mathcal{P}}_k^h(\boldsymbol{\sigma})\|_{0,\Omega} \\ + |\mathbf{u} - \boldsymbol{\mathcal{R}}_k^h(\mathbf{u})|_{1,h} + \|\mathbf{u} - \boldsymbol{\mathcal{P}}_{k+1}^h(\mathbf{u})\|_{0,4,\Omega}\Big\} + \widetilde{C}_{\mathbf{B}}\|\vec{\boldsymbol{\sigma}}\|_{\mathbf{H}}\|\vec{\boldsymbol{\sigma}} - \vec{\boldsymbol{\sigma}}_h\|_{\mathbf{H}}\,, \end{aligned} \tag{3.96}$$

with $\widetilde{C}_{\mathtt{p}} := C_{\mathtt{p}} + 2\rho_0 \widetilde{C}_{\mathbf{B}}$. In this way, replacing (3.94), (3.74) and (3.96) into (3.92), we deduce the estimate (3.91) with

$$C_{\mathtt{d}} := C_{\mathtt{st}} \max\left\{C_{\mathtt{q}}, L_{\mathbf{A}}, \widetilde{C}_{\mathtt{p}}\right\} \quad \text{and} \quad C_{\mathtt{r}} := C_{\mathtt{st}} \max\left\{\widetilde{C}_{\mathbf{B}}, C_{\mathbf{F}}\right\}. \tag{3.97}$$

□

Next, as for the error $\|\varphi - \varphi_h\|_{1,\Omega}$ arising from (3.90), we have the following result.

**Lemma 3.20.** *There exist positive constants $\widetilde{C}_{\mathtt{d}}$ and $\widetilde{C}_{\mathtt{r}}$, independent of $h$, such that*

$$\begin{aligned}\|\varphi - \varphi_h\|_{1,\Omega} \leq\ & \widetilde{C}_{\mathtt{d}} \Big\{ \|\mathbb{K}\nabla\varphi - \boldsymbol{\mathcal{P}}_k^h(\mathbb{K}\nabla\varphi)\|_{0,\Omega} + h\|\mathrm{div}\,(\mathbb{K}\nabla\varphi) - \mathcal{P}_{k+1}^h(\mathrm{div}(\mathbb{K}\nabla\varphi))\|_{0,\Omega} \\ & + |\varphi - \Pi_k^h(\varphi)|_{1,h} + \|\mathbf{u} - \boldsymbol{\mathcal{P}}_{k+1}^h(\mathbf{u})\|_{0,4,\Omega} + \mathrm{dist}(\varphi, \mathcal{Q}_k^h)\Big\} \\ & + \widetilde{C}_{\mathtt{r}}\Big\{\|\vec{\boldsymbol{\sigma}}_h\|_{\mathbf{H}} + \|\varphi\|_{1,\Omega}\Big\}\|(\vec{\boldsymbol{\sigma}}, \varphi) - (\vec{\boldsymbol{\sigma}}_h, \varphi_h)\|\,.\end{aligned} \tag{3.98}$$

*Proof.* We first observe that the boundedness and ellipticity of the bilinear form $\mathbf{a}$ and Lemma 3.11 guarantee that the family $\{\mathbf{a}\} \cup \{\mathbf{a}_h\}_{h>0}$ is uniformly bounded and uniformly elliptic with constants, independent of $h$, given by

$$L_{\mathrm{B}} := \max\left\{1, \alpha^*\right\}\|\mathbf{a}\| \quad \text{and} \quad L_{\mathrm{E}} := \min\{1, \alpha_*\}\alpha_{\mathbf{a}}\,.$$

respectively. Hence, proceeding as in Lemma 3.19, and applying again the first Strang lemma to the context given by (3.90), we find that

$$\begin{aligned}\|\varphi - \varphi_h\|_{1,\Omega} \leq\ & \widetilde{C}_{\mathtt{st}} \left\{ \sup_{\substack{\psi_h \in \mathcal{Q}_k^h \\ \psi_h \neq 0}} \frac{|\mathrm{F}(\mathbf{u}, \varphi; \psi_h) - \mathrm{F}_h(\mathbf{u}_h, \varphi_h; \psi_h)|}{\|\psi_h\|_{1,\Omega}} \right. \\ & \left. + \inf_{\phi_h \in \mathcal{Q}_k^h} \left( \|\varphi - \phi_h\|_{1,\Omega} + \sup_{\substack{\psi_h \in \mathcal{Q}_k^h \\ \psi_h \neq 0}} \frac{|(\mathbf{a} - \mathbf{a}_h)(\phi_h, \psi_h)|}{\|\psi_h\|_{1,\Omega}} \right) \right\},\end{aligned} \tag{3.99}$$

Next, adding and subtracting $\mathrm{F}_h(\mathbf{u} - \mathbf{u}_h, \varphi, \psi_h)$ we find that

$$|\mathrm{F}(\mathbf{u}, \varphi; \psi_h) - \mathrm{F}_h(\mathbf{u}_h, \varphi_h; \psi_h)| = |(\mathrm{F} - \mathrm{F}_h)(\mathbf{u}, \varphi; \psi_h) + \mathrm{F}_h(\mathbf{u}_h, \varphi - \varphi_h; \psi_h) + \mathrm{F}_h(\mathbf{u} - \mathbf{u}_h, \varphi; \psi_h)|\,. \tag{3.100}$$

For the second and third term on the right-hand side of (3.100) we apply the bound of $\mathrm{F}_h$ (cf. (3.63)) to obtain

$$|\mathrm{F}_h(\mathbf{u}_h, \varphi - \varphi_h; \psi_h) + \mathrm{F}_h(\mathbf{u} - \mathbf{u}_h, \varphi; \psi_h)| \leq \widetilde{C}_{\mathrm{F}}\Big\{\|\mathbf{u}_h\|_{1,\Omega}|\varphi - \varphi_h|_{1,\Omega} + \|\mathbf{u} - \mathbf{u}_h\|_{1,\Omega}|\varphi|_{1,\Omega}\Big\}\|\psi_h\|_{1,\Omega}\,.$$

In addition, thanks to (3.87) from Lemma 3.18, and the foregoing inequality, we get

$$\begin{aligned}&\sup_{\substack{\psi_h \in \mathcal{Q}_k^h \\ \psi_h \neq 0}} \frac{|\mathrm{F}(\mathbf{u}, \varphi; \psi_h) - \mathrm{F}_h(\mathbf{u}_h, \varphi_h; \psi_h)|}{\|\psi_h\|_{1,\Omega}} \\ &\quad \leq \widetilde{C}_{\mathtt{q}}\Big\{h\|\mathrm{div}(\mathbb{K}\nabla\varphi) - \mathcal{P}_{k+1}^h(\mathrm{div}(\mathbb{K}\nabla\varphi))\|_{0,\Omega} + |\,\varphi - \Pi_k^h(\varphi)\,|_{1,h} + \|\mathbf{u} - \boldsymbol{\mathcal{P}}_{k+1}^h(\mathbf{u})\|_{0,4,\Omega}\Big\} \\ &\quad + \widetilde{C}_{\mathrm{F}}\Big\{\|\vec{\boldsymbol{\sigma}}_h\|_{\mathbf{H}}\|\varphi - \varphi_h\|_{1,\Omega} + \|\vec{\boldsymbol{\sigma}} - \vec{\boldsymbol{\sigma}}_h\|_{\mathbf{H}}\|\varphi\|_{1,\Omega}\Big\}\,.\end{aligned} \tag{3.101}$$

Then, replacing (3.101) into (3.99), and using the estimate (3.86) from Lemma 3.18, we conclude the proof with

$$\widetilde{C}_{\mathtt{d}} := \widetilde{C}_{\mathtt{st}} \max\left\{\widetilde{C}_{\mathtt{q}}, L_{\mathbf{a}}\right\} \quad \text{and} \quad \widetilde{C}_{\mathtt{r}} := \widetilde{C}_{\mathtt{st}}\widetilde{C}_{\mathrm{F}}\,. \tag{3.102}$$

□

We are now in a position to derive an estimation for the global error (3.72). Indeed, bearing in mind the terms in Lemmas 3.19 and 3.20 that are multiplying $\|(\vec{\boldsymbol{\sigma}},\varphi) - (\vec{\boldsymbol{\sigma}}_h,\varphi_h)\|$, using the bounds for $\|\vec{\boldsymbol{\sigma}}\|_{\mathbf{H}}$, $\|\varphi\|_{1,\Omega}$, and $\|\vec{\boldsymbol{\sigma}}_h\|_{\mathbf{H}}$, given by (3.19), (3.20), and (3.70), respectively, the fact that $\|\mathbf{u}\|_{1,\Omega} \leq \rho_0$ (cf. (3.73)), and performing some algebraic manipulations, we find that

$$C_{\mathtt{r}}\Big\{\|\vec{\boldsymbol{\sigma}}\|_{\mathbf{H}} + \|\mathbf{g}\|_{\infty,\Omega}\Big\} + \widetilde{C}_{\mathtt{r}}\Big\{\|\vec{\boldsymbol{\sigma}}_h\|_{\mathbf{H}} + \|\varphi\|_{1,\Omega}\Big\} \leq \mathbf{C}_{\mathtt{r}}\Big\{\|\mathbf{g}\|_{\infty,\Omega} + \|\mathbf{u}_D\|_{0,\Gamma} + \|\mathbf{u}_D\|_{1/2,\Gamma}\Big\}\,, \tag{3.103}$$

where

$$\begin{aligned}
\mathbf{C}_{\mathtt{r}} &:= \mathbf{C}_{1,\mathtt{r}}\mathbf{C}_{2,\mathtt{r}}\mathbf{C}_{3,\mathtt{r}}\,,\\
\mathbf{C}_{1,\mathtt{r}} &:= \max\left\{C_{\mathtt{r}}, \widetilde{C}_{\mathtt{r}}\right\},\\
\mathbf{C}_{2,\mathtt{r}} &:= \max\left\{1, 2M_{\mathbf{F}}\left(\frac{1}{\alpha_{\mathbf{A}}} + \frac{1}{\widetilde{\alpha}_{\mathbf{A}}}\right), \frac{2M_{\mathrm{F}}}{\alpha_{\mathbf{a}}}\right\},\\
\mathbf{C}_{3,\mathtt{r}} &:= (1+\rho)^2 \max\left\{1, \rho\frac{2M_{\mathbf{F}}}{\alpha_{\mathbf{A}}}\right\}.
\end{aligned} \tag{3.104}$$

In this way, since the constant $\mathbf{C}_{\mathtt{r}}$ depends linearly on the data $\mathbf{g}$, $\mathbf{u}_D$ and $\varphi_N$, we conclude from the foregoing analysis, the following result.

**Theorem 3.21.** *Let $\mathbf{C}_{\mathtt{r}}$ be the constant from (3.104), and assume that the data $\mathbf{g}, \mathbf{u}_D$, and $\varphi_N$ are such that*

$$\mathbf{C}_{\mathtt{r}}\Big\{\|\mathbf{g}\|_{\infty,\Omega} + \|\mathbf{u}_D\|_{0,\Gamma} + \|\mathbf{u}_D\|_{1/2,\Gamma}\Big\} \leq \frac{1}{2}\,. \tag{3.105}$$

*Then, there exists a positive constant $C$, depending on $C_{\mathtt{d}}$ (cf. (3.97)) and $\widetilde{C}_{\mathtt{d}}$ (cf. (3.102)), such that*

$$\begin{aligned}
\|(\vec{\boldsymbol{\sigma}},\varphi) - (\vec{\boldsymbol{\sigma}}_h,\varphi_h)\| \leq\; C\Big\{ &\|\mathbf{div}\,(\boldsymbol{\sigma}) - \boldsymbol{\mathcal{P}}^h_{k+1}(\mathbf{div}\,(\boldsymbol{\sigma}))\|_{0,\Omega} + \|\boldsymbol{\sigma} - \boldsymbol{\mathcal{P}}^h_k(\boldsymbol{\sigma})\|_{0,\Omega} + |\mathbf{u} - \boldsymbol{\mathcal{R}}^h_k(\mathbf{u})|_{1,h}\\
&+ \|\mathbf{u} - \boldsymbol{\mathcal{P}}^h_{k+1}(\mathbf{u})\|_{0,4,\Omega} + \|\mathbb{K}\nabla\varphi - \boldsymbol{\mathcal{P}}^h_k(\mathbb{K}\nabla\varphi)\|_{0,\Omega} + h\|\mathrm{div}(\mathbb{K}\nabla\varphi) - \mathcal{P}^h_{k+1}(\mathrm{div}(\mathbb{K}\nabla\varphi))\|_{0,\Omega}\\
&+ \|\varphi - \mathcal{P}^h_{k+1}(\varphi)\|_{0,\Omega} + |\varphi - \Pi^h_k(\varphi)|_{1,h} + \mathrm{dist}(\vec{\boldsymbol{\sigma}}, \mathbf{H}^h_k) + \mathrm{dist}(\varphi, \mathcal{Q}^h_k)\Big\}\,.
\end{aligned} \tag{3.106}$$

*Proof.* It suffices to add the estimates (3.91) and (3.98) from Lemmas 3.19 and 3.20, respectively, and to use the estimate (3.103) together with the assumption given by (3.105). □

Having established Theorem 3.21, we now provide the corresponding rates of convergence.

**Theorem 3.22.** *Let $(\vec{\boldsymbol{\sigma}},\varphi) := ((\boldsymbol{\sigma},\mathbf{u}),\varphi) \in \mathbf{H} \times \mathrm{H}$ and $(\vec{\boldsymbol{\sigma}}_h,\varphi_h) := ((\boldsymbol{\sigma}_h,\mathbf{u}_h),\varphi_h) \in \mathbf{H}^h_k \times \mathcal{Q}^h_k$ be the unique solutions of the continuous and discrete schemes (3.6) and (3.55), respectively. Assume that for integers $r \in [1, k+1]$, $s \in [2, k+2]$, and $m \in [2, k+2]$, there hold $\boldsymbol{\sigma}|_K \in \mathbb{H}^r(K)$, $\mathbf{div}\,(\boldsymbol{\sigma})|_K \in \mathbf{H}^r(K)$,*

$\mathbf{u}|_K \in \mathbf{H}^s(K)$, $\varphi\big|_K \in \mathrm{H}^m(K)$, *and* $\mathbb{K}\big|_K \in \mathbb{W}^{m-1,\infty}(K)$, *for each* $K \in \mathcal{T}_h$. *Then, there exists a positive constant* $C$, *independent of* $h$, *such that*

$$\|(\vec{\boldsymbol{\sigma}},\varphi) - (\vec{\boldsymbol{\sigma}}_h,\varphi_h)\| \leq C\, h^{\min\{r,s-1,m-1\}} \left\{ \sum_{K\in\mathcal{T}_h} \Big( |\boldsymbol{\sigma}|^2_{r,K} + |\mathbf{div}\,(\boldsymbol{\sigma})|^2_{r,K} + |\mathbf{u}|^2_{s,K} + |\varphi|^2_{m,K} \Big) \right\}^{1/2} + C\, h^{s-1} \left\{ \sum_{K\in\mathcal{T}_h} |\mathbf{u}|^4_{s-1,4,K} \right\}^{1/4} . \tag{3.107}$$

*Proof.* It follows from (3.106) and the approximation properties (3.26), (3.36)-(3.39), (3.51), $(\mathbf{AP}^{\boldsymbol{\sigma}}_h)$, $(\mathbf{AP}^{\varphi}_h)$, and $(\mathbf{AP}^{\mathbf{u}}_h)$. □

### 3.5.2 Computable approximations of $\boldsymbol{\sigma}$, $\mathbf{u}$, $\boldsymbol{\varphi}$ and $p$

We first introduce the fully computable approximations of $\boldsymbol{\sigma}_h$, $\mathbf{u}_h$ and $\varphi_h$ given by

$$\widehat{\boldsymbol{\sigma}}_h := \boldsymbol{\mathcal{P}}^h_k(\boldsymbol{\sigma}_h), \quad \widehat{\mathbf{u}}_h := \boldsymbol{\mathcal{P}}^h_{k+1}(\mathbf{u}_h), \quad \text{and} \quad \widehat{\varphi}_h := \mathcal{P}^h_{k+1}(\varphi_h)\,, \tag{3.108}$$

and establish the corresponding *a priori* error estimates for the errors

$$\|((\boldsymbol{\sigma},\mathbf{u}),\varphi) - ((\widehat{\boldsymbol{\sigma}}_h,\widehat{\mathbf{u}}_h),\widehat{\varphi}_h)\|_{0,\Omega} := \|\boldsymbol{\sigma} - \widehat{\boldsymbol{\sigma}}_h\|_{0,\Omega} + \|\mathbf{u} - \widehat{\mathbf{u}}_h\|_{0,\Omega} + \|\varphi - \widehat{\varphi}_h\|_{0,\Omega}\,,$$

and

$$|(\mathbf{u},\varphi) - (\widehat{\mathbf{u}}_h,\widehat{\varphi}_h)|_{1,h} := |\mathbf{u} - \widehat{\mathbf{u}}_h|_{1,h} + |\varphi - \widehat{\varphi}_h|_{1,h}\,.$$

As shown below in Theorem 3.25, they yield exactly the same rate of convergence given by Theorem 3.22. Then, we begin the analysis with the following result.

**Theorem 3.23.** *Let* $(\vec{\boldsymbol{\sigma}},\varphi) := ((\boldsymbol{\sigma},\mathbf{u}),\varphi) \in \mathbf{H}\times\mathrm{H}$ *and* $(\vec{\boldsymbol{\sigma}}_h,\varphi_h) := ((\boldsymbol{\sigma}_h,\mathbf{u}_h),\varphi_h) \in \mathbf{H}_h \times \mathcal{Q}^h_k$ *be the unique solutions of the continuous and discrete schemes* (3.6) *and* (3.55), *respectively. In addition, let* $\widehat{\boldsymbol{\sigma}}_h$, $\widehat{\mathbf{u}}_h$, *and* $\widehat{\varphi}_h$ *be the discrete approximations introduced in* (3.108). *Then there exists a positive constant* $C > 0$, *independent of* $h$, *such that*

$$\begin{aligned} &\|((\boldsymbol{\sigma},\mathbf{u}),\varphi) - ((\widehat{\boldsymbol{\sigma}}_h,\widehat{\mathbf{u}}_h),\widehat{\varphi}_h)\|_{0,\Omega} + |(\mathbf{u},\varphi) - (\widehat{\mathbf{u}}_h,\widehat{\varphi}_h)|_{1,h} \\ &\leq C \left\{ \|(\vec{\boldsymbol{\sigma}},\varphi) - (\vec{\boldsymbol{\sigma}}_h,\varphi_h)\| + \|\boldsymbol{\sigma} - \boldsymbol{\mathcal{P}}^h_k(\boldsymbol{\sigma})\|_{0,\Omega} \right. \\ &\left. + \left\{ \sum_{K\in\mathcal{T}_h} \|\mathbf{u} - \boldsymbol{\mathcal{P}}^K_{k+1}(\mathbf{u})\|^2_{1,K} \right\}^{1/2} + \left\{ \sum_{K\in\mathcal{T}_h} \|\varphi - \mathcal{P}^K_{k+1}(\varphi)\|^2_{1,K} \right\}^{1/2} \right\}. \end{aligned}$$

*Proof.* It follows by using similar arguments from [69, Theorem 5.4]. □

Next, proceeding as in [69, Section 5.3], and according to (3.5) and the decomposition of $\boldsymbol{\sigma}$ provided by (3.1), we suggest the following computable approximation of the pressure:

$$\widehat{p}_h := -\frac{1}{2}\,\mathrm{tr}\Big(\widehat{\boldsymbol{\sigma}}_h + \widehat{c}_h\mathbb{I} + \widehat{\mathbf{u}}_h\otimes\widehat{\mathbf{u}}_h\Big) \quad \text{in} \quad \Omega\,, \qquad \text{with} \qquad \widehat{c}_h := -\frac{1}{2|\Omega|}\,\|\widehat{\mathbf{u}}_h\|^2_{0,\Omega}\,. \tag{3.109}$$

The following lemma establishes the corresponding *a priori* error estimate.

**Theorem 3.24.** *There exists a positive constant $C > 0$, independent of $h$, such that*

$$\|p - \widehat{p}_h\|_{0,\Omega} \leq C \left\{ \|(\vec{\boldsymbol{\sigma}}, \varphi) - (\vec{\boldsymbol{\sigma}}_h, \varphi_h)\| + \|\boldsymbol{\sigma} - \boldsymbol{\mathcal{P}}_k^h(\boldsymbol{\sigma})\|_{0,\Omega} + \|\mathbf{u} - \boldsymbol{\mathcal{P}}_{k+1}^h(\mathbf{u})\|_{0,4,\Omega} \right\}.$$

*Proof.* See [69, Theorem 5.5]. □

We end this section by providing the theoretical rates of convergence for $\widehat{\boldsymbol{\sigma}}_h$, $\widehat{\mathbf{u}}_h$, $\widehat{\varphi}_h$ and $\widehat{p}_h$.

**Theorem 3.25.** *Let $(\vec{\boldsymbol{\sigma}}, \varphi) := ((\boldsymbol{\sigma}, \mathbf{u}), \varphi) \in \mathbf{H} \times \mathrm{H}$ and $(\vec{\boldsymbol{\sigma}}_h, \varphi_h) := ((\boldsymbol{\sigma}_h, \mathbf{u}_h), \varphi_h) \in \mathbf{H}_h \times \mathcal{Q}_k^h$ be the unique solutions of the continuous and discrete schemes (3.6) and (3.55), respectively. In addition, let $((\widehat{\boldsymbol{\sigma}}_h, \widehat{\mathbf{u}}_h), \widehat{\varphi}_h)$, and $\widehat{p}_h$ be the discrete approximations introduced in (3.108) and (3.109), respectively. Assume that for integers $r \in [1, k+1]$, $s \in [2, k+2]$, and $m \in [2, k+2]$, there hold $\boldsymbol{\sigma}|_K \in \mathbb{H}^r(K)$, $\mathbf{div}(\boldsymbol{\sigma})|_K \in \mathbf{H}^r(K)$, $\mathbf{u}|_K \in \mathbf{H}^s(K)$, $\varphi\big|_K \in \mathrm{H}^m(K)$, and $\mathbb{K}\big|_K \in \mathbb{W}^{m-1,\infty}(K)$, for each $K \in \mathcal{T}_h$. Then, there exists a positive constant $C$, independent of $h$, such that*

$$\begin{aligned} &\|((\boldsymbol{\sigma}, \mathbf{u}), \varphi) - ((\widehat{\boldsymbol{\sigma}}_h, \widehat{\mathbf{u}}_h), \widehat{\varphi}_h)\|_{0,\Omega} + |(\mathbf{u}, \varphi) - (\widehat{\mathbf{u}}_h, \widehat{\varphi}_h)|_{1,h} + \|p - \widehat{p}_h\|_{0,\Omega} \\ &\leq C\, h^{\min\{r, s-1, m-1\}} \left\{ \sum_{K \in \mathcal{T}_h} \left( |\boldsymbol{\sigma}|_{r,K}^2 + |\mathbf{div}(\boldsymbol{\sigma})|_{r,K}^2 + |\mathbf{u}|_{s,K}^2 + |\varphi|_{m,K}^2 \right) \right\}^{1/2} \\ &\quad + C\, h^{s-1} \left\{ \sum_{K \in \mathcal{T}_h} |\mathbf{u}|_{s-1,4,K}^4 \right\}^{1/4}. \end{aligned} \tag{3.110}$$

*Proof.* It follows from Theorems 3.22 to 3.24, and the approximation properties provided along the chapter. In particular, applying (3.36) and (3.37), we readily find that

$$\left\{ \sum_{K \in \mathcal{T}_h} \|\varphi - \mathcal{P}_{k+1}^K(\varphi)\|_{1,K}^2 \right\}^{1/2} \leq C\, h^{m-1} \left\{ \sum_{K \in \mathcal{T}_h} |\varphi|_{m,K}^2 \right\}^{1/2},$$

and

$$\left\{ \sum_{K \in \mathcal{T}_h} \|\mathbf{u} - \boldsymbol{\mathcal{P}}_{k+1}^K(\mathbf{u})\|_{1,K}^2 \right\}^{1/2} \leq C\, h^{s-1} \left\{ \sum_{K \in \mathcal{T}_h} |\mathbf{u}|_{s,K}^2 \right\}^{1/2},$$

respectively. □

### 3.5.3 A convergent approximation of $\boldsymbol{\sigma}$ in the broken $\mathbb{H}(\mathbf{div}; \Omega)$-norm

In what follows we proceed as in [31, Section 5.3] and propose a second approximation $\widetilde{\boldsymbol{\sigma}}_h$ of the pseudostress $\boldsymbol{\sigma}$, which yields the same rate of convergence from Theorems 3.22 and 3.25 in the broken $\mathbb{H}(\mathbf{div}; \Omega)$-norm. For this purpose, for each $K \in \mathcal{T}_h$ we let $(\cdot, \cdot)_{\mathbf{div};K}$ be the usual $\mathbb{H}(\mathbf{div}; K)$-inner product with induced norm $\|\cdot\|_{\mathbf{div};K}$. Then, we let $\widetilde{\boldsymbol{\sigma}}_h \in \mathbb{L}^2(\Omega)$ be the tensor defined locally as $\widetilde{\boldsymbol{\sigma}}_h|_K := \widetilde{\boldsymbol{\sigma}}_{h,K}$, where $\widetilde{\boldsymbol{\sigma}}_{h,K} \in \mathbb{P}_{k+1}(K)$ is the unique solution of the problem

$$(\widetilde{\boldsymbol{\sigma}}_{h,K}, \boldsymbol{\tau}_h)_{\mathbf{div};K} = \int_K \widehat{\boldsymbol{\sigma}}_h : \boldsymbol{\tau}_h + \int_K \mathbf{div}(\boldsymbol{\sigma}_h) \cdot \mathbf{div}(\boldsymbol{\tau}_h) \qquad \forall\, \boldsymbol{\tau}_h \in \mathbb{P}_{k+1}(K). \tag{3.111}$$

Note here that the right-hand side of (3.111), and hence $\widetilde{\boldsymbol{\sigma}}_{h,K}$, is fully computable since both $\widehat{\boldsymbol{\sigma}}_h$ and $\mathbf{div}(\boldsymbol{\tau}_h)$ are. In addition, it is important to remark that $\widetilde{\boldsymbol{\sigma}}_{h,K}$ can be calculated for each $K \in \mathcal{T}_h$, independently. Then, the rate of convergence for the broken $\mathbb{H}(\mathbf{div}; \Omega)$-norm of $\boldsymbol{\sigma} - \widetilde{\boldsymbol{\sigma}}_h$ is established as follows.

**Lemma 3.26.** *Assume that the hypotheses of Theorem 3.22 are satisfied. Then, there exists a positiveconstant $C$, independent of $h$, such that*

$$\left\{ \sum_{K\in\mathcal{T}_h} \|\boldsymbol{\sigma}-\widetilde{\boldsymbol{\sigma}}_{h,K}\|^2_{\mathbf{div};K} \right\}^{1/2} = \mathcal{O}(h^{\min\{r,s-1,m-1\}}) \tag{3.112}$$

*Proof.* See [69, Theorem 5.7]. □

## 3.6 Numerical Examples

In this section we present some numerical examples illustrating the performance of the augmented mixed virtual element scheme (3.55), which was introduced and analized in Section 3.5. In addition, and similarly as in [68], the zero integral mean condition for tensors in the space (3.33) is imposed via a real Lagrange multiplier. Concerning the decompositions of $\Omega$ employed in our computations, we use two families of uniformly generated meshes: distorted squares and uniform triangular (see Figure 3.1).

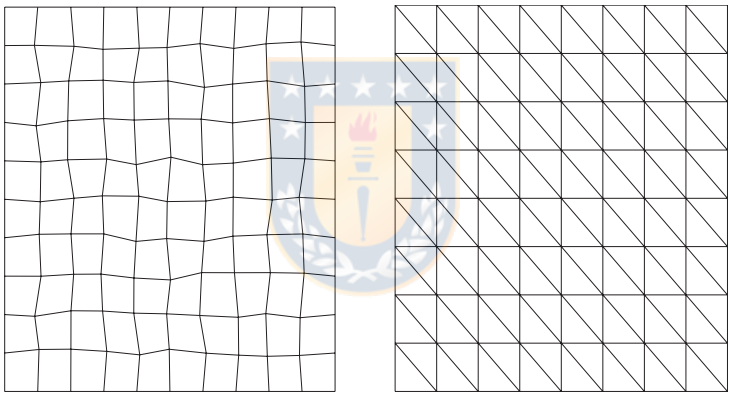

Figure 3.1: Sample meshes: distorted squares (left), triangular (right) (figure produced by the author).

We begin by introducing some notations. In what follows, $N$ stands for the total number of degrees of freedom (unknowns) of (3.55). Further, the individual errors are defined by

$$\mathtt{e}_0(\boldsymbol{\sigma}) := \|\boldsymbol{\sigma}-\widehat{\boldsymbol{\sigma}}_h\|_{0,\Omega}, \quad \mathtt{e}_0(\mathbf{u}) := \|\mathbf{u}-\widehat{\mathbf{u}}_h\|_{0,\Omega}, \quad \mathtt{e}_1(\mathbf{u}) := |\mathbf{u}-\widehat{\mathbf{u}}_h|_{1,\Omega} \quad \mathtt{e}_0(\varphi) := \|\varphi-\widehat{\varphi}\|_{0,\Omega}$$

$$\mathtt{e}_1(\varphi) := |\varphi-\widehat{\varphi}_h|_{1,\Omega}, \quad \mathtt{e}(p) := \|p-\widehat{p}_h\|_{0,\Omega}, \quad \text{and} \quad \mathtt{e}(\widetilde{\boldsymbol{\sigma}}) := \left\{ \sum_{K\in\mathcal{T}_h} \|\boldsymbol{\sigma}-\widetilde{\boldsymbol{\sigma}}_h\|^2_{\mathbf{div};K} \right\}^{1/2},$$

where $\widehat{\boldsymbol{\sigma}}_h, \widetilde{\boldsymbol{\sigma}}_h, \widehat{p}_h, \widehat{\mathbf{u}}_h$ and $\widehat{\varphi}_h$ are computed as in Section 3.5.2, whereas the associated experimental rates of convergence are given by

$$\mathtt{r}(\cdot) := \frac{\log(\mathtt{e}(\cdot)/\mathtt{e}'(\cdot))}{\log(h/h')},$$

where $\mathtt{e}$ and $\mathtt{e}'$ denote the corresponding errors for two consecutive meshes with sizes $h$ and $h'$, respectively. In turn, the nonlinear algebraic systems obtained are solved by the Newton method with a

tolerance of $10^{-6}$ and taking as initial iteration the solution $(\mathbf{u}_h, \varphi_h) = (\mathbf{0}, 0)$. The numerical results presented below were obtained using a MATLAB code.

In Example 1, we consider the square $\Omega := (0,1)^2$, set $\mu = 1$, $\mathbf{g} = (0,1)^{\mathbf{t}}$, the thermal conductivity $\mathbb{K} = \mathbb{I}$ in $\Omega$, and adequately manufacture the data so that the exact solution is given by the smooth functions

$$\varphi(\mathbf{x}) = x_1^2 + x_2^4\,,$$

$$\mathbf{u}(\mathbf{x}) = \begin{pmatrix} 2x_1^2 x_2(2x_2-1)(x_2-1)(x_1-1)^2 \\ -2x_1 x_2^2(x_2-1)^2(2x_1-1)(x_1-1) \end{pmatrix},$$

$$p(\mathbf{x}) = e^{x_2}\left(x_1 - \frac{1}{2}\right)^3$$

for all $\mathbf{x} := (x_1, x_2)^{\mathbf{t}} \in \Omega$. For this first example, we use meshes composed of distorted squares (see Figure 3.1).

In Example 2, we consider the square $\Omega := (-1/2, 3/2) \times (0,2)$, set $\mu = 1$, $\mathbf{g} = (0,1)^{\mathbf{t}}$, the thermal conductivity $\mathbb{K}(\mathbf{x}) = e^{(x_1+x_2)}\mathbb{I} \quad \forall\, \mathbf{x} := (x_1, x_2)^{\mathbf{t}} \in \Omega$. Then, the terms on the right-hand sides are adjusted so that the exact solution is given by the functions

$$\varphi(\mathbf{x}) = x_1^2(x_2^2+1)\,,$$

$$\mathbf{u}(\mathbf{x}) = \begin{pmatrix} 1 - e^{\lambda x_1}\cos(2\pi x_2) \\ \dfrac{\lambda}{2\pi} e^{\lambda x_1}\sin(2\pi x_2) \end{pmatrix},$$

$$p(\mathbf{x}) = -\frac{1}{2}e^{2\lambda x_1} + p_0$$

for all $\mathbf{x} := (x_1, x_2)^{\mathbf{t}} \in \Omega$ where $\lambda := \dfrac{-8\pi^2}{1+\sqrt{1+16\pi^2}}$ and $p_0$ is such that $\int_\Omega p = 0$. Here we make use of triangular meshes (see Figure 3.1).

| $h$ | $N$ | $\mathtt{e}_0(\boldsymbol{\sigma})$ | $\mathtt{r}_0(\boldsymbol{\sigma})$ | $\mathtt{e}_0(\mathbf{u})$ | $\mathtt{r}_0(\mathbf{u})$ | $\mathtt{e}_1(\mathbf{u})$ | $\mathtt{r}_1(\mathbf{u})$ | $\mathtt{e}_0(\varphi)$ | $\mathtt{r}_0(\varphi)$ |
|---|---|---|---|---|---|---|---|---|---|
| 0.2001 | 532 | 4.0438e-02 | −− | 2.0899e-03 | −− | 2.1666e-02 | −− | 8.7405e-03 | −− |
| 0.1008 | 1956 | 2.0448e-02 | 0.9934 | 5.9382e-04 | 1.8331 | 1.0365e-02 | 1.0742 | 2.1844e-03 | 2.0201 |
| 0.0504 | 7492 | 9.9385e-03 | 1.0427 | 1.5886e-04 | 1.9055 | 4.8940e-03 | 1.0845 | 5.4847e-04 | 1.9972 |
| 0.0252 | 29316 | 4.7872e-03 | 1.0539 | 4.0979e-05 | 1.9549 | 2.3559e-03 | 1.0548 | 1.3770e-04 | 1.9940 |
| 0.0126 | 115972 | 2.3363e-03 | 1.0353 | 1.0364e-05 | 1.9839 | 1.1560e-03 | 1.0275 | 3.4472e-05 | 1.9985 |

| $\mathtt{e}_1(\varphi)$ | $\mathtt{r}_1(\varphi)$ | $\mathtt{e}(p)$ | $\mathtt{r}(p)$ | $\mathtt{e}(\widetilde{\boldsymbol{\sigma}})$ | $\mathtt{r}_1(\widetilde{\boldsymbol{\sigma}})$ | iter |
|---|---|---|---|---|---|---|
| 2.0770e-01 | −− | 2.3446e-02 | −− | 1.7541e-01 | −− | 3 |
| 1.0475e-01 | 0.9973 | 1.2254e-02 | 0.9453 | 8.8354e-02 | 0.9991 | 3 |
| 5.2347e-02 | 1.0025 | 6.0438e-03 | 1.0215 | 4.4173e-02 | 1.0019 | 3 |
| 2.6240e-02 | 0.9964 | 2.9143e-03 | 1.0523 | 2.2076e-02 | 1.0007 | 3 |
| 1.3132e-02 | 0.9990 | 1.4191e-03 | 1.0384 | 1.1031e-02 | 1.0012 | 3 |

Table 3.1: Example 1: Convergence history using distorted squares with $k = 0$ (table produced by the author).

In Tables 3.1 and 3.2 we summarize the convergence history of our virtual scheme applied to Example 1 and 2. We notice there that the rate of convergence $\mathcal{O}(h)$ predicted by Theorem 3.25 is achieved by all the unknowns, with exception of $\|\mathbf{u}-\widehat{\mathbf{u}}\|_{0,\Omega}$ and $\|\varphi-\widehat{\varphi}_h\|_{0,\Omega}$, which have rate of convergence $\mathcal{O}(h^2)$. In addition, we can observe that our postprocessed stress $\widetilde{\boldsymbol{\sigma}}_h$ provided the correct order in the broken $\mathbb{H}(\mathbf{div})$-norm. Moreover, we can observe the robustness of our method with respect to the mesh shape. Finally, in order to graphically illustrate the accurateness of our discrete scheme, in Figures 3.2 and 3.3 we display some components of the approximate solutions for the examples. They all correspond to those obtained with the last mesh of each kind (distorted squares and triangles, respectively).

| $h$ | $N$ | $\mathtt{e}_0(\boldsymbol{\sigma})$ | $\mathtt{r}_0(\boldsymbol{\sigma})$ | $\mathtt{e}_0(\mathbf{u})$ | $\mathtt{r}_0(\mathbf{u})$ | $\mathtt{e}_1(\mathbf{u})$ | $\mathtt{r}_1(\mathbf{u})$ | $\mathtt{e}_0(\varphi)$ | $\mathtt{r}_0(\varphi)$ |
|---|---|---|---|---|---|---|---|---|---|
| 0.4000 | 504 | 8.4858e+01 | −− | 4.0905e+00 | −− | 4.8767e+01 | −− | 9.2742e-02 | −− |
| 0.2000 | 1904 | 5.8586e+01 | 0.5345 | 1.3543e+00 | 1.5947 | 3.0955e+01 | 0.6557 | 2.2886e-02 | 2.0187 |
| 0.1000 | 7404 | 3.2513e+01 | 0.8495 | 3.4294e-01 | 1.9816 | 1.6366e+01 | 0.9195 | 5.6053e-03 | 2.0296 |
| 0.5000 | 29204 | 1.6533e+01 | 0.9757 | 9.0330e-02 | 1.9247 | 8.3920e+00 | 0.9636 | 1.3887e-03 | 2.0130 |
| 0.0250 | 116004 | 8.2805e+00 | 0.9975 | 2.3206e-02 | 1.9607 | 4.2200e+00 | 0.9918 | 3.4822e-04 | 1.9957 |

| $\mathtt{e}_1(\varphi)$ | $\mathtt{r}_1(\varphi)$ | $\mathtt{e}(p)$ | $\mathtt{r}(p)$ | $\mathtt{e}(\widetilde{\boldsymbol{\sigma}})$ | $\mathtt{r}_1(\widetilde{\boldsymbol{\sigma}})$ | iter |
|---|---|---|---|---|---|---|
| 1.2798e+00 | −− | 4.5138e+01 | −− | 8.4914e+01 | −− | 5 |
| 6.2869e-01 | 1.0255 | 2.6777e+01 | 0.7533 | 5.8594e+01 | 0.5352 | 6 |
| 3.1236e-01 | 1.0092 | 1.4876e+01 | 0.8481 | 3.2514e+01 | 0.8497 | 8 |
| 1.5595e-01 | 1.0021 | 7.4528e+00 | 0.9971 | 1.6533e+01 | 0.9757 | 8 |
| 7.7953e-02 | 1.0005 | 3.7126e+00 | 1.0054 | 8.2805e+00 | 0.9975 | 8 |

Table 3.2: Example 2: Convergence history using triangles with $k = 0$ (table produced by the author).

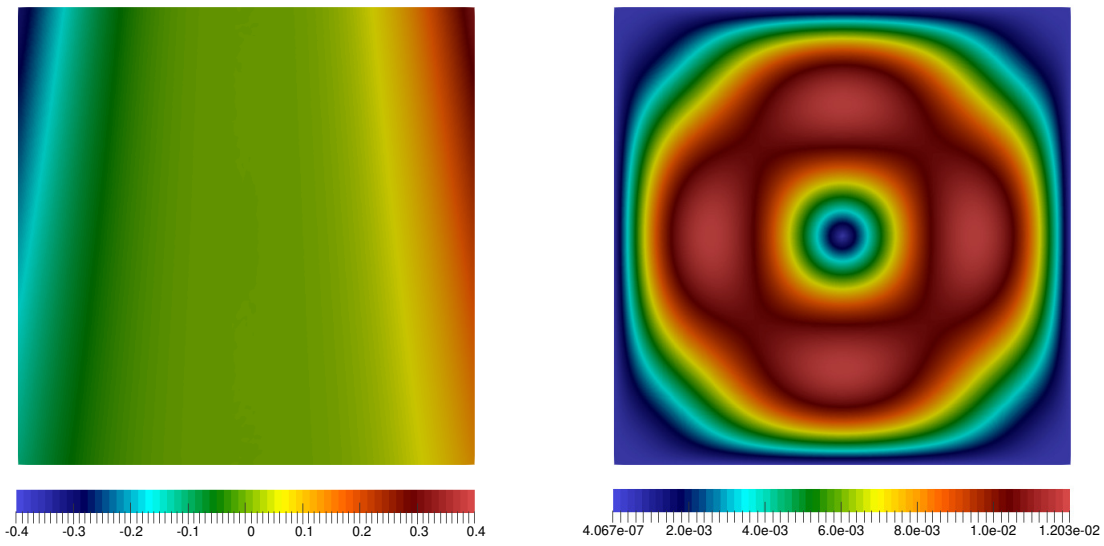


Figure 3.2: Example 1: $\widehat{p}_h$ (left) and $|\widehat{\mathbf{u}}_h|$ (right) with $N = 115972$ (figure produced by the author).

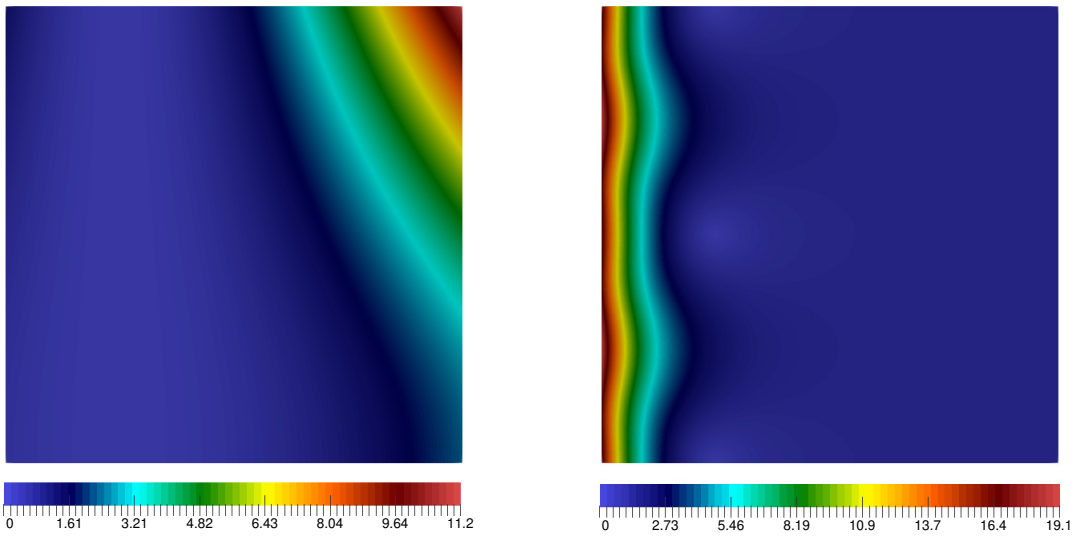


Figure 3.3: Example 2: $\widehat{\varphi}_h$ (left) and $|\widehat{\mathbf{u}}_h|$ (right) with $N = 116004$ (figure produced by the author).

# CHAPTER 4

## A posteriori error estimates for mixed virtual element methods

### 4.1 Introduction

The Virtual Element Method (VEM) was originally introduced in [13] for the solution of elliptic problems, followed by the mixed VEM proposed in [28]. Subsequently, new mixed VEMs have been analysed for the solution of the Stokes, Navier-Stokes, and Brinkman problem [10, 39, 30, 20, 21, 69, 31, 90].

One of the defining characteristics of the VEM is that it allows for the use of very general polygonal and polyhedral meshes. As such, it naturally lends itself as a flexible solution step within automatically adaptive algorithms. Indeed, mesh refinement and coarsening strategies can be implemented very easily and efficiently as, for instance, hanging nodes are simply treated as new nodes, with no detrimental affect on the quality of the approximation. Moreover, it has been shown that the VEM in primal form allows for extremely aggressive mesh adaptation producing strongly solution-adapted polygonal meshes [38]. In this respect, the design and analysis of adaptive mesh refinement strategies based on robust a posteriori error indicators for the VEM approach and, in particular, for the mixed-VEM is an attractive proposition.

Several error estimators have been proposed in the context of VEM for primal forms (see, e.g.,[24, 38, 26, 81, 79, 44]). Firstly, the authors of [24] proposed a posteriori error bounds for the $C^1$-conforming VEM for the two-dimensional Poisson problem. Next, a posteriori error bounds for the $C^0$-conforming VEM for the discretization of second-order linear elliptic reaction-convection-diffusion problems with nonconstant coefficients in two and three dimension were proposed in [38], whereas a residual-based a posteriori error estimator for the VEM discretization of the Poisson problem with discontinuous diffusivity coefficient was introduced and analysed in [26]. Moreover, in [81] and [79], the authors developed a posteriori error analysis of a VEM approach for the Steklov eigenvalue problem and the spectral analysis for the elasticity equations, respectively. Finally, in [44] a general recovery-based a posteriori error estimation framework for the VEM of arbitrary order on general polygonal/polyhedral meshes has been developed. A posteriori analisys of other techniques of mixed-type on general meshes have been presented in [51] for the Mixed High-Order method, in [22] for the Mimetic Finite Difference method, and in [92] for lowest-order locally conservative methods. However, to the best of our knowledge, *no* a posteriori error analysis for mixed VEM is available from the literature.

The aim of this chapter is to introduce the basic tools to develop the a posteriori error analysis for the mixed VEM. To this end, we consider a second order elliptic equation in divergence form with mixed boundary condition, discretised using the basic mixed VEM of [15]. As usual in the VEM approach, we introduce fully computable approximations for the virtual approximation of the flux variable and establish its corresponding a priori error estimates. In particular, in order to improve on the sub-optimal order provided by the computable component of the flux variable in the broken H(div)-norm, observed numerically in [68], we follow [31] and construct by postprocessing second computable approximation of the flux variable, which has an optimal rate of convergence in the aforementioned norm.

The a posteriori error analysis is based on a global inf-sup condition coming from the well-posedness of the continuos problem. Upper bounds are shown for the scalar variable in the $\mathrm{L}^2$-norm, the VEM flux variable in the H(div)-norm, its projection in the $\mathrm{L}^2$-norm, and postprocessing in the broken H(div)-norm. The proof uses properties of the interpolation operator associated to the virtual subspace of the flux variable and Clément-type interpolation operators, together with a suitable Helmholtz decomposition. Moreover, some inverse inequalities and localization techniques based on bubble functions will serve to show a lower bound for the error. In this way, we are able to establish the equivalence up to virtual inconsistency terms between the error and the error estimator for the postprocessing of the virtual element approximation, measured in the broken H(div)-norm.

The remainder of the chapter has been structured as follows. In what is left of this section, we introduce some standard notations and the required functional spaces. In Section 4.2 we introduce the model problem and presents the associate variational formulation. In Section 4.3, we present the mixed virtual element scheme. The a posteriori error analysis is laid down in details in Section 4.5. In Section 4.6, we propose an adaptive algorithm and test its effectiveness with some numerical examples.

Hereafter, we use the following notation for any vector field $\boldsymbol{\tau} = (\tau_i)_{i=1,2}$ and any scalar field $v$:

$$\operatorname{div}\boldsymbol{\tau} := \partial_1\tau_1 + \partial_2\tau_2 \quad \operatorname{rot}\boldsymbol{\tau} := \partial_1\tau_2 - \partial_2\tau_1 \quad \text{and} \quad \mathbf{rot}\, v := (\partial_2 v, -\partial_1 v)^{\mathbf{t}} .$$

Next, given a bounded domain $\mathcal{O} \subseteq \mathrm{R}^2$ with boundary $\partial\mathcal{O}$, we let $\nu$ be the outward unit normal vector on $\partial\mathcal{O}$. Also, for $s \geq 0$, the symbol $|\cdot|_{s,\mathcal{O}}$ stands for the norm of the Hilbertian Sobolev spaces $\mathrm{H}^s(\Omega)$, with the convention $\mathrm{H}^0(\mathcal{O}) := \mathrm{L}^2(\mathcal{O})$. We also define the Hilbert spaces

$$\mathrm{H}(\operatorname{div};\mathcal{O}) := \left\{ \boldsymbol{\tau} \in [\mathrm{L}^2(\mathcal{O})]^2 : \quad \operatorname{div}\boldsymbol{\tau} \in \mathrm{L}^2(\mathcal{O}) \right\},$$

and

$$\mathrm{H}(\operatorname{rot};\mathcal{O}) := \left\{ \boldsymbol{\tau} \in [\mathrm{L}^2(\mathcal{O})]^2 : \quad \operatorname{rot}\boldsymbol{\tau} \in \mathrm{L}^2(\mathcal{O}) \right\},$$

whose norms are given by

$$\|\boldsymbol{\tau}\|^2_{\operatorname{div};\mathcal{O}} := \|\boldsymbol{\tau}\|^2_{0,\mathcal{O}} + \|\operatorname{div}\boldsymbol{\tau}\|^2_{0,\mathcal{O}} \quad \text{and} \quad \|\boldsymbol{\tau}\|^2_{\operatorname{rot};\mathcal{O}} := \|\boldsymbol{\tau}\|^2_{0,\mathcal{O}} + \|\operatorname{rot}\boldsymbol{\tau}\|^2_{0,\mathcal{O}} .$$

In addition, we will denote with $c$ and $C$, with or without subscripts, tildes, or hats, a generic constant independent of the mesh parameter $h$, which may take different values in different occurrences.

## 4.2 The model problem

Let us assume that $\Omega \subset \mathrm{R}^2$ be a bounded domain with polygonal boundary $\Gamma$. We denote by $\nu$ the outward unit normal vector to the boundary $\Gamma$. Moreover, we assume that $\Gamma$ admits a disjoint partition $\Gamma = \overline{\Gamma}_D \cup \overline{\Gamma}_N$, where $\Gamma_D$ and $\Gamma_N$ are open subsets of $\Gamma$, with $|\Gamma_D|, |\Gamma_N| \neq 0$. We consider the problem

$$-\operatorname{div}(\boldsymbol{\kappa}\nabla u) = f \quad \text{in} \quad \Omega, \quad u = g \quad \text{on} \quad \Gamma_D \quad \text{and} \quad (\boldsymbol{\kappa}\nabla u)\cdot\nu = 0 \quad \text{on} \quad \Gamma_N, \tag{4.1}$$

where $f \in \mathrm{L}^2(\Omega)$, $g \in \mathrm{H}^{1/2}(\Gamma_D)$ and $\boldsymbol{\kappa} \in [\mathrm{L}^\infty(\Omega)]^{2\times 2}$ is an uniformly positive definite tensor, which is assumed to be known. In particular, we denote by $\kappa^*$ the positive constant satisfying

$$\boldsymbol{\kappa}^{-1}\boldsymbol{\zeta}\cdot\boldsymbol{\zeta} \geq \kappa^*|\boldsymbol{\zeta}|^2\,, \quad \forall\, \boldsymbol{\zeta} \in [\mathrm{L}^2(\Omega)]^2\,. \tag{4.2}$$

We need to introduce the following spaces

$$H := \Big\{\boldsymbol{\tau} \in \mathrm{H}(\operatorname{div};\Omega) : \quad \boldsymbol{\tau}\cdot\nu = 0 \quad \text{on} \quad \Gamma_N\Big\} \quad \text{and} \quad Q := \mathrm{L}^2(\Omega)\,, \tag{4.3}$$

endorsed with the norms

$$\|\tau\|_H := \|\tau\|_{0,\Omega} + \|\operatorname{div}\tau\|_{0,\Omega} \quad \text{and} \quad \|v\|_Q := \|v\|_{0,\Omega}\,.$$

Furthermore, we make use of the product space $H \times Q$ with the norm

$$\|(\tau, v)\|_{H\times Q} := \|\tau\|_H + \|v\|_Q\,.$$

Then, by introducing the flux variable $\boldsymbol{\sigma} := \boldsymbol{\kappa}\nabla u$ in $\Omega$ as additional unknown, a mixed variational formulation of (4.1) becomes: Find $(\boldsymbol{\sigma}, u) \in H \times Q$ such that

$$\begin{aligned} a(\boldsymbol{\sigma},\boldsymbol{\tau}) + b(\boldsymbol{\tau}, u) &= \langle \boldsymbol{\tau}\cdot\nu, g\rangle_{\Gamma_D} \qquad \forall\, \boldsymbol{\tau} \in H, \\ b(\boldsymbol{\sigma}, v) &= -\int_\Omega fv \qquad \forall\, v \in Q\,, \end{aligned} \tag{4.4}$$

where $\langle\cdot,\cdot\rangle$ stands for the duality pairing between $\mathrm{H}^{-1/2}(\Gamma_D) \to \mathrm{H}^{1/2}(\Gamma_D)$. In turn, $a : H \times H \to \mathrm{R}$ and $b : H \times Q \to \mathrm{R}$ are the bounded bilinear forms defined by

$$a(\boldsymbol{\sigma},\boldsymbol{\tau}) := \int_\Omega \boldsymbol{\kappa}^{-1}\boldsymbol{\sigma}\cdot\boldsymbol{\tau}, \quad \text{and} \quad b(\boldsymbol{\tau}, u) := \int_\Omega u \operatorname{div}\boldsymbol{\tau}. \tag{4.5}$$

Under the assumptions on $\boldsymbol{\kappa}$, $f$ and $g$, the existence and uniqueness of the weak solution of (4.4) is consequence of the Babuška-Brezzi theory.

## 4.3 The virtual element method

Let $\{\mathcal{T}_h\}_{h>0}$ be a family of decompositions of $\Omega$ into open non-overlapping polygonal elements. Then, for each $K \in \mathcal{T}_h$ we denote its diameter by $h_K$, and also, as usual, $h := \max\Big\{h_K : K \in \mathcal{T}_h\Big\}$. In what follows we make the following mesh regularity assumptions which are standard in this context (cf.[13, 28]).

**Assumption 4.1.** *The family of decompositions $\{\mathcal{T}_h\}_{h>0}$ satisfies:*

*a) the ratio between the shortest edge and the diameter $h_K$ of $K$ is bigger than $C_{\mathcal{T}}$, and*

*b) $K$ is star-shaped with respect to a ball $B$ of radius $C_{\mathcal{T}}h_K$ and center $\mathbf{x}_B \in K$.*

**Remark 4.2.** *The above assumptions imply that each $K \in \mathcal{T}_h$ is simply connected and that there exists an integer $N_{\mathcal{T}}$ (depending only on $C_{\mathcal{T}}$), such that the numbers of edges of each $K \in \mathcal{T}_h$ is bounded above by $N_{\mathcal{T}}$. Moreover, as each element $K$ is star-shaped, it admits a sub-triangulation $\mathcal{T}_h^K$ obtained by joining each vertex of $K$ with a point with respect to which $K$ is starred. And the uniform bound on the diamater of the mesh edges ensures that the resulting global triangulation $\widehat{\mathcal{T}_h} := \bigcup_{K\in\mathcal{T}_h} \mathcal{T}_h^K$ is shape-regular. We finally note that the above assumptions allow for very general possibly non-convex polygonal elements. In particular, they permit the natural incorporation of so-called hanging nodes, thus completely avoiding the need of removing hanging nodes typical of standard mesh adaptation algorithms.*

Now, given an integer $\ell \geq 0$ and $\mathcal{O} \subseteq \mathrm{R}^d$, $d = 1, 2$, we denote by $\mathrm{P}_\ell(\mathcal{O})$ the space of polynomials on $\mathcal{O}$ of degree up to $\ell$. Then, given an edge $e \in \partial K$ with barycenter $x_e$ and diameter $h_e$, we denote the following set of $(\ell + 1)$ normalized monomials on $e$

$$\mathcal{B}_\ell(e) \ := \ \left\{ \left( \frac{x - x_e}{h_e} \right)^j \right\}_{0\leq j\leq \ell},$$

which certainly constitutes a basis on $\mathrm{P}_\ell(e)$. Similarly, on $K \in \mathcal{T}_h$ with barycenter $\mathbf{x}_K$, we define the following set of $\frac{1}{2}(\ell + 1)(\ell + 2)$ normalized monomials

$$\mathcal{B}_\ell(K) \ := \ \left\{ \left( \frac{\mathbf{x} - \mathbf{x}_K}{h_K} \right)^{\boldsymbol{\alpha}} \right\}_{0\leq |\boldsymbol{\alpha}|\leq \ell},$$

which is a basis of $\mathrm{P}_\ell(K)$. Notice that in the definition of $\mathcal{B}_\ell(K)$ above, we made use of the multi-index notation, that is, given $\mathbf{x} := (x_1, x_2)^{\mathbf{t}} \in \mathrm{R}^2$ and $\boldsymbol{\alpha} := (\alpha_1, \alpha_2)^{\mathbf{t}}$, with non-negative integers $\alpha_1, \alpha_2$, we set $\mathbf{x}^{\boldsymbol{\alpha}} := x_1^{\alpha_1} x_2^{\alpha_2}$ and $|\boldsymbol{\alpha}| := \alpha_1 + \alpha_2$.

We further let $\mathcal{G}_\ell(K)$ be a basis of $\big(\nabla \mathrm{P}_{\ell+1}(K)\big) \cap [\mathrm{P}_\ell(K)]^2$, whereas with $\mathcal{G}_\ell^\perp(K)$ we denote a basis of the $[\mathrm{L}^2(K)]^2$-orthogonal of $\mathcal{G}_\ell(K)$ in $[\mathrm{P}_\ell(K)]^2$.

Throughout the chapter, we denote by $\Pi_k^0 : \mathrm{L}^2(K) \to \mathrm{P}_k(K)$ the $\mathrm{L}^2(K)$-orthogonal projection onto the space $\mathrm{P}_k(K)$, for any $K \in \mathcal{T}_h$ and $k \geq 0$. In addition, we will make use of a vectorial version of the aforementioned projector, which is denoted by $\boldsymbol{\Pi}_k^0$. The following approximation properties of these projectors are well-known:

$$\|v - \Pi_k^0(v)\|_{0,K} \ \leq \ Ch_K^m |v|_{m,K} \quad \text{and} \quad \|\boldsymbol{\tau} - \boldsymbol{\Pi}_k^0(\boldsymbol{\tau})\|_{0,K} \ \leq \ Ch_K^m |\boldsymbol{\tau}|_{m,K} \tag{4.6}$$

for all $K \in \mathcal{T}_h$, and for all $v \in \mathrm{H}^m(K)$, $\boldsymbol{\tau} \in [\mathrm{H}^m(K)]^2$, with $m \in \{0, 1, \ldots, k + 1\}$.

## 4.4 Virtual subspace and its approximation properties

For any integer $k \geq 0$, we introduce the finite dimensional subspaces of $H$ and $Q$, respectively, given by

$$H_h \ := \ \Big\{ \boldsymbol{\tau} \in H : \quad \boldsymbol{\tau}\big|_K \in H_h^K \quad \forall\, K \in \mathcal{T}_h \Big\}, \tag{4.7}$$

and

$$Q_h \;:=\; \Big\{ v \in Q : \quad v\big|_K \in Q_h^K \quad \forall\, K \in \mathcal{T}_h \Big\}, \tag{4.8}$$

where $Q_h^K := \mathrm{P}_k(K)$, and $H_h^K$ is the virtual element space introduced in [15, Section 3.1]. This is defined by

$$\begin{aligned} H_h^K \;:=\; \Big\{ \boldsymbol{\tau} \in \mathrm{H}(\mathrm{div}; K) \cap \mathrm{H}(\mathrm{rot}; K) \,:\quad & \boldsymbol{\tau}\cdot\nu|_e \in \mathrm{P}_k(e) \quad \forall \text{ edge } e \in \partial K\,, \\ & \mathrm{div}\,\boldsymbol{\tau} \in \mathrm{P}_k(K) \quad \text{and} \quad \mathrm{rot}\,\boldsymbol{\tau} \in \mathrm{P}_{k-1}(K) \Big\}. \end{aligned} \tag{4.9}$$

and is characterised by the following degrees of freedom (cf. [15, 14]):

$$\begin{aligned} &\int_e q\,(\boldsymbol{\tau}\cdot\nu) \quad \forall\, q \in \mathcal{B}_k(e)\,, && \forall \text{ edge } e \quad \text{in} \quad \mathcal{T}_h, \\ &\int_K \boldsymbol{\tau}\cdot\nabla q \quad \forall\, q \in \mathcal{B}_k(K)\setminus\{1\}, && \forall\, K \in \mathcal{T}_h, \\ &\int_K \boldsymbol{\tau}\cdot\eta \quad \forall\, \eta \in \mathcal{G}_k^{\perp}(K)\,, && \forall\, K \in \mathcal{T}_h. \end{aligned} \tag{4.10}$$

As was remarked in [15, Section 3.2] (see also [14, Section 3.5]), the degrees of freedom (4.10) allow the explicit computation of the projection $\boldsymbol{\Pi}_k^0(\boldsymbol{\tau})$ using only the degrees of freedom of $\boldsymbol{\tau}$. Moreover, collected together, the local degrees of freedom (4.10) provide a set of degrees of freedom for the global virtual element space $H_h$.

For each $\boldsymbol{\tau} \in H$ such that $\boldsymbol{\tau}\big|_K \in [\mathrm{H}^1(K)]^2$ for all $K \in \mathcal{T}_h$, we may denote by $\boldsymbol{\tau}_I \in H_h$ the Lagrange interpolant of $\boldsymbol{\tau}$ with respect to the degrees of freedom (4.10). For each $q \in \mathcal{B}_k(K)$ we find that

$$\int_K q\,\mathrm{div}(\boldsymbol{\tau}-\boldsymbol{\tau}_I) \;=\; -\int_K (\boldsymbol{\tau}-\boldsymbol{\tau}_I)\cdot\nabla q + \int_{\partial K} q(\boldsymbol{\tau}-\boldsymbol{\tau}_I)\cdot\nu \;=\; 0,$$

which, thanks to the fact that $\mathrm{div}\,\boldsymbol{\tau}_I \in \mathrm{P}_k(K)$, implies the commutative property

$$\mathrm{div}\,\boldsymbol{\tau}_I \;=\; \Pi_k^0(\mathrm{div}\,\boldsymbol{\tau}) \qquad \forall\, \boldsymbol{\tau} \in [\mathrm{H}^1(K)]^2. \tag{4.11}$$

Hence we have the following approximation error estimates [13, 15].

**Lemma 4.3.** *Let $r$ be an integer such that $1 \le r \le k+1$. Then, there exists a constant $C > 0$, independent of $K$, such that for each $\boldsymbol{\tau} \in [\mathrm{H}^r(K)]^2$ such that $\mathrm{div}\,\boldsymbol{\tau} \in \mathrm{H}^r(K)$ there holds*

$$\|\boldsymbol{\tau}-\boldsymbol{\tau}_I\|_{\mathrm{div};K} \;\le\; C\,h_K^r \Big\{ |\boldsymbol{\tau}|_{r,K} \,+\, |\mathrm{div}\,\boldsymbol{\tau}|_{r,K} \Big\} \qquad \forall\, K \in \mathcal{T}_h\,. \tag{4.12}$$

*Proof.* The bound on the divergence term follows from (4.11) and (4.6). The result then follows from classical arguments [27]. □

### 4.4.1 Discrete formulation

We now aim to define a virtual scheme for our problem (4.4) based on the discrete spaces (4.7) and (4.8). To this end, we first notice that the bilinear form $b$ (cf.(4.5)) is explicitly computable for all

$(\boldsymbol{\tau}, v) \in H_h \times Q_h$, just by accessing the degrees of freedom (4.10). On the contrary, for each $K \in \mathcal{T}_h$, the local version $a^K : H_h^K \times H_h^K \to \mathrm{R}$ of the bilinear form $a$, which, is defined for all $\boldsymbol{\zeta}, \boldsymbol{\tau} \in H_h^K \times H_h^K$ by

$$a^K(\boldsymbol{\zeta}, \boldsymbol{\tau}) := \int_K \boldsymbol{\kappa}^{-1} \boldsymbol{\zeta} \cdot \boldsymbol{\tau}, \tag{4.13}$$

is not explicitly computable for $\boldsymbol{\zeta}, \boldsymbol{\tau} \in H_h^K$ since in general $\boldsymbol{\zeta}$ and $\boldsymbol{\tau}$ are not known explicitly on the whole of $K$. In order to deal with this difficulty, we follow [15, Section 3.3] and introduce a local bilinear form $a_h^K : H_h^K \times H_h^K \to \mathrm{R}$ defined by

$$a_h^K(\boldsymbol{\zeta}, \boldsymbol{\tau}) := a^K(\boldsymbol{\Pi}_k^0(\boldsymbol{\zeta}), \boldsymbol{\Pi}_k^0(\boldsymbol{\tau})) + \mathcal{S}^K(\boldsymbol{\zeta} - \boldsymbol{\Pi}_k^0(\boldsymbol{\zeta}), \boldsymbol{\tau} - \boldsymbol{\Pi}_k^0(\boldsymbol{\tau}))\,, \tag{4.14}$$

where $\mathcal{S}^K : H_h^K \times H_h^K \to \mathrm{R}$ is any symmetric and positive definite bilinear form such that

$$\widehat{c}_0 a^K(\boldsymbol{\zeta}, \boldsymbol{\zeta}) \leq \mathcal{S}^K(\boldsymbol{\zeta}, \boldsymbol{\zeta}) \;\leq\; \widehat{c}_1 a^K(\boldsymbol{\zeta}, \boldsymbol{\zeta}) \qquad \forall\, \boldsymbol{\zeta} \in H_h^K, \quad \text{with} \quad \boldsymbol{\Pi}_k^0(\boldsymbol{\zeta}) = 0\,, \tag{4.15}$$

with constants $\widehat{c}_0, \widehat{c}_1 > 0$ which depend only on the shape regularity constant $C_{\mathcal{T}}$ and on $\boldsymbol{\kappa}$. In particular, to define $\mathcal{S}^K$ we can consider the bilinear form associated to the identity matrix in $\mathrm{R}^{n_k^K}$ with respect to the local basis determined by the degrees of freedom (4.10), and where $n_k^K = \dim H_h^K$. (cf.[13, 28])

The following two lemmas establish the properties of the bilinear form $a_h^K$ and the consistency error between $a_h^K$ and $a^K$, respectively.

**Lemma 4.4.** *For all $K \in \mathcal{T}_h$, there holds*

$$\textbf{(Consistency)} \qquad a_h^K(p, \boldsymbol{\zeta}) = \int_K \boldsymbol{\kappa}^{-1} p \cdot \boldsymbol{\Pi}_k^0(\boldsymbol{\zeta}) \qquad \forall\, p \in [\mathrm{P}_k(K)]^2 \quad \textit{and} \quad \forall\, \boldsymbol{\zeta} \in H_k^K\,,$$

*and further, there exist constants $\alpha_*, \alpha^* > 0$, such that*

$$\textbf{(Stability)} \qquad \alpha_* a^K(\boldsymbol{\zeta}, \boldsymbol{\zeta}) \leq a_h^K(\boldsymbol{\zeta}, \boldsymbol{\zeta}) \leq \alpha^* a^K(\boldsymbol{\zeta}, \boldsymbol{\zeta}) \qquad \forall\, \boldsymbol{\zeta} \in H_h^K, \forall\, K \in \mathcal{T}_h\,.$$

*Proof.* We refer to [15] and [23] for the details. □

**Lemma 4.5.** *There exists a constant $C > 0$, depending only on $\boldsymbol{\kappa}, \widehat{c}_1$ and $\alpha^*$, such that*

$$(a_h^K - a^K)(\boldsymbol{\zeta}, \boldsymbol{\tau}) \leq C \Big\{ \|\boldsymbol{\zeta} - \boldsymbol{\Pi}_k^0(\boldsymbol{\zeta})\|_{0,K} + \|\boldsymbol{\kappa}^{-1}\boldsymbol{\Pi}_k^0(\boldsymbol{\zeta}) - \boldsymbol{\Pi}_k^0(\boldsymbol{\kappa}^{-1}\boldsymbol{\Pi}_k^0(\boldsymbol{\zeta}))\|_{0,K} \Big\} \|\boldsymbol{\tau}\|_{0,K} \tag{4.16}$$

*for all $\boldsymbol{\zeta}, \boldsymbol{\tau} \in H_h^K$ and for all $K \in \mathcal{T}_h$.*

*Proof.* We have that

$$\begin{aligned}(a_h^K - a^K)(\boldsymbol{\zeta}, \boldsymbol{\tau}) \;=\; & -\int_K \Big\{ \boldsymbol{\kappa}^{-1}\boldsymbol{\Pi}_k^0(\boldsymbol{\zeta}) - \boldsymbol{\Pi}_k^0(\boldsymbol{\kappa}^{-1}\boldsymbol{\Pi}_k^0(\boldsymbol{\zeta})) \Big\} \cdot (\boldsymbol{\tau} - \boldsymbol{\Pi}_k^0(\boldsymbol{\tau})) - \int_K \boldsymbol{\kappa}^{-1}(\boldsymbol{\zeta} - \boldsymbol{\Pi}_k^0(\boldsymbol{\zeta})) \cdot \boldsymbol{\tau} \\ & + \mathcal{S}^K(\boldsymbol{\zeta} - \boldsymbol{\Pi}_k^0(\boldsymbol{\zeta}), \boldsymbol{\tau} - \boldsymbol{\Pi}_k^0(\boldsymbol{\tau}))\,.\end{aligned}$$

The results now follows from Cauchy-Schwarz inequality and the properties of the bilinear $\mathcal{S}^K$. □

According to the definition (4.14) the global discrete bilinear form $a_h : H_h \times H_h \to \mathrm{R}$ can now be defined summing together the local contribution (4.14), that is

$$a_h(\boldsymbol{\zeta}, \boldsymbol{\tau}) := \sum_{K \in \mathcal{T}_h} a_h^K(\boldsymbol{\zeta}, \boldsymbol{\tau}) \qquad \forall\, \boldsymbol{\zeta}, \boldsymbol{\tau} \in H_h. \tag{4.17}$$

In this way, the virtual element method associated with the formulation (4.4) reads:

Find $(\boldsymbol{\sigma}_h, u_h) \in H_h \times Q_h$ such that

$$\begin{aligned} a_h(\boldsymbol{\sigma}_h, \boldsymbol{\tau}_h) + b(\boldsymbol{\tau}_h, u_h) &= \langle \boldsymbol{\tau}_h \cdot \nu, g \rangle_{\Gamma_D} \qquad \forall\, \boldsymbol{\tau}_h \in H_h, \\ b(\boldsymbol{\sigma}_h, v_h) &= -\int_\Omega f v_h \qquad \forall\, v_h \in Q_h. \end{aligned} \tag{4.18}$$

The well-posedness of (4.18) follows from Lemma 4.4 and of the well-posedness of (4.4). In addition, we have the following result about the a priori error estimates for the schemes (4.4) and (4.18).

**Theorem 4.6.** *Let $(\boldsymbol{\sigma}, u) \in H \times Q$ and $(\boldsymbol{\sigma}_h, u_h) \in H_h \times Q_h$ be the unique solutions of the continuous and discrete schemes (4.4) and (4.18), respectively. In addition, assume that for some $s \in [1, k+1]$ there hold $\boldsymbol{\sigma}\big|_K \in \mathbf{H}^s(K)$ and $\operatorname{div} \boldsymbol{\sigma}\big|_K, u\big|_K \in \mathrm{H}^s(K)$ for each $K \in \mathcal{T}_h$. Then, there exist a positive constant $C > 0$, independent of $h$, such that*

$$\|(\boldsymbol{\sigma}, u) - (\boldsymbol{\sigma}_h, u_h)\|_{H \times Q} \leq C h^s \left\{ \sum_{K \in \mathcal{T}_h} |\boldsymbol{\sigma}|_{s,K}^2 + |\operatorname{div} \boldsymbol{\sigma}|_{s,K}^2 + |u|_{s,K}^2 \right\}^{1/2}. \tag{4.19}$$

*Proof.* The result is consequence of [28, Theorem 6.1] and of a straightforward application of the approximation properties provided by (4.6) and Lemma 4.3. □

### 4.4.2 Computable approximations

A first fully computable approximation $\widehat{\boldsymbol{\sigma}}_h \in Q$ of the VEM solution $\boldsymbol{\sigma}_h \in H$ is given by

$$\widehat{\boldsymbol{\sigma}}_h := \boldsymbol{\Pi}_k^0(\boldsymbol{\sigma}_h). \tag{4.20}$$

The corresponding a priori error estimates for the error $\|\boldsymbol{\sigma} - \widehat{\boldsymbol{\sigma}}_h\|_Q$ immediately follows from the foregoing Theorem 4.6 and the triangle inequality.

**Theorem 4.7.** *Assume that the hypotheses of Theorem 4.6 are satisfied. Then, there exists a positive constant $C > 0$, independent of $h$, such that*

$$\|\boldsymbol{\sigma} - \widehat{\boldsymbol{\sigma}}_h\|_Q + \|u - u_h\|_Q \leq C h^s \left\{ \sum_{K \in \mathcal{T}_h} |\boldsymbol{\sigma}|_{s,K}^2 + |\operatorname{div} \boldsymbol{\sigma}|_{s,K}^2 + |u|_{s,K}^2 \right\}^{1/2}. \tag{4.21}$$

Next, motivated by the non-satisfactory order provided by $\widehat{\boldsymbol{\sigma}}_h$ in the broken H(div)-norm (see [68, Section 5] for numerical evidences of this fact), we proceed as in [31, Section 5.3] (see also [32]) and construct, by local postprocessing, a second approximation $\boldsymbol{\sigma}_h^\star$ for the flux variable $\boldsymbol{\sigma}$ which has an

optimal rate of convergence in such norm. To this end, for each $K \in \mathcal{T}_h$ we let $(\cdot,\cdot)_{\mathrm{div};K}$ be the usual $\mathrm{H}(\mathrm{div};K)$-inner product with induced norm $\|\cdot\|_{\mathrm{div};K}$ and let $\boldsymbol{\sigma}_h^\star\big|_K := \boldsymbol{\sigma}_{h,K}^\star \in [\mathrm{P}_{k+1}(K)]^2$ be the unique solution of the local problem

$$(\boldsymbol{\sigma}_{h,K}^\star, \boldsymbol{\tau}_h)_{\mathrm{div};K} = \int_K \widehat{\boldsymbol{\sigma}}_h \cdot \boldsymbol{\tau}_h \; + \; \int_K \mathrm{div}\,\boldsymbol{\sigma}_h \,\mathrm{div}\,\boldsymbol{\tau}_h \qquad \forall\, \boldsymbol{\tau}_h \in [\mathrm{P}_{k+1}(K)]^2. \tag{4.22}$$

We stress that $\boldsymbol{\sigma}_{h,K}^\star$ can be explicitly computed for each $K \in \mathcal{T}_h$, independently. Then, the rate of convergence for the broken $\mathrm{H}(\mathrm{div};\Omega)$-norm of $\boldsymbol{\sigma} - \boldsymbol{\sigma}_h^\star$ is established as follows.

**Theorem 4.8.** *Assume that the hypotheses of Theorem 4.6 are satisfied. Then, there exists a positive constant $C$, independent of $h$, such that*

$$\left\{ \sum_{K\in\mathcal{T}_h} \|\boldsymbol{\sigma} - \boldsymbol{\sigma}_{h,K}^\star\|^2_{\mathrm{div};K} \right\}^{1/2} \leq Ch^s \left\{ \sum_{K\in\mathcal{T}_h} |\boldsymbol{\sigma}|^2_{s,K} \; + \; |\mathrm{div}\,\boldsymbol{\sigma}|^2_{s,K} + |u|^2_{s,K} \right\}^{1/2}. \tag{4.23}$$

*Proof.* See [31, Section 5.3,Theorem 5.5]. □

## 4.5 A posteriori error analysis

In this section we develop a residual-based a posteriori error analysis for the mixed virtual element scheme (4.18). The proof of the a posteriori upper bound on the error is based on a global inf-sup condition, (cf. [9]), and a suitable Helmholtz decomposition; the lower bound is derived as usual via techniques based on bubble functions together with inverse inequalities.

### 4.5.1 Preliminaries

We let $\mathcal{E}_h = \mathcal{E}_h(\Omega)\cup\mathcal{E}_h(\Gamma_D)\cup\mathcal{E}_h(\Gamma_N)$ be the set of all edges of $\mathcal{T}_h$, where $\mathcal{E}_h(\Omega) := \{e \in \mathcal{E}_h : \quad e \subseteq \Omega\}$, $\mathcal{E}_h(\Gamma_D) := \{e \in \mathcal{E}_h : \quad e \subseteq \Gamma_D\}$, and $\mathcal{E}_h(\Gamma_N) := \{e \in \mathcal{E}_h : \quad e \subseteq \Gamma_N\}$. And, for a given $K \in \mathcal{T}_h$, we denote by $\mathcal{E}(K) \subset \mathcal{E}_h$ the set of edges of $K$. Given an edge $e \in \mathcal{E}_h$, we let $h_e$ be its length and we fix a unit normal vector $\nu_e := (\nu_1,\nu_2)^{\mathtt{t}}$ and let $s_e := (-\nu_2,\nu_1)^{\mathtt{t}}$ be the corresponding unit tangential vector along $e$. However, when no confusion arises, we simply write $\nu$ and $s$ instead of $\nu_e$ and $s_e$, respectively. Now, given $\boldsymbol{\zeta} \in [\mathrm{L}^2(\Omega)]^2$ such that $\boldsymbol{\zeta}\big|_K \in [\mathrm{C}(K)]^2$ for each $K \in \mathcal{T}_h$. Then, given $K \in \mathcal{T}_h$ and $e \in \mathcal{E}_h(\Omega)\cap\mathcal{E}(K)$ we denote by $[\![\boldsymbol{\zeta}\cdot s]\!]$ the tangential jump of $\boldsymbol{\zeta}$ across $e$, that is $[\![\boldsymbol{\zeta}\cdot s]\!] := (\boldsymbol{\zeta}\big|_K - \boldsymbol{\zeta}\big|_{K'})\big|_e \cdot s$, where $K$ and $K'$ are the elements of $\mathcal{T}_h$ having $e$ as a common edge.

We first recall the conforming VEM spaces from [13], which will be used as an auxiliary space in the a posteriori analysis below. Given $k \geq 0$, we consider the space defined by

$$V_h := \left\{ v \in \mathrm{H}^1(\Omega) : \quad v\big|_{\partial K} \in \mathbb{B}_k(\partial K) \text{ and } \Delta v \in \mathrm{P}_{k-1}(K) \quad \forall K \in \mathcal{T}_h \right\},$$

where

$$\mathbb{B}_k(\partial K) \; := \; \left\{ v \in \mathrm{C}(\partial K) : \quad v|_e \in \mathrm{P}_{k+1}(e) \quad \forall \text{ edge } e \subseteq \partial K \right\}.$$

It has been shown in [80, Section 4, Proposition 4.2] that there exists an interpolation operator $\mathcal{I}_h : \mathrm{H}^1(\Omega) \to V_h$, such that there holds

$$\|v - \mathcal{I}_h(v)\|_{0,K} + h_K|v - \mathcal{I}_h(v)|_{1,K} \leq c_1 h_K \|v\|_{1,K} \quad \forall\, v \in H^1(K). \tag{4.24}$$

From this, using a scaled trace inequality, the Cauchy-Schwarz inequality, and Assumption 4.1 it follows that

$$\|v - \mathcal{I}_h(v)\|_{0,e} \leq c_2 h_e^{1/2} \|v\|_{1,K} \quad \forall\, e \in \mathcal{E}_h. \tag{4.25}$$

We now let $\mathrm{H}^1_{\Gamma_N}(\Omega) := \big\{ v \in \mathrm{H}^1(\Omega) : \ v = 0 \ \text{ on } \ \Gamma_N \big\}$ and consider the virtual element subspace given by

$$\widetilde{V}_h := V_h \cap \mathrm{H}^1_{\Gamma_N}(\Omega). \tag{4.26}$$

Also, we introduce, analogously as before, the interpolation operator $\widetilde{I}_h : \mathrm{H}^1_{\Gamma_N}(\Omega) \to \widetilde{V}_h$ such that $\widetilde{I}_h := I_h\big|_{\mathrm{H}^1_{\Gamma_N}(\Omega)}$. In addition, the following lemma establishes an important relation between the virtual spaces $\widetilde{V}_h$ and $H_h$ (cf.(4.7)).

**Lemma 4.9.** *For $k \geq 0$, given $v \in \widetilde{V}_h$ we have $\mathbf{rot}\, v \in H_h$.*

*Proof.* Given $v \in \widetilde{V}_h$, it is easy to see that $\mathbf{rot}\, v \in H$. Moreover, given $K \in \mathcal{T}_h$, we observe that $\mathrm{rot}(\mathbf{rot}\, v) = -\Delta v \in \mathrm{P}_{k-1}(K)$. Furthermore, following [14, Section 8, Theorem 3], we have that $\mathbf{rot}\, v \cdot \nu\big|_e = \nabla v \cdot s\big|_e \in \mathrm{P}_k(e)$ for all edge $e \in \partial K$ . Hence, we conclude that $\mathbf{rot}\, v\big|_K \in H_h^K$ for all $K \in \mathcal{T}_h$. □

We now recall from [30, Section 3.3] some preliminary notations and technical results. For each element $K \in \mathcal{T}_h$ we first define $\widetilde{K} := T_K(K)$, where $T_K : \mathrm{R}^2 \to \mathrm{R}^2$ is the bijective affine mapping defined by

$$T_K(\mathbf{x}) := \frac{\mathbf{x} - \mathbf{x}_B}{h_K} \quad \forall\, \mathbf{x} \in \mathrm{R}^2\,.$$

Then, as it was remarked in [30, Section 3.3], it is easy to see that the diameter $h_{\widetilde{K}}$ of $\widetilde{K}$ is 1, the shortest edge of $\widetilde{K}$ is bigger than $C_{\mathcal{T}}$ (which follows from Assumption 4.1), and $\widetilde{K}$ is star-shaped with respect to a ball $\widetilde{B}$ of radius $C_{\mathcal{T}}$ and centered at the origin. Then, by connecting each vertex of $\widetilde{K}$ to the center of $\widetilde{B}$, that is to the origin, we generate a partition of $\widetilde{K}$ into $d_{\widetilde{K}}$ triangles $\widetilde{\Delta}_i$, $i \in \{1, 2, \ldots, d_{\widetilde{K}}\}$, where $d_{\widetilde{K}} \leq N_{\mathcal{T}}$, and for which the minimum angle condition is satisfied. The later means that there exists a constant $c_{\mathcal{T}} > 0$, depending only on $C_{\mathcal{T}}$ and $N_{\mathcal{T}}$, such that $\widetilde{h}_i (\widetilde{\rho}_i)^{-1} \leq c_{\mathcal{T}} \quad \forall\, i \in \{1, 2, \ldots, d_{\widetilde{K}}\}$, where $\widetilde{h}_i$ is the diameter of $\widetilde{\Delta}_i$ and $\widetilde{\rho}_i$ is the diameter of the largest ball contained in $\widetilde{\Delta}_i$. We also let $\widehat{\Delta}$ be the canonical triangle of $\mathrm{R}^2$ with corresponding parameters $\widehat{h}$ and $\widehat{\rho}$. In what follows, given $K \in \mathcal{T}_h$ and $\boldsymbol{\zeta} \in [\mathrm{H}^1(K)]^2$, we let $\widetilde{\boldsymbol{\zeta}} := \boldsymbol{\zeta} \circ T_K^{-1} \in [\mathrm{H}^1(\widetilde{K})]^2$. With this notation at hand, we prove the following interpolation error bound for normal components of $\mathrm{H}^1$ fuctions on edges which generalises to the VEM setting on polygons the analogous result for mixed-FEM given by Lemma 3.18 in [56].

**Lemma 4.10.** *There exists a constant $c_3 > 0$, independent of $h$, such that for all $\boldsymbol{\tau} \in [\mathrm{H}^1(\Omega)]^2$, there holds*

$$\|(\boldsymbol{\tau} - \boldsymbol{\tau}_I) \cdot \nu_e\|_{0,e} \leq c_3 h_e^{1/2} |\boldsymbol{\tau}|_{1,K} \quad \forall\, e \in \mathcal{E}_h, \tag{4.27}$$

*where $K$ is any element of $\mathcal{T}_h$ such that $K \in \omega_e$.*

*Proof.* The proof is based on the availability of the sub-triangulation of the scaled element $\widetilde{K}$ (cf. Remark 4.2), and follows along the lines of the proof of Lemma 3.18 in [56]. Let $e \in \mathcal{E}_h$ and $K \in \mathcal{T}_h$ such that $K \in \omega_e$, and let $\widetilde{e}$ be the edge of $\partial\widetilde{K}$, such that $e = T_K^{-1}(\widetilde{e})$. We further define $T_e := T_K\big|_e$.

Now, given $\boldsymbol{\tau} \in [\mathrm{H}^1(K)]^2$, we know from (4.7) and the definition of $\boldsymbol{\tau}_I$, respectively, that $\boldsymbol{\tau}_I \cdot \nu\big|_e \in \mathrm{P}_k(e)$ and

$$\int_e q(\boldsymbol{\tau} - \boldsymbol{\tau}_I) \cdot \nu = 0 \quad \forall\, q \in \mathcal{B}_k(e).$$

In turns, this implies that

$$\boldsymbol{\tau}_I \cdot \nu_e = \Pi_k^e(\boldsymbol{\tau} \cdot \nu_e),$$

where $\Pi_k^e : \mathrm{L}^2(e) \to \mathrm{P}_k(e)$ is the orthogonal projector. Then, it is easy to see that $\widetilde{\Pi_k^e(v)} = \Pi_k^{\widetilde{e}}(\widetilde{v}) \quad \forall\, v \in \mathrm{L}^2(e)$, where $\Pi_k^{\widetilde{e}} : \mathrm{L}^2(\widetilde{e}) \to \mathrm{P}_k(\widetilde{e})$ is the corresponding orthogonal projector. Hence, we obtain

$$\begin{aligned} \|(\boldsymbol{\tau} - \boldsymbol{\tau}_I) \cdot \nu_e\|_{0,e} &= \|\boldsymbol{\tau} \cdot \nu_e - \Pi_k^e(\boldsymbol{\tau} \cdot \nu_e)\|_{0,e} = \frac{h_e^{1/2}}{h_{\widetilde{e}}^{1/2}} \|\widetilde{\boldsymbol{\tau} \cdot \nu_e} - \widetilde{\Pi_k^e(\boldsymbol{\tau} \cdot \nu_e)}\|_{0,\widetilde{e}} \\ &= \frac{h_e^{1/2}}{h_{\widetilde{e}}^{1/2}} \|\widetilde{\boldsymbol{\tau} \cdot \nu_e} - \Pi_k^{\widetilde{e}}(\widetilde{\boldsymbol{\tau} \cdot \nu_e})\|_{0,\widetilde{e}} \leq \frac{h_e^{1/2}}{h_{\widetilde{e}}^{1/2}} \|\widetilde{\boldsymbol{\tau} \cdot \nu_e}\|_{0,\widetilde{e}} \leq \frac{h_e^{1/2}}{h_{\widetilde{e}}^{1/2}} \|\widetilde{\boldsymbol{\tau}}\|_{0,\widetilde{e}}. \end{aligned} \tag{4.28}$$

Now, let $\widetilde{\triangle}$ be the triangle formed by connecting the end points of $\widetilde{e}$ to the center of $\widetilde{B}$ and consider $\widehat{\boldsymbol{\tau}} := \widetilde{\boldsymbol{\tau}}\big|_{\widetilde{\triangle}} \circ F \in [\mathrm{H}^1(\widehat{\triangle})^2$, where $F : \mathrm{R}^2 \to \mathrm{R}^2$ is the bijective linear mapping defined by $F(\mathbf{x}) := B\mathbf{x} \quad \forall\, \mathbf{x} \in \mathrm{R}^2$, with $B \in \mathrm{R}^{2\times 2}$ invertible, such that $F(\widehat{\triangle})$. Let $\widehat{e}$ be the edge of $\partial\widehat{\triangle}$ such that $\widetilde{e} = F(\widehat{e})$, then

$$\|\widetilde{\boldsymbol{\tau}}\|_{0,\widetilde{e}} = \frac{h_{\widetilde{e}}^{1/2}}{h_{\widehat{e}}^{1/2}} \|\widehat{\boldsymbol{\tau}}\|_{0,\widehat{e}} = \widehat{C} h_{\widetilde{e}}^{1/2} \|\widehat{\boldsymbol{\tau}}\|_{0,\widehat{e}}. \tag{4.29}$$

Now, considering $\varphi \in C^\infty(\widehat{\triangle})$ such that $\varphi \equiv 1$ in a neighbourhood of $\widehat{e}$, and $\varphi \equiv 0$ in a neighbourhood of the vertex opposite to $\widehat{e}$, and applying the trace theorem in $\mathrm{H}^1(\widehat{\triangle})$, the Friedrichs-Poincaré inequality, and the Leibniz rule, we get

$$\|\widehat{\boldsymbol{\tau}}\|_{0,\widehat{e}} = \|\widehat{\boldsymbol{\tau}}\varphi\|_{0,\widehat{e}} \leq \|\widehat{\boldsymbol{\tau}}\varphi\|_{0,\partial\widehat{\triangle}} \leq \gamma_{\mathrm{tr}} \|\widehat{\boldsymbol{\tau}}\varphi\|_{1,\widehat{\triangle}} \leq \gamma_{\mathrm{tr}} C_p |\widehat{\boldsymbol{\tau}}\varphi|_{1,\widehat{\triangle}} \leq C_\varphi \gamma_{\mathrm{tr}} C_p |\widehat{\boldsymbol{\tau}}|_{1,\widehat{\triangle}}.$$

Using this to bound (4.29) and replacing the resulting bound in (4.28) we deduce that

$$\begin{aligned} \|(\boldsymbol{\tau} - \boldsymbol{\tau}_I) \cdot \nu_e\|_{0,e} &\leq C_\varphi \gamma_{\mathrm{tr}} C_p \widehat{C} h_e^{1/2} |\widehat{\boldsymbol{\tau}}|_{1,\widehat{\triangle}} \leq \widehat{C}_1 C_\varphi \gamma_{\mathrm{tr}} C_p \widehat{C} h_e^{1/2} |\widetilde{\boldsymbol{\tau}}|_{1,\widetilde{\triangle}} \\ &\leq \widehat{C}_1 C_\varphi \gamma_{\mathrm{tr}} C_p \widehat{C} h_e^{1/2} |\widetilde{\boldsymbol{\tau}}|_{1,\widetilde{K}} \leq c_3 h_e^{1/2} |\boldsymbol{\tau}|_{1,K}, \end{aligned}$$

where $c_3 := C_1 \widehat{C}_1 C_\varphi \gamma_{\mathrm{tr}} C_p \widehat{C}$, with $\widehat{C}_1$ and $C_1$, the $\mathrm{H}^1$-seminorm scaly constants on $\widetilde{\triangle}$ and $K$, respectively, thus concluding the proof. □

### 4.5.2 A posteriori error estimator

Let $(\boldsymbol{\sigma}_h, u_h) \in H_h \times Q_h$ be the unique solution of (4.18). In addition, let $\widehat{\boldsymbol{\sigma}}_h, \boldsymbol{\sigma}_h^\star$ be the discrete approximations introduced in (4.20) and (4.22), respectively. For each $K \in \mathcal{T}_h$, we define the following local and computable error indicators:

$$\Phi_K^2 := \|f + \operatorname{div} \boldsymbol{\sigma}_h\|_{0,K}^2, \quad \Lambda_{1,K}^2 := \|\widehat{\boldsymbol{\sigma}}_h - \boldsymbol{\sigma}_h^\star\|_{0,K}^2, \quad \Upsilon_K^2 := \|(\boldsymbol{\kappa}^{-1} - \boldsymbol{\kappa}_h)\boldsymbol{\sigma}_h^\star\|_{0,K}^2,$$

$$\Psi_K^2 := \sum_{i=1}^{2} \Psi_{i,K}^2, \qquad \eta_K^2 := \sum_{i=1}^{2} \eta_{i,K}^2, \qquad \theta_K^2 := \sum_{i=1}^{3} \theta_{i,K}^2,$$

where

$$\Psi_{1,K}^2 := \mathcal{S}^K(\boldsymbol{\sigma}_h - \widehat{\boldsymbol{\sigma}}_h, \boldsymbol{\sigma}_h - \widehat{\boldsymbol{\sigma}}_h)\,, \qquad \Psi_{2,K}^2 := \|\boldsymbol{\kappa}^{-1}\widehat{\boldsymbol{\sigma}}_h - \boldsymbol{\Pi}_k^0(\boldsymbol{\kappa}^{-1}\widehat{\boldsymbol{\sigma}}_h)\|_{0,K}^2\,,$$

$$\eta_{1,K}^2 := h_K^2\|\boldsymbol{\kappa}_h\boldsymbol{\sigma}_h^\star - \nabla u_h\|_{0,K}^2\,, \qquad \eta_{2,K}^2 := \sum_{e\in\mathcal{E}(K)\cap\mathcal{E}_h(\Gamma_D)} h_e\|u_h - g\|_{0,e}^2\,,$$

$$\theta_{1,K}^2 := h_K^2\|\mathrm{rot}\,(\boldsymbol{\kappa}_h\boldsymbol{\sigma}_h^\star)\,\|_{0,K}^2\,, \qquad \theta_{2,K}^2 := \sum_{e\in\mathcal{E}(K)\cap\mathcal{E}_h(\Omega)} h_e\,\|[\![\boldsymbol{\kappa}_h\boldsymbol{\sigma}_h^\star\cdot s]\!]\|_{0,e}^2\,,$$

$$\theta_{3,K}^2 := \sum_{e\in\mathcal{E}(K)\cap\mathcal{E}_h(\Gamma_D)} h_e\left\|\boldsymbol{\kappa}_h\boldsymbol{\sigma}_h^\star\cdot s - \frac{dg}{ds}\right\|_{0,e}^2\,,$$

and $\boldsymbol{\kappa}_h$ is a piecewise-polynomial approximation of $\boldsymbol{\kappa}^{-1}$.

**Remark 4.11.** *Notice that from the residual character of the indicators, the computability of each local term becomes clear. Also, observe that the term $\Psi_{1,K}$ represents, together with $\Psi_{2,K}$, a bound on the error related to the inconsistency between the continuous and discrete bilinear forms, $a^K$ and $a_h^K$, (cf. Lemma 4.5). We further observe that the last term in $\theta_{3,K}$ requires the trace $g$ to be more regular. This assumption will be stated and clarified below in Lemma 4.18.*

**Remark 4.12.** *If $\boldsymbol{\kappa}$ is piecewise-constant on each $K\in\mathcal{T}_h$, we have that $\Upsilon_K$ and $\Psi_{2,K}$ are null, whereas if we use homogeneous boundary conditions on $\Gamma_D$, we deduce that $\eta_{2,K}$ is null.*

**Remark 4.13.** *We stress here that the approach below can be applied to problems more generals, however, it could be more convenient to start with a simple model, presenting the keys points of our approach. See e.g.* **Chapter 5**.

**Remark 4.14.** *Through the a posteriori analysis below, it will be clear that the same terms but* without *the postprocessing, hence with $\widehat{\boldsymbol{\sigma}}_h$ in place of $\boldsymbol{\sigma}_h^\star$ everywhere, also constitute an a posteriori bound for the error that involves $\widehat{\boldsymbol{\sigma}}_h$. However, as we shall see, the introduction of $\boldsymbol{\sigma}_h^\star$ will permit us to include an optimal bound on the broken* $\mathrm{H}(\mathrm{div};\Omega)$*-norm of computable quantities.*

### 4.5.3 Upper bound

We proceed with the following preliminary estimate

**Lemma 4.15.** *Let $(\boldsymbol{\sigma},u)\in H\times Q$ and $(\boldsymbol{\sigma}_h,u_h)\in H_h\times Q_h$ be the unique solutions of (4.4) and (4.18), respectively. In addition, let $\boldsymbol{\sigma}_h^\star$ be the discrete approximation introduced in (4.22). Then, there exists a positive constant $C$, independent of $h$, such that*

$$C\|(\boldsymbol{\sigma},u)-(\boldsymbol{\sigma}_h,u_h)\|_{H\times Q} \leq \left\{\sum_{K\in\mathcal{T}_h}\Phi_K^2+\Upsilon_K^2+\Psi_K^2+\Lambda_{1,K}^2\right\}^{1/2} + \sup_{\substack{\boldsymbol{\tau}\in H\\ \boldsymbol{\tau}\neq\mathbf{0}}}\frac{E(\boldsymbol{\tau})}{\|\boldsymbol{\tau}\|_H}, \tag{4.30}$$

*where*

$$E(\boldsymbol{\tau}) := -\int_\Omega \boldsymbol{\kappa}_h\boldsymbol{\sigma}_h^\star\cdot(\boldsymbol{\tau}-\boldsymbol{\tau}_h) - \int_\Omega u_h\,\mathrm{div}(\boldsymbol{\tau}-\boldsymbol{\tau}_h) + \langle(\boldsymbol{\tau}-\boldsymbol{\tau}_h)\cdot\nu, g\rangle_{\Gamma_D}, \tag{4.31}$$

*for all $\boldsymbol{\tau}_h\in H_h$ such that $\|\boldsymbol{\tau}_h\|_Q\leq C\|\boldsymbol{\tau}\|_H$ for some positive constant $C$ independent of $\boldsymbol{\tau}$.*

*Proof.* Consider the bounded linear operator $\mathcal{A} : H \times Q \to (H \times Q)'$ induced by the left hand-side of (4.4), that is, the linear operator defined by

$$[\mathcal{A}(\boldsymbol{\rho}, z), (\boldsymbol{\tau}, v)] := a(\boldsymbol{\rho}, \boldsymbol{\tau}) + b(\boldsymbol{\tau}, z) + b(\boldsymbol{\rho}, v). \tag{4.32}$$

From the well-posedness of the variational formulation (4.4), we know that $\mathcal{A}$ is an isomorphism. In particular, there exists a positive constant $C$, such that

$$C\|(\boldsymbol{\rho}, z)\|_{H\times Q} \leq \sup_{\substack{(\boldsymbol{\tau},v)\in H\times Q \\ (\boldsymbol{\tau},v)\neq \mathbf{0}}} \frac{[\mathcal{A}(\boldsymbol{\rho}, z), (\boldsymbol{\tau}, v)]}{\|(\boldsymbol{\tau}, v)\|_{H\times Q}}.$$

Now, applying the foregoing equation to $(\boldsymbol{\rho}, z) := (\boldsymbol{\sigma} - \boldsymbol{\sigma}_h, u - u_h)$, from (4.32), we get

$$\begin{aligned} C\|(\boldsymbol{\sigma}, u) - (\boldsymbol{\sigma}_h, u_h)\|_{H\times Q} &\leq \sup_{\substack{(\boldsymbol{\tau},v)\in H\times Q \\ (\boldsymbol{\tau},v)\neq \mathbf{0}}} \frac{a(\boldsymbol{\sigma} - \boldsymbol{\sigma}_h, \boldsymbol{\tau}) + b(\boldsymbol{\tau}, u - u_h) + b(\boldsymbol{\sigma} - \boldsymbol{\sigma}_h, v)}{\|(\boldsymbol{\tau}, v)\|_{H\times Q}} \\ &\leq \sup_{\substack{v\in Q \\ v\neq \mathbf{0}}} \frac{b(\boldsymbol{\sigma} - \boldsymbol{\sigma}_h, v)}{\|v\|_Q} + \sup_{\substack{\boldsymbol{\tau}\in H \\ \boldsymbol{\tau}\neq \mathbf{0}}} \frac{a(\boldsymbol{\sigma} - \boldsymbol{\sigma}_h, \boldsymbol{\tau}) + b(\boldsymbol{\tau}, u - u_h)}{\|\boldsymbol{\tau}\|_H} \\ &\leq \|f + \operatorname{div} \boldsymbol{\sigma}_h\|_{0,\Omega} + \sup_{\substack{\boldsymbol{\tau}\in H \\ \boldsymbol{\tau}\neq \mathbf{0}}} \frac{a(\boldsymbol{\sigma} - \boldsymbol{\sigma}_h, \boldsymbol{\tau}) + b(\boldsymbol{\tau}, u - u_h)}{\|\boldsymbol{\tau}\|_H}, \end{aligned} \tag{4.33}$$

and it remains to bound the second term above. To this end, given $\boldsymbol{\tau} \in H$ and any $\boldsymbol{\tau}_h \in H_h$, from (4.4) and (4.18), we have that

$$\begin{aligned} a(\boldsymbol{\sigma} - \boldsymbol{\sigma}_h, \boldsymbol{\tau}) + b(\boldsymbol{\tau}, u - u_h) &= -a(\boldsymbol{\sigma}_h, \boldsymbol{\tau}) - b(\boldsymbol{\tau}, u_h) + \langle \boldsymbol{\tau}\cdot\nu, g\rangle_{\Gamma_D} \\ &= \langle \boldsymbol{\tau}_h\cdot\nu, g\rangle_{\Gamma_D} - a(\boldsymbol{\sigma}_h, \boldsymbol{\tau}) - b(\boldsymbol{\tau}, u_h) + \langle (\boldsymbol{\tau} - \boldsymbol{\tau}_h)\cdot\nu, g\rangle_{\Gamma_D} \\ &= a_h(\boldsymbol{\sigma}_h, \boldsymbol{\tau}_h) - a(\boldsymbol{\sigma}_h, \boldsymbol{\tau}) - b(\boldsymbol{\tau} - \boldsymbol{\tau}_h, u_h) + \langle (\boldsymbol{\tau} - \boldsymbol{\tau}_h)\cdot\nu, g\rangle_{\Gamma_D} \\ &= (a_h - a)(\boldsymbol{\sigma}_h, \boldsymbol{\tau}_h) - a(\boldsymbol{\sigma}_h - \boldsymbol{\sigma}_h^\star, \boldsymbol{\tau} - \boldsymbol{\tau}_h) \\ &\quad -a(\boldsymbol{\sigma}_h^\star - \boldsymbol{\kappa}\boldsymbol{\kappa}_h\boldsymbol{\sigma}_h^\star, \boldsymbol{\tau} - \boldsymbol{\tau}_h) \\ &\quad -a(\boldsymbol{\kappa}\boldsymbol{\kappa}_h\boldsymbol{\sigma}_h^\star, \boldsymbol{\tau} - \boldsymbol{\tau}_h) - b(\boldsymbol{\tau} - \boldsymbol{\tau}_h, u_h) + \langle (\boldsymbol{\tau} - \boldsymbol{\tau}_h)\cdot\nu, g\rangle_{\Gamma_D} \\ &=: I + II + III\,. \end{aligned}$$

Now, in what follows we take in particular $\boldsymbol{\tau}_h \in H_h$ with $\|\tau_h\|_Q \leq C\|\tau\|_H$ for some positive constant $C$ independent of $\boldsymbol{\tau}$. For $I$ and $II$, we use the bounds (4.15) and (4.16), and the Cauchy-Schwarz inequality to deduce

$$I := (a_h - a)(\boldsymbol{\sigma}_h, \boldsymbol{\tau}_h) - a(\boldsymbol{\sigma}_h - \boldsymbol{\sigma}_h^\star, \boldsymbol{\tau} - \boldsymbol{\tau}_h) \leq C \left\{ \sum_{K\in\mathcal{T}_h} \Psi_K^2 + \Lambda_{1,K}^2 \right\}^{1/2} \|\boldsymbol{\tau}\|_H\,, \tag{4.34}$$

and

$$II := -a(\boldsymbol{\sigma}_h^\star - \boldsymbol{\kappa}\boldsymbol{\kappa}_h\boldsymbol{\sigma}_h^\star, \boldsymbol{\tau} - \boldsymbol{\tau}_h) \leq C \left\{ \sum_{K\in\mathcal{T}_h} \Upsilon_K^2 \right\}^{1/2} \|\boldsymbol{\tau}\|_H\,, \tag{4.35}$$

whereas bearing mind the functional $E$ (cf.(4.31)), we use the definitions (4.5) to get

$$III := -a(\boldsymbol{\kappa}\boldsymbol{\kappa}_h\boldsymbol{\sigma}_h^\star, \boldsymbol{\tau}-\boldsymbol{\tau}_h) - b(\boldsymbol{\tau}-\boldsymbol{\tau}_h, u_h) + \langle(\boldsymbol{\tau}-\boldsymbol{\tau}_h)\cdot\nu, g\rangle_{\Gamma_D} = E(\boldsymbol{\tau})\,. \tag{4.36}$$

Finally, replacing (4.34)-(4.36) into (4.33), we conclude the proof. □

We now aim to bound the supremum on the right hand-side of (4.30), for which we need a suitable choice of $\boldsymbol{\tau}_h \in H_h$ such that $\|\tau_h\|_Q \leq \|\tau\|_H$. To this end, in what follow we assume that the boundary $\Gamma$ is such that $\Gamma_N$ is contained in a convex part of $\Omega$. More precisely, we make use of the following result.

**Lemma 4.16.** *Assume that $\Omega$ is a connected domain and that $\Gamma_N$ is contained in the boundary of a convex part of $\Omega$, that is there exists a convex domain $B$ such that $\Omega \subset B$ and $\Gamma_N \subseteq \partial B$. Then, for each $\boldsymbol{\tau} \in H$ (cf.(4.3)), there exist $\boldsymbol{\zeta} \in \mathrm{H}^1(\Omega)$ with $\boldsymbol{\zeta}\cdot\nu = 0$ on $\Gamma_N$ and $\chi \in \mathrm{H}^1_{\Gamma_N}(\Omega)$ (cf. Section 4.5.1) such that*

$$\boldsymbol{\tau} = \boldsymbol{\zeta} + \mathbf{rot}\,\chi \quad \text{in} \quad \Omega\,, \quad \mathrm{div}\,\boldsymbol{\zeta} = \mathrm{div}\,\boldsymbol{\tau} \quad \text{in} \quad \Omega\,, \tag{4.37}$$

*and*

$$\|\boldsymbol{\zeta}\|_{1,\Omega} + \|\chi\|_{1,\Omega} \leq C\|\boldsymbol{\tau}\|_{\mathrm{div};\Omega}\,, \tag{4.38}$$

*with a positive constant $C$ independent of $\boldsymbol{\tau}$.*

*Proof.* See [9, Lemma 3.9] for more details. □

Now, for $\boldsymbol{\tau} \in H$ from Lemmas 4.9 and 4.16, we define $\chi_h := \widetilde{\mathcal{I}}_h(\chi) \in \widetilde{V}_h$, and set

$$\boldsymbol{\tau}_h := \boldsymbol{\zeta}_I + \mathbf{rot}\,\chi_h \in H_h\,, \tag{4.39}$$

as its associated discrete Helmholtz decomposition. Now, it follows from (4.39), the triangle inequality, (4.6), (4.24) and (4.38) that

$$\|\boldsymbol{\tau}_h\|_Q \leq \|\boldsymbol{\zeta}-\boldsymbol{\zeta}_I\|_Q + \|\boldsymbol{\zeta}\|_Q + |\chi-\chi_h|_{1,\Omega} + |\chi|_{1,\Omega} \leq C\|\boldsymbol{\tau}\|_H\,,$$

with a positive constant $C$ independent of $\boldsymbol{\tau}$. Next, we can write

$$\boldsymbol{\tau}-\boldsymbol{\tau}_h = \boldsymbol{\zeta}-\boldsymbol{\zeta}_I + \mathbf{rot}(\chi-\chi_h), \tag{4.40}$$

from which, using (4.11), and the fact that $\mathrm{div}\,\boldsymbol{\zeta} = \mathrm{div}\,\boldsymbol{\tau}$ in $\Omega$, we deduce

$$\int_\Omega u_h\,\mathrm{div}(\boldsymbol{\tau}-\boldsymbol{\tau}_h) = \int_\Omega u_h\,\mathrm{div}(\boldsymbol{\zeta}-\boldsymbol{\zeta}_I) = 0. \tag{4.41}$$

Then, using the choice for $\boldsymbol{\tau}_h$ given by (4.39) to bound the supremum in (4.30), replacing (4.40) and (4.41) into (4.31), we find that $E(\boldsymbol{\tau}) = E_1(\boldsymbol{\zeta}) + E_2(\chi)$ where

$$E_1(\boldsymbol{\zeta}) := -\int_\Omega \boldsymbol{\kappa}_h\boldsymbol{\sigma}_h^\star\cdot(\boldsymbol{\zeta}-\boldsymbol{\zeta}_I) + \langle(\boldsymbol{\zeta}-\boldsymbol{\zeta}_I)\cdot\nu, g\rangle_{\Gamma_D}, \tag{4.42}$$

and

$$E_2(\chi) := -\int_\Omega \boldsymbol{\kappa}_h\boldsymbol{\sigma}_h^\star\cdot\mathbf{rot}(\chi-\chi_h) + \langle\mathbf{rot}(\chi-\chi_h)\cdot\nu, g\rangle_{\Gamma_D}. \tag{4.43}$$

The following two lemmas provide the upper bounds for $|E_1(\boldsymbol{\zeta})|$ and $|E_2(\chi)|$.

**Lemma 4.17.** *There exists $C > 0$, independent of $h$, such that*

$$|E_1(\boldsymbol{\zeta})| \leq C \left\{ \sum_{K \in \mathcal{T}} \eta_K^2 \right\}^{1/2} \|\boldsymbol{\tau}\|_{\mathrm{div};\Omega}.$$

*Proof.* We rewrite the second term in $E_1(\boldsymbol{\zeta})$ as:

$$\langle (\boldsymbol{\zeta} - \boldsymbol{\zeta}_I) \cdot \nu, g \rangle_{\Gamma_D} = \sum_{e \in \mathcal{E}_h(\Gamma_D)} \int_e g\, (\boldsymbol{\zeta} - \boldsymbol{\zeta}_I) \cdot \nu. \tag{4.44}$$

Next, since $u_h\big|_K \in \mathrm{P}_k(K)$, we have

$$\int_e u_h (\boldsymbol{\zeta} - \boldsymbol{\zeta}_I) \cdot \nu = 0 \quad \forall\, e \in \mathcal{E}(K) \cap \mathcal{E}_h(\Gamma_D),$$

and

$$\int_K (\boldsymbol{\zeta} - \boldsymbol{\zeta}_I) \cdot \nabla u_h = 0,$$

for all $K \in \mathcal{T}_h$. Hence, using the above expressions, we can write

$$E_1(\boldsymbol{\zeta}) = -\sum_{K \in \mathcal{T}_h} \left\{ \int_K (\boldsymbol{\kappa}_h \boldsymbol{\sigma}_h^\star - \nabla u_h) \cdot (\boldsymbol{\zeta} - \boldsymbol{\zeta}_I) + \sum_{e \in \mathcal{E}(K) \cap \mathcal{E}_h(\Gamma_D)} \int_e (u_h - g)(\boldsymbol{\zeta} - \boldsymbol{\zeta}_I) \cdot \nu \right\},$$

from which, applying the Cauchy-Schwarz inequality, the approximation properties (4.6) and (4.27), and the fact $\|\boldsymbol{\zeta}\|_{1,\Omega} \leq \|\boldsymbol{\tau}\|_{\mathrm{div};\Omega}$, we obtain the required estimate. □

**Lemma 4.18.** *Assume that $g \in \mathrm{H}^1(\Gamma_D)$. Then, there exists $C > 0$, independent of $h$, such that*

$$|E_2(\chi)| \leq C \left\{ \sum_{K \in \mathcal{T}} \theta_K^2 \right\}^{1/2} \|\boldsymbol{\tau}\|_{\mathrm{div};\Omega}.$$

*Proof.* We proceed as in the proof of the Lemma 3.11 in [9]. Integrating by parts on each $K \in \mathcal{T}_h$, using that $\mathbf{rot}(\chi - \chi_h) \cdot \nu = \dfrac{d}{ds}(\chi - \chi_h)$, noting that $\dfrac{dg}{ds} \in \mathrm{L}^2(\Gamma_D)$, and using the fact that $\chi\big|_{\Gamma_N} = \chi_h\big|_{\Gamma_N} = 0$, we get

$$\begin{aligned}
E_2(\chi) &= -\sum_{K \in \mathcal{T}_h} \int_K \boldsymbol{\kappa}_h \boldsymbol{\sigma}_h^\star \cdot \mathbf{rot}(\chi - \chi_h) + \left\langle \frac{d}{ds}(\chi - \chi_h), g \right\rangle_{\Gamma_D} \\
&= -\sum_{K \in \mathcal{T}_h} \left\{ \int_K \mathrm{rot}\,(\boldsymbol{\kappa}_h \boldsymbol{\sigma}_h^\star)\,(\chi - \chi_h) - \int_{\partial K} (\boldsymbol{\kappa}_h \boldsymbol{\sigma}_h^\star \cdot s_K)\,(\chi - \chi_h) \right\} - \int_{\Gamma_D} \frac{dg}{ds}(\chi - \chi_h) \\
&= -\sum_{K \in \mathcal{T}_h} \left\{ \int_K \mathrm{rot}\,(\boldsymbol{\kappa}_h \boldsymbol{\sigma}_h^\star)\,(\chi - \chi_h) - \sum_{e \in \mathcal{E}(K) \cap \mathcal{E}_h(\Omega)} \int_e [\![ \boldsymbol{\kappa}_h \boldsymbol{\sigma}_h^\star \cdot s ]\!] (\chi - \chi_h) \right. \\
&\qquad \left. - \sum_{e \in \mathcal{E}(K) \cap \mathcal{E}_h(\Gamma_D)} \int_e \left( \boldsymbol{\kappa}_h \boldsymbol{\sigma}_h^\star \cdot s - \frac{dg}{ds} \right) (\chi - \chi_h) \right\}.
\end{aligned}$$

In this way, since $\chi_h = \widetilde{\mathcal{I}}_h(\chi)$, applying the Cauchy-Schwarz inequality to each term in the above expression and making use of the approximation properties (4.24) and (4.25) and the fact that the number of elements in $\omega_e$ is bounded, we conclude the proof. □

Finally, from Lemmas 4.15, 4.17 and 4.18 we deduce an upper bound for the global error.

**Theorem 4.19.** *Let $(\boldsymbol{\sigma}, u) \in H \times Q$ and $(\boldsymbol{\sigma}_h, u_h) \in H_h \times Q_h$ be the unique solutions of the problem (4.4) and (4.18), respectively. Then, there exists a positive constant $C$, independent of $h$, such that*

$$\|(\boldsymbol{\sigma}, u) - (\boldsymbol{\sigma}_h, u_h)\|_{H\times Q} \leq C \left\{ \sum_{K\in\mathcal{T}_h} \Phi_K^2 + \Upsilon_K^2 + \Psi_K^2 + \Lambda_{1,K}^2 + \eta_K^2 + \theta_K^2 \right\}^{1/2} .$$

We recall from the discussion in Section 4.4.2 that the corresponding result for the computable quantity $\widehat{\boldsymbol{\sigma}}_h$ is only to be expected in the $\mathrm{L}^2$-norm. Instead, for the error using the postprocessing flux we are able to obtain the following result in line with Theorem 4.19.

**Theorem 4.20.** *Let $(\boldsymbol{\sigma}, u) \in H \times Q$ and $(\boldsymbol{\sigma}_h, u_h) \in H_h \times Q_h$ be the unique solutions of the problem (4.4) and (4.18), respectively. In addition, let $\boldsymbol{\sigma}_h^\star$ be the discrete postprocessing introduced in (4.22). Then, there exists a positive constant $C$, independent of $h$, such that*

$$\left\{ \sum_{K\in\mathcal{T}_h} \|\boldsymbol{\sigma} - \boldsymbol{\sigma}_{h,K}^\star\|_{\mathrm{div};K}^2 \right\}^{1/2} + \|u - u_h\|_Q \leq C \left\{ \sum_{K\in\mathcal{T}_h} \Phi_K^2 + \Upsilon_K^2 + \Psi_K^2 + \Lambda_K^2 + \eta_K^2 + \theta_K^2 \right\}^{1/2} ,$$

*with*

$$\Lambda_K^2 := \sum_{i=1}^{2} \Lambda_{i,K}^2 \quad \textit{where} \quad \Lambda_{2,K}^2 := \|\mathrm{div}\,\boldsymbol{\sigma}_h - \mathrm{div}\,\boldsymbol{\sigma}_h^\star\|_{0,K}^2 .$$

*Proof.* From the triangle inequality, we have

$$\begin{aligned} \|\boldsymbol{\sigma} - \boldsymbol{\sigma}_{h,K}^\star\|_{\mathbf{div};K} &\leq \|\boldsymbol{\sigma} - \boldsymbol{\sigma}_h\|_{\mathrm{div};K} + \|\boldsymbol{\sigma}_h - \boldsymbol{\sigma}_{h,K}^\star\|_{0,K} + \|\mathrm{div}\,\boldsymbol{\sigma}_h - \mathrm{div}\,\boldsymbol{\sigma}_{h,K}^\star\|_{0,K} \\ &\leq \|\boldsymbol{\sigma} - \boldsymbol{\sigma}_h\|_{\mathrm{div};K} + \|\boldsymbol{\sigma}_h - \widehat{\boldsymbol{\sigma}}_h\|_{0,K} + \|\widehat{\boldsymbol{\sigma}}_h - \boldsymbol{\sigma}_{h,K}^\star\|_{0,K} + \|\mathrm{div}\,\boldsymbol{\sigma}_h - \mathrm{div}\,\boldsymbol{\sigma}_{h,K}^\star\|_{0,K} . \end{aligned}$$

Then, since $\mathrm{H}(\mathrm{div};\Omega) \subset \mathrm{H}(\mathrm{div};\mathcal{T}_h)$, the upper bound in (4.15), and using the definition of $\Psi_K^2$ and $\Lambda_K^2$, we get

$$\left\{ \sum_{K\in\mathcal{T}_h} \|\boldsymbol{\sigma} - \boldsymbol{\sigma}_{h,K}^\star\|_{\mathrm{div};K}^2 \right\}^{1/2} \leq C \left\{ \|\boldsymbol{\sigma} - \boldsymbol{\sigma}_h\|_H + \left\{ \sum_{K\in\mathcal{T}_h} \Psi_K^2 + \Lambda_K^2 \right\}^{1/2} \right\} .$$

Threrefore, the result is consequence of the foregoing equation and Theorem 4.19. □

### 4.5.4 Lower bound

In this section we derive suitable upper bounds for the terms defining the local error indicators. First, using that $f = -\mathrm{div}\,\boldsymbol{\sigma}$ in $\Omega$ we have that

$$\Phi_K^2 = \|\mathrm{div}(\boldsymbol{\sigma} - \boldsymbol{\sigma}_h)\|_{0,K}^2 \leq 2\Big\{ \|\boldsymbol{\sigma} - \boldsymbol{\sigma}_h^\star\|_{\mathrm{div};K}^2 + \Lambda_{1,K}^2 \Big\} . \tag{4.45}$$

Moreover, adding and subtracting $\boldsymbol{\sigma}$, we easily have

$$\begin{aligned}\Lambda_K^2 &= \|\widehat{\boldsymbol{\sigma}}_h - \boldsymbol{\sigma}_h^\star\|_{0,K}^2 + \|\mathrm{div}\,\boldsymbol{\sigma}_h - \mathrm{div}\,\boldsymbol{\sigma}_h^\star\|_{0,K}^2 \\ &\leq 2\left\{\|\boldsymbol{\sigma} - \boldsymbol{\Pi}_k^0(\boldsymbol{\sigma})\|_{0,K}^2 + \|\boldsymbol{\sigma} - \boldsymbol{\sigma}_h^\star\|_{\mathrm{div};K}^2 + \|\boldsymbol{\sigma} - \boldsymbol{\sigma}_h\|_{\mathrm{div};K}\right\}.\end{aligned} \tag{4.46}$$

In addition, we deduce

$$\Psi_{2,K}^2 \leq C\left\{\Lambda_{1,K}^2 + \|\boldsymbol{\sigma} - \boldsymbol{\sigma}_h^\star\|_{0,K}^2 + \|\boldsymbol{\kappa}^{-1}\boldsymbol{\sigma} - \boldsymbol{\Pi}_k^0(\boldsymbol{\kappa}^{-1}\boldsymbol{\sigma})\|_{0,K}^2\right\}, \tag{4.47}$$

with $C$ depending only on $\boldsymbol{\kappa}$ and $\widehat{c}_0$.

**Remark 4.21.** *Following [38], we interpret $\Psi_{1,K}^2$ as a sort of oscillation term representing the virtual inconsistency of the method.*

The upper bounds of the terms which depend on the mesh parameters $h_K$ and $h_e$, will be derived next. To this end, we proceed similarly as in [41] and [42] and apply the technique based on bubble functions, together with inverse inequalities. Following [38, Section 4] and [81, Section 3], given $K \in \mathcal{T}_h$, a bubble function $\psi_K$ can be constructed piecewise as the sum of the (polynomial) barycentric bubble functions (cf.[91, 5]) on each triangle of the shape-regular sub-triangulation of the mesh element $K$ discussed in the Section 4.4. Further, an edge bubble function $\psi_e$, $e \in \partial K$, is a piecewise quadratic function attaining the value 1 at the mid-point of $e$ and vanishing on the triangles that do not contain $e$ on their boundary. Furthermore, given $k \geq 0$, there exists an extension operator $L : \mathrm{C}(e) \to \mathrm{C}(K)$ that satisfies $L(p) \in \mathrm{P}_k(K)$ and $L(p)\big|_e = p$ for all $p \in \mathrm{P}_k(e)$ (cf.[81, Remark 3.1]). Further properties of $\psi_K, \psi_e$, and $L$ are stated in the following lemma. See [38, Section 4] and [81, Section 3] for more details.

**Lemma 4.22.** *Given $k \geq 0$ and $K \in \mathcal{T}_h$, there exists a positive constant $C_{\mathrm{bub}}$, independent of $h_K$ such that*

$$C_{\mathrm{bub}}^{-1}\|q\|_{0,K}^2 \leq \|\psi_K^{1/2} q\|_{0,K}^2 \leq C_{\mathrm{bub}}\|q\|_{0,K}^2 \qquad \forall\, q \in \mathrm{P}_k(K), \tag{4.48}$$

*and*

$$C_{\mathrm{bub}}^{-1}\|q\|_{0,K} \leq \|\psi_K q\|_{0,K} + h_K|\psi_K q|_{1,K} \leq C_{\mathrm{bub}}\|q\|_{0,K} \qquad \forall\, q \in \mathrm{P}_k(K). \tag{4.49}$$

*In addition, given $e \in \partial K$, there hold*

$$C_{\mathrm{bub}}^{-1}\|q\|_{0,e}^2 \leq \|\psi_e^{1/2} q\|_{0,e}^2 \leq C_{\mathrm{bub}}\|q\|_{0,e}^2 \qquad \forall\, q \in \mathrm{P}_k(e), \tag{4.50}$$

*and*

$$h_K^{-1/2}\|\psi_e L(q)\|_{0,K} + h_K^{1/2}|\psi_e L(q)|_{1,K} \leq C_{\mathrm{bub}}\|q\|_{0,e} \qquad \forall\, q \in \mathrm{P}_k(e), \tag{4.51}$$

*where $K \in \omega_e$.*

We start the analysis bounding the terms defining $\eta_{1,K}^2$ and $\eta_{2,K}^2$.

**Lemma 4.23.** *There exists a constant $C > 0$, independent of $h$, such that*

$$h_K^2\|\boldsymbol{\kappa}_h\boldsymbol{\sigma}_h^\star - \nabla u_h\|_{0,K}^2 \leq C\left\{h_K^2\|\boldsymbol{\sigma} - \boldsymbol{\sigma}_h^\star\|_{0,K}^2 + h_K^2\|(\boldsymbol{\kappa}^{-1} - \boldsymbol{\kappa}_h)\boldsymbol{\sigma}_h^\star\|_{0,K}^2 + \|u - u_h\|_{0,K}^2\right\} \qquad \forall\, K \in \mathcal{T}_h.$$

*Proof.* It is a slight modification of the proof of the Lemma 6.3 in [41] (see also Lemma 5.5 in [55]). Given $K \in \mathcal{T}_h$ we denote $\gamma_K := \boldsymbol{\kappa}_h \boldsymbol{\sigma}_h^\star - \nabla u_h \in [\mathrm{P}_\ell(K)]^2$ for some $\ell \geq 0$. Then, applying (4.48), using that $\boldsymbol{\kappa}^{-1}\boldsymbol{\sigma} = \nabla u$ in $\Omega$, and integrating by parts, we find that

$$\begin{aligned} C_{\mathrm{bub}}^{-1}\|\gamma_K\|_{0,K}^2 &\leq \|\psi_K^{1/2}\gamma_K\|_{0,K}^2 = \int_K \psi_K \gamma_K \cdot \{\boldsymbol{\kappa}_h \boldsymbol{\sigma}_h^\star - \nabla u_h\} \\ &= \int_K \psi_K \gamma_K \cdot \left\{(\boldsymbol{\kappa}_h - \boldsymbol{\kappa}^{-1})\boldsymbol{\sigma}_h^\star + \boldsymbol{\kappa}^{-1}\boldsymbol{\sigma}_h^\star - \boldsymbol{\kappa}^{-1}\boldsymbol{\sigma} + \nabla(u - u_h)\right\} \\ &= -\int_K \psi_K \gamma_K \cdot (\boldsymbol{\kappa}^{-1} - \boldsymbol{\kappa}_h)\boldsymbol{\sigma}_h^\star - \int_K \psi_K \gamma_K \cdot \boldsymbol{\kappa}^{-1}(\boldsymbol{\sigma} - \boldsymbol{\sigma}_h^\star) \\ &\quad - \int_K \mathrm{div}(\psi_K \gamma_K)(u - u_h). \end{aligned}$$

Then, applying the Cauchy-Schwarz inequality, the estimate (4.49), and setting $C_{\boldsymbol{\kappa}} := \max\left\{1, \|\boldsymbol{\kappa}^{-1}\|\right\}$, we get

$$\begin{aligned} &C_{\mathrm{bub}}^{-1}\|\gamma_K\|_{0,K}^2 \\ &\leq C_{\boldsymbol{\kappa}}\left\{\|\psi_K\gamma_K\|_{0,K}\left\{\|(\boldsymbol{\kappa}^{-1} - \boldsymbol{\kappa}_h)\boldsymbol{\sigma}_h^\star\|_{0,K} + \|\boldsymbol{\sigma} - \boldsymbol{\sigma}_h^\star\|_{0,K}\right\} + |\psi_K\gamma_K|_{1,K}\|u - u_h\|_{0,K}\right\} \\ &\leq C_{\boldsymbol{\kappa}} C_{\mathrm{bub}}\left\{\|(\boldsymbol{\kappa}^{-1} - \boldsymbol{\kappa}_h)\boldsymbol{\sigma}_h^\star\|_{0,K} + \|\boldsymbol{\sigma} - \boldsymbol{\sigma}_h^\star\|_{0,K} + h_K^{-1}\|u - u_h\|_{0,K}\right\}\|\gamma_K\|_{0,K} \\ &\leq 2C_{\boldsymbol{\kappa}} C_{\mathrm{bub}}\left\{\|(\boldsymbol{\kappa}^{-1} - \boldsymbol{\kappa}_h)\boldsymbol{\sigma}_h^\star\|_{0,K}^2 + \|\boldsymbol{\sigma} - \boldsymbol{\sigma}_h^\star\|_{0,K}^2 + h_K^{-2}\|u - u_h\|_{0,K}^2\right\}^{1/2}\|\gamma_K\|_{0,K}, \end{aligned}$$

whence, the proof is concluded. □

**Lemma 4.24.** *There exists a constant $C > 0$, independent of $h$, such that*

$$h_e\|g - u_h\|_{0,e}^2 \leq C\left\{h_K^2\|\boldsymbol{\sigma} - \boldsymbol{\sigma}_h^\star\|_{0,K}^2 + h_K^2\|(\boldsymbol{\kappa}^{-1} - \boldsymbol{\kappa}_h)\boldsymbol{\sigma}_h^\star\|_{0,K}^2 + \|u - u_h\|_{0,K}^2\right\} \quad \forall\, e \in \mathcal{E}_h(\Gamma_D),$$

*where $K \in \mathcal{T}_h$ is such that $e \in \partial K$.*

*Proof.* We proceed as in the proof of the Lemma 4.14 in [63]. We consider $e \in \mathcal{E}_h(\Gamma_D)$ and $K \in \mathcal{T}_h$ such that $e \in \partial K$. Then, applying a trace inequality, together with the fact that $u = g$ on $\Gamma_D$ and $\boldsymbol{\sigma} = \boldsymbol{\kappa}\nabla u$ in $\Omega$, we get

$$\begin{aligned} &\|g - u_h\|_{0,e}^2 = \|u - u_h\|_{0,e}^2 \leq C_{\mathrm{tr}}\left\{h_K^{-1}\|u - u_h\|_{0,K}^2 + h_K|u - u_h|_{1,K}^2\right\} \\ &\leq 2C_{\boldsymbol{\kappa}} C_{\mathrm{tr}}\left\{h_K^{-1}\|u - u_h\|_{0,K}^2 + h_K\left\{\|\boldsymbol{\sigma} - \boldsymbol{\sigma}_h^\star\|_{0,K}^2 + \|\boldsymbol{\kappa}_h\boldsymbol{\sigma}_h^\star - \nabla u_h\|_{0,K}^2 + \|(\boldsymbol{\kappa}^{-1} - \boldsymbol{\kappa}_h)\boldsymbol{\sigma}_h^\star\|_{0,K}^2\right\}\right\}, \end{aligned}$$

with $C_{\boldsymbol{\kappa}}$ as in the proof of Lemma 4.23. From this, using the bound $h_e \leq h_K$ and the estimate of Lemma 4.23 we obtain the result. □

The following result is required in view of proving upper bounds for the terms defining $\theta_K^2$.

**Lemma 4.25.** *Let $\boldsymbol{\zeta}_h \in [\mathrm{L}^2(\Omega)]^2$ be a piecewise polynomial of degree $k \geq 0$ on each $K \in \mathcal{T}_h$. In addition let $\boldsymbol{\zeta} \in [\mathrm{L}^2(\Omega)]^2$ be such that $\mathrm{rot}(\boldsymbol{\zeta}) = 0$ in $\Omega$. Then, there exists $C > 0$, depending only on $C_{\mathrm{bub}}$, such that*

$$\|\mathrm{rot}\,\boldsymbol{\zeta}_h\|_{0,K} \leq C h_K^{-1}\|\boldsymbol{\zeta} - \boldsymbol{\zeta}_h\|_{0,K} \quad \forall\, K \in \mathcal{T}_h\,, \tag{4.52}$$

*and*

$$\|[\![\boldsymbol{\zeta}_h \cdot s_e]\!]\|_{0,e} \leq C h_e^{-1/2} \|\boldsymbol{\zeta} - \boldsymbol{\zeta}_h\|_{0,\omega_e} \quad \forall\, e \in \mathcal{E}_h(\Omega)\,. \tag{4.53}$$

*Proof.* To show (4.52), we proceed as in the proof of Lemma 4.3 in [12]. Applying (4.48), observing that $\psi_K = 0$ on $\partial K$, and using the Cauchy-Schwarz inequality, we get

$$\begin{aligned} C_{\mathrm{bub}}^{-1} \|\mathrm{rot}\, \boldsymbol{\zeta}_h\|_{0,K}^2 &\leq \|\psi_K^{1/2} \mathrm{rot}\, \boldsymbol{\zeta}_h\|_{0,K}^2 = -\int_K \psi_K \mathrm{rot}\, \boldsymbol{\zeta}_h\, \mathrm{rot}(\boldsymbol{\zeta} - \boldsymbol{\zeta}_h) \\ &= \int_K (\boldsymbol{\zeta} - \boldsymbol{\zeta}_h) \cdot \mathbf{rot}(\psi_K \mathrm{rot}\, \boldsymbol{\zeta}_h) \leq \|\boldsymbol{\zeta} - \boldsymbol{\zeta}_h\|_{0,K} |\psi_K \mathrm{rot}\, \boldsymbol{\zeta}_h|_{1,K}\,. \end{aligned}$$

Then, from inverse inequality (4.49), we deduce (4.52).

The estimate (4.53) follows from a slight modification of the proof of [12, Lemma 4.4]. Indeed, given $e \in \mathcal{E}_h(\Omega)$, we let $J_h := [\![\boldsymbol{\zeta}_h \cdot s_e]\!] \in \mathrm{P}_k(e)$. Then, utilizing (4.50), the fact that $[\![\boldsymbol{\zeta} \cdot s_e]\!] = 0$ a.e on $e$, and integrating by parts on each $K \in \mathcal{T}_h$, we get

$$\begin{aligned} C_{\mathrm{bub}}^{-1} \|J_h\|_{0,e}^2 &\leq \|\psi_e^{1/2} J_h\|_{0,e}^2 = \|\psi_e^{1/2} L(J_h)\|_{0,e}^2 = \int_e \psi_e L(J_h) [\![\boldsymbol{\zeta}_h \cdot s]\!] \\ &= \int_{\omega_e} (\boldsymbol{\zeta}_h - \boldsymbol{\zeta}) \cdot \mathbf{rot}(\psi_e L(J_h)) + \int_{\omega_e} \psi_e L(J_h)\, \mathrm{rot}\, \boldsymbol{\zeta}_h\,, \end{aligned}$$

which, using the Cauchy-Schwarz inequality, the estimates (4.51) and (4.52), and the fact that $h_e \leq h_K$, yields

$$\begin{aligned} C_{\mathrm{bub}}^{-1} \|J_h\|_{0,e}^2 &\leq |\psi_e L(J_h)|_{1,\omega_e} \|\boldsymbol{\zeta} - \boldsymbol{\zeta}_h\|_{0,\omega_e} + \|\psi_e L(J_h)\|_{0,\omega_e} \|\mathrm{rot}\, \boldsymbol{\zeta}_h\|_{0,\omega_e} \\ &\leq 2 N_{\mathcal{T}} C_{\mathrm{bub}} h_e^{-1/2} \|\boldsymbol{\zeta} - \boldsymbol{\zeta}_h\|_{0,\omega_e} \|J_h\|_{0,e}\,, \end{aligned}$$

whence, we conclude the proof of (4.53). □

**Lemma 4.26.** *There exists $C > 0$, independent of $h$, such that*

$$h_K^2 \|\mathrm{rot}(\boldsymbol{\kappa}_h \boldsymbol{\sigma}_h^\star)\|_{0,K}^2 \leq C \Big\{ \|\boldsymbol{\sigma} - \boldsymbol{\sigma}_h^\star\|_{0,K}^2 + \|(\boldsymbol{\kappa}^{-1} - \boldsymbol{\kappa}_h)\boldsymbol{\sigma}_h^\star\|_{0,K}^2 \Big\} \quad \forall\, e \in \mathcal{E}_h(\Omega),$$

*and*

$$h_e \|[\![\boldsymbol{\kappa}_h \boldsymbol{\sigma}_h^\star \cdot s_e]\!]\|_{0,e}^2 \leq C \Big\{ \|\boldsymbol{\sigma} - \boldsymbol{\sigma}_h^\star\|_{0,K}^2 + \|(\boldsymbol{\kappa}^{-1} - \boldsymbol{\kappa}_h)\boldsymbol{\sigma}_h^\star\|_{0,K}^2 \Big\} \quad \forall\, e \in \mathcal{E}_h(\Omega),$$

*where $K \in \mathcal{T}_h$ is such that $K \in \omega_e$.*

*Proof.* It suffices to apply Lemma 4.25 with $\boldsymbol{\zeta}_h := \boldsymbol{\kappa}_h \boldsymbol{\sigma}_h^\star$ and $\boldsymbol{\zeta} := \boldsymbol{\kappa}^{-1}\boldsymbol{\sigma} = \nabla u$, and the triangle inequality. □

**Lemma 4.27.** *Assume that $\frac{dg}{ds}$ is piecewise polynomial on $\Gamma_D$. Then, there exists $C > 0$, independent of $h$, such that*

$$h_e \left\| \boldsymbol{\kappa}_h \boldsymbol{\sigma}_h^\star \cdot s - \frac{dg}{ds} \right\|_{0,e}^2 \leq C \Big\{ \|\boldsymbol{\sigma} - \boldsymbol{\sigma}_h^\star\|_{0,K}^2 + \|(\boldsymbol{\kappa}^{-1} - \boldsymbol{\kappa}_h)\boldsymbol{\sigma}_h^\star\|_{0,K}^2 \Big\} \quad \forall\, e \in \mathcal{E}_h(\Gamma_D), \tag{4.54}$$

*where $K \in \mathcal{T}_h$ is such that $K \in \omega_e$.*

*Proof.* We proceed as in the proof of Lemma 4.15 in [63] (see also Lemma 5.7 in [55]). Given $e \in \mathcal{E}_h(\Gamma_D)$ and $K \in \omega_e$, we denote $\gamma_e := \boldsymbol{\kappa}_h \boldsymbol{\sigma}_h^\star \cdot s - \dfrac{dg}{ds} \in \mathrm{P}_\ell(e)$ for some $\ell \geq 0$. Then, applying (4.50), the fact that $\nabla u \cdot s = \dfrac{dg}{ds}$, integrating by parts and using that $\boldsymbol{\kappa}^{-1}\boldsymbol{\sigma} = \nabla u$ in $\Omega$, we obtain that

$$\begin{aligned} C_{\mathrm{bub}}^{-1}\|\gamma_e\|_{0,e}^2 &\leq \|\psi_e^{1/2}\gamma_e\|_{0,e}^2 = \int_e \psi_e \gamma_e \Big\{ \boldsymbol{\kappa}_h \boldsymbol{\sigma}_h^\star \cdot s - \nabla u \cdot s \Big\} \\ &= -\int_{\partial K} \psi_e L(\gamma_e) \left\{ \left( \boldsymbol{\kappa}^{-1}\boldsymbol{\sigma} - \boldsymbol{\kappa}_h \boldsymbol{\sigma}_h^\star \right) \cdot s \right\} \\ &= -\int_K \mathbf{rot}(\psi_e L(\gamma_e)) \cdot (\boldsymbol{\kappa}^{-1} - \boldsymbol{\kappa}_h)\boldsymbol{\sigma}_h^\star - \int_K \mathbf{rot}(\psi_e L(\gamma_e)) \cdot \boldsymbol{\kappa}^{-1} \Big\{ \boldsymbol{\sigma} - \boldsymbol{\sigma}_h^\star \Big\} \\ &\quad + \int_K \psi_e L(\gamma_e) \mathrm{rot}(\boldsymbol{\kappa}_h \boldsymbol{\sigma}_h^\star)\,. \end{aligned}$$

Next, applying the Cauchy-Schwarz inequality, Lemma 4.26, the estimate (4.51), and the fact that $h_e \leq h_K$ we get

$$\begin{aligned} C_{\mathrm{bub}}^{-1}\|\gamma_e\|_{0,e}^2 &\leq C \Big\{ |\psi_e L(\gamma_e)|_{1,K} + h_K^{-1}\|\psi_e L(\gamma_e)\|_{0,K} \Big\} \Big\{ \|\boldsymbol{\sigma} - \boldsymbol{\sigma}_h^\star\|_{0,K} + \|(\boldsymbol{\kappa}^{-1} - \boldsymbol{\kappa}_h)\boldsymbol{\sigma}_h^\star\|_{0,K} \Big\} \\ &\leq C h_e^{-1/2} \Big\{ \|\boldsymbol{\sigma} - \boldsymbol{\sigma}_h^\star\|_{0,K} + \|(\boldsymbol{\kappa}^{-1} - \boldsymbol{\kappa}_h)\boldsymbol{\sigma}_h^\star\|_{0,K} \Big\} \|\gamma_e\|_{0,e}, \end{aligned}$$

and the proof is complete. □

If $\frac{dg}{ds}$ is not piecewise polynomial but sufficiently smooth, Lemma 4.27 can still be proven with higher order terms given by the errors arising from suitable polynomial approximations appearing in (4.54).

Finally, a lower bound is obtained from estimates (4.45)-(4.47), together with Lemmata 4.23 throughout 4.27, after summing up over $K \in \mathcal{T}_h$ and using the fact that the number of elements on each domain $\omega_e$ is bounded.

## 4.6 Numerical Tests

In this section, we present three numerical tests confirming the upper and lower bounds, derived in Section 4.5, for the a posteriori error estimator of Theorem 4.20, and showing the behaviour of the associated adaptive algorithm. We begin by introducing additional notations. In what follows, $N$ stands for the total number of degrees of freedom of (4.18), that is,

$$N := (k+1) \times \{\text{number of edges } e \in \mathcal{T}_h\} + \frac{(k+2)(3k+1)}{2} \times \{\text{number of elements } K \in \mathcal{T}_h\}.$$

Also, the individual errors are defined by

$$\begin{aligned} \mathsf{e}(\boldsymbol{\sigma}) &:= \left\{ \sum_{K \in \mathcal{T}_h} \|\boldsymbol{\sigma} - \boldsymbol{\sigma}_{h,K}^\star\|_{\mathrm{div};K}^2 \right\}^{1/2}, \quad \mathsf{e}(u) := \|u - u_h\|_{0,\Omega}, \quad \text{and} \\ \mathsf{e}(\boldsymbol{\sigma}, u) &:= \Big\{ [\mathsf{e}(\boldsymbol{\sigma})]^2 + [\mathsf{e}(u)]^2 \Big\}^{1/2}, \end{aligned}$$

whereas the associated experimental rates of convergence are given by

$$\mathtt{r}(\cdot) := -2\frac{\log(\mathtt{e}(\cdot)/\mathtt{e}'(\cdot))}{\log(N/N')},$$

where $\mathtt{e}$ and $\mathtt{e}'$ denote the corresponding errors for two consecutive meshes with $N$ and $N'$ denote the corresponding degrees of freedom of each decomposition. Denote by $\Theta$ the a posteriori error estimator of Theorem 4.20. The effectivity of the estimator $\Theta$ is given by

$$\mathtt{eff}(\Theta) := \frac{\mathtt{e}(\boldsymbol{\sigma}, u)}{\Theta}\,.$$

For the tests that include adaptivity, we use the strategy:

(i) Start with a coarse mesh $\mathcal{T}_h$.

(ii) Solve the discrete problem on the current mesh $\mathcal{T}_h$.

(iii) Compute local indicators for each $K \in \mathcal{T}_h$.

(iv) Mark each $K' \in \mathcal{T}_h$ such that

$$\Theta_{K'} \geq \beta \max_{K\in\mathcal{T}_h} \Theta_K,$$

with $\beta \in [0,1]$ and we refine using the midpoint of each edge of each element and connecting this to its barycentre. Here, we use $\beta = 0.5$.

(v) Update $\mathcal{T}_h$ with the new mesh and go to step (ii).

Hereafter, in all numerical tests we have $\boldsymbol{\kappa} = \begin{pmatrix} 1 & 0 \\ 0 & 1 \end{pmatrix}$ and we consider domains $\Omega$ satisfying Lemma 4.16. In this case, we have that $\Upsilon_K^2$ and $\Psi_{2,K}^2$ are null for each $K \in \mathcal{T}_h$ (cf. Remark 4.12 in Section 4.5.2).

### 4.6.1 Test 1. Smooth solution: behaviour of the estimator under uniform refinement

For this test case, we consider $\Omega := (0,1)^2$ with $\Gamma_D := \Big\{(w,0),(0,w) \in \Omega : \quad 0 \leq w \leq 1\Big\}$ and $\Gamma_N := \Gamma \setminus \overline{\Gamma}_D$. The source term $f$ and the boundary data $g$ are chosen such that the exact solution is given by $u(x,y) = \cos(\pi x)\cos(\pi y)$

Table 4.1 shows the convergence history of the error for each variable and the estimator on a sequence of uniformly refined hexagonal meshes, indicating that both converge at the optimal rate for polynomial degrees $k = 0, 1, 2$. Moreover, the effectivity remains bounded. In addition, we see from Table 4.2 that each term of the error estimator converge with optimal order $k+1$.

### 4.6.2 Test 2. Solution with a sharp layer: uniform vs adaptive refinement

We consider $\Omega := (0,1)^2$ with $\Gamma_D := \Big\{(w,0),(0,w) \in \Omega : \quad 0 \leq w \leq 1\Big\}$ and $\Gamma_N := \Gamma \setminus \overline{\Gamma}_D$ , and choose $f$ and $g$ such that the exact solution is given by

$$u(x,y) = (x-1)^2(y-1)^2\left(\frac{1}{x+0.1} + \frac{1}{1+y}\right) \quad \text{in} \quad \Omega\,.$$

| $k$ | $N$ | $\mathtt{e}(\boldsymbol{\sigma})$ | $\mathtt{r}(\boldsymbol{\sigma})$ | $\mathtt{e}(u)$ | $\mathtt{r}(u)$ | $\mathtt{e}(\boldsymbol{\sigma},u)$ | $\mathtt{r}(\boldsymbol{\sigma},u)$ | $\Theta$ | $\mathtt{r}(\Theta)$ | $\mathtt{eff}(\Theta)$ |
|---|---|---|---|---|---|---|---|---|---|---|
| | 589 | 1.0959e+00 | −− | 5.5406e-02 | −− | 1.0973e+00 | −− | 1.2946e+00 | −− | 8.4760e-01 |
| | 3469 | 4.3834e-01 | 1.0336 | 2.1963e-02 | 1.0437 | 4.3889e-01 | 1.0336 | 5.1997e-01 | 1.0288 | 8.4405e-01 |
| 0 | 8749 | 2.7388e-01 | 1.0167 | 1.3708e-02 | 1.0191 | 2.7423e-01 | 1.0167 | 3.2511e-01 | 1.0153 | 8.4348e-01 |
| | 19605 | 1.8247e-01 | 1.0067 | 9.1290e-03 | 1.0077 | 1.8270e-01 | 1.0067 | 2.1667e-01 | 1.0059 | 8.4323e-01 |
| | 43805 | 1.2165e-01 | 1.0087 | 6.0851e-03 | 1.0090 | 1.2180e-01 | 1.0087 | 1.4447e-01 | 1.0082 | 8.4307e-01 |
| | 1766 | 5.9382e-02 | −− | 3.0274e-03 | −− | 5.9459e-02 | −− | 7.2082e-02 | −− | 8.2488e-01 |
| | 10406 | 9.5820e-03 | 2.0569 | 4.8269e-04 | 2.0704 | 9.5941e-03 | 2.0569 | 1.1588e-02 | 2.0611 | 8.2791e-01 |
| 1 | 26246 | 3.7498e-03 | 2.0282 | 1.8859e-04 | 2.0317 | 3.7546e-03 | 2.0282 | 4.5310e-03 | 2.0301 | 8.2863e-01 |
| | 58814 | 1.6674e-03 | 2.0088 | 8.3810e-05 | 2.0103 | 1.6695e-03 | 2.0088 | 2.0135e-03 | 2.0105 | 8.2918e-01 |
| | 131414 | 7.4166e-04 | 2.0154 | 3.7268e-05 | 2.0160 | 7.4260e-04 | 2.0154 | 8.9537e-04 | 2.0159 | 8.2938e-01 |
| | 3384 | 2.2263e-03 | −− | 1.1132e-04 | −− | 2.2290e-03 | −− | 3.6826e-03 | −− | 6.0529e-01 |
| | 19944 | 1.4599e-04 | 3.0718 | 7.2751e-06 | 3.0757 | 1.4618e-04 | 3.0718 | 2.3901e-04 | 3.0835 | 6.1158e-01 |
| 2 | 50304 | 3.5848e-05 | 3.0358 | 1.7855e-06 | 3.0368 | 3.5892e-05 | 3.0358 | 5.8541e-05 | 3.0412 | 6.1312e-01 |
| | 112726 | 1.0645e-05 | 3.0097 | 5.3011e-07 | 3.0101 | 1.0658e-05 | 3.0097 | 1.7356e-05 | 3.0135 | 6.1405e-01 |
| | 251876 | 3.1615e-06 | 3.0200 | 1.5743e-07 | 3.0202 | 3.1654e-06 | 3.0200 | 5.1503e-06 | 3.0222 | 6.1460e-01 |

Table 4.1: Test 1. Convergence history for an uniformly generated sequence of hexagonal meshes (table produced by the author).

| $k$ | $N$ | $\Phi$ | $\mathtt{r}(\Phi)$ | $\eta$ | $\mathtt{r}(\eta)$ | $\theta$ | $\mathtt{r}(\theta)$ | $\Psi$ | $\mathtt{r}(\Psi)$ | $\Lambda$ | $\mathtt{r}(\Lambda)$ |
|---|---|---|---|---|---|---|---|---|---|---|---|
| | 589 | 1.0813e+00 | −− | 2.4480e-01 | −− | 4.1938e-01 | −− | 4.9543e-01 | −− | 1.5941e-01 | −− |
| | 3469 | 4.3269e-01 | 1.0331 | 9.9066e-02 | 1.0204 | 1.7027e-01 | 1.0167 | 1.9984e-01 | 1.0240 | 6.6419e-02 | 0.9874 |
| 0 | 8749 | 2.7038e-01 | 1.0166 | 6.2010e-02 | 1.0129 | 1.0674e-01 | 1.0096 | 1.2490e-01 | 1.0162 | 4.1913e-02 | 0.9954 |
| | 19605 | 1.8014e-01 | 1.0066 | 4.1346e-02 | 1.0047 | 7.1146e-02 | 1.0056 | 8.3291e-02 | 1.0043 | 2.8040e-02 | 0.9963 |
| | 43805 | 1.2010e-01 | 1.0086 | 2.7577e-02 | 1.0075 | 4.7506e-02 | 1.0047 | 5.5492e-02 | 1.0103 | 1.8769e-02 | 0.9987 |
| | 1766 | 5.8895e-02 | −− | 2.6740e-02 | −− | 2.4564e-02 | −− | 1.7131e-02 | −− | 1.0741e-02 | −− |
| | 10406 | 9.5028e-03 | 2.0569 | 4.3181e-03 | 2.0560 | 4.0707e-03 | 2.0268 | 2.3959e-03 | 2.2182 | 1.7408e-03 | 2.0519 |
| 1 | 26246 | 3.7187e-03 | 2.0283 | 1.6914e-03 | 2.0262 | 1.6028e-03 | 2.0150 | 8.9830e-04 | 2.1208 | 6.8185e-04 | 2.0263 |
| | 58814 | 1.6535e-03 | 2.0089 | 7.5239e-04 | 2.0079 | 7.1485e-04 | 2.0014 | 3.8855e-04 | 2.0774 | 3.0292e-04 | 2.0111 |
| | 131414 | 7.3548e-04 | 2.0154 | 3.3486e-04 | 2.0139 | 3.1868e-04 | 2.0097 | 1.6997e-04 | 2.0569 | 1.3484e-04 | 2.0135 |
| | 3384 | 2.1867e-03 | −− | 1.5283e-03 | −− | 7.9424e-04 | −− | 2.3731e-03 | −− | 4.2607e-04 | −− |
| | 19944 | 1.4347e-04 | 3.0713 | 9.9799e-05 | 3.0766 | 5.3189e-05 | 3.0482 | 1.5168e-04 | 3.1008 | 2.7317e-05 | 3.0973 |
| 2 | 50304 | 3.5232e-05 | 3.0356 | 2.4480e-05 | 3.0379 | 1.3119e-05 | 3.0261 | 3.7011e-05 | 3.0494 | 6.6740e-06 | 3.0466 |
| | 112726 | 1.0462e-05 | 3.0096 | 7.2624e-06 | 3.0120 | 3.9066e-06 | 3.0027 | 1.0949e-05 | 3.0189 | 1.9758e-06 | 3.0172 |
| | 251876 | 3.1074e-06 | 3.0200 | 2.1565e-06 | 3.0206 | 1.1618e-06 | 3.0168 | 3.2445e-06 | 3.0257 | 5.8587e-07 | 3.0240 |

Table 4.2: Test 1. Convergence history of the terms composing the estimator using hexagonal meshes (table produced by the author).

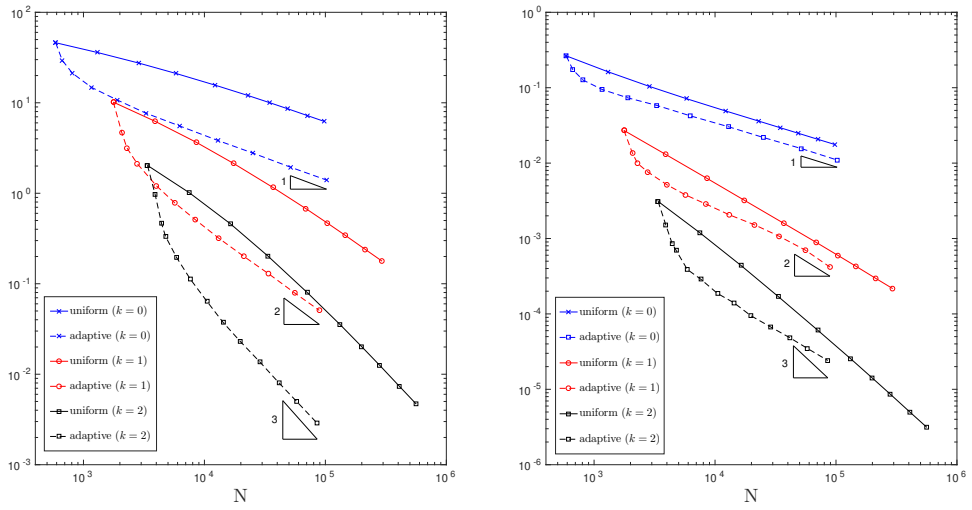


Figure 4.1: Test 2. Convergence history under uniform and the adaptive refinement of hexagonal meshes (cf. Figure 4.3). The error $\mathtt{e}(\boldsymbol{\sigma})$ (left) and $\mathtt{e}(u)$ (right) (figure produced by the author).

Note that $u$ and $\nabla u$ are singular along the lines $x = -0.1$ and $y = -1$. Both such lines are outside $\Omega$, but we expect regions of high gradients in the vicinity of the left boundary. From Figure 4.1 we observe, as expected, that the adaptive methods outperforms uniform refinement. Indeed, initially the adaptive method superconverges until, ones the steep layer is resolved, both methods converge at the theoretical rate, namely $k+1$. This is clearly shown in Table 4.3, where the rates of convergence of the global error and the estimator at each step of the adaptive algorithm are reported together with the effectivity index. As shown in Figure 4.2, all terms in the error estimator follow precisely the same behaviour.

Some intermediate meshes obtained with adaptive strategy are displayed in Figure 4.3. Notice here that the adapted meshes concentrate the refinements in the proximity of the line $x = 0$, confirming that the adaptive algorithm is able to target the regions with high gradients of the solution.

### 4.6.3 Test 3. L-shaped domain solution: adaptive refinement

We consider $\Omega := (-1,1)^2 \setminus (0,1)^2$ with $\Gamma_N := \Big\{(-1,w),(w,-1) \in \Omega : \quad -1 \leq w \leq 1\Big\}$ and $\Gamma_D := \Gamma \setminus \overline{\Gamma}_N$, and choose $f$ and $g$ such that the exact solution is given by

$$u(x,y) = \frac{(x+1)^2(y+1)^2}{\sqrt{(x-0.1)^2+(y-0.1)^2}} \quad \text{in} \quad \Omega\,.$$

Note that $\Omega$ is an L-shaped domain and that $u$ and $\nabla u$ are singular at the point $(0.1, 0.1)$, which is just outside of $\Omega$. Hence, we should expect regions of high gradients around the origin, which is the middle corner of the L-shaped domain. In Figure 4.4 and Table 4.4 we display the convergence history of the adaptive method. Finally, Figure 4.5 shows how the adaptive strategy correctly refines in a neighbourhood of the origin. We also notice that increasing the order of the method allows for a less aggressive refinement.

| $k$ | $N$ | $\mathtt{e}(\boldsymbol{\sigma}, u)$ | $\mathtt{r}(\boldsymbol{\sigma}, u)$ | $\Theta$ | $\mathtt{r}(\Theta)$ | $\mathtt{eff}(\Theta)$ |
|---|---|---|---|---|---|---|
| | 589 | 4.6114e+01 | −− | 4.6592e+01 | −− | 0.9896 |
| | 668 | 2.9471e+01 | 7.1146 | 2.9879e+01 | 7.0595 | 0.9863 |
| | 809 | 2.1279e+01 | 3.4013 | 2.1642e+01 | 3.3681 | 0.9832 |
| 0 | 1163 | 1.4820e+01 | 1.9932 | 1.5118e+01 | 1.9769 | 0.9803 |
| | 1902 | 1.0735e+01 | 1.3112 | 1.0978e+01 | 1.3011 | 0.9779 |
| | 3290 | 7.6690e+00 | 1.2275 | 7.8661e+00 | 1.2165 | 0.9749 |
| | 6272 | 5.5309e+00 | 1.0131 | 5.6850e+00 | 1.0066 | 0.9729 |
| | 12928 | 3.8304e+00 | 1.0158 | 3.9474e+00 | 1.0086 | 0.9704 |
| | 1766 | 1.0162e+01 | −− | 1.0241e+01 | −− | 0.9923 |
| | 2072 | 4.7026e+00 | 9.6441 | 4.7595e+00 | 9.5903 | 0.9880 |
| | 2288 | 3.1654e+00 | 7.9834 | 3.2240e+00 | 7.8561 | 0.9818 |
| | 2782 | 2.1237e+00 | 4.0834 | 2.1691e+00 | 4.0545 | 0.9791 |
| 1 | 4014 | 1.2081e+00 | 3.0775 | 1.2367e+00 | 3.0652 | 0.9769 |
| | 5706 | 7.8010e-01 | 2.4868 | 8.0163e-01 | 2.4652 | 0.9732 |
| | 8368 | 5.1334e-01 | 2.1859 | 5.3063e-01 | 2.1550 | 0.9674 |
| | 13090 | 3.1982e-01 | 2.1151 | 3.3270e-01 | 2.0867 | 0.9613 |
| | 21158 | 2.0077e-01 | 1.9394 | 2.0991e-01 | 1.9183 | 0.9564 |
| | 3384 | 2.0312e+00 | −− | 2.0513e+00 | −− | 0.9902 |
| | 3913 | 9.7026e-01 | 10.1734 | 9.8510e-01 | 10.0996 | 0.9849 |
| | 4422 | 4.6358e-01 | 12.0796 | 4.7458e-01 | 11.9440 | 0.9768 |
| | 4771 | 3.3337e-01 | 8.6810 | 3.4515e-01 | 8.3847 | 0.9659 |
| 2 | 5899 | 1.9436e-01 | 5.0845 | 2.0487e-01 | 4.9154 | 0.9487 |
| | 7640 | 1.1258e-01 | 4.2231 | 1.1729e-01 | 4.3134 | 0.9598 |
| | 10494 | 6.3836e-02 | 3.5747 | 6.6868e-02 | 3.5407 | 0.9547 |
| | 14293 | 3.7310e-02 | 3.4766 | 3.9482e-02 | 3.4105 | 0.9450 |
| | 19800 | 2.3005e-02 | 2.9673 | 2.4509e-02 | 2.9259 | 0.9386 |

Table 4.3: Test 2. The behaviour of the global error and the estimator under adaptive refinement of hexagonal meshes (cf. Figure 4.3). The effectivity of the estimator is reported in the right-most column (table produced by the author).

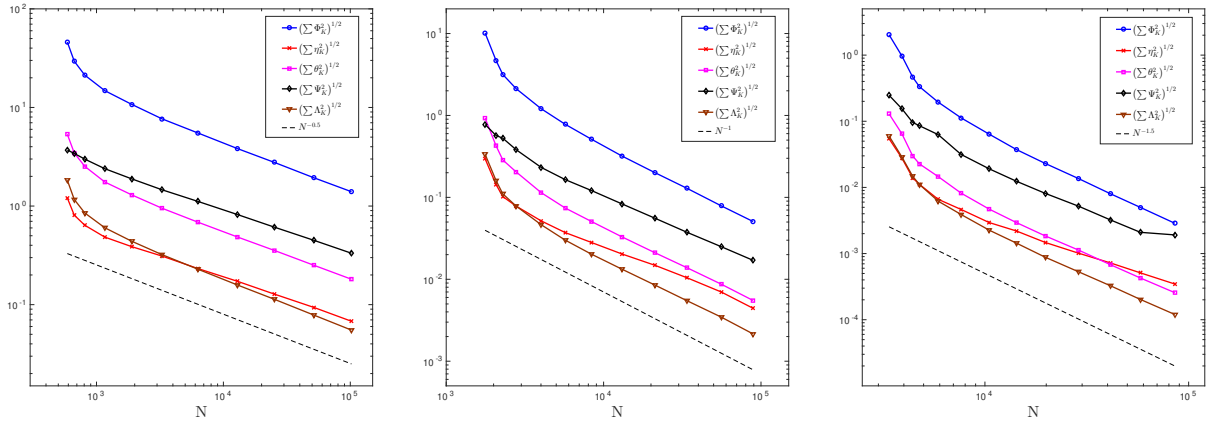


Figure 4.2: Test 2. Convergence history of the components of the estimator under adaptive refinement of hexagonal meshes (cf. Figure 4.3 below). For $k = 0$ (left), $k = 1$ (centre), and $k = 2$ (right) (figure produced by the author).

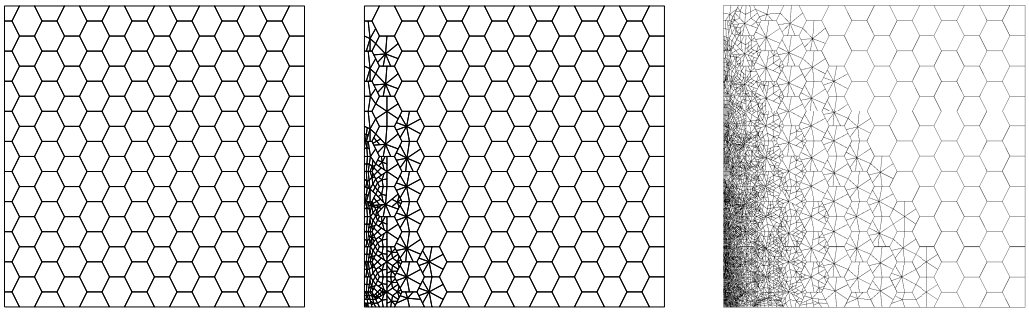

Figure 4.3: Test 2. Some meshes from the adaptive refinement sequence obtained with $k = 1$: initial (left), after 5 refinement steps (centre), and after 10 refinement steps (right) (figure produced by the author).

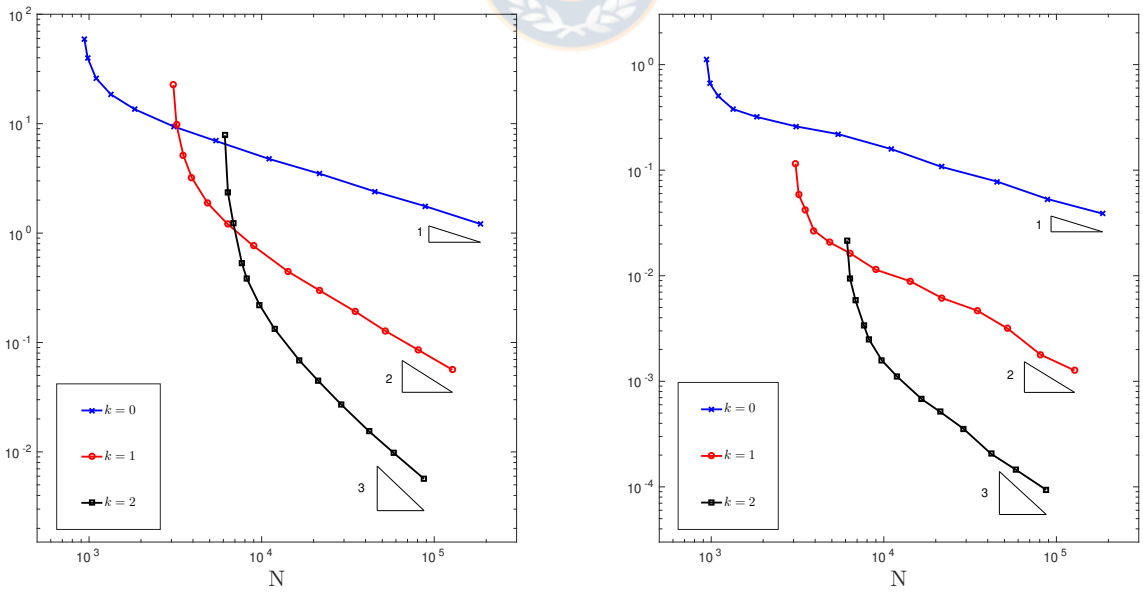


Figure 4.4: Test 3. Errors curves for the adaptive strategy using distorted quadrilateral meshes, (cf. Figure 4.5 below). The error $\mathsf{e}(\boldsymbol{\sigma})$ (left) and the error $\mathsf{e}(u)$ (right) (figure produced by the author).

| $k$ | $N$ | $\mathtt{e}(\boldsymbol{\sigma}, u)$ | $\mathtt{r}(\boldsymbol{\sigma}, u)$ | $\Theta$ | $\mathtt{r}(\Theta)$ | $\mathtt{eff}(\Theta)$ |
|---|---|---|---|---|---|---|
| | 940 | 5.9057e+01 | −− | 6.1812e+01 | −− | 0.9554 |
| | 982 | 3.9730e+01 | 18.1365 | 4.1712e+01 | 17.9953 | 0.9525 |
| | 1096 | 2.6136e+01 | 7.6263 | 2.7724e+01 | 7.4387 | 0.9427 |
| 0 | 1337 | 1.8521e+01 | 3.4653 | 2.0096e+01 | 3.2376 | 0.9216 |
| | 1838 | 1.3548e+01 | 1.9650 | 1.4905e+01 | 1.8783 | 0.9090 |
| | 3098 | 9.4108e+00 | 1.3959 | 1.0536e+01 | 1.3286 | 0.8932 |
| | 5420 | 6.9603e+00 | 1.0786 | 7.8716e+00 | 1.0426 | 0.8842 |
| | 11100 | 4.7501e+00 | 1.0659 | 5.4231e+00 | 1.0395 | 0.8759 |
| | 3080 | 2.2588e+01 | −− | 2.4078e+01 | −− | 0.9381 |
| | 3212 | 9.7746e+00 | 39.9209 | 1.0379e+01 | 40.1065 | 0.9418 |
| | 3516 | 5.1580e+00 | 14.1379 | 5.6331e+00 | 13.5160 | 0.9157 |
| | 3936 | 3.2117e+00 | 8.3964 | 3.5285e+00 | 8.2911 | 0.9102 |
| 1 | 4866 | 1.8770e+00 | 5.0650 | 2.1510e+00 | 4.6667 | 0.8726 |
| | 6342 | 1.2110e+00 | 3.3083 | 1.4262e+00 | 3.1021 | 0.8491 |
| | 8966 | 7.6293e-01 | 2.6687 | 9.0810e-01 | 2.6076 | 0.8401 |
| | 14202 | 4.4611e-01 | 2.3334 | 5.5115e-01 | 2.1714 | 0.8094 |
| | 21684 | 2.9875e-01 | 1.8948 | 3.6841e-01 | 1.9037 | 0.8109 |
| | 6120 | 7.8275e+00 | −− | 8.6432e+00 | −− | 0.9056 |
| | 6378 | 2.3483e+00 | 58.3131 | 2.5850e+00 | 58.4627 | 0.9084 |
| | 6851 | 1.2364e+00 | 17.9329 | 1.4322e+00 | 16.5094 | 0.8633 |
| | 7676 | 5.3466e-01 | 14.7464 | 6.6401e-01 | 13.5204 | 0.8052 |
| 2 | 8200 | 3.8435e-01 | 9.9969 | 4.6526e-01 | 10.7732 | 0.8261 |
| | 9738 | 2.2031e-01 | 6.4748 | 2.7509e-01 | 6.1138 | 0.8009 |
| | 11895 | 1.3259e-01 | 5.0756 | 1.7407e-01 | 4.5744 | 0.7617 |
| | 16581 | 6.8309e-02 | 3.9936 | 9.0940e-02 | 3.9096 | 0.7512 |
| | 21183 | 4.4949e-02 | 3.4173 | 6.1021e-02 | 3.2578 | 0.7366 |

Table 4.4: Test 3. The behaviour of the global error and the estimator using the adaptive strategy. The effectivity of the estimator is reported in the right-most column (table produced by the author).

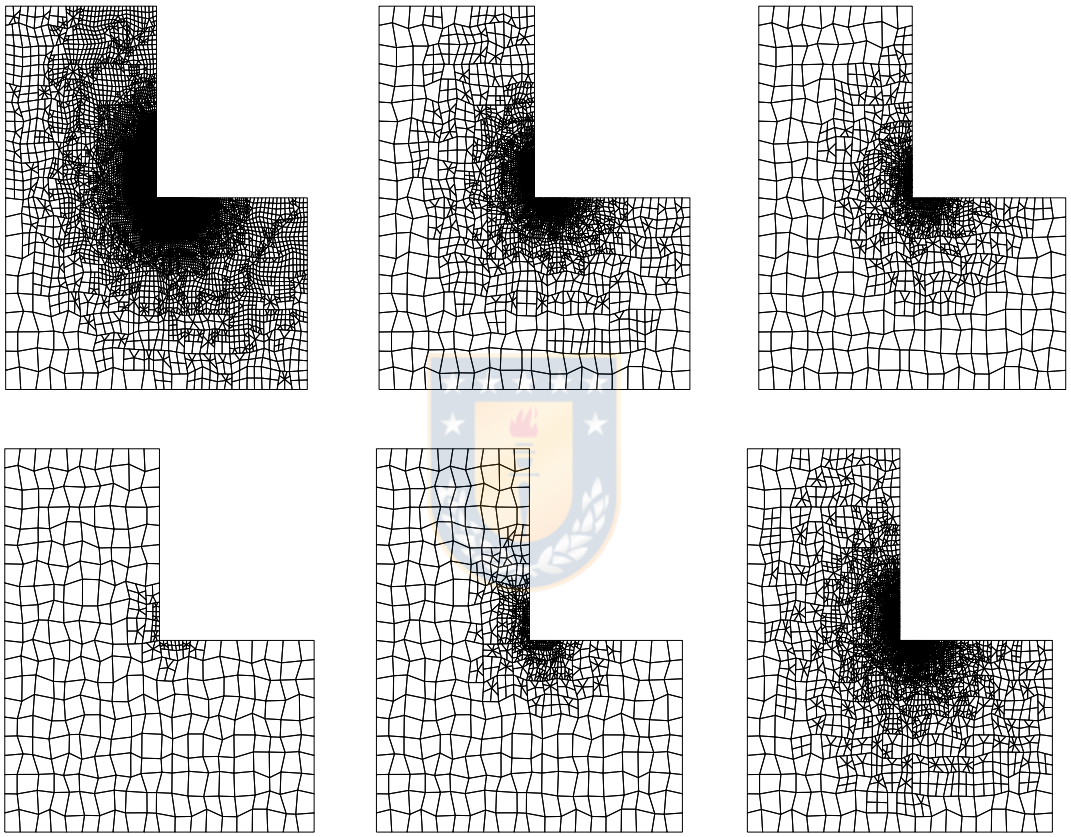

Figure 4.5: Test 3. (Top) The mesh after ten adaptive refinements with $k = 0$ (left), $k = 1$ (centre) and $k = 2$ (right). (Below) Some meshes from the adaptive refinement sequence for $k = 2$: after 3 refinement steps (left), 8 refinement steps (centre), and 15 refinement steps (right) (figure produced by the author).

# CHAPTER 5

# A posteriori error analysis of a mixed virtual element method for a nonlinear Brinkman model of porous media flow

## 5.1 Introduction

The Virtual Element Method (VEM) is a novel technique used for the approximation of partial differential equations, which was originally introduced in [13] and later extended in [28] to handle mixed methods. Its applications to fluid mechanics has become a very active research subject in recent years. Indeed, regarding the Stokes equations, we can cite to [10, 39, 20, 30, 32]. The Brinkman model has been addressed in [31, 90, 68], whereas VEM-discretizations for the Navier-Stokes equations have been developed in [21, 69, 76]. Recently, a mixed-VEM for the Boussinesq problem has been proposed in [67].

The main motivation to use VEM is to construct Galerkin schemes with the capability to use general polygonal/polyhedral meshes, naturally including hanging nodes and non-convex shapes. In this way, the VEM approach offers several advantages due to the flexibility allowed to deal with general meshes. Firstly, this flexibility ensures that adaptive strategies can be implemented very easily and efficiently. On the other hand, the use of hanging nodes introduced by the refinement of a neighbouring element are simply treated as new nodes, which has been proved does not affect the quality of the approximation [38]. Hence, the design and analysis of adaptive mesh refinement strategies based on a posteriori error indicators for the VEM approach and particularly for the mixed-VEM is an attractive task. However, the literature on a posteriori analysis for VEM is focused on primal schemes. In this regard, we can mention the following works [24, 38, 26, 81, 78, 44]. In particular, the authors of [24] proposed a posteriori error bounds for the $C^1$-conforming VEM for the two-dimensional Poisson problem. Next, a posteriori error bounds for the $C^0$-conforming VEM for the discretization of second-order linear elliptic reaction-convection-diffusion problems with nonconstant coefficients in two and three dimensions were proposed in [38], whereas a residual-based a posteriori error estimator for the VEM discretization of the Poisson problem with discontinuous diffusivity coefficient was introduced and analyzed in [26]. Moreover, in [81] and [78], the authors developed an a posteriori error analysis of a VEM approach for the Steklov eigenvalue problem and the spectral analysis for the elasticity equations, respectively. Finally, in [44] a general recovery-based a posteriori error estimation framework for the VEM of arbitrary order on general polygonal/polyhedral meshes has been developed.

On the other hand, in the context of mixed methods using the VEM approach, in [40] was recently developed an a posteriori error analysis, applying to second order elliptic equations in divergence form with mixed boundary conditions. More precisely, the authors propose a framework to incorporate adaptive strategies to mixed-VEM on polygonal meshes. They employed techniques based in Helmholtz decomposition, local approximation properties of interpolation operators, inverse inequalities and localization arguments based on bubble functions to construct a posteriori error estimates.

According to the above discussion, the main purpose of the present **Chapter** is to apply the approach from [40] to develop an a posteriori error analysis and the corresponding adaptive strategy for the nonlinear Brinkman model of porous media flow proposed in [68]. To this end, we propose a residual-type estimator, which involves fully computable approximations of the pseudostress variable. The behavior of our estimator is analyzed with several numerical tests. The remainder of this paper is organized as follows. In Section 5.2 we introduce the model problem, the associated variational formulation and its respective mixed virtual element scheme. The a posteriori error analysis of our method, which constitutes the main contribution of this **Chapter**, is presented in details in Section 5.3. Finally, we propose an adaptive algorithm and validate its effectiveness with some numerical examples in Section 5.4.

We end this section with several notations to be used throughout the paper. Firstly, we let $\mathbb{I}$ be the identity matrix in $\mathrm{R}^{2\times 2}$, and for any $\boldsymbol{\tau} := (\tau_{ij})$, $\boldsymbol{\zeta} := (\zeta_{ij}) \in \mathrm{R}^{2\times 2}$, we set

$$\boldsymbol{\tau}^{\mathrm{t}} := (\tau_{ji}), \quad \mathrm{tr}(\boldsymbol{\tau}) := \sum_{i=1}^{2} \tau_{ii}, \quad \boldsymbol{\tau}^{\mathrm{d}} := \boldsymbol{\tau} - \frac{1}{2}\mathrm{tr}(\boldsymbol{\tau})\,\mathbb{I} \quad \text{and} \quad \boldsymbol{\tau} : \boldsymbol{\zeta} := \sum_{i,j=1}^{2} \tau_{ij}\zeta_{ij},$$

which denote, respectively, the transpose, the trace, the deviator of the tensor $\boldsymbol{\tau}$, and the tensorial product between $\boldsymbol{\tau}$ and $\boldsymbol{\zeta}$. Next, given a bounded domain $\mathcal{O} \subseteq \mathrm{R}^2$, with polygonal boundary $\partial\mathcal{O}$, we utilize standard notations for Lebesgue spaces $\mathrm{L}^p(\mathcal{O})$, $p > 1$, and Sobolev spaces $\mathrm{H}^s(\mathcal{O})$, $s \in \mathrm{R}$, with norm $\|\cdot\|_{s,\mathcal{O}}$ and seminorm $|\cdot|_{s,\mathcal{O}}$. In particular, $\mathrm{H}^{1/2}(\partial\mathcal{O})$ is the space of traces of functions of $\mathrm{H}^1(\mathcal{O})$ and $\mathrm{H}^{-1/2}(\partial\mathcal{O})$ denotes its dual. Moreover, by $\mathbf{M}$ and $\mathbb{M}$ we will refer to the corresponding vector and tensorial counterparts of the generic scalar functional space M, and $\|\cdot\|$, with no subscripts, will stand for the natural norm of either an element or an operator in any product functional space. Furthermore, we recall that

$$\mathbb{H}(\mathbf{div};\mathcal{O}) := \left\{\boldsymbol{\tau} \in \mathbb{L}^2(\mathcal{O}) : \quad \mathbf{div}(\boldsymbol{\tau}) \in \mathbf{L}^2(\mathcal{O})\right\},$$

equipped with the usual norm

$$\|\boldsymbol{\tau}\|^2_{\mathbf{div};\mathcal{O}} := \|\boldsymbol{\tau}\|^2_{0,\mathcal{O}} + \|\mathbf{div}(\boldsymbol{\tau})\|^2_{0,\mathcal{O}} \qquad \forall\, \boldsymbol{\tau} \in \mathbb{H}(\mathbf{div};\mathcal{O}),$$

is a Hilbert space. Also, we define

$$\mathbb{L}^2_{\mathrm{tr}}(\mathcal{O}) := \left\{\mathbf{s} \in \mathbb{L}^2(\mathcal{O}) : \quad \mathrm{tr}(\mathbf{s}) = 0\right\}, \tag{5.1}$$

and

$$\mathbb{H}_0(\mathbf{div};\mathcal{O}) := \left\{\boldsymbol{\tau} \in \mathbb{H}(\mathbf{div};\mathcal{O}) : \quad \int_{\mathcal{O}} \mathrm{tr}(\boldsymbol{\tau}) = 0\right\}. \tag{5.2}$$

Furthermore, we recall (see [29, 56]) that there holds the decomposition

$$\mathbb{H}(\mathbf{div};\mathcal{O}) = \mathbb{H}_0(\mathbf{div};\mathcal{O}) \oplus \mathrm{R}\,\mathbb{I}, \tag{5.3}$$

which, for each $\boldsymbol{\tau} \in \mathbb{H}(\mathbf{div};\mathcal{O})$ indicates that there exist unique $\boldsymbol{\tau}_0 \in \mathbb{H}_0(\mathbf{div};\mathcal{O})$ and $c := \frac{1}{2|\mathcal{O}|}\int_{\mathcal{O}} \mathrm{tr}(\boldsymbol{\tau}) \in \mathrm{R}$, where $|\mathcal{O}|$ denotes the measure of $\mathcal{O}$, such that $\boldsymbol{\tau} = \boldsymbol{\tau}_0 + c\,\mathbb{I}$. Finally, we employ $\mathbf{0}$ to denote a generic null vector, null tensor or null operator, and use $C$ and $c$, with or without subscripts to denote generic constants independent of the discretization parameters, which may take different values at different places.

## 5.2 The nonlinear Brinkman model

In this section we briefly describe the augmented formulation considered in this **Chapter** for the nonlinear Brinkman model. Firstly, in Section 5.2.1 we recall the system of partial differential equations modeling the problem, and its corresponding variational formulation. Then, the mixed-VEM discretization is discussed in Section 5.2.2.

### 5.2.1 The model problem and its continuous formulation

Let $\Omega \subseteq \mathrm{R}^2$ be a bounded domain with polygonal boundary $\Gamma$. Then, a nonlinear Brinkman model of porous media flow is given by the following system of partial differential equations

$$\begin{aligned} \boldsymbol{\sigma} &= \mu(|\nabla \mathbf{u}|)\nabla\mathbf{u} - p\,\mathbb{I} \quad \text{in} \quad \Omega\,, \qquad \alpha\mathbf{u} - \mathbf{div}(\boldsymbol{\sigma}) = \mathbf{f} \quad \text{in} \quad \Omega\,, \\ \mathrm{div}(\mathbf{u}) &= 0 \quad \text{in} \quad \Omega\,, \qquad \mathbf{u} = \mathbf{g} \ \text{ on } \ \Gamma \qquad \text{and} \qquad \int_\Omega p = 0\,, \end{aligned} \tag{5.4}$$

where the unknowns are given by the pseudostress $\boldsymbol{\sigma}$, the velocity $\mathbf{u}$ and the pressure $p$ of a fluid occupying the region $\Omega$. The nonlinear function $\mu : \mathrm{R}^+ \to \mathrm{R}$ represents the kinematic viscosity function of the fluid, $\alpha > 0$ is a constant approximation of the viscosity divided by the permeability, $\mathbf{f} \in \mathbf{L}^2(\Omega)$ and $\mathbf{g} \in \mathbf{H}^{1/2}(\Gamma)$ is a boundary data. Notice that the data $\mathbf{g}$ must satisfy the compatibility condition $\int_\Gamma \mathbf{g}\cdot\boldsymbol{\nu} = 0$, where $\boldsymbol{\nu}$ is the unit outward normal on $\Gamma$, whereas the uniqueness of a pressure solution is ensured by the last equation of (5.4).

In what follows, we let $\psi_{ij} : \mathrm{R}^{2\times 2} \to \mathrm{R}$ be the mapping given by $\psi_{ij}(\mathbf{r}) := \mu(|\mathbf{r}|)r_{ij}$ for each $\mathbf{r} := (r_{ij}) \in \mathrm{R}^{2\times 2}$. Then, throughout this paper we assume that $\mu$ is of class $C^1$ and that there exist $\gamma_0, \alpha_0 > 0$ such that for each $\mathbf{r} := (r_{ij}), \mathbf{s} := (s_{ij}) \in \mathrm{R}^{2\times 2}$, there hold

$$|\psi_{ij}(\mathbf{r})| \ \leq\ \gamma_0\,|\mathbf{r}|\,, \qquad \left|\frac{\partial}{\partial r_{kl}}\psi_{ij}(\mathbf{r})\right| \ \leq\ \gamma_0 \qquad \forall\, i,j,k,l \in \{1,2\}\,,$$

and

$$\sum_{i,j,k,l=1}^{2} \frac{\partial}{\partial r_{kl}}\psi_{ij}(\mathbf{r})s_{ij}s_{kl} \ \geq\ \alpha_0\,|\mathbf{s}|^2.$$

We recall here that the assumptions above allow us to define a nonlinear operator $\mathbb{A} : \mathbb{L}^2(\Omega) \to [\mathbb{L}^2(\Omega)]'$ given by

$$[\mathbb{A}(\mathbf{r}), \mathbf{s}] \ :=\ \int_\Omega \boldsymbol{\psi}(\mathbf{r}) : \mathbf{s} \ =\ \int_\Omega \mu(|\mathbf{r}|)\mathbf{r} : \mathbf{s} \qquad \forall\, \mathbf{r}, \mathbf{s} \in \mathbb{L}^2(\Omega)\,, \tag{5.5}$$

which is Lipschitz-continuous and strongly monotone (cf. [64, Lemma 2.1]). More precisely, there hold

$$\|\mathbb{A}(\mathbf{r}) - \mathbb{A}(\mathbf{s})\|_{[\mathbb{L}^2(\Omega)]'} \ \leq\ \gamma_0\|\mathbf{r}-\mathbf{s}\|_{0,\Omega} \qquad \text{and} \qquad [\mathbb{A}(\mathbf{r}) - \mathbb{A}(\mathbf{s}), \mathbf{r}-\mathbf{s}] \ \geq\ \alpha_0\|\mathbf{r}-\mathbf{s}\|^2_{0,\Omega}\,, \tag{5.6}$$

for each $\mathbf{r},\mathbf{s}\in\mathbb{L}^2(\Omega)$.

Now, as was explained in [58], using the incompressibility condition to eliminate the pressure, and introducing the auxiliary unknown $\mathbf{t}:=\nabla\mathbf{u}$ in $\Omega$, we can rewrite (5.4) as follows:

$$\begin{array}{rcl} \mathbf{t} = \nabla\mathbf{u} \quad \text{in} \quad \Omega, & \boldsymbol{\sigma}^{\mathrm{d}} = \mu(|\mathbf{t}|)\mathbf{t} \quad \text{in} \quad \Omega, & \alpha\mathbf{u}-\mathbf{div}(\boldsymbol{\sigma}) = \mathbf{f} \quad \text{in} \quad \Omega, \\ \mathrm{tr}(\mathbf{t}) = 0 \quad \text{in} \quad \Omega, & \mathbf{u} = \mathbf{g} \quad \text{on} \quad \Gamma & \text{and} \quad \displaystyle\int_\Omega \mathrm{tr}(\boldsymbol{\sigma}) = 0\,. \end{array} \tag{5.7}$$

We recall that the pressure can be obtained using the formula (cf. [68, Section 2.2])

$$p = -\frac{1}{2}\mathrm{tr}(\boldsymbol{\sigma}) \quad \text{in} \quad \Omega\,. \tag{5.8}$$

Note from the fourth and last equation of (5.7) that $\mathbf{t}$ and $\boldsymbol{\sigma}$ must belong to $\mathbb{L}^2_{\mathrm{tr}}(\Omega)$ (cf. (5.1)) and $\mathbb{H}_0(\mathbf{div};\Omega)$ (cf. (5.2)), respectively. In what follows, we make use of the notation $X:=\mathbb{L}^2_{\mathrm{tr}}(\Omega)$ and $H:=\mathbb{H}_0(\mathbf{div};\Omega)$. Then, proceeding as in [68, Section 2.2], that is, testing the first two equations of (5.7) by suitable test functions, integrating by parts, using the Dirichlet conditions for $\mathbf{u}$, the fact that the velocity can be replaced from the third equation of (5.7) as $\mathbf{u}=\frac{1}{\alpha}\{\mathbf{f}+\mathbf{div}(\boldsymbol{\sigma})\}$, and adding the following redundant term

$$\kappa\int_\Omega\{\boldsymbol{\sigma}^{\mathrm{d}}-\mu(|\mathbf{t}|)\mathbf{t}\}:\boldsymbol{\tau}^{\mathrm{d}} = 0 \qquad \forall\,\boldsymbol{\tau}\in H\,,$$

with $\kappa$ a positive parameter to be specified later, we arrive at the augmented variational formulation: Find $(\mathbf{t},\boldsymbol{\sigma})\in X\times H$ such that

$$[\mathbf{A}(\mathbf{t},\boldsymbol{\sigma}),(\mathbf{s},\boldsymbol{\tau})] = [\mathbf{F},(\mathbf{s},\boldsymbol{\tau})] \qquad \forall\,(\mathbf{s},\boldsymbol{\tau})\in X\times H\,, \tag{5.9}$$

where $\mathbf{A}:X\times H\to(X\times H)'$ and $\mathbf{F}:X\times H\to\mathrm{R}$ are given by

$$\begin{aligned}[\mathbf{A}(\mathbf{t},\boldsymbol{\sigma}),(\mathbf{s},\boldsymbol{\tau})] &:= [\mathbb{A}(\mathbf{t}),\mathbf{s}-\kappa\boldsymbol{\tau}^{\mathrm{d}}] - \int_\Omega\mathbf{s}:\boldsymbol{\sigma}^{\mathrm{d}} + \int_\Omega\mathbf{t}:\boldsymbol{\tau}^{\mathrm{d}} + \kappa\int_\Omega\boldsymbol{\sigma}^{\mathrm{d}}:\boldsymbol{\tau}^{\mathrm{d}} \\ &\quad + \frac{1}{\alpha}\int_\Omega\mathbf{div}(\boldsymbol{\sigma})\cdot\mathbf{div}(\boldsymbol{\tau})\,,\end{aligned} \tag{5.10}$$

and

$$[\mathbf{F},(\mathbf{s},\boldsymbol{\tau})] := -\frac{1}{\alpha}\int_\Omega\mathbf{f}\cdot\mathbf{div}(\boldsymbol{\tau}) + \langle\boldsymbol{\tau}\boldsymbol{\nu},\mathbf{g}\rangle\,, \tag{5.11}$$

respectively, where $\langle\cdot,\cdot\rangle$ stands for the duality pairing between $\mathbf{H}^{-1/2}(\Gamma)$ and $\mathbf{H}^{1/2}(\Gamma)$.

In addition, the analysis of the continuous formulation (5.9) is based in results of nonlinear analysis (cf. [68, Section 2.2]). More precisely, it was proved there the Lipschitz-continuity of the operator $\mathbf{A}$, that is, there exists $L_{\mathbf{A}}>0$ (cf [68, eq. 2.18]), depending only on $\kappa,\gamma_0$ and $\alpha$, such that

$$\|\mathbf{A}(\mathbf{r},\boldsymbol{\zeta})-\mathbf{A}(\mathbf{s},\boldsymbol{\tau})\|_{(X\times H)'} \leq L_{\mathbf{A}}\,\|(\mathbf{r},\boldsymbol{\zeta})-(\mathbf{s},\boldsymbol{\tau})\|_{X\times H}\,, \qquad \forall\,(\mathbf{r},\boldsymbol{\zeta}),\,(\mathbf{s},\boldsymbol{\tau})\in X\times H\,. \tag{5.12}$$

Furthermore, for $\kappa\in\left(0,\frac{2\delta\alpha_0}{\gamma_0}\right)$ with $\delta\in\left(0,\frac{2}{\gamma_0}\right)$ there exists $C_{SM}>0$ (cf. [68, Lemma 2.2]), depending only on $\kappa,\alpha_0,\gamma_0,\delta,\Omega$ and $\alpha$, such that

$$[\mathbf{A}(\mathbf{r},\boldsymbol{\zeta})-\mathbf{A}(\mathbf{s},\boldsymbol{\tau}),(\mathbf{r},\boldsymbol{\zeta})-(\mathbf{s},\boldsymbol{\tau})] \geq C_{SM}\|(\mathbf{r},\boldsymbol{\zeta})-(\mathbf{s},\boldsymbol{\tau})\|^2_{X\times H} \qquad \forall\,(\mathbf{r},\boldsymbol{\zeta}),(\mathbf{s},\boldsymbol{\tau})\in X\times H\,,$$

which yielded the strong monotonicity of the operator $\mathbf{A}$. In this way, the well-posedness of the variational formulation (5.9) is established by the following theorem.

**Theorem 5.1.** Assume that $\mathbf{f} \in \mathbf{L}^2(\Omega), \mathbf{g} \in \mathbf{H}^{1/2}(\Gamma)$, and that given $\delta \in \left(0, \frac{2}{\gamma_0}\right)$, the parameter $\kappa$ lies in $\left(0, \frac{2\delta\alpha_0}{\gamma_0}\right)$. Then, there exists a unique $(\mathbf{t}, \boldsymbol{\sigma}) \in X \times H$ solution of (5.9). Moreover, there exists a positive constant $C$, depending only on $\Omega, \alpha_0, \gamma_0, \kappa$ and $\alpha$, such that

$$\|(\mathbf{t}, \boldsymbol{\sigma})\|_{X \times H} \ \leq \ C\big\{\|\mathbf{f}\|_{0,\Omega} \ + \ \|\mathbf{g}\|_{1/2,\Gamma}\big\}.$$

*Proof.* See [68, Theorem 2.1]). □

### 5.2.2 The mixed virtual element method

Regarding the mesh, given $\{\mathcal{T}_h\}_{h>0}$ a family of partitions of $\Omega$ into an open non-overlapping polygonal elements and $K \in \mathcal{T}_h$, we denote its barycenter, diameter and number of edges by $\mathbf{x}_K$, $h_K$, and $d_K$, respectively, and define, as usual, $h := \max\{h_K : K \in \mathcal{T}_h\}$. In addition, in what follows we assume that there exists a constant $C_{\mathcal{T}} > 0$ such that for each partition $\mathcal{T}_h$ and for each $K \in \mathcal{T}_h$ there hold:

a) the ratio between the shortest edge and the diameter $h_K$ of $K$ is bigger than $C_{\mathcal{T}}$, and

b) $K$ is star-shaped with respect to a ball $B$ of radius $C_{\mathcal{T}} h_K$ and center $\mathbf{x}_B \in K$.

We recall here, from the above assumptions, that it is possible to show that each $K \in \mathcal{T}_h$ is simply connected, and that there exists an integer $N_{\mathcal{T}}$ (depending only on $C_{\mathcal{T}}$), such that the numbers of edges of each $K \in \mathcal{T}_h$ is bounded above by $N_{\mathcal{T}}$. Furthermore, the assumption b) implies that each element $K$ admits a sub-triangulation $\mathcal{T}_h^K$, obtained by joining each vertex of $K$ with the point with respect to which $K$ is starred. In this way, since we are also assuming a), we have that the resulting global triangulation $\widehat{\mathcal{T}_h} := \bigcup_{K \in \mathcal{T}_h} \mathcal{T}_h^K$ is shape-regular. Finally, partitions including non-convex elements are allowed, as also meshes with hanging nodes.

Now, given an integer $\ell \geq 0$ and $\mathcal{O} \subseteq \mathrm{R}^2$, we let $\mathrm{P}_\ell(\mathcal{O})$ be the space of polynomials on $\mathcal{O}$ of degree up to $\ell$, we set $\mathbf{P}_\ell(\mathcal{O}) := [\mathrm{P}_\ell(\mathcal{O})]^2$ and $\mathbb{P}_\ell(\mathcal{O}) := [\mathrm{P}_\ell(\mathcal{O})]^{2\times 2}$. In addition, given an edge $e$ of $\mathcal{T}_h$ with barycentric $x_e$ and diameter $h_e$, we introduce the following set of $(\ell+1)$ normalized monomials on $e$

$$\mathcal{B}_\ell(e) \ := \ \left\{ \left( \frac{x - x_e}{h_e} \right)^j \right\}_{0 \leq j \leq \ell},$$

which certainly constitutes a basis on $\mathrm{P}_\ell(e)$. Similarly, given $K \in \mathcal{T}_h$ with barycenter $\mathbf{x}_K$, we define the following set of $\frac{1}{2}(\ell+1)(\ell+2)$ normalized monomials

$$\mathcal{B}_\ell(K) \ := \ \left\{ \left( \frac{\mathbf{x} - \mathbf{x}_K}{h_K} \right)^{\boldsymbol{\alpha}} \right\}_{0 \leq |\boldsymbol{\alpha}| \leq \ell},$$

which is a basis of $\mathrm{P}_\ell(K)$. Notice that in the definition of $\mathcal{B}_\ell(K)$ above, we have made use of the multi-index notation, that is, given $\mathbf{x} := (x_1, x_2)^{\mathrm{t}} \in \mathrm{R}^2$ and $\boldsymbol{\alpha} := (\alpha_1, \alpha_2)^{\mathrm{t}}$, with non-negative integers $\alpha_1, \alpha_2$, we set $\mathbf{x}^{\boldsymbol{\alpha}} := x_1^{\alpha_1} x_2^{\alpha_2}$ and $|\boldsymbol{\alpha}| := \alpha_1 + \alpha_2$. Furthermore, for $e$ and $K$ as indicated, we define

$$\boldsymbol{\mathcal{B}}_\ell(e) \ := \ \big\{(q,0)^{\mathrm{t}} : \quad q \in \mathcal{B}_\ell(e)\big\} \cup \big\{(0,q)^{\mathrm{t}} : \quad q \in \mathcal{B}_\ell(e)\big\},$$

and

$$\boldsymbol{\mathcal{B}}_\ell(K) \;:=\; \big\{(q,0)^{\mathrm{t}} \;:\quad q\in\mathcal{B}_\ell(K)\big\}\,\cup\,\big\{(0,q)^{\mathrm{t}}:\quad q\in\mathcal{B}_\ell(K)\big\}\,.$$

In addition, for each integer $\ell\geq 0$, we let $\mathcal{G}_\ell(K)$ be a basis of $\big(\nabla\mathrm{P}_{\ell+1}(K)\big)^{\perp}\cap\mathbf{P}_\ell(K)$, which is the $\mathbf{L}^2(K)$-orthogonal of $\nabla\mathrm{P}_{\ell+1}(K)$ in $\mathbf{P}_\ell(K)$, and denote its tensorial counterpart as follows:

$$\boldsymbol{\mathcal{G}}_\ell(K) \;:=\; \left\{\begin{pmatrix}\mathbf{q}^{\mathrm{t}}\\ \mathbf{0}\end{pmatrix}:\quad \mathbf{q}\in\mathcal{G}_\ell(K)\right\}\,\cup\,\left\{\begin{pmatrix}\mathbf{0}\\ \mathbf{q}^{\mathrm{t}}\end{pmatrix}:\quad \mathbf{q}\in\mathcal{G}_\ell(K)\right\}\,.$$

We remark that, alternatively, one could also consider another choices, not necessarily orthogonal, that have been proposed recently, such as $\mathbf{P}_k(K)=\nabla\mathrm{P}_{k+1}\oplus\mathbf{x}^{\perp}\mathrm{P}_{k-1}(K)$, where, given $\mathbf{x}:=(x_1,x_2)^{\mathrm{t}}\in\mathrm{R}^2$, $\mathbf{x}^{\perp}$ denotes the rotated vector $(-x_2,x_1)^{\mathrm{t}}$. Actually, it is not difficult to see that it suffices to choose any space $\mathcal{G}(K)$ such that $\mathbf{P}_\ell(K)=\nabla\mathrm{P}_{\ell+1}\oplus\mathcal{G}(K)$.

Throughout the paper, we denote by $\mathcal{P}_k^K:\mathbf{L}^2(K)\to\mathbf{P}_k(K)$ the $\mathbf{L}^2(K)$-orthogonal projection onto the space $\mathbf{P}_k(K)$, for any $K\in\mathcal{T}_h$ and $k\geq 0$. In addition, we will make use of a tensorial version of the aforementioned projector, which is denoted by $\boldsymbol{\mathcal{P}}_k^K$. The following approximation properties of these projectors are well-known:

$$\|\mathbf{v}-\mathcal{P}_k^K(\mathbf{v})\|_{0,K}\;\leq\;Ch_K^s|\mathbf{v}|_{s,K}\qquad\text{and}\qquad\|\boldsymbol{\zeta}-\boldsymbol{\mathcal{P}}_k^K(\boldsymbol{\zeta})\|_{0,K}\leq Ch_K^s|\boldsymbol{\zeta}|_{s,K}\tag{5.13}$$

for all $K\in\mathcal{T}_h$, and for all $\mathbf{v}\in\mathbf{H}^s(K),\boldsymbol{\zeta}\in\mathbb{H}^s(K)$ with $s\in\{0,\ldots,k+1\}$. Finally, we now denote by $\mathcal{P}_k^h$ and $\boldsymbol{\mathcal{P}}_k^h$, respectively, their global counterparts, that is, given $\mathbf{v}\in\mathbf{L}^2(\Omega)$ and $\boldsymbol{\zeta}\in\mathbb{L}^2(\Omega)$, we let

$$\mathcal{P}_k^h(\mathbf{v})\big|_K\;:=\;\mathcal{P}_k^K(\mathbf{v}\big|_K)\qquad\text{and}\qquad\boldsymbol{\mathcal{P}}_k^h(\boldsymbol{\zeta})\big|_K\;:=\;\boldsymbol{\mathcal{P}}_k^K(\boldsymbol{\zeta}\big|_K)\qquad\forall\,K\in\mathcal{T}_h\,.$$

**The virtual element space and its approximation properties**

Let $k\geq 0$ be an integer. Then, we define the finite dimensional subspaces of $X$ and $H$, respectively, as

$$X_k^h\;:=\;\big\{\mathbf{s}\in X:\quad\mathbf{s}\big|_K\in X_k^K\quad\forall\,K\in\mathcal{T}_h\big\}\tag{5.14}$$

and

$$H_k^h\;:=\;\big\{\boldsymbol{\tau}\in H:\quad\boldsymbol{\tau}\big|_K\in H_k^K\quad\forall\,K\in\mathcal{T}_h\big\}\,,\tag{5.15}$$

where, given $K\in\mathcal{T}_h$, $X_k^K:=\mathbb{P}_k(K)$ and $H_k^K$ is the space introduced in [15, Section 3.1], given by

$$\begin{aligned}H_k^K\;:=\;\big\{\boldsymbol{\tau}\in\mathbb{H}(\mathbf{div};K)\cap\mathbb{H}(\mathbf{rot};K):\quad&\boldsymbol{\tau}\boldsymbol{\nu}|_e\in\mathbf{P}_k(e)\quad\forall\text{ edge }e\in\partial K\,,\\ &\mathbf{div}(\boldsymbol{\tau})\in\mathbf{P}_k(K)\quad\text{and}\quad\mathbf{rot}(\boldsymbol{\tau})\in\mathbf{P}_{k-1}(K)\big\}\,.\end{aligned}\tag{5.16}$$

The degrees of freedom guaranteeing unisolvency for each $\boldsymbol{\tau}\in H_k^K$ are defined by (see, e.g., [14], [15])

$$\begin{aligned}&\int_e\boldsymbol{\tau}\boldsymbol{\nu}\cdot\mathbf{q}\qquad&&\forall\,\mathbf{q}\in\boldsymbol{\mathcal{B}}_k(e)\,,\quad\forall\text{ edge }e\in\partial K\,,\\ &\int_K\boldsymbol{\tau}:\nabla\mathbf{p}\qquad&&\forall\,\mathbf{p}\in\boldsymbol{\mathcal{B}}_k(K)\setminus\{(1,0)^{\mathrm{t}},(0,1)^{\mathrm{t}}\}\,,\\ &\int_K\boldsymbol{\tau}:\boldsymbol{\rho}\qquad&&\forall\,\boldsymbol{\rho}\in\boldsymbol{\mathcal{G}}_k(K)\,.\end{aligned}\tag{5.17}$$

We now introduce the interpolation operator $\boldsymbol{\Pi}_k^K : \mathbb{H}^1(K) \to H_k^K$, which is defined for each $\boldsymbol{\tau} \in \mathbb{H}^1(K)$ as the unique $\boldsymbol{\Pi}_k^K(\boldsymbol{\tau})$ in $H_k^K$ such that

$$\begin{aligned}
\int_e (\boldsymbol{\tau} - \boldsymbol{\Pi}_k^K(\boldsymbol{\tau}))\boldsymbol{\nu} \cdot \mathbf{q} &= 0 \qquad \forall\, \mathbf{q} \in \boldsymbol{\mathcal{B}}_k(e)\,, \quad \forall \text{ edge } e \in \partial K\,,\\
\int_K (\boldsymbol{\tau} - \boldsymbol{\Pi}_k^K(\boldsymbol{\tau})) : \nabla \mathbf{p} &= 0 \qquad \forall\, \mathbf{p} \in \boldsymbol{\mathcal{B}}_k(K) \setminus \{(1,0)^{\mathrm{t}}, (0,1)^{\mathrm{t}}\}\,,\\
\int_K (\boldsymbol{\tau} - \boldsymbol{\Pi}_k^K(\boldsymbol{\tau})) : \boldsymbol{\rho} &= 0 \qquad \forall\, \boldsymbol{\rho} \in \boldsymbol{\mathcal{G}}_k(K)\,.
\end{aligned} \tag{5.18}$$

Concerning the approximation properties of $\boldsymbol{\Pi}_k^K$, we first recall from [15, eq. 3.19] that for each $\boldsymbol{\tau} \in \mathbb{H}^s(K)$, with $s \in \{1, \ldots, k+1\}$, there holds

$$\|\boldsymbol{\tau} - \boldsymbol{\Pi}_k^K(\boldsymbol{\tau})\|_{0,K} \;\leq\; C\, h_K^s\, |\boldsymbol{\tau}|_{s,K}\,. \tag{5.19}$$

Now, from (5.13) and the following conmutative property

$$\mathbf{div}(\boldsymbol{\Pi}_k^K(\boldsymbol{\tau})) \;=\; \mathcal{P}_k^K(\mathbf{div}(\boldsymbol{\tau})) \qquad \forall\, \boldsymbol{\tau} \in \mathbb{H}^1(K)\,, \tag{5.20}$$

we deduce, for each $\boldsymbol{\tau} \in \mathbb{H}^1(K)$ such that $\mathbf{div}(\boldsymbol{\tau}) \in \mathbf{H}^s(K)$, with $s \in \{0, \ldots, k+1\}$, that there holds

$$\|\mathbf{div}(\boldsymbol{\tau}) - \mathbf{div}(\boldsymbol{\Pi}_k^K(\boldsymbol{\tau}))\|_{0,K} \;\leq\; C\, h_K^s\, |\mathbf{div}(\boldsymbol{\tau})|_{s,K}\,. \tag{5.21}$$

In addition (cf. [40, Lemma 5.2]), for each $\boldsymbol{\tau} \in \mathbb{H}^1(\Omega)$ there holds

$$\|\boldsymbol{\tau}\boldsymbol{\nu} - \boldsymbol{\Pi}_k^K(\boldsymbol{\tau})\boldsymbol{\nu}\|_{0,e} \leq C\, h_e^{1/2} \|\boldsymbol{\tau}\|_{1,K} \qquad \forall \text{ edge } e \in \mathcal{T}_h\,, \tag{5.22}$$

where $K$ is any element of $\mathcal{T}_h$ such that $e$ is an edge of $K$.

### The discrete scheme and the a priori error estimates

We now recall the discrete formulation proposed in [68, Section 3.3]. Indeed, using the fact that the degrees of freedom introduced in (5.17) allow us the explicit computation of the orthogonal projection on $\mathbb{P}_k(K)$ for each $\boldsymbol{\tau} \in H_k^K$ (cf. [15, Section 3.2]), we define the local discrete nonlinear operator $\mathbf{A}_h^K : (X_k^K \times H_k^K) \to (X_k^K \times H_k^K)'$ given by

$$\begin{aligned}
[\mathbf{A}_h^K(\mathbf{r}, \boldsymbol{\zeta}), (\mathbf{s}, \boldsymbol{\tau})] \;:=\; & [\mathbb{A}(\mathbf{r}), \mathbf{s} - \kappa(\boldsymbol{\mathcal{P}}_k^K(\boldsymbol{\tau}))^{\mathrm{d}}] - \int_K (\boldsymbol{\mathcal{P}}_k^K(\boldsymbol{\zeta}))^{\mathrm{d}} : \mathbf{s} + \int_K (\boldsymbol{\mathcal{P}}_k^K(\boldsymbol{\tau}))^{\mathrm{d}} : \mathbf{r}\\
& + \kappa \int_K (\boldsymbol{\mathcal{P}}_k^K(\boldsymbol{\zeta}))^{\mathrm{d}} : (\boldsymbol{\mathcal{P}}_k^K(\boldsymbol{\tau}))^{\mathrm{d}} + \frac{1}{\alpha} \int_K \mathbf{div}(\boldsymbol{\zeta}) \cdot \mathbf{div}(\boldsymbol{\tau})\\
& + \mathcal{S}^K(\boldsymbol{\zeta} - \boldsymbol{\mathcal{P}}_k^K(\boldsymbol{\zeta}), \boldsymbol{\tau} - \boldsymbol{\mathcal{P}}_k^K(\boldsymbol{\tau}))
\end{aligned} \tag{5.23}$$

for all $(\mathbf{r}, \boldsymbol{\zeta}), (\mathbf{s}, \boldsymbol{\tau}) \in X_k^K \times H_k^K$, where $\mathcal{S}^K : H_k^K \times H_k^K \to \mathrm{R}$ is any symmetric and positive bilinear form verifying (see [13, Section 4.6] or [15, Section 3.3])

$$\widehat{c}_0 \|\boldsymbol{\zeta}\|_{0,K}^2 \;\leq\; \mathcal{S}^K(\boldsymbol{\zeta}, \boldsymbol{\zeta}) \;\leq\; \widehat{c}_1 \|\boldsymbol{\zeta}\|_{0,K}^2 \qquad \forall\, \boldsymbol{\zeta} \in H_k^K, \tag{5.24}$$

with constants $\widehat{c}_0$, $\widehat{c}_1 > 0$ depending only on $C_{\mathcal{T}}$. More precisely, for the numerical results reported below in Section 5.4 we take $\mathcal{S}^K$ as:

$$\mathcal{S}^K(\boldsymbol{\zeta},\boldsymbol{\tau}) := \sum_{j=1}^{n_k^K} m_{j,K}(\boldsymbol{\zeta})\, m_{j,K}(\boldsymbol{\tau}) \qquad \forall\, (\boldsymbol{\zeta},\boldsymbol{\tau}) \in H_k^K \times H_k^K\,.$$

where $n_k^K$ denote the dimension of $H_k^K$ and $m_{j,K}$, $j \in \{1,2,\ldots,n_k^K\}$ collects the degrees of freedom given by (5.17). Then, according to (5.23), we now introduce the global discrete nonlinear operator $\mathbf{A}_h : (X_k^h \times H_k^h) \to (X_k^h \times H_k^h)'$ as:

$$[\mathbf{A}_h(\mathbf{r},\boldsymbol{\zeta}),(\mathbf{s},\boldsymbol{\tau})] := \sum_{K\in\mathcal{T}_h} [\mathbf{A}_h^K(\mathbf{r},\boldsymbol{\zeta}),(\mathbf{s},\boldsymbol{\tau})] \qquad \forall\, (\mathbf{r},\boldsymbol{\zeta}),(\mathbf{s},\boldsymbol{\tau}) \in X_k^h \times H_k^h\,. \tag{5.25}$$

Therefore, the mixed virtual element scheme associated with the augmented formulation (5.9) reads: Find $(\mathbf{t}_h,\boldsymbol{\sigma}_h) \in X_k^h \times H_k^h$ such that

$$[\mathbf{A}_h(\mathbf{t}_h,\boldsymbol{\sigma}_h),(\mathbf{s}_h,\boldsymbol{\tau}_h)] \;=\; [\mathbf{F},(\mathbf{s}_h,\boldsymbol{\tau}_h)] \qquad \forall\, (\mathbf{s}_h,\boldsymbol{\tau}_h) \in X_k^h \times H_k^h\,. \tag{5.26}$$

The inconsistency between $\mathbf{A}$ and $\mathbf{A}_h$ is established by the following result.

**Lemma 5.2.** There exists a constant $C > 0$, depending only on $\kappa$ and $\widehat{c}_1$ (cf. (5.24)), such that

$$\begin{aligned}&[\mathbf{A}_h(\mathbf{r}_h,\boldsymbol{\zeta}_h) - \mathbf{A}(\mathbf{r}_h,\boldsymbol{\zeta}_h),(\mathbf{s}_h,\boldsymbol{\tau}_h)]\\ &\qquad \leq\; C\left\{\|\boldsymbol{\zeta}_h - \boldsymbol{\mathcal{P}}_k^h(\boldsymbol{\zeta}_h)\|_{0,\Omega} \,+\, \|(\boldsymbol{\mathcal{P}}_k^h(\boldsymbol{\zeta}_h))^{\mathrm{d}} - \mu(|\mathbf{r}_h|)\,\mathbf{r}_h\|_{0,\Omega}\right\}\|(\mathbf{s}_h,\boldsymbol{\tau}_h)\|_{X\times H}\end{aligned}$$

for all $(\mathbf{r}_h,\boldsymbol{\zeta}_h),(\mathbf{s}_h,\boldsymbol{\tau}_h) \in X_k^h \times H_k^h$.

*Proof.* It is a light modification of [68, Lemma 4.1]. □

The unique solvability and stability of the virtual scheme (5.26) is established now.

**Theorem 5.3.** Assume that given $\delta \in \left(0, \frac{2}{\gamma_0}\right)$, the parameter $\kappa$ lies in $\left(0, \frac{2\delta\alpha_0}{\gamma_0}\right)$. Then, there exists a unique $(\mathbf{t}_h,\boldsymbol{\sigma}_h) \in X_k^h \times H_k^h$ solution of (5.26), and there exists a positive constant $C$, independent of h, such that

$$\|(\mathbf{t}_h,\boldsymbol{\sigma}_h)\|_{X\times H} \;\leq\; C\left\{\|\mathbf{f}\|_{0,\Omega} \,+\, \|\mathbf{g}\|_{1/2,\Gamma}\right\}.$$

*Proof.* See [68, Theorem 3.1]. □

Now, we recall that the respective a priori error estimates for (5.9) and the corresponding rate of convergence was developed in [68, Section 4]. More precisely, we have the following result.

**Theorem 5.4.** Let $(\boldsymbol{\sigma},\boldsymbol{\tau}) \in X \times H$ and $(\boldsymbol{\sigma}_h,\boldsymbol{\tau}_h) \in X_k^h \times H_h^h$ be the unique solutions of the continuous and discrete schemes (5.9) and (5.26), respetively. Assume that for some $s \in [1, k+1]$ there hold $\mathbf{t}\big|_K, \boldsymbol{\sigma}\big|_K \in \mathbb{H}^s(K)$, and $\mathbf{div}(\boldsymbol{\sigma}) \in \mathbf{H}^s(K)$ for each $K \in \mathcal{T}_h$. Then, there exists $C > 0$, independent of $h$, such that

$$\|\mathbf{t} - \mathbf{t}_h\|_X \,+\, \|\boldsymbol{\sigma} - \boldsymbol{\sigma}_h\|_H \;\leq\; Ch^s \sum_{K\in\mathcal{T}_h}\left\{|\mathbf{t}|_{s,K} \,+\, |\boldsymbol{\sigma}|_{s,K} \,+\, |\mathbf{div}(\boldsymbol{\sigma})|_{s,K}\right\}.$$

*Proof.* See [68, Theorem 4.2]. □

Next, as usual in VEM discretizations it is neccesary to get error estimates for computable approximations of the virtual solution. To this end, we construct two approximations from the virtual solution $\boldsymbol{\sigma}_h$, which are computed locally. The first one is obtained as its $\mathbf{L}^2(\Omega)$-orthogonal projection on $\mathbb{P}_k(K)$, namely

$$\widehat{\boldsymbol{\sigma}}_{h,K} \;:=\; \boldsymbol{\mathcal{P}}_k^K(\boldsymbol{\sigma}_h|_K) \qquad \forall\, K \in \mathcal{T}_h\,, \tag{5.27}$$

whereas the second one, which is denoted by $\boldsymbol{\sigma}^\star_{h,K}$ and belong to $\mathbb{P}_{k+1}(K)$, is computed as the unique solution of the local problem

$$(\boldsymbol{\sigma}^\star_{h,K}, \boldsymbol{\tau}_h)_{\mathbf{div};K} \;=\; \int_K \widehat{\boldsymbol{\sigma}}_{h,K} : \boldsymbol{\tau}_h \;+\; \int_K \mathbf{div}(\boldsymbol{\sigma}_h)\cdot\mathbf{div}(\boldsymbol{\tau}_h) \qquad \forall\, \boldsymbol{\tau}_h \in \mathbb{P}_{k+1}(K)\,, \tag{5.28}$$

where $(\cdot,\cdot)_{\mathbf{div};K}$ stands for the usual $\mathbb{H}(\mathbf{div};K)$-inner product induced by norm $\|\cdot\|_{\mathbf{div};K}$. We remark here that the two approximations of $\boldsymbol{\sigma}_h$ can be explicitly computed for each $K \in \mathcal{T}_h$ using only its degrees of freedom. For more details see [68, Section 4.3] or [31, Section 5.3].

In what follows, for the approximation $\widehat{\boldsymbol{\sigma}}_{h,K}$ introduced in (5.27), we denote by $\widehat{\boldsymbol{\sigma}}_h$ its global counterpart, that is, $\widehat{\boldsymbol{\sigma}}_h\big|_K := \widehat{\boldsymbol{\sigma}}_{h,K}$ for all $K \in \mathcal{T}_h$. In this way, the following theorems provide the theoretical rates of convergence for $\widehat{\boldsymbol{\sigma}}_h$, $\boldsymbol{\sigma}^\star_{h,K}$ and the postproccesing variables $p_h$ and $\mathbf{u}_h$ (cf. [68, Section 4.1]), which are given by

$$p_h \;:=\; -\int_\Omega \mathrm{tr}(\widehat{\boldsymbol{\sigma}}_h) \qquad \text{and} \qquad \mathbf{u}_h \;:=\; \frac{1}{\alpha}\Big\{\mathcal{P}_k^h(\mathbf{f}) + \mathbf{div}(\boldsymbol{\sigma}_h)\Big\}\,. \tag{5.29}$$

**Theorem 5.5.** Let $(\mathbf{t},\boldsymbol{\sigma}) \in X \times H$ and $(\mathbf{t}_h,\boldsymbol{\sigma}_h) \in X_k^h \times H_k^h$ be the unique solutions of the continuous and discrete schemes (5.9) and (5.26), respectively. In addition, let $\widehat{\boldsymbol{\sigma}}_h$ and $(p_h,\mathbf{u}_h)$ be the discrete approximations introduced in (5.27) and (5.29), respectively. Assume that for some $s \in [1, k+1]$ there hold $\mathbf{t}\big|_K$, $\boldsymbol{\sigma}\big|_K \in \mathbb{H}^s(K)$, $\mathbf{div}(\boldsymbol{\sigma})\big|_K \in \mathbf{H}^s(K)$, and $\mathbf{u}\big|_K \in \mathbf{H}^s(K)$ for each $K \in \mathcal{T}_h$. Then, there exist positive constants $C_1$ and $C_2$, independent of $h$, such that

$$\|\boldsymbol{\sigma} - \widehat{\boldsymbol{\sigma}}_h\|_{0,\Omega} \;+\; \|p - p_h\|_{0,\Omega} \;\leq\; C_1\, h^s \sum_{K\in\mathcal{T}_h} \Big\{|\mathbf{t}|_{s,K} \;+\; |\boldsymbol{\sigma}|_{s,K} \;+\; |\mathbf{div}(\boldsymbol{\sigma})|_{s,K}\Big\}\,, \tag{5.30}$$

and

$$\|\mathbf{u} - \mathbf{u}_h\|_{0,\Omega} \;\leq\; C_2\, h^s \sum_{K\in\mathcal{T}_h} \Big\{|\mathbf{u}|_{s,K} \;+\; |\mathbf{t}|_{s,K} \;+\; |\boldsymbol{\sigma}|_{s,K} \;+\; |\mathbf{div}(\boldsymbol{\sigma})|_{s,K}\Big\}\,. \tag{5.31}$$

*Proof.* See [68, Theorem 4.3]. □

**Theorem 5.6.** Assume that the hypotheses of Theorem 5.5 are satisfied. Then, there exists a positive constant $C$, independent of $h$, such that

$$\Big\{\sum_{K\in\mathcal{T}_h} \|\boldsymbol{\sigma} - \boldsymbol{\sigma}^\star_{h,K}\|^2_{\mathbf{div};K}\Big\}^{1/2} \;\leq\; C\, h^s \sum_{K\in\mathcal{T}_h} \Big\{|\mathbf{t}|_{s,K} \;+\; |\boldsymbol{\sigma}|_{s,K} \;+\; |\mathbf{div}(\boldsymbol{\sigma})|_{s,K}\Big\}\,. \tag{5.32}$$

*Proof.* See [68, Theorem 4.4]. □

Finally, we recall here that the approximation $\boldsymbol{\sigma}^\star_{h,K}$ is introduced to improve the non-satisfactory order provided by the first approximation $\widehat{\boldsymbol{\sigma}}_{h,K}$ with respect to the broken $\mathbb{H}(\mathbf{div})$-norm. This fact was substantiated numerically in [68, Section 5].

## 5.3 A posteriori error analysis

In this section we present details about an a posteriori error analysis for the mixed virtual element scheme (5.26). For this purpose, we follow the approach from [40], which allows us to establish an adaptive strategy bearing in mind the two approximations of $\boldsymbol{\sigma}_h$ introduced in Section 5.2.2.

We start by introducing some useful notation. Let $\mathcal{E}_h$ be the set of all edges of $\mathcal{T}_h$, and $\mathcal{E}(K)$ denotes the set of edges of a given $K \in \mathcal{T}_h$. Then $\mathcal{E}_h = \mathcal{E}_h(\Omega) \cup \mathcal{E}_h(\Gamma)$, where $\mathcal{E}_h(\Omega) := \{e \in \mathcal{E}_h : \quad e \subseteq \Omega\}$ and $\mathcal{E}_h(\Gamma) := \{e \in \mathcal{E}_h : \quad e \subseteq \Gamma\}$ . Moreover, $h_e$ stands for the length of a given edge $e$. Also, for each edge $e \in \mathcal{E}_h$ we fix a unit normal vector $\boldsymbol{\nu}_e := (\nu_1, \nu_2)^{\mathrm{t}}$, and let $\boldsymbol{s}_e := (-\nu_2, \nu_1)^{\mathrm{t}}$ be the corresponding fixed unit tangential vector along $e$. However, when no confusion arises, we simply write $\boldsymbol{\nu}$ and $\boldsymbol{s}$ instead of $\boldsymbol{\nu}_e$ and $\boldsymbol{s}_e$, respectively. Now, given $\boldsymbol{\zeta} \in \mathbb{L}^2(\Omega)$ such that $\boldsymbol{\zeta}\big|_K \in \mathbb{C}(K)$ for each $K \in \mathcal{T}_h$ and $e \in \mathcal{E}_h(\Omega)$, we denote by $[\![\boldsymbol{\zeta}\boldsymbol{s}]\!]$ the tangential jump of $\boldsymbol{\zeta}$ across $e$, that is $[\![\boldsymbol{\zeta}\boldsymbol{s}]\!] := (\boldsymbol{\zeta}\big|_K - \boldsymbol{\zeta}\big|_{K'})\big|_e \boldsymbol{s}$, where $K$ and $K'$ are the elements of $\mathcal{T}_h$ having $e$ as a common edge. Finally, given scalar, vector and tensor valued fields $v, \boldsymbol{\varphi} := (\varphi_1, \varphi_2)^{\mathrm{t}}$ and $\boldsymbol{\tau} := (\tau_{ij})$, respectively, we let

$$\mathbf{curl}(v) := \begin{pmatrix} \frac{\partial v}{\partial x_2} \\ -\frac{\partial v}{\partial x_1} \end{pmatrix}^{\mathrm{t}}, \qquad \underline{\mathbf{curl}}(\boldsymbol{\varphi}) := \begin{pmatrix} \mathbf{curl}(\varphi_1)^{\mathrm{t}} \\ \mathbf{curl}(\varphi_2)^{\mathrm{t}} \end{pmatrix} \qquad \text{and} \qquad \mathrm{curl}(\boldsymbol{\tau}) := \begin{pmatrix} \frac{\partial \tau_{12}}{\partial x_1} - \frac{\partial \tau_{11}}{\partial x_2} \\ \frac{\partial \tau_{22}}{\partial x_1} - \frac{\partial \tau_{21}}{\partial x_2} \end{pmatrix}.$$

In what follows we assume the hypotheses of Theorems 5.1 and 5.3 and let $(\mathbf{t}, \boldsymbol{\sigma}) \in X \times H$ and $(\mathbf{t}_h, \boldsymbol{\sigma}_h) \in X_k^h \times H_k^h$ be the unique solutions of (5.9) and (5.26), respectively. In addition, let $\widehat{\boldsymbol{\sigma}}_{h,K}$, $\boldsymbol{\sigma}^{\star}_{h,K}$ and $\mathbf{u}_h$ be the approximations introduced in Section 5.2.2. Then, we define for each $K \in \mathcal{T}_h$ the local a posteriori error indicators

$$\Psi_K^2 := \Lambda_{1,K}^2 + \Lambda_{2,K}^2 + \Lambda_{3,K}^2 + \|\boldsymbol{\sigma}^{\star,\mathrm{d}}_{h,K} - \mu(|\mathbf{t}_h|)\mathbf{t}_h\|_{0,K}^2 ,$$

and

$$\begin{aligned} \theta_K^2 := \; & \Lambda_{4,K}^2 + h_K^2 \|\mathbf{t}_h - \nabla \mathbf{u}_h\|_{0,K}^2 + h_K^2 \|\mathrm{curl}(\mathbf{t}_h)\|_{0,K}^2 + \sum_{e \in \mathcal{E}(K) \cap \mathcal{E}_h(\Omega)} h_e \|[\![\mathbf{t}_h \boldsymbol{s}]\!]\|_{0,e}^2 \\ & + \sum_{e \in \mathcal{E}(K) \cap \mathcal{E}_h(\Gamma)} h_e \left\{ \|\mathbf{g} - \mathbf{u}_h\|_{0,e}^2 + \left\| \frac{d\mathbf{g}}{d\boldsymbol{s}} - \mathbf{t}_h \boldsymbol{s} \right\|_{0,e}^2 \right\} , \end{aligned}$$

where $\boldsymbol{\sigma}^{\star,\mathrm{d}}_{h,K}$ is denoting the deviator tensor of $\boldsymbol{\sigma}^{\star}_{h,K}$, and

$$\begin{aligned} \Lambda_{1,K}^2 &:= \mathcal{S}^K(\boldsymbol{\sigma}_h - \widehat{\boldsymbol{\sigma}}_{h,K}, \boldsymbol{\sigma}_h - \widehat{\boldsymbol{\sigma}}_{h,K}) , & \Lambda_{2,K}^2 &:= \|\boldsymbol{\sigma}^{\star}_{h,K} - \widehat{\boldsymbol{\sigma}}_{h,K}\|_{0,K}^2 , \\ \Lambda_{3,K}^2 &:= \|\mathbf{div}(\boldsymbol{\sigma}_h - \boldsymbol{\sigma}^{\star}_{h,K})\|_{0,K}^2 , & \Lambda_{4,K}^2 &:= \frac{1}{\alpha^2} \|\mathbf{f} - \mathcal{P}_k^K(\mathbf{f})\|_{0,K}^2 . \end{aligned} \tag{5.33}$$

We observe that the term $\frac{d\mathbf{g}}{d\boldsymbol{s}}$ in $\theta_K^2$ requires the trace $\mathbf{g}$ to be more regular, in particular, we need that $\mathbf{g} \in \mathbf{H}^1(\Gamma)$. Then, we introduce the global error estimator given by

$$\boldsymbol{\eta} := \left\{ \sum_{K \in \mathcal{T}_h} \left\{ \Psi_K^2 + \theta_K^2 \right\} \right\}^{1/2} . \tag{5.34}$$

The following theorem constitutes the main result of this section

**Theorem 5.7.** Let $(\mathbf{t},\boldsymbol{\sigma}) \in X \times H$ and $(\mathbf{t}_h,\boldsymbol{\sigma}_h) \in X_k^h \times H_k^h$ be the unique solutions of the problem (5.9) and (5.26), respectively. In addition, let $\boldsymbol{\sigma}^\star_{h,K}$ be the discrete approximation introduced in (5.28). Furthermore, assume that the data $\mathbf{g} \in \mathbf{H}^1(\Gamma)$ and $\dfrac{d\mathbf{g}}{d\boldsymbol{s}}$ is piecewise polynomial. Then, there exist positives constants $C_{\mathtt{eff}}$ and $C_{\mathtt{rel}}$, independent of $h$, such that

$$\|\mathbf{u}-\mathbf{u}_h\|_{0,\Omega} + \|(\mathbf{t},\boldsymbol{\sigma})-(\mathbf{t}_h,\boldsymbol{\sigma}_h)\|_{X\times H} + \left\{\sum_{K\in\mathcal{T}_h}\|\boldsymbol{\sigma}-\boldsymbol{\sigma}^\star_{h,K}\|^2_{\mathbf{div};K}\right\}^{1/2} \leq C_{\mathtt{rel}}\boldsymbol{\eta} \tag{5.35}$$

and

$$C_{\mathtt{eff}}\boldsymbol{\eta} \leq \|\mathbf{u}-\mathbf{u}_h\|_{0,\Omega} + \|(\mathbf{t},\boldsymbol{\sigma})-(\mathbf{t}_h,\boldsymbol{\sigma}_h)\|_{X\times H} + \left\{\sum_{K\in\mathcal{T}_h}\|\boldsymbol{\sigma}-\boldsymbol{\sigma}^\star_{h,K}\|^2_{\mathbf{div};K}\right\}^{1/2} + \|\boldsymbol{\sigma}-\boldsymbol{\mathcal{P}}^h_k(\boldsymbol{\sigma})\|_{0,\Omega}\,. \tag{5.36}$$

The proof of the Theorem 5.7 is separated into the two parts given by the next subsections. More precisely, we show lower and upper bounds for the error that involves the discrete approximations $\boldsymbol{\sigma}^\star_{h,K}$, which were introduced in Section 5.2.2, and the global error estimator defined in (5.34). In Section 5.3.1 we prove that $\boldsymbol{\eta}$ satisfy reliability properties, whereas the corresponding efficiency properties are derived in Section 5.3.2.

### 5.3.1 Reliability

We proceed with the following preliminary estimate.

**Lemma 5.8.** Let $(\mathbf{t},\boldsymbol{\sigma}) \in X \times H$ and $(\mathbf{t}_h,\boldsymbol{\sigma}_h) \times X_k^h \times H_k^h$ be the unique solutions of (5.9) and (5.26), respectively. Then, there exists a positive constant C, such that

$$C\|(\mathbf{t},\boldsymbol{\sigma})-(\mathbf{t}_h,\boldsymbol{\sigma}_h)\|_{X\times H} \leq \left\{\sum_{K\in\mathcal{T}_h}\left\{\Lambda^2_{1,K}+\Lambda^2_{2,K}+\|\boldsymbol{\sigma}^{\star,\mathrm{d}}_{h,K}-\mu(|\mathbf{t}_h|)\mathbf{t}_h\|^2_{0,K}\right\}\right\}^{1/2} + \sup_{\substack{\boldsymbol{\tau}\in H\\ \boldsymbol{\tau}\neq\mathbf{0}}}\frac{\mathcal{R}(\boldsymbol{\tau})}{\|\boldsymbol{\tau}\|_H}\,, \tag{5.37}$$

where

$$\mathcal{R}(\boldsymbol{\tau}) := -\int_\Omega \mathbf{t}_h : (\boldsymbol{\tau}-\boldsymbol{\tau}_h) + \langle(\boldsymbol{\tau}-\boldsymbol{\tau}_h)\boldsymbol{\nu},\mathbf{g}\rangle - \frac{1}{\alpha}\int_\Omega(\mathbf{f}+\mathbf{div}(\boldsymbol{\sigma}_h))\cdot\mathbf{div}(\boldsymbol{\tau}-\boldsymbol{\tau}_h) \tag{5.38}$$

for all $(\mathbf{s},\boldsymbol{\tau}_h) \in X_k^h \times H_k^h$ such that $\|(\mathbf{s}_h,\boldsymbol{\tau}_h)\|_{X\times H} \leq C\|(\mathbf{s},\boldsymbol{\tau})\|_{X\times H}$ for some positive constant C independent of $(\mathbf{s},\boldsymbol{\tau})$.

*Proof.* Proceeding as in [58, Section 5.2], together with the fact that the nonlinear operator $\mathbb{A}$ (cf. (5.5)), has Gâteaux derivative $\mathcal{D}\mathbb{A}(\widetilde{\mathbf{r}})$ at any $\widetilde{\mathbf{r}} \in X$, it is possible to deduce that the linear operator $\mathcal{M} : X \times H \to (X\times H)'$ defined by

$$[\mathcal{M}(\mathbf{s},\boldsymbol{\tau}),(\mathbf{r},\boldsymbol{\zeta})] := \mathcal{D}\mathbb{A}(\widetilde{\mathbf{r}})(\mathbf{r},\mathbf{s}-\kappa\boldsymbol{\tau}^{\mathrm{d}}) - \int_\Omega \mathbf{s}:\boldsymbol{\zeta}^{\mathrm{d}} + \int_\Omega \mathbf{r}:\boldsymbol{\tau}^{\mathrm{d}} + \kappa\int_\Omega \boldsymbol{\zeta}^{\mathrm{d}}:\boldsymbol{\tau}^{\mathrm{d}} + \frac{1}{\alpha}\int_\Omega \mathbf{div}(\boldsymbol{\zeta})\cdot\mathbf{div}(\boldsymbol{\tau})$$

for all $(\mathbf{s},\boldsymbol{\tau}),(\mathbf{r},\boldsymbol{\zeta}) \in X\times H$, satisfies a global inf-sup condition. More precisely, there exists a constant $C>0$, independent of $h$, such that

$$C\|(\mathbf{r},\boldsymbol{\zeta})\|_{X\times H} \leq \sup_{\substack{(\mathbf{s},\boldsymbol{\tau})\in X\times H\\ (\mathbf{s},\boldsymbol{\tau})\neq\mathbf{0}}}\frac{[\mathcal{M}(\mathbf{s},\boldsymbol{\tau}),(\mathbf{r},\boldsymbol{\zeta})]}{\|(\mathbf{s},\boldsymbol{\tau})\|_{X\times H}}\,. \tag{5.39}$$

for all $\widetilde{\mathbf{r}} \in X$ and for all $(\mathbf{r},\boldsymbol{\zeta}) \in X \times H$. Next, since $\mathbf{t}, \mathbf{t}_h \in X$, the mean value theorem ensure the existence of $\widetilde{\mathbf{r}}_h \in X$, such that

$$\mathcal{D}\mathbb{A}(\widetilde{\mathbf{r}}_h)(\mathbf{t}-\mathbf{t}_h,\mathbf{s}) \;=\; [\mathbb{A}(\mathbf{t})-\mathbb{A}(\mathbf{t}_h),\mathbf{s}] \qquad \forall\, \mathbf{s}\in X\,.$$

Then, applying (5.39) to the error $(\mathbf{r},\boldsymbol{\zeta}) := (\mathbf{t}-\mathbf{t}_h, \boldsymbol{\sigma}-\boldsymbol{\sigma}_h)$, we get

$$C\|(\mathbf{t},\boldsymbol{\sigma})-(\mathbf{t}_h,\boldsymbol{\sigma}_h)\|_{X\times H} \;\leq\; \sup_{\substack{(\mathbf{s},\boldsymbol{\tau})\in X\times H\\ (\mathbf{s},\boldsymbol{\tau})\neq \mathbf{0}}} \frac{[\mathbf{A}(\mathbf{t},\boldsymbol{\sigma})-\mathbf{A}(\mathbf{t}_h,\boldsymbol{\sigma}_h),(\mathbf{s},\boldsymbol{\tau})]}{\|(\mathbf{s},\boldsymbol{\tau})\|_{X\times H}}\,. \tag{5.40}$$

Furthermore, from (5.9), (5.26), and adding and subtracting suitable terms, we realize that

$$\begin{aligned}
[\mathbf{A}(\mathbf{t},\boldsymbol{\sigma})-\mathbf{A}(\mathbf{t}_h,\boldsymbol{\sigma}_h),(\mathbf{s},\boldsymbol{\tau})] &= [\mathbf{F},(\mathbf{s},\boldsymbol{\tau})]-[\mathbf{A}(\mathbf{t}_h,\boldsymbol{\sigma}_h),(\mathbf{s},\boldsymbol{\tau})]\\
&= [\mathbf{F},(\mathbf{s}-\mathbf{s}_h,\boldsymbol{\tau}-\boldsymbol{\tau}_h)]+[\mathbf{F},(\mathbf{s}_h,\boldsymbol{\tau}_h)]-[\mathbf{A}(\mathbf{t}_h,\boldsymbol{\sigma}_h),(\mathbf{s},\boldsymbol{\tau})]\\
&= [\mathbf{F},(\mathbf{s}-\mathbf{s}_h,\boldsymbol{\tau}-\boldsymbol{\tau}_h)]+[\mathbf{A}_h(\mathbf{t}_h,\boldsymbol{\sigma}_h),(\mathbf{s}_h,\boldsymbol{\tau}_h)]\\
&\quad -[\mathbf{A}(\mathbf{t}_h,\boldsymbol{\sigma}_h),(\mathbf{s},\boldsymbol{\tau})]\\
&= [\mathbf{F},(\mathbf{s}-\mathbf{s}_h,\boldsymbol{\tau}-\boldsymbol{\tau}_h)]+[\mathbf{A}_h(\mathbf{t}_h,\boldsymbol{\sigma}_h)-\mathbf{A}(\mathbf{t}_h,\boldsymbol{\sigma}_h),(\mathbf{s}_h,\boldsymbol{\tau}_h)]\\
&\quad -[\mathbf{A}(\mathbf{t}_h,\boldsymbol{\sigma}_h),(\mathbf{s}-\mathbf{s}_h,\boldsymbol{\tau}-\boldsymbol{\tau}_h)]
\end{aligned} \tag{5.41}$$

for a given $(\mathbf{s},\boldsymbol{\tau}) \in X \times H$ and any $(\mathbf{s}_h,\boldsymbol{\tau}_h) \in X_k^h \times H_k^h$

Now, in what follows we assume that $(\mathbf{s}_h,\boldsymbol{\tau}_h) \in X_k^h \times H_k^h$ is chosen such that $\|(\mathbf{s}_h,\boldsymbol{\tau}_h)\|_{X\times H} \leq C\|(\mathbf{s},\boldsymbol{\tau})\|_{X\times H}$ for some positive constant $C$ independent of $(\mathbf{s},\boldsymbol{\tau})$. Hence, from Lemma 5.2, the inequality (5.24), and the expresions in (5.33), we deduce

$$[\mathbf{A}_h(\mathbf{t}_h,\boldsymbol{\sigma}_h)-\mathbf{A}(\mathbf{t}_h,\boldsymbol{\sigma}_h),(\mathbf{s}_h,\boldsymbol{\tau}_h)] \;\leq\; C\Big\{\sum_{K\in\mathcal{T}_h}\Big\{\Lambda_{1,K}^2+\Lambda_{2,K}^2+\|\boldsymbol{\sigma}_{h,K}^{\star,\mathrm{d}}-\mu(|\mathbf{t}_h|)\mathbf{t}_h\|_{0,K}^2\Big\}\Big\}^{1/2}\|(\mathbf{s},\boldsymbol{\tau})\|_{X\times H}\,, \tag{5.42}$$

with a constant $C>0$, independent of $h$. On the other hand, from (5.10) and (5.11), adding and subtracting suitable terms, and then performing some algebraic manipulations, we find that

$$\begin{aligned}
&[\mathbf{F},(\mathbf{s}-\mathbf{s}_h,\boldsymbol{\tau}-\boldsymbol{\tau}_h)]-[\mathbf{A}(\mathbf{t}_h,\boldsymbol{\sigma}_h),(\mathbf{s}-\mathbf{s}_h,\boldsymbol{\tau}-\boldsymbol{\tau}_h)]\\
&\qquad = \int_\Omega \big\{\widehat{\boldsymbol{\sigma}}_h^{\mathrm{d}}-\mu(|\mathbf{t}_h|)\mathbf{t}_h\big\}:\big\{(\mathbf{s}-\mathbf{s}_h)-\kappa(\boldsymbol{\tau}-\boldsymbol{\tau}_h)^{\mathrm{d}}\big\}\\
&\qquad\quad + \int_\Omega(\boldsymbol{\sigma}_h-\widehat{\boldsymbol{\sigma}}_h):\big\{(\mathbf{s}-\mathbf{s}_h)-\kappa(\boldsymbol{\tau}-\boldsymbol{\tau}_h)^{\mathrm{d}}\big\}+\mathcal{R}(\boldsymbol{\tau})\,,
\end{aligned} \tag{5.43}$$

where $\mathcal{R}(\boldsymbol{\tau})$ is given by (5.38). Then, from (5.40)–(5.43), using the Cauchy-Schwarz inequality, adding and subtracting locally $\boldsymbol{\sigma}_{h,K}^{\star,\mathrm{d}}$, and recalling that $\|(\mathbf{s}_h,\boldsymbol{\tau}_h)\|_{X\times H} \leq C\|(\mathbf{s},\boldsymbol{\tau})\|_{X\times H}$, we conclude the proof. □

We now aim to bound the supremum on the right-hand side of (5.37). In order to do that, we need a suitable choice of $(\mathbf{s}_h,\boldsymbol{\tau}_h) \in X_k^h \times H_k^h$. To this end, given $(\mathbf{s},\boldsymbol{\tau}) \in X \times H$, we take for simplicity $\mathbf{s}_h := \boldsymbol{\mathcal{P}}_k^h(\mathbf{s}) \in X_k^h$, whereas the choice of $\boldsymbol{\tau}_h$ requires the use of a type Clément interpolant and the Helmholtz decomposition in $H$.

Then, proceeding as in [40, Section 5], we make use of the interpolation operator $\mathcal{I}_k^h : \mathbf{H}^1(\Omega) \to V_k^h$, where $V_k^h$ (cf. [13]) is defined for all $k \geq 0$ as

$$V_k^h \ := \ \big\{ \mathbf{v} \in \mathbf{H}^1(\Omega) : \quad \mathbf{v}\big|_{\partial K} \in \mathbb{B}_k(\partial K) \quad \text{and} \quad \Delta \mathbf{v} \in \mathbf{P}_{k-1}(K) \quad \forall K \in \mathcal{T}_h \big\} \, ,$$

with

$$\mathbb{B}_k(\partial K) \ := \ \big\{ \mathbf{v} \in \mathbf{C}(\partial K) \ : \quad \mathbf{v}|_e \in \mathbf{P}_{k+1}(e) \quad \forall \text{ edge } e \subseteq \partial K \big\} \, .$$

Next, the following lemma establishes the local approximation properties of $\mathcal{I}_h$.

**Lemma 5.9.** There exist constants $c_1, c_2 > 0$, independent of $h$, such that for all $\mathbf{v} \in \mathbf{H}^1(\Omega)$ there hold

$$\|\mathbf{v} - \mathcal{I}_k^h(\mathbf{v})\|_{0,K} \ \leq \ c_1 h_K \|\mathbf{v}\|_{1,\omega_K} \qquad \forall \, K \in \mathcal{T}_h \, , \tag{5.44}$$

and

$$\|(\mathbf{v} - \mathcal{I}_k^h(\mathbf{v})) \cdot \boldsymbol{\nu}_e\|_{0,e} \ \leq \ c_2 h_e^{1/2} \|\mathbf{v}\|_{1,\omega_e} \qquad \forall \, e \in \mathcal{E}_h \, , \tag{5.45}$$

where $\omega_K := \{K' \in \mathcal{T}_h : \ K \cap K' \neq \varnothing\}$ and $\omega_e := \{K \in \mathcal{T}_h : \ e \in \mathcal{E}(K)\}$.

*Proof.* See [81, Section 4, Proposition 4.2] and [40, Section 5, eq. 24] for more details. □

Now, for each $\boldsymbol{\tau} \in H$ we consider its Helmholtz decomposition (see, e.g, [63, Section 4])

$$\boldsymbol{\tau} \ = \ \nabla \mathbf{z} + \underline{\mathbf{curl}}\,(\boldsymbol{\varphi}) \, , \tag{5.46}$$

where $\mathbf{z} \in \mathbf{H}^2(\Omega)$ and $\boldsymbol{\varphi} \in \mathbf{H}^1(\Omega)$, are such that $\mathbf{div}\,(\nabla \mathbf{z}) = \mathbf{div}\,(\boldsymbol{\tau})$ in $\Omega$, and there holds

$$\|\mathbf{z}\|_{2,\Omega} \ + \ \|\boldsymbol{\varphi}\|_{1,\Omega} \ \leq \ C \|\boldsymbol{\tau}\|_{\mathbf{div};\Omega} \, , \tag{5.47}$$

with $C$ a positive constant independent of all the foregoing variables. Then, recalling that $\mathcal{I}_k^h : \mathbf{H}^1(\Omega) \to V_k^h$ and $\boldsymbol{\Pi}_k^h : \mathbb{H}^1(\Omega) \to H_k^h$ are the respective interpolation operators on $V_k^h$ and $H_k^h$, letting $\boldsymbol{\zeta} := \nabla \mathbf{z} \in \mathbb{H}^1(\Omega)$, $\boldsymbol{\varphi}_h := \mathcal{I}_k^h(\boldsymbol{\varphi})$, and using Lemma 5.1 in [40, Section 5], we set

$$\boldsymbol{\tau}_h \ := \ \boldsymbol{\Pi}_k^h(\boldsymbol{\zeta}) + \underline{\mathbf{curl}}\,(\boldsymbol{\varphi}_h) + c_h \mathbb{I} \, , \tag{5.48}$$

where $c_h \in \mathrm{R}$ is chosen so that $\boldsymbol{\tau}_h \in H_k^h$. Equivalently, $\boldsymbol{\tau}_h$ is the $\mathbb{H}_0(\mathbf{div};\Omega)$-component of $\underline{\mathbf{curl}}(\boldsymbol{\varphi}_h) + \boldsymbol{\Pi}_k^h(\boldsymbol{\zeta})$. In addition, it follows from our chosen for $(\mathbf{s}_h, \boldsymbol{\tau}_h)$, by applying of the triangle inequality, the estimates (5.19), (5.44), and the property (5.47), that there holds $\|(\mathbf{s}_h, \boldsymbol{\tau}_h)\|_{X \times H} \leq C \|(\mathbf{s}, \boldsymbol{\tau})\|_{X \times H}$ for some $C > 0$ independent of $(\mathbf{s}, \boldsymbol{\tau})$.

Now, according to (5.46), (5.48), and the linearity of $\mathcal{R}$ (cf. (5.38)), we deduce that the expression $\mathcal{R}(\boldsymbol{\tau})$ can be rewritten as

$$\mathcal{R}(\boldsymbol{\tau}) \ = \ \mathcal{R}(\boldsymbol{\zeta} - \boldsymbol{\Pi}_k^h(\boldsymbol{\zeta})) + \mathcal{R}(\underline{\mathbf{curl}}(\boldsymbol{\varphi} - \boldsymbol{\varphi}_h)) + c_h \mathcal{R}_{\mathbb{I}} \, ,$$

where

$$\mathcal{R}_{\mathbb{I}} \ := \ \int_\Omega \mathbf{t}_h : \mathbb{I}^{\mathrm{d}} \ - \ \langle \mathbb{I}\boldsymbol{\nu}, \mathbf{g} \rangle \ + \ \frac{1}{\alpha} \int_\Omega (\mathbf{f} + \mathbf{div}(\boldsymbol{\sigma}_h)) \cdot \mathbf{div}(\mathbb{I}) \, .$$

Then, using that $\mathbb{I}^{\mathrm{d}} = \mathbf{0}$, $\mathbf{div}(\mathbb{I}) = \mathbf{0}$ and the fact that $\langle \mathbb{I}\boldsymbol{\nu}, \mathbf{g} \rangle = 0$ (which is a consequence of the compatibility condition for the Dirichlet datum $\mathbf{g}$ explained in Section 5.2.1), we obtain

$$\mathcal{R}(\boldsymbol{\tau}) \ = \ \mathcal{R}(\boldsymbol{\zeta} - \boldsymbol{\Pi}_k^h(\boldsymbol{\zeta})) + \mathcal{R}(\underline{\mathbf{curl}}(\boldsymbol{\varphi} - \boldsymbol{\varphi}_h)) \, . \tag{5.49}$$

Next, the following lemma yields the required bound for the supremum on the right-hand side of (5.37).

**Lemma 5.10.** Assume that $\mathbf{g} \in \mathbf{H}^1(\Gamma)$. Then, there exists $C > 0$, independent of $h$, such that

$$|\mathcal{R}(\boldsymbol{\tau})| \;\leq\; C\Big\{ \sum_{K\in\mathcal{T}_h} \theta_K^2 \Big\}^{1/2} \|\boldsymbol{\tau}\|_H \,.$$

*Proof.* It is follows after to bound the modules of the two expressions on the right-hand side of (5.49). To bound $|\mathcal{R}(\boldsymbol{\zeta} - \boldsymbol{\Pi}_k^h(\boldsymbol{\zeta}))|$, we use the ideas from Lemma 5.8 in [40, Section 5], together to the identity

$$\mathbf{div}(\boldsymbol{\zeta} - \boldsymbol{\Pi}_k^h(\boldsymbol{\zeta})) \;=\; (\mathbf{I} - \mathcal{P}_k^h)(\mathbf{div}(\boldsymbol{\tau}))\,,$$

which is consequence of (5.20), and the fact that $\mathbf{div}(\boldsymbol{\zeta}) = \mathbf{div}(\boldsymbol{\tau})$ in $\Omega$, and where $\mathbf{I}$ is denoting a generic identity operator. In addition, following similar arguments to the proof of Lemma 5.4 in [58, Section 5] (see also [40, Lemma 5.9]), in join with Lemma 5.9, and the fact that the number of elements in $\omega_e$ is bounded, the term $|\mathcal{R}(\underline{\mathbf{curl}}(\boldsymbol{\varphi} - \boldsymbol{\varphi}_h))|$ is suitably bounded. □

Then, as a consequence of Lemmas 5.8 and 5.10, the triangle inequality, and the lower bound in (5.24), we conclude that there exists $C > 0$, independent of $h$, such that

$$\begin{aligned} \|(\mathbf{t},\boldsymbol{\sigma}) - (\mathbf{t}_h,\boldsymbol{\sigma}_h)\|_{X\times H} \,+\, \Big\{ \sum_{K\in\mathcal{T}_h} \|\boldsymbol{\sigma} - \boldsymbol{\sigma}_{h,K}^{\star}\|^2_{\mathbf{div};K} \Big\}^{1/2} & \\ \leq\; C\Big\{ \|(\mathbf{t},\boldsymbol{\sigma}) - (\mathbf{t}_h,\boldsymbol{\sigma}_h)\|_{X\times H} \,+\, \Big\{ \sum_{K\in\mathcal{T}_h} \Big\{ \Lambda_{1,K}^2 + \Lambda_{2,K}^2 + \Lambda_{3,K}^2 \Big\} \Big\}^{1/2} \Big\} & \\ \leq\; C\,\boldsymbol{\eta} & \end{aligned} \tag{5.50}$$

where $\boldsymbol{\eta}$ is the global estimator defined by (5.34). Now, in order to incorporate the error $\|\mathbf{u} - \mathbf{u}_h\|_{0,\Omega}$, we recall that from (5.4) and (5.29), we have that

$$\mathbf{u} \;=\; \frac{1}{\alpha}\Big\{ \mathbf{f} + \mathbf{div}\,(\boldsymbol{\sigma}) \Big\} \qquad \text{and} \qquad \mathbf{u}_h \;=\; \frac{1}{\alpha}\Big\{ \mathcal{P}_k^h(\mathbf{f}) + \mathbf{div}\,(\boldsymbol{\sigma}_h) \Big\}\,, \tag{5.51}$$

whence,

$$\|\mathbf{u} - \mathbf{u}_h\|_{0,\Omega} \;\leq\; \frac{1}{\alpha}\Big\{ \|\mathbf{f} - \mathcal{P}_k^h(\mathbf{f})\|_{0,\Omega} + \|\boldsymbol{\sigma} - \boldsymbol{\sigma}_h\|_H \Big\}\,. \tag{5.52}$$

Finally, from (5.50) and (5.52) we have that there exists $C_{\mathtt{rel}} > 0$, independent of $h$, such that

$$\|\mathbf{u} - \mathbf{u}_h\|_{0,\Omega} \,+\, \|(\mathbf{t},\boldsymbol{\sigma}) - (\mathbf{t}_h,\boldsymbol{\sigma}_h)\|_{X\times H} \,+\, \Big\{ \sum_{K\in\mathcal{T}_h} \|\boldsymbol{\sigma} - \boldsymbol{\sigma}_{h,K}^{\star}\|^2_{\mathbf{div};K} \Big\}^{1/2} \;\leq\; C_{\mathtt{rel}}\boldsymbol{\eta}\,,$$

which proves the reliability of the estimator $\boldsymbol{\eta}$.

### 5.3.2 Efficiency

In this section we prove the efficiency of our a posteriori error estimator $\boldsymbol{\eta}$ (lower bound in (5.36)). For this purpose, we derive suitable upper bounds for the terms defining the local error indicators.

First, using the upper bound in (5.24), the estimate (5.51), and adding and subtracting suitable terms, we get

$$\begin{aligned}
\Lambda_{1,K}^2 &\leq 4\,\widehat{c}_1\Big\{\|\boldsymbol{\sigma}-\boldsymbol{\sigma}_{h,K}^{\star}\|_{0,K}^2+\Lambda_{2,K}^2+\|\boldsymbol{\sigma}-\boldsymbol{\sigma}_h\|_{0,K}^2\Big\}\,,\\
\Lambda_{2,K}^2 &\leq 4\Big\{\|\boldsymbol{\sigma}-\boldsymbol{\sigma}_{h,K}^{\star}\|_{0,K}^2+\|\boldsymbol{\sigma}-\boldsymbol{\sigma}_h\|_{0,K}^2+\|\boldsymbol{\sigma}-\boldsymbol{\mathcal{P}}_k^K(\boldsymbol{\sigma})\|_{0,K}^2\Big\}\,,\\
\Lambda_{3,K}^2 &\leq 2\Big\{\|\mathbf{div}(\boldsymbol{\sigma}-\boldsymbol{\sigma}_{h,K}^{\star})\|_{0,K}^2+\|\mathbf{div}(\boldsymbol{\sigma}-\boldsymbol{\sigma}_h)\|_{0,K}^2\Big\}\,,\\
\Lambda_{4,K}^2 &\leq 4\max\{1,\alpha^2\}\Big\{\|\mathbf{u}-\mathbf{u}_h\|_{0,K}^2+\|\mathbf{div}(\boldsymbol{\sigma}-\boldsymbol{\sigma}_{h,K}^{\star})\|_{0,K}^2+\Lambda_{3,K}^2\Big\}\,.
\end{aligned}\tag{5.53}$$

Moreover, procceding as in [58, Section 5.3, eq. 5.26], that is, adding and subtracting $\boldsymbol{\sigma}^{\mathrm{d}}$, using the second equation in (5.7), the fact that $\|\boldsymbol{\zeta}^{\mathrm{d}}\|_{0,K}\leq\|\boldsymbol{\zeta}\|_{0,K}$ for all $\boldsymbol{\zeta}\in\mathbb{L}^2(K)$, and the Lipschitz-continuity of the operator $\mathbb{A}$ (cf. (5.6)), but restricted to the element $K\in\mathcal{T}_h$ instead of $\Omega$, we deduce that

$$\|\widehat{\boldsymbol{\sigma}}_{h,K}^{\star,\mathrm{d}}-\mu(|\mathbf{t}_h|)\mathbf{t}_h\|_{0,K}^2\;\leq\;2\Big\{\|\boldsymbol{\sigma}-\boldsymbol{\sigma}_{h,K}^{\star}\|_{0,K}^2\;+\;\gamma_0^2\,\|\mathbf{t}-\mathbf{t}_h\|_{0,K}^2\Big\}\,.\tag{5.54}$$

Next, the upper bounds of the terms which depend on the mesh parameters $h_K$ and $h_e$, will be derived below. For this purpose, we make use of the results and estimates proved in [40, Section 5.4], whose proofs use techniques based on bubble functions, extension operators, and discrete trace and inverse inequalities. More precisely, it was used the following Lemma (see [38, 40, 81] for more details).

**Lemma 5.11.** Given $k\geq 0$ and $K\in\mathcal{T}_h$, there exists a positive constant $C_{\mathrm{bub}}$, independent of $h_K$, such that

$$C_{\mathrm{bub}}^{-1}\|q\|_{0,K}^2\;\leq\;\|\psi_K^{1/2}q\|_{0,K}^2\;\leq\;C_{\mathrm{bub}}\|q\|_{0,K}^2\qquad\forall\,q\in\mathbf{P}_k(K)\,,$$

and

$$C_{\mathrm{bub}}^{-1}\|q\|_{0,K}\;\leq\;\|\psi_K q\|_{0,K}+h_K|\psi_K q|_{1,K}\;\leq\;C_{\mathrm{bub}}\|q\|_{0,K}\qquad\forall\,q\in\mathbf{P}_k(K)\,.$$

In addition, given $e\in\partial K$, there hold

$$C_{\mathrm{bub}}^{-1}\|q\|_{0,e}^2\;\leq\;\|\psi_e^{1/2}q\|_{0,e}^2\;\leq\;C_{\mathrm{bub}}\|q\|_{0,e}^2\qquad\forall\,q\in\mathbf{P}_k(e)\,,$$

and

$$h_K^{-1/2}\|\psi_e L(q)\|_{0,K}+h_K^{1/2}|\psi_e L(q)|_{1,K}\;\leq\;C_{\mathrm{bub}}\|q\|_{0,e}\qquad\forall\,q\in\mathbf{P}_k(e)\,,$$

where $K\in\omega_e$ and $\omega_e$ is as in Lemma 5.9.

**Lemma 5.12.** Assume that $\dfrac{d\mathbf{g}}{d\boldsymbol{s}}$ is piecewise polynomial. Then, there exist $C_i>0$, $i=1,\ldots,4$, independent of $h$, such that

$$\begin{aligned}
h_K^2\|\mathrm{curl}(\mathbf{t}_h)\|_{0,K}^2 &\leq C_1\|\mathbf{t}-\mathbf{t}_h\|_{0,K}^2\qquad\forall\,K\in\mathcal{T}_h\,,\\
h_e\big\|[\![\mathbf{t}_h\boldsymbol{s}]\!]\big\|_{0,e}^2 &\leq C_2\|\mathbf{t}-\mathbf{t}_h\|_{0,\omega_e}^2\qquad\forall\,e\in\mathcal{E}_h(\Omega)\,,\\
h_K^2\|\mathbf{t}_h-\nabla\mathbf{u}_h\|_{0,K}^2 &\leq C_3\Big\{\|\mathbf{u}-\mathbf{u}_h\|_{0,K}^2+h_K^2\|\mathbf{t}-\mathbf{t}_h\|_{0,K}^2\Big\}\qquad\forall\,K\in\mathcal{T}_h\,,\\
h_e\left\{\|\mathbf{g}-\mathbf{u}_h\|_{0,e}^2+\left\|\frac{d\mathbf{g}}{d\boldsymbol{s}}-\mathbf{t}_h\boldsymbol{s}\right\|_{0,e}^2\right\} &\leq C_4\Big\{\|\mathbf{u}-\mathbf{u}_h\|_{0,\omega_e}^2+h_{K_e}^2\|\mathbf{t}-\mathbf{t}_h\|_{0,\omega_e}^2\Big\}\qquad\forall\,e\in\mathcal{E}_h(\Gamma)\,,
\end{aligned}$$

where $\omega_e$ is as in Lemma 5.9.

*Proof.* The first two estimates are consequence of [40, Lemma 5.17] through an adaptation of [40, Lemma 5.16]. The third inequality follows from a slight modification of the proof of Lemma 5.14 in [40]. Finally, the last estimate follows the same arguments used in the proof of Lemmas 5.15 and 5.18 of [40]. We remark here that all these proofs makes use of Lemma 5.11. □

Consequently, the efficiency of $\boldsymbol{\eta}$ (lower bound in Lemma 5.7) follows straightforwardly from estimates (5.53)–(5.54), together with Lemma 5.12, after summing up over $K \in \mathcal{T}_h$. We observe here that this bound shows the efficiency of the estimator $\boldsymbol{\eta}$ up to data oscillation. This fact can be interpreted as a quasi-efficiency (see, e.g, [9, 83]).

## 5.4 Numerical results

In this section, we present several numerical examples confirming reliability and efficiency of the a posteriori error estimator $\boldsymbol{\eta}$ derived in Section 5.3, and showing the behavior of the associated adaptive algorithm. We recall here that the condition $\int_\Omega \mathrm{tr}(\boldsymbol{\tau}_h) = 0$ for each $\boldsymbol{\tau}_h \in H_k^h$ was imposed as usual, that is, via a real Lagrange multiplier (see [68, Section 5] for more details). In what follows $N$ stands for the total number of degrees of freedom of (5.26), that is,

$$N := 2(k+1) \times \{\text{number of edges } e \in \mathcal{T}_h\} + \frac{(k+2)(7k+3)}{2} \times \{\text{number of elements } K \in \mathcal{T}_h\} + 1.$$

Also, the individual errors are defined by

$$\mathtt{e}(\mathbf{u}) := \|\mathbf{u} - \mathbf{u}_h\|_{0,\Omega}\,, \qquad \mathtt{e}(\mathbf{t}) := \|\mathbf{t} - \mathbf{t}_h\|_{0,\Omega}\,, \qquad \mathtt{e}(p) := \|p - p_h\|_{0,\Omega}\,,$$

$$\mathtt{e}(\boldsymbol{\sigma}) := \left\{ \sum_{K \in \mathcal{T}_h} \|\boldsymbol{\sigma} - \boldsymbol{\sigma}^\star_{h,K}\|^2_{\mathbf{div};K} \right\}^{1/2} \quad \text{and} \quad \mathtt{e}(\mathbf{u},\mathbf{t},\boldsymbol{\sigma}) := \left\{ [\mathtt{e}(\mathbf{u})]^2 + [\mathtt{e}(\mathbf{t})]^2 + [\mathtt{e}(\boldsymbol{\sigma})]^2 \right\}^{1/2},$$

where $\mathbf{u}_h$ and $p_h$ are computed by the postprocessing formulae (5.29), whereas the effectivity index with respect $\boldsymbol{\eta}$ is given by

$$\mathtt{eff}(\boldsymbol{\eta}) := \frac{\mathtt{e}(\mathbf{u},\mathbf{t},\boldsymbol{\sigma})}{\boldsymbol{\eta}}\,.$$

Observe that this quantity is not a true efficiency index, however, it gives information on the behavior of $\boldsymbol{\eta}$. Moreover, in this case, some of the local indicators defined in (5.33) can be interpreted as oscillation terms . At least they must have the same rate of convergence of the global error if the exact solution is smooth enough (see, e.g. [40, Section 5.4]). In Example 1 it is proved numerically.

Then, we define the experimental rates of convergence

$$\mathtt{r}(\cdot) := -2\,\frac{\log(\mathtt{e}(\cdot)/\mathtt{e}'(\cdot))}{\log(N/N')}\,,$$

where $\mathtt{e}$ and $\mathtt{e}'$ denote the corresponding errors for two consecutive meshes with $N$ and $N'$ the respective degrees of freedom of each decomposition. Similarly, we define:

$$\mathtt{r}(\Lambda_i) := -2\,\frac{\log(\Lambda_i/\Lambda_i')}{\log(N/N')}\,,$$

where $\Lambda_i := \left\{ \sum_{K\in\mathcal{T}_h} \Lambda_{i,K}^2 \right\}^{1/2}$. For the tests that include adaptivity, we use for the local a posteriori error indicator $\boldsymbol{\eta}_K := \boldsymbol{\eta}|_K$, the strategy:

(i) Start with a coarse mesh $\mathcal{T}_h$.

(ii) Solve the discrete problem on the current mesh $\mathcal{T}_h$.

(iii) Compute local indicators for each $K \in \mathcal{T}_h$.

(iv) Mark each $K' \in \mathcal{T}_h$ to be refined appyling the rule

$$\boldsymbol{\eta}_{K'} \geq \beta \max_{K\in\mathcal{T}_h} \boldsymbol{\eta}_K,$$

with $\beta \in (0,1)$. Here we use $\beta = 0.35$.

(v) Define the new mesh as actual mesh $\mathcal{T}_h$ and go to step (ii).

Regarding adaptive strategy, for each $K \in \mathcal{T}_h$ that has been marked for refinement, we subdivide it using the midpoint of each edge of the boundary of $K$ and connecting these to its barycenter. Observe that all meshes used for the numerical examples in this section (see Figure 5.1) are composes of convex elements, therefore, the barycenter of $K$ is an internal point of it. In this way, each new element generated with this strategy is a quadrilateral. Now, since for meshes with non-convex elements, it is possible that some barycenter is outside its respective element, we can use the barycenter of $Ker(K)$ to subdivide $K$.

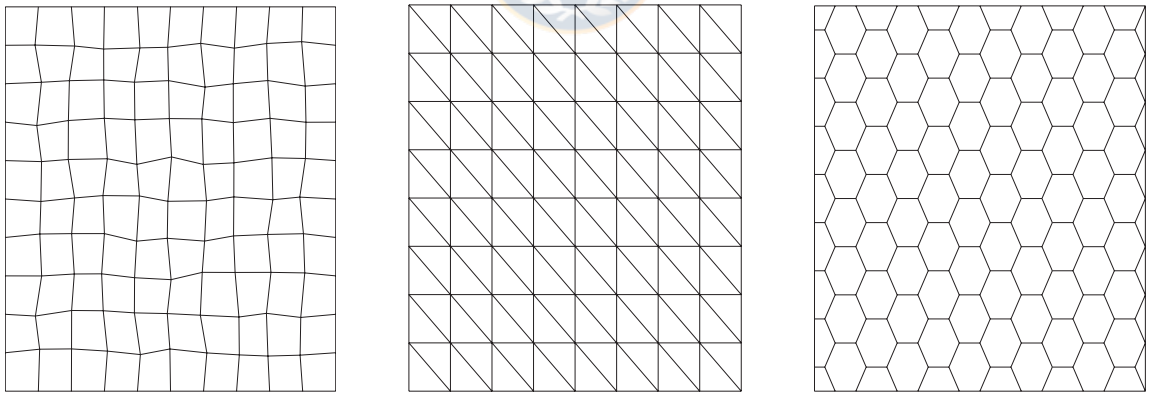

Figure 5.1: Sample meshes: distorted squares (left), triangular (center) and hexagonal (right) (figure produced by the author).

In turn, the nonlinear algebraic systems are solved by the Newton method with a tolerance of $10^{-6}$ and taking as initial iteration the solution of the linear Brinkman problem with $\mu = 1$. The numerical results presented below were obtained using a MATLAB code. For all the numerical tests we use $\alpha = 1$ and $\kappa = 0.4$, where the value of $\kappa$ is chosen according to the Theorems 5.3 and 5.4.

### 5.4.1 Example 1

First, we consider the unit square $\Omega := (0,1)^2$, and choose $\mathbf{f}$ and $\mathbf{g}$ such that the exact solution is given by

$$\mathbf{u}(\mathbf{x}) := \begin{pmatrix} -\cos(\pi x_1)\sin(\pi x_2) \\ \sin(\pi x_1)\cos(\pi x_2) \end{pmatrix} \qquad \text{and} \qquad p(\mathbf{x}) := x_1^2 + x_2^2 - p_0$$

for all $\mathbf{x} := (x_1, x_2)^{\mathrm{t}} \in \Omega$, where $p_0 \in \mathrm{R}$ is such that $\int_\Omega p = 0$. Moreover, we consider the nonlinear viscosity $\mu$ given by

$$\mu(s) := 2 + (1+s^2)^{-1/6} \qquad \forall\, s \geq 0\,. \tag{5.55}$$

The aim of this test is to verify the asymptotic behavior of the estimator with a smooth solution and under uniform refinements. To this end, we use three families of uniformly generated meshes: distorted squares, uniform triangular and hexagonal (see Figure 5.1).

Tables 5.1 to 5.3 show the convergence history of the errors and the estimator on the three sequence of uniformly refined meshes, indicating that all converge at the optimal rate for polynomial degrees $k = 0, 1, 2$. We can observe the robustness of the estimator with respect to the mesh shape. Moreover, the effectivity of $\boldsymbol{\eta}$ remains bounded. In addition, we see from Table 5.4–5.6 that each term $\Lambda_{i,K}$ for $i = 1, ..., 4$, converge with optimal order $k+1$, with exception of $\Lambda_{3,K}$, which converge with order $k+2$. Also, the robustness of the terms with respect to the mesh shape is verified.

| $k$ | $N$ | $\mathtt{e}(\mathbf{u},\mathbf{t},\boldsymbol{\sigma})$ | $\mathtt{r}(\mathbf{u},\mathbf{t},\boldsymbol{\sigma})$ | $\boldsymbol{\eta}$ | $\mathtt{r}(\boldsymbol{\eta})$ | $\mathtt{eff}(\boldsymbol{\eta})$ |
|---|---|---|---|---|---|---|
| | 741 | 4.9184e+00 | −− | 5.5400e+00 | −− | 0.8878 |
| | 2881 | 2.4631e+00 | 1.0186 | 2.7848e+00 | 1.0131 | 0.8845 |
| 0 | 6421 | 1.6443e+00 | 1.0084 | 1.8597e+00 | 1.0076 | 0.8842 |
| | 11361 | 1.2342e+00 | 1.0056 | 1.3961e+00 | 1.0050 | 0.8840 |
| | 17701 | 9.8742e-01 | 1.0061 | 1.1173e+00 | 1.0047 | 0.8837 |
| | 2381 | 4.2581e-01 | −− | 4.7037e-01 | −− | 0.9053 |
| | 9361 | 1.0858e-01 | 1.9963 | 1.1968e-01 | 1.9995 | 0.9072 |
| 1 | 20941 | 4.8948e-02 | 1.9790 | 5.3847e-02 | 1.9840 | 0.9090 |
| | 37121 | 2.7384e-02 | 2.0290 | 3.0154e-02 | 2.0256 | 0.9081 |
| | 57901 | 1.7577e-02 | 1.9948 | 1.9348e-02 | 1.9963 | 0.9084 |
| | 4721 | 4.7913e-02 | −− | 4.9194e-02 | −− | 0.9740 |
| | 18641 | 9.4987e-03 | 2.3566 | 9.6137e-03 | 2.3775 | 0.9880 |
| 2 | 41761 | 3.0449e-03 | 2.8209 | 3.0779e-03 | 2.8241 | 0.9893 |
| | 74081 | 1.2901e-03 | 2.9964 | 1.3039e-03 | 2.9968 | 0.9894 |
| | 115601 | 6.5711e-04 | 3.0321 | 6.6436e-04 | 3.0307 | 0.9891 |

Table 5.1: Example 1. Convergence history for a uniformly generated sequence of meshes composed of distorted squares (table produced by the author).

| $k$ | $N$ | $\mathtt{e}(\mathbf{u},\mathbf{t},\boldsymbol{\sigma})$ | $\mathtt{r}(\mathbf{u},\mathbf{t},\boldsymbol{\sigma})$ | $\boldsymbol{\eta}$ | $\mathtt{r}(\boldsymbol{\eta})$ | $\mathtt{eff}(\boldsymbol{\eta})$ |
|---|---|---|---|---|---|---|
| | 801 | 5.0103e+00 | −− | 5.6443e+00 | −− | 0.8877 |
| | 3137 | 2.5110e+00 | 1.0120 | 2.8399e+00 | 1.0063 | 0.8842 |
| 0 | 7009 | 1.6749e+00 | 1.0074 | 1.8961e+00 | 1.0050 | 0.8834 |
| | 12417 | 1.2565e+00 | 1.0053 | 1.4229e+00 | 1.0039 | 0.8830 |
| | 19361 | 1.0053e+00 | 1.0042 | 1.1387e+00 | 1.0033 | 0.8828 |
| | 2753 | 4.0703e-01 | −− | 4.7947e-01 | −− | 0.8489 |
| | 10881 | 1.0774e-01 | 1.9342 | 1.2502e-01 | 1.9561 | 0.8618 |
| 1 | 24385 | 4.8734e-02 | 1.9663 | 5.6304e-02 | 1.9772 | 0.8656 |
| | 43265 | 2.7545e-02 | 1.9902 | 3.1787e-02 | 1.9942 | 0.8666 |
| | 67521 | 1.7659e-02 | 1.9976 | 2.0370e-02 | 1.9994 | 0.8669 |
| | 5601 | 4.4640e-02 | −− | 5.0546e-02 | −− | 0.8832 |
| | 22209 | 1.0416e-02 | 2.1128 | 1.0857e-02 | 2.2331 | 0.9594 |
| 2 | 49825 | 3.3845e-03 | 2.7825 | 3.5066e-03 | 2.7973 | 0.9652 |
| | 88449 | 1.4448e-03 | 2.9665 | 1.4962e-03 | 2.9681 | 0.9656 |
| | 138081 | 7.4558e-04 | 2.9705 | 7.7186e-04 | 2.9720 | 0.9660 |

Table 5.2: Example 1. Convergence history for a uniformly generated sequence of triangular meshes (table produced by the author).

| $k$ | $N$ | $\mathtt{e}(\mathbf{u},\mathbf{t},\boldsymbol{\sigma})$ | $\mathtt{r}(\mathbf{u},\mathbf{t},\boldsymbol{\sigma})$ | $\boldsymbol{\eta}$ | $\mathtt{r}(\boldsymbol{\eta})$ | $\mathtt{eff}(\boldsymbol{\eta})$ |
|---|---|---|---|---|---|---|
| | 903 | 5.1548e+00 | −− | 5.5410e+00 | −− | 0.9303 |
| | 3891 | 2.3753e+00 | 1.0608 | 2.5969e+00 | 1.0377 | 0.9147 |
| 0 | 7806 | 1.6636e+00 | 1.0230 | 1.8278e+00 | 1.0089 | 0.9102 |
| | 13071 | 1.2797e+00 | 1.0178 | 1.4098e+00 | 1.0074 | 0.9078 |
| | 19686 | 1.0399e+00 | 1.0137 | 1.1474e+00 | 1.0057 | 0.9063 |
| | 2723 | 3.7773e-01 | −− | 4.2442e-01 | −− | 0.8810 |
| | 11669 | 8.4064e-02 | 2.0651 | 9.3206e-02 | 2.0835 | 0.9019 |
| 1 | 23414 | 4.1853e-02 | 2.0029 | 4.6318e-02 | 2.0083 | 0.9036 |
| | 39209 | 2.4964e-02 | 2.0045 | 2.7602e-02 | 2.0080 | 0.9044 |
| | 59054 | 1.6562e-02 | 2.0038 | 1.8302e-02 | 2.0065 | 0.9049 |
| | 5257 | 5.2896e-02 | −− | 5.3776e-02 | −− | 0.9836 |
| | 22471 | 6.9311e-03 | 2.7980 | 6.9875e-03 | 2.8096 | 0.9919 |
| 2 | 45091 | 2.5194e-03 | 2.9062 | 2.5381e-03 | 2.9082 | 0.9926 |
| | 75511 | 1.1781e-03 | 2.9484 | 1.1865e-03 | 2.9496 | 0.9929 |
| | 113731 | 6.4129e-04 | 2.9700 | 6.4576e-04 | 2.9707 | 0.9931 |

Table 5.3: Example 1. Convergence history for a uniformly generated sequence of hexagonal meshes (table produced by the author).

| $k$ | $N$ | $\Lambda_1$ | $\mathtt{r}(\Lambda_1)$ | $\Lambda_2$ | $\mathtt{r}(\Lambda_2)$ | $\Lambda_3$ | $\mathtt{r}(\Lambda_3)$ | $\Lambda_4$ | $\mathtt{r}(\Lambda_4)$ |
|---|---|---|---|---|---|---|---|---|---|
| | 741 | 1.8477e+00 | −− | 7.5024e-01 | −− | 1.5379e-02 | −− | 4.9244e+00 | −− |
| | 2881 | 9.3401e-01 | 1.0048 | 3.7905e-01 | 1.0056 | 3.8945e-03 | 2.0229 | 2.4657e+00 | 1.0188 |
| 0 | 6421 | 6.2345e-01 | 1.0087 | 2.5285e-01 | 1.0104 | 1.7304e-03 | 2.0244 | 1.6465e+00 | 1.0078 |
| | 11361 | 4.6799e-01 | 1.0053 | 1.8981e-01 | 1.0051 | 9.7493e-04 | 2.0110 | 1.2359e+00 | 1.0054 |
| | 17701 | 3.7456e-01 | 1.0044 | 1.5192e-01 | 1.0043 | 6.2437e-04 | 2.0098 | 9.8875e-01 | 1.0063 |
| | 2381 | 1.0284e-01 | −− | 5.7518e-02 | −− | 6.9336e-04 | −− | 4.2232e-01 | −− |
| | 9361 | 2.7016e-02 | 1.9529 | 1.4446e-02 | 2.0185 | 8.7022e-05 | 3.0319 | 1.0808e-01 | 1.9910 |
| 1 | 20941 | 1.2218e-02 | 1.9710 | 6.4404e-03 | 2.0066 | 2.5888e-05 | 3.0115 | 4.8795e-02 | 1.9753 |
| | 37121 | 6.9260e-03 | 1.9831 | 3.6282e-03 | 2.0048 | 1.0944e-05 | 3.0080 | 2.7314e-02 | 2.0270 |
| | 57901 | 4.4529e-03 | 1.9873 | 2.3227e-03 | 2.0065 | 5.6063e-06 | 3.0093 | 1.7539e-02 | 1.9930 |
| | 4721 | 4.1684e-03 | −− | 4.1204e-03 | −− | 5.5974e-05 | −− | 4.7853e-02 | −− |
| | 18641 | 6.0907e-04 | 2.8010 | 5.1934e-04 | 3.0162 | 3.4255e-06 | 4.0684 | 9.4926e-03 | 2.3558 |
| 2 | 41761 | 1.9152e-04 | 2.8687 | 1.5552e-04 | 2.9898 | 6.7610e-07 | 4.0235 | 3.0429e-03 | 2.8209 |
| | 74081 | 8.3109e-05 | 2.9129 | 6.4689e-05 | 3.0606 | 2.0539e-07 | 4.1571 | 1.2894e-03 | 2.9959 |
| | 115601 | 4.2959e-05 | 2.9660 | 3.3209e-05 | 2.9969 | 8.4115e-08 | 4.0125 | 6.5675e-04 | 3.0323 |

Table 5.4: Example 1. Convergence history of some terms using a uniformly generated sequence of meshes composed of distorted squares (table produced by the author).

| $k$ | $N$ | $\Lambda_1$ | $\mathtt{r}(\Lambda_1)$ | $\Lambda_2$ | $\mathtt{r}(\Lambda_2)$ | $\Lambda_3$ | $\mathtt{r}(\Lambda_3)$ | $\Lambda_4$ | $\mathtt{r}(\Lambda_4)$ |
|---|---|---|---|---|---|---|---|---|---|
| | 801 | 1.8756e+00 | −− | 6.6290e-01 | −− | 1.1960e-02 | −− | 4.9732e+00 | −− |
| | 3137 | 9.4552e-01 | 1.0035 | 3.3426e-01 | 1.0031 | 3.0154e-03 | 2.0186 | 2.4931e+00 | 1.0117 |
| 0 | 7009 | 6.3131e-01 | 1.0049 | 2.2319e-01 | 1.0048 | 1.3423e-03 | 2.0135 | 1.6631e+00 | 1.0072 |
| | 12417 | 4.7374e-01 | 1.0042 | 1.6749e-01 | 1.0042 | 7.5547e-04 | 2.0103 | 1.2476e+00 | 1.0052 |
| | 19361 | 3.7909e-01 | 1.0036 | 1.3403e-01 | 1.0036 | 4.8362e-04 | 2.0083 | 9.9822e-01 | 1.0042 |
| | 2753 | 1.5275e-01 | −− | 5.3977e-02 | −− | 6.0926e-04 | −− | 4.0644e-01 | −− |
| | 10881 | 3.8424e-02 | 2.0084 | 1.3587e-02 | 2.0074 | 7.6697e-05 | 3.0159 | 1.0766e-01 | 1.9332 |
| 1 | 24385 | 1.7101e-02 | 2.0064 | 6.0479e-03 | 2.0061 | 2.2760e-05 | 3.0110 | 4.8702e-02 | 1.9661 |
| | 43265 | 9.6244e-03 | 2.0051 | 3.4039e-03 | 2.0049 | 9.6074e-06 | 3.0084 | 2.7527e-02 | 1.9901 |
| | 67521 | 6.1611e-03 | 2.0042 | 2.1791e-03 | 2.0041 | 4.9203e-06 | 3.0068 | 1.7648e-02 | 1.9976 |
| | 5601 | 9.6676e-03 | −− | 3.3427e-03 | −− | 2.9024e-05 | −− | 4.4573e-02 | −− |
| | 22209 | 1.3049e-03 | 2.9075 | 4.4608e-04 | 2.9241 | 1.9316e-06 | 3.9342 | 1.0411e-02 | 2.1114 |
| 2 | 49825 | 3.9533e-04 | 2.9558 | 1.3486e-04 | 2.9609 | 3.8905e-07 | 3.9663 | 3.3828e-03 | 2.7825 |
| | 88449 | 1.6788e-04 | 2.9847 | 5.7233e-05 | 2.9870 | 1.2382e-07 | 3.9897 | 1.4440e-03 | 2.9665 |
| | 138081 | 8.6179e-05 | 2.9941 | 2.9370e-05 | 2.9957 | 5.0834e-08 | 3.9974 | 7.4520e-04 | 2.9705 |

Table 5.5: Example 1. Convergence history of some terms using a uniformly generated sequence of triangular meshes (table produced by the author).

| $k$ | $N$ | $\Lambda_1$ | $\mathtt{r}(\Lambda_1)$ | $\Lambda_2$ | $\mathtt{r}(\Lambda_2)$ | $\Lambda_3$ | $\mathtt{r}(\Lambda_3)$ | $\Lambda_4$ | $\mathtt{r}(\Lambda_4)$ |
|---|---|---|---|---|---|---|---|---|---|
| | 903 | 1.8103e+00 | −− | 7.6139e-01 | −− | 1.6158e-02 | −− | 5.0494e+00 | −− |
| | 3891 | 8.8261e-01 | 0.9836 | 3.5881e-01 | 1.0301 | 3.5023e-03 | 2.0936 | 2.3539e+00 | 1.0450 |
| | 7806 | 6.2697e-01 | 0.9824 | 2.5287e-01 | 1.0052 | 1.7330e-03 | 2.0210 | 1.6545e+00 | 1.0129 |
| | 13071 | 4.8602e-01 | 0.9880 | 1.9519e-01 | 1.0045 | 1.0307e-03 | 2.0161 | 1.2752e+00 | 1.0102 |
| | 19686 | 3.9676e-01 | 0.9911 | 1.5892e-01 | 1.0039 | 6.8250e-04 | 2.0131 | 1.0374e+00 | 1.0078 |
| | 2723 | 1.4070e-01 | −− | 6.1339e-02 | −− | 7.7155e-04 | −− | 3.7815e-01 | −− |
| | 11669 | 3.0868e-02 | 2.0848 | 1.3240e-02 | 2.1072 | 7.6419e-05 | 3.1778 | 8.4359e-02 | 2.0619 |
| | 23414 | 1.5308e-02 | 2.0143 | 6.5354e-03 | 2.0276 | 2.6446e-05 | 3.0475 | 4.2013e-02 | 2.0020 |
| | 39209 | 9.1135e-03 | 2.0117 | 3.8807e-03 | 2.0219 | 1.2089e-05 | 3.0367 | 2.5064e-02 | 2.0038 |
| | 59054 | 6.0396e-03 | 2.0091 | 2.5678e-03 | 2.0166 | 6.5029e-06 | 3.0280 | 1.6630e-02 | 2.0033 |
| | 5257 | 5.8995e-03 | −− | 3.3259e-03 | −− | 3.3573e-05 | −− | 5.2785e-02 | −− |
| | 22471 | 6.2194e-04 | 3.0975 | 3.4240e-04 | 3.1302 | 1.5341e-06 | 4.2484 | 6.9226e-03 | 2.7969 |
| | 45091 | 2.2035e-04 | 2.9797 | 1.1957e-04 | 3.0212 | 3.6877e-07 | 4.0937 | 2.5165e-03 | 2.9059 |
| | 75511 | 1.0208e-04 | 2.9849 | 5.4821e-05 | 3.0249 | 1.2775e-07 | 4.1120 | 1.1768e-03 | 2.9482 |
| | 113731 | 5.5393e-05 | 2.9850 | 2.9538e-05 | 3.0199 | 5.5315e-08 | 4.0876 | 6.4060e-04 | 2.9699 |

Table 5.6: Example 1. Convergence history of some terms using a uniformly generated sequence of hexagonal meshes (table produced by the author).

### 5.4.2 Example 2

We consider again the unit square $\Omega := (0,1)^2$, and choose $\mathbf{f}$ and $\mathbf{g}$ such that the exact solution is given by

$$\mathbf{u}(\mathbf{x}) := \begin{pmatrix} (1+x_1-e^{x_1})(1-\cos(x_2)) \\ (1-e^{x_1})(\sin(x_2)-x_2) \end{pmatrix} \quad \text{and} \quad p(\mathbf{x}) := \frac{1}{x_1+0.1} - p_0$$

for all $\mathbf{x} := (x_1, x_2)^{\mathrm{t}} \in \Omega$, where $p_0 \in \mathrm{R}$ is such that $\int_\Omega p = 0$ and we use again the same nonlinearity $\mu$ from Example 1 (cf. (5.55)). In this example, whereas that $\mathbf{u}$ is smooth, the variable $p$ is singular along the line $x_1 = -0.1$, therefore, we should expect regions of high gradients along the line $x_1 = 0$. For this test, we make use of hexagonal meshes (see Figure 5.5).

First, we show that the adaptive methods decrease faster than those obtained by uniforms. This fact is better illustrated in Figure 5.2. In addition, the order of convergence of the estimator is shown in Figure 5.3. Also, the effectivity index remain bounded from above and below, which confirms the reliability and efficiency of $\boldsymbol{\eta}$. More precisely, we can observe that the effectivity for $\boldsymbol{\eta}$ is very near to 1, which is highly desirable because this determine the good quality of the estimator. Next, the Figure 5.4 show the orders of convergence of all variables under the refinement. We notice that the rate of convergence $O(h^{k+1})$ is attained by all the unknowns, including the postprocessed $\mathbf{u}$ and $p$.

Also, some intermediate meshes obtained with this adaptive strategy are displayed in Figure 5.5. Notice there that the adapted meshes concentrate the refinements along the line $x_1 = 0$, which means that the method is able to recognize the regions with high gradients of the solutions.

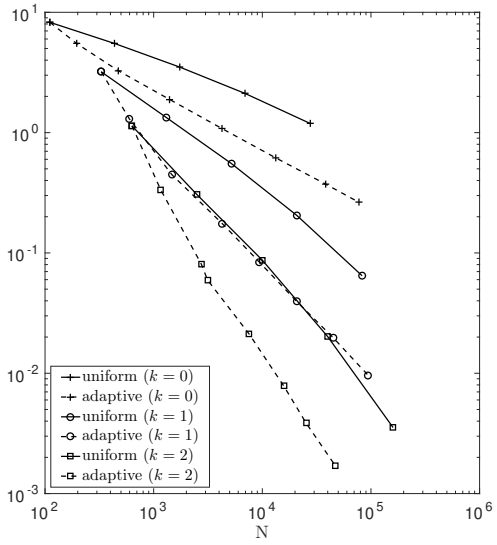


Figure 5.2: Example 2. Convergence history under uniform and adaptive refinement of the error $\mathsf{e}(\mathbf{u}, \mathbf{t}, \boldsymbol{\sigma})$ using hexagonal meshes (figure produced by the author).

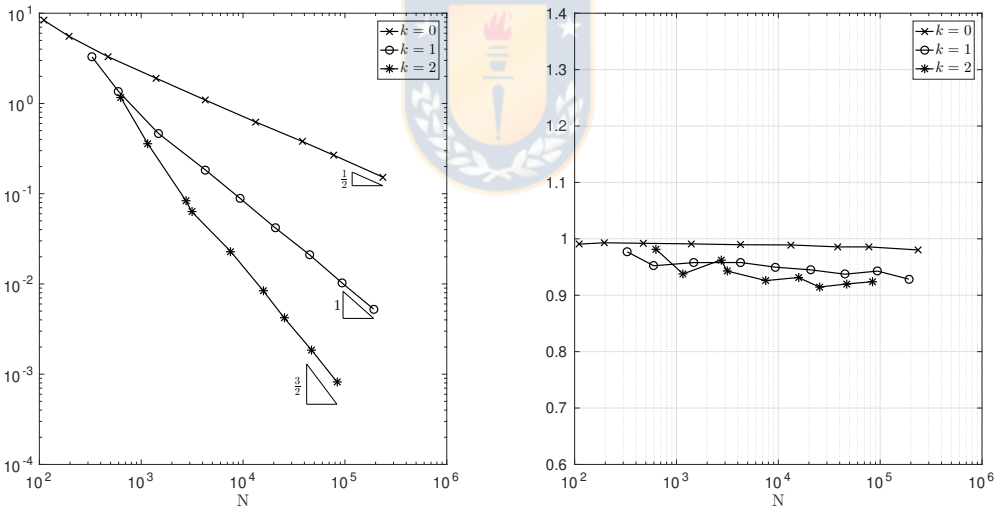


Figure 5.3: Example 2. Behavior under adaptive refinement (left). Effectivity of the estimator (right) (figure produced by the author).

### 5.4.3 Example 3

We take the L-shaped domain $\Omega := (-1, 1)^2 \setminus (0, 1)^2$, and choose $\mathbf{f}$ and $\mathbf{g}$ such that the exact solution is given by

$$\mathbf{u}(\mathbf{x}) \;:=\; \mathbf{curl}\big(\sqrt{(x_1 - 0.01)^2 + (x_2 - 0.01)^2}\big) \qquad \text{and} \qquad p(\mathbf{x}) \;:=\; \frac{1}{x_2 + 1.1} - p_0$$

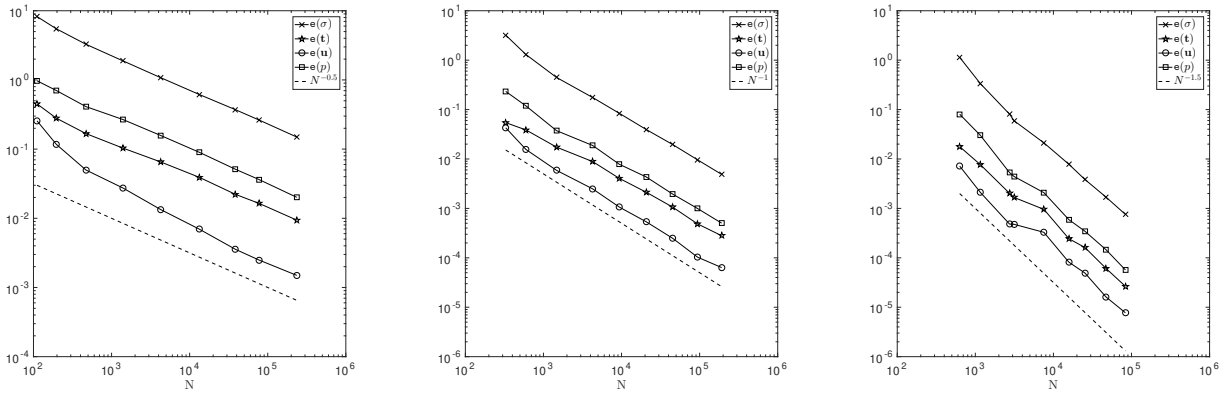


Figure 5.4: Example 2. Convergence history of the variables using an adaptive strategy based in the estimator $\boldsymbol{\eta}$ (figure produced by the author).

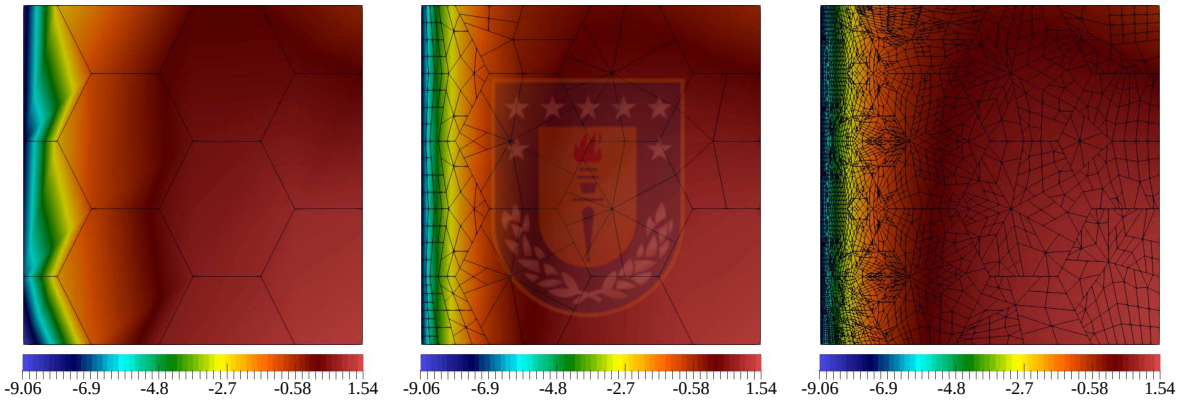


Figure 5.5: Example 2. Approximate pseudostress component $\boldsymbol{\sigma}^{\star}_{11,h}$. Some meshes from the adaptive refinement sequence obtained with $k = 1$: initial (left), after 3 refinement steps (center), and after 7 refinement steps (right) (figure produced by the author).

for all $\mathbf{x} := (x_1, x_2)^{\mathrm{t}} \in \Omega$, where $p_0 \in \mathrm{R}$ is such that $\int_\Omega p = 0$. Moreover, we consider the nonlinear viscosity $\mu$ given by

$$\mu(s) \ := \ \frac{1}{2} + \frac{1}{2}(1 + s^2)^{-1/4} \qquad \forall\, s \geq 0\,. \tag{5.56}$$

Note in this example that $\mathbf{u}$ and $p$ are singular near to the origin, and along the line $x_2 = -1.1$, respectively. Hence, we should expect regions of high gradients around $(0, 0)$, and along the line $x_2 = -1$. For this test, we use meshes composed of distorted squares (see Figure 5.9).

Firstly, as expected, the error of the adaptive method decrease faster than the obtained by the uniform one. This fact is illustrated in Figure 5.6. In addition, from Figure 5.7, we can observe how the effectivity index remain again bounded from above and below, which confirms again the reliability and efficiency of the estimator for the associated adaptive algorithm as well. Here we can see a similar behavior to the observed in the Example 2, in connection with the optimality properties of the

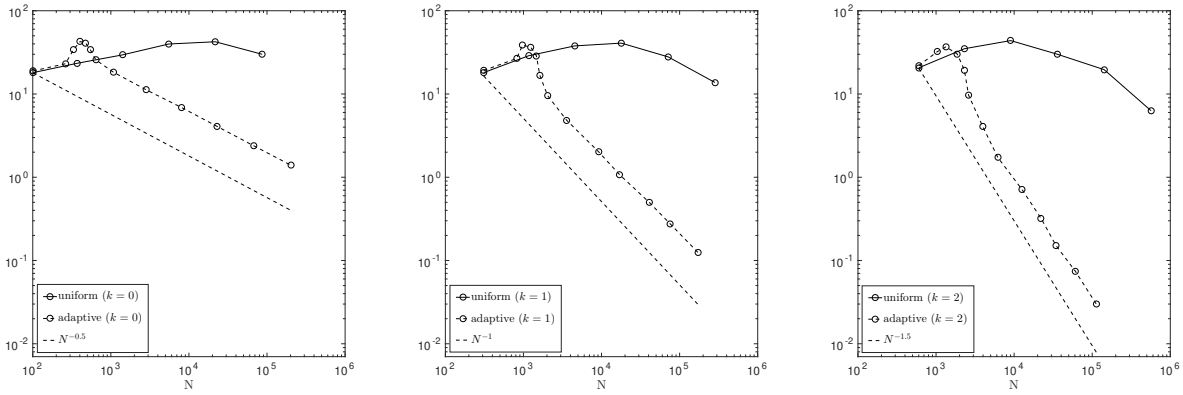


Figure 5.6: Example 3. Convergence history under uniform and adaptive refinement of the error $\mathbf{e}(\mathbf{u}, \mathbf{t}, \boldsymbol{\sigma})$ using the estimator $\boldsymbol{\eta}$ and meshes composed of distorted squares (figure produced by the author).

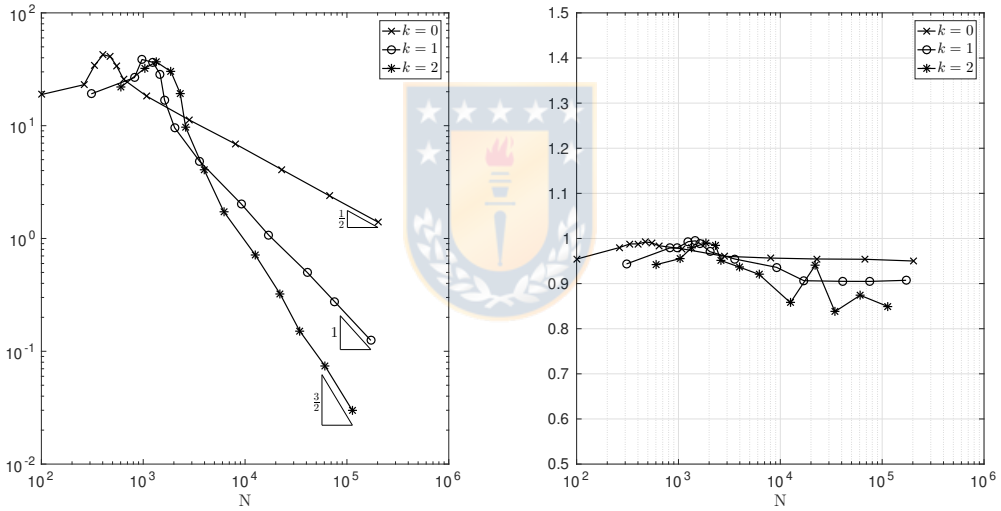


Figure 5.7: Example 3. Behavior under adaptive refinement (left). Effectivity of the estimator (right) (figure produced by the author).

estimator. Also, the robustness with respect to the nonlinearity is established.

On the other hand, Figure 5.8 shows the orders of convergence of all variables under refinement. We notice that the rate of convergence $O(h^{k+1})$ is attained by all the unknowns, including the postprocessed $\mathbf{u}$ and $p$. Finally, some intermediate meshes obtained with this adaptive strategy are displayed in Figures 5.9. Notice there that the adapted meshes concentrate the refinements around the origin and the line $x_2 = -1$, which means that the method is able to recognize the regions with high gradients of the solutions.

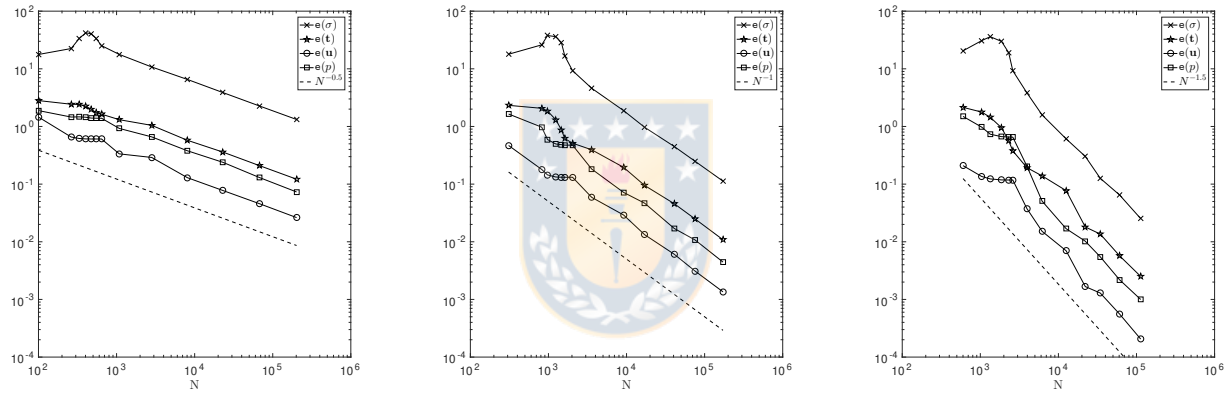


Figure 5.8: Example 3. Convergence history of the variables using an adaptive strategy based in the estimator $\boldsymbol{\eta}$ (figure produced by the author).

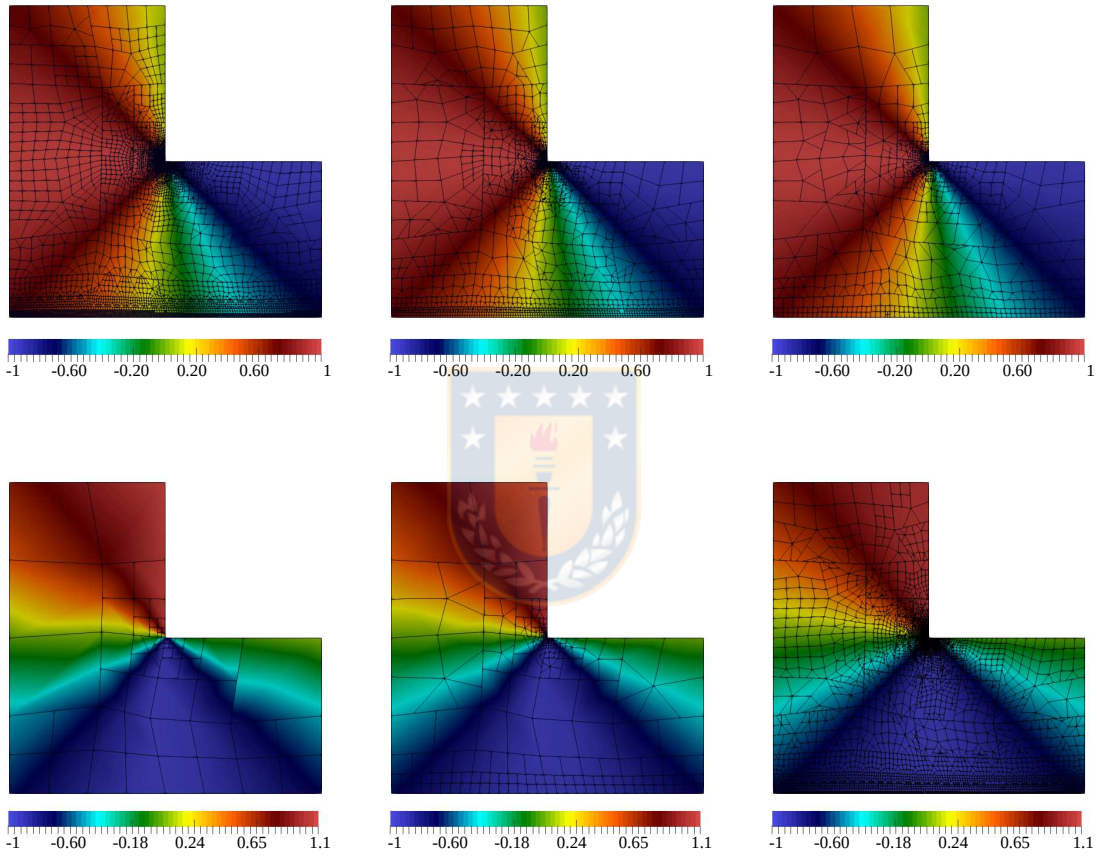


Figure 5.9: Example 3. Approximate velocity component $\mathbf{u}_{2,h}$. (Top) The mesh after eleven adaptive refinements with $k = 0$ (left), $k = 1$ (center) and $k = 2$ (right). Approximate velocity component $\mathbf{u}_{1,h}$ (Below) Some meshes from the adaptive refinement sequence obtained with $k = 1$: after 4 refinement steps (left), after 8 refinement steps (center), and after 12 refinement steps (right) (figure produced by the author).

# Summary and Future work

## Summary

In this thesis we developed mixed virtual element methods for a set of partial differential equations of physical interest in fluid mechanics. We have focused our analysis on some nonlinear problems, in particular, we considered Brinkman, Navier-Stokes, and Boussinesq models. Here, the solvability analysis of both continuous and discrete problems as well as their convergence are presented. As a summary of our main contributions, we state the following:

1. We have introduced a mixed-VEM for a dual-mixed formulation of a nonlinear Brinkman model of porous media flow, in which the main unknowns were given by the gradient of the velocity and the pseudostress, whereas the velocity and the pressure are computed via postprocessing formulae. The discrete scheme was derived using a virtual subspace for the pseudostress and piecewise-polynomials for the gradient of the velocity. Furthermore, concepts of nonlinear functional analysis were used to prove the well-posedness of it. The corresponding a priori error estimates were derived, also. In addition, we introduced an element-by-element postprocessing formula for the pseudostress, which provided an optimally convergent approximation of this unknown with respect to the broken $\mathbb{H}(\mathbf{div})$-norm. Finally, several numerical tests were reported to valid the good perfomance of the proposed scheme, as well as the predicted convergence orders.

2. We have proposed and analyzed a mixed-VEM for a pseudostress-velocity formulation of the Navier-Stokes problem. In this way, the pressure were easily recovered through a simple postprocessing. The virtual scheme was obtained through the incorporation of virtual spaces for $\mathbf{H}^1$ and $\mathbb{H}(\mathbf{div})$, in order to approximate the velocity and the pseudostress, respectively. The corresponding solvability analysis was carried out using fixed point strategies. In turn, Strang-type estimates were used to obtain error bounds for both the involved variables and the postprocessed ones. Finally, some numerical examples confirming the theoretical error bounds and illustrating the performance of the proposed discrete scheme were reported.

3. We have introduced and analyzed a mixed-VEM for a pseudostress-based formulation based of the Boussinesq problem, in which the pseudostress, the velocity and the temperature represented the main unknowns. The pressure was computed using a postprocessing procedure. The discrete problem was proposed using three virtual subspaces for $\mathrm{H}^1$, $\mathbf{H}^1$ and $\mathbb{H}(\mathbf{div})$ in order to approximate the unknows. Fixed point strategies were used to establish the solvability analysis of the associated scheme. Further, Strang-type estimates were applied to derive the a priori error

estimates for the components of the virtual element solution as well as for the fully computable projections of them and the postprocessed pressure.

4. We have derived a posteriori error estimates for a mixed-VEM approach for a second order elliptic equation in divergence form with mixed boundary conditions. We have proved upper and lower bounds for the error between the true solution and both the VEM approximation and a computable postprocessing of it. In particular, the postprocessing permitted us to obtain optimal error estimates in the broken H(div)-norm, whereas for the directly computable projection of the virtual element approximation, it is only possible to prove error estimates in the $L^2$-norm. Arguments based in the global inf-sup condition, suitable Helmholtz decompositions and a Clément-type interpolant were used to derive the upper bound. The lower bound was obtained by using localisation techniques of bubble functions. We have also proposed an adaptive algorithm based on the fully local and computable error estimator derived from the a posteriori error analysis. Its performance and effectiveness were illustrated through numerical tests.

5. We have established the a posteriori error analysis for a mixed virtual element method associated to a nonlinear Brinkman model of porous media flow. We derived a reliable and efficient estimator up to some virtual inconsistency terms for the respective scheme. In addition, several numerical results were provided in order to illustrate the reliability and efficiency of the estimator, together with the expected behavior of the associated adaptive algorithm.

## Future work

The methods developed and the results obtained in this thesis have motivated several ongoing and future projects. Some of them are described below:

1. To provide details concerning to the implementation of the mixed-VEM described in **Chapter** 2, together with several numerical examples confirming the respective analysis.

2. To complement the mixed-VEM described in **Chapter** 3 with its respective numerical computations. The aim is to obtain several numerical tests confirming the theoretical error bounds and illustrating the performance of the proposed discrete scheme. Moreover, we plan to implement adapative strategies for this problem.

3. To study new VEM for the Boussinesq problem and related problems. On the one hand, we are interested in extending the ideas proposed in [21] for this problem. On the other hand, we would like to study non-augmented approaches where Banach instead of Hilbert spaces are used for the unknows.

4. To extend our study to the Navier-Stokes-Brinkman problem proposed in [72]. Here, our aim is to apply the ideas from [69] to present a mixed-VEM where virtual subspaces are used to approximate the pseudostress and the velocity. In contrast to [69] and [67], we plan to approximate the velocity using the approach from [21].

5. To study anisotropic error estimates for virtual element methods. We plan to analyze the behavior of mixed-VEM under uniform and adaptive refinement with highly anisotropic meshes. Also, we would like to take advantage of the flexibility of VEM to use general meshes, and to explore new adaptive refinement strategies.

6. To analyze the coupling of mixed-VEM and Boundary Element Methods. From [66] and [65], we plan to extend this approach to mixed methods, in particular them problems involving nonlinear equations.

# Sumario y trabajo futuro

## Sumario

En esta tesis desarrollamos métodos de elementos virtuales mixtos para un conjunto de ecuaciones diferenciales parciales de interés físico en mecánica de fluidos. Hemos enfocado nuestro análisis en algunos problemas no lineales, en particular, consideramos los modelos de Brinkman, Navier-Stokes y Boussinesq. Se presenta el análisis de solubilidad tanto del problema continuo como del discreto, así como el respectivo análisis de convergencia. Como un resumen de nuestras principales contribuciones presentamos lo siguiente:

1. Hemos introducido un mixed-VEM para una formulación dual-mixta de un modelo no lineal del problema de Brinkman para flujo en medios porosos, en el cual las principales incógnitas estaban dadas por el gradiente de la velocidad y el pseudoesfuerzo, mientras que la velocidad y la presión son computadas vía formulas de postprocesamiento. Se derivó el esquema discreto usando un espacio virtual para el pseudoesfuerzo y polinomios a trozos para el gradiente de la velocidad. De este modo, se usaron conceptos de análisis funcional no lineal para probar que dicho esquema estaba bien puesto. Adicionalmente, se introdujo un post-procesamiento para el pseudoesfuerzo, con el cual se obtiene una aproximación con convergencia óptima para esta incógnita, con respecto a la norma $\mathbb{H}(\mathbf{div})$ por tramos. Finalmente, se presentaron varios ejemplos numéricos, los cuales validaron el buen rendimiento del esquema propuesto, así como los órdenes de convergencia predichos.

2. Hemos propuesto y analizado un mixed-VEM para una formulación pseudoesfuerzo-velocidad del problema de Navier-Stokes. De esta manera, la presión fue fácilmente recuperada a través de un postproceso. El esquema virtual fue prupuesto a través de la incorporación de espacios virtuales para $\mathbf{H}^1$ y $\mathbb{H}(\mathbf{div})$, con el fin de aproximar la velocidad y el pseudoesfuerzo, respectivamente. Luego, se obtuvo el correspondiente análisis de solubilidad usando estrategias de punto fijo. Se usaron estimaciones tipo Strang para obtener cotas de error tanto para las variables involucradas como para las postprocesadas. Finalmente, se presentaron algunos ejemplos ejemplos numéricos que confirmaron las cotas de error e ilustraron el buen rendimiento del esquema discreto propuesto.

3. Hemos introducido y analizado un mixed-VEM para una formulación basada en pseudoesfuerzos del problema de Boussinesq, en el cual el pseudoesfuerzo, la velocidad y la temperatura representaron las principales incógnitas. La presión fue computada usando postprocesamiento. El problema discreto fue planteado usando tres subespacios virtuales para $\mathrm{H}^1$, $\mathbf{H}^1$ y $\mathbb{H}(\mathbf{div})$, con

el fin de aproximar la temperatura, velocidad y el pseudoesfuerzo, respectivamente. Se usaron estrategias de punto fijo para establecer el análisis de solubilidad del esquema asociado. Además, se aplicaron estimaciones tipo Strang para obtener cotas de error tanto para las variables involucradas como para las postprocesadas.

4. Hemos derivado estimaciones de error a posteriori para una discretización con elementos virtuales mixtos de una ecuación elíptica de segundo orden en forma de divergencia y con condiciones de frontera mixta. Hemos probado cotas superios e inferiores para el error entre la solución verdadera y ambas, la aproximación virtual y un postproceso computable de ésta. En particular, el postprocesamiento nos permitió obtener estimas de error óptimas en la norma H(div) por tramos, mientras que para la proyección computable de la aproximación virtual, solo fue posible probar estimas de error en la norma $L^2$. Se usaron argumentos basados en la condición inf-sup global, descomposiciones de Helmholtz adecuadas, y un interpolante tipo Clément para derivar la cota superior. La cota inferior se obtuvo mediante el uso de técnicas de localización basados en funciones de burbuja. También hemos propuesto un algoritmo adaptativo basado en el estimador de error totalmente local y computable derivado del análisis de error a posteriori. Su rendimiento y efectividad se ilustraron mediante algunas pruebas numéricas.

5. Hemos establecido el análisis de error a posteriori para un método de elementos virtuales mixto asociado a un modelo no lineal del problema de Brinkman de flujo en medios porosos. Derivamos un estimadore de error confiable y eficiente hasta ciertos términos de oscilación para el esquema respectivo. Adicionalmente, se presentaron varios resultados numéricos con el fin de ilustrar la confiabilidad y eficiencia del estimador, junto con el comportamiento esperado del algoritmo adaptativo asociado.

## Trabajo futuro

Los métodos desarrollados y los resultados obtenidos en esta tesis han motivado varios trabajos en desarrollo y proyectos futuros. Algunos de ellos se describen a continuación.

1. Proveer los detalles relacionados con la implementación del mixed-VEM descrito en el **Capítulo** 2, junto con varios ejemplos numéricos que respalden el análisis.

2. Complementar el mixed-VEM descrito en el **Capítulo** 3 con sus respectivos cálculos numéricos. La finalidad es presentar varios ejemplos numéricos que confirmen los resultados teóricos obtenidos y que respalden las tasas de convergencia predichas. También se pretende implementar estrategias adaptativas.

3. Estudiar nuevas discretizaciones VEM para las ecuaciones de Boussinesq y problemas relacionados. Por un lado, estamos interesados en extender las ideas propuestas en [21] para aplicarlas al problema mencionado. Por otro lado, nos gustaría estudiar enfoques no aumentados donde se usan espacios de Banach en lugar de espacios de Hilbert.

4. Extender nuestro estudio al problema de Navier-Stokes-Brinkman propuesto en [72]. La finalidad es aplicar las ideas expuestas en [69] para presentar una discretización mixed-VEM donde tanto el

pseudoesfuerzo como la velocidad se busquen en espacios virtuales. En contraste con [69] y [67], se pretende usar nuevos espacios virtuales para aproximar la velocidad. Para este fin, planeamos aplicar el enfoque estudiado en [21].

5. Estudiar estimaciones de error anisótropicas para métodos de elementos virtuales mixtos. Se pretende analizar el comportamiento de esquemas virtuales mixtos bajo refinamiento uniforme y adaptativo de mallas con altos grados de anisotropía. Tambien se quiere aprovechar la flexibilidad que ofrece el enfoque VEM para explorar nuestras estrategias de refinamiento adaptativo.

6. Analizar el acople de métodos virtuales mixtos con métodos de elementos de frontera. Tomando como base los trabajos [66] y [65], la idea es extender este enfoque a metodos mixtos, y en particular a aquellos que involucran problemas no lineales.

# References


[1] B. Adams and T. Olson, *The mesostructure-properties linkage in polycrystals*, Prog. Mater. Sci., 43 (1998), pp. 1–88.

[2] R. A. Adams and J. J. F. Fournier, *Sobolev spaces*, vol. 140 of Pure and Applied Mathematics (Amsterdam), Elsevier/Academic Press, Amsterdam, second ed., 2003.

[3] P. Adler and J. Thovert, *Fractures and Fracture Networks*, Kluwer Academic, Dordrecht, 1999.

[4] B. Ahmad, A. Alsaedi, F. Brezzi, L. D. Marini, and A. Russo, *Equivalent projectors for virtual element methods*, Comput. Math. Appl., 66 (2013), pp. 376–391.

[5] M. Ainsworth and J. T. Oden, *A posteriori error estimation in finite element analysis*, Pure and Applied Mathematics (New York), Wiley-Interscience [John Wiley & Sons], New York, 2000.

[6] J. Almonacid and G. N. Gatica, *A fully-mixed finite element method for the boussinesq problem with temperature-dependent parameters*, Comput. Methods Appl. Mech. Engrg. DOI: https://doi.org/10.1515/cmam-2018-0187.

[7] J. A. Almonacid, G. N. Gatica, and R. Oyarzúa, *A mixed–primal finite element method for the Boussinesq problem with temperature-dependent viscosity*, Calcolo, 55 (2018), pp. Art. 36, 42.

[8] J. A. Almonacid, G. N. Gatica, R. Oyarzúa, and R. Ruiz-Baier, *A new mixed finite element method for the n-dimensional boussinesq problem with temperature-dependent viscosity*, Preprint 2018-18, Centro de Investigación en Ingeniería Matemática, Universidad de Concepción, Chile [available at: `https://www.ci2ma.udec.cl/publicaciones/prepublicaciones`].

[9] M. Alvarez, G. N. Gatica, and R. Ruiz-Baier, *A posteriori error analysis for a viscous flow-transport problem*, ESAIM Math. Model. Numer. Anal., 50 (2016), pp. 1789–1816.

[10] P. F. Antonietti, L. Beirão da Veiga, D. Mora, and M. Verani, *A stream virtual element formulation of the Stokes problem on polygonal meshes*, SIAM J. Numer. Anal., 52 (2014), pp. 386–404.

[11] D. N. Arnold, F. Brezzi, B. Cockburn, and L. D. Marini, *Unified analysis of discontinuous Galerkin methods for elliptic problems*, SIAM J. Numer. Anal., 39 (2001/02), pp. 1749–1779.

[12] T. P. Barrios, G. N. Gatica, M. González, and N. Heuer, *A residual based a posteriori error estimator for an augmented mixed finite element method in linear elasticity*, M2AN Math. Model. Numer. Anal., 40 (2006), pp. 843–869 (2007).

[13] L. Beirão da Veiga, F. Brezzi, A. Cangiani, G. Manzini, L. D. Marini, and A. Russo, *Basic principles of virtual element methods*, Math. Models Methods Appl. Sci., 23 (2013), pp. 199–214.

[14] L. Beirão da Veiga, F. Brezzi, L. D. Marini, and A. Russo, *$H(div)$ and $H(\mathbf{curl})$-conforming virtual element methods*, Numer. Math., 133 (2016), pp. 303–332.

[15] L. Beirão da Veiga, F. Brezzi, L. D. Marini, and A. Russo, *Mixed virtual element methods for general second order elliptic problems on polygonal meshes*, ESAIM Math. Model. Numer. Anal., 50 (2016), pp. 727–747.

[16] L. Beirão da Veiga, F. Brezzi, L. D. Marini, and A. Russo, *Virtual element method for general second-order elliptic problems on polygonal meshes*, Math. Models Methods Appl. Sci., 26 (2016), pp. 729–750.

[17] L. Beirão da Veiga, K. Lipnikov, and G. Manzini, *The mimetic finite difference method for elliptic problems*, vol. 11 of MS&A. Modeling, Simulation and Applications, Springer, Cham, 2014.

[18] L. Beirão da Veiga, C. Lovadina, and D. Mora, *A virtual element method for elastic and inelastic problems on polytope meshes*, Comput. Methods Appl. Mech. Engrg., 295 (2015), pp. 327–346.

[19] L. Beirão da Veiga, C. Lovadina, and A. Russo, *Stability analysis for the virtual element method*, Math. Models Methods Appl. Sci., 27 (2017), pp. 2557–2594.

[20] L. Beirão da Veiga, C. Lovadina, and G. Vacca, *Divergence free virtual elements for the Stokes problem on polygonal meshes*, ESAIM Math. Model. Numer. Anal., 51 (2017), pp. 509–535.

[21] L. Beirão da Veiga, C. Lovadina, and G. Vacca, *Virtual elements for the Navier-Stokes problem on polygonal meshes*, SIAM J. Numer. Anal., 56 (2018), pp. 1210–1242.

[22] L. Beirão da Veiga and G. Manzini, *An a posteriori error estimator for the mimetic finite difference approximation of elliptic problems*, Internat. J. Numer. Methods Engrg., 76 (2008), pp. 1696–1723.

[23] L. Beirão da Veiga and G. Manzini, *A virtual element method with arbitrary regularity*, IMA J. Numer. Anal., 34 (2014), pp. 759–781.

[24] L. Beirão da Veiga and G. Manzini, *Residual a posteriori error estimation for the virtual element method for elliptic problems*, ESAIM Math. Model. Numer. Anal., 49 (2015), pp. 577–599.

[25] L. Beirão da Veiga, D. Mora, G. Rivera, and R. Rodríguez, *A virtual element method for the acoustic vibration problem*, Numer. Math., 136 (2017), pp. 725–763.

[26] S. Berrone and A. Borio, *A residual a posteriori error estimate for the Virtual Element Method*, Math. Models Methods Appl. Sci., 27 (2017), pp. 1423–1458.

[27] S. C. Brenner and L. R. Scott, *The mathematical theory of finite element methods*, vol. 15 of Texts in Applied Mathematics, Springer, New York, third ed., 2008.

[28] F. Brezzi, R. S. Falk, and L. D. Marini, *Basic principles of mixed virtual element methods*, ESAIM Math. Model. Numer. Anal., 48 (2014), pp. 1227–1240.

[29] F. Brezzi and M. Fortin, *Mixed and hybrid finite element methods*, vol. 15 of Springer Series in Computational Mathematics, Springer-Verlag, New York, 1991.

[30] E. Cáceres and G. N. Gatica, *A mixed virtual element method for the pseudostress-velocity formulation of the Stokes problem*, IMA J. Numer. Anal., 37 (2017), pp. 296–331.

[31] E. Cáceres, G. N. Gatica, and F. A. Sequeira, *A mixed virtual element method for the Brinkman problem*, Math. Models Methods Appl. Sci., 27 (2017), pp. 707–743.

[32] ——, *A mixed virtual element method for quasi-Newtonian Stokes flows*, SIAM J. Numer. Anal., 56 (2018), pp. 317–343.

[33] J. Camaño, G. N. Gatica, R. Oyarzúa, and R. Ruiz-Baier, *An augmented stress-based mixed finite element method for the steady state Navier-Stokes equations with nonlinear viscosity*, Numer. Methods Partial Differential Equations, 33 (2017), pp. 1692–1725.

[34] J. Camaño, G. N. Gatica, R. Oyarzúa, and G. Tierra, *An augmented mixed finite element method for the Navier-Stokes equations with variable viscosity*, SIAM J. Numer. Anal., 54 (2016), pp. 1069–1092.

[35] J. Camaño, R. Oyarzúa, and G. Tierra, *Analysis of an augmented mixed-FEM for the Navier-Stokes problem*, Math. Comp., 86 (2017), pp. 589–615.

[36] A. Cangiani, P. Chatzipantelidis, G. Diwan., and E. H. Georgoulis, *Virtual element method for quasilinear elliptic problems*, arXiv:1707.01592 [math.NA] (2017).

[37] A. Cangiani, Z. Dong, E. H. Georgoulis, and P. Houston, *hp-version discontinuous Galerkin methods on polygonal and polyhedral meshes*, SpringerBriefs in Mathematics, Springer, Cham, 2017.

[38] A. Cangiani, E. H. Georgoulis, T. Pryer, and O. J. Sutton, *A posteriori error estimates for the virtual element method*, Numer. Math., 137 (2017), pp. 857–893.

[39] A. Cangiani, V. Gyrya, and G. Manzini, *The nonconforming virtual element method for the Stokes equations*, SIAM J. Numer. Anal., 54 (2016), pp. 3411–3435.

[40] A. Cangiani and M. Munar, *A posteriori error estimates for mixed virtual element methods*, Preprint 2019-10, Centro de Investigación en Ingeniería Matemática, Universidad de Concepción, Chile [available at: `https://www.ci2ma.udec.cl/publicaciones/prepublicaciones`].

[41] C. Carstensen, *A posteriori error estimate for the mixed finite element method*, Math. Comp., 66 (1997), pp. 465–476.

[42] C. Carstensen and G. Dolzmann, *A posteriori error estimates for mixed FEM in elasticity*, Numer. Math., 81 (1998), pp. 187–209.

[43] S. Caucao, G. N. Gatica, R. Oyarzúa, and I. Šebestová, *A fully-mixed finite element method for the Navier-Stokes/Darcy coupled problem with nonlinear viscosity*, J. Numer. Math., 25 (2017), pp. 55–88.

[44] H. Chi, L. Beirão da Veiga, and G. H. Paulino, *A simple and effective gradient recovery scheme and a posteriori error estimator for the virtual element method (VEM)*, Comput. Methods Appl. Mech. Engrg., 347 (2019), pp. 21–58.

[45] P. G. Ciarlet, *The finite element method for elliptic problems*, vol. 40 of Classics in Applied Mathematics, Society for Industrial and Applied Mathematics (SIAM), Philadelphia, PA, 2002. Reprint of the 1978 original [North-Holland, Amsterdam].

[46] E. Colmenares, G. N. Gatica, and R. Oyarzúa, *Analysis of an augmented mixed-primal formulation for the stationary Boussinesq problem*, Numer. Methods Partial Differential Equations, 32 (2016), pp. 445–478.

[47] ——, *Fixed point strategies for mixed variational formulations of the stationary Boussinesq problem*, C. R. Math. Acad. Sci. Paris, 354 (2016), pp. 57–62.

[48] ——, *An augmented fully-mixed finite element method for the stationary Boussinesq problem*, Calcolo, 54 (2017), pp. 167–205.

[49] E. Colmenares and M. Neilan, *Dual-mixed finite element methods for the stationary Boussinesq problem*, Comput. Math. Appl., 72 (2016), pp. 1828–1850.

[50] D. Copeland, U. Langer, and D. Pusch, *From the boundary element domain decomposition methods to local Trefftz finite element methods on polyhedral meshes*, in Domain decomposition methods in science and engineering XVIII, vol. 70 of Lect. Notes Comput. Sci. Eng., Springer, Berlin, 2009, pp. 315–322.

[51] D. A. Di Pietro and R. Specogna, *An a posteriori-driven adaptive mixed high-order method with application to electrostatics*, J. Comput. Phys., 326 (2016), pp. 35–55.

[52] A. R. Diaz and A. Bénard, *Designing materials with prescribed elastic properties using polygonal cells*, Internat. J. Numer. Methods Engrg., 57 (2003), pp. 301–314.

[53] M. Discacciati and R. Oyarzúa, *A conforming mixed finite element method for the Navier-Stokes/Darcy coupled problem*, Numer. Math., 135 (2017), pp. 571–606.

[54] L. E. Figueroa, G. N. Gatica, and A. Márquez, *Augmented mixed finite element methods for the stationary Stokes equations*, SIAM J. Sci. Comput., 31 (2008/09), pp. 1082–1119.

[55] G. N. Gatica, *A note on the efficiency of residual-based a-posteriori error estimators for some mixed finite element methods*, Electron. Trans. Numer. Anal., 17 (2004), pp. 218–233.

[56] ——, *A simple introduction to the mixed finite element method*, SpringerBriefs in Mathematics, Springer, Cham, 2014. Theory and applications.

[57] G. N. Gatica, L. F. Gatica, and A. Márquez, *Analysis of a pseudostress-based mixed finite element method for the Brinkman model of porous media flow*, Numer. Math., 126 (2014), pp. 635–677.

[58] G. N. Gatica, L. F. Gatica, and F. A. Sequeira, *Analysis of an augmented pseudostress-based mixed formulation for a nonlinear Brinkman model of porous media flow*, Comput. Methods Appl. Mech. Engrg., 289 (2015), pp. 104–130.

[59] ——, *A* $\mathbb{RT}_k - \mathbf{P}_k$ *approximation for linear elasticity yielding a broken* $H(\mathbf{div})$ *convergent post-processed stress*, Appl. Math. Lett., 49 (2015), pp. 133–140.

[60] ——, *A priori and a posteriori error analyses of a pseudostress-based mixed formulation for linear elasticity*, Comput. Math. Appl., 71 (2016), pp. 585–614.

[61] G. N. Gatica, M. González, and S. Meddahi, *A low-order mixed finite element method for a class of quasi-Newtonian Stokes flows. I. A priori error analysis*, Comput. Methods Appl. Mech. Engrg., 193 (2004), pp. 881–892.

[62] G. N. Gatica, A. Márquez, R. Oyarzúa, and R. Rebolledo, *Analysis of an augmented fully-mixed approach for the coupling of quasi-Newtonian fluids and porous media*, Comput. Methods Appl. Mech. Engrg., 270 (2014), pp. 76–112.

[63] G. N. Gatica, A. Márquez, and M. A. Sánchez, *Analysis of a velocity-pressure-pseudostress formulation for the stationary Stokes equations*, Comput. Methods Appl. Mech. Engrg., 199 (2010), pp. 1064–1079.

[64] ——, *A priori and a posteriori error analyses of a velocity-pseudostress formulation for a class of quasi-Newtonian Stokes flows*, Comput. Methods Appl. Mech. Engrg., 200 (2011), pp. 1619–1636.

[65] G. N. Gatica and S. Meddahi, *Coupling of virtual element and boundary element methods for the solution of acoustic scattering problems*, Preprint 2019-22, Centro de Investigación en Ingeniería Matemática, Universidad de Concepción, Chile [available at: `https://www.ci2ma.udec.cl/publicaciones/prepublicaciones`].

[66] ——, *On the coupling of vem and bem in two and three dimensions*, Preprint 2018-33, Centro de Investigación en Ingeniería Matemática, Universidad de Concepción, Chile [available at: `https://www.ci2ma.udec.cl/publicaciones/prepublicaciones`].

[67] G. N. Gatica, M. Munar, and F. A. Sequeira, *A mixed virtual element method for the boussinesq problem on polygonal meshes*, Preprint 2019-32, Centro de Investigación en Ingeniería Matemática, Universidad de Concepción, Chile [available at: `https://www.ci2ma.udec.cl/publicaciones/prepublicaciones`].

[68] G. N. Gatica, M. Munar, and F. A. Sequeira, *A mixed virtual element method for a nonlinear Brinkman model of porous media flow*, Calcolo, 55 (2018), pp. Art. 21, 36.

[69] ——, *A mixed virtual element method for the Navier-Stokes equations*, Math. Models Methods Appl. Sci., 28 (2018), pp. 2719–2762.

[70] G. N. Gatica and F. A. Sequeira, *Analysis of an augmented HDG method for a class of quasi-Newtonian Stokes flows*, J. Sci. Comput., 65 (2015), pp. 1270–1308.

[71] ——, *A priori and a posteriori error analyses of an augmented HDG method for a class of quasi-Newtonian Stokes flows*, J. Sci. Comput., 69 (2016), pp. 1192–1250.

[72] L. F. Gatica, R. Oyarzúa, and N. Sánchez, *A priori and a posteriori error analysis of an augmented mixed-FEM for the Navier-Stokes-Brinkman problem*, Comput. Math. Appl., 75 (2018), pp. 2420–2444.

[73] S. Giani, *Solving elliptic eigenvalue problems on polygonal meshes using discontinuous Galerkin composite finite element methods*, Appl. Math. Comput., 267 (2015), pp. 618–631.

[74] J. S. Howell, *Dual-mixed finite element approximation of Stokes and nonlinear Stokes problems using trace-free velocity gradients*, J. Comput. Appl. Math., 231 (2009), pp. 780–792.

[75] J. S. Howell and N. J. Walkington, *Dual-mixed finite element methods for the Navier-Stokes equations*, ESAIM Math. Model. Numer. Anal., 47 (2013), pp. 789–805.

[76] X. Liu and Z. Chen, *The nonconforming virtual element method for the Navier-Stokes equations*, Adv. Comput. Math., 45 (2019), pp. 51–74.

[77] A. F. D. Loula and J. a. N. C. Guerreiro, *Finite element analysis of nonlinear creeping flows*, Comput. Methods Appl. Mech. Engrg., 79 (1990), pp. 87–109.

[78] D. Mora and G. Rivera, *A priori and a posteriori error estimates for a virtual element spectral analysis for the elasticity equations*, IMA Journal of Numerical Analysis. DOI: https://doi.org/10.1093/imanum/dry063.

[79] D. Mora and G. Rivera, *A priori and a posteriori error estimates for a virtual element spectral analysis for the elasticity equations*, IMA Journal of Numerical Analysis. DOI: https://doi.org/10.1093/imanum/dry063.

[80] D. Mora, G. Rivera, and R. Rodríguez, *A virtual element method for the Steklov eigenvalue problem*, Math. Models Methods Appl. Sci., 25 (2015), pp. 1421–1445.

[81] ——, *A posteriori error estimates for a virtual element method for the Steklov eigenvalue problem*, Comput. Math. Appl., 74 (2017), pp. 2172–2190.

[82] L. Mu, J. Wang, Y. Wang, and X. Ye, *Interior penalty discontinuous Galerkin method on very general polygonal and polyhedral meshes*, J. Comput. Appl. Math., 255 (2014), pp. 432–440.

[83] R. Oyarzúa, M. Solano, and P. Zúñiga, *A priori and a posteriori error analyses of a high order unfitted mixed-fem for Stokes flow*, Preprint 2019-15, Centro de Investigación en Ingeniería Matemática, Universidad de Concepción, Chile [available at: `https://www.ci2ma.udec.cl/publicaciones/prepublicaciones`].

[84] A. Quarteroni and A. Valli, *Numerical approximation of partial differential equations*, vol. 23 of Springer Series in Computational Mathematics, Springer-Verlag, Berlin, 1994.

[85] S. Rjasanow and S. Weisser, *Higher order BEM-based FEM on polygonal meshes*, SIAM J. Numer. Anal., 50 (2012), pp. 2357–2378.

[86] ——, *FEM with Trefftz trial functions on polyhedral elements*, J. Comput. Appl. Math., 263 (2014), pp. 202–217.

[87] J. E. Roberts and J.-M. Thomas, *Mixed and hybrid methods*, in Handbook of numerical analysis, Vol. II, Handb. Numer. Anal., II, North-Holland, Amsterdam, 1991, pp. 523–639.

[88] D. Sandri, *Sur l'approximation numérique des écoulements quasi-newtoniens dont la viscosité suit la loi puissance ou la loi de Carreau*, RAIRO Modél. Math. Anal. Numér., 27 (1993), pp. 131–155.

[89] N. Sukumar and A. Tabarraei, *Conforming polygonal finite elements*, Internat. J. Numer. Methods Engrg., 61 (2004), pp. 2045–2066.

[90] G. Vacca, *An $H^1$-conforming virtual element for Darcy and Brinkman equations*, Math. Models Methods Appl. Sci., 28 (2018), pp. 159–194.

[91] R. Verfurth, *A review of a posteriori error estimation and adaptive mesh-refinement techniques*, Chichester : Wiley, 1996.

[92] M. Vohralík and S. Yousef, *A simple a posteriori estimate on general polytopal meshes with applications to complex porous media flows*, Comput. Methods Appl. Mech. Engrg., 331 (2018), pp. 728–760.

[93] E. L. Wachspress, *A rational basis for function approximation*, J. Inst. Math. Appl., 8 (1971), pp. 57–68.

[94] ——, *A rational finite element basis*, Academic Press, Inc. [A subsidiary of Harcourt Brace Jovanovich, Publishers], New York-London, 1975. Mathematics in Science and Engineering, Vol. 114.

[95] S. Weisser, *BEM-based Finite Element Approaches on Polytopal Meshes*, vol. 130 of Lecture Notes in Computational Science and Engineering, Springer International Publishing, 2019.

[96] D. Wirasaet, E. J. Kubatko, C. E. Michoski, S. Tanaka, J. J. Westerink, and C. Dawson, *Discontinuous Galerkin methods with nodal and hybrid modal/nodal triangular, quadrilateral, and polygonal elements for nonlinear shallow water flow*, Comput. Methods Appl. Mech. Engrg., 270 (2014), pp. 113–149.

[97] E. Zeidler, *Nonlinear functional analysis and its applications. II/B*, Springer-Verlag, New York, 1990. Nonlinear monotone operators, Translated from the German by the author and Leo F. Boron.